SANDIA REPORT
SAND2018-4664 Unlimited Release | Printed May 2018

Feasibility of the Zero-V:

A Zero-Emission, Hydrogen Fuel-Cell, Coastal Research Vessel

Leonard E. Klebanoff, Joseph W. Pratt, Robert T. Madsen, Sean A.M. Caughlan, Timothy S. Leach, T. Bruce Appelgate, Jr., Stephen Zoltan Kelety, Hans-Christian Wintervoll, Gerd Petra Haugom and Anthony T.Y. Teo

Prepared by
Sandia National Laboratories,
Livermore, California 94550

Sandia National Laboratories is a multimission laboratory managed and operated by National Technology and Engineering Solutions of Sandia, LLC, a wholly owned subsidiary of Honeywell International, Inc., for the U.S. Department of Energy's National Nuclear Security Administration under contract DE-NA0003525.

Sandia National Laboratories

Issued by Sandia National Laboratories, operated for the United States Department of Energy by National Technology and Engineering Solutions of Sandia, LLC.

Available to DOE and DOE contractors from

- U.S. Department of Energy
  Office of Scientific and Technical Information
  P.O. Box 62
  Oak Ridge, TN 37831

  Telephone: (865) 576-8401
  Facsimile: (865) 576-5728
  E-Mail: reports@osti.gov
  Online ordering: http://www.osti.gov/scitech

Available to the public from

- U.S. Department of Commerce
  National Technical Information Service
  5301 Shawnee Rd
  Alexandria, VA 22312

  Telephone: (800) 553-6847
  Facsimile: (703) 605-6900
  E-Mail: orders@ntis.gov
  Online order: https://classic.ntis.gov/help/order-methods/

Feasibility of the Zero-V:

A Zero-Emission, Hydrogen Fuel-Cell, Coastal Research Vessel

Leonard E. Klebanoff[1]*, Joseph W. Pratt[1], Robert T. Madsen[2], Sean A.M. Caughlan[2], Timothy S. Leach[2], T. Bruce Appelgate, Jr.[3], Stephen Zoltan Kelety[3], Hans-Christian Wintervoll[4], Gerd Petra Haugom[4] and Anthony T.Y. Teo[4]

Sandia National Laboratories

[1]Hydrogen and Materials Science (8367)
Sandia National Laboratories
P.O. Box 969, Livermore, CA 94550

Glosten

[2]Glosten
1201 Western Avenue, Seattle, WA 98101

[3]The Scripps Institution of Oceanography, U.C. San Diego
9500 Gilman Drive, La Jolla, CA 92093

DNV·GL

[4]DNV GL
P.O. Box 300
1322 Hovik, Norway

*Author to whom correspondence should be addressed.

Acknowledgements

It is our pleasure to acknowledge and thank many people who contributed their time and expertise to the Zero-V feasibility study. First, we wish to thank Sujit Ghosh at the U.S. Department of Transportation Maritime Administration (MARAD). Sujit has been the technical project manager for the Zero-V study, and we thank him for his technical contributions, his encouragement and his talent for asking the right questions at the right times. We also thank Michael Carter at MARAD for support of this work, and Tom Thompson, David Palacios and Regina Farr at MARAD for assistance with organizing the final project report-out at MARAD on November 28, 2017.

The authors especially thank Krissy Galbraith, Creative Designer at Sandia National Laboratories for all her hard work assembling this report and making it look great.

Several staff at DNV GL contributed to the regulatory review of the Zero-V. They include Marius Leisner and Torill Grimstad Osberg. We especially acknowledge the efforts of Tomas Tronstad, formerly of DNV GL, who led the DNV GL activity in the first half of the Zero-V project.

The authors thank Ryan Sookhoo of Hydrogenics for invaluable technical discussions about the PEM fuel cells considered in the feasibility study. Ryan provided important details about the fuel-cell operational characteristics, their assembly into "racks," track record in the field, approach to ventilation and safety, required power conditioning electronics and strategies for fuel-cell refurbishment. This information was vital for placing the study on solid technical ground. We also thank Ryan for his consistent encouragement of the work and being Canadian.

The authors thank Catharine Farish and Ian McCauley of Glosten for assistance with the Zero-V design work and project support. Special thanks are extended to Kevin Jirak and Stelios Ambargis of Chart Inc., who provided essential information on the anticipated price of liquid hydrogen (LH_2) tanks on the Zero-V, the expected tank dimensions and weight required to hold the Zero-V LH_2 fuel load, and other tank characteristics such as the maximum allowable working pressure.

The project team received critical support from Kyle McKeown of Linde. The LH_2 tanks considered for the Zero-V are of the type previously used for land-based storage of hydrogen, and also liquid hydrogen transport trailers. Kyle shared his expertise with these systems, important information about how such tanks are refueled with LH_2 and what the requirements are for trailer depressurization before driving on public roads. This refueling information directly impacted feasibilty assessments of refueling the Zero-V in the time required and at the desired locations. Kyle also provided important information on how the tank plumbing needs to be configured to ensure safe operation of these vessels.

The authors also thank Air Products hydrogen experts Dave Farese, Brian Bonner and Brian O'Neil (retired) for discussions of how the LH_2 tanks on the Zero-V could be best refueled using LH_2 trailers. We also thank Jim Mullen from Gardner Cryogenics for providing cost information on LH_2 tanks.

The Zero-V project team received important feedback from University of California San Diego (UCSD) faculty members and Scripps operational staff who attended the September 28, 2017 report/feedback meetings at Scripps. These include Gabi Laske, Mark Ohman, Ken Melville and Rob Pinkel from UCSD. We thank Paul Mauricio from Scripps operations for providing hands-on information about the practical and safe operation of research vessels, as well as their refueling, restocking, and maintenance.

The United States Coast Guard (USCG) assisted in reviewing the technical design of the Zero-V from the standpoint of marine safety. We thank Tim Meyers, Thane Gilman, Capt. John Miller and Lt. James Carter for providing this technical review and attending our project final report-out meeting at MARAD. We appreciate Tim Meyers presenting a review of the USCG findings at this meeting.

We thank a number of organizations and individuals for engaging with the project team on possible locations for refueling the Zero-V with LH_2. These discussions helped us to assess the feasibility of refueling the Zero-V at expected ports of call. Rich Berman of the Port of San Francisco has been incredibly supportive of hydrogen vessel initiatives, and of the Zero-V in particular. Rich technically reviewed the prospects of refueling the vessel at Pier 54 at the Port of San Francisco. We also thank Mike Giari and Giorgio Garilli of the Port of Redwood City for their technical feedback and assessment of refueling the Zero-V at Wharf 5 of the Port of Redwood City. We thank Paul Maricio (again) for evaluation of refueling the Zero-V at the Nimitz Marine Facility at the Scripps campus in La Jolla. We are grateful to Mike Prince, Brian Ackerman and Jim Harvey of the Moss Landing Marine Laboratory for evalu-

ating the Zero-V refueling at the MBARI Pier and elsewhere within their facilities and providing feedback on the Zero-V design.

We thank Emre Veziroglu, Editor-in-Chief of the International Journal of Hydrogen Energy for permission to reproduce the article appearing as Appendix A. We also thank Mikhail Chester, Associate Editor of the Journal Transportation Research D for permission to reproduce the article appearing in Appendix D.

Finally, we thank Tom Escher of the Red and White fleet for inspiring Sandia's work in hydrogen powered vessels, his encouragement of this work in particular, and being a thought and fashion leader in maritime environmental issues.

Abbreviations and Acronyms

AB: Airborne

ABL: Above Baseline

ABS: American Bureau of Shipping

AC: Alternating Current

ACH: Air Changes per Hour

AFFF: Aqueous Film Forming Foam

AIP: Approval in Principle

ARB: Air Resources Board

AUV: Autonomous Underwater Vehicle

BC: Black Carbon

BHP: Brake Horsepower

BSGC: Brake Specific Gas Consumption

CAIP: Conditional Approval in Principle

CCC: Carriage of Cargoes and Containers

CDR: Commander

CEC: California Energy Commission

CFD: Computational Fluid Dynamics

COI: Certificate of Inspection

CONN: Connection

COTP: Captain of the Port

CTD: Conductivity, Temperature and Depth (instrument)

DC: Direct Current

DDT: Deflagration to Detonation Transition

DF: Demand Factor

DOT: Department of Transportation (United States)

DP: Dynamic Positioning

DWL: Design Waterline

EBM: Ecosystem-based Management

ECA: Emission Control Area

ELA: Electrical Load Analysis

EOS: Electrical and Engineering Operator Station

EPA: Environmental Protection Agency (United States)

ESD: Emergency Shutdown

ET: Electronic Technician

EU: European Union

FC: Fuel Cell

FCPM: Fuel Cell Power Module

FLA: Full Load Amperes

FLIP: Floating Instrument Platform

FMEA: Failure Mode and Effects Analysis

FSB: First Structureborne

Gg: Gigagrams = 1 x 10^9 grams

GM: Metacentric Height

GSU: Gas Supply Unit

HAZID: Hazard Identification

HC: Hydrocarbons

HVAC: Heating, Ventilation and Air Conditioning

HVO: Hydrogenated Vegetable Oil

ICE: Internal Combustion Engine

ICES: International Council of the Exploration of the Sea

IGF: International Gas Fueled (Ships)

IJHE: International Journal of Hydrogen Energy

IMCA: International Marine Contractors Association

IMO: International Maritime Organization

IPCC: Intergovernmental Panel on Climate Change

ITTC: International Towing Tank Conference

Kts: Knots

LCG: Longitudinal Center of Gravity

LCH_4: Liquid Methane

LEL: Lower Explosion Limit

LFL: Lower Flammability Limit

LH_2: Liquid Hydrogen

LHV: Lower Heating Value

LNG: Liquid Natural Gas

LKR: Locker

LT: Long Tonnes

MARAD: Maritime Administration (U.S. DOT)

MarFac: Marine Facility

MARVS: Maximum Allowable Relief Valve Setting

MBARI: Monterey Bay Aquarium Research Institute

MLML: Moss Landing Marine Laboratory

NASA: National Aeronautics and Space Administration

NBP: Normal Boiling Point

NCE: Noise Control Engineering

NG: Natural Gas

nm: Nautical Miles

NTP: Normal Temperature and Pressure

O&M: Operations and Maintenance

Ops: Operations

PEM: Proton Exchange Membrane

PBU: Pressure Building Unit

PFSA: Polyfluorinated Sulfonic Acid

PM: Particulate Matter, or Permanent Magnet

PM_{10}: Particulate Matter with Diameter Less Than 10 Microns

RCRV: Regional Class Research Vessel

REMUs: Remote Environmental Monitoring Units

ROV: Remotely Operated Vehicle

R&M: Repair & Maintenance

SAWE: Society of Allied Weight Engineers

SEA: Statistical Energy Analysis

SF-BREEZE: San Francisco Bay Renewable Energy Electric Vessel with Zero Emissions

SIO: Scripps Institution of Oceanography

SMR: Steam Methane Reforming

SOLAS: Safety of Life at Sea

SS4: Sea State 4

SS5: Sea State 5

SSB: Secondary Structureborne

ST: Short Tons

STBD: Starboard

SURR: Surrounding

SWATH: Small Water Area Twin Hull

SWBD: Switchboard

SWBS: Ship Work Breakdown System

SWL: Safe Working Load

TCG: Transverse Center of Gravity

TCS: Tank Connection Space

TRD: Transportation Research Part D

UAV: Unmanned Aerial Vehicle

UC: University of California

UCSD: University of California San Diego

UEL: Upper Explosion Limit

UFL: Upper Flammability Limit

URN: Underwater Radiated Noise

USCG: United States Coast Guard

VAC: Volts Alternating Current

VCG: Vertical Center of Gravity

VDC: Volts Direct Current

WTT: Well-to-Tank

WTW: Well-to-Waves

Executive Summary

The goals of this feasibility study are to determine the technical, regulatory, and economic feasibility of a coastal research vessel powered solely by hydrogen fuel cells, assess the environmental benefits and determine the prospects for refueling such a vessel at the expected ports of call.

For a research vessel, the potential advantages of using hydrogen fuel cells are considerable. For example, zero emissions hydrogen technology allows the collection of air samples with no interference from vessel engine emission. Hydrogen can be readily used in Arctic Oceanographic exploration because hydrogen is not susceptible to the waxing/freezing problems of the petroleum-based fuels. Also, the complete elimination of vessel particulate emissions avoids the formation of "black ice" which is a major concern for increased solar absorbance leading to increased rates of ice melting. Since fuel cells are very low noise power systems, such research vessels are quieter, allowing more accurate sonar mapping operations and reduced noise risk for marine life. PEM fuel cells, being electrical devices, offer faster power response than internal combustion engine technology, which is an advantage in vessel handling and positioning. Fuel cells generate pure, deionized water which can be captured for other purposes such as drinking water for the scientific staff and crew, or for experimental and analytical purposes. This can offset the weight of potable or experimental water needed to be carried on-board. This myriad of potential benefits motivates a detailed exploration of the technical, regulatory, and economic feasibility of designing, building, and operating a practical, commercial, zero-emission coastal research vessel.

The project team consists of Sandia National Laboratories (Project Lead and hydrogen fuel cell technical expertise), Glosten (naval architect), the Scripps Institution of Oceanography (oceanographic research expertise and end user) and DNV GL (maritime regulatory expertise, marine hydrogen systems).

The research missions for the Zero-V were determined by Scripps, and included 14 research activities of particular significance in coastal oceanography that require a modern, capable, general-purpose coastal research vessel. These research areas included coastal and nearshore oceanography, ecosystem-based management, marine microbiology, physical oceanography, ocean chemistry, Hypoxia/anoxia zone research, biodiversity, biotechnology, seismic and tsunami risk research, ocean acoustics, sensor technology development, and ephemeral event response. These missions translated into the primary Zero-V vessel requirements shown in Table I against which technical feasibility of the Zero-V is assessed.

The primary ports of call for the vessel were determined by Scripps in consultation with Sandia, which visited these ports in order to assess refueling and servicing feasibility. These primary ports of call include the Nimitz Marine

Table I: Primary Vessel Requirements to Perform the Scripps Science Missions

Characteristic	Requirement
Cruise	10 kts, calm water
Speed	12 kts, calm water (sprint) 9 kts, SS4 7 kts, SS5
Range	2400 nm
DP	2 kts beam current, 25 kts wind at best heading
Endurance	15 days
Main Lab	800 sq ft
Wet Lab	500 sq ft
Computer Lab	120 sq ft
Aft Deck	1200 sq ft

Characteristic	Requirement
Portable Vans	2
Crew Berths	11
Scientist Berths	18
A-Frame	12,000 ST SWL
Main Crane	8,000 lbs @ 12' over the side
Portable Crane	4,000 lbs SWL
Side Frame	5,000 lbs SWL
Trawl Winch	10,000m 3/8 3x19
Hydro Winch	10,000m 0.322 EM, 10,000m 1/4 3x19

Facility at the Scripps Institution of Oceanography in San Diego CA; Moss Landing Marine Laboratory in Monterey CA, Pier 54 at the Port of San Francisco, San Francisco CA and Wharf 5 at the Port of Redwood City, Redwood City CA.

With the technical performance goals thus formulated, and the ports of call determined, the Zero-V design activity commenced.

The design of the Zero-V that satisfies all of the Scripps science missions, and can visit all the anticipated ports of call is

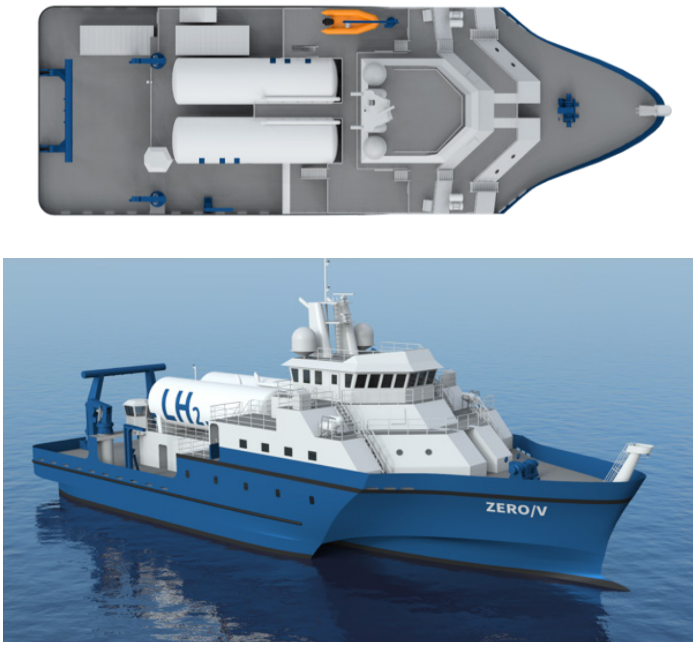

Figure 1: Renderings of the Zero-V zero-emission hydrogen fuel cell research vessel.

shown in Figures 1 and 2.

Three hull-forms were evaluated for the Zero-V: monohull, catamaran and trimaran. The trimaran hullform was selected because it enabled a vessel that could meet all of the space and volume requirements as well as fitment of the machinery, service, and control spaces necessary for operation of the vessel. The arrangements consider the operations of the vessel such as access between science spaces, the working deck, and science handling systems as well as visibility and sight lines from control stations to the working areas and equipment.

To reduce weight, the vessel has to be constructed of aluminum. The beam and length requirements were driven by the requirement that the vessel be able to dock at all primary ports of call for the vessel. Of these ports of call, the most restrictive refueling location is the Monterey Bay Aquarium Research Institute (MBARI) Pier at the Moss Landing Marine Laboratory (MLML). The beam (width) of the Zero-V is 56 feet, with a length of 170 feet. The vessel displacement is 1,175 LT. The draft is 12 feet, limited primarily by the water depths at the Moss Landing Harbor channel and MBARI Pier, as well as the water depth at Pier 54. The cruising speed is 10 knots as determined by the science mission requirements. With 10,900 kg of consumable LH_2 stored in two LH_2 tanks, the range of the vessel is 2400 nm, or an endurance of 15 days. The Zero-V is designed to be home to 18 scientists, 11 crew and to be truly zero-emissions on the water. The vessel performs "station keeping" by dynamic positioning.

The Zero-V design follows traditional arrangements for a research vessel even given the trimaran hull type. A cut-away view of the Zero-V is shown in Figure 3, giving the locations of the mechanical and propulsion system components.

An integrated fuel-cell electric plant supplemented with small lithium-ion bridging batteries provides both propulsion and ship service electrical. The fuel cells are Hydrogenics HyPM HD 30 fuel-cell power modules arranged into power racks with each rack holding six fuel-cell modules. Each rack has a total power output of 180 kW. With ten racks total, the vessel has 1,800 kW of installed power. The 10 hydrogen fuel-cell racks are evenly distributed between Starboard and Port fuel cell rooms, allowing the vessel to continue operation at reduced power if one space must be taken out of service for maintenance. The fuel cells provide DC power, which must be conditioned, converted and inverted to provide bus DC and AC power, respectively.

To provide the required position keeping for on-station science work, the vessel is fitted with a retractable azimuthing bow thruster as well as stern thrusters in each outer hull. Additionally, high-lift flap rudders are provided to maximize steering forces produced from the main propellers during station keeping. The Zero-V uses one propulsion motor to power each of its two propellers. Based on the resistance and powering calculations, it was determined that 500 kW motors provide sufficient power for the various mission requirements and also have enough reserve power for safe operation in heavy seas and for dynamic positioning. High-torque alternating current (AC) permanent magnet type motors were selected as the propulsion motors. These motors can be directly coupled to the propeller shaft to provide efficient and quiet operation.

The vessel is outfitted with two fixed pitch propellers. Each propeller is approximately 2.1 m in diameter. Fixed pitch propellers are chosen for their simplicity, low capital and operating cost, and quiet operation. The propellers are of wake-adapted design to minimize underwater noise as well

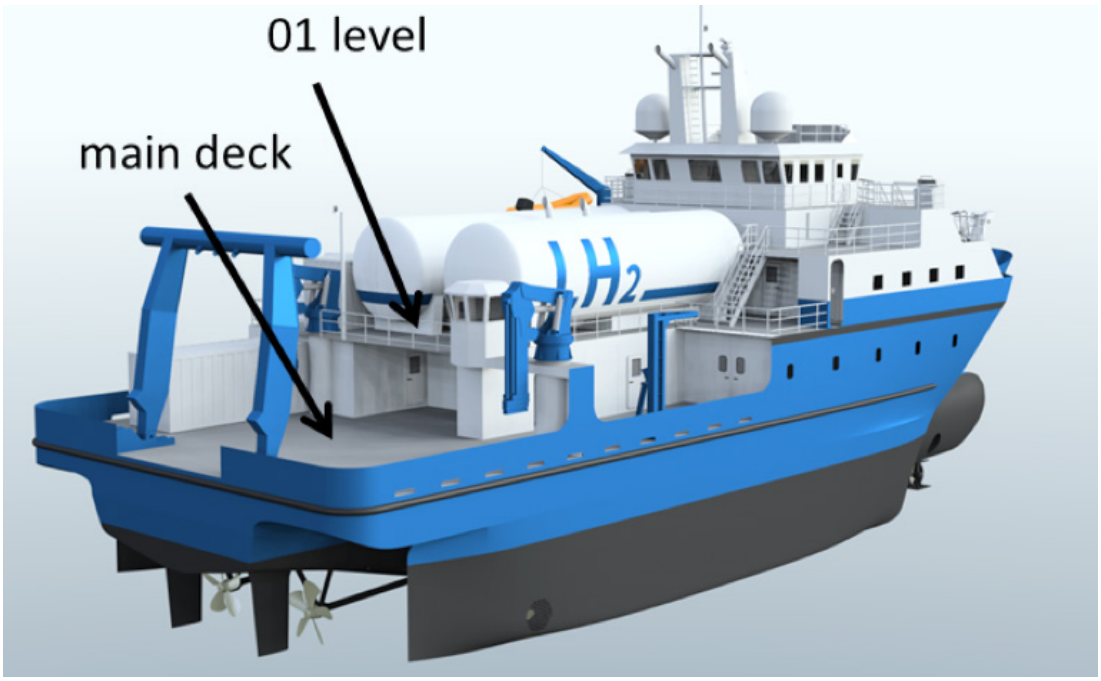

Figure 2: Aft view of the Zero-V showing deck specification and LH_2 tank location detail.

as maximize efficiency. The propellers are fully non-cavitating at speeds of up to 8 knots.

High-lift flap rudders are used for maneuvering the vessel. Compared to conventional spade rudders, the flap rudders provide both high turning forces underway and superior thrust control for position keeping. The bow thruster is a 500 kW retractable azimuthing thruster. This thruster provides sufficient maneuvering and dynamic positioning capability for the vessel under the required operating conditions. The bow thruster is powered by a permanent magnet AC motor for maximum efficiency.

To increase docking and position keeping performance, stern tunnel thrusters are installed in each trimaran side hull. Conventional electric motor driven tunnel thrusters were selected for the stern thrusters. To increase compactness and efficiency, permanent magnet AC motors are used. Because of the trimaran's center hull, thrust directed inward by the stern thrusters would suffer significant thrust loss due to hydrodynamic effects and would also likely create excessive noise. To avoid this problem, it has been assumed that the stern thrusters will only be operated to provide outward thrust away from the vessel.

A preliminary dynamic positioning (DP) capability study for the Zero-V was performed and indicates 500 kW tunnel thrusters provide satisfactory DP capability. The vessel can maintain position with 1 knot beam current and more than 25 knots wind and waves from any heading. With 2 knots beam current, the vessel can still maintain position with significant wind and waves at best heading.

The use of hydrogen fuel cells offer the potential for low-noise operation of the vessel. This is important not only for the safety of marine life and integrity of acoustic measurments, but also for the comfort of those onboard the vessel. To establish a noise estimate for the Zero-V, the predictions from a prior study of a diesel-powered research vessel's underwater radiated noise were adjusted to account for the removal of the noise source from the diesel engines (since the Zero-V does not have diesel engines). The result suggests that, with noise treatments such as damping material on the hull and vibration isolation of large rotating machinery, the Zero-V can meet the limits in ICES Report 209.

Both the CO_2(eq.) and criteria pollutant (smog) emissions were estimated for the Zero-V based on a complete "well-to-waves" (WTW) analysis. Here CO_2(eq.) emissions refers to the sum of CO_2, CH_4 and N_2O emissions multiplied by their radiative trapping weighting factors. Criteria pollutant emissions refer to NO_x, hydrocarbons and particular matter emissions. The annual WTW CO_2(eq.) emissions from the Zero-V fueled with LH_2 from fossil natural gas (NG) would be 2.16 Gigagrams (Gg) of CO_2 (eq.) per year, produced entirely by the production and delivery of the LH_2 fuel. This is slightly worse than the equivalent vessel running on fossil diesel, with WTW CO_2(eq.) emissions of 1.91 Gg CO_2 (eq.)/year, despite the fact that the fuel-cell-powered Zero-V is 22% more energy efficient than the equivalent diesel vessel. This WTW CO_2(eq.) emission increase is due to the facts that making hydrogen from NG is energy intensive in the first place, the carbon in NG is released into the atmosphere as CO_2 during the hydrogen manufacturing process, and hydrogen liquefaction involves significant energy and associated emissions. These

factors conspire to produce undesirable emissions for the Zero-V along the fuel production and delivery path when the hydrogen is produced by steam methane reforming of fossil-based natural gas.

The situation is dramatically improved using renewable hydrogen, such as that made from biogas, or by water electrolysis using wind or low-carbon nuclear power. Our analysis shows the annual WTW CO_2(eq.) emissions from the Zero-V using renewable LH_2 becomes 0.164 Gg CO_2 (eq.)/year. This is 91.4% less than the WTW CO_2(eq.) emissions from the equivalent diesel vessel running on conventional diesel fuel. In our discussions with the gas suppliers Linde and Air Products, renewable LH_2 can be made available to the Zero-V today in the quantities required. The gas suppliers are currently working to make renewable hydrogen more broadly available. Summarizing the CO_2(eq.) results, hydrogen PEM fuel-cell technology can dramatically reduce the CO_2(eq.) emissions from operation of the Zero-V. However, nearly 100% renewable hydrogen must be used to achieve the desired deep cuts in CO_2(eq.) emissions that are commensurate with the challenge presented by increased levels of infra-red radiation trapping gases in the atmosphere.

We also performed an analysis of the criteria pollutant (NO_x, HC, PM) emissions from the Zero-V. The results indicate that Hydrogen PEM fuel-cell technology can dramatically reduce WTW NO_x and hydrocarbon (HC) emissions below the most advanced Tier 4 criteria pollutant emissions requirements, regardless of whether the hydrogen is made by NG reforming or using more renewable means.

The economic (cost) feasibility of the Zero-V was analyzed from the vessel capital cost and operations and maintenance (O&M) perspectives. Based on this analysis, the "Low Labor Rate" construction cost of the Zero-V is estimated to be $76 million dollars ($76M). The "High Labor Rate" construction cost is estimated to be $82M. The average of these construction estimates is $79M. Comparing the Zero-V construction cost to diesel-fueled research vessels revealed that although somewhat more expensive, the Zero-V construction costs are not unreasonable when compared to other modern research vessels of similar size and capabilities. The O&M costs of the Zero-V were estimated and compared to a comparable diesel powered vessel, the New Horizon, which was retired from the Scripps fleet in 2014. We found that the total annual O&M cost for Zero-V is 7.7% higher than operating the New Horizon, at today's fuel prices for fossil-NG non-renewable LH_2. Using renewable LH_2, the total annual O&M costs for operating the Zero-V are 41.9% higher than operating the New

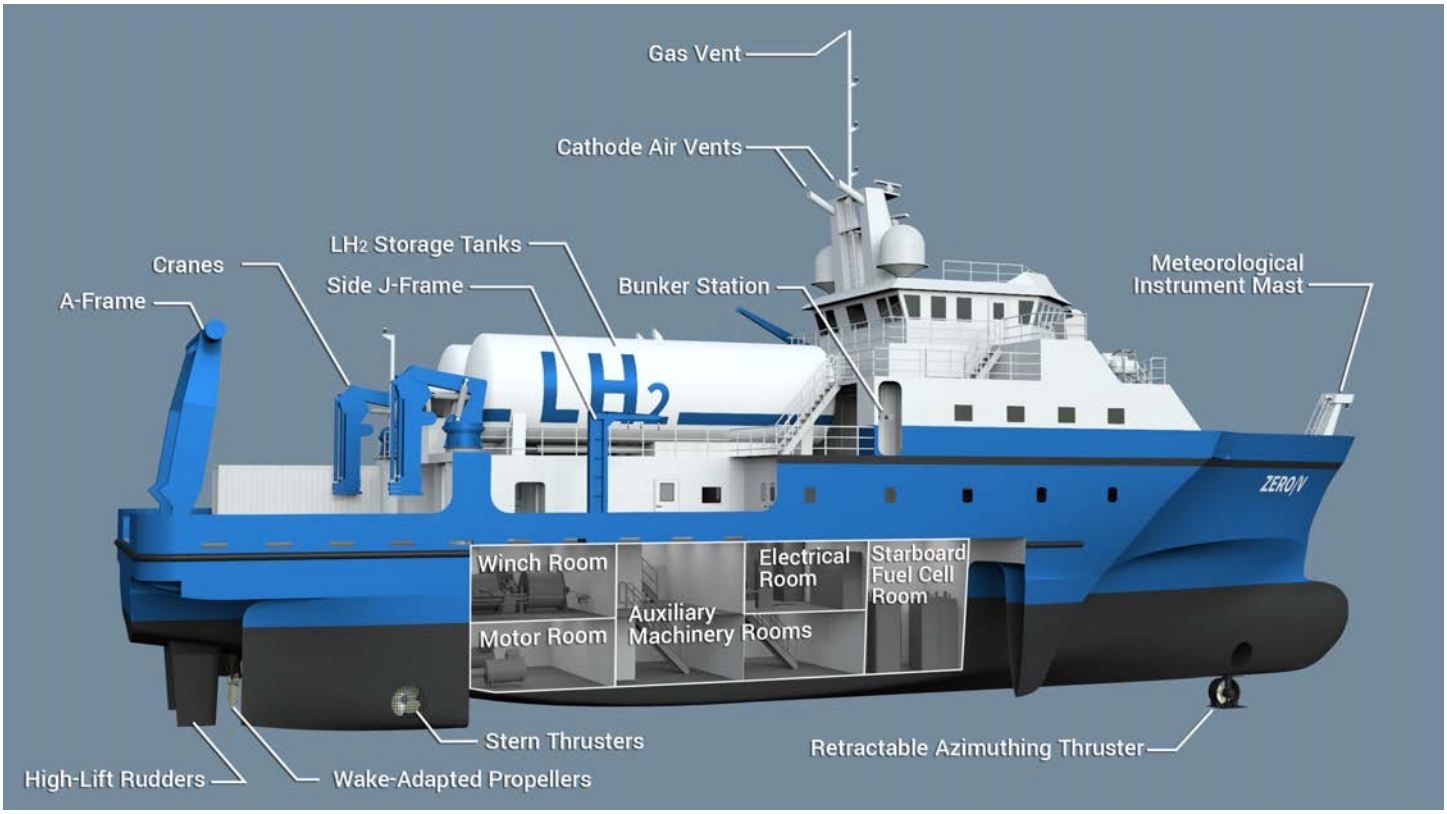

Figure 3: Cut-away view of the Zero-V showing locations of mechanical and propulsion system components

Horizon, due to the current high cost of renewable LH_2 fuel.

To refuel the Zero-V, LH_2 must be delivered to the vessel's LH_2 tanks in a timely way, preferably within an 8 hour shift. Both Linde and Air Products concluded that the best strategy for refueling the Zero-V would be using direct trailer refueling. In this scenario, LH_2 trailers pull onto the pier area where the Zero-V is docked, the trailers hook up to a dock stationary fueling stanchion that decouples the trailer hoses from a moving vessel. Both gas suppliers indicated that refueling of the Zero-V could take place within a 9 hour timeframe, and both could provide access to renewable LH_2, although it would initially be expensive. Both fuel suppliers stated that a large reliable single customer for renewable LH_2 such as the Zero-V would greatly encourage these companies to make renewable LH_2 more available nationwide.

We found it helpful in considering the capabilities of the Zero-V to understand the context of the vessel in comparison to other diesel-powered research vessels that have been deployed in the recent past. All of the diesel-fueled vessels have a superior range, which is a consequence of diesel fuel having ~ 4 times the volumetric energy density as LH_2. Apart from range, in other aspects the Zero-V is quite competitive with these other vessels, particularly with regard to the scientific capabilities and the number of scientists it can berth. One design criterion of the Zero-V was to make a vessel that the scientists and crew would be comfortable in, and enjoy being on. The feedback we received from the Scripps science team is that the Zero-V design has succeeded in those regards.

A vessel design package was submitted to both the USCG and to DNV GL for their evaluation. In general, the response from both reviews was that while additional development would be necessary to gain approval as an alternative design, there were no fundamental or "show-stopping" design concerns that would prevent eventual deployment of the Zero-V. Furthermore, DNV GL provided a conditional approval in principle (CAIP) for the Zero-V design.

Summarizing, as a result of this study we deem it feasible from technical, regulatory, and economic perspectives to design, build and operate a coastal research vessel powered solely by hydrogen fuel cells. Such a vessel would offer dramatic environmental benefits, have low airborne and under water noise signatures, and could be conveniently refueled at a number of ports of call by LH_2 refueling trailers.

Table of Contents

I. Introduction

Project Goals

The goals of this project are to determine the technical, regulatory, and economic feasibility of a coastal research vessel powered solely by hydrogen fuel cells, assess the environmental benefits and determine the prospects for refueling such a vessel at the expected ports of call.

The anticipated attendant benefits of this project are to establish technology and know-how, in particular:

- Increase H_2 technology expertise within the U.S. maritime industries and promote new jobs.
- Develop maritime regulations for H_2 vessel technology based on sound science.
- Promote class society capability for examining the safe operation of H_2 vessels.
- Promote the development of fuel-cell technology for marine applications.

If the Zero-V research vessel were to be built and operated, the operational benefits would be to:

- Eliminate vessel carbon-based and criteria pollutant (smog) emissions, while reducing noise risk to wildlife and vessel operation.
- Increase awareness among U.S. H_2 suppliers of maritime applications.
- Stimulate H_2 production and delivery in the U.S., especially renewable H_2.

Motivation

Pratt and Klebanoff [1,2] have reviewed maritime-related emissions of infra-red radiation trapping gases (CO_2(eq.)) and criteria pollutants (nitric oxides, hydrocarbons, particulate matter), and how vessels based on hydrogen fuel cell power dramatically reduce such emissions. Harbor craft (which excludes ocean going tankers, but includes coastal vessels) account for ~ 0.35% of California CO_2(eq.) emissions and about 0.1% of the state's criteria pollution. Although these numbers may seem small, as noted by Corbett and Farrell [3], emissions from harbor-craft constitute a highly visible pollution source in close proximity to dense population areas where emissions most adversely affect human health. It is clear that because of the expected growth in maritime transportation in the coming years, partial reductions of today's vessel emission levels, even reductions as much as 50% per vessel, cannot lead to long term reductions in global maritime emissions because of expected growth in the number of vessels on the world's oceans, lakes, and waterways. As a result, incremental efficiency improvement in fossil-fuel power technology will be unable to provide reduced emissions in the face of increased sizes of the maritime vessel fleets. Instead, a move away from fossil-fuel derived power is required. Only then can large reductions in emissions, stable against growth in maritime fleets, be obtained.

Thinking beyond emissions, there are other problems with our fossil-fuel based maritime power technology. These problems include dependence on a dwindling natural resource which leads to fuel resource insecurity and the fact that such resources are not evenly shared amongst the nations of the world, which introduces a political aspect to our energy insecurity problems. These problems are in addition to the environmental sustainability problems that are more widely known and discussed.

Keller et al. [4] have provided a compelling argument that if the global community is going to solve its fuel resource insecurity, political energy insecurity and environmental sustainability problems that accompany the current fossil-fuel-based energy systems, hydrogen-based energy technology will be needed. For significant environmental benefits, particularly with regard to reduction of CO_2(eq.) emissions, the hydrogen will need to be produced by renewable methods with minimal (close to zero) pathway CO_2(eq.) emissions. One can define a zero-carbon energy solution as an energy system in which there is no net release of CO_2 or other radiation trapping gases into the atmosphere, either at the point of technical use, or along the path used to produce the fuel. Unless we have a new maritime transportation technology with emissions reductions approaching ~ 80% or more, the emission reductions will not be robust against growth. Such deep cuts are generally consistent with recommendations from the Intergovernmental Panel on Climate Change (IPCC) [5] and U.S National Academy of Sciences [6].

Hydrogen enables a zero-CO_2 and zero-criteria pollutant en-

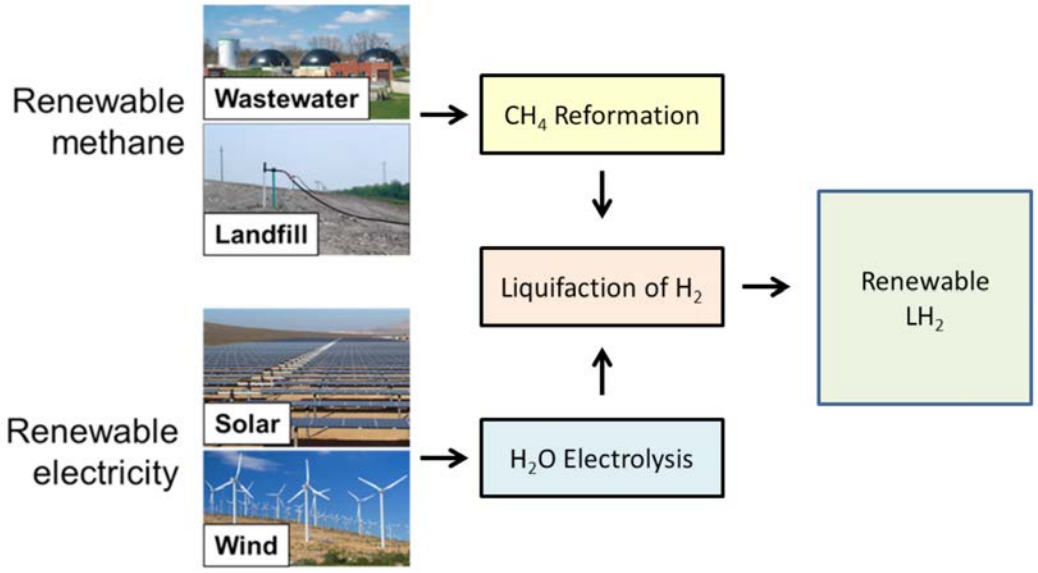

Figure 4: Example pathways for renewable (zero CO_2(eq.)) liquid hydrogen production based on steam methane reforming of biomethane feedstock or electrolysis of water using renewable electricity.

ergy pathway. Figure 4 depicts how renewable (zero carbon and criteria pollutant) liquid hydrogen can be obtained.

If the other energy inputs to the process are renewable (such as electricity for compression or liquefaction) and the hydrogen is then transported in a renewable way (via biofuel or hydrogen-powered truck) to the vessel and used in a fuel cell, there are no CO_2(eq.) or criteria pollutant emissions throughout the production and use cycle.

Hydrogen can also be made from non-renewable natural gas through steam reformation. However, the well-to-waves CO_2(eq.) emissions associated with obtaining the natural gas and reforming it results in only modest CO_2(eq.) reductions compared to using fossil fuels directly in combustion engines.

As reviewed by Klebanoff et al. [7], high efficiency hydrogen energy conversion devices that convert hydrogen into electrical or shaft power are powerful drivers for hydrogen technology. These conversion devices include hydrogen internal combustion engines (ICEs), both spark ignition and turbine hydrogen engines, along with hydrogen fuel cells [7]. Hydrogen internal combustion engines, while a basically proven technology, do not eliminated NO_x because there is air burning of hydrogen in ICE's which leads to NO_x. As a result, hydrogen ICE's are not considered "zero-emission" power sources and will not be considered further. On the other hand Proton Exchange Membrane (PEM) fuel cells (which do not involve burning) are already finding use in the first fuel-cell vehicles, portable power, backup power, material handling equipment and fuel-cell mobile lighting [7]. The use of hydrogen fuel-cell technology for maritime applications was reviewed in the Final Report of the SF-BREEZE project [1], and we consider it here for a zero-emission research vessel.

Besides CO_2(eq.) reduction, using hydrogen for maritime transport has many more potential benefits. These were explored at the Zero Emission Hydrogen Vessel Workshop held February 26, 2016 hosted by Sandia National Laboratories at the US DOT/Maritime Administration in Washington, DC. Workshop participants were a mix of public and private entities and included government representatives, regulators, class society, vessel owners and operators, hydrogen suppliers, and technology companies. The participants produced a list of hydrogen fuel cell attributes and attendant benefits of zero-emission hydrogen vessels. The complete list is provided in the SF-BREEZE report [1] and can be briefly summarized as follows:

- Since there is no air pollution from H_2/fuel cell exhaust, the air is clean for passengers and it is easy to comply with current criteria pollutant emission regulations and perhaps future regulations on CO_2(eq.) emissions (which are currently not regulated).
- Money can be saved because there is no need for exhaust scrubbing equipment.
- Hydrogen is non-toxic, has no odor, is not an infra-red radiation trapping gas, and there are no fuel fumes (which improves the passenger experience).
- Polluting fuel spills are impossible since LH_2, if spilled, quickly evaporates and dissipates. Because hydrogen is so light, any released hydrogen eventually escapes into space. The impossibility of a polluting fuel spill,

which completely eliminates the risk of contamination of sensitive ecological areas, is a unique and highly beneficial aspect of using hydrogen as a maritime fuel.

For a research vessel, the advantages of using hydrogen fuel cells are considerable. For example, zero emissions hydrogen technology allows the collection of air samples with no interference from vessel engine emissions. Hydrogen is readily used in Arctic Oceanographic exploration because hydrogen is not susceptible to the waxing/freezing problems of the petroleum-based fuels. Also, the complete elimination of particulate emissions avoids the formation of "black ice" which is a major concern for increased solar absorbance leading to increased rates of ice melting [2]. Since fuel cells are very low noise power systems, such research vessels are quieter, which broaden the capability for scientific operations that use acoustic systems (sonars) by enabling greater sensitivity in receiving very quiet sounds. Reducing mechanical sounds associated with internal combustion propulsion systems also reduces the levels of sounds radiated into the environment, which may be heard by marine wildlife. PEM fuel cells, being electrical devices, offer faster power response than engine technology, which is an advantage in vessel handling and positioning. Fuel cells generate pure, deionized water which can be captured used for other purposes such as drinking water for the scientific staff and crew, or for experimental and analytical purposes. This can offset weight of potable or experimental water needed to be carried on-board.

This myriad of potential benefits motivates a detailed exploration into the technical, regulatory, and economic feasibility of designing, building, and operating a practical, commercial, zero-emission coastal research vessel.

Project Team

The project team consisted of Sandia National Laboratories (Project Lead and hydrogen fuel cell technical expertise), Glosten (naval architect), the Scripps Institution of Oceanography (oceanographic research expertise and end user) and DNV GL (maritime regulatory expertise, marine hydrogen systems).

Sandia National Laboratories

Sandia National Laboratories (aka Sandia) is one of the three U.S. national security laboratories. Sandia is operated and managed by National Technology and Engineering Solutions of Sandia, LLC., a wholly owned subsidiary of Honeywell International, Inc. National Technology and Engineering Solutions of Sandia operates Sandia as a contractor for the U.S. Department of Energy's National Nuclear Security Administration (NNSA) and supports numerous federal, state, and local government agencies, companies, and organizations. For more than 60 years, Sandia has delivered essential science and technology to resolve the most challenging U.S. security issues. With a strong science, technology and engineering foundation, Sandia enjoys a reputation as the premier science and engineering laboratory in the U.S. for national security work, technology innovation and unbiased technical assessment.

Sandia National Laboratories; (top) Lennie Klebanoff, Zero-V Project Lead; (bottom) Joe Pratt

Although most of Sandia's approximately 10,000 employees work at Sandia's headquarters in Albuquerque, New Mexico, approximately 1000 employees work at the second Sandia laboratory in Livermore, California. Among Sandia's many research and development initiatives is its Hydrogen and Fuel-cell (H_2FC) program, which has been in existence since the 1960's. Sandia has provided the science-based knowledge needed for the development of hydrogen storage technology, efficient hydrogen production methods, and the underlying science for rational hydrogen safety codes and standards development. In addition, Sandia, within its Fuel Cell Market Transformation Activity, has for the past 15 years investigated the feasibility of using hydrogen fuel cells as emergency power and hotel power on commercial aircraft, in mining equipment, mobile lighting, and more recently in providing zero-emission power at ports and as the primary propulsive energy for vessels.

Dr. Lennie Klebanoff (Sandia) serves as the Zero-V Project Lead, with assistance from Dr. Joe Pratt.

Glosten

Glosten, located in Seattle, Washington, is a full-service consulting firm of naval architects, marine engineers, and ocean engineers. Glosten has a staff of 87 associates including 35 professionally licensed engineers supported by other engi-

neers, marine designers and administrative staff. Consulting and design services include hull, structural, mechanical, and electrical systems design, as well as construction management. Founded in 1958, the firm's design experience includes tugs, barges, research vessels, passenger/car ferries, and special-purpose platforms. The firm also offers noise and vibration measurement and control for marine applications through its subsidiary, Noise Control Engineering, LLC, a premier acoustical and structural engineering consultancy.

The firm offers specialized expertise in hydrodynamic analysis, climatology, risk analysis, and consulting to civil engineers and marine construction contractors for floating and coastal structures. For these projects, Glosten draws on in-house expertise in wave mechanics and fluid-structure interaction to define the hydrodynamic loads from waves, current and wind. Glosten provides design guidance on marine construction and assembly strategies, and also assists in construction logistics planning, particularly where large modules or floating structures are to be constructed off-site.

Supporting clients in complex marine operations is a Glosten specialty. Glosten works with clients in areas such as loading and unloading of large and valuable cargoes, seafastening design, and reducing overall risks of challenging marine operations. Glosten's strong technical staff, coupled with deep experience in design and construction, offers clients critical insights into the operations of marine vessels and structures.

Glosten Naval Architects: (Top) Tim Leach; (Bottom) Sean Caughlan (Left) and Robin Madsen.

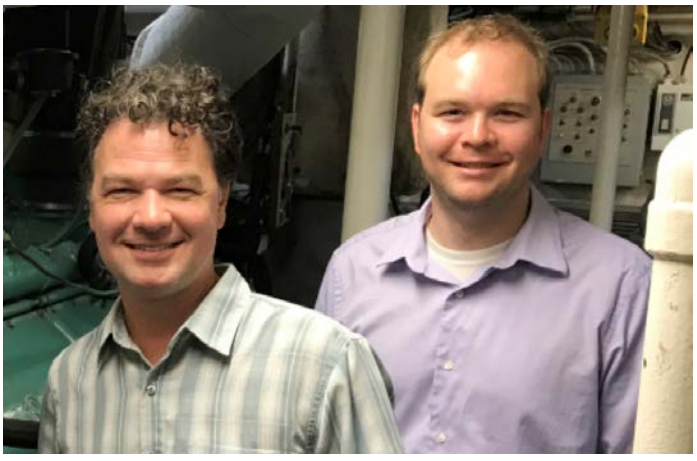

Glosten has experienced engineers and technical personnel who are thoroughly familiar with marine vessel construction. Many Glosten associates have prior shipyard and contract management experience, enhancing Glosten's ability to effectively communicate with the builder on all construction matters. Glosten routinely represents Owners on-site to ensure contract compliance and technical suitability, and provides complete on-site technical program management assistance including provision of qualified technical program managers and construction inspection teams.

Long-standing relationships with clients provide opportunities for involvement in various marine operations. Many of the firm's engineers have had seagoing experience and have assisted and directed transportation, emplacement, and salvage operations, enhancing our design and analysis capabilities. The Zero-V project is led from the Glosten side by Sean Caughlan, Robin Madsen, and Tim Leach.

Scripps Institution of Oceanography: Bruce Appelgate (top) and Stephen "Zoltan" Kelety (bottom).

Scripps Institution of Oceanography, University of California at San Diego

Founded in 1903 as an independent research laboratory, Scripps today is a major research and training institution organized within UC San Diego (UCSD). Scripps is the largest oceanographic institution in the United States, with 186 professors, researchers and project scientists, 329 graduate students, 1,160 academic, technical, and administrative personnel, plus 587 volunteers. Scripps maintains outstanding research facilities and support infrastructure, including the largest fleet of oceanographic research vessels and platforms of any U.S. academic institution, operating from a world-class home port at Nimitz Marine Facility on San Diego Bay. Ongoing research programs in physical, chemical, biological, atmospheric, geological, and geophysical studies of the oceans and Earth expended more than $193 million in FY10-11. Dr. Bruce

DNV GL: (Left) Gerd Petra Haugom (L) and Hans-Christian Koch-Wintervoll (R); and (Right) Anthony Teo.

Appelgate is the Scripps technical lead for the Zero-V project, with support from CDR Steven "Zoltan" Kelety.

DNV GL

DNV GL is a Norwegian global quality assurance and risk management company. Driven by the purpose of safeguarding life, property and the environment, DNV GL enables customers to advance the safety and sustainability of their business. DNV GL provides classification, technical assurance, software and independent expert advisory services to the maritime, oil & gas, power and renewables industries, all with a commitment to teamwork, customer service and care, with high technical excellence and integrity in their work.

DNV GL offers classification services for ships including those introducing alternative fuels and new technologies, such as fuel cells, natural gas and batteries based on their class rules. They offer maritime advisory services on environmental technologies including feasibility studies, technology qualification, emission analyses and assessments.

DNV GL also provides certification, supply chain and data management services to customers across a wide range of industries. Combining technical, digital and operational expertise, risk methodology and in-depth industry knowledge, DNV GL empowers their customers' decisions and actions with trust and confidence. DNV GL continuously invests in research and collaborative innovation to provide customers and society with operational and technological foresight. With origins stretching back to 1864 and operations in more than 100 countries, as illustrated with our presence in the United States [8], our experts are dedicated to helping customers make the world safer, smarter and greener.

The DNV GL project leads are Gerd Petra Haugom and Hans-Christian Koch-Wintervoll , with support from Anthony Teo.

Though not a formal partner in this study, Hydrogenics played a critical role in enabling fuel-cell integration into the Zero-V vessel by providing fuel-cell and hydrogen expertise as well as guidance for safety and control strategies. Through previous experience in deploying systems for maritime applications, Hydrogenics has showcased its' leadership for the adoption of fuel cells in the marine industry. The Hydrogenics participant is Ryan Sookhoo.

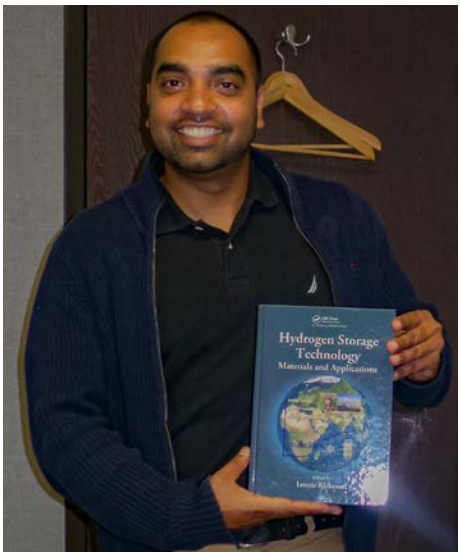

Ryan Sookhoo of Hydrogenics.

II. Research Vessel Background

The Mission of Coastal Research Vessels

Shipboard research offers the transformative potential to understand fundamental processes upon which human well-being depends. From short-term local events to long-lasting global impacts, the processes occurring in the oceans affect everyone on our planet. Our civilization faces an unprecedented situation in the history of human events. We as a species have always altered our environment to suit our needs, but human impacts have accelerated in recent decades to reach global proportions. We know that impacts on the ocean environment have sweeping consequences, including depletion of fisheries, loss of biodiversity, drought, deforestation, ocean acidification, sea level rise, and increased levels of infra-red radiation trapping gases in the atmosphere.

Coastal oceanography is especially significant. The United States is a coastal nation. Fifty-three percent of United States population lived in coastal counties in 2010. By 2020, that percentage is expected to grow to 63 percent. Our oceans provide food, jobs, and recreation for millions of Americans. The oceans produce the majority of the oxygen in our atmosphere, control weather, store and redistribute heat, and interact with infra-red radiation trapping gases in ways that influence the lives of everyone on the planet.

It is prudent to use the best available science and knowledge to inform decisions affecting the oceans and coasts, and enhance our capacity to understand, respond and adapt to a changing environmental conditions [9]. To fulfill this objective, we must increase scientific understanding of ocean and coastal ecosystems as part of the global interconnected systems of air, land, ice, and water, including their relationships to humans and their activities.

In order to make the kinds of observations needed to drive our understanding of the coastal ocean, we need the right observing tools. Coastal oceanography is multidisciplinary due to the inter-relatedness of processes in the ocean. Biological, chemical, geological and physical processes in the earth, ocean and atmosphere influence each other in both profound and subtle ways. A complete understanding of any one scientific issue often requires a theoretical framework and experimental approach that crosscuts many disciplines. Because observing and sampling methods for each of these disciplines differ, a broad variety of sensors, sampling systems, and instruments are required. To deploy all of these sensors in the dynamic, unpredictable and sometimes unforgiving coastal ocean requires a broadly capable general-use research vessel.

Coastal research vessels have historically played an important role in Scripps's educational mission. Professors routinely make use of coastal research vessels to demonstrate field methods to students, moving them beyond the classroom and onto the ocean to learn how to sample, measure and observe the ocean, and acquire information that can be used ashore in courses in geology, geophysics, fisheries, chemistry, physics, engineering, and other topics. Coastal vessels are also integral to student-led research, in which graduate students develop and lead seagoing scientific programs to acquire data for their dissertation research. Coastal vessels at Scripps are ideally suited to these applications because they are based full-time in San Diego (in contrast to our larger ships, which range globally), and can be flexibly adapted to the needs of classes and small groups of students. Our coastal vessel *Robert Gordon Sproul* is currently a vital part of our undergraduate and graduate teaching and student research.

Renewal of Research Vessels at Scripps Institution of Oceanography

Scripps is currently involved in the early planning for a new coastal research vessel to replace the aging *Robert Gordon Sproul*. Built in 1981 as an oilfield workboat, *Robert Gordon Sproul* was converted for scientific research by Scripps in 1984 and has operated continuously since then from the Scripps home port, the Nimitz Marine Facility (MarFac), in San Diego. Research vessels are typically designed for a 30-year service life. Scripps has taken meticulous care of *Robert Gordon Sproul* to keep the ship capable to date (36 years), but now is the time to consider renewing our capability with a next-generation vessel. The pressing need for a new research vessel is depicted in Figure 5, which shows the recent retirement of Scripps's Intermediate Class ship *New Horizon* (removed from service in 2015) and of Moss Landing Marine Laboratory's Regional Class ship *Pt Sur* (removed from service in 2014).

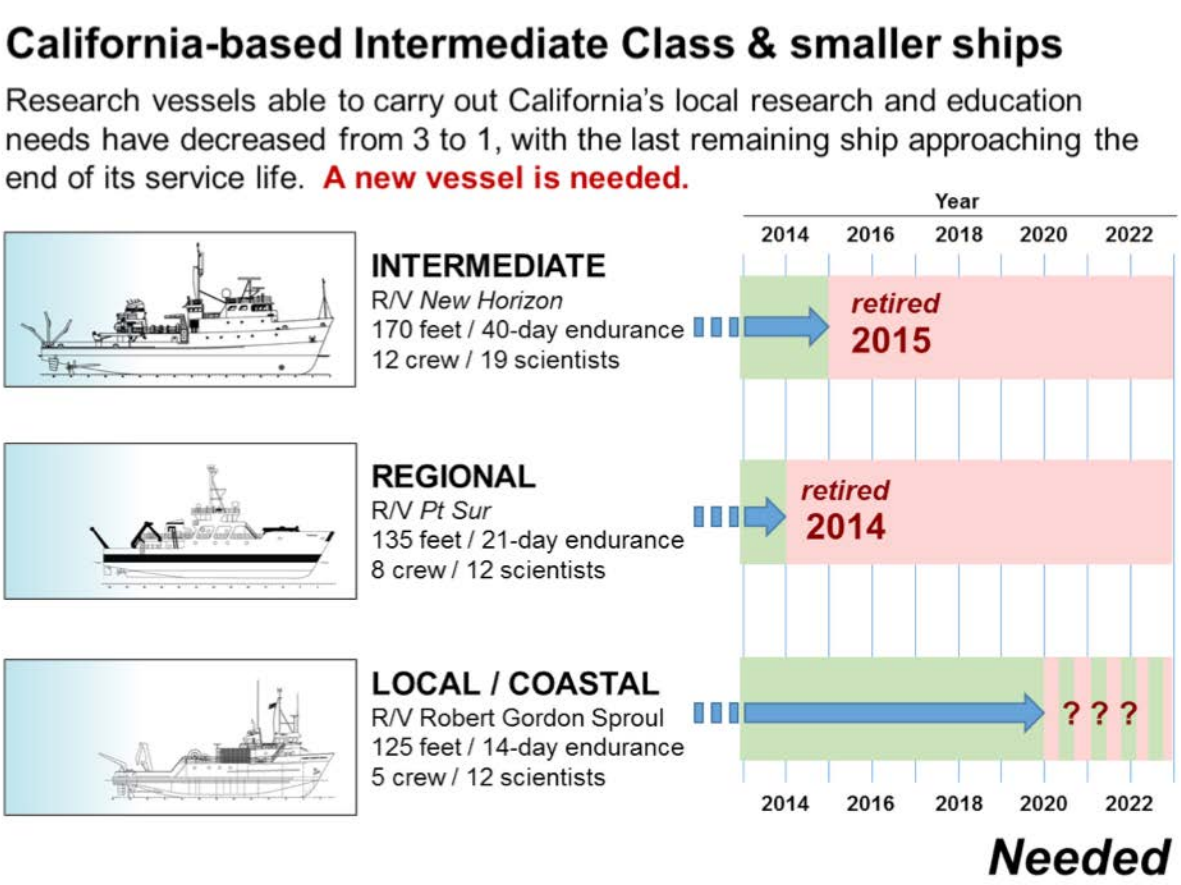

Figure 5: Description of the attrition of the research vessels serving the West Coast of the United States, and the need for a new zero-emissions vessel.

Both of those vessels served ocean scientists on the US West Coast. With the removal of those vessels from the US Academic Research Fleet, as well as the impending retirement of *Robert Gordon Sproul,* scientists at Scripps and other institutions who study the coastal ocean on the west coast have a large and growing need for a new vessel to provide capable scientific access to the sea.

Scientific Themes Supported by Coastal Research Vessels

An imperative for the scientific community is understanding the biological, chemical and physical complexity of coastal oceans. Coastal ocean systems extend from estuaries and river mouths to bays, onto the continental shelf and the continental slope. Physical, geochemical and ecosystem processes in these regions are dynamic, complex and variable in space and time. In order for us to understand significant, societally-relevant issues here (the causes of coastal changes, the role of coastal margins in the global carbon cycle, strategies for managing coastal resources) we must quantify the coupled physical, chemical, and biological processes active here, as well as the physical forcing mechanisms between oceans, land and the atmosphere.

Coastal oceans impact and are impacted by changes in the Earth's climate. The ocean stores heat and carbon dioxide, and redistributes them via large-scale circulation. Both the storage capacity and redistribution patterns are affected by climate change and the ocean in turn may modify climate through feedback mechanisms. Variability in ocean-atmosphere feedback on climate time scales may have profound effects on ecosystems through habitat change and the modulation of shorter time scale phenomena. Key elements of climate research are shipboard sampling and observing of coupled climate processes (ocean, atmosphere, biosphere), data assimilation including air-sea interaction, statistical climatology and prediction, marine micrometeorology and dynamical meteorology. Nowhere are these processes more complex than in coastal seas, and nowhere are the impacts on human interests more profound.

Within these broad themes are several research areas of particular significance in coastal oceanography that require a modern, capable, general-purpose coastal research vessel.

Coastal and nearshore oceanography

Coastal studies and considerations of land-sea interactions are growing areas of research. Environmental issues include pollution from oil spills, sewage entry and river runoff, damage from storms and increased sea surface height and temperature, and biological productivity and harmful algal blooms. The rapid detection of pathogens, toxins, and harmful chemicals is of growing importance, as is the accurate characterization and prediction of coastal circulation and pollution dispersal patterns.

Ecosystem-based management

The past several decades have witnessed dramatic declines in populations of marine organisms in U.S. waters, and indeed around the world. Equally dramatic conservation efforts will be required in the future to preserve dwindling fisheries stocks and many different marine ecosystems. A key initiative in coastal oceanography is the establishment of ecosystem-based management (EBM), a field that includes fish and fisheries as well as coastal biogeochemistry, climate, and the lower trophic levels. New developments in acoustic technology, such as three-dimensional, multibeam acoustics and shelf-scale water-column mapping are necessary for major advances in fishery oceanography [10].

Marine microbiology

Nearly simultaneously with this recognition of catastrophic species loss, we have begun to understand that much of the web of life is represented in marine flora, fauna, protists, prokaryotes and viruses. Understanding life at all levels, from its origins and evolution to its development, symbiotic interactions and biotechnological exploitation, necessitates the ongoing study of marine life. Dynamic coastal and shelf environments are especially important, and require research that will extend beyond the next decade.

Physical oceanography

New observing capabilities coupled with numerical models are driving research towards a better understanding of the transitions in ocean dynamics from the coast to the open ocean, the air-sea interface to the interior of the ocean, and the submesoscale to gyre circulations. Emergent themes that will drive research over the next decade include the need to understand cross-shelf transport (to constrain biological productivity contaminant dispersal in coastal oceans); upper ocean processes predominantly energized by atmospheric forcing (wind stress and buoyancy loss due to evaporation and cooling); benthic boundary layers (significant for the fate of sinking organic matter, redistribution of material on continental shelves, and accurate high-resolution circulation models); and mesoscale eddies that contribute significantly to larger-scale property transport. Understanding the broader set of eastern boundary current problems is essential for climate change-related issues like ocean acidification, which may well impact the eastern boundary and its ecosystems sooner and more forcefully than other regions.

Ocean chemistry

Improved chemical measurements in the marine sciences are being undertaken to study the nature of recalcitrant organic material present at depth, the constituents of sea water-derived aerosols, the rapid detection of trace nutrients in the oceans, and organic and inorganic pollutants in the atmosphere. Chemical measurements of microbial activity, such as those related to metal transformations, the deep biosphere and aspects of geobiology are of growing interest, with strong ties to shipboard programs.

Hypoxia/anoxia zones

Hypoxic (low oxygen) and anoxic (no oxygen) waters have existed throughout geologic time in many of the ocean's deeper environs. The occurrence of hypoxia and anoxia in shallow, coastal and estuarine areas, however, appears to be increasing, most likely accelerated by human activities, and no other environmental variable of such ecological importance to estuarine and coastal marine ecosystems around the world as dissolved oxygen has changed so drastically and in such a short period of time [11]. Hypoxia and anoxia have pervasive, devastating ecological effects on shallow coastal waters [12]. A major oceanic suboxic zone occurs in the north eastern tropical Pacific off Baja California. Understanding the forcing mechanisms and impacts of suboxic conditions is important for these biogeochemically important regions.

Biodiversity

The imperative for finding, cataloging, and understanding margin diversity derives from the many key functions, goods, and services provided by continental margin ecosystems and by an increasingly deep human footprint on our continental slopes [13]. As our living and mineral resources become depleted on land and on continental shelves, we have turned to deeper water to provide energy and food. A frontier mentality, and limited regulatory structure on continental margins, has led to the wholesale removal of fisheries stocks or physical disruption of their habitat, more or less out of sight and often in areas whose faunas and habitats are understudied. Overprinting the direct human contact are changing hydrographic and productivity conditions that are harbingers of climate damage. Many of the expected climate-induced alterations in deep water, such warming, acidification, and deoxygenation, will have their greatest impact on the ocean margins.

Biotechnology

Marine biotechnology is the industrial, medical or environmental application of biological resources from the sea. Biomedicine, biofuels, genomics, molecular genetics and bioin-

formatics hold promise across a broad range of applications ranging from fuels to treating human disease. Marine natural products have fueled explosive growth in biomedical science, for example, yet the physically and biologically diverse coastal oceans still represent a frontier for new and exotic species and organic molecules with societally-significant applications.

Seismic and tsunami risk

The west coast of North America is tectonically and seismically active, being host to boundaries between the Pacific, North American, Cocos, and Juan de Fuca tectonic plates. Earthquakes on these plate boundaries, and associated tsunamis, pose a grave threat to coastal populations. A greater understanding of the tectonic architecture is vitally important to society's ability to manage these risks.

Ocean Acoustics

Acoustic data communications has important relevance to emerging scientific efforts, for instance in support of the Ocean Observing Initiative supported by the National Science Foundation. Target applications include the retrieval of environmental data from in situ sensors, the exchange of data and control information between autonomous underwater vehicles and other off-board/distributed sensing systems and relay nodes (e.g. surface buoys), and submarine communications.

Sensor technologies

Measurements from satellites, unmanned aircraft, and free-drifting profiling floats continue to serve the nation's science interests. Programs such as the Ocean Observing Initiative emphasize the need to develop and deploy a greater variety of sensors at the sea surface, in the water column, and at or beneath the seafloor. Sensor development and testing require specialized research vessels that can provide rapid access to both coastal and deep water environments appropriate for sensor tests.

Ephemeral event response

The scientific community must have the capacity to respond rapidly to sudden research needs driven by natural or anthropogenic events, which can often have extreme human significance. For example, assessing the environmental effects of catastrophic oil spills (Deepwater Horizon, Odyssey, Mandoil I spills on the Gulf, East and West coasts), the after effects of natural disasters (2011 Japanese tsunami, the 2010 Chilean earthquake) and the cause and consequences of significant ephemeral events (harmful algal blooms, transport and fate of coastal pollutants). Our ability to respond to and learn from these events requires research vessels, instruments, and individuals capable of providing scientifically useful information to government agencies, legislators and leaders.

The research needs of scientists will continue to evolve as

Table II: The Scripps Science Missions that defined the vessel performance requirements for the Zero-V.

Mission	Hours per Mission	Missions per Year	Total Hours per Year	Total Days per Year
Coastal Mooring	24	6	144	6
Deep Moorings (400 m) & towed sonar	120	2	240	10
Mapping (multibeam & towed CHIRP)	120	2	240	10
Class Cruise Biology	12	6	72	3
Class Cruise Geology	12	6	72	3
Class Cruise ROV	12	4	48	2
ROV Survey	168	2	336	14
Geology Sampling	120	2	240	10
Support for R/P FLIP	72	6	432	18
UAV Flight Ops	96	2	192	8
AUV Ops (REMUS, Wave Glider, Spray, etc.)	96	5	480	20
Physical Oceanography	192	4	768	32
Biochemical Survey	192	2	384	16
Yearly Totals		**49**	**3,648**	**152**

Table III: Primary Vessel Requirements to Perform the Scripps Science Missions

Characteristic	Requirement	Characteristic	Requirement
Cruising Speed	10 kts, calm water	Portable Vans	2
Maximum Speed in Varying Sea States	12 kts, calm water (sprint) 9 kts, SS4 7 kts, SS5	Crew Berths	11
Range	2400 nm	Scientist Berths	18
DP	2 kts beam current, 25 kts wind at best heading	A-Frame	12,000 ST SWL
Endurance	15 days	Main Crane	8,000 lbs @ 12' over the side
Main Lab	800 sq ft	Portable Crane	4,000 lbs SWL
Wet Lab	500 sq ft	Side Frame	5,000 lbs SWL
Computer Lab	120 sq ft	Trawl Winch	10,000m 3/8 3x19
Aft Deck	1200 sq ft	Hydro Winch	10,000m 0.322 EM, 10,000m 1/4 3x19

technological advances bring new opportunities for observation and measurement. Natural and human catastrophes catalyze shifts in research foci. Evolving funding paradigms drive shifts in research methods. For all of these reasons, creating a coastal research vessel that can adapt to the changing needs of research scientists is an imperative.

Definition of Zero-V Performance Requirements

Taking into account the breadth of science missions a new vessel must be able to execute, Scripps defined the science missions required of the Zero-V (Table II), which translates to the vessel performance requirements as listed in Table III.

The primary ports of call for the vessel were specified as the Nimitz Marine Facility (MarFac) at the Scripps Institution of Oceanography in San Diego CA; Moss Landing Harbor, Moss Landing, CA, Pier 54 at the Port of San Francisco, San Francisco CA and Wharf 5 at the Port of Redwood City, Redwood City CA.

The feasibility study plan was generally divided into six tasks whose strategy is described in the following section.

III. Zero-V Feasibility Study Approach

Task 1: Technical Feasibility

In Task 1 we examined whether or not such a vessel can be built that satisfies the Scripps scientific mission requirements (Table II), thereby meeting the Zero-V performance requirements of Table III. The primary questions have centered on the weight and volume of the hydrogen fuel-cell system and its impact on vessel size and performance. While fuel-cell sizes have continued to decrease, they are still not as compact as diesel engines on a power-per-weight or power-per-volume basis. Similarly, hydrogen storage systems take up to ~ 5 times the space as the analogous diesel fuel tanks and are about four times heavier. Here, Glosten, with input from Sandia and Hydrogenics on hydrogen storage and fuel cell power systems, would provide a "Qualitative Hull Comparison Study" to evaluate three candidate hulls (monohull, catamaran, and trimaran) across various performance characteristics. For the selected hull configuration, Glosten would further provide:

- Outboard Profile and General Arrangement (including a 3-D rendering of the vessel with a hull cut-away to show hydrogen tanks, fuel cell, switchboard/transformer and propulsion motor)
- Weight Estimate
- Design Details for Regulatory Review by the DNV GL and the USCG
- Stability Assessment
- Speed and Powering Calculations
- Construction Capital Cost Estimate
- Vessel Energy consumption allowing CO_2(eq.) and criteria H_2 production pathway emissions estimate.

Task 2: Refueling Feasibility

In this task, the project team examined the technical feasibility of refueling the Zero-V at the likely ports of call in its oceanographic research missions. Using the selected hull configuration and the anticipated hydrogen fuel needs from Glosten, Sandia would assess the feasibility of refueling the Zero-V with either fossil-based hydrogen or renewable hydrogen. The ports of call would be specified by Scripps, and on-site visit to these ports would be conducted by Sandia to determine the acceptability of Zero-V refueling at these sites, vessel size requirements for accessing these ports and any other issues associated with successful hydrogen refueling. The best strategy for refueling the Zero-V (e.g. using refueling trailers or fixed refueling installations) would be developed in discussions with the hydrogen gas suppliers Linde and Air Products. These discussions would also examine the refueling times needed for the Zero-V based on the expected fuel needs and the proposed fuel delivery method. Finally, the discussions with the gas suppliers would reveal if sufficient amounts of fossil-based and renewable hydrogen could be made available for the Zero-V science missions.

Task 3: CO_2(eq.) and Criteria Pollutant Emissions

Hydrogen PEM fuel cells are truly zero-emission power devices at the technical point of use. However, the CO_2(eq.) and criteria pollutant emissions associated with hydrogen fuel production and delivery must also be considered, so that the analysis is inclusive of all emission from "well-to-waves" (WTW). Such fuel production emissions are also associated with diesel fuel, but are typically less than the emissions with actually burning the fossil fuel on the vessel. Sandia was tasked with developing the full WTW emissions associated with yearly use of the Zero-V, based on hydrogen fuel consumption estimates from Glosten for the finally accepted vessel design. The WTW emissions includes atmospheric heat trapping emissions (CO_2 (eq.)) and the emissions of NO_x, HC and PM would be calculated for the Zero-V, and compared to emissions from a comparably capable diesel-fueled research vessel.

Task 4: Economics

The cost of designing, building, and operating the Zero-V must be understood to determine the feasibility of making the Zero-V a reality, and for the end-users to fully understand the recurring operational and maintenance costs such a vessel would incur. Glosten was charged with estimating the vessel design and construction costs for building the Zero-V today. Sandia and Scripps would collaborate on examining the recurring yearly operating costs expected for the Zero-V in order to compare with Scripp's experience in operating diesel-fueled research vessels.

Task 5: Regulatory Requirements

The regulatory (environmental, safety, permitting) aspects of the Zero-V are critical feasibility topics. DNV GL led the regulatory review, based on design input from Glosten and general hydrogen and fuel cell technology information from Sandia and Hydrogenics. The objective of the DNV GL review was to assess the design of the Zero-V relative to existing maritime regulations, and to give feedback to Glosten, Scripps and Sandia. Given the feasibility-level design work in the project, it was not expected that an Approval In Principle (AIP) would result from the DNV GL review. Rather, the ultimate objective was to advance the Zero-V design and provide sufficient information for DNV GL to consider issuing a conditional AIP. In addition to the DNV GL review, the design package would be submitted to the U.S. Coast Guard (USCG) for their technical review and feedback.

Task 6: Feedback from the Scripps Science Community and Operations Staff

During the execution of the Zero-V project, it was important to get feedback from the Scripps science community on the Zero-V design and capabilities. This was to be collected on two occasions. The first was early in the project when the hull form options and properties were first identified. This initial review was conducted by Bruce Appelgate with the Scripps Science community in April of 2017. Based on that feedback, the hull-form was finalized and more detailed design pursued. After the Zero-V design was finalized for the purposes of the feasibility study, two meetings would be held at the Scripps Institution of Oceanography to present the Zero-V project results to the Scripps science community (in the morning) and to the Scripps research vessel operations staff (in the afternoon). Each meeting would begin with a summary presentation of the feasibility results, followed by a question and answer session to solicit feedback and ideas for improvement. Appendix H captures the feedback from these meetings with the Scripps science community and operations staff.

IV. Hydrogen Fuel-Cell Technology Background

Before presenting the results of the Zero-V feasibility study and in particular the design of the Zero-V research vessel, it is important to introduce those aspects of the hydrogen vessel technology that are dramatically different than the diesel vessels that are so familiar. These aspects are 1) how hydrogen is stored, to better understand the tankeage used and how that influences the Zero-V design; 2) what the safety-related properties of hydrogen are, to better understand the design philosophy and approach to safety on the Zero-V; and finally 3) PEM fuel-cell technology, to appreciate how this zero-emissions power technology is incorporated into a high-performance research vessel.

Hydrogen Storage Selection

The task of the hydrogen storage system is to hold as much hydrogen as required by the energy utilization profile of the Zero-V within the desired refueling schedule. There are three ways of storing hydrogen: as a high-pressure gas, within a compound or chemical host that can store and release hydrogen, or as cryogenic liquid hydrogen [1,14]. The SF-BREEZE report [1] examined these three options in detail, and explained why liquid hydrogen (LH_2) is the best method for storing hydrogen for the quantities required for the Zero-V science mission. Liquid hydrogen storage has the highest gravimetric density and volumetric density of the options available for storing large quantities of hydrogen. These gravimetric and volumetric specifications (specs) can be defined as:

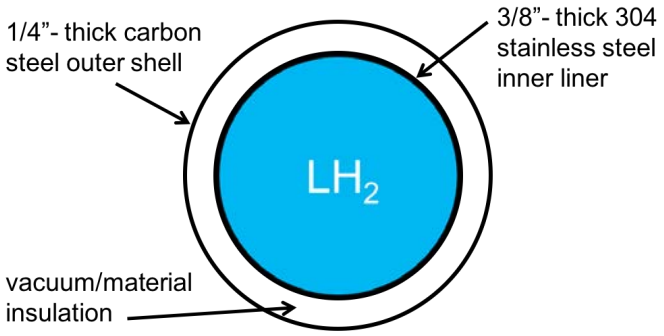

Figure 6: Cross section of a typical road-transport LH_2 tank showing the double liner approach (not to scale). The double liner provides ultra-insulation properties as well as extremely high resistance to damage. The Zero-V will use the same kind of tank.

Gravimetric Spec =
[Empty Tank Mass (kg)]/[Mass of Stored Hydrogen (kg)]

An ideal storage system would have a value of zero for the gravimetric spec. Similarly, one can define a volumetric storage specification as:

Volumetric Spec =
[Outer Tank Volume (L)]/[Mass of Stored Hydrogen (kg)].

An ideal storage system volumetric spec would be hydrogen's density at the pressure and temperature of the storage. As an example, for liquid hydrogen, these gravimetric and volumetric efficiencies for the LH_2 refueling trailer tanks made by Gardner Cryogenics are 8.7 kg Tank/kgH, and 24.8 L/kgH [1], respectively.

LH_2 is a cryogenic liquid with boiling point of 20 K (-253.1 °C). The tanks which hold it can be thought of as highly engineered Thermos™ bottles, with an inner metal liner, separated from an outer metal liner with vacuum and a typically proprietary insulation in-between. A diagram of the arrangement is shown in Figure 6.

The insulation is not perfect, so there is always a small heat leak from the room temperature outer liner through the insulating spacer layer, through the inner metal liner and eventually to the LH_2 itself. Heat leak to the LH_2 causes boiling, with buildup of H_2 pressure within the inner tank. This H_2 must eventually be consumed or vented to relieve the tank pressure, resulting in lost hydrogen through "boil-off." The heat leak is less severe for larger LH_2 tanks because the quantity of hydrogen stored scales with the tank volume, (i.e., as the cube of the tank radius assuming a spherical tank) whereas the heat leak though the outer surface scales with the tank surface area (i.e., as the square of the spherical tank radius). Thus, LH_2 has been the traditional and successful method for storing large quantities of hydrogen (thousands of kilograms) with minimal and acceptable loss of hydrogen through boil-off. Spherically shaped tanks maximize hydrogen storage volume while minimizing surface area, and are thus ideal tank shapes. However, cylindrical tanks are much easier to manufacture (and therefore less expensive) and the surface area/volume ratio is only somewhat greater than that for spherical

shapes. Thus, cylindrical LH_2 tanks are much more common. The heat leak problem is more severe for small LH_2 tanks as the radius shrinks. Thus, LH_2 storage is more challenging for storing small H_2 quantities such as the 5 kg considered for fuel-cell vehicles.

Figure 7 shows examples of existing LH_2 tanks.

Apart from the benefits of minimal weight and volume, there are many other attendant benefits of choosing LH_2 as the storage method of hydrogen. These benefits include:

Figure 7: Examples of LH_2 tanks: (Top, Left) Chart Inc. LH_2 tank; (Top, Right) Linde Group LH_2 tank at the AC Transit Hydrogen Station in Emeryville CA and (Bottom) Linde LH_2 refueling trailer at the AC Transit Hydrogen Station

- LH_2 storage does not require high pressures. While the high-pressure composite hydrogen tanks are very safe, and the composite tank manufacturers deserve a lot of credit for making such a reliable product, there can be perceptions about the safety of having such high pressures (5,000 - 10,000 psi) near people. The highest system pressure for LH_2 storage is typically determined by the tank's hydrogen vent pressure relief valve, which is a modest 150 psi.

- LH_2 storage has been used for decades for space applications (both the Apollo Saturn V and Space Shuttle launch vehicles used very large quantities of LH_2), and has also been transported on the roads in tankers for decades with an excellent safety record. The properties of LH_2 are well understood, and LH_2 storage and transport are mature technologies.

- LH_2 tank technology scales well. Building much larger LH_2 tanks does not introduce new problems, and can be readily accomplished.

- LH_2 is very similar in its physical and combustion properties to liquid natural gas (LNG). Since LNG ships are already being designed by naval architects, and approved by the international and domestic regulatory shipping authorities, LH_2 is a natural extension of LNG maritime technology. Indeed, maritime authorities and international regulatory bodies have already formulated the codes and standards for safe use of LNG on vessels. Theses codes provide a basis for consideration to allow for the safe use of LH_2 on hydrogen fuel vessels based on similarity with LNG. This provides the benefit that naval architects such as Glosten, having LNG design experience, can readily acquire the new learning needed to design hydrogen fuel-cell vessels.

Physical Properties of Hydrogen

Here we provide a brief discussion of the physical and combustion properties of hydrogen, which provide context for understanding the design philosophy of the Zero-V and the fire safety technology it incorporates. A more comprehensive discussion of these properties has been recently published by Klebanoff et al. [15]. This publication is reproduced in this report with journal permission as Appendix A. Comparison is made to the physical and combustion properties of methane (CH_4, the major component of natural gas), which may be more familiar to the reader.

Gaseous Hydrogen

Hydrogen is the lightest gas, with a density of 0.08376 kg/m^3 at normal temperature and pressure (NTP), 293.15K, 1 atmosphere pressure. By comparison methane is considerably heavier, with a density at NTP of 0.65119 kg/m^3. Note that 80% of the atoms in methane are hydrogen atoms. Both

gases at NTP are more buoyant than air, which has a NTP density of 1.204 kg/m^3.

Being a homolytic diatomic molecule, hydrogen has no dipole moment, and vibrations of the molecule cannot produce charge separation along the bond axis. Consequently, hydrogen does not interact with infrared radiation, and is not a heat trapping gas. In contrast, since methane (CH_4) is a heterolytic molecule with different elements bonded together, the bonds are inherently polar, and stretches and bends of C-H bonds produce charge fluctuations that can couple to infrared electromagnetic radiation. This character makes methane a potent heat trapping gas, ~ 23 times more capable of trapping heat in the atmosphere than CO_2. This fundamental difference between hydrogen and methane makes methane leaks from LNG infrastructure a serious concern from environmental, safety and economic perspectives, whereas leaks from a hydrogen infrastructure raise safety and economic concerns without environmental impact.

Liquid Hydrogen (LH_2)

As described previously, the most volumetrically efficient method of storing large quantities of hydrogen is as a liquid, which in the case of hydrogen is a cryogenic liquid. A defining characteristic of molecular hydrogen is the very weak attractive van der Waals interactions between H_2 molecules. The normal boiling point for hydrogen is a very cold 20 K; the normal boiling point for LCH_4 is 111 K. An important consequence for the difference in boiling points is that liquid methane (at its boiling point) cannot liquefy air, whereas LH_2 can liquefy air, whose components N_2 and O_2 condense at 77.3 K and 90.2 K, respectively. These atmospheric gases can also solidify when exposed to LH_2, as the melting points for solid N_2 and solid O_2 are 63.3 K and 54.8 K, respectively. The potential for liquefying or solidifying air introduces safety concerns arising from clogging hydrogen lines with condensed air, as well as concerns about reactivity stemming from condensed oxygen. As a practical matter, these air condensation issues are routinely handled in LH_2 fueling operations by purging the LH_2 plumbing lines with hydrogen or helium (more typically hydrogen due to its availability at the site and lower cost).

Both hydrogen and methane are less dense than air at room temperature and pressure. An important safety-related question is: when these liquids evaporate, producing either cold hydrogen gas at 20 K, or cold methane gas at 111 K, how much do these gases have to warm before they become more buoyant than ambient air? If we assume that for small leaks, the ambient air is not cooled too much and remains near NTP, then hydrogen will become more buoyant than NTP air (with density 1.204 kg/m^3) at 22.07 K. In other words, small hydrogen releases from LH_2 need only warm up by ~ 2 K in order to become more buoyant than air at NTP conditions. In contrast, methane needs to warm up 53.3 K, from 111 K to 164.3 K, before its gas-phase density equals that of NTP air [15]. As a result, when LCH_4 evaporates at 111 K, the cold methane gas stays non-buoyant for significantly longer times than does LH_2. Both LH_2 and LNG at their NBP expand considerably when warmed to NTP. The volume expansion factor for hydrogen is 847.6 and that for methane is 648.0 when a given mass is warmed from the NBP to NTP.

Cryogenic Spills

The weak intermolecular attractions between hydrogen molecules leads to the enthalpy of vaporization ΔH_{vap} of LH_2 being a very low 0.92 kJ/mole, 9.2 times less than that of LCH_4, whose ΔH_{vap} value is 8.5 kJ/mole. For comparison, the ΔH_{vap} of liquid water is 40.66 kJ/mole, due to the strong hydrogen bonding found between water molecules. The extraordinarily low ΔH_{vap} value for hydrogen means that it takes very little energy to evaporate it, and as a result, LH_2 spills are very short duration events. Theoretical models have predicted that spilling ~2800 kg of LH_2 would produce a pool with a lifetime of ~ 13 seconds [15].

Permeation

Hydrogen permeation arises from the dissociation of molecular hydrogen at metal and oxide surfaces into hydrogen atoms, and the subsequent diffusion of hydrogen atoms through materials involved in hydrogen storage and plumbing lines. Hydrogen atoms produced in this way can also lead to hydrogen embrittlement, which is a very important phenomenon in materials science. Many misinterpret hydrogen permeation (even in the absence of embrittlement) as a leak risk. The concern is that hydrogen diffusing through stainless steel tubing and other fittings can pass though the material and exit as hydrogen gas, thereby constituting a leak. Permeation as a source of leaking is not an issue for the practical performance of stainless steel tubing, valves or other hardware at the pressures involved in the Zero-V because the quantities of gas exiting in this way are infinitesimal [15].

Hydrogen Embrittlement

Hydrogen solution, permeation and diffusion, even though involving vanishingly small quantities of hydrogen from a leak perspective, are key ingredients to the phenomenon of hydrogen embrittlement. Hydrogen embrittlement is a significant area of materials science. Excellent reviews exist and are referenced in Appendix A. Hydrogen atoms produced by the dissociation of H_2 at metallic surfaces can diffuse into the bulk of the material, and accumulate at defect sites in the presence of material strain (which all practical materials have to some extent). Because of the combination of hydrogen, pre-existing defects and strain, hydrogen atoms can accumulate at defect sites, locally weakening the material and promoting crack growth. This is a problem for ferritic (body-centered cubic, bcc) steels, but is a vastly smaller problem

for austenitic (face-centered cubic, fcc) steels, or copper or aluminum.

As a practical matter, hydrogen embrittlement is circumvented in hydrogen technology by using 304 or 316 stainless steels, aluminum or copper in all hydrogen storage systems and piping. Decades of industrial experience show these materials are robust to hydrogen embrittlement. This materials choice is similar in spirit to choosing copper over iron in the manufacture of electrical wiring. Copper has a higher electrical and thermal conductivity than iron, and using copper reduces resistive losses and promotes thermal control. Analogously, the correct materials must be chosen for hydrogen service. The practical experience of the gas providers is that hydrogen embrittlement is not a maintenance issue for LH_2 or other hydrogen plumbing (tubing, piping) when type 316 or 304 stainless steel materials choices are properly implemented. Like most commercial LH_2 tanks, the interior liners of the LH_2 tank of the Zero-V will be 304 stainless steel.

Combustion Properties of Hydrogen and Methane

The physical properties just discussed for hydrogen and methane are the foundation for the discussion of the combustion properties of these two fuels. Table IV provides values for "classic" physical and combustion properties of hydrogen and methane, with more details given in Appendix A.

In order to discuss combustion caused by specific ignition sources, some definitions are in order:

Weak (Thermal) Ignition Sources: Matches, sparks, hot surfaces, open flames with initiation energy of < 50 mJ are called "weak" or "thermal" ignition sources. These are the ignition sources of accidents.

Strong (Shock Wave) Ignition Sources: blasting caps, TNT, high-voltage capacitor shorts (exploding wires), lightning are all examples of "strong" ignition sources with initiation energy of > 4 MJ. Note that strong ignition sources are ~ 10^8 times stronger than weak initiators. This is an enormous difference in ignition input energy. Other than lightning, strong ignition sources are the sources of intentional ignition, not accidental ignition.

Fire: Fire is the term for ordinary combustion familiar in everyday life where the flame propagates through the unburned fuel/air mix at low speeds (~ 20 m/s or less). Fires are not loud, and produce negligible overpressure in the surrounding air. Fires are produced by weak ignition sources in contact with flammable mixtures of fuel and air. Despite their familiarity, it is important from a safety perspective to remember that fires are dangerous.

Deflagration: Fast combustion where the flame propagates through the unburned fuel/air mix rapidly, but at subsonic speeds (~ 100 - 400 m/s). Deflagrations can be loud, and can produce overpressures that can rupture eardrums and cause other injury. Under the right conditions, deflagrations are initiated by weak ignition sources. From a safety perspective, deflagrations are very dangerous.

Explosion or Detonation: Technically, detonation is the more properly defined term for extremely fast combustion events where the flame propagates through the unburned fuel/air mix at supersonic speeds (> 700 m/s). Explosion has been loosely used to label fast combustion events where the flame propagates through the unburned fuel/air mix at subsonic speeds (< 700 m/s), and can produce loud bangs and very damaging overpressures. The terms explosion and detonation have often been used interchangeably (especially in the older literature referenced in this work), and will be so used here. "Direct" explosions are instantaneous events caused by strong ignition sources with specific conditions of fuel/air mix and confinement. From a safety perspective, explosions and detonations are very, very dangerous.

Before discussing the combustion of these fuels by explicit ignition sources, we consider the phenomenon where releases of these gases can spontaneously ignite even in the absence of specific ignition sources.

Spontaneous Ignition

Hydrogen, when suddenly released, can undergo "spontaneous ignition" for pressures higher than ~ 41 bar [15]. Spontaneous ignition is a particular safety concern, because it represents an ignition pathway that can persist even if one has successfully removed all explicit ignition sources from the design of a particular application involving hydrogen. While spontaneous ignition may be a concern for high-pressure (350 bar, 700 bar) hydrogen systems such as those used in light-duty fuel cell vehicles, we shall see that the Zero-V employs LH_2 storage of hydrogen for which the hydrogen pressure in the fueling system is everywhere less than 10 bar, which corresponds to the pressure relief for the LH_2 tank vent. As a result, the overall hydrogen system pressures on the Zero-V are too low for spontaneous hydrogen ignition to come into play. The mechanistic cause of spontaneous ignition is not definitively known, and continues to be an active research topic.

Fires

Both H_2 and CH_4 mixtures with air ignite easily using weak ignition sources to produce fires. Fire regulations focus on

Table IV: Physical and Combustion Property Values for Hydrogen and Methane.

Quantity	Hydrogen	Methane
Molecular Weight	2.016	16.043
Density of Gas at NTP, kg/m^3	0.08376	0.65119
Temperature to Achieve NTP Neutral Buoyancy in Air (1.204 kg/m^3), K	22.07	164.3
Normal Boiling Point (NBP), K	20	111
Liquid Denisty at NBP, g/L	71	422
Enthalpy of Vaporization at NBP, kJ/mole	0.92	8.5
Lower Heating Value, MJ/kg	119.96	50.02
Limits of Flammability in Air, vol%	4 – 75	5.3 – 15
Explosive Limits in Air, vol%	18.3 – 59.0	6.3 – 13.5
Minimum Spontaneous Ignition Pressure, bar	~41	~100
Stoichiometric Composition in Air, vol%	29.53	9.48
Minimum Ignition Energy, J	0.02	0.29
Flame Temperature in Air, K	2318	2148
Autoignition Temperature, K	858	813
Burning Velocity in NTP Air, m/s	2.6 – 3.2	0.37 – 0.45
Diffusivity in Air, cm^2/s	0.63	0.2

the "Lower Flammability Limit" (LFL), expressed as a volume percentage (vol%):

$$\text{vol\%} = [\text{Volume (Fuel)}/\text{Volume (Fuel + Air)}] \times 100$$

The LFL is the focus of safety regulations, since the risk of fire typically comes from the accumulation of flammable gas in initially clean air. The classic values [15] for the flammability range LFL to upper flammability limit (UFL) for H_2 = 4.0 – 75.0 % at 298 K (see Table IV). The LFL to UFL of methane is = 5.3 – 15.0 % at room temperature. For context, the LFL – UFL values for gasoline are 1 – 7.6%. Thus, while hydrogen has a much wider flammability range than methane (making it more of a fire risk), from the perspective of building up flammable gas in an initially clean environment, hydrogen and methane have similar LFLs, with similar threshold gas accumulations that can be ignited.

Buoyancy effects can modify the LFL of these gases slightly [15]. For example, for sustained hydrogen fires in a quiescent mixture, the hydrogen/air mix needs to be ~ 8% for combustion to propagate in all three directions with complete combustion of the fuel. Active mixing of hydrogen returns the LFL to 4 % for hydrogen [15]. The minimum ignition energy for H_2 is 0.020 mJ; that for CH_4 is 0.29 mJ. Static discharges from human beings are ~ 10 mJ, so both CH_4 and H_2, when present between the LFL – UFL limits, ignite easily when exposed to common (weak) ignition sources. Table IV lists these combustion properties for hydrogen and methane.

Overall, from the point of view of fire risk coming from fuel release into initially clean air, hydrogen and methane have very similar ignition risks because their LFLs are similar.

Thermal Flame Radiation

One of the striking differences between hydrogen and natural gas is the radiant nature of their fires. When hydrogen burns, the product of combustion is primarily water vapor, with other species such as OH and H radicals, and HO_2 and H_2O_2 produced in trace (< 1 %) amounts. As a result, the vast majority of thermal radiation from hydrogen fires originates from vibrationally excited water molecules. In contrast, when methane burns, although some water is produced, most of the thermal radiation comes from carbon-containing species, and especially carbon soot, which is an efficient radiator of thermal energy. As a result, the thermal radiation emitted from methane fires is (on a fuel LHV basis) 2 - 3 times higher than for a hydrogen fire. Thus, one can get closer to a hydrogen fire because it radiates less thermal energy. In addition, there is more atmospheric absorption of the thermal radiation from a hydrogen fire. Since a hydrogen fire is emitting infrared (IR) radiation from the vibrational (bending, stretching) modes of thermally excited water vapor, residual water in the atmosphere (i.e. humidity) can absorb some of radiation from hydrogen fires, reducing the transmission of radiant heat. Over a 4.7-meter path length, ~30% of the thermal radiation issuing from a hydrogen fire is effectively blocked by atmospheric water vapor [15]. The two effects of reduced emitted radiation and higher atmospheric absorption of fire radiation more than compensate for the slightly higher flame tempera-

ture of hydrogen compared to methane (Table IV), making hydrogen fires less damaging in terms of radiant energy on surrounding structures and personnel than methane fires.

Explosion and Detonation

Hydrogen and methane can both detonate given the right conditions of fuel/air mixture, confinement and strong ignition source [15]. The lower explosion limit (LEL) to upper explosion limit (UEL) of H_2 at room temperature (% by volume) is 18.3 – 59.0 % at room temperature. The LEL to UEL of methane is = 6.3 – 13.5 % at room temperature [15]. Thus, hydrogen has a much wider explosive range than methane, making it more of an explosion risk in general. From the perspective of a leak building up flammable gas in an initially clean environment, the LEL of methane (6.3%) is reached considerably sooner than that of hydrogen (18.3%).

As reviewed by Klebanoff et al. [15], the A.D. Little Company evaluated the practical explosion risk from large-scale releases of hydrogen in confined and unconfined environments in a series of experiments and modeling studies for the U.S. Air Force and the NASA Lewis Research Center over the period 1960 – 1982. The conclusion from this work is that both confinement (e.g., storage in a balloon) and explosive initiation (e.g., using blasting caps) are required for the direct explosion of confined hydrogen/air mixtures in which explosion occurs instantaneously. Furthermore, the Little work showed that hydrogen vapor clouds could not be detonated even with initiation by explosive charges. These observations led the authors to conclude that "even with shock-wave initiation, detonation is unlikely of the hydrogen-air cloud from a large-scale spill." Summarizing these early tests of practical hydrogen combustion risks, direct detonation requires strong ignition sources, confinement, and hydrogen/air mixes within the LEL - UEL range. Weak ignition sources (the sources of accidents) produce fires even when the hydrogen/air mix is within the explosive range and confined.

These experimental results from the 1960s already help frame the anticipated hydrogen fire safety issues for the Zero-V. We shall see that on the 01 level where the LH_2 is stored, fire is the only significant combustion risk, (rather than detonation, explosion or deflagration) because of the open environment on the 01 level and the absence of strong ignition sources. In the confined Starboard and Port Fuel Cell Rooms, direct detonation is not possible because of the lack of strong (intentional) ignition sources.

Deflagration to Detonation Transition (DDT):

The LEL-UEL range listed in Table IV is for direct detonation of a gas mixture assuming confinement and use of a strong ignition source. The absence of strong (intentional) ignition sources precludes the direct detonation of hydrogen and methane in accident scenarios. However, under certain circumstances it is possible to have a detonation for fuel/air mixes even below the LEL of Table IV if obstacles or internal structures are present within the confined reacting volume. Unlike direct detonation, which requires a strong ignition source, this type of explosion can start with a normal fire. In the confined/obstructed environment, the speed of the combustion accelerates over time and distance to a deflagration due to turbulent mixing of the unburnt fuel-air mixture near the obstacles. With further acceleration, the deflagration transitions to a detonation, producing a Deflagration to Detonation Transition (DDT). For H_2, DDT can only occur for 12% fuel /air mix or higher [15]. Both H_2 and methane can experience DDT, although it is easier for hydrogen.

The presence of obstacles induces an acceleration of the flame velocity at H_2/air concentrations that would otherwise not experience flame acceleration. The role of obstacles is to increase the rate of formation of turbulent structures which improve fuel/air mixture and can also increase the flame area. The advancing flame affects the unburnt flow field ahead of the flame by radiation, generating turbulence at obstacles that alters the combustion within the flame when the advancing flame passes through the turbulent region. Given obstacles and a run-up distance of 10 meters or more, the flame speeds for hydrogen concentrations greater than 12% accelerate from normal fire speeds to deflagration speeds. With more run time and distance, even at mixtures as low as 15.5%, very fast deflagration velocities of ~ 700 m/s are observed if obstacles are present, corresponding to DDT.

Table V: Types of Fuel Cells.

Fuel Cell Type	Mobile Ion	Operating Temp
Proton Exchange Membrane (PEM)	H^+	50 – 100 °C
Alkaline (AFC)	OH^-	50 – 200 °C
Phosphoric Acid (PAFC)	H^+	~220 °C
Molten Carbonate (MCFC)	CO_3^{2-}	~650 °C
Solid Oxide (SOFC)	O^{2-}	500 – 1000 °C

We shall see that in the Zero-V design, the Starboard and Port Fuel Cell Rooms have dimensions 3.35 m wide x 5.18 m tall x 4.27 m long. Distributing the PEM fuel cells amongst these two rooms not only creates redundancy in the vessel power system (as required by U.S. Coast Guard regulations), but also limits the run-up distance available to a hydrogen fire should

one break out in one of these rooms.

From a safety perspective, it is not that important if a highly accelerated flame has actually undergone DDT because the overpressures accompanying these phenomena can be similar, producing the same safety hazard. Similarly, ordinary fires are dangerous and need to be avoided. Since fire requires the most easily realized set of circumstances, the design philosophy of the Zero-V is to prevent fires, which automatically prevents deflagrations, DDTs and detonations.

The Hindenburg and Space Shuttle Accidents

When considering hydrogen for a new application, for example as a propulsion fuel for the Zero-V, the existing community for that application usually references the Hindenburg accident in 1937 as a concern for hydrogen use in general. Most people have seen the newsreel images from the accident that tragically claimed the lives of 35 people. A common misconception is that the Hindenburg exploded. The Hindenburg accident was an ordinary fire, not that an ordinary fire made the situation any less tragic. Also, in discussions with the maritime community, it has been helpful to provide context for the Hindenburg accident, particularly noting the tremendous science and engineering advancements in hydrogen technology since 1937. The method of storing hydrogen for the airship (rubberized gas bags) bears no resemblance to the engineered and rugged DOT-approved stainless steel LH_2 tanks in use on the roads today and used in the Zero-V design.

In another arena, for the past 60 years, NASA has mastered the use of hydrogen, the "signature fuel" of the American Space Program. The Space Shuttle held 102,900 kg of LH_2, 9.4 times more than the Zero-V. Although there have been two tragic accidents involving the Space Shuttles Challenger and Columbia, these accidents did not originate from the onboard storage or use of LH_2.

Through science-based safety engineering and a sound understanding of hydrogen physical and combustion phenomena, hydrogen technology can be used safely in maritime applications. The 50-year record of transporting LNG throughout the world is excellent: 8 accidents involving spills, with no fires and no fatalities [15]. Since LH_2 and LNG are very similar in their physical and combustion properties, minor augmentation of the proven and effective international regulations for LNG transport will enable regulated and safe use of hydrogen fuel cell technology in maritime applications.

Hydrogen Fuel Cells

Here we provide an introduction to proton exchange membrane (PEM) fuel-cell technology, and also describe in a general way the layout of one of the 10 fuel cell racks used to power the Zero-V Research Vessel. The Zero-V is based on the PEM fuel-cell offerings of Hydrogenics, who provided detailed information on their design enabling the conduct of this study.

An excellent presentation of the science and engineering of fuel cells can be found in the book "Fuel Cell Systems Explained" by Larminie and Dicks [16]. A review of hydrogen fuel cells can also be found by Klebanoff et al. in Reference [7], upon which a lot of this discussion is based.

A hydrogen fuel cell is an electrochemical device that executes the hydrogen/oxygen reaction (1) without direct combustion:

$$2H_2\,(g) + O_2\,(g) \rightarrow 2H_2O\,(g) + Q \qquad (1)$$

where Q is the heat released by the reaction, which can be turned into useful work such as electrical work. In a fuel cell, instead of direct combustion of H_2 and O_2 which would involve a flame, the reaction (1) is made to happen in two spatially separated "half-reactions" (2) and (3):

$$2H_2\,(g) \rightarrow 4H^+ + 4\,e^- \quad \text{(occurring at the anode)} \qquad (2)$$

$$O_2\,(g) + 4\,e^- \rightarrow 2O^{2-} \quad \text{(occurring at the cathode)} \qquad (3)$$

Initially, the products H^+ (proton) and O^{2-} are created at separate electrode sites, but subsequently H^+ diffuses from the anode to the cathode through a proton conducting membrane. The last step of the reaction occurs spontaneously at the cathode, as represented by reaction (4):

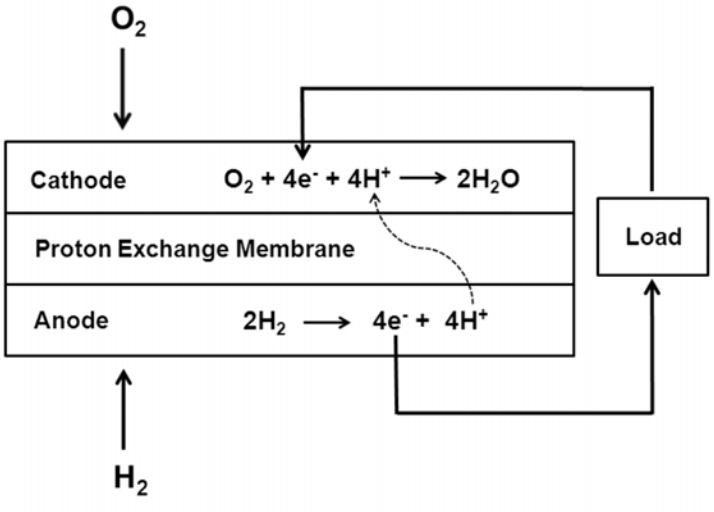

Figure 8: Schematic Diagram of a Proton Exchange Membrane (PEM) Fuel Cell, from Reference 7.

$$4H^{+} + 2O^{2-} \rightarrow 2H_2O\ (g) \qquad (4)$$

These reaction steps of oxidation of H_2 (Reaction (2)) and reduction of O_2 (Reaction (3)) happen not in the gas phase, but at physically separate locations with no flame ever being created. The physical separation is the key point, and this separation allows the thermodynamic tendency for each half reaction to express itself as a half-cell voltage, allowing an overall cell voltage and external current to be developed. Figure 8 shows the relevant reactions in a H_2 PEM fuel cell [7], where reactions (3) and (4) are shown combined at the cathode.

The efficiency of the electrochemical process can be significantly higher than traditional combustion of H_2 and O_2. However, given no constraints on the temperature of combustion, both hydrogen internal combustion engines and fuel cells have equivalent thermal efficiencies [7]. Whereas traditional gasoline combustion has a thermal efficiency of ~35%, limited primarily by the temperatures achievable in traditional combustion systems, the thermal efficiency of the electrochemical process can be ~ 50%. Thus, 50% of the reaction energy can be converted to electricity, with the remaining 50% constituting "waste heat" which is removed from the system by cooling air or liquid.

Fuels cells and batteries share some of the same principles regarding the generation of electricity, with a basic difference being that the fuel cell consumes fuel (i.e. hydrogen and oxygen from air) from external sources, whereas a battery contains all of the reactive species required for power generation. The separation of the fuel sources for a fuel cell provides a distinct safety advantage over batteries, since there is very little chemical energy within a fuel cell at any given time, and in the event of a concern, the fuel supply to the fuel cell can be simply shut off.

Although there are five types of fuel cells, as indicated in Table V, only the PEM fuel cell combines all the advantages of being commercially available, having a strong track record, having fast turn on times, and with the smallest weight and volume for the delivered power. Thus, only PEM fuel cells were considered for the Zero-V.

PEM Fuel Cells

At the PEM anode (site of oxidation) hydrogen gas ionizes (oxidizes), releasing protons and electrons to the external circuit, as shown in Figure 8. At the cathode (site of reduction), oxygen molecules are reduced in an acidic environment by electrons from the circuit, forming water molecules. Protons pass through the proton exchange membrane, from anode to cathode, completing the circuit.

Traditional PEM fuel cells use a solid proton conducting polymer membrane called Nafion, a type of polyfluorinated sulfonic acid (PFSA) material, which allows proton transfer between the anode and cathode. Nafion-based fuel cells operate at low temperatures, around 80°C. The low-temperature operation provides for rapid start-up, which is essential for

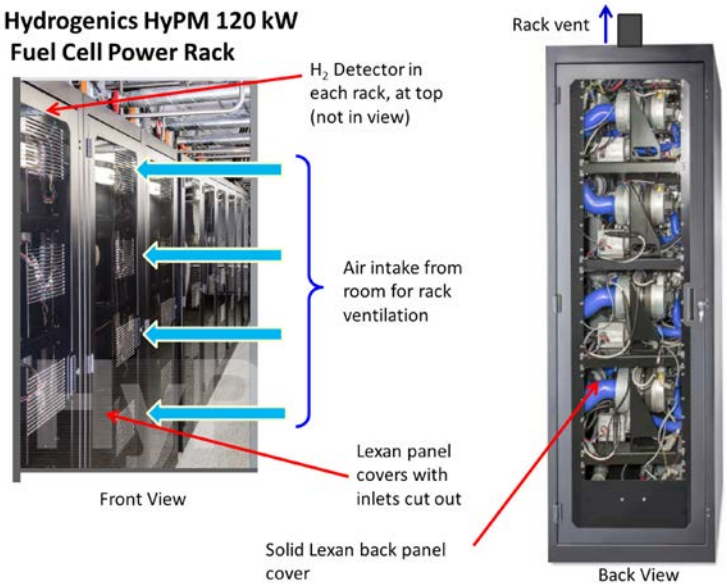

Figure 9: Hydrogenics HyPM-R 120S PEM Fuel Cell Rack Component Installation in South Korea. Photo courtesy of Ryan Sookhoo, Hydrogenics.

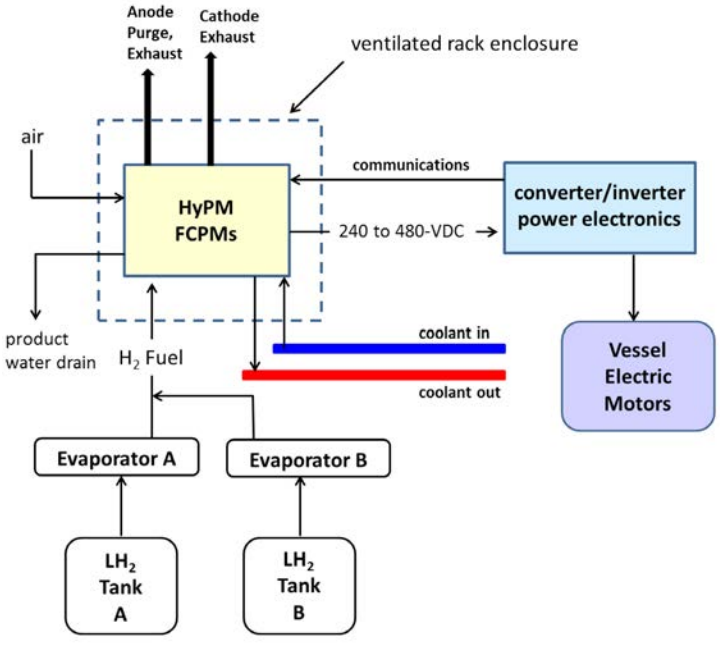

Figure 10: Hydrogenics HyPM-R 120S PEM Fuel Cell Rack Component System Block Diagram. This figure is a modification of a diagram supplied by Ryan Sookhoo of Hydrogenics.

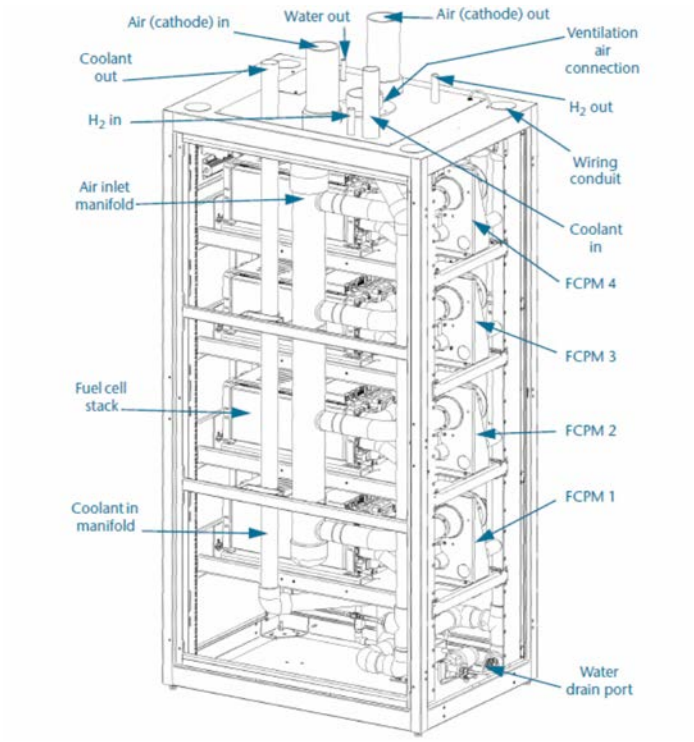

Figure 11: Hydrogenics HyPM-R 120S PEM Fuel Cell Rack Component Locations (front ISO view). Note that in the Zero-V design, the racks will hold 6 fuel-cell power modules (FCPMs) instead of the 4 shown. Figure provided courtesy of Ryan Sookhoo of Hydrogenics.

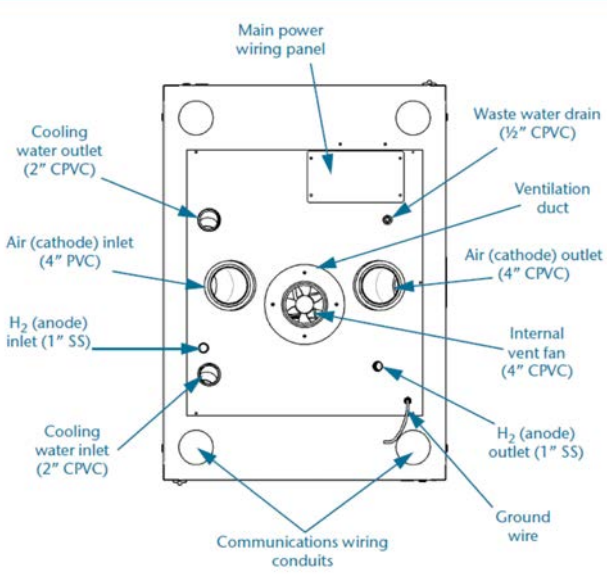

Figure 12: Hydrogenics HyPM-R 120S PEM Fuel Cell Rack Component Locations (top assembly view). Diagram courtesy of Ryan Sookhoo, Hydrogenics.

most relatively low-power and mobile applications. However, for temperatures at or below ~80 °C, the reaction product is liquid water, making management of liquid water an important issue.

In the fuel-cell power racks used in the Zero-V, individual fuel-cell power modules (FCPMs) of nominal power ~ 30 kW are integrated together into power "racks." The commercial system that is purchased are power racks which integrate together the H_2 and air supply lines, the liquid coolant lines to remove waste heat, water discharge lines for the waste water, the exhaust gases from the anode and cathode spaces within the fuel cells, as well as hydrogen detectors and ventilation systems for safety. The operation of each FCPM is monitored by the control system. For maintenance purposes, the FCPMs are easily removed and replaced, typically through a service contract with the fuel-cell manufacturer.

Overview of Rack Development

Hydrogenics is a leading supplier of PEM fuel cell systems for mobile and stationary power applications alike. Since 2006, Hydrogenics has spent a lot of effort working with the certification organizations such as UL to review their products for mobile and stationary power applications. As a result of this process, The HyPM-R 120S Rack complies with the American National Standard/CSA America Standard for Stationary Fuel Cell Power Systems, ANSI/CSA America FC 1-2004. Note that the ANSI/CSA America FC 1-2004 regulation covers operation/service, installation, material compatibility and components to ensure the rack can be safely operated

The HyPM-R 120S rack also complies with the IEC 60079-10-1 code of 2015, which refers to the classification of areas where flammable gas or vapor hazards may arise. It provides guidance for classifying the areas on the basis of chemical properties, process installation and process conditions. The IEC 60079-10-1 code is used to determine the ventilation and classification of the rack and surrounding environment to ensure safe operation and installation. When the rack is installed with other components (balance of plant), this standard is used for classification of components of the overall system (rack + balance of plant) for stationary power applications.

Figure 9 shows a picture of installed HyPM-R 120S power racks for an operational 1 MW fuel cell stationary power application in South Korea with an indication of the required rack ventilation to provide safety in the event of a small leak of flammable H_2 gas.

One can see in Figure 9 that the FCPMs are enclosed in a rack covered with Lexan panels, with ventilation slots cut in to allow air intake for ventilation only. The ventilation is largely around the perimeter of the FCPMs located within the rack.

A hydrogen sensor is located at the top of each rack, within the rack enclosure, and its activation can be used to shut down the FCPMs and shutoff the hydrogen supply. While one could envision the possibility that each FCPM has a hydrogen detector, such duplication of detection is unnecessary since hydrogen rises when released. The layout of hydrogen detectors and the ventilation strategy is described more fully later in the report.

Figure 10 shows the overall block diagram for the power train incorporating an individual power rack for the Zero-V application. The hydrogen is stored in LH_2 tanks at a nominal temperature of 20 K. The fuel cells require room temperature hydrogen, so evaporators (heat exchangers) are used to convert LH_2 and cold hydrogen gas to room temperature hydrogen gas at ~ 100 psig. Note that there are many hardware items such as valves, safety shutoff valves, pressure relief devices and a hydrogen detector which are not shown in Figure 10. The room temperature hydrogen is directed to the HyPM rack where the electrochemical reactions take place. The waste water from the reaction is removed by the water drain. Sometimes water tends to collect in the anode region, which blocks H_2 gas. This water is removed by a brief pulse of hydrogen called the "anode purge." The fuel cell contains an exhaust line for this purge (the anode purge) and also an exhaust line for the cathode which consists of oxygen depleted air and water vapor. The rack also provides for strong ventilation of the entire rack space, generally with flow from bottom to top. The power out of the rack is typically conditioned with a DC-DC converter, and then transformed to AC power by a DC-AC inverter.

Figure 11 shows a diagram of the rack layout, showing locations of individual FCPMs as well as inlets and outlets for fuel cell cooling water, rack ventilation, hydrogen (anode) and air (cathode) inputs and other utilities.

Figure 12 shows an assembly view of the top of one HyPM-R 120S power racks, with the types of piping (CPVC, stainless steel, etc.) and dimensions indicated.

V. Essential Results from the Zero-V Feasibility Study

Figure 13(a): Side rendering of the Zero-V zero-emission hydrogen fuel cell research vessel.

In this section we provide the essential results for the Zero-V feasibility study, and provide descriptions of the Zero-V design that emerged from the study.

General Zero-V Design

The design of the Zero-V that satisfies all of the Scripps science missions, and can visit all the anticipated ports of call is shown in Figures 13 and 14. A complete description of the Zero-V design is given in Glosten's Design Report, presented in Appendix B.

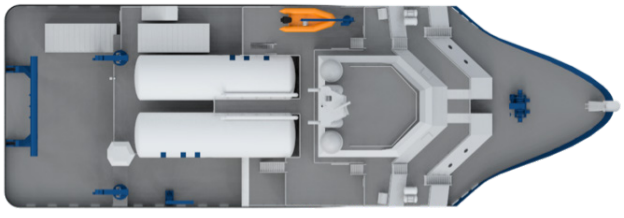

Figure 13(b): Top rendering of the Zero-V.

Three hull-forms were evaluated for the Zero-V: monohull, catamaran and trimaran. The trimaran was selected because it enabled a design such that the vessel could meet all of the space and volume requirements of the vessel as well as for fitment of the machinery, service, and control spaces necessary for operation of the vessel.

The Zero-V design performance specifications are shown in Table VI. To meet speed and range requirements, the vessel has to be constructed of aluminum to reduce its weight. The beam and length were driven by the requirement that the vessel be able to dock at all primary ports of call, namely: the Nimitz Marine facility at the Scripps Institution of Oceanography in San Diego CA; the MBARI Pier at the Moss Landing Harbor, Moss Landing CA, Pier 54 at the Port of San Francisco, San Francisco CA and Wharf 5 at the Port of Redwood City, Redwood City CA. Of these ports of call, the most restrictive refueling location is the MBARI Pier. As described in Table VI,

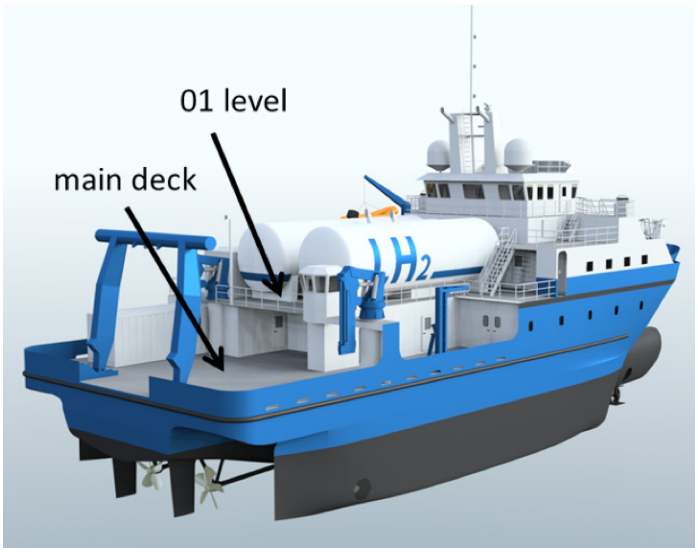

Figure 14: Aft view of the Zero-V showing deck specification and LH_2 tank location detail.

Table VI: Zero-V Overall Design Specifications

Hull Type	Trimaran
Material	Aluminum
Length	170 ft.
Beam	56 ft.
Draft	12 ft.
Freeboard	9 ft.
Displacement	1,175 LT
Cruise Speed	10 knots
Range	2,400 nm
Endurance	15 days
Station Keeping	Dynamic positioning
Berths	18 Science (8 double, 2 single) 11 Crew (single)
Air Emissions	Water vapor

the beam of the Zero-V is 56 feet, with a length of 170 feet. The draft is 12 feet, limited primarily by the water depths at the Moss Landing Harbor channel and MBARI Pier, as well as the water depth at Pier 54. The cruising speed is 10 knots as determined by the science mission requirements. With a total of 10,900 kg of consumable LH_2 stored in two LH_2 tanks, the range of the vessel is 2400 nm, or an endurance of 15 days. The vessel performs "station keeping" by dynamic positioning. The Zero-V is designed to be home to 18 scientists, 11 crew and to be truly zero-emissions on the water.

Zero-V Design Specifics

Arrangements and Propulsion System

Arrangements for the Zero-V were developed to meet all of the space and volume requirements of the vessel as well as for fitment of the machinery, service, and control spaces necessary for operation of the vessel. Additionally, the arrangements consider the operations of the vessel such as access between science spaces, the working deck, and science handling systems as well as visibility and sight lines from control stations to the working areas and equipment. The arrangements also incorporate special requirements specific to the use of liquefied gas fuel. The most significant of these special requirements are hazardous areas, and the restriction that the hydrogen storage tanks be located no closer to the sides of the vessel than 20% of the overall width (beam) of the vessel. For example if the vessel's beam is 50 feet, the hydrogen tanks shall be no closer than 10 feet from the sides of the vessel.

The Zero-V design follows traditional arrangements for a research vessel even given the trimaran hull type. A cut-away view of the Zero-V is shown in Figure 15, giving the locations of the mechanical and propulsion system components. The inboard profile diagram of the Zero-V is shown in Figure 16.

The propulsion power plant, machinery, machinery operating station, stores, main winches, and scientific acoustic equipment are located below the main deck in the hull. The main deck contains the working deck, laboratories, main service spaces, and science berthing. The upper decks contain the crew berthing and navigation spaces. The location of the large LH_2 tanks was driven primarily by their size.

LH_2, because it is a cryogenic liquid stored at pressure, is stored in vacuum-insulated Type C cylindrical pressure vessels. The fitment of cylindrical type C storage tanks into a prismatic hull is both challenging and space inefficient. It is desirable to have fewer large LH_2 storage tanks because large diameter tanks are more volume, weight, and cost efficient.

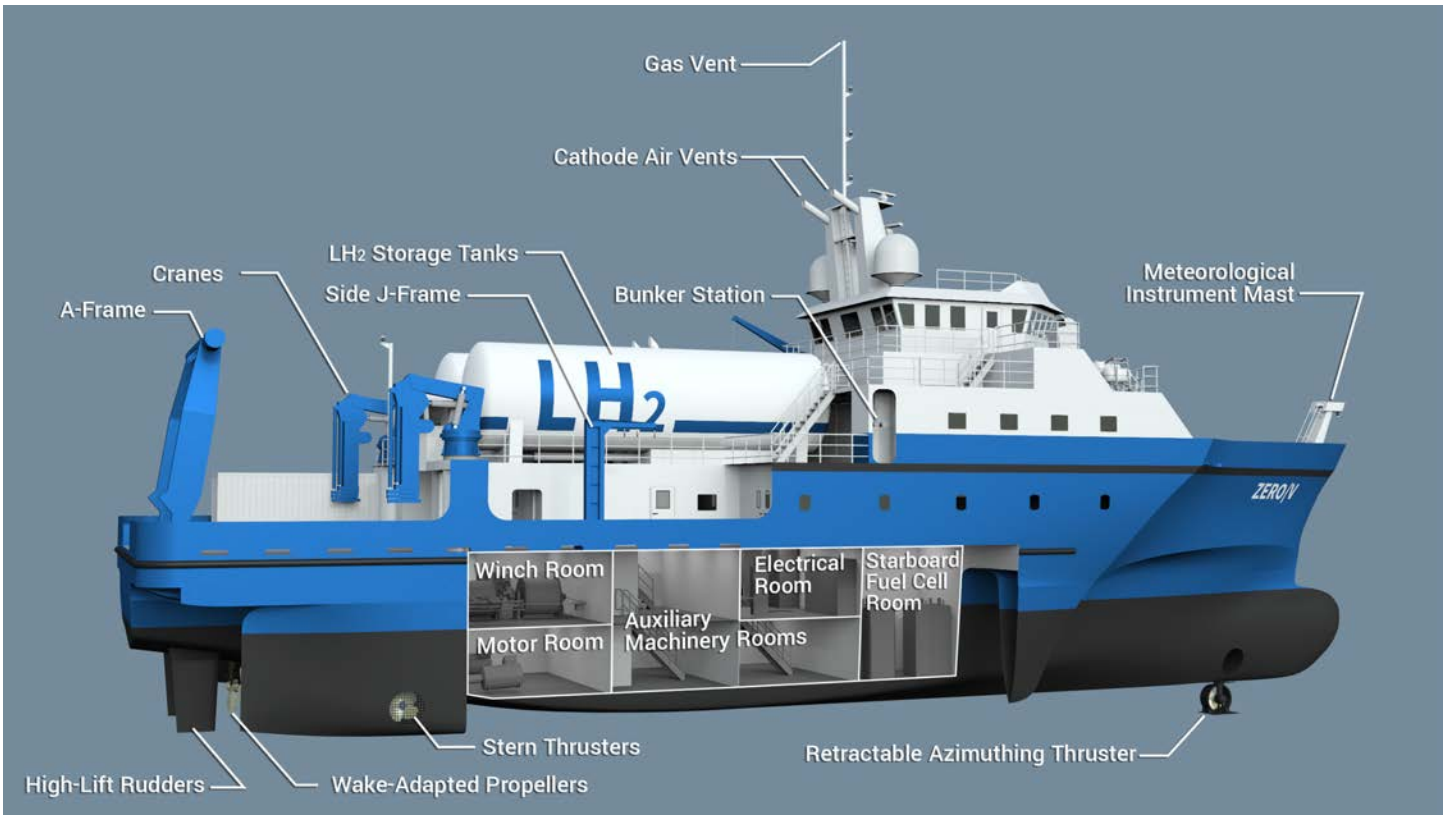

Figure 15: Cut-away view of the Zero-V showing locations of mechanical and propulsion system components.

In addition, the heat leakage from large diameter LH_2 tanks is, as a percentage of the amount of LH_2 stored, smaller than from smaller cryogenic vessels. Thus, undesirable "boil off" of the LH_2 is lower for larger LH_2 tanks than for smaller tanks. Furthermore, the volumetric energy density (energy in the fuel per unit of volume) of LH_2 is 4.2 times lower than that of diesel fuel, making the amount of tankage for an equivalent fuel energy more than four times the volume. Because of these factors, it was found that the size of the storage fuel tanks required to meet range was too large to fit inside the hull of a vessel that met the dimensional limitations. For this reason, the fuel tanks are located above the deck in the weather. On research vessels, the Main Deck is the most valuable working and laboratory spaces. Because large storage tanks located on the Main Deck would be too disruptive to the working spaces and science operations, the tanks were located on the 01 Level aft weather deck. Two evaporators (not shown) convert the cold hydrogen gas to room temperature hydrogen gas which is preferred by the PEM fuel cells.

Details of the vessel's arrangements can be seen in the General Arrangement Drawing in Appendix B. Diagrams of the Zero-V Main Deck and 01 deck are shown in Figures 17 and 18, respectively.

The propulsion system overall electrical architecture is depicted in Figure 19. The system is configured to provide redundancy and flexibility for different operating conditions. The primary objective of the hydrogen fuel-cell propulsion system selection is to allow the vessel to achieve the mission and design requirements. An electric, direct drive, twin propeller arrangement was selected. In this arrangement, each propeller shaft is directly driven by a high-torque permanent magnet motor. This arrangement is simple, efficient, and quiet.

An integrated fuel-cell electric plant supplemented with small lithium-ion bridging batteries provides both propulsion and ship service electrical. The fuel-cell racks have been described previously. The fuel cells are Hydrogenics HyPM HD 30 fuel cell power modules arranged into power racks each holding six fuel-cell modules. Each rack has a total power output of 180 kW. With ten racks total, the vessel has 1,800 kW of installed power.

The ten hydrogen fuel-cell racks are evenly distributed between Starboard and Port fuel-cell rooms, allowing the vessel to continue operation at reduced power if one space must be taken out of service for maintenance or in response to a hydrogen leak or other maintenance problem in the space. The fuel cells provide DC power, which much be conditioned, converted and inverted to provide bus DC and AC power, re-

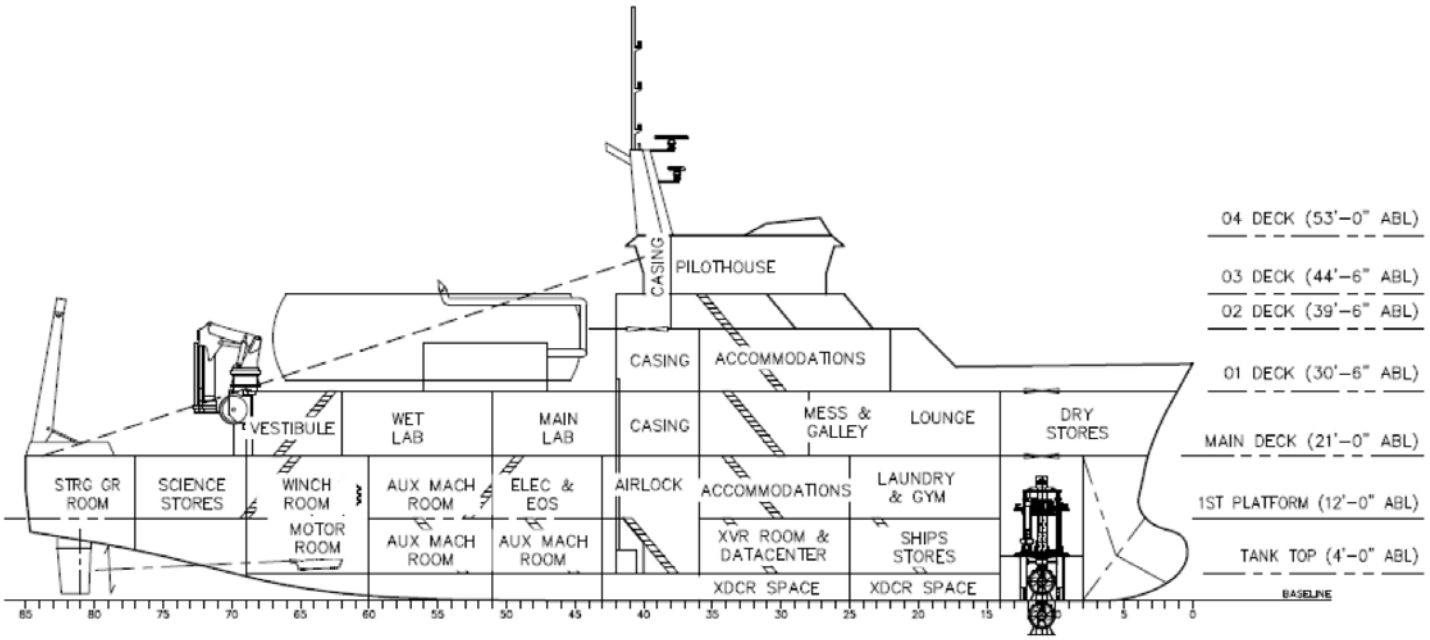

Figure 16: Inboard profile arrangements for the Zero-V.

spectively. There are two switchboards (SWBD) in the Zero-V electrical system: a 900 VDC propulsion SWBD and a 480 VAC ship service SWBD.

The fuel-cell power modules have an operating voltage between 60 and 100 VDC. All the modules in a rack operate in series making the output of the power rack 360-600 VDC. Each power rack supplies power to the propulsion switchboard through a DC-DC converter that converts the voltage to a steady nominal voltage of 900 VDC. The various large loads such as propulsion, thruster, and winch motors are supplied from the propulsion switchboard through DC-AC drives. Additionally, the ship service electrical power is supplied to the 480 VAC ship service switchboard by redundant DC-AC power converters. Smaller loads such as lighting, fans, or pumps are supplied from the ship service switchboard.

Fuel cells can assume load fairly quickly. The fuel cells take approximately 5 seconds to go from offline to standby and less than 30 seconds to go from standby to rated power output. However, operations such as dynamic positioning can have very fast, transient spikes in vessel propulsion electrical load that could challenge the ability of the fuels cells to respond quickly enough. To account for these transient loads, the electrical plant also has two lithium-ion battery banks as depicted in Figure 19. Batteries are able to provide large amounts of power nearly instantaneously in response to load demands. With the fuel cells providing the base load power, the batteries will charge or discharge as required to manage transient loads. Additionally, the batteries can be used as a power sink for dynamic braking of large motors such as propulsion motors or winches. This allows energy to be recovered during operations such as paying out a winch, thereby increasing overall vessel efficiency.

The overall specifications for the propulsion equipment are given in Table VII. To provide the required position keeping ability for on-station science work, the vessel is fitted with a retractable azimuthing bow thruster as well as stern thrusters in each outer hull. A typical retractable bow thruster is shown in Figure 20.

Additionally, high-lift flap rudders are provided to maximize steering forces produced from the main propellers during station keeping. The Zero-V uses two propulsion motors to power to its propellers. Based on the resistance and powering calculations, it was determined that 500 kW motors will provide sufficient power for the various mission requirements and also have enough reserve power for safe operation in heavy seas and for dynamic positioning. High-torque alternating current (AC) permanent magnet type motors were selected as the propulsion motors. These motors can be directly coupled to the propeller shaft to provide efficient and quiet operation.

The vessel is outfitted with two fixed pitch propellers. Each

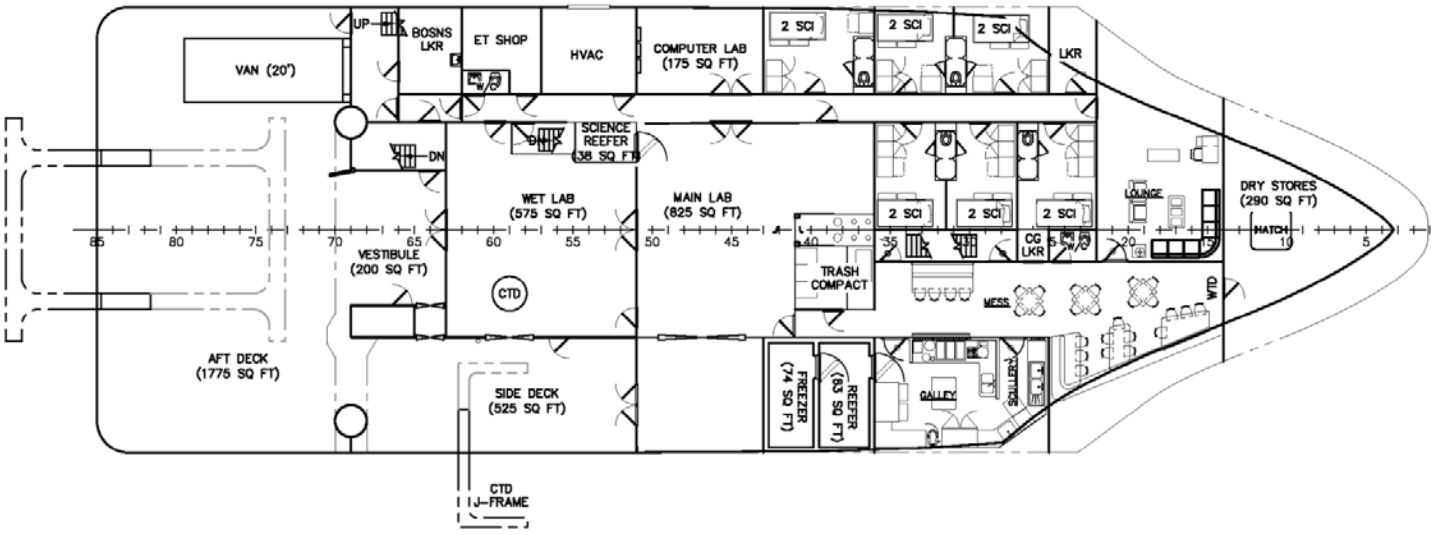

Figure 17: Zero-V arrangement for the Main Deck.

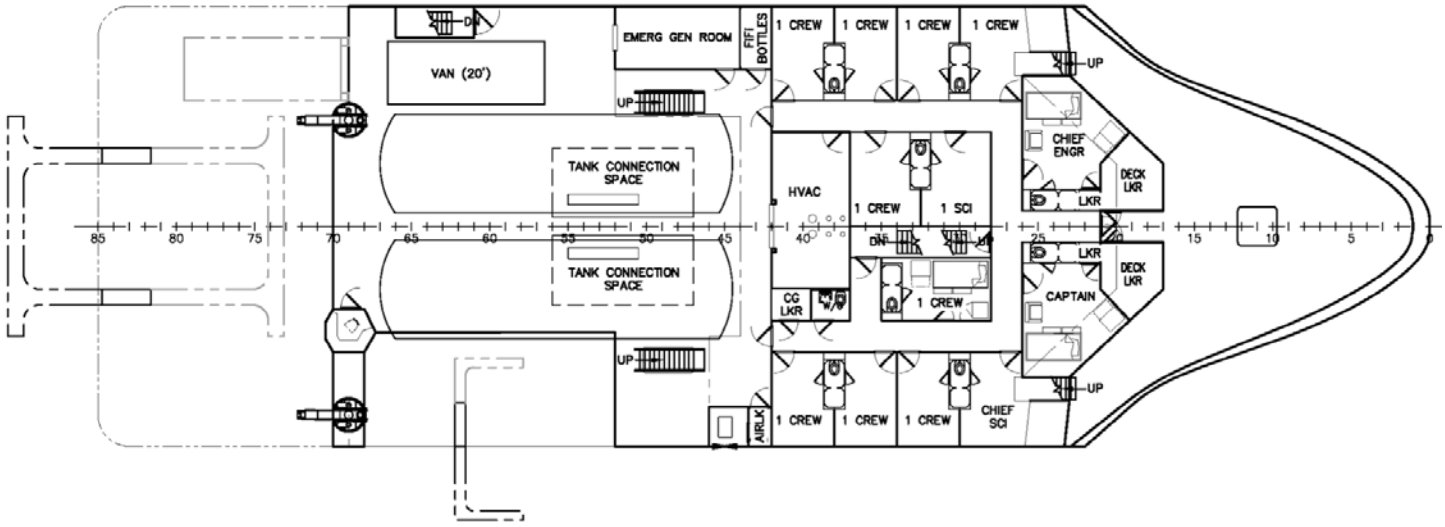

Figure 18: Zero-V arrangement for the 01 Deck.

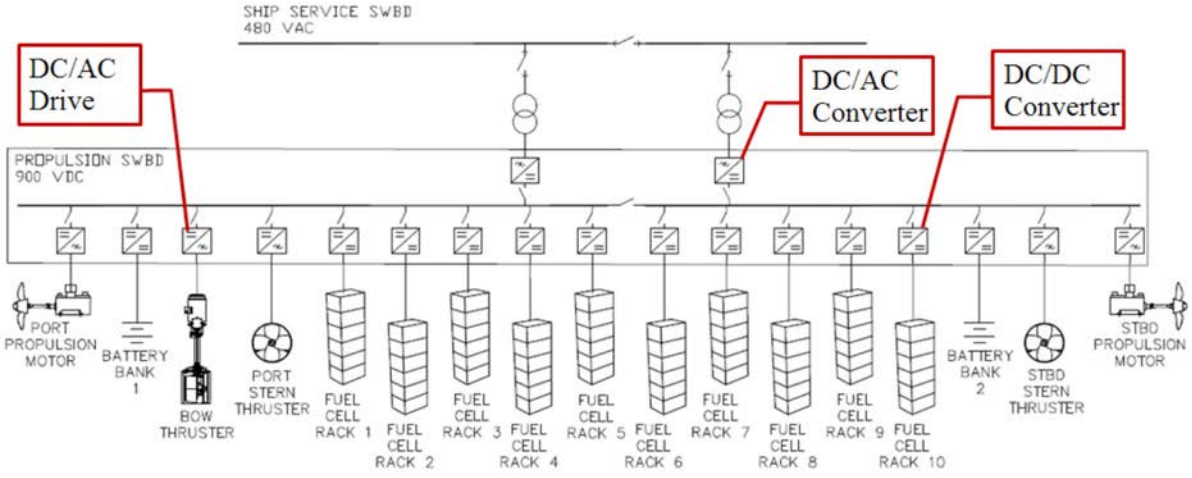

Figure 19: Propulsion system electrical architecture block diagram

Figure 20: Brunvoll Azimuth Combi Thruster

Figure 21: Electric motor driven tunnel thruster (Schottel STT)

propeller is approximately 2.1 m in diameter. Fixed pitch propellers are chosen for their simplicity, low capital and operating cost, and quiet operation. The propellers are of wake-adapted design to minimize underwater noise as well as maximize efficiency. The propellers are fully non-cavitating at speeds of up to 8 knots.

High-lift flap rudders are used for maneuvering the vessel. Compared to conventional spade rudders, the flap rudders provide both high turning forces underway and superior thrust control for position keeping. The bow thruster is a 500 kW retractable azimuthing thruster. This thruster provides sufficient maneuvering and dynamic positioning capability for the vessel under the required operating conditions. The bow thruster is powered by a permanent magnet AC motor for maximum efficiency.

To increase docking and position keeping performance, stern tunnel thrusters are installed in each side hull. An example of a tunnel thruster is shown in Figure 21. Conventional electric motor driven tunnel thrusters were selected for the stern thrusters. To increase compactness and efficiency, permanent magnet AC motors are used. Because of the trimaran's center hull, thrust directed inward by the stern thrusters would suffer significant thrust loss due to hydrodynamic effects and would also likely create excessive noise. For this reason, it has been assumed that the stern thrusters will only be operated to provide outward thrust away from the vessel. Table VII summarizes the propulsion equipment specifications.

Science Capabilities and Vessel Performance

Table VIII summarizes the Zero-V capabilities in performing its science missions. The installed science packages and material handling equipment are chosen as required by the Scripps science missions. The laboratory spaces on the vessel are quite large. Early in the design process we received feedback from Scripps science staff that this was a particularly desirable feature for a new vessel.

Table VII: Propulsion Equipment Specifications

Power	10 x 180 kW hydrogen fuel cell racks
LH_2 Tanks	2 x 28,800 gal type C
Propulsion	2 x 500 kW PM motors
Bow Thruster	500 kW, retractable azimuthing
Stern Thrusters	2 x 500 kW tunnel
Propellers	Wake-adapted fixed pitch
Rudders	High-lift

Seakeeping

Good seakeeping performance is important for research vessels to maximize the operability of the vessel for mission activities. Although the scope of this project did not include seakeeping analysis, prior research vessel design work by Glosten provides some general expectations for the Zero-V.

Glosten previously investigated variants of a research vessel design including both a 170' x 41' monohull with a displacement of 1,250 long tons and a 170' x 56' trimaran with a displacement of 1,175 long tons. Because of the similarity in size of these vessels to the Zero-V, this prior study provides applicable expectations of seakeeping performance for the Zero-V.

In this study it was found that while there were some differences in the seakeeping performance of the variants, they both provided excellent seakeeping in conditions up to Sea State 4 (4 ft to 8 ft significant wave height). An operability analysis for central California offshore conditions found that both the monohull and the trimaran exceeded 95% operability with respect to operating limitations for motions (displacement, velocity, and acceleration) at the A-frame and to motion sickness incidence in the Main Lab and the Pilothouse. In other words, the expectation is that the Zero-V would be

Table VIII: Summary of Zero-V Science Mission Capabilities

A-Frame	20,000 lbs. SWL 20' vertical clearance 12' outboard reach
Main Cranes (2)	8,000 lbs. SWL over the side
Portable Crane	8,000 lbs. SWL
Side Frame	5,000 lbs. SWL
Trawl Winch	10,000m 3/8 3x19 wire
Hydro Winch	10,000m 0.322 EM 10,000 1/4" 3x19 wire
Multi Beam Sonar	Kongsberg EM712
Underwater Noise	ICES up 8 knots
Main Lab	825 ft^2
Wet Lab	575 ft^2
Computer Lab	175 ft^2
Aft Deck	1,775 ft^2
Side Deck	525 ft^2
Van Spaces	2
Science Payload	50 LT

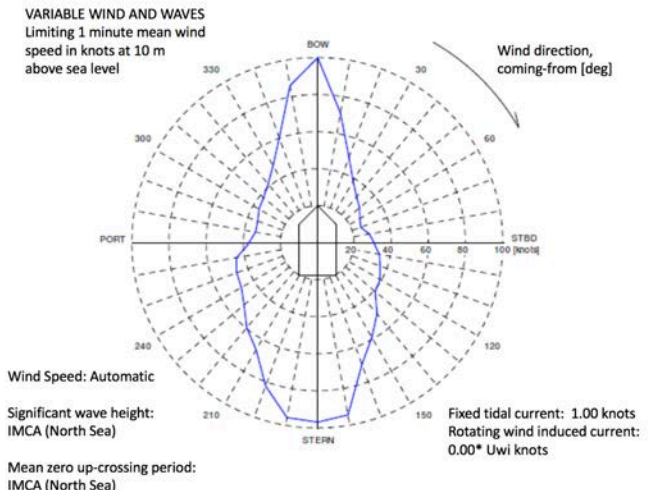

Figure 22: Dynamic positioning capability in 1 knot of beam current.

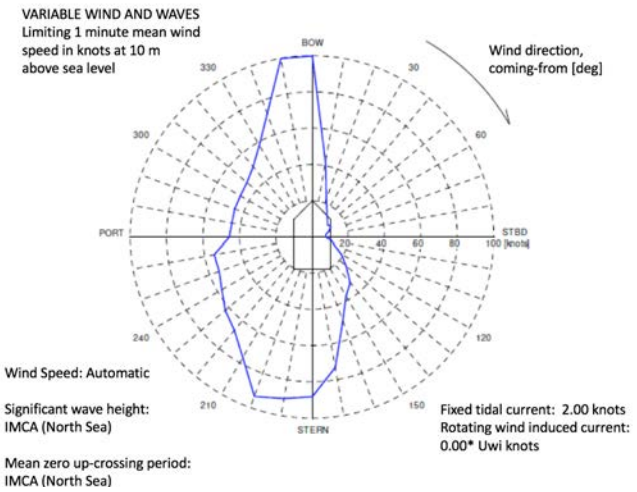

Figure 23: Dynamic positioning capability in 2 knots of beam current.

operable for science work in 95% of the annual expected of sea conditions in central California waters.

Positioning

A preliminary dynamic positioning (DP) capability study for the Zero-V was performed by Kongsberg and indicates 500 kW tunnel thrusters will provide satisfactory DP capability. The vessel is able to maintain position with 1 knot beam current and more than 25 knots wind and waves from any heading. With 2 knots beam current, the vessel can still maintain position with significant wind and waves at best heading. Figures 22 and 23 show the DP capability plots of the Zero-V for these conditions.

These DP capabilities are expected to be sufficient for performing the typical on-station work this vessel would engage in.

Underwater Radiated Noise

One of the benefits of hydrogen fuel cells is that they are very quiet compared to diesel engines. Unlike an internal combustion engine, hydrogen PEM fuel cells contain no moving parts, although there are mechanical devices for the "balance-of-plant" which includes pumps for waste water, electronic fans, and recirculating pumps for fuel-cell coolant and for the cryogen evaporators, etc. It is expected that fuel cell technology should provide significantly reduced noise signature in comparison to diesel compression ignition technology.

The reduction in noise from elimination of diesel engines, one of the largest noise sources onboard conventional vessels, has two significant benefits. The reduction in airborne noise from the engine and the engine exhaust improves habitability

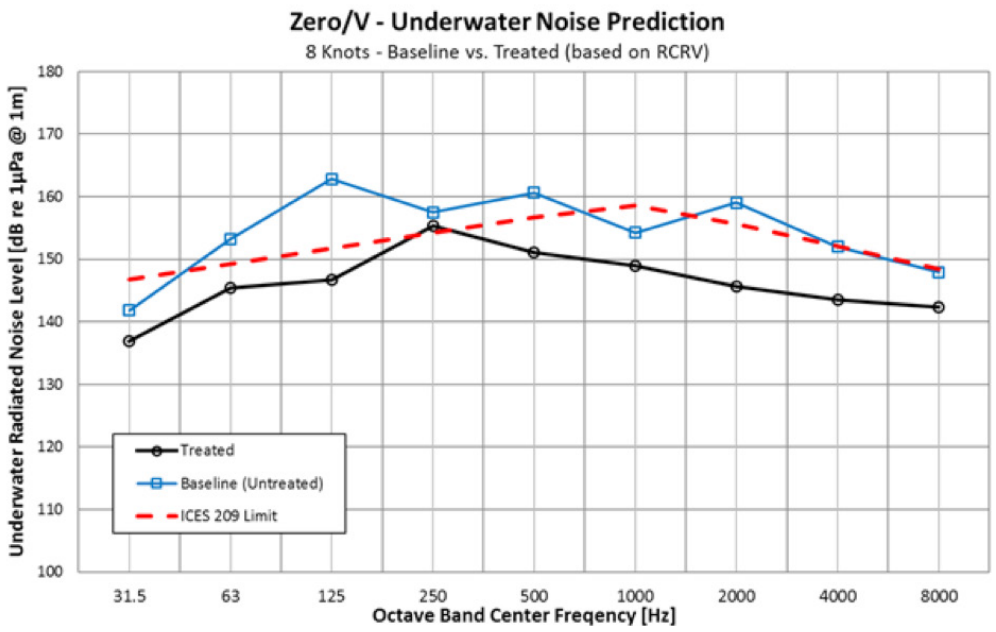

Figure 24: Result of initial underwater radiated noise assessment for the Zero-V travelling at 8 knots speed. The Zero-V with no noise treatment is shown by the blue curve; the Zero-V with nominal (typical) noise treatment is shown by black curve. Comparison is made to the limits recommended by the International Council of the Exploration of the Sea (ICES) Report 209, as this is often used benchmark for underwater radiated noise.

both inside the vessel and on the working decks. Additionally, the reduction in noise helps the vessel achieve underwater radiated noise (URN) limits.

Low URN is very important for research vessels to avoid interference with scientific instruments such as sonars and to minimize detection from marine wildlife. Based on discussions with Scripps, the URN goal for the Zero-V is to meet the limits from the International Council for the Exploration of the Sea (ICES) Report 209 at a speed of 8 knots. The ICES Report 209 limits are a commonly used standard for URN limits of research vessels. Noise Control Engineering (NCE), a Glosten subsidiary, developed an estimate of the URN levels for the Zero-V. The estimate was developed using the URN predictions for the RCRV, developed for Oregon State University, as a baseline because the vessels are of similar size and propulsion power.

To establish an estimate for the Zero-V, the RCRV URN predictions were adjusted to account for the removal of the noise source from the diesel engines. This method provides a relatively rough estimate, but as can be seen in Figure 24, the result suggests that, with noise treatments such as damping material on the hull and vibration isolation of large rotating machinery, the Zero-V can meet the limits in ICES Report 209. The Zero-V URN estimate was done for a steel hull and was not revised to account for the aluminum hull. The aluminum hull may require additional damping material to achieve ICES Report 209 limits. To establish a more accurate estimate, a full DesignerNOISE ™ model is required. This is beyond the scope of this feasibility study.

Well-to-Waves CO_2(eq.) and Criteria Pollutant Emissions

As discussed previously, hydrogen has the potential to form the basis for a zero-carbon energy system. Here we summarize the results of our analysis, given in its entirety in Appendix C, revealing the well-to-waves (WTW) CO_2(eq.) and criteria pollutant emissions of the Zero-V using hydrogen PEM fuel-cell technology. Here CO_2(eq.) emissions refers to the sum of CO_2, CH_4 and N_2O emissions multiplied by their radiative trapping weighting factors. Criteria pollutant emissions refer to NO_x, hydrocarbons and particular matter emissions. We use methods published previously by Klebanoff et al. [2]. This publication is reproduced with journal permission in this report as Appendix D. CO_2(eq.) and criteria pollutant emissions are determined and directly compared with those from an equivalent diesel-powered vessel, as well as a vessel fueled with biodiesel fuel.

Since the Zero-V is powered with PEM fuel cells, the vessel emits zero CO_2(eq.) and criteria pollutants during vessel operation. However, one must take into account the emissions associated with LH_2 fuel production and delivery, which depends dramatically on how the fuel is manufactured [2]. The CO_2(eq.) emissions from use of diesel fuel have two sources, namely the emission associated with fuel production and delivery, and the CO_2 release from the vessel upon combustion. Both sources contribute to the WTW emissions associate with diesel fuel use.

We conducted our WTW analysis assuming two production methods for LH_2: hydrogen derived from the steam methane reforming of natural gas (fossil NG LH_2) and hydrogen derived using low-carbon "renewable" methods, such as using elec-

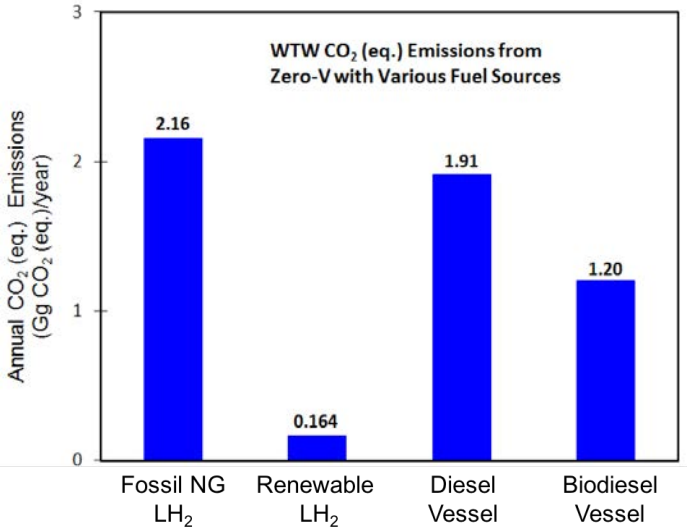

Figure 25; Predicted annual well-to-waves (WTW) CO_2(eq.) emissions for the Zero-V operating on Fossil NG LH_2 and renewable LH_2 compared to the equivalent vessel operating on diesel fuel and biodiesel fuel.

trolysis of water using low-carbon electricity. Appendices C and D give further details of the analysis. A comparison of the annual CO_2(eq.) WTW emissions for the Zero-V running on fossil NG LH_2 and renewable LH_2 and CO_2(eq.) emission from an equivalent vessel powered with diesel fuel and biofuel are shown in Figure 25.

Figure 25 shows that the annual WTW CO_2(eq.) emissions from the Zero-V fueled with LH_2 from fossil NG would be 2.16 Gigagrams (Gg) of CO_2 (eq.) per year, produced entirely during the production and delivery of the LH_2 fuel. Recall that a "Gigagram" is $1x10^9$ grams. This is slightly worse than the equivalent vessel running on fossil diesel, with WTW CO_2(eq.) emissions of 1.91 Gg CO_2 (eq.)/year, despite the fact that the Zero-V is 22% more energy efficient than the equivalent diesel vessel. This increase is due to the facts that making hydrogen is energy intensive in the first place, the carbon in NG is released into the atmosphere as CO_2 during the hydrogen manufacturing process, and hydrogen liquefaction involves significant energy and associated emissions. These factors conspire to produce undesirable emissions for the Zero-V along the fuel production and delivery path when the hydrogen is produced by steam methane reforming of natural gas.

The situation is dramatically improved using renewable hydrogen. Taking the average value of the renewable production pathways discussed in Appendix D, Figure 25 shows the annual WTW CO_2(eq.) emissions from the Zero-V using renewable LH_2 becomes 0.164 Gg CO_2 (eq.)/year. This is 91.4% less than the WTW CO_2(eq.) emissions from the Diesel Vessel running on conventional diesel fuel.

Figure 25 shows that the real potential in hydrogen technology to reduce maritime CO_2(eq.) lies NOT in the use of hydrogen derived from fossil NG, but rather in using renewable hydrogen. The renewable hydrogen considered for Figure 25 is nearly 100% renewable. In our discussions with the gas suppliers Air Products and Linde, renewable LH_2 can be made available to the Zero-V today in the quantities required, and these companies are currently working to make renewable hydrogen more broadly available.

One could consider using biodiesel to power an "equivalent biodiesel vessel." Figure 25 shows that the well-to-waves CO_2(eq.) emissions are indeed reduced, from 1.91 Gg CO_2 (eq.)/year for diesel fuel to 1.20 Gg CO_2 (eq.)/year for biodiesel. This represents a 37% reduction in CO_2(eq.) emissions. The reduction is not as large as one might expect from a biofuel because making biodiesel is energy intensive.

Traditional biodiesel is the fatty acid methyl ester product that results from the transesterification of vegetable oil or animal fats with methanol. The oils themselves are not compatible with diesel engine operation due to their higher viscosities, thus requiring the transesterification processing. In the ~2010 timeframe, there emerged alternative methods of oil processing that produced fuels whose composition more closely resembled fossil diesel [2]. These products are called "renewable diesel" or "green diesel". In Europe, the product is called "hydrotreated vegetable oil" (HVO). A 2013 EU commission study [2] reports that the WTT CO_2(eq.) emissions (grams CO_2 (eq.)/MJ_{fuel}) for HVO and biodiesel are essentially the same [2]. This means that the WTW CO_2(eq.) emissions for the "equivalent vessel" operating on renewable diesel would be essentially the same as that depicted in Figure 25 for biodiesel.

Summarizing the CO_2(eq.) results of Figure 25, hydrogen PEM fuel cell technology can dramatically reduce the CO_2(eq.) emissions from a high-performance research vessel. However, nearly 100% renewable hydrogen must be used to achieve the desired deep cuts in CO_2(eq.) emissions that are commensurate with the challenge presented by increased levels of infra-red radiation trapping gases in the atmosphere.

Criteria pollutant emissions from the combustion of fossil fuels, among them nitrogen oxides (NO_x), hydrocarbons (HC) and particulate matter (PM) continues to be of concern due to their immediate adverse health effects. Since the PEM fuel cell does not involve combustion, it is incapable of producing criteria pollutants at the point of use. As a result, any criteria pollutant emissions associated with the Zero-V arise entirely from emissions associated with the production and transport of LH_2 to the vessel. Criteria pollutant emissions can arise from combustion used to create the process heat needed to heat the reactants of the SMR process or as a byproduct of the SMR process. Alternatively, combustion could be used to

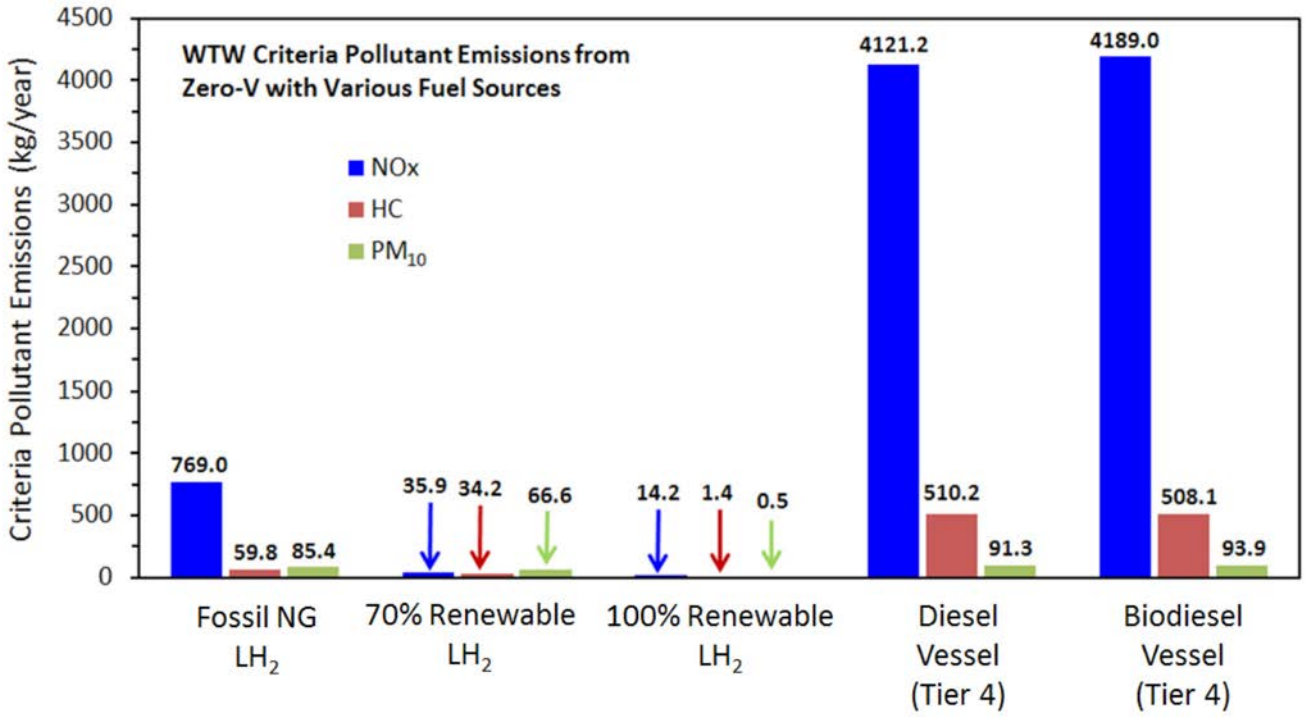

Figure 26: Predicted annual well-to-waves (WTW) criteria pollutant emissions for the Zero-V operating on various hydrogen fuels, and the equivalent diesel and biodiesel vessels constrained to Tier 4 emission limits. PM_{10} indicates emission of particles with diameter less than 10 microns.

generate the electricity used in hydrogen liquefaction.

Analogously, criteria pollutant emissions are associated with the production and delivery of diesel fuel. For example, the diesel-fueled tanker truck delivering diesel fuel is a source of diesel pathway criteria pollutant emissions. If the diesel fuel originates from petroleum ("fossil diesel"), then there is the additional criteria pollutant emissions associated with burning the fuel in the research vessel diesel engines. As a result, criteria pollutant emissions from an equivalent diesel-powered vessel using fossil diesel fuel involve two sources: (1) production and delivery of the diesel fuel and (2) combustion of the fuel onboard the vessel [2]. If the diesel fuel originates from biomass ("biodiesel"), there are still criteria pollutant emissions released on the vessel, even though biodiesel reduces CO_2(eq.) emissions because the carbon released on the vessel originated recently from CO_2 in the air, making biodiesel "carbon neutral" in this sense.

In comparing the Zero-V to an "equivalent" diesel or biodiesel vessel, we constrain both the diesel and biodiesel engine emissions to be at the Tier 4 criteria pollutant emission limits. In this way, we are comparing the Zero-V to a new vessel build (one based on either fossil diesel or biodiesel) which must meet the Tier 4 limits by regulation. While the hydrogen PEM fuel cell technology automatically satisfies the Tier 4 criteria emission requirements because it is zero-emission technology at the point of use, the WTW hydrogen analyses capture important fuel production pathway and delivery emissions.

The results for the annual WTW criteria pollutant emissions analyses are presented graphically in Figure 26. The first aspect of Figure 26 to notice is that the WTW criteria pollutant emissions for the "equivalent vessel" running on diesel fuel or biodiesel are very nearly the same. Although the "well-to-tank" (WTT) criteria pollutant emissions for the production and delivery of biodiesel are higher than those for fossil diesel, due to the increased process energy required, the WTT criteria pollutant emissions are only a small fraction of the overall WTW criteria pollutant emissions. This finding, combined with the onboard criteria pollutant emissions for the equivalent vessel running on fossil diesel or biodiesel set equal to each other at the Tier 4 limits, produces the similarity for these fuels seen in Figure 26.

There have been no published analyses of the WTT criteria pollutant emissions associated with the production and delivery of renewable diesel. However, as noted previously, a recent EU Commission study reports that the WTT energy required to make HVO (renewable diesel) and biodiesel are very nearly the same [2]. This suggests that the WTW criteria pollutant emissions from the equivalent vessel operating on renewable diesel would be similar to that reported in Figure

26 for the vessel operating on biodiesel. This finding is analogous to the similarity of renewable diesel and biodiesel in the WTW CO_2(eq.) emissions discussed previously in connection with Figure 25.

Figure 26 shows that the Zero-V operating on LH_2 derived from NG SMR reduces annual WTW NO_x by ~ 81.3% below that of the equivalent vessel operating on fossil diesel fuel (but held to Tier 4 emission standards). Using 70% Renewable LH_2 on the SF-BREEZE, the WTW NO_x is reduced 99.1% below the equivalent vessel fossil diesel levels. These reductions in NO_x can be traced to relatively less NO_x being produced when NG is burned for SMR process heat, and dramatically less NO_x associated with electrolysis of water using 70% renewable electricity.[2]. Annual WTW HC is reduced ~ 88.3% below that of the equivalent vessel operating on fossil diesel fuel (but held to Tier 4 emission standards) when the Zero-V is operated on LH_2 derived from NG SMR. Using 70% Renewable LH_2, the WTW HC is reduced 93.3% below the Tier 4 equivalent vessel fossil diesel levels.

Figure 26 shows that the WTW PM emissions (PM_{10}, particle diameters less than 10 microns) associated with the Zero-V using 70% Renewable LH_2 are only slightly smaller than the WTW PM emissions of the equivalent vessel running on fossil diesel. In the TIAX study [2], it was noted for this fuel pathway that there exists somewhat high PM emissions for natural gas combined cycle power plants which constitute 44.5% of the California grid mix.

Using 100% renewable electricity, the WTW criteria pollutant emissions for the Zero-V collapse to those for LH_2 trailer transport operating on diesel fuel. Thus, using 100% renewable electricity, the Zero-V WTW emissions would represent a 99.6% reduction in NO_x, a 99.7% reduction in HC and a 99.4% reduction in PM compared to the equivalent vessel running on diesel fuel with Tier 4 emission constraints. If the LH_2 trailer ran on 100% renewable hydrogen instead of diesel fuel, the criteria pollutant emissions could be essentially eliminated.

Summarizing these criteria pollutant emission results, the Zero-V goes far beyond the Tier 4 criteria pollutant emissions requirements for new vessel construction in the U.S. because the powerplant is zero emissions at the point of use. Hydrogen PEM fuel cell technology can dramatically reduce WTW NO_x and HC emissions below the most advanced Tier 4 criteria pollutant emissions requirements regardless of whether the hydrogen is made by NG reforming or using more renewable means. Overall, the results show that operating a hydrogen fuel cell research vessel on nearly 100% renewable hydrogen provides the dramatic reduction in vessel CO_2(eq.) and criteria pollutant emissions commensurate with the problems of increased levels of infra-red radiation trapping gases in the atmosphere and increasing maritime air pollution worldwide.

Table IX: Estimates of Zero-V construction costs using Low and High labor rates.

Construction at Low Labor Rate	
Construction cost at $60 per man-hour	$66,300,00
Builder's risk insurance (1%)	$663,000
Contingency (15%)	$9,300,000
Total	**$76,000,000**
Construction at High Labor Rate	
Construction cost at $75 per man-hour	$71,000,000
Builder's risk insurance (1%)	$713,000
Contingency (15%)	$10,000,000
Total	**$82,000,000**

Capital Costs and Operations and Maintenance Costs

The costs associated with constructing and operating/maintain the Zero-V were estimated. For the Zero-V capital costs, we leveraged as a basis the prior cost estimate data from the Regional Class Research Vessel (RCRV) that Glosten designed for Oregon State University. The RCRV provided a good basis for the Zero-V cost estimate because the size, outfitting, science mission equipment, and vessel capabilities are very similar and the RCRV project involved significant effort in development of cost estimates.

The cost estimates for major systems were developed in several ways including built up from major equipment quotations, parametric from materials and dimensions, scaling and adjustment of RCRV estimated costs, or best engineering judgment estimates. The cost estimate was developed considering the equipment and material costs as well as labor hours for construction or installation. While the material costs are considered constant, the labor rates for shipbuilding can vary significantly based on geographic location and economic climate in the shipbuilding industry. To capture this variation, the cost estimate was developed using both high ($75 per man-hour) and low ($60 per man-hour) labor rates to bracket the construction cost estimate. Included in the cost estimate was also a 15% shipyard markup on materials and subcontractors, the cost of builders risk insurance (1% of

contract value), and a contingency allowance (15% of contract value). A summary is given in Table IX.

Based on this analysis, the "Low Labor Rate" construction cost of the Zero-V is estimated to be $76 million dollars ($76M). The "High Labor Rate" construction cost is estimated to be $82M. The average of these construction estimates is $79M. A more detailed summary of the cost estimate is contained in Glosten's Report, Appendix B. A high-level examination of the Zero-V construction cost compared to other vessels revealed that although somewhat more expensive, The Zero-V construction costs are not unreasonable when compared to other modern research vessels of similar size and capabilities, but not possessing the environmental benefits of the Zero-V.

The operations and maintenance (O&M) costs were estimated as described in Appendix E. Summarizing that analysis, we based the analysis on the known 2014 O&M costs associated with the R/V New Horizon, which is similar in size with the Zero-V and has the same 12 member crew. We took the New Horizon budget, removed items that could easily be attributed to the use of diesel engines (such as diesel engine maintenance and overhaul costs, cost of diesel fuel) and added back costs associated with hydrogen use, including the cost of LH_2, maintenance of the fuel cell balance-of-plant and the cost of fuel cell refurbishment. All other vessel costs, such as ships payroll, non-diesel maintenance and repair, "other ship costs" (food, insurance, stores travel), distributed costs (such as employee benefits, shore support) and indirect costs were kept equal to the New Horizon cost numbers. In this way, a reality-based estimate for the Zero-V O&M costs could be made.

The O&M estimate assumes the Zero-V is at sea 152 days a year, the number of days it requires to satisfy the annual roster of Scripps science missions. Furthermore, we assume a fuel-cell lifetime of 12,500 hours, midway between the commercial estimates [17] of 10,000 – 15,000 hours from Hydrogenics. If all of the fuel cells were being used during the 3648 hours of operation in 152 days, then the entire complement of Zero-V fuel cells would need to be replaced every 3.43 years.

However, this is not the case. Glosten has calculated that the average total energy output of the Zero-V fuel cells over the 152 days in performing the Scripps science mission is only 623 kW. Thus, it turns out that on average only 34.6% of the 1.8 MW of installed fuel cell power is being used over the course of a year. Of course, some vessel operations require all the fuel cells to be used. Other operations require a lot fewer. But the average is 34.6%. This means that instead of all the fuel cells needing to be replaced in 3.43 years, they will all need to be replaced in 9.91 years. The ability to distribute the Zero-V power load in a way that extends the fuel cell lifetime dramatically reduces the O&M cost from what it might otherwise be.

We estimate the annual costs associated with the fuel cell balance-of-plant to be 2.5% of the fuel cell powerplant capital cost, as recommended by Hydrogenics. As for LH_2 fuel costs, we assume for non-renewable hydrogen produced from

Figure 27: (a) Linde LH_2 Refueling Trailer providing hydrogen to the Emeryville CA hydrogen station stationary LH_2 tank. (b) Linde personnel preparing hose connection; (c) Linde LH_2 Refueling Trailer. Pictured (L-R) are Kyle Mckeown and Nitan Natesan (Linde), Lennie Klebanoff (Sandia), and Tom Escher and Joe Burgard of the Red and White Fleet.

natural gas, a delivered LH_2 price of \$6.87/kgH_2 [1]. If we used renewable LH_2, we assume a quoted price of \$16.38/kg at today's prices [1].

Pulling these (and other) costs together as described in Appendix E, we find that the increase in total annual O&M cost for Zero-V is 7.7% higher than operating the New Horizon, at today's fuel prices for fossil-NG non-renewable LH_2. Using renewable LH_2, the total annual O&M costs for operating the Zero-V are 41.9% higher than operating the New Horizon. This larger increase is due to the current high cost of renewable LH_2.

The 7.7% O&M increase in running the Zero-V (compared to the New Horizon) is encouraging. We have heard feedback from both the Scripps science team and scientists at Moss Landing Marine Laboratory that a 5 - 10% increase in O&M costs could be tolerated for the benefits afforded by the Zero-V. These benefits include: zero-emission operation, no risk of fuel spills and quieter operation. Furthermore, in comparison to the New Horizon, the Zero-V offers, 33% increase in deck working area, 4.3% increase in lab space and a 11% increase in speed. However, the Zero-V also has a 75% reduction in range.

Bunkering and Ports of Call

The Zero-V will primarily operate along the coast of California, although it has the range to transit from San Francisco, CA to Honolulu, HI. The vessel holds two LH_2 tanks with hydrogen storage capacity 5840 kg each, for a total of 11,680 kg. Although the tanks can hold 11,600 kg, typically only 10,900 kg of the fuel is consumable, as discussed in Appendix B. Since road LH_2 trailers typically can deliver 4,000 kg each, three trailers will be required to refuel the Zero-V at maximum. We recognize that many refueling operations would require only two trailers, as most of the vessel's missions involve less than 8,000 kg of hydrogen fuel consumption.

The first bunkering feasibility question that the project answered was if this supply of LH_2 (both fossil NG based hydrogen and renewable hydrogen) could be supplied by the major hydrogen gas suppliers. A second feasibility question is if the Zero-V refueling operation could physically take place at the sites identified by Scripps as likely refueling sites. For example, is there sufficient space for two LH_2 trailers to be refueling the Zero-V at the same time at the anticipated ports of call? A third refueling question is if the refueling could take place within the desired time. Scripps indicated that the preferred refueling time was 8 hours or less, as this is the duration of a typical work shift.

A picture of a Linde LH_2 tanker refueling a stationary LH_2 tank at the Emeryville CA hydrogen station is shown in Figure 27.

In addition to LH_2 refueling, there are other activities on-

Figure 28: Location of the Nimitz Marine Facility (MarFac) at the Scripps Institution of Oceanography, San Diego CA. (a) General MarFac location; (b) general view of MarFac facility with the Zero-V docked and (c) close-up view of the Zero-V docked at MarFac with two LH_2 trailers and refueling stanchion shown in red. The refueling stanchion is notional only. The relative sizes of the Zero-V, LH_2 trailers and dock are properly rendered. Satellite images are courtesy of Google Maps.

board the Zero-V that must be accommodated by the refueling site. These activities include: bringing 18-wheel trucks onto the site to deliver science equipment, using forklifts to off-load equipment from the supply trucks, and loading new equipment onboard, using cranes to load/off-load science equipment, storing science equipment in anticipation of vessel arrival in an onsite warehouse (or other enclosed structure).

Needed facilities in support of this work includes power, sewage, water, internet, all of which must be provided at the refueling location. Another activity is adding/replacing crew and scientists for work on the vessel, which should be supported by proximity to hotels and restaurants.

With these issues in mind, we examined the feasibility of refueling the Zero-V by first speaking with representatives from the major gas suppliers Linde and Air Products. Then, we visited the likely ports of call, to brief them on the hydrogen fuel cell vessel technology, and to examine their facilities to see if there were any major problems with refueling the Zero-V there.

We start with the questions concerning LH_2 supply and refueling rates and overall refueling logistics and requirements. Two industrial gas suppliers were contacted with regard to the Zero-V refueling: Linde Gas and Air Products. The meeting with Kyle McKeown (Linde) took place on March 21, 2017 in their Pleasanton CA offices. The conversation with Dave Farese and Brian Bonner (both Air Products) took place on the telephone on March 23, 2017. A full account of these meetings is provided in Appendix F.

Both Linde and Air Products indicated that the best strategy for refueling the Zero-V would be using direct trailer refueling. In this scenario, LH_2 trailers pull onto the Pier area where the Zero-V is docked, the trailers hook up to a dock stationary fueling stanchion that decouples the trailer hoses from a moving vessel. Both gas suppliers indicated that complete refueling of the Zero-V could take place within a 9-hour timeframe, and both could provide access to renewable LH_2, although it would initially be expensive. Both fuel suppliers intimated that a large reliable single customer for renewable LH_2 such as the Zero-V would greatly encourage these companies to make renewable LH_2 more available nationwide.

Sandia (Klebanoff) then visited a number of marine facilities and ports to engage the local stakeholders and to determine their interest in the Zero-V project, make them aware of the nature of LH_2 refueling, and to assess the compatibility of the Zero-V with berthing at these sites. A full account of these site meetings is provided in Appendix F.

Nimitz Marine Facility (MarFac), San Diego, CA

The home port for the Zero-V would be the Nimitz Marine Facility (MarFac) of the Scripps Institution of Oceanography in San Diego CA. Figure 28(a) shows the general location of within the greater San Diego area. Figure 28(b) provides a general view of MarFac facility with the Zero-V docked while Figure 28(c) gives a close-up view of the Zero-V docked at MarFac along with two LH_2 trailers and refueling stanchion shown in red. The refueling stanchion recommended by the gas providers is notional only. The relative sizes of the Zero-V, LH_2 trailers and docks are properly rendered to allow an assessment of available space for the LH_2 refueling operation.

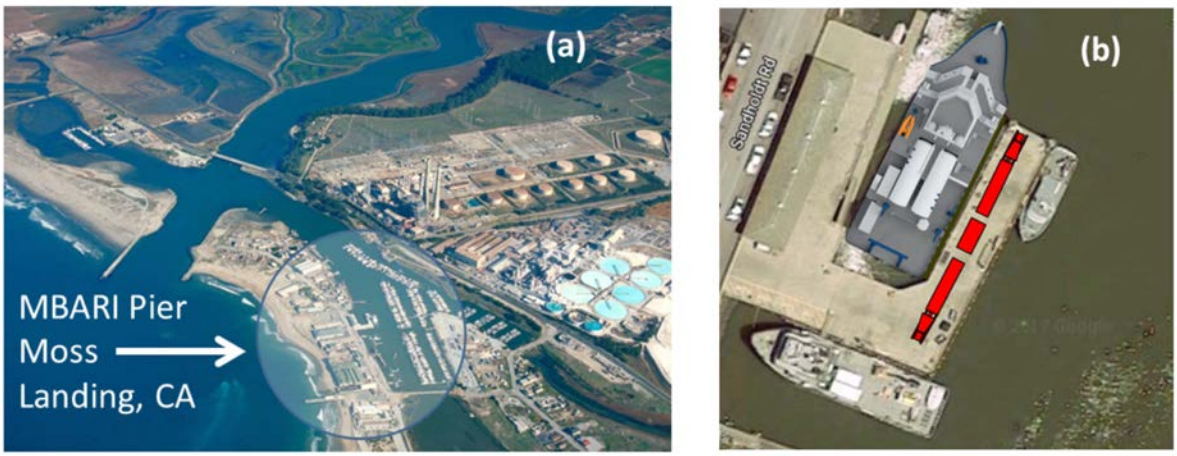

Figure 29: Location of the Monterey Bay Aquarium Research Institute (MBARI), within Moss Landing, 15 miles north of Monterey CA. (a) General MBARI location; (b) close-up view of the Zero-V docked at MBARI Pier along with two LH_2 trailers and refueling stanchion show in red. The refueling stanchion is notional only. The relative sizes of the Zero-V, LH_2 trailers and dock are properly rendered. Satellite images are courtesy of Google Maps.

Figure 30: Location of Pier 54, San Francisco CA. (a) General Pier 54 location relative to the City of San Francisco; (b) general view of Pier 54 with the Zero-V docked and (c) close-up view of the Zero-V docked at Pier 54 along with two LH_2 trailers and refueling stanchion show in red. The refueling stanchion is notional only. The relative sizes of the Zero-V, LH_2 trailers and dock are properly rendered. Satellite images are courtesy of Google Maps.

Figure 28 shows that there is ample room at MarFac to refuel the Zero-V. The water depth off the pier is 17-25 feet, more than enough to accommodate the 12 foot draught of the Zero-V. The facility already allows for refueling and restocking of research vessels, and there is ample room for all of the activities anticipated for the Zero-V, as suggested by Figure 28(c). Paul Mauricio, the Port Engineer at MarFac after hearing a full briefing on the Zero-V on September 28, 2017, concluded that all aspects of Zero-V refueling operations are readily accommodated at MarFac.

Moss Landing Marine Laboratories (MLML) and Monterey Bay Aquarium Research Institute (MBARI), Moss Landing, CA

The MLML is a graduate school in Marine Sciences of the California State University System (CSU) located within Moss Landing Harbor, approximately 15 miles north of Monterey California. The Monterey Bay Aquarium Research Institute (MBARI) is a private, non-profit research center, funded by The David and Lucile Packard Foundation also located in Moss Landing with pier facilities supporting research vessels. Since the Zero-V can perform science missions in support of MLML and MBARI oceanographic research and educational objectives, we anticipate the Zero-V will need to dock and refuel at the MBARI Pier indicated in Figure 29.

The Zero-V can successfully transit to and from the MBARI Pier. However, the MBARI Pier is much more physically constrained than the other refueling sites, both with regard to vessel navigation from the sea through Moss Landing Harbor, to docking at the MBARI Pier itself. In addition, there are buildings near the berth, which must be examined with regard to the fire and safety codes NFPA 55 and NFPA 2 pertaining to LH_2 refueling.

Pier 54, Port of San Francisco, San Francisco, CA

The Zero-V project was briefed to Rich Berman of the Port of San Francisco on April 7, 2017. The Port of San Francisco was very enthusiastic and supportive. In addition to being a way of bringing zero-emission maritime technology to San Francisco Bay, they also were attracted by the educational component. Bay Area universities working with Scripps are: U.C. Berkeley, Stanford, San Francisco State, San Jose State and U.C. Santa Cruz. Scripps is the oceanographic lead for all the U.C. schools. There is a current initiative to increase collaboration between the U.C. and Cal State Universities in the area of ocean science and the Port of San Francisco was excited to be host to such a zero-emissions hydrogen vessel that can support this research.

Figure 31: Location of Wharf 5, Port of Redwood City, Redwood City CA. (a) General Wharf 5 location relative to the San Francisco Bay; (b) close-up view of the Zero-V docked at Wharf 5 along with two LH_2 trailers and refueling stanchion show in red. The refueling stanchion is notional only. The relative sizes of the Zero-V, LH_2 trailers and dock are properly rendered. Satellite images are courtesy of Google Maps.

	Zero-V	Sally Ride	RCRV	New Horizon	Sharp	Sproul
Length, ft.	170	238	192	170	146	125
Beam, ft.	56	50	41	36	32	32
Size	•	+	≈	-	-	--
Range	•	++	++	++	+	+
Science Berths	•	+	≈	≈	-	-
Lab Space	•	≈	-	-	--	--
Deck Space	•	+	-	-	-	-
Over Side Handling	•	+	≈	≈	-	--
Station Keeping	•	≈	+	-	≈	-
Sonars	•	+	≈	×	-	×
Payload	•	++	≈	+	-	--
Year Built	NA	2014	NA	1978	2005	1981

++ much greater + greater -- much less - less ≈ equivalent × none

Figure 32: Qualitative comparison of the Zero-V features with five diesel-fueled research vessels. The diesel vessel properties are given in comparison to the Zero-V. Thus, ++ means much greater than the Zero-V, + means greater than the Zero-V, -- means much less than the Zero-V, - means less than the Zero-V, and ~ means approximately the same as the Zero-V. An x indicates the property is not present on the vessel in question.

The Port of San Francisco recommended using Pier 54, as shown in Figure 30. Figure 30 shows that there is sufficient space at Pier 54 to refuel the Zero-V. Pier 54 has direct vessel access from the San Francisco Bay. There are three aspects of Pier 54 that need to be considered. First, the south side is exposed to very rough swells during storms so the ideal location for the bunkering is on the north side, as indicated in Figure 30. Second, a structural assessment performed by the Port of San Francisco in 2013 revealed deterioration of some piles and other concrete support members on Pier 54. As a result, the pier was classified as Restricted Use and there is currently a 10-ton (gross) limit on vehicle traffic. This means that repairs are needed if the pier is to support the weight three LH_2 refueling trailers. Nonetheless, such repairs would be straightforward. Third, the current depth of the water on the north side of Pier 54 is estimated to be 10 - 12 feet, not enough for the Zero-V with a draught of 12 feet, so the area near the Pier would need to be dredged.

Wharf 5, Port of Redwood City, Redwood City, CA

The Port of Redwood City is in the South San Francisco Bay, and is another option for Zero-V refueling in the San Francisco Bay. It is an attractive destination because of its proximity to universities in the area (Stanford, San Jose State, U.C. Berkeley and U.C. Santa Cruz) with oceanographic research interests. In addition there are ample hotels and restaurants nearby to support Zero-V crew exchange. The Zero-V project was briefed to Mike Giari (Port Director) and Giorgio Garilli (Assistant Manager of Operations) on May 9, 2017.

The Port of Redwood City is a deep-water port. Mike Giari and Giorgio Garilli identified Wharf 5 as the best location for Zero-V refueling. Wharf 5 is shown in Figure 31.

Wharf 5 is a large open, structurally-sound pier. Wharf 5 is 60 feet wide, and access is excellent - an LH_2 trailer could come in one side and drive out the other. The depth of the water at Wharf 5 is adequate for the Zero-V, with minimum depth of 18 – 20 feet at the Wharf and 30 feet within the channel connecting the dock to the San Francisco Bay.

Wharf 5 is currently set up for shore-power of 480V/60A as this is what prior vessels used. Zoltan Kelety of Scripps stated that 480V/400A is more typical for research vessels like the Zero-V. Thus, we anticipate an upgrade to the Wharf 5 electrical facilities would be needed for the Zero-V to berth there. The weight limit for Wharf 5 is 500 lbs/ft^2. This is more than sufficient as the LH_2 trailers have a weight footprint of ~ 150 lbs/ft^2.

Zero-V Comparison with Other Research Vessels

We found it helpful in considering the capabilities of the Zero-V to understand the context of the vessel in comparison to other research vessels that have been deployed in the recent past. Figure 32 provides a high-level (qualitative) comparison of five diesel-fueled research vessels using the Zero-V proper-

ties as a comparative norm. In Figure 32, the Zero-V is compared to the R/V *Sally Ride*, the RCRV vessel recently designed by Glosten, the R/V New Horizon, which was just decommissioned in 2015, the R/V *Hugh R. Sharp*, and to the R/V *Robert Gordon Sproul* which is nearing its retirement. The properties of these other vessels are given in comparison to the Zero-V. All of the diesel-fueled vessels have a superior range, which is a consequence of diesel fuel having ~ 4 times the volumetric energy density as LH_2. Apart from the range limitations of the Zero-V, in other aspects, the Zero-V is quite competitive with these other vessels, particularly with regard to the scientific capabilities and the number of scientists it can hold. One design criterion of the Zero-V was to make a vessel that the scientists and crew would be comfortable in, and enjoy being on. The feedback we received from the Scripps science team is that the Zero-V has succeeded in these regards.

Regulatory Review

As part of this study, we wanted to establish a regulatory feasibility of the concept developed. A challenge for regulatory review of the Zero-V design is that there are currently no specific and comprehensive rules governing hydrogen installations on ships. Indeed, one objective of this project was to promote hydrogen "technology transfer" to the maritime industry, and regulatory and classification societies in order to provide information they need for a science-based development of maritime H_2 regulations. Such rules are currently the subject of development by the International Maritime Organization (IMO) and ship classification societies. The DNV GL rules for gas fueled vessels [18] and the IMO IGF code [19] govern gas fueled vessels, but are primarily specific to natural gas applications. The DNV GL rules do have some regulations pertaining to hydrogen in Part 6 Chapter 2 Section 3, of Reference 18.

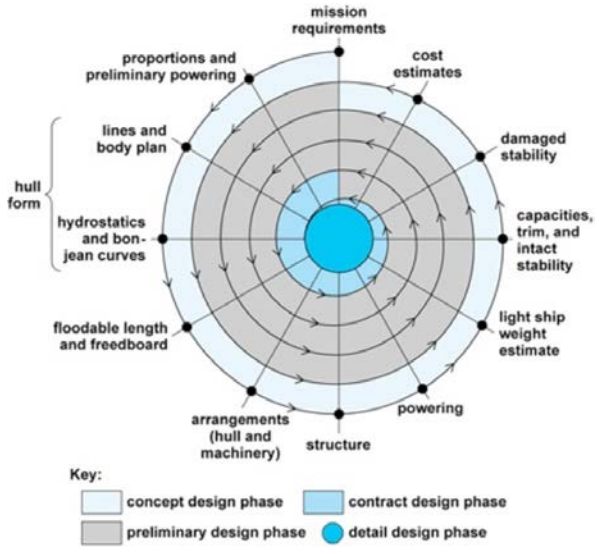

Figure 33: Design Spiral for Vessels, reproduced from Reference 20.

However, these rules are by no means comprehensive. 46 CFR are the federal regulations pertaining to design and operation of US flagged vessels which and are enforced by the United States Coast Guard (USCG). These federal regulations have no specific requirements for hydrogen fuel applications. Due to the lack of a comprehensive rule set, DNV GL and USCG have both indicated that the design would need to be developed as an alternative design approach whereby the equivalency of the vessel safety, reliability and dependability to that of a conventional oil-fueled vessel would need to be demonstrated. This approach requires a significant and time-consuming level of analysis that is well beyond the scope of this feasibility study.

In order to provide some basis for the design of the vessel, it was decided that the design would be developed for compliance with the DNV GL Rules for Classification: Ships with specific attention to Part 6 Chapter 2 Section 3, Fuel Cell Installations and Part 6 Chapter 2 Section 5, Gas Fueled Ship Installations as well as the IMO IGF Code Part A-1. While these rules are primarily for natural gas installation, they are considered to provide a reasonable baseline level of requirements for hydrogen fuel as well because the properties of hydrogen and natural gas are similar. There is the expectation that there will be additional requirements for hydrogen that will evolve as the rules are developed or as requirements become evident from rigorous risk analysis of a hydrogen fuel design. In addition to these rules, the general requirements of the vessel were developed from 46 CFR Subchapter U (USCG rules for oceanographic research vessels).

With the understanding of the aforementioned limitations of the available rules, the basic Zero-V design was submitted independently to both the US Coast Guard and DNV GL for review. The goal of these regulatory reviews was to identify any regulatory or safety areas of concern given consideration of the fundamental design, the physical and combustion properties of hydrogen, and the current state-of-the-art in PEM fuel cell technology. The following documents were provided.

- General Arrangement
- Preliminary Hazardous Zone Plan
- Electrical One-Line Diagram
- Concept Gas System Architecture
- Draft Design Study Report (including fire safety systems)

As a project partner, DNV GL also was involved in discussions with Sandia, which focused on the physical and combustion properties of LH_2 and gaseous hydrogen, ventilation strategies for the fuel-cell spaces and for refueling operations, and other technical topics.

Both USCG and DNV GL provided review comments that are included in Appendix G. In general, the response from both reviewers was that while additional development would be necessary to gain approval as an alternative design, there were no identified fundamental or "show-stopping" concerns that would prevent eventual deployment of the Zero-V. Furthermore, DNV GL provided a conditional approval in principle (CAIP) for the Zero-V design, which is also provided in Appendix G.

Future Technical Work Required Before Full Class and USCG Approval and Vessel Construction

The vessel design process is often described as a design spiral, as depicted in Figure 33, reproduced from Reference [20]. The project starts at the outside of the spiral and works around through the vessel requirements, design and performance. Each trip around the spiral takes the outcomes of the prior and refines them. In such a manner the project works inward through the spiral in ever increasing detail and rigor until the final design is achieved.

The Zero-V project, to provide a very fundamental design basis as an evaluation of the feasibility of a hydrogen fuel cell research vessel, represents the first trip around the design spiral. From this feasibility design, there is significant amount of additional work that is required to flesh out and refine the design especially in the areas peculiar to the gas system and the trimaran design in order for the vessel to achieve an unconditional (full) AIP and to receive full approval by the USCG.

A key step to moving the project forward is to conduct a risk assessment of the gas systems. Because the vessel must be developed and reviewed under the regulatory framework of an alternative design, both the USCG and classification societies will require a comprehensive and detailed risk assessment of gas systems and related fire and safety systems to demonstrate an equivalent level of operability and safety to a conventional oil fueled vessel. The first step of this is a comprehensive design of the systems. Following this, a hazard-identification (HAZID) workshop involving major project and regulatory stakeholders would need to be held to identify potential risks and hazards. This would likely result in many specific areas requiring further analysis to further asses the level of risk. It is anticipated that at a minimum the following analyses would be required:

Failure modes and effects analysis (FMEA) of the gas system, fuel cells, propulsion electrical/control systems, gas detection systems, fire detection systems, ventilation systems, fire suppression systems, and emergency shutdown systems.

Gas dispersion modeling of gas releases from the vent mast and leaks in enclosed spaces (i.e. fuel cell rack, Fuel Cell Room, tank connection space), and in the weather, including:

- Explosion analysis of the Fuel Cell Room.
- Probabilistic damage assessment of gas system.
- Fire risk assessment especially in way of the storage tanks.

A refined assessment of the ability of the Zero-V to meet the Scripps mission requirements would be needed, particularly to understand the vessel speed and range. Computational Fluid Dynamics (CFD) analysis of resistance is important along these lines because of the limited availability of parametric resistance estimation methods for trimarans, especially in low Froude number operating regimes. A comprehensive CFD study would provide improved confidence in resistance predictions as well as a more comprehensive understanding of the impact of hull form features, such as hull spacing, on the vessel resistance. In addition, to better define the seakeeping performance of the vessel, a computation seakeeping analysis would be required. In this analysis, a geometric model of the vessel will be analyzed in a seakeeping analysis software package to establish the expected vessel motions in a variety of sea states and to compare these motions to operation criteria.

Additionally, CFD could be used to optimize the hull form.

Figure 34: Robin Madsen (Glosten) presents results of the Zero-V study to facility at The Scripps Institution of Oceanography.

Figure 35: Attendees at the Final Project Report Out of the Zero-V Project to the U.S. DOT Maritime Administration on November 28, 2017. (L-R): Gerd-Michael Wursig (DNV GL), Tim Meyers (USCG), Tom Escher (Red and White Fleet), Thane Gilman (USCG), Robin Madsen (Glosten), Lennie Klebanoff (Sandia), Bruce Appelgate (Scripps), Zoltan Kelety (Scripps), Joe Pratt (Sandia), John Miller (USCG), Hans-Christian Koch-Wintervoll (DNV GL), James Carter (USCG), Anthony Teo (DNV GL) and Tom Thompson (MARAD).

Because the fuel storage capacity is a large driver in the vessel design, minimizing resistance of the vessel is particularly critical for the Zero-V. In several Glosten vessel design projects, including research vessels, hull form optimization studies have been conducted using CFD. In these studies, the geometry of a parent hull form is manipulated within imposed constraints to seek a reduction in resistance. In past projects hull form optimization has resulted in resistance reductions of as much as 15%.

A structural design is required to take the design to the next phase of development. Because the hull structure is a significant driver of both the vessel weight and construction cost, developing a comprehensive hull structural arrangement would greatly improve accuracy of both the weight and cost estimates.

This feasibility study only examined vessel systems that are directly affected by or unique to the use of hydrogen fuel and fuel cells. Additionally, these systems were only examined at a high level to assess feasibility, not to develop the full system details that would be required for vessel construction. To take the vessel design forward, all vessel systems would require a preliminary level of design to develop the system requirements and sizing. Additionally, optimization of the energy efficiency to minimize the ship service electrical loads of the vessel will be very important for the Zero-V. Through a rigorous focus on reducing electrical energy use, it may be possible to realize significant improvement in range or reduction in required fuel storage tank size.

Zero-V Feedback Meeting at the Scripps Institution of Oceanography, San Diego, CA.

On September 28, 2017 two meetings were held at the Scripps Institution of Oceanography to present the Zero-V project results to the Scripps science community (in the morning) and to the Scripps research vessel operations staff (in the afternoon). Each meeting began with a summary presentation of the feasibility results, followed by a question

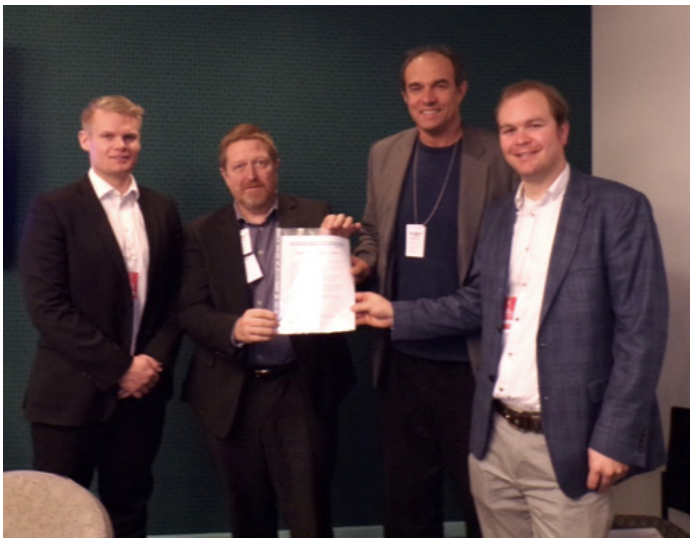

Figure 36: (L-R), Hans-Christian Koch Wintervoll and Gerd-Michael Wursig present the DNV GL Conditional Approval in Principal to Lennie Klebanoff and Robin Madsen.

Figure 37: Tim Meyers (L) of the USCG presents results from the USCG review of the Zero-V. Tim is being assisted by David Palacios of MARAD (R).

and answer session, and lasted approximately 2 hours each.

For the morning meeting, beginning at 9:00am, there were 18 in attendance, including representatives of the Scripps science staff, Lt. William Hawn from the U.S. Coast Guard as well as a representative from Clean Cities organization of San Diego. Sujit Ghosh from MARAD attended by telephone. These questions followed a Zero-V summary presentation given by Bruce Appelgate, Lennie Klebanoff, Robin Madsen and Sean Caughlan, as shown in the Figure 34.

At 3:00 pm in the afternoon, a presentation was given to the Scripps operations staff. There were 16 in attendance, including Scripps operations staff, Mike Prince from Moss Landing Marine Laboratories, Ryan Sookhoo from Hydrogenics, Joe Pratt from Sandia and a representative from Clean Cities San Diego. Appendix H gives a full account of these meetings and the questions and answers that were discussed.

Figure 38: Michael Carter (center) of MARAD describes the current state of MARAD funded programs and directions of further interest.

Zero-V Final Project Reporting to the U.S. Department of Transportation Maritime Administration (MARAD), Washington D.C.

The findings of the Zero-V project were reported on November 28, 2017 at the Washington D.C. headquarters of the U.S. Department of Transportation, Maritime Administration (MARAD). Attendees included representatives from Sandia National Laboratories, Glosten, the Scripps Institution of Oceanography, DNV GL, the U.S. Coast Guard, the Red and White Fleet, and MARAD. A picture of the attendees is shown in Figure 35.

After introductions, Bruce Appelgate described the roles that research vessels play in ocean science, Scripp's need for a new research vessel, the desire for zero emissions, and a description of the science missions that the Zero-V would be required to execute. The Scripps presentation was followed by Lennie Klebanoff (Sandia) presenting the origin of the Zero-V project and summarizing briefly the physical and combustion properties of hydrogen and PEM fuel cell technology. With this introductory material established, Robin Madsen from Glosten gave an in-depth report out on the design, performance, noise level, well-to-waves CO_2(eq.) and criteria pollutant emissions, capital and O&M costs for the hydrogen fuel-cell Zero-V research vessel.

Following a break, Lennie Klebanoff summarized the two technical feedback meetings that were held at Scripps on September 17, 2017 in La Jolla California. The morning meeting engaged the Scripps science community (morning meeting) for feedback, wheras the Scripps operations staff was engaged in the afternoon.

The meeting then turned to the regulatory review and approval for the Zero-V. Hans-Christian Koch-Wintervoll presented the process that DNV GL used to examine the Zero-V, a process that led to their issuing a conditional approval in principle (CAIP) for the vessel. Hans-Christian, Gerd-Michael Wursig and Anthony Teo (all DNV GL) presented a copy of the CAIP Letter to Lennie Klebanoff and Robin Madsen, in recognition of attaining that project milestone, as shown in Figure 36.

The DNV GL presentation was followed by an analogous presentation by Tim Meyers of the USCG (Figure 37), describing the USCG review of the Zero-V.

Importantly, after reviewing detailed schematics, renderings and supporting material, neither the USCG nor DNV GL found

any “show-stopping” problems with the use of hydrogen fuel cell technology onboard a research vessel, as represented by the Zero-V. Both DNV GL and Coast Guard also concluded that a more detailed vessel design (suitable as a basis for construction) would be required for the next step in the approval process, called an unconditional Approval in Principal from DNV GL, or a Design Basis Letter from U.S. Coast Guard.

After lunch, there was a discussion led by Scripps on what the “next steps” were for the Zero-V, with the goal of taking the vessel from a feasibility study to a real vessel on the water. Finally, Michael Carter from MARAD provided an update of the budget situation at MARAD, and future technical areas of interest as shown in Figure 38.

VI. References

1. J.W. Pratt and L.E. Klebanoff, "*Feasibility of the SF-BREEZE: A Zero-emission, Hydrogen Fuel Cell, High-speed Passenger Ferry,*" Sandia Report SAND2016-9719, September 2016.

2. L.E. Klebanoff , J.W. Pratt, C.M. Leffers, K.T. Sonerholm, T. Escher, J. Burgard, and S. Ghosh, "*Comparison of the Greenhouse Gas and Criteria Pollutant Emissions from the SF-BREEZE High-Speed Fuel-Cell Ferry with a Diesel Ferry*," Transportation Research D **54**, 250-268 (2017).

3. J. J. Corbett and A. Farrell, "*Mitigating Air Pollution Impacts of Passenger Ferries,*" Transportation Research Part D **7**, 197 (2002).

4. J.O. Keller, L.E. Klebanoff, S. Schoenung, and M. Gillie, "*The Need for Hydrogen-based Energy Technologies in the 21st Century,*" Chapter 1 in "*Hydrogen Storage Technology, Materials and Applications*" Ed. L.E. Klebanoff, (Taylor and Francis, Boca Raton, 2012), p. 3.

5. IPCC (Intergovernmental Panel on Climate Change Report: Climate Change 2007: The Physical Science Basis. Contribution of Working Group I to the Fourth Assessment Report of the IPCC, S. Solomon, D. Qin, M. Manning, Z. Chen, M. Marquis, K. B. Averyt, M. Tignor, and H. L. Miller, eds. Cambridge, U.K.: Cambridge University Press, 996 pp.

6. America's Climate Choices, Panel on Advancing the Science of Climate Change, National Research Council, ISBN: 0-309-14589-9 (2010).

7. L.E. Klebanoff, J.O. Keller, M.H. Fronk and P. Scott, "*Hydrogen Conversion Technologies and Automotive Applications,*" Chapter 2 in "*Hydrogen Storage Technology, Materials and Applications*," Ed. L.E. Klebanoff, (Taylor and Francis, Boca Raton, 2012) p. 31.

8. A map of DNV GL offices in the United States can be found at: https://www.dnvgl.com/contact/find-our-offices.html)

9. A notice for the national ocean policy implementation plan can be found at: https://www.federalregister.gov/documents/2012/03/14/2012-6215/national-ocean-council-national-ocean-policy-draft-implementation-plan

10. J.A. Koslow, "*The Role of Acoustics in Ecosystem-based Fishery Management,*" ICES Journal of Marine Science **66**, 966-973 (2009).

11. R. Diaz and R. Rosenberg, Rutger, " *Marine Benthic Hypoxia: A Review of its Ecological Effects and the Behavioural Response of Benthic Macrofauna,*" Oceanography and Marine Biology: An annual Review **33** 245-303 (1995).

12. N.N. Rabalais, R.E. Turner, and W.J. Wiseman Jr., "*Gulf of Mexico Hypoxia*, A.K.A. "The Dead Zone", Annual Review of Ecology and Systematics **33** 235-263 (2002).

13. L.A. Levin and M. Sibuet, "*Understanding Continental Margin Biodiversity: A New Imperative,*" Annual Review of Marine Science **4** 79-112 (2012).

14. "*Hydrogen Storage Technology, Materials and Applications,*" Editor-in-Chief L.E. Klebanoff, (Taylor and Francis, Boca Raton) published December 12, 2012.

15. L.E. Klebanoff, J.W. Pratt and C.B. LaFleur, "*Comparison of the Safety Related Physical and Combustion Properties of Liquid Hydrogen and Liquid Natural Gas in the Context of the SF-Breeze High-Speed Fuel-Cell Ferry,*" Int. J. Hydrogen Energy **42**, 757-774 (2017).

16. J. Larminie and A. Dicks, in "*Fuel Cell Systems Explained,*" (John Wiley & Sons Ltd., New York, 2000).

17. Private communication from Ryan Sookhoo to Lennie Klebanoff, November 27, 2017.

18. Rules for Classification: Ships, Part 6 Chapter 2, Propulsion, power generations, and auxiliary systems, DNV GL, January 2017

19. International Code of Safety for Ships Using Gases or Other Low-Flashpoint Fuels (IGF Code) as Amended by Resolution MSC.391 (95), International Maritime Organization (IMO)

20. J. H. Evans, "*Basic Design Concepts," Journal of the American Society for Naval Engineers,*" **71** 671-678 (1959).

VII. Appendices

Appendix A: IJHE Article on the Safety of Combustion Properties of LH_2 Compared to LNG

Appendix B: 17003.01 Glosten | Sandia Zero-V Design Study Report

Appendix C: Emissions of Radiation Trapping Gases and Criteria Pollutants

Appendix D: TRD Article on CO_2(eq.) and Criteria Pollutant Emissions from the SF-BREEZE

Appendix E: Operations Cost Estimates for the Zero-V

Appendix F: Feasibility of Refueling the Zero-V at Identified Sites

Appendix G: DNV GL Statement of Conditional Approval in Principal and USCG Feedback

Appendix H: Zero-V Project Report-Out Meetings at the Scripps Institution of Oceanography, San Diego CA

Appendix: A

IJHE Article on the Safety and Combustion Properties of LH_2 Compared to LNG

Presented here is a paper published in the International Journal of Hydrogen Energy (IJHE) that compares and contrasts the physical and combustion properties of LH_2 in comparison to LNG. The article is referenced: "Comparison of the Safety-related Physical and Combustion Properties of Liquid Hydrogen and Liquid Natural Gas in the Context of the SF-BREEZE High-Speed Fuel-Cell Ferry," L.E. Klebanoff, J.W. Pratt and C.B. LaFleur, International Journal of Hydrogen Energy **42**, 757 (2017).

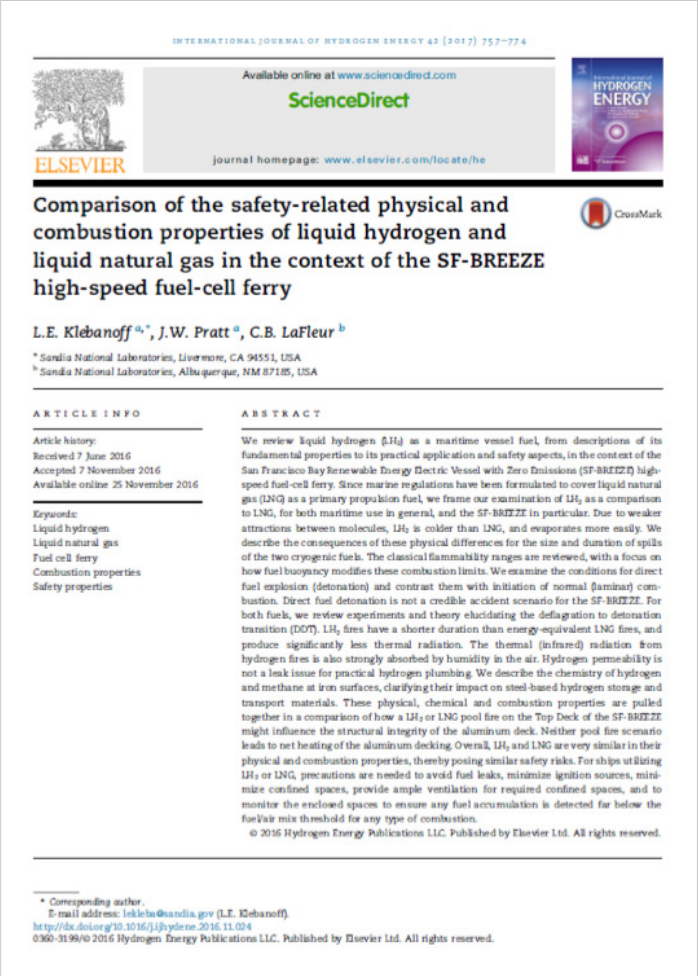

INTERNATIONAL JOURNAL OF HYDROGEN ENERGY 42 (2017) 757–774

Available online at www.sciencedirect.com

ScienceDirect

journal homepage: www.elsevier.com/locate/he

Comparison of the safety-related physical and combustion properties of liquid hydrogen and liquid natural gas in the context of the SF-BREEZE high-speed fuel-cell ferry

L.E. Klebanoff [a,*], J.W. Pratt [a], C.B. LaFleur [b]

[a] Sandia National Laboratories, Livermore, CA 94551, USA
[b] Sandia National Laboratories, Albuquerque, NM 87185, USA

ARTICLE INFO

Article history:
Received 7 June 2016
Accepted 7 November 2016
Available online 25 November 2016

Keywords:
Liquid hydrogen
Liquid natural gas
Fuel cell ferry
Combustion properties
Safety properties

ABSTRACT

We review liquid hydrogen (LH_2) as a maritime vessel fuel, from descriptions of its fundamental properties to its practical application and safety aspects, in the context of the San Francisco Bay Renewable Energy Electric Vessel with Zero Emissions (SF-BREEZE) high-speed fuel-cell ferry. Since marine regulations have been formulated to cover liquid natural gas (LNG) as a primary propulsion fuel, we frame our examination of LH_2 as a comparison to LNG, for both maritime use in general, and the SF-BREEZE in particular. Due to weaker attractions between molecules, LH_2 is colder than LNG, and evaporates more easily. We describe the consequences of these physical differences for the size and duration of spills of the two cryogenic fuels. The classical flammability ranges are reviewed, with a focus on how fuel buoyancy modifies these combustion limits. We examine the conditions for direct fuel explosion (detonation) and contrast them with initiation of normal (laminar) combustion. Direct fuel detonation is not a credible accident scenario for the SF-BREEZE. For both fuels, we review experiments and theory elucidating the deflagration to detonation transition (DDT). LH_2 fires have a shorter duration than energy-equivalent LNG fires, and produce significantly less thermal radiation. The thermal (infrared) radiation from hydrogen fires is also strongly absorbed by humidity in the air. Hydrogen permeability is not a leak issue for practical hydrogen plumbing. We describe the chemistry of hydrogen and methane at iron surfaces, clarifying their impact on steel-based hydrogen storage and transport materials. These physical, chemical and combustion properties are pulled together in a comparison of how a LH_2 or LNG pool fire on the Top Deck of the SF-BREEZE might influence the structural integrity of the aluminum deck. Neither pool fire scenario leads to net heating of the aluminum decking. Overall, LH_2 and LNG are very similar in their physical and combustion properties, thereby posing similar safety risks. For ships utilizing LH_2 or LNG, precautions are needed to avoid fuel leaks, minimize ignition sources, minimize confined spaces, provide ample ventilation for required confined spaces, and to monitor the enclosed spaces to ensure any fuel accumulation is detected far below the fuel/air mix threshold for any type of combustion.

© 2016 Hydrogen Energy Publications LLC. Published by Elsevier Ltd. All rights reserved.

* Corresponding author.
E-mail address: lekleba@sandia.gov (L.E. Klebanoff).
http://dx.doi.org/10.1016/j.ijhydene.2016.11.024
0360-3199/© 2016 Hydrogen Energy Publications LLC. Published by Elsevier Ltd. All rights reserved.

Comparison of the Safety-related Physical and Combustion Properties of Liquid Hydrogen and Liquid Natural Gas in the Context of the SF-BREEZE High-Speed Fuel-Cell Ferry

L.E. Klebanoff,[1],* J.W. Pratt[1] and C.B. LaFleur[2]

[1]Sandia National Laboratories, Livermore CA 94551

[2]Sandia National Laboratories, Albuquerque, NM 87185

*Author to whom correspondence should be addressed

Abstract

We review liquid hydrogen (LH_2) as a maritime vessel fuel, from descriptions of its fundamental properties to its practical application and safety aspects, in the context of the San Francisco Bay Renewable Energy Electric Vessel with Zero Emissions (SF-BREEZE) high-speed ferry. Since marine regulations have been formulated to cover liquid natural gas (LNG) as a primary propulsion fuel, we frame our examination of LH_2 as a comparison to LNG, for both maritime use in general, and the SF-BREEZE in particular. Due to weaker attractions between molecules, LH_2 is colder than LNG, and evaporates more easily. We describe the consequences of these physical differences for the size and duration of spills of the two cryogenic fuels. The classical flammability ranges are reviewed, with a focus on how fuel buoyancy modifies these combustion limits. We examine the conditions for direct fuel explosion (detonation) and contrast them with initiation of normal (laminar) combustion. Direct fuel detonation is not a credible accident scenario for the SF-BREEZE. For both fuels, we review experiments and theory elucidating the deflagration to detonation transition (DDT). LH_2 fires have a shorter duration than energy-equivalent LNG fires, and produce significantly less thermal radiation. The thermal (infrared) radiation from hydrogen fires is also strongly absorbed by humidity in the air. Hydrogen permeability is not a leak issue for practical hydrogen plumbing. We describe the chemistry of hydrogen and methane at iron surfaces, clarifying their impact on steel-based hydrogen storage and transport materials. These physical, chemical and combustion properties are pulled together in a comparison of how a LH_2 or LNG pool fire on the Top Deck of the SF-BREEZE might influence the struc-

tural integrity of the aluminum deck. Neither pool fire scenario leads to net heating of the aluminum decking. Overall, LH_2 and LNG are very similar in their physical and combustion properties, thereby posing similar safety risks. For ships utilizing LH_2 or LNG, precautions are needed to avoid fuel leaks, minimize ignition sources, minimize confined spaces, provide ample ventilation for required confined spaces, and to monitor the enclosed spaces to ensure any fuel accumulation is detected far below the fuel/air mix threshold for any type of combustion.

Introduction

Keller et al. [1] have provided a compelling argument that if we are going to solve our fuel resource insecurity, political energy insecurity and environmental sustainability problems that accompany our current fossil-fuel-based energy infrastructure, we as a civilization are going to need to turn to hydrogen. For significant environmental benefits, particularly reduction of greenhouse gas (GHG) emissions, the hydrogen will need to be produced by renewable methods with minimal (close to zero) pathway GHG emissions. One can define a zero-carbon energy solution as an energy system in which there is no net release of CO_2 or other GHGs into the atmosphere, either at the point of technical use, or along the path used to produce the fuel. Unless we have a new transportation technology with emissions reductions approaching 80% or more, the emission reductions will not be robust against growth in either population, or growth in the intensity with which technology uses energy [1]. While use of fossil-based hydrogen allows the introduction of the hydrogen-based power conversion technology [2], ultimately, renewable hydrogen is required. The time-scales for technological change and the ~ 50-year horizon associated with our limited fossil fuel resources indicate that we have to start the conversion to a renewable hydrogen technology now, and we need to be going much faster than we are [1].

As reviewed by Klebanoff et al. [2], high efficiency hydrogen energy conversion devices that convert hydrogen into electrical or shaft power are powerful drivers for hydrogen technology. These conversion devices include hydrogen internal combustion engines (ICEs), both spark ignition and turbine hydrogen engines, along with hydrogen fuel cells [2]. Proton Exchange Membrane (PEM) fuel cells in particular are already finding use in the first fuel cell vehicles, portable power, backup power, material handling equipment and fuel cell mobile lighting [2]. The use of hydrogen fuel cell technology for maritime applications is currently being considered.

The San Francisco Bay Area Renewable Energy Electric Vessel with Zero Emissions (SF-BREEZE) is a conceptual high-speed hydrogen fuel cell ferry designed for commercial use in the San Francisco Bay. The SF-BREEZE combines renewable liquid hydrogen (LH_2), PEM fuel cell technology, and a catamaran hull design to provide high-speed ferry service for 150 passengers at 35-knot top speed. The feasibility of such a vessel has been proven in a project funded by the Maritime Administration (MARAD) within the U.S. Department of Transportation. The technical and economic feasibility of the vessel, its initial design, as well as the extent to which new maritime regulations will be required to permit safe use of hydrogen fuel cell technology in the ferry application are reported elsewhere [3].

During the project, we analyzed the use of LH_2 onboard the SF-BREEZE with a focus on safety. Another cryogenic fuel, liquid natural gas (LNG), has found increased use as a primary propulsion fuel for maritime vessels. Since maritime regulations have been formulated to cover LNG use as a primary propulsion fuel, it was natural that our examination of the safe use of LH_2 as a primary fuel for ferries be couched as a comparison to LNG, for both the maritime environment generally, and specifically for the SF-BREEZE. This comparison required pulling information from many sources in order to form a complete picture of the differences between LH_2 and LNG as practical maritime fuels. Here we review both the physical and chemical nature of these fuels that impact safety, as well as the very different character of the fires derived from burning LH_2 and LNG. We supplement this existing information with new analyses that shed additional light on the uses of LH_2 and LNG in marine applications.

It is timely to compare and contrast the physical and combustion properties of LH_2 and LNG. In 1978, Hord provided [4] an excellent and comprehensive comparison of the safety properties of hydrogen and methane (the primary constituent of NG), with both fuels being compared to gasoline. In 1981, Donakowski [5] assessed LH_2 and LNG physical and combustion properties with regard to safety. Also in the early 1980's NASA sponsored separate work by Lockheed and the Arthur D. Little Company to investigate hydrogen-fueled commercial aircraft. Both studies involved technical and safety comparisons between LH_2, LNG and conventional jet fuel (Jet-A) in their use as primary aviation fuels. Brewer has published the results of the Lockheed work in both journal [6] and book [7] form. The results of the A.D. Little study were summarized in several NASA reports in 1960, 1964 and 1982 [8 - 10]. The comparative properties of LH_2 and liquid methane (LCH_4, often considered a conceptual substitute for LNG) for aviation were later reviewed by Contreras and co-workers in 1997 [11], who also reviewed some subsequent designs for LH_2 aircraft conceived by the Airbus consortium and Boeing. In many ways, hydrogen use in aircraft is similar to its use in high-speed ferries, as both aircraft and high-speed watercraft are very weight-sensitive applications, favoring storing hydrogen on-board as a liquid. Safety comparisons between

compressed natural gas and compressed hydrogen as automotive fuels were reported by Karim in 1983 [12].

Since these prior comparisons, there has been significant progress in elucidating the combustion properties of hydrogen, particularly with regard to the effects of buoyancy and turbulent mixing on combustion and the "deflagration to detonation transition" (DDT). Advanced modeling studies have also clarified how cryogenic fuels spread and vaporize when spilled on the ground or other surfaces. In addition, there have been a couple of decades of further experience handling LH_2 and LNG, and development of associated codes and standards. Here we provide an updated review with these new developments, with a focus appropriate for the comparison of LH_2 and LNG in maritime applications generally, and for the specific case of the SF-BREEZE.

Design of the SF-BREEZE as a Model of Hydrogen Use in Maritime Applications

Figure 1 displays engineering models of the SF-BREEZE [3]: The Top Deck holds a cylindrical 1200 kg capacity LH_2 tank, with enough hydrogen for 4 hours of continuous operation. A desire to refuel only a couple of times per day drives the 1200 kg capacity specification. The high-speed (35 knots) requirements of the design requires the lightest method of storing 1200 kg of hydrogen, namely LH_2 storage in a DOT-approved double walled cryogenic tank. The fuel cell racks are located on the Main Deck, adjacent to the passenger compartment. The fuel cells are of the PEM variety, selected for their fast turn on, minimal weight, commercial availability, established track record and ability to run on pure hydrogen. LH_2 is typically 99.9995% pure, which is better than the specification for hydrogen fuel purity required for PEM fuel cell vehicles (> 99.99 %) documented in SAE J2719.

Unlike hydrogen derived from LH_2, LNG is a mixture with composition that varies depending on place of origin. LNG is typically ~ 93% methane, ~ 5% ethane, with the balance being propane, butane, nitrogen and other trace gases. The percentage of methane runs from 87% to 96% depending on source [13]. While in some cases the approximation is made that the physical and combustion properties of LNG can be fairly represented by those of liquid methane (LCH_4), it is worth noting that the composition variations do have observable effects (typically modest) on the combustion properties [14] and the net GHG emissions associated with LNG combustion [13]. The fact that LNG consists of a mixture introduces the phenomenon of compositional "stratification" whereby density and temperature differences arising from the mixture can lead to increased local vaporization (called rollover) [15].

Physical Properties of Hydrogen and Methane

Gaseous State

Hydrogen is the lightest gas, with a density of 0.08376 kg/m^3 at normal temperature and pressure (NTP), 293.15 K, 1 atmosphere pressure. Methane is considerably heavier, with a density at NTP of 0.65119 kg/m^3. Both gases at NTP are more buoyant than air, which has a NTP density of 1.204 kg/m^3. It is generally not possible to accurately specify the "rising velocity" of a practical hydrogen or methane release, because the terminal rising velocity is established as a balance of the buoyant force (pointed up), gravitational force (pointed down), and the atmospheric drag (pointed down) on the gas volume as it rises. The atmospheric drag depends on the shape and cross-sectional area of the released gas volume, which in practical releases is unknown and can depend on the initial conditions of the release, turbulence and wind conditions. Furthermore, the density of air depends on relative humidity. To give a sense of the relative rising rates for hydrogen and methane at NTP for spherical volumes of released gas in the absence of wind or turbulence,

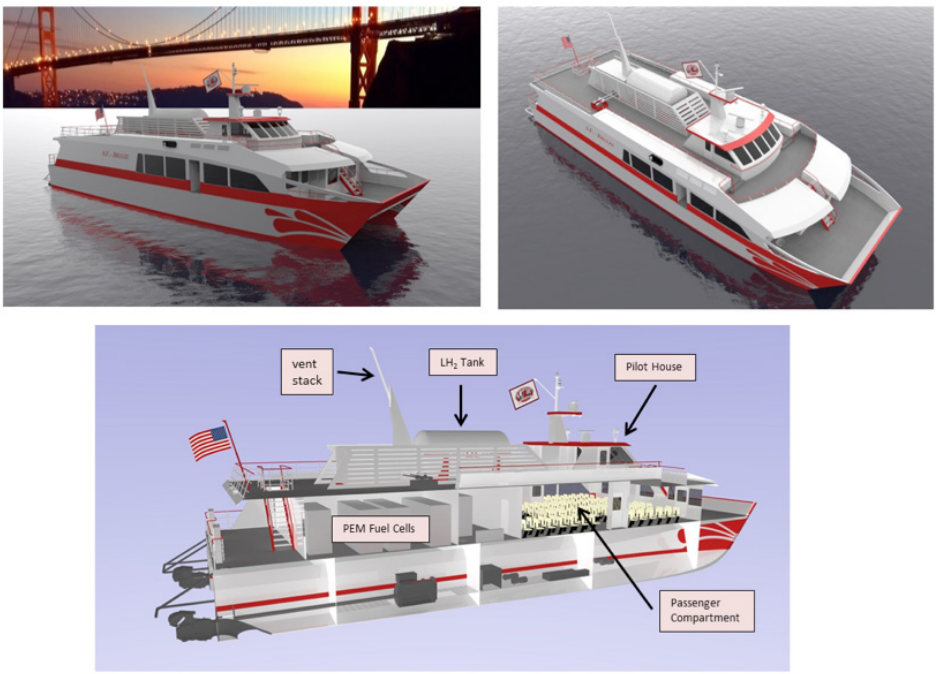

Figure 1: Engineering Models of the SF-BREEZE. The Top Deck holds the LH_2 storage tank, the associated vent stack, evaporation equipment, and the Pilot House of the vessel. The Main Deck holds the PEM fuel cell power racks and the passenger compartment.

we show in Figure 2 a plot of the terminal rising velocity in air (under these assumptions) for both gases as a function of the sphere radius. For the hydrogen fuel complement of the SF-BREEZE (1200 kg), this mass of hydrogen would, at NTP, occupy a sphere with radius 15.07 m, with a terminal rising velocity of 27.92 m/s. The same mass of methane would occupy a sphere of radius 7.61 m with terminal rising velocity of 13.93 m/s. Clearly, hydrogen is significantly more buoyant than methane, although both rise quickly in air at NTP.

Being a homolytic diatomic molecule, hydrogen has no dipole moment, and vibrations of the molecule cannot produce

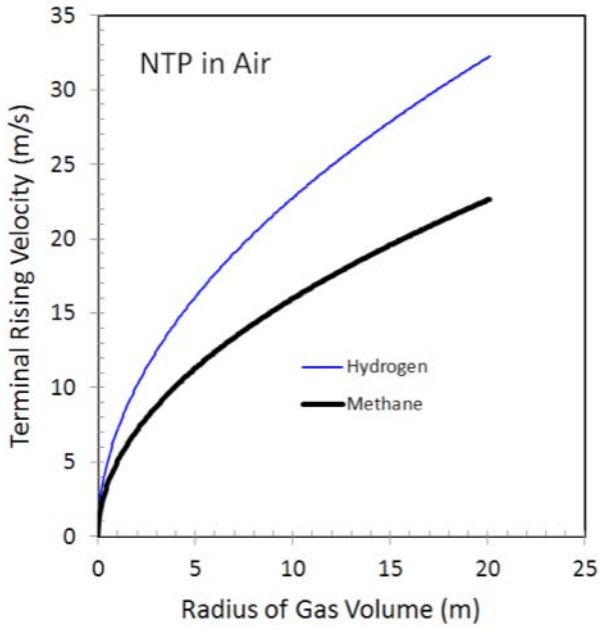

Figure 2: The terminal rising velocity for spherical volumes of hydrogen and methane in air at NTP (293.15 K, 1 atmosphere pressure). The figure uses NTP gas densities of 1.204 kg/m³ for air, 0.08376 kg/m³ for hydrogen and 0.65119 kg/m³ for methane.

charge separation along the bond axis. Consequently, hydrogen does not interact with infrared radiation, and is not a greenhouse gas. In contrast, since methane is a heterolytic molecule with different elements bonded together, the bonds are inherently polar, and stretches and bends of C-H bonds produce charge fluctuations that can couple to infrared electromagnetic radiation. This character makes methane a potent greenhouse gas, ~ 23 times more capable of trapping heat in the atmosphere than CO_2. This fundamental difference between hydrogen and methane makes methane leaks from LNG infrastructure a serious concern from environmental, safety and economic perspectives, whereas leaks from a hydrogen infrastructure raise safety and economic concerns without environmental impact.

Liquid State

A defining characteristic of molecular hydrogen is the very weak attractive van der Waals interactions between H_2 molecules. The intermolecular attractions between H_2 molecules are weaker than those between CH_4 molecules, which explains the lower boiling temperature for LH_2 compared to LCH_4 (LNG). The normal boiling point for hydrogen is 20 K; the normal boiling point for LCH_4 is 111 K. An important consequence for the difference in boiling points is that liquid methane (at its boiling point) cannot liquefy air, whereas LH_2 can liquefy air, whose components N_2 and O_2 condense at 77.3 K and 90.2 K, respectively. These atmospheric gases can also solidify when exposed to LH_2, as the melting points for solid N_2 and solid O_2 are 63.3 K and 54.8 K, respectively. The potential for liquefying or solidifying air introduces safety concerns arising from clogging hydrogen lines with condensed air, as well as concerns about reactivity stemming from condensed oxygen. As a practical matter, these air condensation issues are routinely handled in LH_2 fueling operations by purging the LH_2 plumbing lines with hydrogen or helium (more typically hydrogen due to its availability at the site and lower cost).

The weak intermolecular attraction between H_2 molecules, combined with hydrogen's low mass, makes LH_2 a low-density fluid. The density of LH_2 is 71 g/L at its normal boiling point (NBP) of 20 K at 1 atmosphere pressure. The density of LCH_4 at its NBP of 111 K at 1 atmosphere pressure is 422 g/L. For comparison, the density of liquid water is 1000 g/L. For the same amount of stored energy, LH_2 has 0.38 times the mass of LCH_4, but has 2.4 times the volume.

Both hydrogen and methane are less dense than air at room temperature and pressure. An important safety-related question is: when these liquids evaporate, producing either cold hydrogen gas at 20 K, or cold methane gas at 111 K, how much do these gases have to warm before they become more buoyant than ambient air? If we assume that for small leaks, the ambient air is not cooled too much and remains near NTP, then hydrogen will become more buoyant than NTP air (with density 1.204 kg/m³) at 22.07 K [16]. In other words, hydrogen release from LH_2 need only warm up by ~ 2 K in order to become more buoyant than air at NTP conditions. In contrast, methane needs to warm up 53.3 K, from 111 K to 164.3 K, before its gas-phase density equals that of NTP air [16]. As a result, when LCH_4 evaporates at 111 K, the cold methane gas stays non-buoyant for significantly longer times than does LH_2. Both LH_2 and LNG at their NBP expand considerably when warmed to NTP. The volume expansion factor for hydrogen is 847.6 and that for methane is 648.0 when a given mass is warmed from the NBP to NTP.

Cryogenic Spills

The weak intermolecular attractions between hydrogen molecules leads to the enthalpy of vaporization ΔH_{vap} of LH_2 being only 0.92 kJ/mole, 9.2 times less than that of LCH_4, whose ΔH_{vap} value is 8.5 kJ/mole [17]. For comparison, the ΔH_{vap} of liquid water is 40.66 kJ/mole, due to the strong hydrogen bonding found between water molecules. The extraordinarily low ΔH_{vap} value for hydrogen has important consequences for its use as a fuel and its behavior during spills. For equal amounts of stored energy (to be discussed), LH_2 takes 3 times less thermal energy to evaporate than LCH_4. Thus, in a spill, LH_2 will cool surrounding surfaces much less than a LCH_4 (LNG) spill. This is an important consideration for structural elements of a ferry, as mild ferritic steels can undergo brittle fracture when exposed to cryogenic temperatures [18]. The Top Deck of the SF-BREEZE is made of aluminum, which does not suffer brittle fracture [19].

We have analyzed the effect of spilling the entire 1200 kg LH_2 fuel complement onto the Top Deck of the SF-BREEZE, although we note that since the cryogenic tanks designed for LH_2 have no history of catastrophically failing in this way, the U.S. Coast Guard does not consider such a spill a credible accident scenario. In such a spill, the SF-BREEZE Top Deck, with area 162.65 m^2, thickness 0.794 cm and mass 3483 kg would be cooled from 298 K to 168 K. The cooling of the aluminum deck is deeper if LCH_4 is spilled, due to the significantly higher ΔH_{vap} value of 8.5 kJ/mole. For the same Top Deck, spilling an energy-equivalent mass of LCH_4 (3198 kg) cools the Top Deck from 298 K to 111 K. Thus, due to the higher ΔH_{vap} value for methane, spills of LCH_4 will produce deeper reductions in temperature of structural items than spills of LH_2. The chemistry and physics of how LH_2 and LNG behave when spilled are important for understanding not only thermal effects on the surroundings, but also the behavior of such pools if their vapors are ignited (so called "pool fires.") We will return to this topic later when we discuss the nature of pool fires in the maritime application.

The A.D. Little Company [10] performed an early comparison of LH_2 and LNG (LCH_4) in the context of cryogenically fueled commercial aircraft. This work concentrated on the combined problem of fluid flow when in contact with the ground along with ignition. Witcofski and Chirivella at NASA Langley [20] conducted the first large-scale spill tests of LH_2 in the absence of ignition, with a focus on the measured hydrogen content of vapor clouds at varying distances from the pool spill. This NASA work motivated subsequent work on predicting the duration and physical extent of LH_2 spills, as well as those of other cryogens including LCH_4. Verfonden and Dienhart performed pioneering model studies of the NASA experiments and conducted controlled spill tests focusing on the extent and duration of LH_2 spilled onto water and aluminum [21, 22], two surfaces very relevant for the SF-BREEZE application. These workers also developed a mathematical model called LAuV to address the relevant phenomena involved in cryogenic pool spreading and vaporization. The LAuV model predictions for pool radius and duration received prior validation by comparison with LNG pool spreading experiments.

The NASA spill tests did not emphasize the size and duration of the LH_2 pool, but one spill trial did provide data that a spill of 5.7 m^3 (404.7 kg) of LH_2 produced a maximal radius of 2 - 3 meters and the entire pool evaporated within 5 seconds after cessation of active spilling (which occurred after 38 seconds). Verfonden and Dienhart's model of this spill test predicted a LH_2 radius of 6.5 m, and excellent agreement with the duration data [21, 22]. These foundational studies point to LH_2 spills having very short durations and relatively small physical extents, both attributable to the high vaporization rate produced by the low ΔH_{vap} value. Heat conduction from the ground is the dominant contributor to evaporation of spilled pools of cryogenic liquids [21, 22].

The LAuV model gave an excellent account of the controlled LH_2 spill tests on both water and aluminum [21, 22]. Experimentally, the duration of the pool was determined mostly by the practical speed at which LH_2 could be physically spilled, which was 62 seconds in these tests. For example, for 0.31 m^3 (22.0 kg) of LH_2 spilled on water, the observed and calculated pool radii were both ~ 0.6 m, and the model predicted the pool completely evaporated at 62.9 seconds, within 1 second of completion of fuel spill. Spills onto water had a larger radius (0.6 m vs. 0.4 m) than those on aluminum due to ice formation and the subsequent poorer heat transfer to the LH_2 pool. Overall, spill results on water or solid surfaces were comparable in size and duration.

Table I: Predicted Size and Duration of Instantaneous LH_2 and LNG Spills from LAuV Model, from Reference [21].

Pool Characteristic	LH_2 (17,040 kg)	LH_2 (2,840 kg)	LNG (40,725 kg)*	LNG (18,000 kg)*
Radius (m)	42	20	49	38
Duration (s)	25	13	80	65

*assumes an LNG density of 450 g/L

The LAuV model was also used to predict the pool radii and vaporization times (duration) for 40 m^3 instantaneous spills of the LH_2 and LNG (modeled as 87% methane and 13% propane) on solid ground. Table I summarizes these results [21].

It is clear from Table I that due to the exceptionally low ΔH_{vap} value, LH_2 spills are very short duration events. Using the duration and size predictions in Table I for 2,840 kg of LH_2 as a basis for linear interpolation to 1200 kg, we estimate for the SF-BREEZE that if the entire 1200 kg contents of the LH_2 tank instantaneously spilled onto the Top Deck, the cryogenic pool would last ~ 6 seconds and spread to a maximal radius of ~ 8 meters.

More recently, theory was extended to account not only for the dimensions of the LH_2 pool, but also for the composition of the vapor phase immediately above the pool. Middha and co-workers [23] used a 3-D computational fluid dynamics (CFD) code named FLACS to simulate the NASA and the Verfonden and Dienhart experiments for both pool formation and hydrogen content in the air above the pool and downrange. The FLACS and LAuV models were in general agreement with each other with regard to pool formation (radius, duration), although the FLACS model had higher evaporation rates and smaller pool radii due to the inclusion of thermal effects other than ground conduction. The FLACS model gave a reasonable account (with factors of 2) of the gas dispersion data that was available. The FLACS model did not take into account possible gas-phase complications such as the condensation of air components (oxygen, nitrogen) in the hydrogen cloud or perhaps N_2 and O_2 freezing very close to the LH_2 pool, or in the pool itself. Condensation or freezing of atmospheric water was not included the FLACS model studies [23]. The condensation/freezing of atmospheric components (water, O_2, N_2) is at the edge of the state-of-the-art in theoretical modeling of spilled cryogenic pools.

Two other physical phenomena need to be described for hydrogen use in maritime applications: hydrogen permeation and hydrogen embrittlement.

Permeation

Hydrogen permeation arises from the dissociation of molecular hydrogen at metal and oxide surfaces into hydrogen atoms, and the subsequent diffusion of hydrogen atoms through materials involved in hydrogen storage and plumbing lines. Hydrogen atoms produced in this way can also lead to hydrogen embrittlement, which is a very important phenomenon in materials science. Many misinterpret hydrogen permeation (even in the absence of embrittlement) as a leak risk. The concern is that hydrogen diffusing through tubing and other fittings can pass though the material and exit as hydrogen gas, thereby constituting a leak.

Permeation as a source of leaking is not an issue for the practical performance of tubing, valves or other hardware because the quantities of gas exiting in this way are infinitesimal. San Marchi, and co-workers have described hydrogen permeation in stainless steels at high pressure [24], reviewing the fundamental thermodynamics and kinetics of hydrogen permeation, diffusion and solubility in a material supporting a hydrogen pressure differential. Hydrogen permeation is defined as the product D•K, where D is the diffusivity and K is the equilibrium constant for hydrogen dissolving from the gas phase into a material. We now assess hydrogen dissolution, permeation and diffusion in metals as a leak risk using experimentally determined values for solubility and diffusion in steel alloys [24].

We ask the question: "If the entire 1200 kg fuel complement of the SF-BREEZE LH_2 tank were vaporized to room temperature, and compressed to 150 psi (the maximal pressure to be found anywhere on the SF-BREEZE), what would the rate of hydrogen diffusion be through 1/16" thick 300 series (304, 316) stainless steel?" This corresponds to the maximal hydrogen permeation conditions (highest temperature, highest pressure, smallest hardware wall thickness) that could exist in the SF-BREEZE hydrogen-fueling manifold. Studies show the solubility, permeation and diffusion of hydrogen in 304 and 316 alloys are the same to within experimental accuracy [24]. If one takes the entire 1200 kg of hydrogen, vaporizes it to room temperature, and enclosed it in a spherical 316 container and compressed the gas to 150 psi, the sphere would have a radius of 7.0 m. Assuming a 1/16" wall thickness for the sphere, we can calculate the rate of passage of hydrogen from the interior of the sphere to the exterior, exiting the sphere as hydrogen gas "leaking" across its entire external surface area. Under these circumstances, the flux of hydrogen out of the sphere in steady state would be 1.56×10^{-9} moles/s. Hydrogen diffusion is a thermally activated process, and drops off drastically as the temperature is lowered. At 200 K, the rate of flux would be 1.13×10^{-14} moles/s, which shows how dramatically this thermally activated process is reduced for even mildly cryogenic conditions.

This leakage rate of 1.56×10^{-9} moles/s needs context. If one were to fill a classic model KS-21716 AT+T telephone booth (dimensions H x W x D = 211 cm x 85 cm x 85 cm) with this permeation leakage of hydrogen, it would take 60 years to reach the 4% LFL. One might ask how much hydrogen the 150 passengers on the SF-BREEZE are releasing. Hydrogen is a well-known product of human metabolism, produced at ~ 3 ppm levels in human respiration. Assuming an average human lung tidal volume of 0.5 liters/breath, and a respiration rate of 20 breaths /minute, one can readily calculate that it would take 10.3 days for the hydrogen from passenger respiration, directed into the KS-21716 phone booth, to reach the 4% LFL. This assumes of course that only hydrogen from the

respiration enters the phone booth. The point of this discussion is that permeation in the context of the SF-BREEZE is not an issue for leakage from plumbing systems such as valves, fittings, tubes, pipes, etc. because it is infinitesimal. Passenger breathing represents a vastly larger source of hydrogen. It is also worth noting that welds do not strongly affect the rate of diffusion in metal samples, and there is some evidence microscopic defects in welds can actually act as hydrogen traps, slowing diffusion.

One might reasonably ask if CH_4 containment can lead to molecular dissociation, releasing hydrogen atoms into a vessel wall material where they can then diffuse, resulting in permeation and perhaps even hydrogen embrittlement. The surface science of methane adsorbed on iron is very different from hydrogen adsorbed on iron. In investigations both experimental [25] and theoretical [26], methane bonds to iron films in a very weakly bound "physisorbed" state, characterized by thermal desorption from the surface at 130 K. Methane does not adsorb to iron surfaces at room temperature. Even for temperatures below 130 K in which methane is bound to iron, there is no dissociation into hydrogen and carbon, because the energy barrier for breaking the C-H bonds is unfavorable [27]. In contrast, hydrogen is dissociated at iron surfaces as revealed in theoretical [27] and experimental [28] studies, forming bound chemisorbed H atoms that are stable at room temperature and desorb only if the temperature is raised to greater than ~ 625 K. This basic surface science explains why methane does not dissociate at stainless steel surfaces (with majority component iron), and as a result is not a source of hydrogen atom production at internal natural gas plumbing or storage surfaces that would lead to hydrogen permeation or hydrogen embrittlement.

Hydrogen Embrittlement

Hydrogen solution, permeation and diffusion, even though involving vanishingly small quantities of hydrogen from a leak perspective, are key ingredients to the phenomenon of hydrogen embrittlement. Hydrogen embrittlement is a significant area of materials science, and it is beyond the scope of this review to cover it in a comprehensive manner. Excellent reviews exist [29]. As described above, hydrogen embrittlement does not exist for materials carrying LNG, NG or methane because there is no methane dissociation at the metallic surface. On the other hand, hydrogen atoms produced by the dissociation of H_2 at metallic surfaces can diffuse into the bulk of the material, and accumulate at defect sites in the presence of material strain (which all practical materials have to some extent). Because of the combination of hydrogen, pre-existing defects and strain, hydrogen atoms can accumulate at defect sites, and form brittle metal hydrides such as FeH_2 and CoH_2. If the pre-existing defect is a small crack, the hydriding of the surrounding metal can lead to facile crack growth and eventual material failure. This is a problem for ferritic (body-centered cubic, bcc) steels, but not for austenitic (face-centered cubic, fcc) steels, or copper or aluminum.

As a practical matter, hydrogen embrittlement is circumvented in hydrogen technology by using 304 or 316 stainless steels, aluminum or copper in hydrogen storage systems and piping. Decades of industrial experience show these materials are robust to hydrogen embrittlement. This materials choice is similar in spirit to choosing copper over iron in the manufacture of electrical wiring. Copper has a higher electrical and thermal conductivity than iron, and using copper reduces resistive losses and promotes thermal control. Similarly, the correct materials must be chosen for hydrogen service.

The practical experience of the gas providers is that hydrogen embrittlement is not a maintenance issue for LH_2 or other hydrogen plumbing (tubing, piping) when type 316 or 304 stainless steel materials choices are properly implemented [30]. Like most commercial LH_2 tanks, the interior liner of the LH_2 tank of the SF-BREEZE will be 304 stainless steel. One could contemplate using lighter weight aluminum for the inner liner, but it is structurally weaker and requires using thicker liners (which mostly defeats the lighter weight advantage), and has an undesirable larger thermal conductivity which increases heat leak.

Combustion Properties of Hydrogen and Methane

The physical properties just discussed for hydrogen and methane are the foundation for the discussion of the combustion properties of these two fuels. Table II provides values for "classic" physical and combustion properties of hydrogen and methane. The combustion properties are taken in part from Reference 31.

Before discussing the combustion of these fuels by explicit ignition sources, we consider the phenomenon where releases of these gases can spontaneously ignite even in the absence of specific ignition sources.

Spontaneous Ignition

Dryer and coworkers [32] were among the first to recognize that compressed hydrogen and methane, when suddenly released, can undergo "spontaneous ignition." Spontaneous ignition is a particular safety concern, because it represents an ignition pathway that can persist even if one has successfully removed all explicit ignition sources from the design of a particular application involving these fuels. A number of different mechanisms have been considered [33]. The

Table II: Physical and Combustion Property Values for Hydrogen and Methane.

Quantity	Hydrogen	Methane
Molecular Weight	2.016	16.043
Density of Gas at NTP, kg/m^3	0.08376	0.65119
Temperature to Achieve NTP Neutral Buoyancy in Air (1.204 kg/m^3), K	22.07	164.3
Normal Boiling Point (NBP), K	20	111
Liquid Density at NBP, g/L	71	422
Enthalpy of Vaporization at NBP, kJ/mole	0.92	8.5
Lower Heating Value, MJ/kg	119.96	50.02
Limits of Flammability in Air, vol%	4 – 75	5.3 - 15
Explosive Limits in Air, vol%	18.3 – 59.0	6.3 – 13.5
Minimum Spontaneous Ignition Pressure, bar	~ 41	~ 100
Stoichiometric Composition in Air, vol%	29.53	9.48
Minimum Ignition Energy, J	0.02	0.29
Flame Temperature in Air, K	2318	2148
Autoignition Temperature, K	858	813
Burning Velocity in NTP Air, m/s	2.6 – 3.2	0.37 – 0.45
Diffusivity in Air, cm^2/s	0.63	0.2

evolving picture is that spontaneous ignition arises when a sufficiently high pressure boundary between the compressed gaseous fuel and surrounding (lower pressure) air results in a shock wave that can rapidly mix and heat fuel and oxygen, leading to ignition and flame propagation fed by the continuing fuel release. Dryer and co-workers [32], along with other investigators [34], have examined spontaneous ignition as a function of release pressure, and downstream hardware configuration, which can affect the course of the shock propagation and reactant mixing. The results show that the tendency to spontaneously ignite is higher for hydrogen than methane. The minimum pressure for which spontaneous ignition has been observed, independent of downstream hardware geometry, is ~ 41 bar for hydrogen and ~ 100 bar for methane.

While spontaneous ignition may be a concern for high-pressure (350 bar, 700 bar) hydrogen systems, the SF-BREEZE employs LH_2 storage of hydrogen. The highest pressure in the SF-BREEZE fueling system will be ~ 10 bar, which corresponds to the pressure relief for the LH_2 tank vent. The manifold inlet pressure to the PEM fuel cells will be ~7 bar. As a result, the overall SF-BREEZE system pressures are too low for spontaneous hydrogen ignition to come into play. The mechanistic cause of spontaneous ignition continues to be an active research topic.

Explicit Ignition

In order to discuss combustion caused by specific ignition sources, some definitions are in order:

Weak (Thermal) Ignition Sources: Matches, sparks, hot surfaces, open flames with initiation energy of < 50 mJ are called "weak" or "thermal" ignition sources. These are the ignition sources of accidents.

Strong (Shock Wave) Ignition Sources: blasting caps, TNT, high-voltage capacitor shorts (exploding wires), lightning are all examples of "strong" ignition sources with initiation energy of > 4 MJ. Note that strong ignition sources are ~ 10^8 times stronger than weak initiators. This is an enormous difference in ignition input energy. Other than lightning, strong ignition sources are the sources of intentional ignition, not accidental ignition.

Fire: Fire is the term for ordinary combustion familiar in everyday life where the flame propagates through the unburned fuel/air mix at low speeds (~ 20 m/s or less). Fires are not loud, and produce negligible overpressure in the surrounding air. Fires are produced by weak ignition sources in contact with flammable mixtures of fuel and air. Despite their familiarity, it is important from a safety perspective to remember that fires are dangerous.

Deflagration: Fast combustion where the flame propagates through the unburned fuel/air mix rapidly, but at subsonic speeds (~ 100 - 400 m/s). Deflagrations can be loud, and can produce overpressures that can rupture eardrums and cause other injury. Under the right conditions, deflagrations are initiated by weak ignition sources. From a safety perspective, deflagrations are very dangerous.

Explosion or Detonation: Technically, detonation is the more properly defined term for extremely fast combustion events where the flame propagates through the unburned fuel/air mix at supersonic speeds (> 700 m/s). Explosion has been loosely used to label fast combustion events where the flame propagates through the unburned fuel/air mix at subsonic speeds (< 700 m/s), and can produce loud bangs and very damaging overpressures. The terms explosion and detonation have often been used interchangeably (especially in the older literature referenced in this work), and will be so used here. "Direct" explosions are instantaneous events caused by strong ignition sources with specific conditions of fuel/air mix and confinement. From a safety perspective, explosions and detonations are very, very dangerous.

Fires

Both H_2 and CH_4 mixtures with air ignite easily using weak ignition sources to produce fires. Fire regulations focus on the "Lower Flammability Limit" (LFL), expressed as a volume percentage (vol%):

$$\text{vol\%} = [\text{Volume (Fuel)}/\text{Volume (Fuel + Air)}] \times 100$$

The LFL is the focus of safety regulations, since the risk of fire typically comes from the accumulation of flammable gas in initially clean air. The classic values [31] for the flammability

range (LFL to upper flammability limit (UFL)) for H_2 = 4.0 – 75.0 % at 298 K. The LFL to UFL of methane is = 5.3 – 15.0 % at room temperature [31]. For context, the LFL – UFL values for gasoline are 1 – 7.6% [31]. Thus, while hydrogen has a much wider flammability range than methane (making it more of a fire risk), from the perspective of building up flammable gas in an initially clean environment, hydrogen and methane have similar LFLs, with similar threshold gas accumulations that can be ignited. The minimum ignition energy for H_2 is 0.020 mJ; that for CH_4 is 0.29 mJ. Static discharges from human beings are ~ 10 mJ, so both CH_4 and H_2, when present between the LFL – UFL limits, ignite easily when exposed to common (weak) ignition sources. Table II lists these combustion properties for hydrogen and methane.

As described by Cashdollar and co-workers [35], in quiescent mixtures of fuel and air, fuel buoyancy alters the LFL required for self-sustaining fires. In a self-sustaining fire, combustion advances at nearly the same speed for upward, horizontal and downward directions. Upward flame propagation is intrinsically faster than other propagation directions because combustion products are hotter and less dense than the original fuel and air mixture. However, for sufficient concentrations of fuel, the combustion is hot enough that flame propagation is facile in all directions. Hydrogen mixtures ignited at 4 % produce very little heat, and flame propagation is almost exclusively upward. Thus, for a spherical hydrogen/air mixture, weak initiation at the sphere center at the LFL will only produce combustion for a relatively small upper slice of the spherical volume, producing fire that cannot sustain itself to the point of complete combustion of the fuel. For sustained hydrogen fires, the hydrogen/air mix needs to be ~ 8% for combustion to propagate in all three directions with complete combustion of the fuel [35]. Since methane is less buoyant than hydrogen, buoyancy effects are correspondingly less, and full-three dimensional flame propagation is achieved at a methane/air mix of ~ 6%, up from the classic LFL value of 5.3 %.

Interestingly, intentional active mixing of the fuel/air mixture can largely counteract the effects of buoyancy. In some of the experiments of Cashdollar et al. [35], a mixing fan produced flows of order 1 – 1.5 m/s along the fan rotation axis. In this mildly turbulent condition, the threshold for a self-sustaining fire in hydrogen returned to 4%. The effect of the active mixing is to introduce a velocity element that can overcome the influence of buoyancy and promote mixing, which produces hotter burning, and faster flame speeds that propagate well in all three directions. For methane, for which buoyancy effects are small to begin with, mild turbulent mixing produced the same ignition concentration threshold as quiescent conditions (5.3%).

In typical accidental scenarios involving slow releases of hydrogen in the SF-BREEZE fuel cell rooms, we anticipate the conditions will correspond more closely to the quiescent scenario, suggesting a LFL for sustained hydrogen combustion to be closer to ~ 8%. Even with ventilation producing the 30 room air exchanges required by U.S. Coast Guard regulations, the average air speed during ventilation would only be ~ 0.02 m/s, which is unlikely to produce strong turbulent flow.

Laboratory experiments have shown that the LFL holds even if the ignition source is highly intermittent. Schefer and coworkers [36] have shown that in ignition tests on hydrogen and methane turbulent jets using a 100-mJ laser with a 9-ns pulsewidth, ignition is not possible unless the instantaneous concentration of fuel present at the time of the laser pulse is above the classic LFL.

Overall, from the point of view of fire risk coming from fuel release into initially clean air, hydrogen and methane have very similar ignition risks because their LFLs are similar.

Explosion and Detonation

Hydrogen and methane can both detonate given the right conditions of fuel/air mixture, confinement and strength of ignition source. Ng and Lee [37] have discussed the explosion risk for hydrogen in the transportation setting. The lower explosion limit (LEL) of H_2 at room temperature (% by volume) - upper explosion limit (UEL) = 18.3 – 59.0 % at room temperature [31]. The LEL to UEL of methane is = 6.3 – 13.5 % at room temperature [31]. Thus, hydrogen has a much wider explosive range than methane, making it more of an explosion risk in general. From the perspective of building up flammable gas in an initially clean environment, the LEL of methane (6.3%) is reached considerably sooner than that of hydrogen (18.3%).

In the SF-BREEZE design, hydrogen release is a concern for two locations. On the Top Deck where the LH_2 tank is situated, we have an essentially unconfined environment in which a release of H_2 would be free to disperse upward without blockage. In contrast, the Main Deck holds the PEM fuel cells, which are distributed into a Starboard (right, facing forward) and Port (left, facing forward) Fuel Cell Rooms. A cutaway view of the Main Deck of the SF-BREEZE is shown in Figure 3:

In these fuel cell rooms, there exists a confined situation where hydrogen (if released) would enter an enclosed room, albeit with installed ventilation providing 30 room exchanges of air per hour. We examine combustion beyond normal fires to include assessment of explosions and deflagrations with varying degrees of confinement.

The A.D. Little Company evaluated the practical explosion risk from large-scale releases of hydrogen in confined and unconfined environments in a series of experiments and modeling

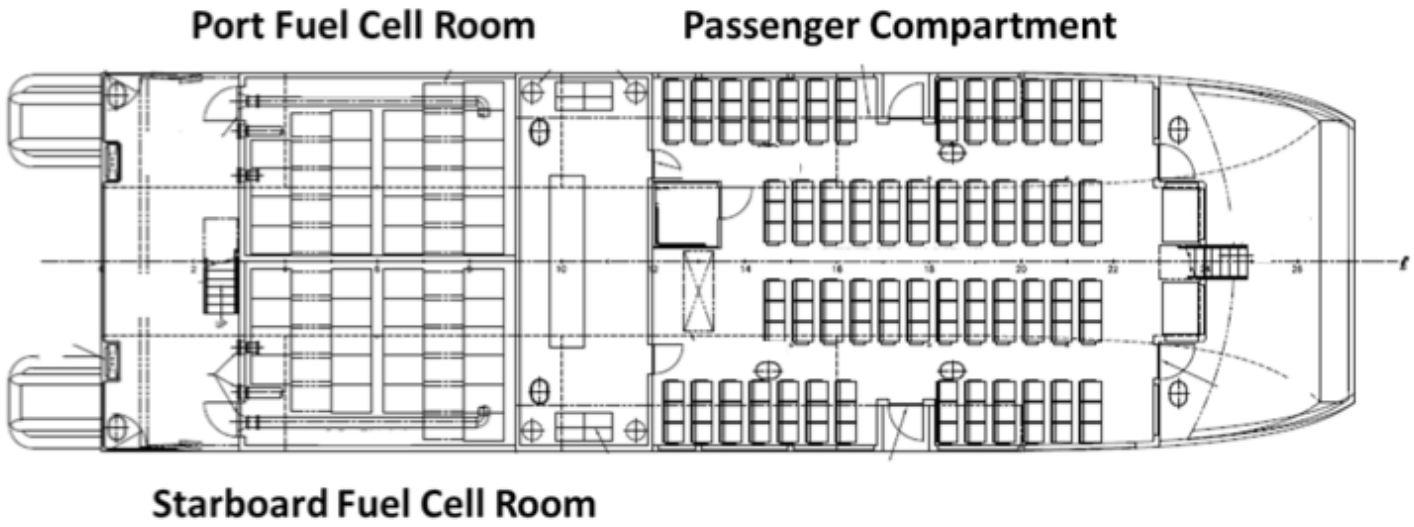

Figure 3: Cutaway view of the Main Deck of the SF-BREEZE. The PEM fuel cells are distributed into a Starboard Fuel Cell Room and a Port Fuel Cell Room, with ~ 20 fuel cell racks in each room. The Passenger Compartment holds 150 passengers. The "beam" (width) of the SF-BREEZE is 10 m. The dimensions of each Fuel Cell Room are 7.4 m long x 5.1 m wide x 2.7 m tall.

studies for the U.S. Air Force and the NASA Lewis Research Center over the period 1960 – 1982 [8 - 10]. These impressive and comprehensive tests represent the first modern scientific investigations of the consequences of spilling and igniting large quantities of LH_2. The original work, published in 1960 [8] with aspects reported again in 1964 [9], reported the combustion of stoichiometric mixtures of hydrogen and air confined in large balloons with diameters ranging from 5 to 8 feet. Though clearly "confined," such balloons were a departure from the highly confined small tube experiments that had been used up to that time, and gave an indication of combustion properties in "free space." For the 5-ft balloon, detonation of the stoichiometric H_2/air mix required a strong ignition source (2 grams of pentolite explosive). This data revealed that a three-dimensional shock wave could be propagated in "free space" in a H_2/air mix if a sufficiently strong initiator were used. Importantly, ignition of these confined H_2/air stoichiometric mixtures via weak ignition sources (sparks) yielded only fires with no measureable overpressure.

The Little investigators assessed if a larger volume balloon could provide a sufficient path length to allow a transition from fire to deflagration to detonation. Using an 8-foot diameter balloon containing a stoichiometric mixture of hydrogen and air, ignition by weak spark sources produced again only fire with negligible overpressure. The conclusion from this work is that both confinement and explosive initiation are required for the direct explosion of confined hydrogen/air mixtures in which explosion occurs instantaneously. Furthermore, in free space (with no obstacles present), over a distance of ~ 4 feet (the balloon radius), there is no transition of the combustion from fire to deflagration to detonation using weak ignition sources.

In the LH_2 spill tests using 32 gallons in which a vapor cloud forms in the open (no confinement of any kind), the Little researchers found no detonation or tendency towards detonation even when strong explosive initiators were used to ignite the vapor cloud. Since detonation using explosive charges was observed in the 5-foot balloon tests, they concluded that the vapor clouds above real spills had non-ideal mixing that inhibits direct detonation. These observations led the authors to conclude [8], "even with shock-wave initiation, detonation is unlikely of the hydrogen-air cloud from a large-scale spill."

Summarizing these early tests of practical hydrogen combustion risks, direct detonation requires strong ignition sources, confinement, and hydrogen/air mixes within the LEL - UEL range. Weak ignition sources produce fires even when the hydrogen/air mix is within the explosive range and confined in a balloon. Ignition of vapor clouds above sizeable LH_2 releases using strong or weak ignition sources produces only fires. Experimental results for ordinary combustion and detonation were consistent with the LFL – UFL and LEL –UEL ranges listed in Table II. For LNG, ignition tests over LNG pools conducted at Sandia National Laboratories as part of the "Phoenix Program" [38] gave similar results. Ignition of LNG vapors above pools with weak ignition sources produced fires, not deflagrations or explosions.

These experimental results from the 1960s already help

frame the hydrogen fire safety issues for the SF-BREEZE. On the Top Deck where the LH_2 is stored, fire is the only significant combustion risk, (rather than detonation, explosion or deflagration) because of the open environment on the Top Deck and the absence of strong ignition sources. In the confined Starboard and Port Fuel Cell Rooms, direct detonation is not possible because of the lack of strong (intentional) ignition sources. Although these rooms would have constant ventilation (30 room exchanges per hour) and hydrogen monitoring tied to redundant hydrogen shut-off valves in the event of a hydrogen leak, it is instructive to examine these fuel cell rooms to assess conceptually the role of confinement and internal obstacles on the acceleration of ordinary fires to deflagrations, with possible subsequent deflagration to detonation transition (DDT).

In the decades since the 1960s, there has been enormous growth in the scientific understanding of hydrogen and methane flammability, deflagration and detonation, which supports and helps understand the A.D. Little test results. This foundational understanding is essential for the design of hydrogen technology systems [37]. Matsui and Lee quantitatively determined [39] the minimum ignition energy required for direct detonation of hydrogen/air and methane/air mixtures and how this threshold energy varies with the fuel/air mix. The minimum ignition energy occurs near the stoichiometric mix (29.53 % for H_2, 9.48 % for methane), and is 4.16×10^6 J for hydrogen and 2.28×10^8 J for methane. The value for methane is orders of magnitude larger than any other hydrocarbon, making methane exceptionally insensitive to direct detonation. The minimum detonation energy for both hydrogen and methane are ~ 10^8 times larger than the energy required to start normal burning-- an enormous ignition energy requirement essentially precluding direct detonation of hydrogen or methane in accident scenarios.

So far, we have considered three physical limitations to the direct detonation of hydrogen or methane, namely the fuel/air mixture has to be within the range LEL – UEL, a strong (shock wave) initiator is required and the fuel/air mix must be confined. A fourth physical requirement has been discovered over the past several decades: the combustion volume must be larger than the "detonation cell size" of the explosive mixture. As discussed previously by Ng and Lee [37] and Yang [40], it has been experimentally observed that detonations form distinctive physical patterns called "detonation cells" which can be observed in experiments as a "smoke foil" record [41]. For a detonation to occur, the spatial extent of the reacting system must be larger than one cell dimension. For a stoichiometric mix (equivalence ratio = 1) for hydrogen, at room temperature and atmospheric pressure, the detonation cell size is ~ 1.5 cm [41]. The detonation cell size for methane at room temperature and atmospheric pressure is ~ 33 cm [41]. For the SF-BREEZE Top Deck, and the Starboard and Port Fuel Cell Rooms, the physical dimensions are significantly larger than these detonation cell sizes, meeting the geometry requirement imposed by the detonation cell size. The detonation cell size determines how wide experimental tube reactors must be in the transverse direction (normal to the flame propagation) in order to study tube-based detonations in these gases. If the tube diameter is ~ 13 times the detonation cell size, then a confined planar detonation can transform into an unconfined spherical detonation wave upon exit from the tube [41]. The larger detonation cell size for methane requires using significantly larger tubes or tunnels for experiments than required for hydrogen, making it technically more challenging to examine detonation phenomena in methane.

Deflagration to Detonation Transition (DDT)

The LEL-UEL range listed in Table II is for direct detonation of a gas mixture assuming confinement and use of a strong ignition source. The absence of strong (intentional) ignition sources precludes the direct detonation of hydrogen and methane in accident scenarios. However, under certain circumstances it is possible to have a detonation for fuel/air mixes even below the LEL of Table II if obstacles or internal structures are present within the confined reacting volume. Unlike direct detonation, which requires a strong ignition source, this type of explosion can start with a normal fire. In the confined/obstructed environment, the speed of the combustion accelerates over time and distance to a deflagration due to turbulent mixing of the unburnt fuel-air mixture near the obstacles. With further acceleration, the deflagration transitions to a detonation, producing a Deflagration to Detonation Transition (DDT). For H_2, DDT can only occur for 12% fuel /air mix or higher. Both H_2 and NG can experience DDT, although it is easier for hydrogen. Note that for the A.D. Little balloon tests, which showed no acceleration of combustion for either the 5-foot balloon or the 8-foot balloon, there were no internal structures or obstacles which would have promoted a DDT.

The SF-BREEZE Starboard and Port Fuel Cell Rooms (Figure 3) each measure 7.4 m long x 5.1 m wide x 2.7 m tall. These rooms each hold twenty 120 kW fuel cell racks each, which constitute obstacles and potential weak ignition sources for the present discussion. If there were to be a significant hydrogen leak into one of these fuel cell rooms that was not detected by the hydrogen monitors (triggering shutoff of the H_2 supply), or could not be handled by the ventilation system, a legitimate question is whether or not the hydrogen buildup, presence of confinement, obstacles and ignition sources could potentially lead to a fire that evolved into a DDT.

An early and particularly illuminating series of DDT tests for H_2/air mixtures was performed at Sandia in the early-mid 1980s in the "FLAME Facility " [42]. Figure 4 gives a diagram

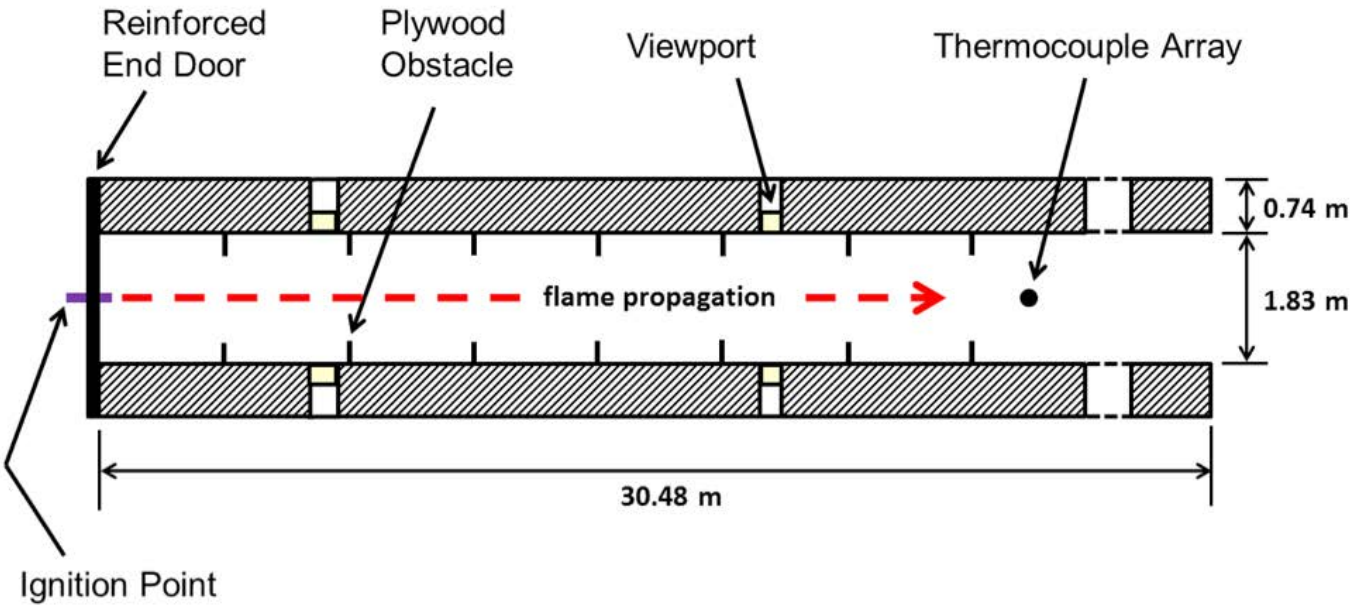

Figure 4: Schematic of the Sandia FLAME facility. Figure is reproduced with modification from Reference 42.

of the FLAME facility.

The FLAME tunnel was 1.83 m wide, 2.44 m tall and 30.48 m long, and constructed of heavily reinforced concrete. The transverse dimensions are similar to the 5.1 m x 2.7 m transverse dimensions of the SF-BREEZE Starboard and Port Fuel Cell Rooms. Sherman et al. placed flow obstacles in the tunnel, blocking one third of the cross section of the tunnel (33% blockage ratio), and monitored the speed of combustion as it traversed the FLAME tunnel using thermocouples. The experiments were conducted at atmospheric pressure and ambient temperature.

Figure 5 shows results for the planar flame speed as a function of distance downrange from the ignition end for various H_2/air mixtures in the tunnel with obstacles removed [42].

This figure shows that for hydrogen concentrations of 12.9% or less, the flame velocities are slow, less than ~ 20 m/s. There is no change in the flame velocity as the flame propagates down the tunnel, and thus no flame acceleration occurs with run distance. This is the propagation of an ordinary fire.

However, given confinement, significant downrange run distance and an increase in the hydrogen concentration to 18.4%, one can see in Figure 5 that the flame velocity increases with distance from the ignition end, reaching 162 m/s at the end of the tunnel. Increasing the hydrogen concentration to 24.7%, the flame accelerates to 367 m/s at 25 meters. Qualitatively, we refer to flame speeds in the range ~100 – 400 m/s as "deflagrations" in comparison to the slower "fire" flame speeds at ~ 100 m/s or less. For the 30% mix, a near-stoichiometric mix of hydrogen and air, one sees significant acceleration to 307 m/s at a run distance of 16.6 meters. Thereafter a dramatic jump in flame speed occurs, and the velocity measured 26 meters down the tunnel is a supersonic 927 m/s. This represents the transition from deflagration to detonation. We qualitatively refer to flame speeds from ~ 400 – 700 m/s as being in the "DDT" range, and velocities higher than ~700 m/s as a "detonation." Figure 5 shows how confinement, increasing hydrogen concentration and run distance can cause acceleration from normal fire to deflagration to detonation in relatively confined spaces even if obstacles are absent.

Figure 6 shows the same experiment, only with obstacles placed in the flame propagation path.

The presence of obstacles induces an acceleration of the flame velocity at H_2/air concentrations that would otherwise not experience flame acceleration. Given obstacles and a run-up distance of 10 meters, the flame speeds for concentrations greater than 12% accelerate from normal fire speeds to deflagration speeds. With more run time and distance, even at mixtures as low as 15.5%, very fast deflagration velocities of ~ 700 m/s are observed if obstacles are present, corresponding to DDT. The lowest H_2/air mix for which DDT was observed in the Sandia tests was 15% when obstacles where present. Note that the experiment corresponding to 10 – 15 % hydrogen was one in which a mixing fan lost power,

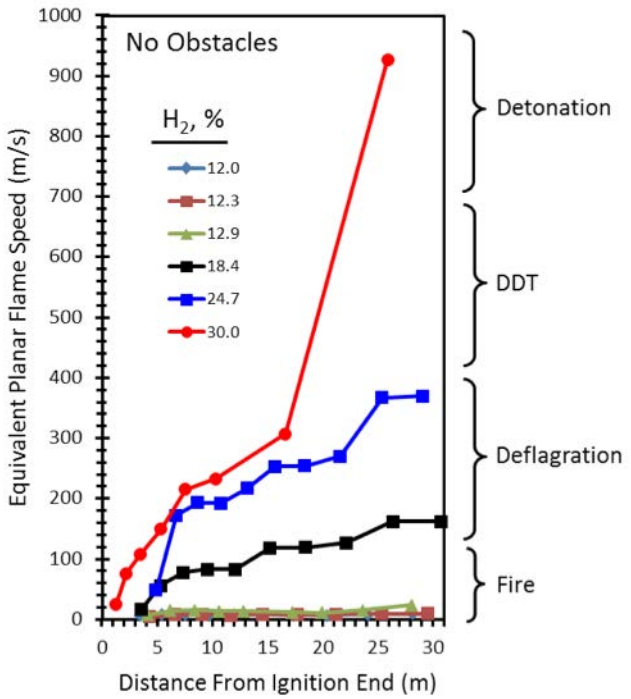

Figure 5: Planar flame speed plotted against distance from the ignition end in FLAME experiments. Obstacles were removed from the tunnel for these measurements. The figure uses data reported in Reference 42.

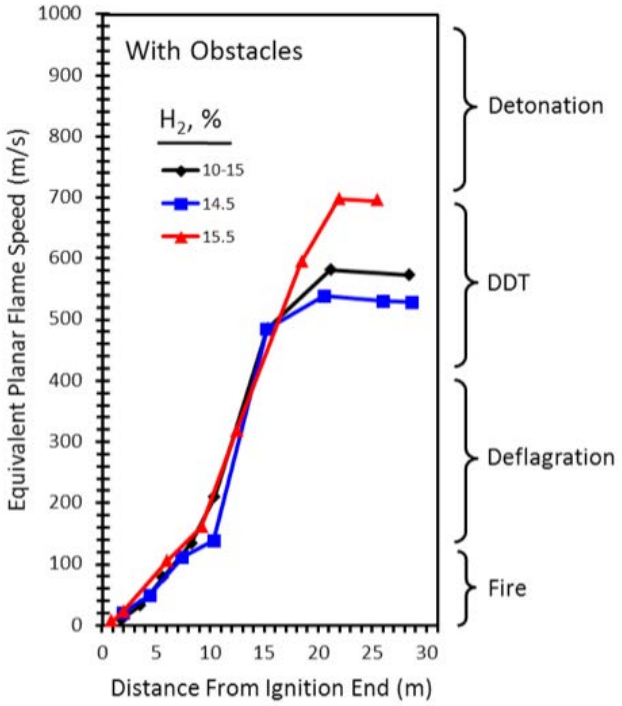

Figure 6: Planar flame speed plotted against distance from the ignition end in FLAME experiments. Obstacles were placed in the tunnel for these measurements. The figure uses data reported in Reference 42. The experiment corresponding to 10 – 15% hydrogen was one in which a mixing fan lost power, producing an inhomogeneous mixture in which the lower part of the tunnel had 10% hydrogen and the upper part had 15% hydrogen. See Reference 42 for further details.

producing an inhomogeneous mixture in which the lower part of the tunnel had 10% hydrogen and the upper part had 15% hydrogen [42]. Other studies [43] of large-scale hydrogen/air mixtures have found a lower concentration threshold for hydrogen DDT to be ~ 12.5% in the presence of obstacles.

Recent studies using sophisticated experimental and theoretical approaches have revealed the basic mechanism for DDT [37, 44, 45, 46, 47]. Flame acceleration requires a feedback mechanism between the advancing (initially low-speed laminar) flame and the unburnt fuel/air mix ahead of the flame. Consider the tunnel geometry of the FLAME apparatus in Figure 4. At any given position and moment in time, the flame influences the temperature and pressure in the unburnt flow field ahead of the flame (towards the right in Figure 4). This interaction produces small turbulent structure in the unburnt flow field. When the flame advances and engulfs this turbulence, the flame will burn hotter because the turbulence increases the area of the boundary between flame and unburnt fuel/air (i.e. the flame area increases), and the combustion itself becomes hotter because the fuel and air are better mixed. This increased flame area and temperature affects the new unburnt flow field ahead even more than before, which in turn further increases the combustion energy when, at a later time and downrange distance, the flame encounters this new turbulent area. This feedback continues, increasing the flame speed until the flow reaches the sonic limit consistent with the composition of the combustion products. When the flame speed approaches the speed of sound, shock waves form and shock-flame interactions become an important mechanism for flame wrinkling and further turbulence generation. The deflagration transitions to a detonation at this point.

The role of obstacles is to increase the rate of formation of turbulent structures. For example, obstacles can induce vortices in the upstream flow field, reminiscent of the turbulent structures issuing from aircraft wingtips. As flow moves past the edge of an obstacle, the shear layer can roll up into a spiraling turbulent structure that provides the feedback to the flame needed for an accelerated flame velocity as the flame moves down the tunnel.

Recently, Johansen and Ciccarelli [45] have captured the creation of a turbulent flow field ahead of the advancing flame for stoichiometric methane-air mixtures using a high-speed schlieren video system. The images show directly how the advancing flame affects the unburnt flow field ahead of the flame, the creation of turbulence at obstacles, and how this turbulence alters the combustion within the flame once the flame passes through the turbulent region. Such experiments have also been successfully modeled theoretically [46].

Figures 5 and 6 showed the importance of "run up distance" in the DDT phenomena. The Sandia FLAME results explain why there was no significant flame acceleration in the prior A.D. Little balloon experiments [9]: there was insufficient run-up distance provided by the balloon radii of only 2.5 – 4 feet for significant hydrogen flame acceleration to occur. For the Sandia FLAME experiments, 10 meters of run-up distance is needed to attain deflagration speeds of 100 – 200 m/s. In the SF-BREEZE design, the Starboard and Port Fuel Cell Rooms have dimensions 5.1m wide x 2.7 m tall x 7.4 m long. Distributing the PEM fuel cells amongst these two rooms not only creates redundancy in the vessel power system (as required by U.S. Coast Guard regulations), but also limits the run-up distance available to a hydrogen fire should one break out in one of these rooms.

The studies of Groethe and coworkers [48] demonstrate the importance of limited "run-up" in limiting the acceleration of hydrogen combustion caused by obstacles. Their experimental setup is shown in Figure 7:

A hemispherical tent of radius 5.7 meters (300 m^3 total volume) was outfitted with a weak ignition source (40 J spark) at the hemisphere center, along with 18 cylindrical aluminum cylinders measuring 0.46 m diameter by 3 m height. The cylinders were arranged around a central point of ignition as shown in the Figure 7. Experiments on hydrogen combustion were conducted with and without the cylinders present to assess the role of obstacles in producing DDT in this geometry.

Figure 8 shows optical video images of the combustion using a 30% hydrogen-air volumetric mix [48].

These images show the flame velocity with obstacles present was ~ 85 m/s, consistent with a fast laminar flame. The form of the flame looks like an ordinary fire. Pressure sensors outside the hemispherical tent showed no overpressure produced by the fire of Figure 8 with or without the obstacles placed inside. A reasonable explanation for the lack of obstacle-induced acceleration is that the geometry of Figure 7 does not provide sufficient run-up distance. With only 5.7 m of run-up available, there is insufficient distance for obstacle-induced flame acceleration to occur.

Although the tent provided confinement and an optimal near stoichiometric 30% H_2/air mix, there was no detonation or explosion. This is because a weak ignition source was used. In one experiment, the researchers replaced the weak ignition source with 10 g of C-4 high explosive to initiate the combustion. With a strong ignition source, confinement, the H_2/air mix in the LEL –UEL range, and a geometry larger than the detonation cell size, all the necessary ingredients were in place for a detonation. Figure 9 shows high-speed video images of the detonation.

The time scales in Figure 9 are much shorter than for Figure

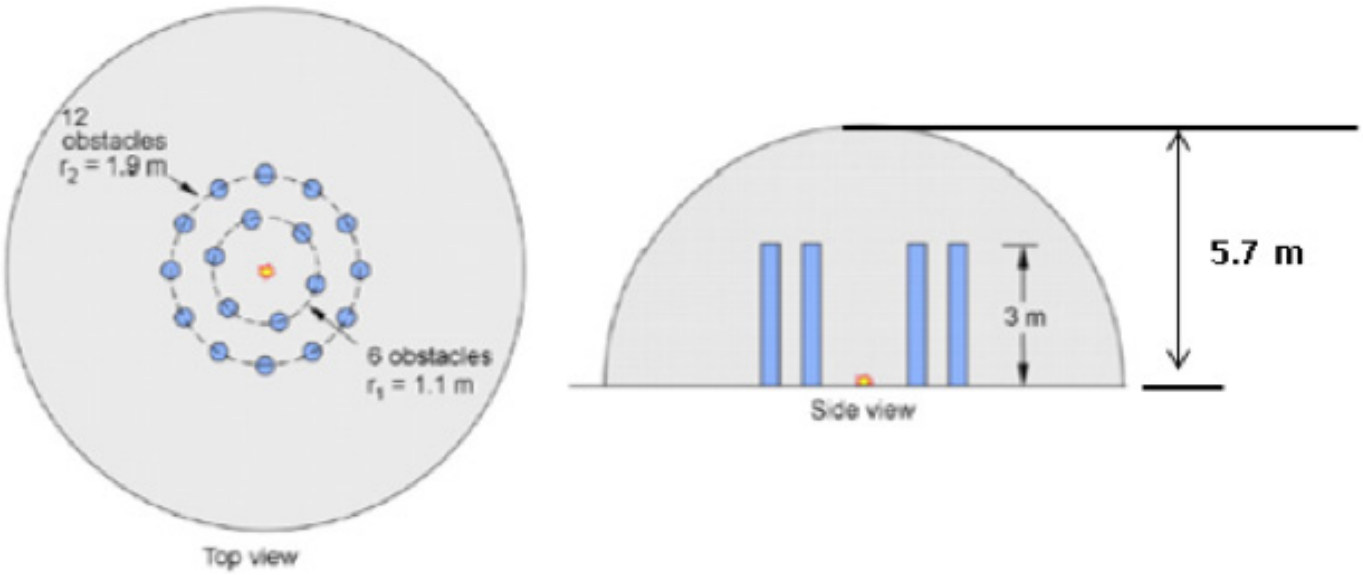

Figure 7: Experimental setup for the experiments reported in Reference 48. Figure reproduced from Reference 48.

Figure 8: High-speed optical video images of hydrogen combustion for a 30% hydrogen/air mixture, ignited with a 40 J spark. Figure reproduced from Reference 48.

8. The video images show that the flame velocity is 1980 m/s, well into the detonation range. Also, note the completely spherical shape of the detonation wave. In a detonation, the flame front advances so rapidly that the fuel/air mixture has essentially no time to move in response to the combustion event. Over the 5088 microseconds of the detonation event, the gas is essentially motionless, with no turbulent structures developed. A nearly perfectly spherical combustion front is created. In contrast, using a weak initiator in Figure 8, over the 65-millisecond duration of the photography the gas volume has time to react to the combustion, producing irregular flame structures. The work of Goethe provides a very educational and intuitive picture of the difference between ordinary combustion and a detonation, in addition to revealing how short run distances can limit DDT even when obstacles are present. This data supports our view that a fire is the primary risk on the Top Deck of the SF-BREEZE where the environment is relatively open. Although there are obstacles on the Top Deck (for example the evaporator that converts LH_2 to gaseous H_2 for the fuel cells) that could possibly induce flame acceleration, the run distances are short where obstacles exist. A quantitative assessment of flame acceleration would require a detailed hardware layout, which is not available at this point in the SF-BREEZE design process.

As noted by Sherman et al. [42], from a safety perspective, it is not that important if a highly accelerated flame has actually undergone DDT because the overpressures accompanying these phenomena can be similar, producing the same safety hazard. Indeed, we have described the physical phenomena of fire, deflagration, DDT and detonation (explosion) to provide the scientific basis for how hydrogen and natural gas may behave in an accident scenario. All of these combustion phenomena can be dangerous and need to be prevented.

Pool Fires

One of the striking differences between hydrogen and natural gas is the radiant nature of their fires. When hydrogen burns, the product of combustion is primarily water vapor, with other species such as OH and H radicals, and HO_2 and H_2O_2 produced in trace (< 1 %) amounts. As a result, the vast majority of thermal radiation from hydrogen fires originates from vibrationally excited water molecules. In contrast, when methane burns, although some water is produced, most of the thermal radiation comes from carbon-containing species, and especially carbon soot, which is an efficient radiator of thermal energy. As a result, the thermal radiation emitted from methane fires is (on a fuel LHV basis) 2 - 3 times higher than for a hydrogen fire. This property is quantified as the "radiant fraction," which gives the fraction of fuel combustion energy that is released as radiation. We estimate that for a pool fire involving combustion of the entire 1200 kg of the LH_2 fuel complement, the radiant fraction would be 0.045. A pool fire burning an energy equivalent amount of methane (3198.9 kg) would have a radiant fraction of 0.10. Thus, the methane fire would release 2.2 times more radiant energy than a hydrogen fire for the same combustion energy.

Because a hydrogen fire is emitting infrared (IR) radiation from the vibrational (bending, stretching) modes of thermally excited water vapor, residual water in the atmosphere (i.e. humidity) can absorb some of radiation from hydrogen fires, reducing the transmission of radiative heat. The spectral match between atmospheric water absorption and flame water emission is not perfect due to the well-known red-shift that occurs in the emission spectra, as described by Tilotta and co-workers [49]. However, the shift is relatively small, producing substantial absorption of water IR emission from flames by atmospheric water. Gerritsma and Haanstra [50] made quantitative measurements of the IR transmission of atmospheric air at room temperature with a relative humidity of 62%. Over a 4.7-meter path length, the average transmission in the regions for the water emission bands is ~ 70%. Thus, ~30% of the thermal radiation issuing from a hydrogen

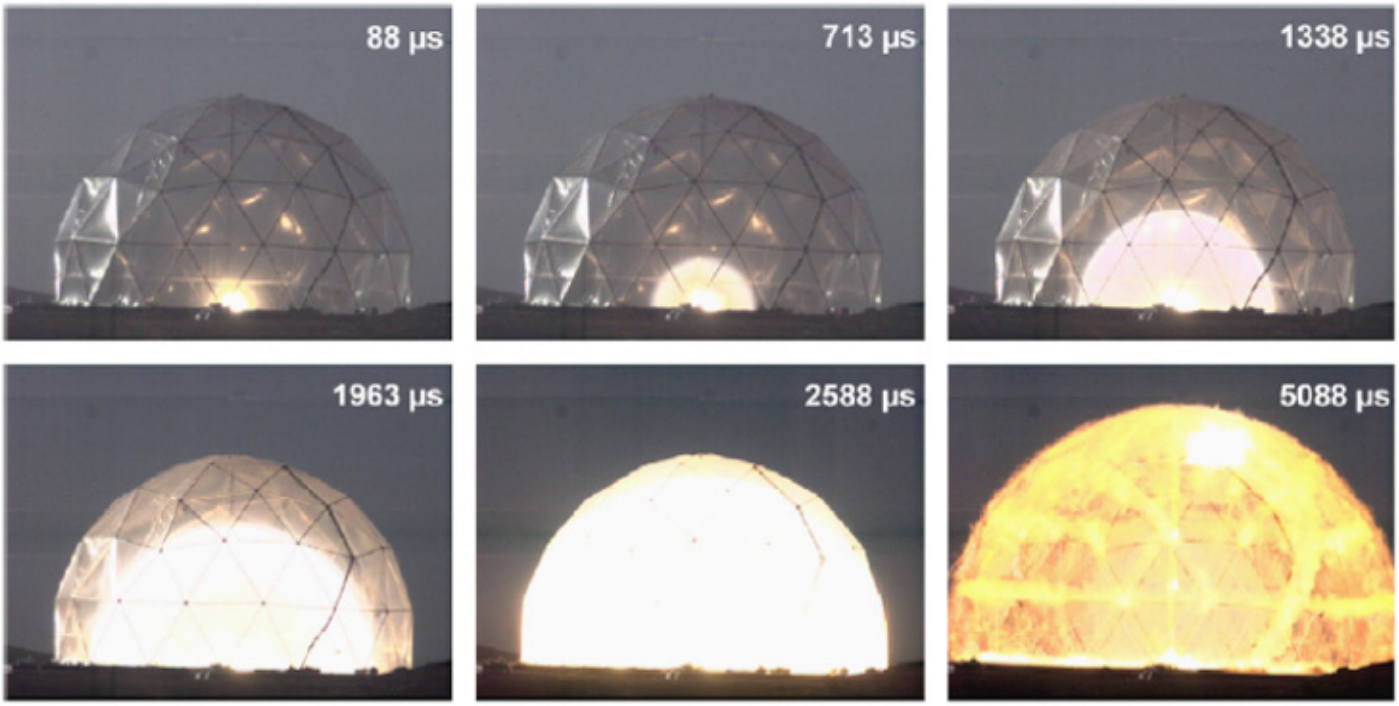

Figure 9: High-speed optical video images of hydrogen combustion for a 30% hydrogen/air mixture, ignited with 10 grams of C-4 high explosive. Figure reproduced from Reference 48.

fire over a 4.7 m distance would be blocked by atmospheric water vapor [49]. Wayne [51] confirmed this result and provided a convenient means of calculating atmospheric infrared transmissivities for a variety of humidity and temperature combinations. The atmospheric absorption of thermal radiation from a methane fire would be less, as noted in the original modeling work of A.D. Little [10], where the explicit calculation of radiative heat transfer from hydrogen and methane fires was reported using atmospheric transmissivity data.

This difference in radiant energy has consequences for the impact fire has on surrounding structures and personnel. In their 1982 study [10], A.D. Little calculated the closest approach one could get to a pool fire of LH_2 and LCH_4 and still not suffer a thermal skin injury (whose threshold was assumed to be 5 kW/m^2) for varying quantities of fuel burned. For a fuel heat content of 144 GJ, corresponding to 1200 kg of LH_2 and 3198.9 kg of LCH_4, calculations were made of the closest approach to the fire in the horizontal direction at grade. For 1200 kg of burning hydrogen, the closest approach is ~ 19 m. For LCH_4, the closest approach is ~ 58 m. One can get closer to a hydrogen fire because it radiates less thermal energy and there is more atmospheric absorption of the thermal radiation. These two effects more than compensate for the slightly higher flame temperature of hydrogen compared to methane (Table II).

To bring together the concepts that have been discussed thus far for fuel buoyancy, pool formation, fuel combustion, and fire radiation, it is useful to compare and contrast two hypothetical accident scenarios where the entire 1200 kg LH_2 fuel complement of the SF-BREEZE and the energy equivalent in LNG is instantaneously spilled and ignited on the Top Deck of the vessel. This is a pool fire scenario, which has been the subject of many studies given its importance in fuel and fire safety [52-57]. It was of initial interest to the SF-BREEZE project, because aluminum was used as the material for the Top Deck (to reduce weight), but aluminum is not a structurally strong as steel in traditional (diesel) fires, which initially raised some concerns. Indeed, as specified by Alcan [58], "if a load-bearing structure made from age hardened aluminum alloys is exposed to temperature above 150 °C for several hours, then the residual mechanical characteristics of components made from alloys belonging to the 6000 series will have to be tested after fire." It turns out that the U.S. Coast Guard does not consider the spilling and ignition of the entire fuel complement to be a credible accident scenario for the SF-BREEZE, because there is no history of LH_2 tanks catastrophically failing in this way. Nonetheless, considering this scenario pulls together the hydrogen and methane physical and combustion properties discussed thus far into a worked

example.

The energy produced by burning 1200 kg of H_2 is 143,952 MJ, using a LHV value of 119.96 MJ/kg for hydrogen. In the 1982 A.D. Little study [10] of crash scenarios for LH_2 aircraft, predictions were made for pool diameters, duration and flame heights for such an accident. According to the Little study, 4.5% of the hydrogen combustion energy is converted to thermal radiation (radiant fraction = 0.045). Thus, the thermal energy radiated from burning the 1200 kg of hydrogen from the SF-BREEZE would be 6477.8 MJ. The Little modeling work predicts that spilling 1200 kg (16.90 m^3) of LH_2 would result in a pool of radius of 7.5 m, yielding a pool fire of duration 7.2 seconds, and a flame height of 105 m. Given these dimensions for the fire column, and the 6477.8 MJ of radiant energy, the emissive power of the hydrogen fire would be 169.8 kW/m^2 averaged over the entire flame surface during the fire duration of 7.2 seconds. These estimates for the pool diameter and duration for an LH_2 pool fire are consistent with estimates inferred from the cryogen spill investigations and modeling of Verfondern and Dienhart [22]. The result of the instantaneous spill and ignition is to produce a very tall fire. Tall fires do exist, as shown in Figure 10 for a 10-m diameter LNG (consisting of 99% methane) pool fire from the recent Sandia Phoenix tests [56].

The average concentration of hydrogen within the 105 m tall and 15 m diameter combustion column would be 41.9%, well within the LFL – UFL range for hydrogen. The radiant fraction estimated by Little for hydrogen is in reasonable accord with the expectations (13 msec) for the flame residence time calculated for a hydrogen fire column of the dimensions given.

The combustion column is so tall because hydrogen gas is so buoyant. As a result, most of the thermal radiation emitted from the flame surface is directed well above and away from the vessel, with only a small fraction directed downward towards the deck. The percentage of the entire flame area at the base of the fire column is 3.3%. Therefore, thermal radiation directed from the fire to the deck is 213.7 MJ. None of this IR radiation is absorbed directly by the LH_2 pool, because hydrogen is inactive in the IR. The lack of IR absorption by LH_2 pools is an important consideration for quantitative models of LH_2 pool fires. The 213.7 MJ of IR radiation directed downwards passes through the LH_2 pool and strikes the aluminum deck that can absorb the IR radiation. Assuming a conservative (more highly absorbing) emissivity value of 0.4 for aluminum [59], the total thermal energy absorbed by the aluminum Top Deck is 85.5 MJ.

Figure 10: A 10-m diameter LNG pool fire from the Sandia Phoenix Tests. Figure reproduced from Reference 56.

When LH_2 spills (instantaneously in this example) onto the Top Deck of the SF-BREEZE, the hydrogen cools the aluminum deck via the enthalpy of vaporization of the liquid. For a conservative estimate (one that leads to the least cooling, and therefore the highest final temperature for the aluminum) we assume a liquid initially at 29 K under pressure, for which the enthalpy of vaporization is 323.9 kJ/kg. Thus, 388 MJ is needed to fully evaporate the 1200 kg of LH_2 fuel. With the dimensions of the Top Deck being 0.794 cm thick, with an area of 162.5 m^2, there is sufficient thermal energy contained in the structure to evaporate all the LH_2. Using the temperature-dependent heat capacity of aluminum, we estimate the final aluminum deck temperature induced by spilling the cryogenic LH_2 fluid would be 168 K.

With 85.5 MJ of radiant energy available to warm up the deck, combined with the energy required to evaporate the LH_2 (which initially cooled the deck) we calculate the final temperature to be 199 K after the sequential LH_2 spill and fire. Thus, through spilling and igniting the LH_2 fuel load on the SF-BREEZE, the final temperature of the deck is below room temperature. There is no structural risk to the aluminum deck, since the temperature during the spill/fire never approaches 150 °C. There is no risk of brittle fracture, since the aluminum Top Deck is not susceptible to brittle fracture [19].

One can perform a similar analysis using an energy equivalent amount of LCH_4, namely 3198.90 kg of LCH_4. Assuming a fuel LHV of 45 kJ/kg to be representative of LNG, the energy produced by burning 3198.9 of methane is 143,952 MJ (same as for burning 1200 kg of hydrogen). Methane fires emit more thermal radiation, since the fuel is based on carbon. We adopt a radiant fraction of 0.10 for methane combustion. Thus, the thermal energy radiated from burning the 3198.9 kg of methane would be 14,395.2 MJ. Scaling results from the analyses of Verfondern and Dienhart [22] we estimate this quantity of LNG would occupy a diameter of 14.0 m and the pool would last 12.3 seconds on the deck. If the fire column height were 87 m (shorter than for H_2 because methane is less buoyant), then the flame surface, for this duration,

would have an emissive power of 286 kW/m^2, which is what has been measured in the Phoenix LNG pool fire tests [56].

Note that the average concentration of methane within a column that was 87 m tall and 14 m in diameter would be 25%, outside the UFL range for methane. However, there is little doubt the combination of ignition and density fluctuations within the vapor above the pool would lead to full column combustion. The radiant fraction of 0.10 estimated for methane is in accord with the expectations (34 milliseconds) for the flame residence time calculated for a methane fire column of the dimensions given.

The percentage of the entire methane flame area at the base of the column is 3.7%. Therefore, thermal radiation directed from the fire to the deck is 533 MJ. This value is higher than for hydrogen because of the higher radiant fraction for methane combustion. Unlike the case for hydrogen, LCH_4 is capable of absorbing IR radiation because CH_4 vibrations do involve the creation of a dipole moment. We will ignore this for the present, and assume that all the IR is directed onto the aluminum deck. Assuming an emissivity of 0.4 for the IR emissivity of aluminum, the total thermal energy absorbed by the aluminum deck is 213 MJ.

When LNG spills (instantaneously in this example) on the Top Deck of the SF-BREEZE, the liquid methane cools the aluminum deck via the enthalpy of vaporization of the liquid. Using the ΔH_{vap} value for LCH_4 of 531 kJ/kg, to evaporate 3198.90 kg of LCH_4 requires 1698 MJ of thermal energy from the SF-BREEZE aluminum deck. This is much larger than the 388 MJ needed to vaporize the LH_2, because the stronger intermolecular forces for methane lead to its higher enthalpy of vaporization. Because the ΔH_{vap} of LCH_4 is so much larger than that for LH_2, the aluminum deck will be cooled down to 111 K, the boiling temperature of LNG, and there will still be LNG left over.

With 213 MJ of radiant energy available from the methane fire to warm up the deck, combined with the energy required to evaporate the LNG (which initially cooled the deck) we can calculate the final temperature to be 198 K, again below room temperature. This is actually quite similar to that calculated for LH_2 (199 K). As was the case with LH_2, there is no structural risk to the Al deck, since the temperature during the spill/fire never approaches 150 °C. There is no risk of brittle fracture, since aluminum does not suffer this materials failure mode [19].

The LH_2 and LNG spill/ignition scenarios produce very similar final temperatures (199 K for LH_2, 198 K for LNG). This is because the 1200 kg of LH_2 cools the 0.794-cm thick aluminum deck less (via its lower ΔH_{vap}) and heats the deck less (via its lower radiant fraction) than the case for spilling and burning 3198.9 kg of LNG. Liquid methane cools the deck significantly more (via its larger ΔH_{vap}), but also warms the deck significantly more (via its larger radiant fraction), with the two effects balancing to produce a similar final aluminum deck temperature as for LH_2.

The Hindenburg

When considering hydrogen for a new application, for example as a propulsion fuel in the high-speed ferry SF-BREEZE, the existing community for that application usually references the Hindenburg accident in 1937 as a concern for hydrogen use in general. Most people have seen the newsreel images from the accident that tragically claimed the lives of 35 people. In discussions with the maritime community, a common misconception is that the Hindenburg exploded. With the hydrogen combustion properties now sufficiently described, one can look again at the Hindenburg accident with an eye toward the combustion phenomena involved.

It is clear from the photographic record of the event that the accident consisted of a fire, not an explosion. Unlike explosions that are extremely fast (see Figure 9), the airship initially stayed aloft while burning. This is consistent with a fire. The burning airship descended tail-first, because there was still unburned hydrogen in the nose of the airship, due to the relatively slow flame velocity. This also is consistent with a fire. Since the airship provided confinement of the hydrogen, we can conclude that a weak ignition source initiated the hydrogen combustion, not a strong ignition source that would have produced a detonation. Furthermore, there is no evidence for a DDT from the film record of the event. The lack of explosion and the presence of an ordinary fire do not make the accident any less tragic. Fires are dangerous too, and all effort needs to be directed to preventing hydrogen-based fires. Vessel designs that prevent fires also work to prevent other more dangerous events such as DDT or direct detonation.

In discussions with the maritime community, it has been helpful to provide context for the Hindenburg accident. The Hindenburg held ~15 times more H_2 than the SF-BREEZE. The method of storing hydrogen for the airship (rubberized gas bags) bears no resemblance to the engineered and rugged DOT-approved stainless steel LH_2 tanks in use on the roads today and used in the SF-BREEZE design. Over the past 60 years, NASA has mastered the use of hydrogen, the "signature fuel" of the American Space Program [60]. The Space Shuttle held 102,900 kg of LH_2, 86 times more than the SF-BREEZE [61]. Although there have been two tragic accidents involving the Space Shuttles Challenger and Columbia, these accidents did not originate from the onboard storage or use of LH_2.

Through science-based safety engineering and a sound

understanding of hydrogen physical and combustion phenomena, hydrogen technology can be used safely in maritime applications. The 50-year record of transporting LNG throughout the world is excellent: 8 accidents involving spills, with no fires and no fatalities [62]. Since LH_2 and LNG are very similar in their physical and combustion properties, minor augmentation of the proven and effective international regulations for LNG transport will enable regulated and safe use of hydrogen fuel cell technology in maritime applications such as the SF-BREEZE high-speed fuel-cell ferry.

Summary

The safety-related physical and combustion properties of LH_2 and LNG have been reviewed in the context of the SF-BREEZE high-speed fuel-cell ferry. Due to weaker interaction between molecules, LH_2 is colder than LNG, and evaporates more easily. If spilled, LH_2 cools surfaces less than LNG due to its smaller enthalpy of vaporization, ΔH_{vap}. LH_2 spills are smaller and shorter-lived compared to energy-equivalent LNG spills. LH_2 pool dispersal times for the full 1200 kg of LH_2 spilled on the SF-Breeze deck would be ~ 6 sec, with a cryogenic pool radius of ~ 8 m. Permeability is not a leak issue for hydrogen or LNG piping. Hydrogen embrittlement is surmounted by using 304 and 316 stainless steel components for hydrogen rated hardware. Hydrogen embrittlement does not exist for LNG because methane does not dissociate on the iron-based surfaces (e.g. stainless steel) of pipelines and conventional storage tanks.

LH_2 and LNG are similar in their combustion properties, with hydrogen having a wider flammability range. Vapors of both are easily ignited by weak (thermal) ignition sources and become flammable at low percent volume mixtures with air. H_2 and NG vapors can both directly explode, but require confinement with a geometry larger than the detonation cell size, a strong (shock wave) initiation source and a fuel/air mixture in the LEL – UEL range for direct detonation. Both fuels can experience DDT depending on the geometry with hydrogen being more susceptible to DDT than methane due in part to its smaller detonation cell size. DDT would be unlikely in the SF-BREEZE application (even in the event of failures in the H_2 leak detection, H_2 shut-off and ventilation systems) because of the lack of confinement on the Top Deck, limited "run-up" distances and the reduced physical dimensions in the Starboard and Port Fuel Cell Rooms that also limit "run-up." LH_2 fires burn out faster than LNG fires, and produce significantly less thermal radiation, with the hydrogen fire thermal radiation also strongly absorbed by humidity in the air. In a hypothetical scenario (judged not to be a credible accident threat by the U.S. Coast Guard) where the entire 1200 kg fuel complement of the SF-BREEZE were released and ignited, the temperature of the Top Deck would still be below room temperature due to the combined effects of cryogenic cooling and hydrogen fire radiant heating. Although an analogous LNG spill would cool the aluminum deck more, the higher radiant flux would heat the deck more, producing a similar final temperature. The results show it is safe to use aluminum for the Top Deck of the SF-BREEZE from the point of view of large fuel pool fires because the Top Deck does not approach 150 °C if the fuel complement were spilled and ignited.

Since LH_2 and LNG are similar in their physical and combustion properties, they pose similar safety risks. For both LH_2 and LNG ships, precautions are needed to avoid fuel leaks, minimize ignition sources, minimize run-up distances and confined spaces through design, provide ample ventilation for confined spaces, and monitor the enclosed spaces to ensure any fuel accumulations are detected and controlled (via H_2 supply shutoff) far below the fuel/air mix thresholds for any type of combustion.

Acknowledgements

The authors thank Samantha Lawrence and Paul Gibbs (both at Sandia), as well as Jay Keller (Zero Carbon Energy Solutions), Kyle McKeown (Linde), Dave Farese and Brian O'Neil (Air Products), Jim Mullen (Gardner Cryogenics), Karl Verfondern (Research Center Julich) and James Fesmire (NASA) for very helpful discussions. The U.S. Department of Transportation (DOT), Maritime Administration (MARAD) funded the SF-BREEZE project through MARAD's Maritime Environmental and Technical Assistance (META) program. The authors gratefully acknowledge Sujit Ghosh (MARAD) for skillfully managing the project. The work was performed at Sandia National Laboratories, which is a multi-program laboratory managed and operated by Sandia Corporation, a wholly owned subsidiary of Lockheed Martin Corporation, for the U.S. Department of Energy's National Nuclear Security Administration under contract DE-AC04-94AL85000.d

References

[1]. J. Keller, L. Klebanoff, S. Schoenung and M. Gillie, "*The Need for Hydrogen-based Energy Technologies in the 21st Century*", Chapter 1 in Hydrogen Storage Technology, Materials and Applications, Ed. L.E. Klebanoff (Boca Raton: Taylor & Francis; 2012), p. 3.

[2]. L. Klebanoff, J. Keller, M. Fronk and P. Scott, "*Hydrogen Conversion Technologies and Automotive Applications*," Chapter 2 in Hydrogen Storage Technology, Materials and Applications, Ed. L.E. Klebanoff (Boca Raton: Taylor & Francis; 2012),

p. 31.

[3]. J.W. Pratt and L.E. Klebanoff, "*Feasibility of the SF-BREEZE: a Zero Emission, Hydrogen Fuel Cell, High-speed Passenger Ferry,*" Sandia National Laboratories Report #: SAND2016-9719, September 2016.

[4]. J. Hord, "*Is Hydrogen a Safe Fuel?*," Int. J. Hydrogen Energy **3**, 157-176 (1978).

[5]. T.D. Donakowski, "*Is Liquid Hydrogen Safer Than Liquid Methane?,*" Fire Technology **17**, 183-188 (1981).

[6]. G.D. Brewer, "*An Assessment of the Safety of Hydrogen-Fueled Aircraft,*" J. Aircraft **20**, 935-939 (1983).

[7]. G.D. Brewer, "*Hydrogen Aircraft Technology,*" (CRC Press, Boca Raton, 1991).

[8]. A.D. Little, Inc., "*Final Report On An Investigation of Hazards Associated with the Storage and Handling of Liquid Hydrogen,*" Report to the U.S. Air Force, C-61092, (1960).

[9]. L.H. Cassutt, F.E. Maddocks, W.A. Sawyer, "*A Study of the Hazards in Storage and Handling of Liquid Hydrogen,*" Report to the U.S. Air Force, Report No. 61-05-5182, (1964).

[10]. A.D. Little, Inc., "*An Assessment of the Crash Fire Hazard of Liquid Hydrogen Fueled Aircraft*," Final Report to the National Aeronautics and Space Administration, NASA CR-165526 (1982).

[11]. A. Contreras, S. Yigit, K.Ozay and T.N. Veziroglu, "*Hydrogen as Aviation Fuel: A Comparison with Hydrocarbon Fuels,*" Int. J. Hydrogen Energy **22**, 1053-1060 (1997).

[12]. G.A. Karim, "*Some Considerations of the Safety of Methane, (CNG), as an Automotive Fuel- Comparison with Gasoline, Propane and Hydrogen Operation,*" SAE Technical Paper Series 830267 (1983).

[13]. See for example: M. Hajbabaei, G. Karavalakis, K.C. Johnson, L. Lee and T.D. Durbin, "*Impact of Natural Gas Fuel Composition on Criteria, Toxic and Particle Emissions from Transit Buses Equipped with Lean Burn and Stoichiometric Engines,*" Energy **62**, 425-434 (2013).

[14]. J.D. Naber, D.L. Siebers, S.S. DiJulio and C.K. Westbrook, "*Effects of Natural Gas Composition on Ignition Delay Under Diesel Conditions,*" Combustion and Flame **99**, 192-200 (1994).

[15]. S. Bates and D.S. Morrison, "*Modelling the Behavior of Stratified Liquid Natural Gas in Storage Tanks: A Study of the Rollover Phenomenon*," Int. J. Heat Mass Transfer **40**, 1875-1884 (1997).

[16]. The densities of cold hydrogen and methane gases are taken from the NIST database: http://webbook.nist.gov/cgi/fluid.cgi?T=160+K&PLow=0.99+atm&PHigh=1.03+atm&PInc=.1&Applet=on&Digits=5&ID=C74828&Action=Load&Type=IsoTherm&TUnit=K&PUnit=atm&DUnit=kg%2Fm^3&HUnit=kJ%2Fmol&WUnit=m%2Fs&VisUnit=uPa*s&STUnit=N%2Fm&RefState=DEF).

[17]. B. Bowman and L. Klebanoff, "*Historical Perspectives on Hydrogen, Its Storage, and Its Applications*," Chapter 3 in Hydrogen Storage Technology, Materials and Applications, Ed. L.E. Klebanoff (Boca Raton: Taylor & Francis; 2012), p. 65.

[18]. R.E. Reed-Hill and R. Abbaschian, "*Physical Metallurgy Principles,*" (PWS Publishing, Boston, 1994), p.740.

[19]. M.G. Zabetakis, "*Safety with Cryogenic Fluids,*" (Plenum, New York, 1967), p. 25.

[20]. R.D. Witcofski and J.E. Chirivella, "*Experimental and Analytical Analyses of the Mechanisms Governing the Dispersion of Flammable Clouds Formed by Liquid Hydrogen Spills,*" Int. J. Hydrogen Energy **9**, 425-435 (1984).

[21]. K. Verfondern and B. Dienhart, "*Experimental and Theoretical Investigations of Liquid Hydrogen Pool Spreading and Vaporization*," Int. J. Hydrogen Energy **22**, 649-660 (1997).

[22]. K. Verfondern and B. Dienhart, "*Pool Spreading and Vaporization of Liquid Hydrogen,*" Int. J. Hydrogen Energy **32**, 2106 – 2117 (2007).

[23]. P. Middha, M. Ichard and B. J. Arntzen, "*Validation of CFD Modelling of* LH_2 *Spread and Evaporation Against Large-scale Spill Experiments,*" Int. J. Hydrogen Energy **36**, 2620-2627 (2011).

[24]. C. San Marchi, B.P. Somerday and S.L. Robinson, "*Permeability, Solubility and Diffusivity of Hydrogen Isotopes in Stainless Steels at High Gas Pressures,*" Int. J. Hydrogen Energy **32**, 100-116 (2007).

[25]. G. Wedler and M. Mengel, "*The Adsorption of Methane on Polycrystalline Iron Films*," Surface Science **131**, L423-L428 (1983).

[26]. D.C. Sorescu, "*First-principles Calculations of the Adsorption and Hydrogenation Reactions of* CH_x *(x = 0, 4) Species on a Fe(100) Surface,*" Phys. Rev. B **73**, 155420 (2006).

[27]. A. Staykov, J. Yamabe and B.P. Somerday, "*Effect of Hydrogen Gas Impurities on the Hydrogen Dissociation on Iron*

Surface," Int. J. Quantum Chemistry **114**, 626-635 (2014).

[28]. F. Bozso, G. Ertl, M. Grunze and M. Weiss, "*Chemisorption of Hydrogen on Iron Surfaces,*" Appl Surf. Sci. **1**, 103-119 (1977).

[29]. The hydrogen embrittlement of metals is extensively reviewed in the books: "*Gaseous Hydrogen Embrittlement of Materials in Energy Technologies,*" Vol. 1 and 2, ed. R.P. Gangloff and B.P. Somerday (Woodhead Publishing Ltd., Cambridge, 2012).

[30]. Kyle McKeown (Linde), private communication to L.E. Klebanoff on November 2, 2015.

[31]. Some of the gaseous hydrogen properties listed are from: L.M. Das, "*Hydrogen Engines: A View of the Past and a Look Into the Future,*" Int. J. Hydrogen Energy **15**, 425-443 (1990).

[32]. F.L. Dryer, M. Chaos, Z. Zhao, J.N. Stein, J.Y. Alpert and C.J. Homer, "*Spontaneous Ignition of Pressurized Releases of Hydrogen and Natural Gas into Air,*" Combust. Sci. and Tech. **179**, 663-694 (2007).

[33]. G.R. Astbury and S.J. Hawksworth, "*Spontaneous Ignition of Hydrogen Leaks: A Review of Postulated Mechanisms,*" Int. J. Hydrogen Energy **32**, 2178-2185 (2007).

[34]. T. Mogi, Y. Wada, Y. Ogata and A. K. Hayashi, "*Self-ignition and Flame Propagation of High-pressure Hydrogen Jet During Sudden Discharge from a Pipe,*" Int. J. Hydrogen Energy **34**, 5810-5816 (2009).

[35]. K.L. Cashdollar, I.A. Zlochower, G.M. Green, R.A. Thomas and M. Hertzberg, "*Flammability of Methane, Propane and Hydrogen Gases,*" J. Loss Prevention in the Process Industries **13**, 327-340 (2000).

[36]. R.W.Schefer, G.H. Evans, J. Zhang, A.J. Ruggles and R. Greif, "*Ignitability Limits for Combustion of Unintended Hydrogen Releases: Experimental and Theoretical Results,*" Int. J. Hydrogen Energy **36**, 2426-2435 (2011).

[37]. H.D. Ng and J.H.S. Lee, "*Comments on Explosion Problems for Hydrogen Safety*," J. Loss Prevention in the Process Industries," **21**, 136-146 (2008).

[38]. A. Luketa and T. Blanchat, "*The Phoenix Series Large Scale Methane Gas Burner Experiments and Liquid Methane Pool Fire Experiments on Water,*" Combustion and Flame **162**, 4497-4513 (2015).

[39]. H. Matsui and J.H. Lee, "*On the Measure of the Relative Detonation Hazards of Gaseous Fuel-Oxygen and Air Mixtures,*" Symposium (International) on Combustion **17**, 1269-1280 (1979).

[40]. J.M. Yang, "*An Improved Analytical Approach to Determine the Explosive Effects of Flammable Gas-Air Mixtures*," Report UCRL-TR-217005 Lawrence Livermore National Laboratory, November 2005 (available from osti.gov).

[41]. R. Knystautas, C. Guirao, J.H. Lee and A. Sulmistras, "*Measurements of Cell Size in Hydrocarbon-Air Mixtures and Predictions of Critical Tube Diameter, Critical Initiation Energy and Detonability Limits*," Progress in Astronautics and Aeronautics, Volume 94, American Institute of Aeronautics and Astronautics (AIAA), 1984.

[42]. M.P. Sherman, S.R. Tieszen and W.B. Benedick, "*FLAME Facility: The Effect of Obstacles and Transverse Venting on Flame Acceleration and Transition to Detonation for Hydrogen-Air Mixtures at Large Scale,*" Sandia National Laboratories Report SAND85-1264 R3, 1989.

[43]. S.B. Dorofeev, V.P. Sidorov, A.E. Dvoinishnikov and W. Breitung, "*Deflagration to Detonation Transition in Large Confined Volume of Lean Hydrogen-Air Mixtures,*" Combustion and Flame **104**, 95-110 (1996).

[44]. E.S. Oran and V.N. Gamezo, "*Origins of the Deflagration-to-Detonation Transition in Gas-phase Combustion*," Combustion and Flame **148**, 4 – 47 (2007).

[45]. C.T. Johansen and G. Ciccarelli, "*Visualization of Unburned Gas Flow Field Ahead of An Accelerating Flame in an Obstructed Square Channel,*" Combustion and Flame **156**, 405-416 (2009).

[46]. D.A. Kessler, V.N. Gamezo and E.S. Oran, "*Simulations of Flame Acceleration and Deflagration-to-Detonation Transitions in Methane-Air Systems,*" Combustion and Flame **157**, 2063-2077 (2010).

[47]. P. Middha and O.R. Hansen, "*Predicting Deflagration to Detonation Transition in Hydrogen Explosions,*" Process Safety Progress **27**, 192 -204 (2008).

[48]. M. Groethe, E. Merilo, J. Colton, S. Chiba, Y. Sato and H. Iwabuchi, "*Large-scale Hydrogen Deflagrations and Detonations,*" Int. J. Hydrogen Energy **32**, 2125-2133 (2007).

[49]. D.C. Tilotta, K.W. Busch and M.A. Busch, "*Fourier Transform Flame Infrared Emission Spectroscopy,*" Applied Spectroscopy **43**, 704-709 (1989).

[50]. C.J. Gerritsma and J.H. Haanstra, "*Infrared Transmission*

of Air Under Laboratory Conditions," Infrared Physics **10**, 79-90 (1970).

[51]. F. David Wayne, "*An Economical Formula for Calculating Atmospheric Infrared Transmissivities,*" J. Loss Prev. Process Ind. **4**, 86 - 92 (1991).

[52]. V. Babrauskas, "*Estimating Large Pool Fire Burning Rates*," Fire Technology **19**, 251 – 261 (1983).

[53]. D.W. Hissong, "*Keys to Modeling LNG Spills on Water,*" J. Hazardous Materials **140**, 465-477 (2007).

[54]. A. Luketa-Hanlin, "*A Review of Large-scale LNG Spills: Experiments and Modeling*," J. Hazardous Materials **A132**, 119-140 (2006).

[55]. J.A. Fay, "*Model of Large Pool Fires,*" J. Hazardous Materials **B136**, 219-232 (2006).

[56]. A. Luketa, "*Recommendations on the Prediction of Thermal Hazard Distances from Large Liquefied Natural Gas Pool Fires on Water for Solid Flame Models,*" Sandia National Laboratories Report SAND2011-9415, (2011).

[57]. P.K. Raj, "*Large Hydrocarbon Pool Fires: Physical Characteristics and Thermal Emission Variations with Height,*" J. Hazardous Materials **140**, 280-292 (2007).

[58]. A summary of the fire properties of Aluminum has been written by Alcan Marine, and can be found at: http://www.ansatt.hig.no/henningj/materialteknologi/Lettvektdesign/Al%20and%20the%20sea/Alcan+anglais+chap.09.pdf

[59]. C.-D. Wen and I. Mudawar, "*Emissivity Characteristics of Roughened Aluminum Alloy Surfaces and Assessment of Multispectral Radiation Thermometry (MRT) Emissivity Models,*" Int. J. of Heat and Mass Transfer **47**, 3591-3605 (2004).

[60]. A description of LH_2 becoming the signature fuel for NASA can be found at: http://www.nasa.gov/topics/technology/hydrogen/hydrogen_fuel_of_choice.html

[61]. James Fesmire (NASA), private communication to J.W. Pratt on April 22, 2016.

[62]. M. Hightower, L. Gritzo, A. Luketa-Hanlin, J. Covan, S. Tieszen, G. Wellman, M. Irwin, M. Kaneshige, B. Melof, C. Morrow and D. Ragland, "*Guidance on Risk Analysis and Safety Implications of a Large Liquefied Natural Gas (LNG) Sill Over Water,*" Sandia National Laboratories Report: SAND2004-6258, December (2004).

(This page left intentionally blank.)

Appendix: B

17003.01 Glosten | Sandia Zero-V Design Study Report

(This page left intentionally blank.)

Glosten

SANDIA ZERO-V

DESIGN STUDY REPORT

PREPARED FOR

SANDIA NATIONAL LABORATORIES
LIVERMORE, CALIFORNIA

25 NOVEMBER 2017
FILE NO. 17003.01
REV. A

PREPARED

Digitally Signed 26-Nov-2017

ROBER T. MADSEN, PE

PROJECT ENGINEER

CHECKED

Digitally Signed 26-Nov-2017

SEAN A. CAUGHLAN, PE

PROJECT ENGINEER

APPROVED

Digitally Signed 27-Nov-2017

TIMOTHY S. LEACH, PE

PRINCIPAL-IN-CHARGE

ROBERT T. MADSEN
STATE OF WASHINGTON
48955
REGISTERED
PROFESSIONAL ENGINEER

Digitally Signed 27-Nov-2017

Table of Contents

Revision History

Section	Rev	Description	Date	Approved
All	-	Initial Issue.	11/22/17	TSL
4.7	A	Added Section 4.7	11/25/17	TSL

References

1. Rules for Classification: Ships, Part 6 Chapter 2, Propulsion, power generations, and auxiliary systems, DNV GL, January 2017
2. International Code of Safety for Ships Using Gases or Other Low-Flashpoint Fuels (IGF Code) as Amended by Resolution MSC.391 (95), International Maritime Organization (IMO)
3. Zero-V, General Arrangement, Glosten, Drawing No. 17003.01-070-01, Rev -, 2017
4. Zero-V, Preliminary Hazardous Zone Plan, Glosten, Drawing No. 17003.01-0-01, Rev -, 2017
5. Zero-V, Electrical One-Line Diagram, Glosten, Drawing No. 17003.01-300-01, Rev -, 2017
6. Zero-V, Concept Gas System Architecture, Glosten, Drawing No. 17003.01-540-01, Rev -, 2017
7. Fuel Cell Power Generation HyPM Rack, Hydrogenics Corp, October 2013
8. HyPM-R 30/60/90/120 kW (P/Ns 1045646/7/8/9) Specification Sheet, Hydrogenics Corp, 25 November 2014
9. HyPM® HD 30 (P/N 1042848) Specification Sheet, Hydrogenics Corp, 28 February 2014
10. *Resistance and Propulsion of Ships*, Harvald, Svend Aage, 1983.
11. *Principles of Naval Architecture,* Society of Naval Architecture, Volume II Resistance, Propulsion and Vibration, 1988.
12. Molland, AD; Wellicome, JF; Crouser, PR; "Resistance Experiments on a Systematic Series of High-speed Displacement Catamaran Forms: Variation of Length-Displacement Ratio and Breadth-Draught ratio", Trans. RINA, 1996.
13. *Weight Estimating and Margin Manual for Marine Vehicles*, International Society of Allied Weight Engineers, Inc., Recommended Practice Number 14, 22 May 2001.
14. Pratt, J. W; Klebanoff, L. E; *Feasibility of the SF-BREEZE: a Zero-Emission, Hydrogen Fuel Cell, High-Speed Passenger Ferry*, Sandia National Laboratories, September 2016.
15. Guidance related to Vessels and Waterfront Facilities Conducting Liquified Natural Gas (LNG) Marine Fuel Transfer (Bunkering) Operations, CG-OES Policy Letter 02-15, United State Coast Guard, 19 February 2015.
16. Guidelines for Liquefied Natural Gas Fuel Transfer Operations and Training of Personnel on Vessels Using Natural Gas as Fuel, CG-OES Policy Letter 01-15, United State Coast Guard, 19 February 2015.
17. *LNG Bunkering: Technical and Operational Advisory*, American Bureau of Shipping.

Executive Summary

Sandia National Laboratories (Sandia) in collaboration with the U.S. Department of Transportation Maritime Administration (MARAD) has been working to advance marine hydrogen fuel cell applications for a number of years. Previous projects have included fuel cell power for refrigerated intermodal shipping containers and a fuel cell passenger ferry feasibility study. Sandia seeks to build on these prior developments and tasked Glosten to assess the feasibility of a hydrogen fuel cell powered oceanographic research vessel, nicknamed the Zero-V.

Glosten, in partnership with the Scripps Institution of Oceanography (SIO), the DNV GL marine classification society, Sandia, and MARAD has established the fundamental requirements and regulatory framework for a ground-breaking design of a hydrogen fueled oceanographic research vessel for operations in the coastal waters of the State of California. A concept design using liquefied hydrogen fuel was developed in order to assess the feasibility of such a vessel. The design efforts examined the hydrogen storage and fuel systems, vessel arrangements, hydrogen safety, powering and operational performance, access to key ports of call, weights and stability, vessel cost, and regulatory requirements. Through this examination, it was determined that it is feasible to build and operate a zero-emissions hydrogen fuel cell powered coastal research vessel using commercially established technology. The resulting design of the Zero-V is a highly capable oceanographic research vessel meeting all the owner (SIO) requirements for diverse oceanographic work.

The vessel developed is a 170 foot aluminum trimaran. The design evolved to this size and type primarily from the space requirements for the storage of the hydrogen fuel. Because the trimaran design has a wide beam, it provides the stability needed for fuel storage tanks on the 01 Deck and also benefits from ample space for large laboratory, working, and accommodation spaces as well as high capability science mission equipment. The primary performance limitation is the range limit of 2,400 nautical miles, the minimum required based on the mission requirements from Scripps. The construction cost of the Zero-V, estimated at $76-82M, was found to be reasonable for a vessel of this size and capability when compared to other modern, diesel fueled, research vessels.

The design of the Zero-V was reviewed by both DNV GL and the United Stated Coast Guard to assess the regulatory feasibility. The process revealed gaps in applicability of current regulations to a hydrogen fueled vessel but uncovered no fundamental concerns for either the vessel design or a path to approval for such a novel vessel. Based on the design, DNV GL issued a conditional approval in principal (CAIP).

Overall, the design and review of the Zero-V has shown that from a technical and regulatory standpoint it is feasible to build and operate a zero-emissions hydrogen fuel cell powered coastal research vessel.

Section 1 Introduction

Sandia National Laboratories (Sandia) in collaboration with the U.S. Department of Transportation Maritime Administration (MARAD) has been working on the development of marine hydrogen fuel cell applications for a number of years. Previous projects have included hydrogen fuel cell power for refrigerated intermodal shipping containers and a fuel cell passenger ferry feasibility study. Sandia seeks to build on these prior developments with additional fuel cell vessel design development for differing types of vessels including an oceanographic research vessel.

Sandia's interest in a hydrogen fuel cell powered research vessel coincides with Scripps Institution of Oceanography's need for a new coastal research vessel and the University of California's Carbon Neutrality Initiative.

The Scripps Institution of Oceanography (Scripps) at the University of California San Diego is one of the world's premier oceanographic research institutions and operates fleet of research vessel from coastal to global class ships. Scripps' current coastal research vessel is the R/V *Robert Gordon Sproul.* Built in 1981, the R/V *Sproul* is nearing the end of its service life and will require replacement soon. Scripps and Sandia are both interested in exploring the feasibility of a new hydrogen fuel cell powered coastal research vessel to replace the R/V *Robert Gordon Sproul* and support the University of California's goals to reduce emissions of air pollutants and greenhouse gasses.

The purpose of this study was to evaluate the feasibility of a hydrogen fuel cell powered research vessel considering required vessel mission performance, cost, regulatory acceptance, and access to key ports of call.

Section 2 Vessel Requirements

The vessel requirements came from a combination of general requirements that are typical of oceanographic research vessels, specific requirements from Scripps to meet the requirements of a new California coastal research vessel, and facility limitations for intended operating locations.

The general vessel requirements are the following.

- US flagged.
- United States Coast Guard inspected vessel, 46 CFR Subchapter U oceanographic research vessel.
- Classed by DNV GL ✠ A1, E0, FC (Power), Gas Fueled, Battery (safety).
- Zero air emissions

Table 1 Science mission requirements

Cruise Speed	10 knots cruise, calm water
Speed in Seaway	12 knots, calm water (sprint) 9 knots, SS4 (sea state 4) 7 knots, SS5
Range	2,400 nm (nautical miles)
Station Keeping	2 knots beam current, 25 knots wind at best heading
Endurance	15 days
Main Lab Space	800 ft^2
Wet Lab Space	500 ft^2
Computer Lap Space	120 ft^2
Working Deck Space	1,200 ft^2
Portable Vans	2
Crew Berths	11
Scientist Berths	18
A-Frame	12,000 ST SWL (safe working load)
Main Crane	8,000 lbs @ 12' over the side
Portable Crane	4,000 lbs SWL
Side Frame	5,000 lbs SWL
Trawl Winch	10,000m 3/8 3x19 wire
Hydro Winch	10,000m 0.322 EM Wire, 10,000m 1/4 3x19 wire
Science Payload	50 LT

Scripps additionally provided operational profiles for 14 notional missions that the vessel must be capable of performing.

Table 2 Notional Science Missions

Mission	Length (Days)	Participants Science,	Techs	Number of Missions Per Year
Coastal Mooring	1	15	1	6
Deep Moorings (4000 m) & towed sonar	5	13	2	2
Mapping (multibeam & towed CHIRP)	5	7	1	2
Class cruise: biology	1	40	4	6
Class cruise: geology	1	40	4	6
Class cruise: ROV	1	20	4	4
ROV survey	7	12	4	2
Geology sampling	5	10	2	2
FLIP anchor handling	3	2	2	6
UAV flight ops (aerial drones)	4	10	1	2
AUV ops (Remus, Wave glider, Spray etc)	4	10	1	5
Physical oceanography	8	14	1	4
Biogeochemical survey	8	14	1	2

2.1 Dimensional Limitations

Other research institutions in addition to Scripps would use the Zero-V California coastal research vessel. Specifically the Moss Landing Marine Laboratory (MLML) located in Moss Landing Harbor in Monterey Bay, CA, would use the vessel frequently. The primary marine facility in Moss Landing Harbor is currently the Monterey Bay Aquarium Research Institute (MBARI). Accessing this facility imposes some dimensional constraints on the vessel, as the navigation channel in Moss Landing Harbor is narrow and relatively shallow. The MBARI pier is a horseshoe-shaped pier and the vessel would be required to tie up inside. Moss Landing Harbor and the MBARI pier can be seen in Figure 1. Accessing Moss Landing and the MBARI pier imposes the following maximum dimensions on the vessel.

Table 3 Dimension constraints for accessing MBARI pier

Dimension	Maximum
Length	170'
Beam	56'
Draft	12'

The MBARI Pier was found to be the most dimensionally restrictive of the expected ports of call. Designing the vessel to access MBARI guarantees its accessibility to other Ports such as the Mar-Fac Facility at Scripps, or Pier 54 in the Port of San Francisco, or Wharf 5 of the Port of Redwood City.

Figure 1 Moss Landing Harbor, Monterey Bay CA

(Imagery ©2017 Google, TerraMetrics, Data SCUMB SFML, CA OPC, Map Data ©2017 Google)

Section 3 Vessel Design

3.1 Hull Type

Hull type options for ocean-going vessels include monohulls, catamarans, and trimarans. Monohulls are the most common type of ocean-going vessel and the vast majority of large oceanographic research vessels are monohulls. There are, however, numerous ocean-going multi-hull vessels in service around world including some oceanographic research vessels. A monohull design for the Zero-V was initially investigated because it is the most conventional research vessel hull. However as the project progressed, it was apparent that the monohull design could not support the space needed for the hydrogen storage tanks while meeting both the vessel space requirements and the dimensional constraints. For this reason the design evolved to a trimaran design because it offers significantly more space on deck due to a greater beam. A catamaran hull was also considered but not pursued. The benefits, drawbacks, and limitations of each hull type as applicable to the Zero-V are discussed in more details in the following sections.

3.1.1 Monohull

Monohulls offer the largest amount of volume within the hull below the main deck and have relatively simple and efficient hull structure, making a monohull typically less expensive to build than a multihull of the same displacement. This is the primary reason that monohulls are the most common and conventional hull for large ocean-going research vessels. Additionally, monohulls of conventional proportions (ratios of length, beam, draft, and displacement) can have excellent seakeeping performance and maneuverability. However, monohulls are often stability limited. This is especially true of research vessels, which tend to have very large superstructures and deckhouses with a high center of gravity.

For the Zero-V it was determined that due to the large size of the hydrogen fuel storage tanks, the tanks would need to be located above deck rather than inside the hull. A monohull would not have the necessary stability to accommodate the substantial weight of the fuel tanks at a high location in the vessel. Increasing the stability would require unusual vessel proportions such as a very wide shallow hull, which would have significant adverse effects of the vessel's resistance as well as motions and seakeeping performance. For this reason, a monohull was not well suited for this particular vessel's requirements and constraints.

Figure 2 Monohull research vessel R/V *New Horizon* (photo from www.unols.org)

3.1.2 Catamaran

Catamarans are the most common multihull. They offer a wide vessel affording significantly more above-deck space compared to a monohull. Catamarans have excellent stability due to the wide separation of the waterplane areas (intersection area of the hull and the water) of the two hulls. This creates higher righting forces (forces restoring the vessel to vertical position) than can be achieved with a monohull of equal displacement. Catamarans are typically designed for high-speed operations with very slender hulls to reduce the vessel resistance at high speed. However, the slenderness of the hulls also causes catamarans to have much lower displacements and waterplane areas compared to similar sized monohulls, making them weight sensitive i.e. small changes in weight significantly affect the vessel's draft, heel and trim. Additionally, the slenderness of the hulls affords little space below decks for machinery, equipment, accommodations, or service spaces. While this is not a problem for a vessel like a passenger ferry, which is dominated by above-deck cabins, it makes the arrangement of a research vessel requiring large volumes both above and below the deck difficult. Another significant drawback of a conventional catamaran design is that they tend to have poorer seakeeping performance than both monohulls and trimarans and tend to have very abrupt motions. This is undesirable for a research vessel that requires the ability to perform work on deck and in the labs both on station and underway.

Figure 3 Catamaran passenger ferry

3.1.3 Trimaran

The trimaran design with a center hull and two smaller side hulls is something of a blend between the monohull and the catamaran. The center hull, while more slender than a monohull, still has substantial breadth and can accommodate the machinery, storage, control and science spaces that are typically located in the hull of a research vessel. Additionally the trimaran has a wide deck allowing for a large deckhouse and superstructure for accommodations, laboratory, and service spaces.

The trimaran has excellent stability characteristics due to the righting forces from the widely spaced water planes of the outer hulls. This allows the vessel to have a higher center of gravity than a monohull, thereby accommodating the fuel storage tanks in an elevated, above-deck location. The increased righting forces of the outer hulls does result in increased seakeeping motion responses, especially roll response in beam seas, when the direction of waves is coming from the side of the vessel. However, the seakeeping performance can still be excellent with greater than 95% vessel operability. Seakeeping is further discussed in Section 4.5.

Due to the slenderness of the outer hulls, the trimaran is more weight sensitive than a monohull. However, the substantial center hull mitigates this significantly, making the trimaran less weight-sensitive than a typical catamaran. Additionally because the Zero-V will operate at a relatively low speed for a trimaran, the hull can be fuller (less slender) than typical of a high-speed trimaran. This also serves to mitigate the sensitivity of the design to weight.

The design of the trimaran also results in significant directional stability, which is good for course-keeping but makes maneuvering more difficult than either a catamaran or a trimaran. This results in increased thrust required for station keeping and turning. However, these limitations can be overcome by proper selection and arrangement of maneuvering equipment such as high-lift rudders, bow thrusters, and stern thrusters, all of which are incorporated into the Zero-V design.

In the case of the Zero-V, the dimensional limitations of the vessel restricted the beam and therefore forced the hull spacing of the trimaran to be less than is optimal for resistance based on some of the design literature available. However, the impact of this on the Zero-V is estimated to be mitigated greatly by the relatively low speed operation of this vessel with the expectation that the hydrodynamic interaction between the hulls is less important at low speeds. Ultimately, it is expected that for the Zero-V operating conditions, the resistance of a monohull and a

trimaran of similar length and displacement is nearly equivalent. Resistance and powering is further discussed in Section 4.1.

Figure 4 Trimaran research vessel Zero-V

3.2 Arrangements

Arrangements for the vessel were developed to meet all of the space and volume requirements of the vessel as well as for fitment of the machinery, service, and control spaces necessary for operation of the vessel. Additionally, the arrangements consider the operations of the vessel such as access between science spaces, the working deck, and science handling systems as well as visibility and sight lines from control stations to the working areas and equipment. The arrangements also incorporate special requirements specific to the use of liquefied gas fuel. The most significant of these special requirements are hazardous areas, discussed in Section 3.7.2, and the restriction that the hydrogen storage tanks be located no closer to the sides of the vessel than 20% of the overall width (beam) of the vessel. For example if the vessel's beam is 50 feet, the hydrogen tanks shall be no closer than 10 feet from the sides of the vessel.

The Zero-V design follows traditional arrangements for a research vessel despite the trimaran hull type. The power plant, machinery, machinery operating station, stores, main winches, and scientific acoustic equipment are located below the main deck in the hull. The main deck contains the working deck, laboratories, main service spaces, and science berthing. The upper decks contain the crew berthing and navigation spaces. The major deviation from conventional research vessel arrangements is that the fuel storage is located on the 01 Deck rather than in the inner bottom of the hull.

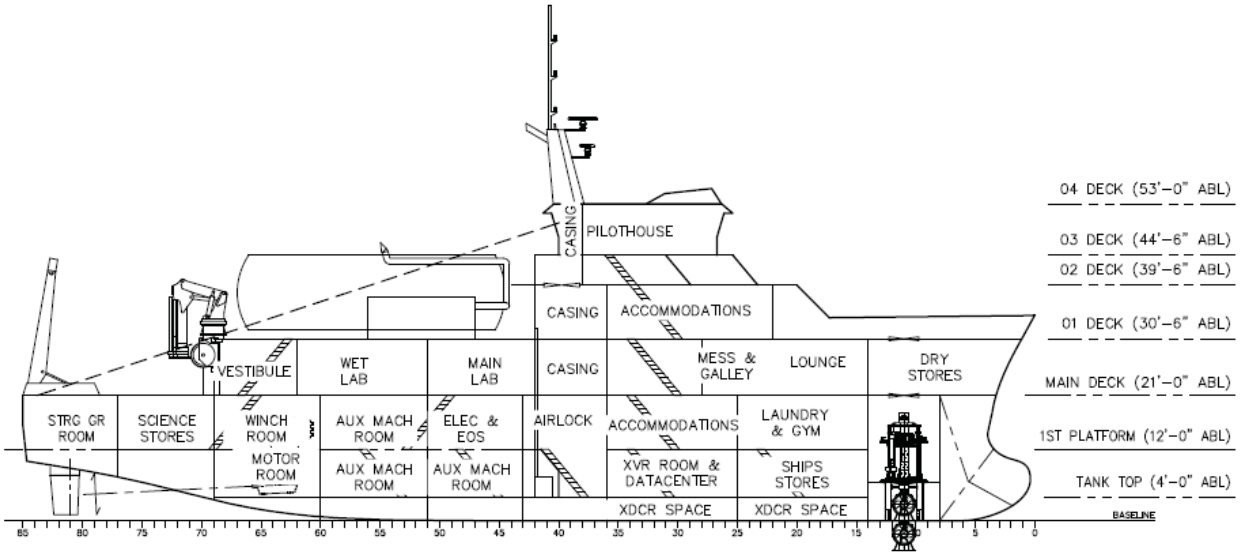

Figure 5 Zero-V Inboard Profile

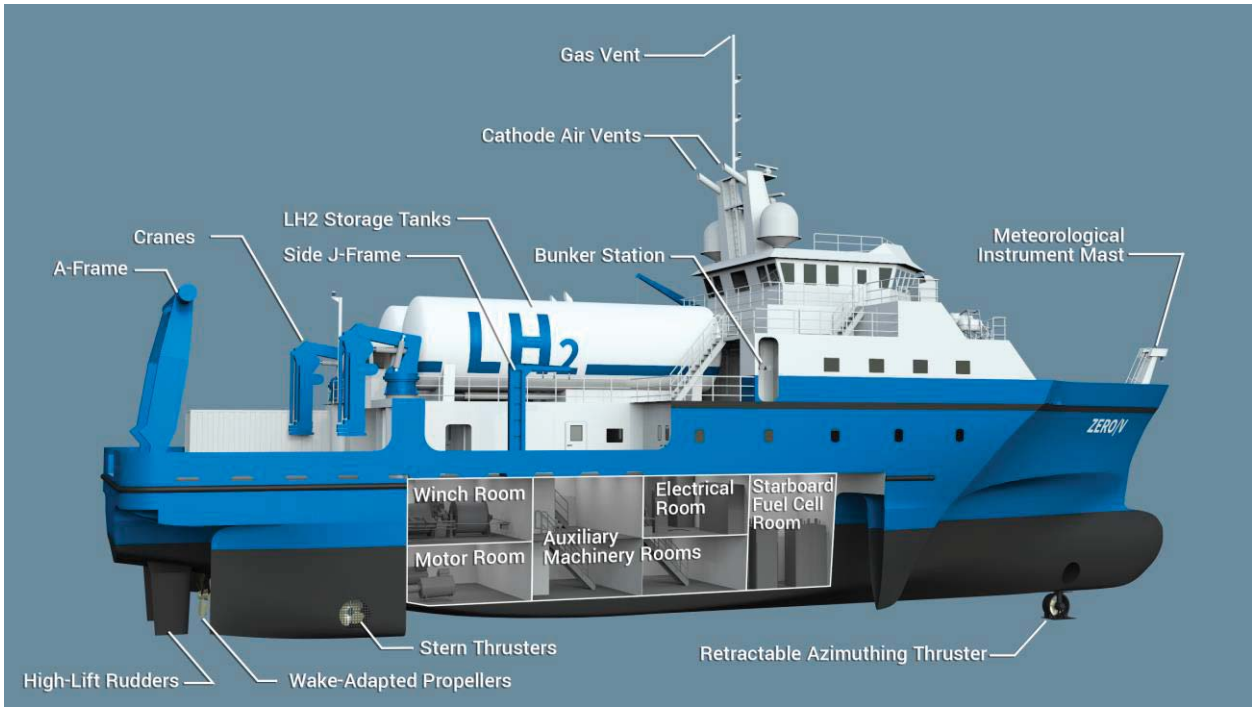

Figure 6 Zero-V 3D Arrangement

The location of the fuel storage was driven by a combination of factors. Conventionally, the diesel fuel oil tanks are in the inner bottom of the hull against the shell. These tanks therefore are of limited height and have odd but generally prismatic shapes. The diesel fuel storage is typically split into many tanks to accommodate the vessel watertight subdivision, arrangements, and stability limitations. Figure 7 shows an example diesel fuel oil storage arrangement with 11 storage tanks that is illustrative of a typical research vessel.

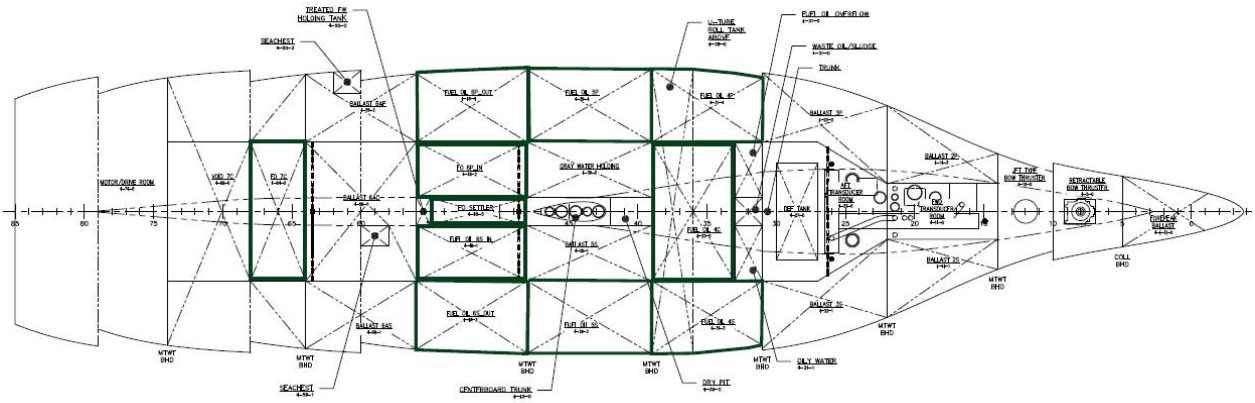

Figure 7 Example of typical inner bottom diesel fuel oil storage tank arrangement for a research vessel. (Diesel fuel tanks indicated with bold green outlines)

LH_2, because it is a cryogenic liquid stored at pressure, is stored in vacuum-insulated Type C cylindrical pressure vessels. The fitment of cylindrical type C storage tanks into a prismatic hull is both challenging and space inefficient. It is desirable to have fewer large LH_2 storage tanks because large diameter tanks are more volume, weight, and cost efficient. In addition, the heat leakage from large diameter LH2 tanks is, as a percentage of the amount of LH_2 stored, smaller than from smaller cryogenic vessels. Thus, undesirable "boil off" of the LH_2 is less for larger LH_2 tanks than for smaller tanks. Furthermore, the volumetric energy density (energy in the fuel per unit of volume) of LH_2 is 4.2 times lower than that of diesel fuel, making the amount of tankage for an equivalent fuel energy more than four times the volume. Because of these factors, it was found that the size of the storage fuel tanks required to meet range was too large to fit inside the hull of a vessel that met the dimensional limitations. For this reason, the fuel tanks are located above the deck in the weather. On research vessels, the Main Deck is the most valuable real estate for working and laboratory spaces. Because large storage tanks located on the Main Deck would be too disruptive to the working spaces and science operations, the tanks are located on the 01 Level aft weather deck.

Details of the vessel's arrangements can be seen in the General Arrangement Drawing in Appendix A.

3.3 Propulsion System

3.3.1 Objectives and Requirements

The primary objective of the propulsion system selection is to allow the vessel to achieve the mission and design requirements given in Section 2. An electric, direct drive, twin propeller arrangement was selected. In this arrangement, each propeller shaft is directly driven by a high-torque permanent magnet motor. This arrangement is simple, efficient, and quiet. An integrated hydrogen fuel cell electric plant provides both propulsion and ship service electrical power.

To provide the required position keeping ability for on-station science work, the vessel is fitted with a retractable azimuthing (rotating 360 degrees) bow thruster as well as stern thrusters in each outer hull. These thrusters provide thrust at the bow and stern ends of the vessel to help control the ship's heading and position during maneuvering, docking, and station keeping. Additionally, high-lift flap rudders are provided to maximize steering forces produced from the main propellers during station keeping.

Table 4 summarizes the propulsion equipment specifications.

Table 4 Propulsion system equipment

Equipment	Type	Description
Electrical Power	10 fuel cell racks	Each Rack contains six (6) FC modules. Each FC module delivers 30 kW (kilowatts), for a total rack power of 180 kW, and a total installed power of 1,800 kW.
Propulsion Motors	Two (2) electric motors	High torque permanent magnet, 500 kW
Bow Thruster	One (1) retractable azimuthing thruster	Fixed pitch ducted propeller, electric motor driven L-drive, 500 kW
Stern Lateral Thrusters	Two (2) identical tunnel thrusters	Fixed pitch, mounted in side hulls, 500 kW
Propellers	Two (2) identical fixed pitch propellers	Approx. 2.1 m in diameter
Rudders	Two (2) identical, high-lift rudders	Flap type

The propulsion system block diagram showing the main propulsion switchboard (SWBD) and the ship service switchboard is depicted in Figure 8. The propulsion switchboard provides power to all the major propulsion loads and well as to the ship service switchboard. The ship service switchboard provides power to the vessel's auxiliary equipment, hotel, and lighting systems. The propulsion system is configured to provide redundancy and flexibility for different operating conditions. This creates a capable propulsion system that can operate efficiently for the varied operational and mission demands of a general-purpose research vessel.

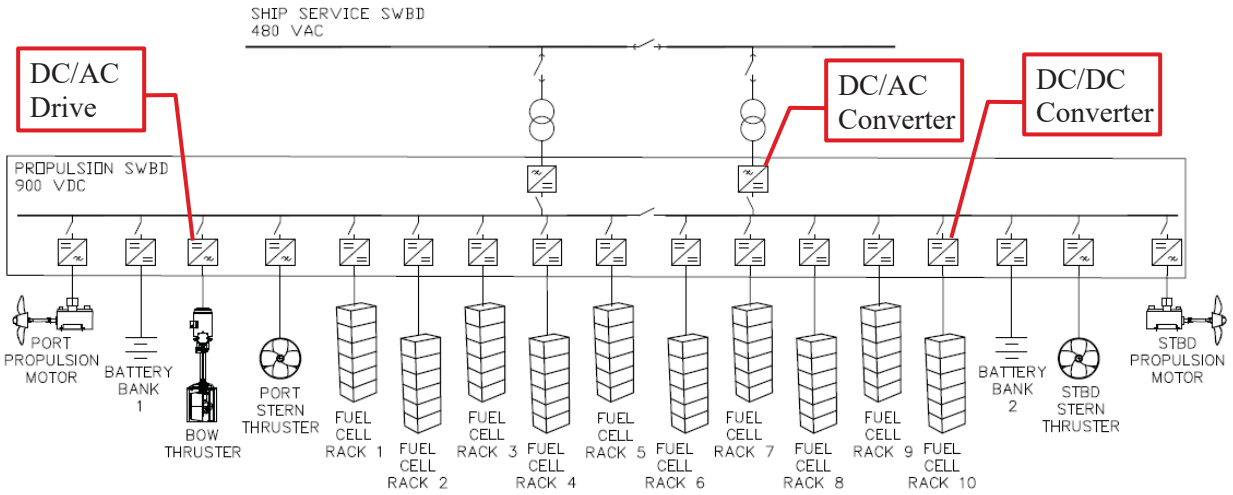

Figure 8 Propulsion system block diagram

3.3.2 Propulsion Motors

The Zero-V will use two propulsion motors to power to its propellers. Based on the resistance and powering calculations, it was determined that 500 kW motors will provide sufficient power for the various mission requirements and also have enough reserve power for safe operation in heavy seas and for dynamic positioning. There are several manufacturers offering marine propulsion motors of this size.

High-torque alternating current (AC) permanent magnet type motors were selected as the propulsion motors. These motors can be directly coupled to the propeller shaft to provide

efficient and quiet operation. AC permanent magnet motors were preferred over DC motors for several reasons. AC motors, especially permanent magnet type, are lighter, more compact, and more efficient than typical DC motors. Additionally AC motors tend to require less maintenance. The propulsion motors would be resiliently mounted in the hull to reduce the transmission of structure-borne underwater noise.

3.3.3 Propulsors

The vessel is outfitted with two fixed pitch propellers. Each propeller is approximately 2.1 m in diameter. Fixed pitch propellers were chosen for their simplicity, low capital and operating cost, and quiet operation. The propellers should be of wake-adapted design to minimize underwater noise as well as maximize efficiency. The propellers are assumed to be fully non-cavitating at speeds up to 8 knots.

3.3.4 Rudders

High-lift flap rudders are used for maneuvering the vessel. Compared to conventional spade rudders, the flap rudders provide both high turning forces underway and superior thrust control for position keeping.

3.3.5 Bow Thrusters

A 500 kW retractable azimuthing bow thruster is located in the forward section of the center hull. This thruster provides sufficient maneuvering and dynamic positioning (ability to hold vessel position relative to a fixed position on the seabed) capability for the vessel under the required operating conditions. The bow thruster can provide thrust in both a lowered position, or while retracted into a thruster tunnel in the hull. While in the lowered position, the thruster extends below the bottom of the hull and can rotate 360 degrees to provide thrust in any direction. For operation in shallow water such as when docking, the thruster can operate while retracted into a tunnel within the hull. In this position, the thruster can only provide sideways thrust. The bow thruster is powered by a permanent magnet AC motor for maximum efficiency and minimum size. A typical retractable bow thruster is shown in Figure 9.

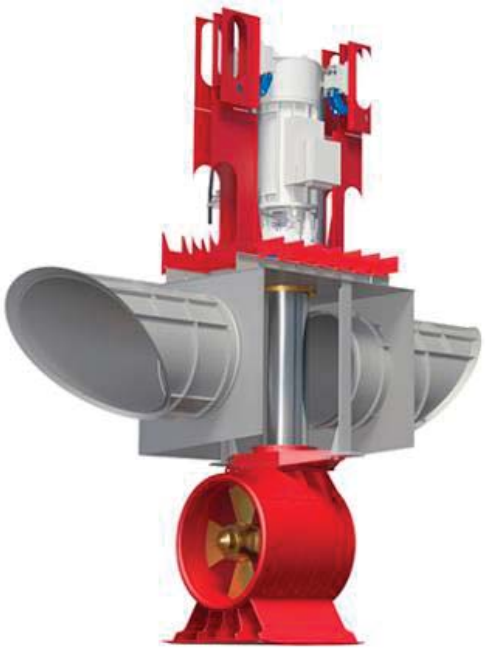

Figure 9 Brunvoll Azimuth Combi Thruster

3.3.6 Stern Transverse Thrusters

To increase docking and position keeping performance, stern thrusters are provided in each side hull. Because of the trimaran's center hull, thrust directed inward by the stern thrusters would suffer significant thrust loss due to hydrodynamic effects and would likely create excessive noise. For this reason, it is assumed that the stern thrusters will only be operated to provide outward thrust away from the vessel and therefore only one of them would be operating at a time.

Conventional electric motor driven tunnel thrusters were selected for the stern thrusters. To increase compactness and efficiency, permanent magnet AC motors are used.

Rim drive tunnel thrusters were also considered but not selected. A rim drive tunnel thruster is a permanent magnet (PM) motor, where the stator of the electric motor is integrated into the tunnel and the thruster blades are fastened to the inside of the rotor. This reduces the necessary space above the impeller where a typical induction motor would be installed. The compact rim drive is an attractive option for the space constrained side hulls. Advantageous characteristics also include reduced noise and vibration, as well as high efficiency PM motors. However, rim drive thruster are three to four times the cost of conventional thrusters. Because conventional thrusters provide satisfactory performance for this vessel, the added cost of rims drives is not justified.

Figure 10 Electric motor driven tunnel thruster (Schottel STT)

Figure 11 Rim thruster (Schottel SRT)

3.4 Integrated Electric Plant

Propulsion power for Zero-V is supplied by an integrated electric plant consisting of hydrogen proton exchange membrane (PEM) fuel cells and lithium ion batteries. The fuel cells are 30kW Hydrogenics HyPM HD 30 fuel cell power modules arranged into power racks each holding six modules. Each rack has a total power output of 180 kW. With ten racks total, the vessel has 1,800 kW of installed power.

The fuel cell racks are distributed with five racks in each of two separate fuel cell spaces. This allows the vessel to continue operation at reduced power if one space must be taken out of service for maintenance or in response to a hydrogen leak or a failure in the space.

Figure 12 Rendering of one fuel cell power module and a four-module rack (Hydrogenics Corporation)

The fuel cell power modules have an operating voltage between 60 and 100 VDC (Volts Direct Current). All the modules in a rack operate in series making the output of the power rack 360-600 VDC. Each power rack supplies power to the propulsion switchboard through a DC-DC converter that converts the voltage to a steady nominal voltage of 900 VDC. The various large loads such as propulsion, thruster, and winch motors are supplied from the propulsion switchboard through DC-AC drives. Additionally the ship service electrical power is supplied to the 480 VAC (Volts Alternating Current) ship service switchboard by redundant DC-AC power converters. Smaller loads such as lighting, fans, or pumps are supplied from the ship service switchboard. The electrical system architecture can be seen in Figure 8 and in the electrical one-line diagram (Reference 5) that is included in Appendix A.

The efficiency of the PEM fuel cells varies with power output. The fuel cell power modules have a peak efficiency of approximately 51%. However, when operating at rated power output, the efficiency is closer to 43%. The fuel cell efficiency will be slightly higher at the beginning of service but degrades over time. Figure 13 shows the typical performance of the fuel cell power modules at the end of their service life.

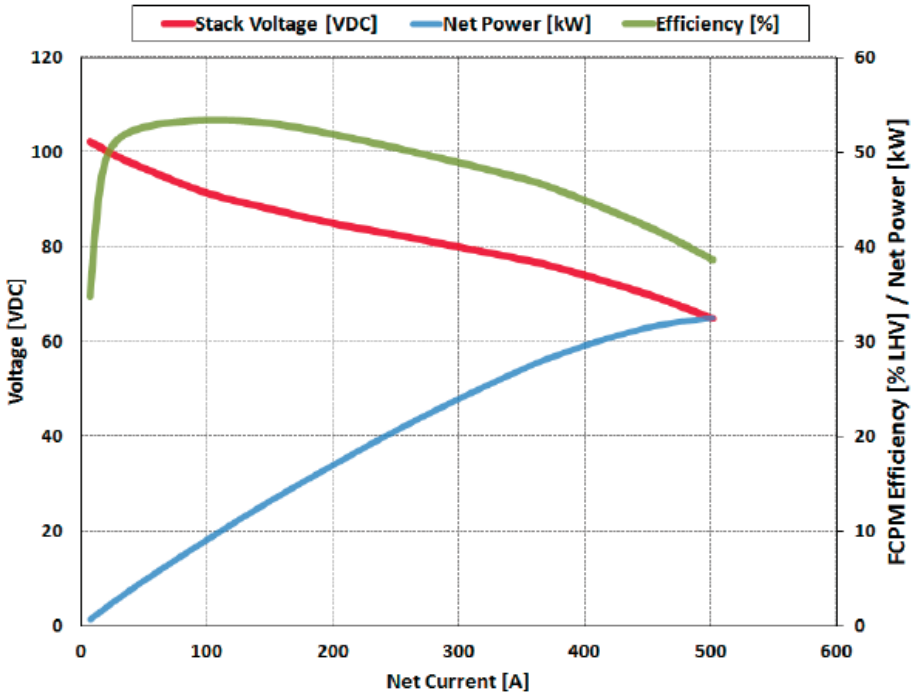

Figure 13 Typical HyPM® HD 30 performance (Hydrogenics Corporation)

The service life for the fuel cell is driven by lifetime of the proton exchange membrane inside the fuel cell module and is based on the operating hours of the cell stack. The fuel cells can achieve 10,000 to 15,000 hours of operation before requiring reconditioning to replace the membranes. The voltage of the cells degrades throughout its service life. They will continue to produce power, but at increased current and lower efficiency. At the end of the service life, the membranes must be replaced. The service life of the membranes is only consumed when the fuel cell is producing power. When the fuel cells are in standby, they are not consuming the operating life.

Fuel cells can assume load fairly quickly. From a cold, turned-off state, the PEM fuel cells take approximately 5 seconds to go from offline to standby and less than 30 seconds to go from standby to full rated power output. However, operations such as dynamic positioning can have very fast, transient spikes in vessel propulsion electrical load that could challenge the ability of the fuels cells to respond quickly enough. To account for these transient loads, the electrical plant also has two lithium-ion battery banks. The battery banks are each able to provide 100 kW of power nearly instantaneously in response to load demands. With the fuel cells providing the base load power, the batteries will charge or discharge as required to manage transient loads. Additionally, the batteries can be used as a power sink for dynamic braking of large motors such as propulsion motors or winches. This allows energy to be recovered during operations such as paying out a winch, thereby increasing overall vessel efficiency.

3.5 Fuel Gas Systems

Hydrogen gas is used for the fuel cell fuel. The hydrogen is stored as liquefied hydrogen gas (LH_2) in two storage tanks located in the weather on the 01 Level aft deck as shown in Figure 14. The hydrogen is bunkered and stored as cryogenic liquid at -253°C (–423°F) and then vaporized to gas, warmed to above 0°C and delivered to the fuel cells. The fuel gas system consists of storage tanks, gas vaporization equipment, a gas distribution system, and a bunkering system. For redundancy, the gas storage and distribution systems are arranged as two parallel systems.

Each system is fed primarily by one tank and serves one fuel cell space. Crossovers between the systems allow either tank to serve both Fuel Cell Rooms.

A concept of the fundamental fuel gas system architecture was developed leveraging to a large extent the arrangements of marine liquefied natural gas (LNG) fuel systems, as well as industrial liquefied hydrogen systems. A concept sketch of the fuel gas system architecture is included in Appendix A. While this sketch is useful to communicate the fundamental philosophy of the fuel gas system architecture, significant additional development of the fuel gas system will be required to flesh out the details and support a comprehensive operational and risk assessment of the system. A cryogenic gas systems supplier experienced with both industrial LH_2 systems and marine LNG systems would be a critical partner in this effort.

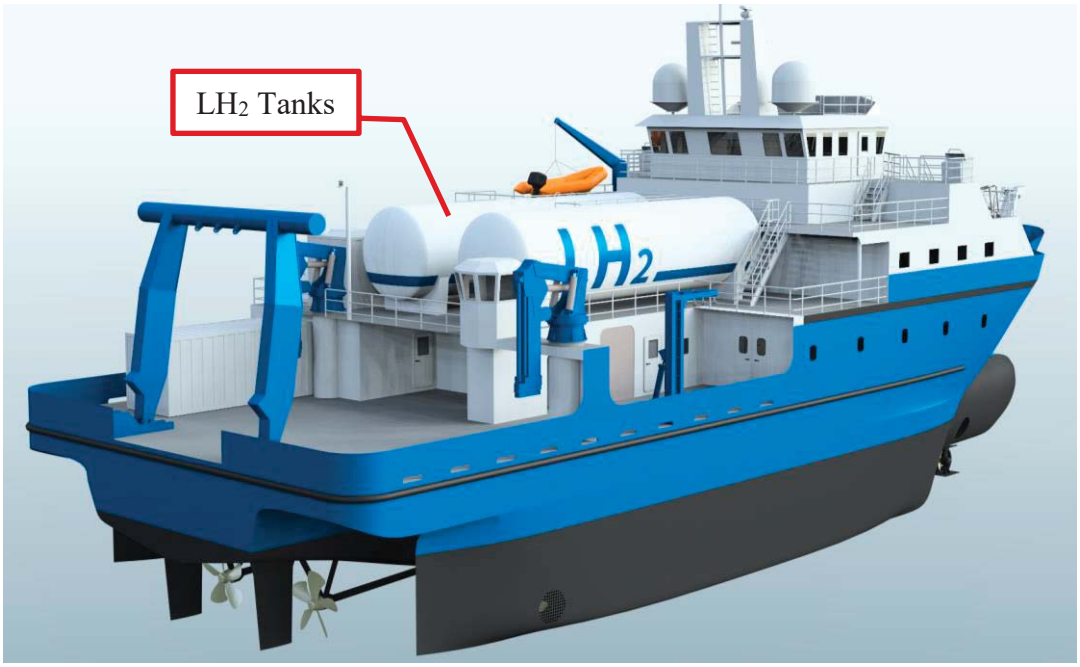

Figure 14 Fuel storage tank location

3.5.1 Gas Storage

The LH_2 is stored in two cylindrical pressure vessel storage tanks each with a molded volume (water volume) of 28,800 gallons. This gives each tank a capacity of 5,840 kg of LH_2. The tanks are Type C independent tanks of fully stainless steel double wall construction with vacuum insulation between the primary containment and the outer shell. The tanks will have a design pressure of 150 pounds per square inch gage (psig), and a typical operating pressure around 100 psig. A tank connection space, sometimes called a cold box, is located on the inboard side of each tank. The tank connection space contains all the pipe penetrations into the tank below the full liquid level. In this way, any liquid leaks resulting from a failure of a pipe penetration into the tank would be contained by the tank connection space.

3.5.2 Gas Distribution System

Each tank connection space will contain all of the gas piping and equipment that processes liquefied gas. This includes a pressure-building unit (PBU), a gas vaporizer, and gas delivery piping and valves.

In normal operation, pressurized LH_2 fuel is conveyed from the bottom of the tank to the vaporizer where it is evaporated to "warm" hydrogen vapor at a temperature of approximately 0°C. The "warm" gas vapor is then delivered to the fuel cells by way of the gas supply piping and a gas supply unit (GSU). The vaporizer is a shell and tube heat exchanger that is specifically designed for cryogenic services and uses ambient seawater as the heating medium. The Zero-V uses commercially available Thermax Cold Water Cryogenic Vaporizers model P25-20. The vaporizer is capable of delivering the gas within 10°F of the incoming seawater temperature and can operate with seawater temperature as low as 50°F. While this is anticipated to be sufficient for operations in the coastal areas of California, a detailed climatology study of the sea temperature in the operating area would be required. If necessary, the seawater could be heated using waste heat recovered from the fuel cell cooling system.

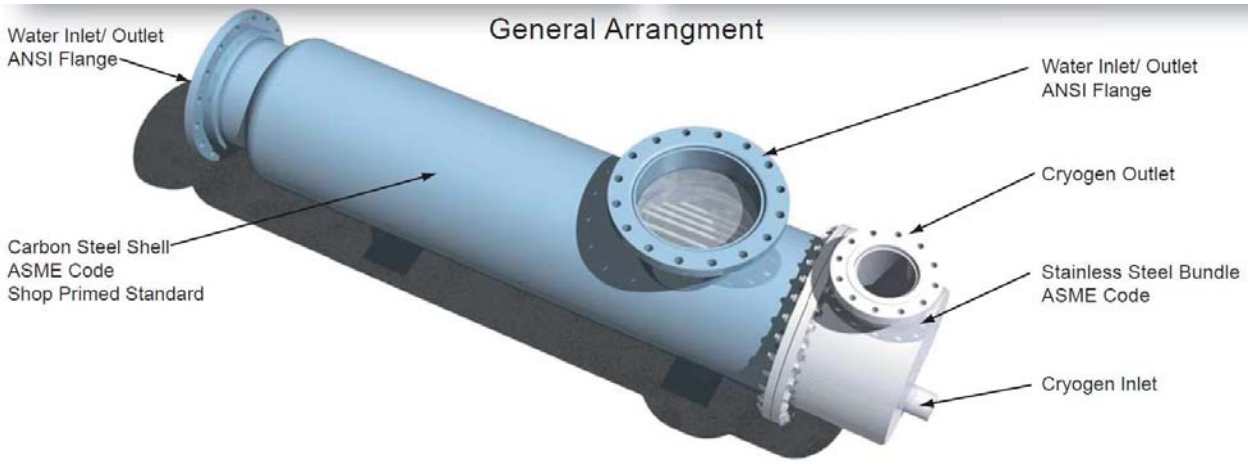

Figure 15 Thermax Cold Water Cryogenic Vaporizer

The LH_2 is pushed through the vaporizer by increasing the pressure in the storage tank to the operating pressure using a pressure-building unit (PBU). The PBU is a small evaporator that takes a small amount of LH_2 from the tank, vaporizes it, and sends the vapor back into the gas cushion at the top of the tank to increase the pressure in the tank. This type of delivery system is commonly used on LNG fueled vessels and cryogenic delivery trucks. Cryogenic pumps are expensive and are typically only used where necessary, such as high pressure applications.

Each gas system is fitted with a remotely operated tank isolation valve immediately at the liquid piping penetration into the tank. This valve can be used to shut off supply of LH_2 in an emergency. Additionally, each gas system is also fitted with a master gas valve where the gas vapor piping exits the tank connection space. This valve can be used for emergency shutdown of vaporized gas. Typically, the master gas valve would be used for emergency shutdown of the gas supply system unless a leak detection alarm has occurred inside the tank connection space.

The gas supply piping is led from each of the tank connection spaces to the master gas valves and then down to the GSU for each fuel cell space, which are located adjacent to the Fuel Cell Rooms. From the GSUs, the piping is led into the fuel cell spaces and to the fuel cell racks. Everywhere gas piping is led inside the vessel, it is inside of gas-tight ventilated ducts. There will be one GSU, inside a dedicated enclosure, for each of the Fuel Cell Rooms.

All of the gas supply piping will be low pressure piping, with the gas pressure not exceeding 150 psig and typically operating around 100 psig. Pressure relief valves inside the GSU will ensure that the gas pressure does not exceed the maximum allowable pressure.

The gas supply unit (GSU) will consist of the double block-and-bleed valve, pressure control valve, and a nitrogen purging connection. On either side of the double block-and-bleed valve will be a vent valve that allows the gas supply piping upstream and downstream of the double block-and-bleed valve to be vented to the gas vent mast. The nitrogen injection valve will be located upstream of the double block-and-bleed valve, to facilitate inerting the gas supply line between the double block-and-bleed valve and the storage tank, as well as from the GSU to the fuel cells. Nitrogen inerting of the piping would only be done if required for maintenance and is only done for "warm" gas piping. In normal operation, the gas supply piping would always contain hydrogen. The double block-and-bleed valve is used to secure the hydrogen supply to each fuel cell space for both normal shutdown of the equipment in the space or for emergency shutdown.

The GSU for each fuel cell space will be installed inside a gas tight enclosure in the GSU room adjacent to the Fuel Cell Rooms. The ventilation ducting around the gas supply piping will be connected to the GSU enclosure thereby ventilating the enclosure. The GSU enclosure will be considered a Zone 1 hazardous area, and will not have access doors. Hazardous areas are further discussed in Section 3.7.2. Maintenance and service access to the enclosure will be through a bolted hatch that will only be opened when the gas supplying line has been inerted with nitrogen. After the gas supply lines are inerted, the GSU enclosure is not a hazardous space.

The gas supply piping from the GSUs enters each fuel cell space where it branches to the fuel cell racks. Each fuel cell rack supply branch contains a block-and-bleed valve near the fuel cell rack connection. This valve is remotely operated and is used to isolate the fuel supply to each fuel cell rack for normal shutdown of the fuel cell. This allows the branch piping to each fuel cell rack to be depressurized whenever the rack is not operating. This significantly reduces both the risk and consequence of a leak within the fuel cell rack. An additional manual isolation valve is located upstream of the block-and-bleed valve for maintenance isolation of each fuel cell rack.

3.5.3 Gas Vents

There are several gas vents in the gas system. The vents are either from pressure relief valves or from bleed lines for purging gas supply and bunkering lines. All the gas vents lead to a gas vent mast.

3.5.3.1 Gas Vent Mast

Because of the hazardous nature of vented gas, all gas vents are connected to a gas vent mast. In accordance with regulations, the gas vent mast must be located such that the gas outlet is sufficiently far from any potential ignition source (4.5m), working deck (6m), or a ventilation intake (10m). The gas vent mast will be located at the top of the vessel navigation and communication mast and will be the highest point of the vessel. It has been assumed that due to the buoyant nature and rapid dispersion characteristics of hydrogen gas, the hazardous area associated with the vent mast is a hemisphere of radius 4.5m above the vent outlet with a cylindrical skirt that extends 3m below the outlet (Reference 4). This assumption requires additional support though gas dispersion modeling to validate the approach for regulatory approval.

3.5.3.2 Bleed Vents

Bleed vents are used to bleed hydrogen from fuel gas piping and are designed for safe venting and/or purging of gas lines for fuel cell shutdown, bunkering, and in response to a gas system alarm.

The gas supply line will be vented by bleed valves in the GSU enclosure and at the fuel cell racks. When gas supply to a fuel cell rack or a Fuel Cell Room is stopped with the double block-and-bleed valve, the bleed valve will open to vent the pipe between the stop valves. The bleed valve will be connected via the vent pipe to the gas vent mast. All gas vent piping within the interior of the vessel will run through the ventilated gas pipe ducts.

In addition to the bleed line from the double block-and-bleed valve, there will also be bleed valves on either side of the double block-and-bleed valve that vent the gas supply piping in case of an automatic closure of the master gas valve. These bleed valves will be connected to the vent pipe.

A vent valve in the bunkering line will be located near the tanks. The bunkering vent will be used for purging the bunkering pipe to the vent mast with hydrogen before and after the bunkering process.

The storage tanks will be connected to the vent mast by bleed valves located in the tank connection spaces. These valves will be normally closed, but can be opened to allow purging of the tanks for maintenance.

3.5.3.3 Pressure Relief Valves

There are several pressure relief valves in the system to prevent the hydrogen pressure from exceeding the maximum allowable pressure of the fuel system (150 psig). There will be two sets of pressure relief valves and rupture discs on the tanks with one set active at all times. The relief valves and rupture discs are set at progressively higher pressure to provide multiple levels of protection of the tank. Additionally, there are pressure relief valves in all sections of liquid piping in which LH_2 could become trapped and a pressure relief valve from each GSU. If any pressure relief valve lifts, the gas is vented to the gas mast through the vent piping.

Gas Release

With marine LNG fuel applications, routine venting of gas to the vent mast is not permitted. The vent mast is solely to be used for emergency or pressure relief valve releases. This LNG gas venting philosophy is not aligned with current widely accepted industrial practices for LH_2 handling. In industrial LH_2 storage and transfer, hydrogen gas is routinely and safely vented to atmosphere during normal operating procedures. One key difference in the release of hydrogen verses natural gas vapors is that the methane vented from LNG is a significant air pollutant and greenhouse gas, while hydrogen is neither. Additionally, unlike natural gas, hydrogen is buoyant in air even for temperatures only a few degrees above the boiling point of -253°C. This prevents hydrogen from ever settling or pooling in low points.

Because there is no established regulatory standard for venting of hydrogen fuel gas in marine applications, it is proposed that the accepted industrial procedures be adapted to marine applications. This proposal is supported by other accepted marine practices involving release of hydrogen gas. One such example is the venting of hydrogen gas that is formed as a byproduct of large scale electrochlorination-type ballast water treatment systems. Electrochlorination systems generate hypochlorite disinfectant products by electrolyzing seawater. In this process, hydrogen gas is evolved as a byproduct and is entrained in the disinfectant process stream. To avoid accumulation of hydrogen gas in the vessel's ballast tanks, the hydrogen gas is separated and vented to weather. The considerations for arrangement and safety of the hydrogen venting in ballast treatment applications is codified in the various shipbuilding rules of the major marine classification societies. With the appropriate diligence and risk assessment, it is reasonable that the practices established for venting of hydrogen in ballast water treatment systems could be

extended to venting of hydrogen gas fuel. In fact, for some very large ballast water treatment systems, the amount of hydrogen vented may be comparable to or greater than the amount of boil off gas from the Zero-V LH_2 tanks.

One of the principle methodologies for handling of hydrogen venting in electrochlorination systems is the use of hydrogen dilution systems. The dilution systems consists of redundant blowers that force sufficient quantity of air into the hydrogen vent system to dilute the hydrogen to a level that is safely below the lower flammability limit. A similar dilution system could be employed for routine venting of hydrogen fuel gas.

Alternatively, there are provisions in the various classification society rules including the DNV GL rules (Reference 1) for venting flammable concentrations of hydrogen from ballast water treatment systems. It is not unreasonable that this could also be extended to venting of hydrogen fuel gas through careful analysis and risk assessment. Hydrogen gas disperses quite rapidly when released to the atmosphere. Sandia National Laboratories is currently examining the dispersion of vented hydrogen using computational fluid dynamics. Through such analysis and prudent placement of the vent mast outlet, it is plausible to demonstrate that the quantities of hydrogen released through routine operations such as from boil-off gas or purging of bunker lines can be released safely.

3.5.4 Bunker Process and Piping

Discussions with the gas suppliers Linde and Air Products revealed that the preferred and most flexible way to refuel the Zero-V is by LH_2 trailer trucks. Tanker truck refueling also eliminates the burden to ports of call of having to establish hydrogen fueling infrastructure at their sites. Truck trailers are currently used for filling of industrial and hydrogen fueling station LH_2 storage tanks across United States and several suppliers are operating in the California market. According to one of the LH_2 fuel suppliers serving California, an LH_2 trailer can deliver approximately 4,000 kg of LH_2. With a total of 10,900 kg of consumable fuel, three trailers would be required to fully fuel the Zero-V. However, most mission profiles require less than 8,000 kg of fuel, allowing typical bunkering with two trailers. Delivery of a full trailer load of fuel takes approximately 3.5 to 4 hours. To expedite the bunkering, the bunker piping system and process will facilitate two LH_2 trailers simultaneously bunkering the vessel with one trailer bunkering each tank. Having each trailer independently bunker a separate tank was the much-preferred method by the LH_2 suppliers who indicated that ganging trucks together to bunker a single tank, while possible, is challenging from a pressure management perspective.

The hydrogen is bunkered into the storage tanks as liquid hydrogen. A bunkering station containing the bunkering hose connection flanges is located on the starboard side of the 01 Level. The bunkering station is open to the weather to provide for good natural ventilation and will be constructed with a sloped, smooth overhead such that any released hydrogen vapor will be naturally directed to weather and cannot become trapped. The bunker station consists of hose connections with dry-break emergency release couplings, pressure gauges, manual stop valves, and remotely operated emergency stop valves.

The bunker piping is led from the bunker station to the tanks. To accommodate the cryogenic temperature in the liquid state, all bunker piping is constructed of austenitic stainless steel and is double walled and vacuum insulated as is standard industry practice. The double wall vacuum insulated pipe serves to provide secondary containment and to minimize heat ingress into the LH_2 during bunkering. To allow for simultaneous but independent bunkering of both tanks, each tank has a dedicated bunkering pipe from a bunker flange to the tank. A crossover between the two bunker lines would allow a single bunker flange to be used to fill both tanks.

Several discussions were had with Linde and Air Products regarding the bunkering process to gain understanding of the current operations for filling of industrial and fueling station LH_2 storage tanks and potential operations for marine vessel bunkering. It is anticipated that marine bunkering will be similar to filling the storage tanks at hydrogen vehicle refueling stations, with some differences.

One notable difference is that the LH_2 suppliers expressed some uncertainty about connecting a hose directly from the trailer to the vessel bunkering station for several reasons. First, the current experience of the LH_2 trailer operators is to connect to a stationary fueling connection. There was some concern about deviating from standard operations and training to connect to a moving vessel. Additionally, the typical LH_2 transfer hoses are very short in order to manage the heat influx through the hose and would likely be inadequate to reach from the truck on a pier to the bunker flange on the vessel. As such, it was recommended to have some intermediate LH_2 transfer infrastructure, such as a fueling stanchion, available at the port facilities where the vessel will bunker.

It is anticipated that the intermediate transfer equipment would be similar to loading arms that are already widely used in the marine industry. These have already been developed for cryogenic liquefied gasses such as LNG and could reasonably be extended to LH_2. Potentially, the loading arm would be mobile trailer-based infrastructure that could be moved to various ports where bunkering occurs. Figure 16 shows an example of a mobile marine loading arm. This particular loading arm is a Wiese Europe model Atlanta arm customized for a mobile application. According to Wiese Europe literature, the Atlanta arm is rated for -196°C. Ideally, something similar could be developed with vacuum-insulated transfer piping to handle the -253°C temperature required for LH_2. Because both tanks can be bunkered simultaneously from two trucks, it would be necessary for the arm to have two sets of transfer piping.

Figure 16 Mobile marine loading arm (Wiese Europe)

With a shore-based loading arm, the LH_2 trailers would connect to the stationary arm and the arm would be connected to the vessel via flexible hoses. Because the arm can be positioned close to the bunker flanges, only short hoses would be required.

Bunkering operations would be similar to bunkering of LNG that is currently done by vessels in the United States and around the world. Several authorities have developed guidelines for bunkering of LNG including USCG (References 15 and 16) and ABS (Reference 17). In general this guidance can be extended to LH_2 bunkering as well, however some differences will exist due to differing properties and risks of LH_2. Because marine bunkering of LH_2 is not yet an established practice, detailed bunkering operations and facilities plans including risk assessment would be required to be developed in coordination with the cognizant authorities in all locations where bunkering is to occur.

The following conceptual bunkering procedure is adapted with modification from the current practices for LNG bunkering:

Bunkering Procedure

1. Vessel is moored with the starboard side to the pier and made ready for bunkering. The cognizant authorities such as the local Captain of the Port (COTP) shall be notified that bunkering of LH_2 will be performed.
2. Safety checks are performed of all equipment involved in the bunkering process to ensure it is in good operating condition and properly aligned for bunkering operations. This also includes testing of sensing and alarm systems, emergency shutdown systems, and communications systems.
3. Loading arm is brought into position and connected to the vessel bunker flanges.
4. LH_2 trucks are brought into position and connected to the loading arm.
5. The trucks build pressure in the LH_2 trailers to the transfer pressure.
6. Bunkering piping valves are aligned to the vessel's vent mast and the truck pushes cold hydrogen vapor through the bunkering hoses and piping and to the vent mast. This is necessary to purge the bunkering piping of any contaminant gasses and to cool them down before liquid transfer commences. The use of the vessel vent mast during bunkering is a notable divergence from LNG bunkering procedures. This is further discussed in Section 3.5.3.
7. Once the pipes are purged and cooled, the bunker piping valves are aligned to the LH_2 storage tanks and liquid transfer begins.
8. Pressure is controlled in LH_2 tanks by alternating between bottom filling and top filling though spray bars to collapse the vapor in the head space.
9. Once the tanks are filled to the desired level, liquid transfer is stopped. Cold hydrogen gas is used to push remaining liquid to the tanks to the greatest extent possible. Any liquid remaining in the transfer piping must be vented to the vessel's vent mast.
10. Bunkering and transfer piping, now containing only cold gas, is isolated from the LH_2 storage tanks and the LH_2 trailer. The pipe is then vented to the vent mast to depressurize all bunkering and LH_2 transfer piping and hoses.
11. Valves at the bunkering flange are secured and hose connections to the loading arm are broken and hoses removed.
12. The truck is moved to a designated safe area at the port facility to depressurize the trailer tank before the trailer drives on public roads (as required by DOT regulations). This may require a fixed vent mast at the port facility.

3.6 Auxiliary Systems

This section will address aspects of the design of auxiliary systems that are peculiar to a hydrogen fueled vessel. It will not address aspects of the of the auxiliary systems design that are standard vessel systems. The seawater cooling, cathode air, and ventilation systems are unique propulsion support systems on the Zero-V and are discussed in the following sections.

3.6.1 Seawater Cooling

The seawater cooling system provides cooling for the fuel cell racks. Each Fuel Cell Room will have a dedicated seawater cooling system.

A Sperre Rack Cooler heat exchanger will be installed in the double bottom of the vessel, below each Fuel Cell Room. Deionized water is primary coolant and circulated through the fuel cells and through the hot side of the rack cooler by the cooling pumps in the fuel cell racks. Seawater is the secondary coolant and is pumped through the cool side of the rack cooler. This system serves to transfer the waste heat from the hydrogen fuel cells to the seawater.

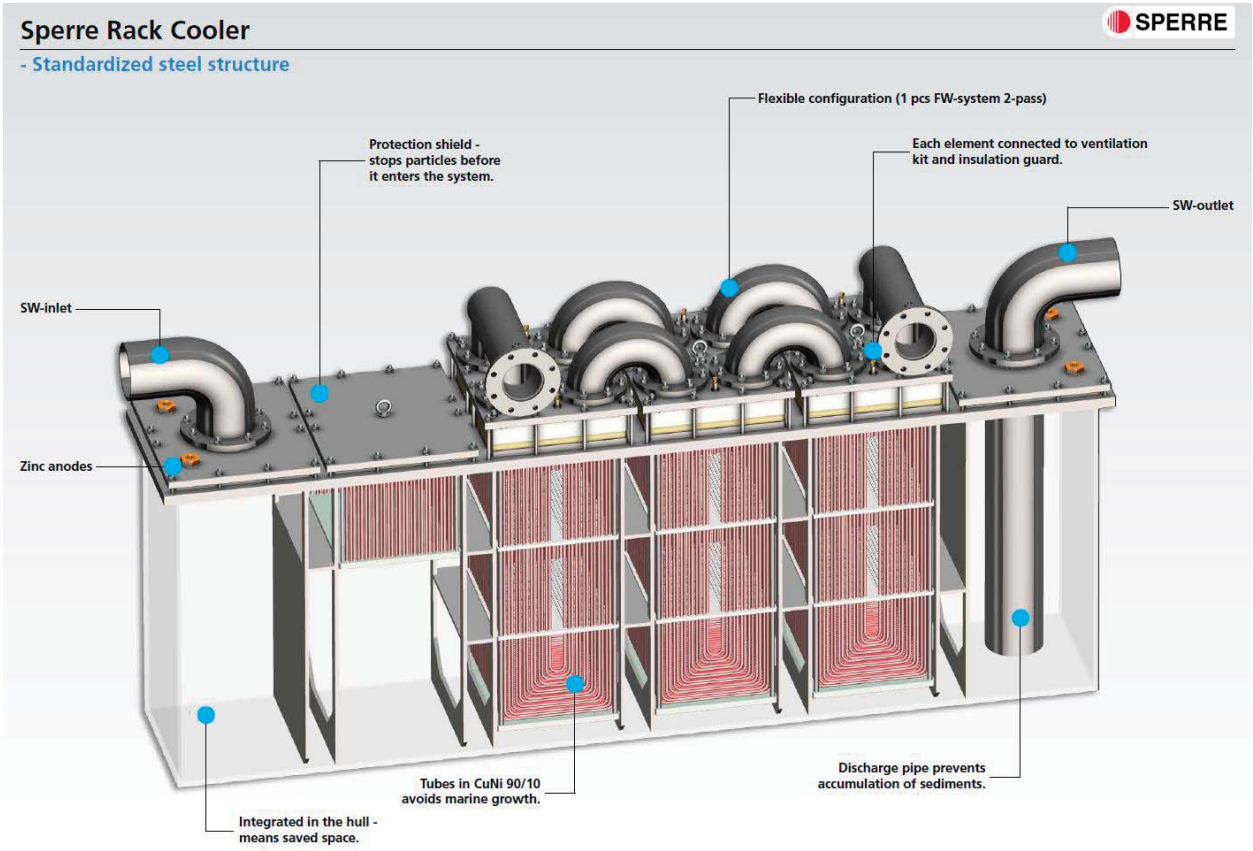

Figure 17 Sperre Rack Cooler heat exchanger

The cooler has two elements which service the five fuel cells for a total heat transfer of 1,560 kW of heat dissipation for each Fuel Cell Room. This will require a seawater flow rate of 1,695 gpm (gallons per minute) at the maximum electrical production. Because the rack cooler requires very high flow rates with relatively low pressure drop, axial flow pumps are well suited for this application. Each seawater pump would be approximately 10 horsepower.

3.6.2 Cathode Air

Air must be supplied to the fuel cells to provide oxygen to the cathodes. The cathode air is ambient outdoor air that is filtered but otherwise requires no special preparation. Each fuel cell

rack requires a supply of 530 cfm (cubic feet per minute) for a total of 2650 cfm per Fuel Cell Room. This is a similar quantity to the combustion air that would be required by an equivalent diesel generator set. The cathode air would be supplied by two supply fans to a common supply plenum leading to the Fuel Cell Room and branch supply ducts to each fuel cell rack. The supply fans would have variable frequency drives to permit modulation of the flow rate depending on the air demand of the fuel cells.

The air from the cathode is then exhausted by an exhaust fan in each fuel cell module. The oxygen levels in the exhausted air is reduced to about 12%. With this level of oxygen, exhausting the air to a well-ventilated location in the weather where it can rapidly mix with fresh air poses little risk of adverse effects on personnel. This is accomplished by exhaust ducts from each rack that are led to a common exhaust plenum in each Fuel Cell Room and then lead to weather. Because the fuel cell cathode air exhaust fans have very low static pressure, two exhaust fans in each cathode air exhaust system would ensure that the plenum is always under slight negative pressure. The exhaust fans would be configured to modulate flow in order to maintain a set point pressure in the exhaust plenum.

3.6.3 Ventilation

Ventilation is very important in a gas fueled vessel as it is used to mitigate the effects of any gas leaks within the vessel. There are two primary ventilation systems serving this purpose. One is for ventilation of the Fuel Cell Rooms. The other is for ventilation of the secondary containment duct around the fuel gas supply and vent piping.

Each Fuel Cell Room has an independent ventilation system consisting of powered supply and powered exhaust. The supply to the space provides outdoor air from a safe location in the weather located on the forward end of the 02 Deck as shown in Reference 4. Redundant supply fans are required to ensure that ventilation of the space is not interrupted due to equipment failures. Redundant fans are also used to exhaust air from the Fuel Cell Room to a location in the weather on the aft end of the deckhouse on the 01 Level as shown in Reference 4. Because hydrogen is highly buoyant, the exhaust air is taken from the high point in the space. In accordance with DNV GL requirements (Reference 1) for fuel cell spaces where hydrogen is present, the overhead of the space will be smooth with no obstructing structures and arranged to be upward sloping up towards the ventilation outlet. Under normal conditions both the supply and exhaust ducting and weather terminals are not considered hazardous areas. However, under gas detection event in the fuel cell space, they would become classified as gas hazardous. Any electrical equipment that impacts the hazardous area would either need to be rated for use in a hydrogen atmosphere or electrically disconnected as part of the emergency shutdown (ESD) sequence. Hazardous areas and emergency shutdown are further discussed in Section 3.7.2.

In accordance with DNV GL regulations (Reference 1) for spaces containing hydrogen pipes the ventilation rate must be sufficient to avoid gas concentration in the flammable range in all leakage scenarios, including pipe rupture. It is anticipated that the rate of 30 air changes per hour required for spaces containing other flammable gas pipes, such as for natural gas, is sufficient to achieve this requirement. However, a detailed analysis of potential hydrogen releases and the ventilation rate is required in future development.

All hydrogen gas piping routed through enclosed spaces in the vessel will be contained within a gas tight duct that provides a secondary containment of any gas that is leaked from the pipe. Similar to the fuel cell spaces, the gas pipe ducting will be ventilated throughout its entire length at a rate sufficient to avoid gas concentration in the flammable range in all leakage scenarios, including pipe rupture. It is again anticipated that the rate of 30 air changes per hour is sufficient to achieve this requirement but a detailed analysis is required to confirm. The ventilation of the

gas pipe ducts is by fully redundant exhaust fans that maintain the ducting under a slight negative pressure and exhaust the air to a location in the weather.

3.7 Electrical

3.7.1 Load Analysis

The electrical load analysis (ELA) was developed using estimates for the ship service, emergency, propulsion and science system electrical loads. Electrical load and demand factor estimates from other similar sized research vessels including the Regional Class Research Vessel (RCRV) developed for Oregon State University were used as a reference. The ship service electrical load estimate reflects the expectation that substantial efforts will be made to increase the energy efficiency of the Zero-V to minimize both required fuel storage volume and environmental impact. The ELA is preliminary, and requires further refinement as the vessel design is developed and specific equipment is selected. The ELA can be seen in Appendix B.

The main propulsion and ship service loads are supplied with power from 10 racks of 6 fuel cells. Because the fuel cells operate with a unity power factor (the ratio of real and apparent power), much like a battery, and the propulsion and ship service loads typically have a power factor between 0.8 and 0.9, the limits on apparent power (kVA) governs utilization of the fuel cells. The fuel cells provide 1,800 kVA for the vessel. Under calm water cruise conditions, approximately 470 kVA are used for the vessel propulsion, while 250 kVA supplies the ship's service loads. However, under sprint conditions, maximum propulsion power, the total electrical load is 1500 kVA. Adding in a 10% design margin and a 10% growth margin for future modification, this requires the full 1,800 kVA capacity of the electrical plant. To ensure that as the ship service loads fluctuate the total power demanded does not exceed the plant capacity, an automated power management system would control and limit the power to the propulsion motors under sprinting conditions.

The fuel cell racks supply DC power to the main propulsion switchboard at 360VDC - 720VDC. The propulsion switchboard supplies power to the propulsion motors, thrusters, and ship service switchboard through an inverter and transformer. Reference 5 and Figure 8 show the details of the electrical system architecture.

There are seven operating profiles considered in the ELA. The *Transit* scenario is applicable when the vessel is transiting between stations, and not performing science operations. The *Towing* scenario represents when the vessel is moving at slow speed (2 knots) and using the towing winch. The *Loitering* and *On Station* profiles represent light and heavy dynamic positioning respectively. In these scenarios, the bow and stern thrusters are being utilized, along with heavy science equipment demands. The *In Port* scenario represents the vessel's electrical demands while in port. *Sprint* was also included in the ELA but is not a normal operating profile.

The most demanding normal operating profiles are *Transit* and *On Station (DP).* These scenarios will require a minimum of 5 and 7 fuel cell racks respectively to be operating to supply sufficient power.

The small emergency load of 162 kVA can be accommodated by two fuel cell racks

The shore power load for the vessel is 180 kVA. The shore power connection will be sized to accommodate this load.

3.7.2 Electrical Safety and Hazardous Areas

In addition to the standard marine vessel electrical safety considerations, there are several additional considerations that are specific to the use of gas fuel including hydrogen. The primary considerations are designation of hazardous areas and the safety of electrical appliance or equipment installed in those areas. The hazardous areas are areas that either have hydrogen gas atmospheres under normal conditions (i.e. the inside of fuel piping) or potentially may have hydrogen gas atmospheres under normal or abnormal conditions do to a fault or failure. The IGF code (Reference 2) provides definitions of the zonal classification and size of various hazardous area associated with the use of natural gas fuel. This hazardous area classification was considered to be applicable to hydrogen gas as well. A gas dispersion analysis of releases of hydrogen is required to validate this assumption. The designation of hazardous areas for the Zero-V can be seen in the Hazardous Zone Plan drawing (Reference 4) which is included in Appendix A. Figure 17 shows a 3D representation of the hazardous areas. As can be seen, care was taken in the locations of sources of hazardous areas to avoid hazardous areas impinging on science working areas or entrances into the interior of the vessel.

To prevent ignition of flammable gasses, electrical equipment installations in hazardous zones is restricted. Electrical wiring and equipment is generally prohibited from installation in hazardous areas unless it is essential to operation of equipment within the hazardous area. Where electrical equipment is installed in hazardous areas, it must be certified safe for use in the applicable hazardous zone.

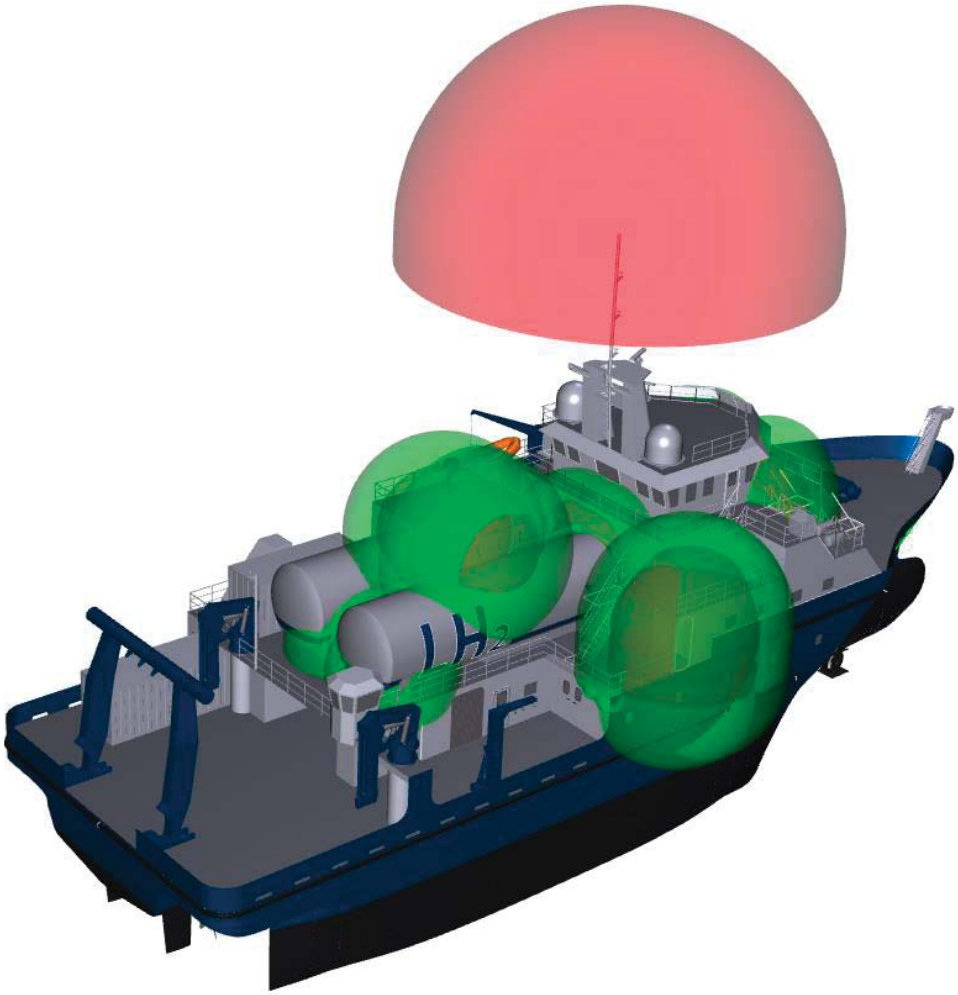

Figure 18 Hazardous areas

The Fuel Cell Rooms of the Zero-V require additional consideration. Under normal operating conditions, the atmospheres of the Fuel Cell Rooms would contain no hydrogen and are gas safe. However, the construction of the fuel cells is such that a single failure could result in the release of hydrogen into the Fuel Cell Room causing the space to become gas hazardous. This single failure release potential requires the fuel cell spaces to be arranged as emergency shutdown (ESD) protected machinery spaces. In the event of abnormal conditions involving gas hazards, emergency shutdown of non-safe equipment (ignition sources) and machinery must be automatically executed. Any equipment that must remain in use or operating during these conditions must be of a certified safe type. The emergency shutdown of equipment is achieved by complete and immediate disconnection of electrical power to all non-gas safe equipment in the Fuel Cell Room. In general all electrical equipment that is not essential for the safe operation of the vessel would be part of the ESD circuits. ESD of a Fuel Cell Room would be initiated upon detection of a gas leak or fire within the space or from a failure of the ventilation serving the space. In addition to electrical disconnection, ESD of a Fuel Cell Room would initiate immediate shutdown of the hydrogen supply to the space.

3.8 Fire Safety Specification

This section has been developed using the International Code of Safety for Ships using Gases or other Lower-flashpoint Fuels (IGF Code, Reference 2) and the DNV GL regulations for Gas Fuelled Ship Installations (Reference 1) and Fuel Cell Installations (Reference 1). Gas fueled vessels have several safety requirements beyond those of diesel fueled ships that have been developed by the regulatory bodies to address the risks of gas fueled propulsion.

IGF code is the primary international construction and safety code for gas-fueled ships. The majority of the rules in the IGF code are contained in Part A-1 which covers specific requirements for ships using natural gas fuel. There is no part specific to hydrogen fuel. However, much of part A-1 can reasonably be extended to hydrogen fuel as a baseline level of requirements. On this basis, the IGF code Part A-1 has been applied to this vessel as guidance for hydrogen fuel cell installations. However, there may be some additional or differing requirements that come about as hydrogen fueled vessel regulation progresses.

The additional requirements beyond conventional ship fire safety systems pertaining to Zero-V involve additional structural fire protection surrounding the storage tanks and Fuel Cell Rooms, a substantial water-spray system, specific firemain configuration, additional dry-chemical fire-extinguishing capabilities and additional fire detection and alarm capabilities. The following sub-sections provide more information on the detailed requirements and how the vessel's design and arrangement will meet them.

3.8.1 Structural Fire Protection

There are additional structural fire protection regulations for gas fueled vessels. These are summarized below:

- All boundaries facing the fuel tanks on the open deck will be shielded by A-60 class divisions. These spaces include, but are not limited to:
    - Bulkhead forward of the tanks on 01 Deck.
    - Bulkhead forward of the tanks on 02 Deck.
    - Aft bulkhead of the Pilothouse.
    - Deck of the Pilothouse.

- Pilothouse windows will be rated A-0.
- 01-Deck below tanks.
- Control station bulkheads.
- Control station windows will be rated A-0.
- Emergency generator room bulkheads.

- The boundaries of the Fuel Cell Rooms will be insulated to A-60 rating.
- Fuel Cell Rooms will have gas-tight steel bulkheads.
- The ventilation trunks into the Fuel Cell Rooms will be insulated A-60.

3.8.2 Water-Spray System

The vessel is required by regulatory requirements to have a water spray system for cooling and fire prevention that covers all exposed parts of the fuel storage tanks located on the open deck. Additionally, the water spray system also provides coverage for boundaries of the superstructures, control spaces, bunkering station, and occupied deckhouses facing the storage tanks and within 10m of the tanks.

The following sketches show the areas which will be protected by the water spray system.

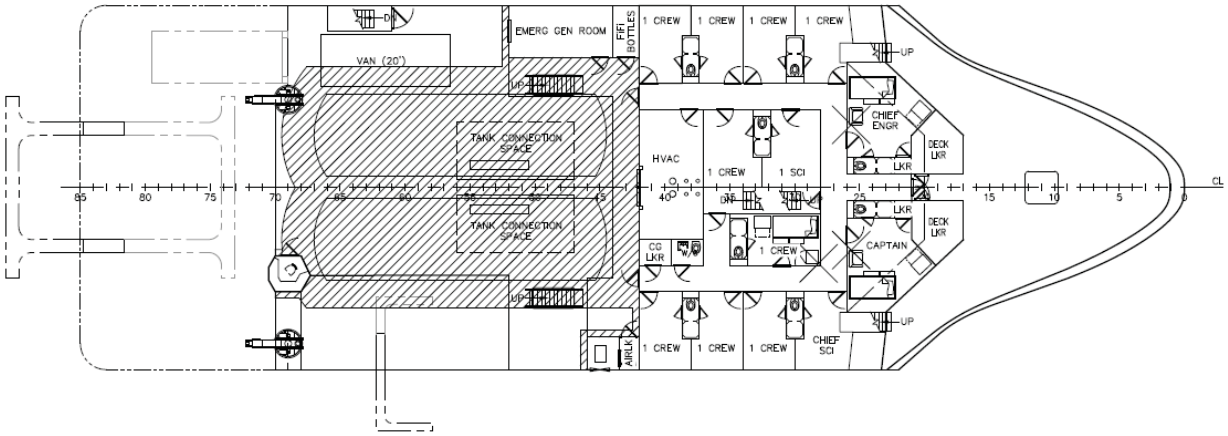

Figure 19 Area protected by water spray system: 02 Deck

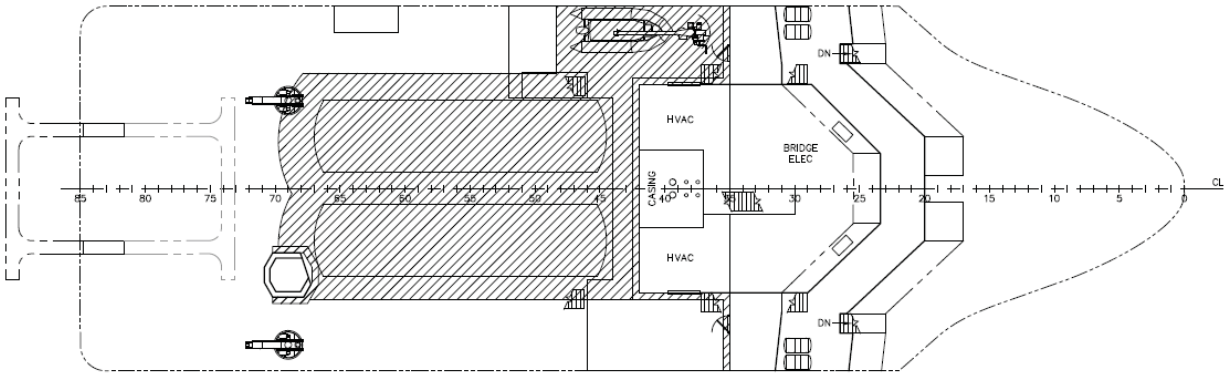

Figure 20 Area protected by water spray system: 01 Deck

The water spray and firemain will be a combined system, with a pump capacity capable of serving both systems simultaneously. The combined system will have isolation valves installed to isolate damaged sections near the fuel storage tanks.

The water spray system will be sized at 10 L/min/m^2 for horizontal projected surfaces and 4 L/min/m^2 for vertical surfaces in accordance with regulatory requirements for LNG fueled vessels (References 1 and 2). There will be isolation valves at least every 40 m to isolate damaged sections as necessary.

The water-spray system will have remote start of the pumps from the Pilothouse, and the Electrical and Engineers Operating Station (EOS). Any normally closed valves in the system will also be controlled from the Pilothouse and the EOS.

The nozzles of this system will be an approved full bore type and arranged to provide effective distribution of water throughout the spaces.

In other hydrogen fueled projects (Reference 14), the use of aqueous film forming foam (AFFF) fire suppression has been discussed. The current IGF code only specifies the use of a water system. However, the use of an AFFF system around the tank location certainly warrants consideration during a fire risk assessment to determine if it would appreciably reduce the risk or consequence of a fire in the storage tank location.

3.8.3 Firemain

The vessel will be fitted with a firemain system serving all parts of the vessel. The firemain will be configured such that it can be isolated should any part of the system be damaged near the tanks. The isolation of this section will not impede the ability of the firemain to service the rest of the vessel.

3.8.4 Fixed Fire Suppression

The Fuel Cell Rooms will be fitted with clean agent fixed fire suppression systems. 3M NOVEC 1230 is the recommended agent because it safe for personnel, does not damage electronics or leave residue, and has zero ozone depleting potential and zero global warming potential. The fixed fire suppression system would be manually deployed. Upon deployment, ventilation to the Fuel Cell Rooms would be automatically shut down to prevent removal of the clean agent from the space. Consideration should be given during risk assessments in future phases as to whether some passive vents at the top of the space should remain open to allow for natural escape of hydrogen gas. This could be accomplished by shutdown of fans without closure of the dampers in the ventilation exhaust ducts. Deployment of the fixed fire suppression system would also result in emergency shutdown of the fuel gas supply to the affected space.

3.8.5 Dry Chemical Fire-Extinguishing

A portable dry powder extinguisher of at least 5 kg will be located near the bunkering station. As the bunkering station onboard Zero-V is on the open deck, an enclosed system to flood the space is not practical.

3.8.6 Fire Detection and Alarm

In addition to the standard vessel fire detection system, additional fire detection will be installed in the Fuel Cell Rooms. The fire detection will be installed such that it is evident from the Pilothouse and EOS which detectors have alarmed.

Upon active fire detection in the Fuel Cell Room, the automatic shutdown of the fuel gas supply to the Fuel Cell Room will occur. Following typical shutdown procedures in the activation of a fire detector, the ventilation to this space will stop automatically, and the fire dampers will close.

Fire detection of hydrogen fires presents some challenges. Hydrogen fires do not emit smoke, are nearly invisible to the naked eye, and have little infrared heat radiation. For these reasons, specialized fire detectors specifically for hydrogen fire detection applications will be required in the Fuel Cell Rooms and other locations where there is risk of a hydrogen fire. There are several technologies available for hydrogen flame detection including multispectrum IR, UV, and combination IR/UV detectors. Because the consequence of false alarms is emergency shutdown of the Fuel Cell Room, special care will be required to select a flame detection system and to minimize all potential sources of false alarm detections.

3.8.7 Gas Detection and Alarm

A hydrogen gas detection and alarm system is required to monitor areas where a potential hydrogen gas atmosphere could occur. This includes detection in each fuel cell rack, Fuel Cell Rooms, GSU enclosures, gas pipe ducts, and tank connection spaces. In many cases, multiple detectors will be required depending on the size and arrangement of the protected space. A gas dispersion analysis will be required to determine the quantity and locations for gas detection. Because the Fuel Cell Room is an ESD protected space, a gas detection event in a Fuel Cell Room would trigger immediate shutdown of the gas supply to the space as well as disconnection of all electrical equipment in the space that are not certified safe for use in a hydrogen gas atmosphere.

Section 4 Vessel Performance

4.1 Speed and Power

Estimating the speed and power requirements of the vessel is very important for determining the fuel consumption of the vessel underway. This is especially important for the Zero-V because the low volumetric energy density of LH_2 make the fuel storage requirements to meet range a major design driver. At this level of design, the best industry practice for determining powering is to rely upon parametric hull series data for similar hull designs. Using regression analysis, typically in a program like NavCad®, one can develop a fairly accurate estimate of the hull resistance using the vessel's principal hull dimensions. The regressions help to account for the shape of the hull to more accurately estimate the overall resistance of the design.

Unfortunately there is limited data on trimaran hull forms with little to no available data in the speed range of this vessel (Froude number < 0.3). Consequently, a simplified approach was used to estimate the speed and power of this vessel.

Instead of using regressions, the resistance of the hull was calculated directly using the ITTC method. Using the ITTC method (Reference 11) for estimating hull drag, hull resistance can be broken down into multiple components based upon the source of the drag; frictional resistance (R_f), residuary or wave-making resistance (R_r), appendage resistance (R_{app}), and air resistance (R_{air}). The ITTC method uses coefficients, which as a function of wetted surface area can be used to calculate the various drag components. The Frictional Coefficient (C_f) is calculated using the Reynolds number. In the ITTC method, a form factor (1+k) is introduced to modify C_f to help account for the form (shape) of the hull. This form factor can be modified further to also help account for the interaction effects between the hulls (1+βk).

Without specific regression equations from similar trimaran hull-forms to estimate the appropriate form factor, the Molland algorithm (Reference 12) for catamarans was used instead. The Molland Algorithm is a regression equation that can be used to calculate the form factor for each hull, based upon their slenderness ratio. Once the individual C_f's were calculated, the frictional resistance was calculated for each of the three hulls based upon their respective wetted surface area and then summed together to estimate the total frictional resistance of the trimaran.

The residuary resistance was similarly calculated for each of the three hulls and then summed together to estimate the total wave-making resistance. Again without regression data, the residuary resistance had to be calculated more generically. Design charts from Harvald's "Resistance and Propulsion of Ships" (Reference 10) that define the residuary resistance coeffeicient (C_r) as a function of prismatic coefficient were referenced. The Residuary Resistance coefficients were interpolated from these charts and then the Correlation allowance (C_a) of 0.0004 was added to each C_r before calculating R_r.

As the level of the Zero-V design is not far enough along to accurately calculate the appendage drag (R_{app}), and air resistance (R_a), it was assumed that the combined effect of the two drag components would add 20% to the total resistance of the vessel. Consequently, after frictional and residuary resistance were added together, a factor of 1.2 was applied to the total to calculate the total resistance including R_{app} and R_a.

Figure 18 below shows the breakdown of the resistance components over the operational speed range of the vessel. The total resistance is not predicted to drastically increase until after the design speed of 10 knots

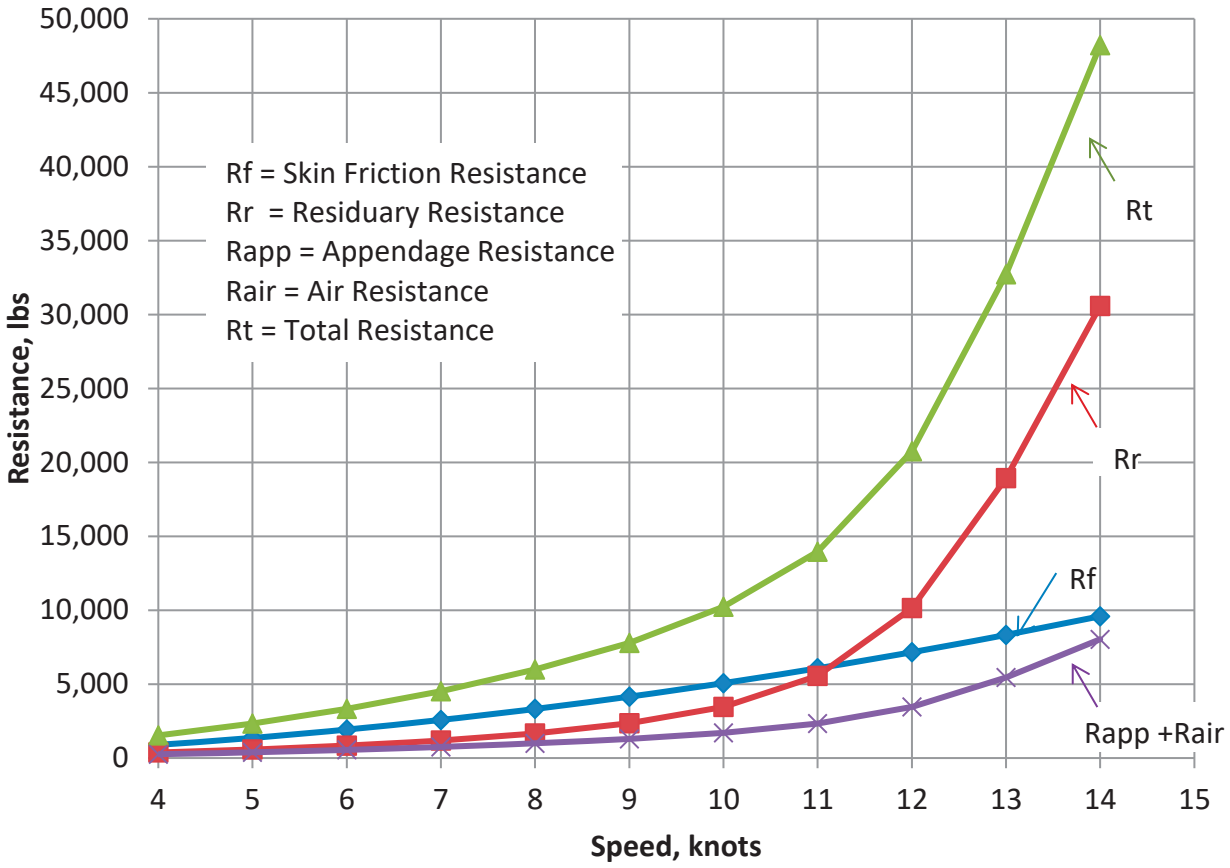

Figure 21 Speed and resistance

Assuming a 0.64 quasi propulsive coefficient, and a 98% mechanical efficiency, the required brake horsepower (BHP) per shaft is plotted in Figure 19 below. At the calm water design speed of 10 knots the BHP per shaft is estimated to be 250 horsepower.

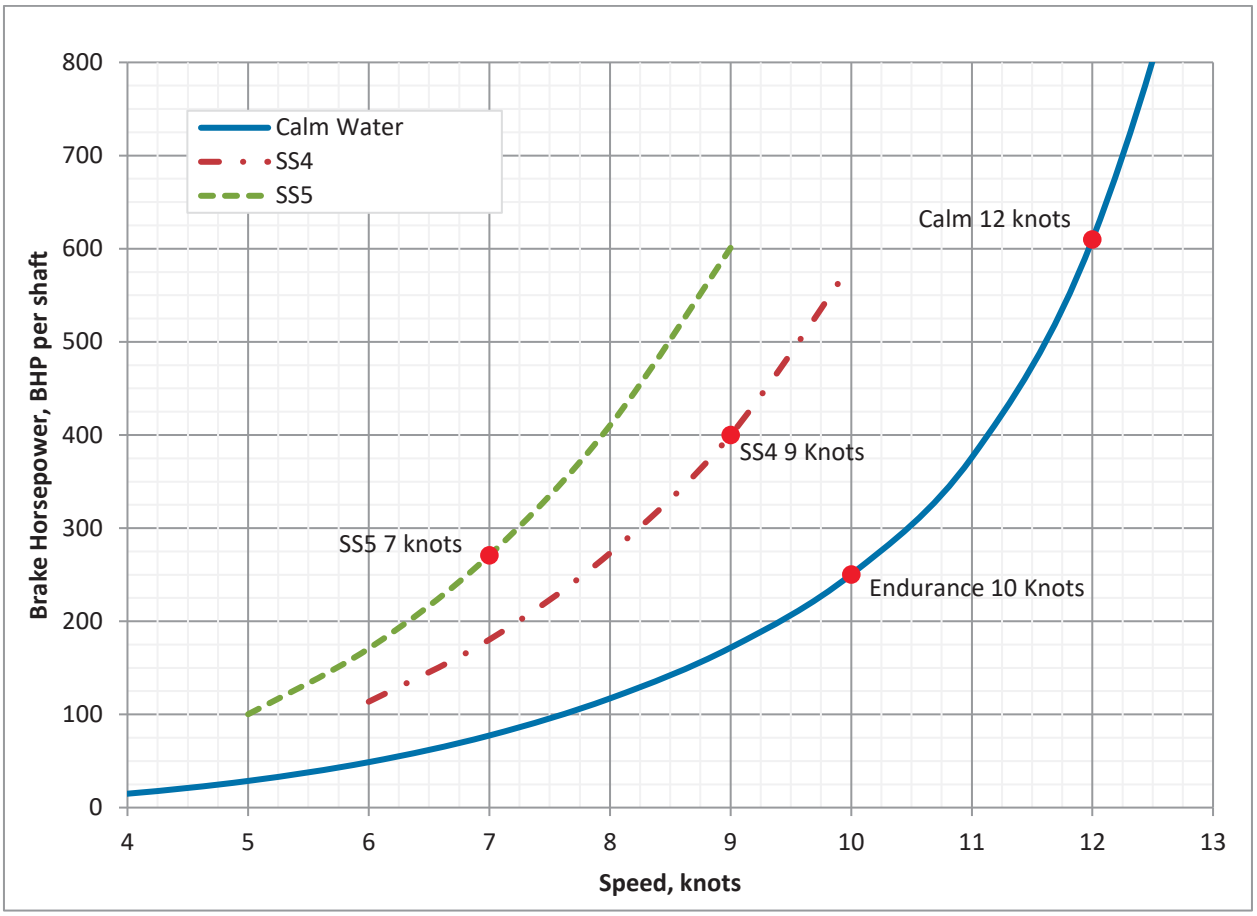

Figure 22 Speed and power

This resistance and powering assessment is a high-level estimate. A detailed analysis using computational fluid dynamics (CFD) and model testing will be required to optimize the hullform and accurately determine the propulsion requirements for this vessel. This is especially important for the Zero-V design due to the uniqueness of a low speed trimaran.

4.2 Range and Endurance

To accomplish repositioning of the vessel, the range was established in the mission requirements as 2,400 nautical miles. Additionally SIO provided 13 different typical mission profiles the vessel needed to accomplish. The fuel consumption for each of the mission profiles as well as for 2,400 nm endurance cruise at 10 knots was calculated. It was found that the governing condition for fuel consumption was the endurance cruise. The fuel consumption of each mission profile is given in Table 4. The detailed calculation can be seen in Appendix B.

Table 5 Fuel consumption

Mission	Hydrogen Consumed, kg
Coastal Mooring	1,208
Deep Moorings (4000m) & towed sonar	5,352
Mapping (multibeam & towed CHIRP)	4,015
Class Cruise biology	492
Class Cruise geology	492
Class Cruise ROV	492
ROV Survey	7,670
Geology Sampling	5,979
FLIP Anchor Handling	2,605
UAV Flight Ops	3,000
AUV Ops (REMUS, Wave Flider, Spray etc)	2,279
Physical oceanography	8,243
Biochemical Survey	7,654
Endurance	10,664

The fuel storage tank sizing was based on this fuel consumption.

However, LH_2 tank filling and storage must be carefully calculated and controlled due to some unique properties of cryogenic liquefied gasses. Because the fuel is delivered and stored at cryogenic temperatures, the tanks must undergo a special cool down procedure before they can be filled with LH_2 for the first time. Once the tanks are filled with LH_2, they must always be kept cold. To accomplish this, some amount of liquid fuel remains in the tanks at the end of every voyage. This liquid amount is known as a "heel". With LNG applications, a heel of approximately 5% is fairly common and it has been assumed that a 5% heel is sufficient for the Zero-V LH_2 tanks.

Additionally, the density of LH_2 changes substantially with temperature, which makes it necessary to account for the expansion of the liquid in the storage tank. The LH_2 that is loaded into the tanks is typically cooled to a temperature at or below –423°F, the saturation temperature at atmospheric pressure. However, heat ingress into the tanks causes the fuel to boil. If the boiloff gas is always removed from the tanks the fuel would remain at a steady temperature until all the fuel is boiled off. However, if the pressure is allowed to increase in the tank, the corresponding saturation temperature increases and the fuel can warm and expand. As the pressure builds in the tanks, the fuel can continue to warm and expand up to the point at which it reaches the Maximimum Allowable Relief Valve Setting (MARVS) and the tanks start venting the boil off gas. To prevent the tank from becoming liquid full when the fuel expands, there must be sufficient volume in the tank for the fuel to expand from the density at the loading condition to the density at the saturation temperature associated MARVS. This temperature is referred to as the reference temperature. The regulations require that the maximum fill level of the tanks is such that at the reference temperature, the tank will not be more than 98% full.

Because the fuel is delivered at -253°C from the trucks, the tanks can only be loaded to 75.5% full to prevent the tank from being liquid full when the gas warms up to the reference temperature of -243°C at the 115 psia MARVS.

The combined effect of the loading limit and the heel is that the consumable volume of the storage tanks is only 70.5% of the molded volume. Based on this and the fuel consumption, the

tanks were sized at molded volume of 28,825 gallons which equate to a total consumable fuel amount of 10,900 kg of hydrogen between the two tanks.

The standard tank loading limits previously discussed were used as the basis for the tank sizing because they are conservative. There are allowances in the rules that may permit increased loading of the tanks up to 95% full at loading conditions. Both the DNV GL rules and the IGF code allow a higher loading limit to be used when the tanks are located where there is a very small probability of an external fire and there is a means of controlling the tank pressure other than by fuel consumers. The tank location on the weather deck of the 01 level is a low fire risk location. Although there is not active pressure control devices like a reliquifaction system or a thermal oxidizer to manage pressure in the tanks from boil off gas, venting of the boil off through the vent mast has been considered. Venting of boil off gas to weather is currently standard practice for industrial LH_2 storage and could reasonably be extended to marine installations with careful application. Venting of hydrogen is discussed more in Section 3.5.3.

The use of increased loading limits would significantly increase the useable fuel and the range of the vessel. Additionally, the range of the vessel can be increased by slowing down to an economical cruise speed of 9 knots. Table 5 presents the range available at both standard and increased loading for speeds of 9 and 10 knots.

Table 6 Comparison of vessel ranges at 9 or 10 knots cruising speed

Loading	Speed, kts	Consumable LH_2, kg	Range, nm
Standard Loading (75.5%)	10	10,902	2,454
Increased Loading Limit (85%)	10	12,368	2,784
Max Increased Loading Limit (95%)	10	13,914	3,132
Standard Loading (75.5%)	9	10,902	2,729
Increased Loading Limit (85%)	9	12,368	3,096
Max Increased Loading Limit (95%)	9	13,914	3,483

Using the maximum increased loading limit and a cruise speed of 9 knots increases the range by more than 40%. It is recommended that the use of an increased loading limit for the Zero-V be further explored with regulatory bodies.

4.3 Weights Estimate

Trimarans are known for being weight sensitive, and this vessel is no exception. A preliminary structural weight model was developed for an all steel vessel and was found to be too heavy for the design to be feasible. Consequently the structure model was re-evaluated considering variants with a steel hull with partial-aluminum superstructure and an all-aluminum vessel. The results of this evaluation showed that the only viable option was an all-aluminum structure. This is consistent with other trimaran designs like the trimaran variant of the US Navy's Littoral Combat Ship which is also made completely from aluminum.

Glosten has recently designed a mono-hull research vessel of similar proportions to the Zero-V. Given the similarities in size, mission, and crew compliment, the weight estimate for the existing design was exploited as a basis to build out a weight estimate for this vessel. Where the designs digressed, such as with the propulsion system and the hull type and material, the appropriate weight items were replaced/added/removed as necessary to accurately represent the actual components in the Zero-V. Additionally, the center of gravity of the remaining weight items were moved to correctly locate them in the vessel.

Weight and VCG (vertical center of gravity) margins for this design were selected per the SAWE's suggested margins (Reference 13). While the complete vessel design is only at a feasibility level, the weight estimate is closer to a concept level weight estimate. Consequently, an 18% weight margin and 12% VCG margin were assumed for all weight groups, assuming a low risk concept level design. A breakdown of the lightship weight, including post-delivery mods can be found below. The weight estimate, organized following the Ship Work Breakdown System (SWBS), details the breakdown of the weights and their longitudinal center of gravity (LCG), transverse center of gravity (TCG) and vertical center of gravity (VCG).

Table 7 Lightship Weight Estimate

SWBS	Entry Description		Weight (LT)	LCG (ft-FR 0)	TCG (ft-CL +S)	VCG (ft-ABL)
100	Hull Structure		270.00	91.71	-0.88	19.00
	Welding Allowance	1.5%	4.05	91.71	-0.88	19.00
	Mill Tolerance Allowance	2.0%	5.40	91.71	-0.88	19.00
	Brackets, Inserts and Doublers Allowance	2.0%	5.40	91.71	-0.88	19.00
	Total Hull Structure		284.85	91.71	-0.88	19.00
	Weight/VCG Margin	18.0%	51.27		12.0%	2.28
	Total Hull Structure w/ margins		**336.12**	**91.71**	**-0.88**	**21.28**
200	Propulsion System		10.94	137.74	0.00	6.21
	Weight/VCG Margin	18.0%	1.97		12.0%	0.74
	Propulsion System w/ margins		**12.91**	**137.74**	**0.00**	**6.95**
300	Electrical System		59.26	90.22	0.70	18.69
	Weight/VCG Margin	18.0%	10.67		12.0%	2.24
	Electrical System w/ margins		**69.93**	**90.22**	**0.70**	**20.93**
400	Command and Surveillance		9.07	66.57	-1.24	38.29
	Weight/VCG Margin	18.0%	1.63		12.0%	4.60
	Command and Surveillance w/ margins		**10.71**	**66.57**	**-1.24**	**42.89**
500	Auxiliary Systems		198.74	73.31	-0.23	20.02
	Weight/VCG Margin	18.0%	35.77		12.0%	2.40
	Auxiliary Systems w/ margins		**234.52**	**73.31**	**-0.23**	**22.43**
600	Outfitting and Furnishings		152.26	77.36	-0.93	24.78
	Weight/VCG Margin	18.0%	27.41		12.0%	2.97
	Outfitting and Furnishings w/ margins		**179.67**	**77.36**	**-0.93**	**27.76**
700	Mission Equipment		69.43	137.70	4.98	26.52
	Weight/VCG Margin	18.0%	12.50		12.0%	3.18
	Mission Equipment w/ margins		**81.93**	**137.70**	**4.98**	**29.70**
	Lightship Subtotal w/o margins		**784.56**	**88.57**	**-0.08**	**21.07**
	Net Margins	18.0%	141.22		12%	2.53
	Lightship at Delivery w/ margins		**925.78**	**88.57**	**-0.08**	**23.60**
1200	Post Delivery Outfit		14.99	109.85	9.19	16.53
	Weight/VCG Margin	6.7%	1.00		3.03%	0.50
	Post Delivery Outfit w/ margins		**15.99**	**109.85**	**9.19**	**17.03**
	Operational Lightship Subtotal w/o margins		**799.55**	**88.97**	**0.09**	**20.98**
	Operational Lightship w/margins		**941.77**	**88.94**	**0.08**	**23.49**

In addition to the lightship weights, the operation weights for the vessel were estimates

Table 8 Operating weights

Item	Weight, LT	LCG	TCG	VCG
Science Payload	50.00	160.00	0.00	21.00
Crew & Effects	5.00	60.00	0.00	30.00
Fuel	20.00	112.50	0.00	37.50
Tanks	25.00	90.00	0.00	5.00
Consumables	12.50	90.00	0.00	21.00
Total Operating Weights	**112.50**	**123.78**	**0.00**	**20.78**

Because research vessel typical are planned to be in use for a long time, a 60 LT service life allowance was also included for future modification to the vessel throughout its life.

Table 9 Departure weight summary

Item	Weight, LT	LCG	TCG	VCG
Operational Lightship w/margins	941.77	88.94	0.08	23.49
Operating Weights	112.50	123.78	0.00	20.78
New Departure Weight	**1054.27**	**92.65**	**0.07**	**23.20**
Contract Mod & Service Life Allowance	60.00	88.94	0.08	23.49
End of Life Departure Weight	**1114.27**	**92.45**	**0.07**	**23.21**

4.4 Stability

As a research vessel, the Zero-V will be designated a USCG subchapter U vessel. This means that it must meet the intact stability criteria of CFR46 170.170 (Weather) and 170.173 (Unusual proportions and Form). These stability criteria were evaluated to determine the maximum VCG that the vessel may have and still pass the criteria. The vessel was evaluated in GHS™ (General Hydrostatics) to determine the maximum operational VCG over its range of operational displacements. A plot was developed from the results of this analysis and can be found below.

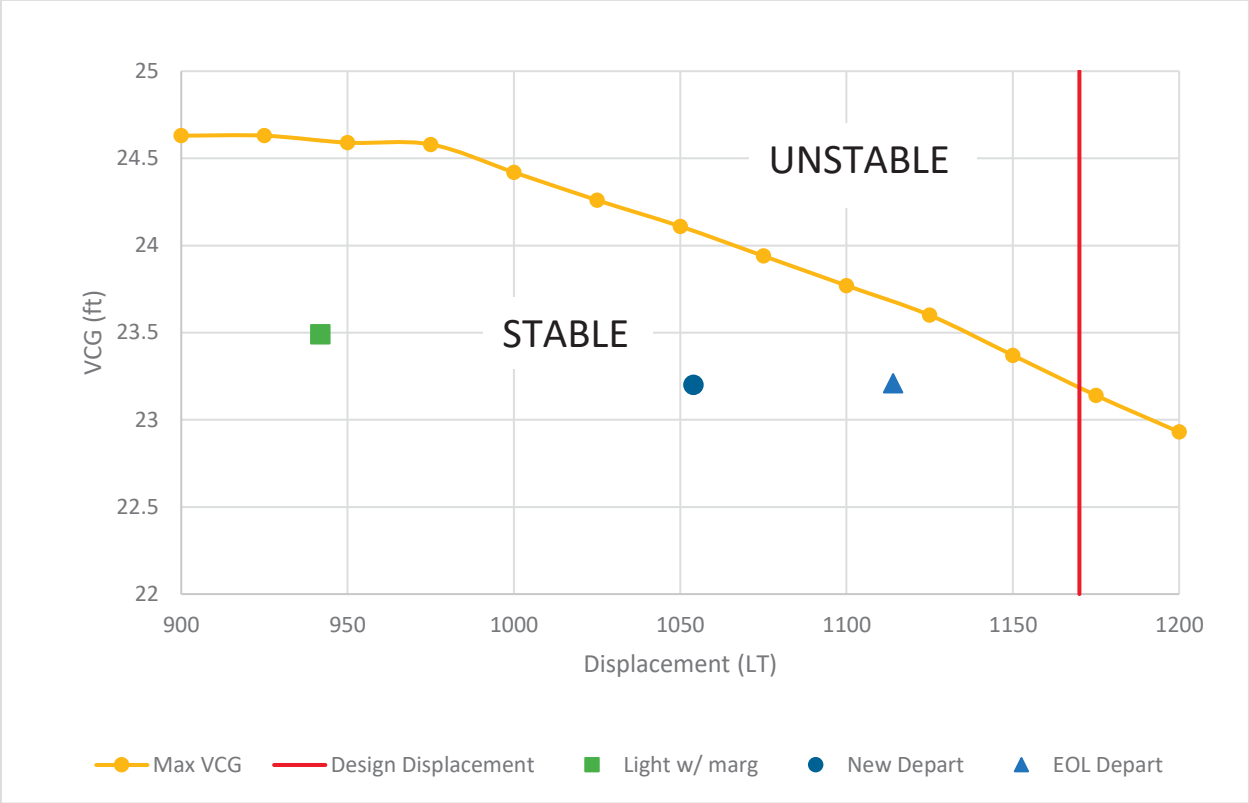

Figure 23 Stability Plot

The figure also includes three load cases (Lightship, Departure, and End of Life Departure). Only the departure conditions need to be shown due to the fact that the fuel is positioned high on the vessel, and as it is consumed, the VCG will decrease, improving stability. This is a feature of this design which is atypical to conventionally fueled vessels. Normally conventional vessels see their VCG increase as they consume fuel, which can cause them to become unstable if the VCG is not properly controlled and offset with ballast.

Concerning ballast, a minimal system will be needed to adjust trim and heel to accommodate the variable science equipment and stores weights that will be loaded on board for each mission.

It should also be noted that the LCB (longitudinal center of buoyancy) and LCG are not currently coincident. This will lead to an unacceptable amount of forward trim if not addressed in future work. To improve the numbers, the weight estimate will need to be refined by developing a full structural weight model and adjustments made to the arrangements to shift weights aft. Additionally, as part of hullform optimization, there should also be a focus on moving the LCB forward to better align with the LCG. That modification in combination with an improved weight estimate should correct the discrepancy between LCB and LCG.

4.5 Seakeeping

Good seakeeping performance is important for research vessels to maximize the operability of the vessel for mission activities. Although the scope of this project did not include seakeeping analysis, prior research vessel design work by Glosten provides some general expectations.

Glosten performed a study for a client that investigated variants of a research vessel design including both a 170' x 41' monohull with a displacement of 1,250 long tons and a 170'x56' trimaran with a displacement of 1,175 long tons. Because of the similarity in size of these

vessels to the Zero-V, this study provides applicable expectations of seakeeping performance for the Zero-V.

In this study it was found that while there were some differences in the seakeeping performance of the variants, they both provided excellent seakeeping in conditions up to Sea State 4 (4 ft to 8 ft significant wave height). An operability analysis for central California offshore conditions found that both the monohull and the trimaran exceeded 95% operability with respect to operating limitations for motions (displacement, velocity, and acceleration) at the A-frame and to motion sickness incidence in the Main Lab and the Pilothouse. In other words, the expectation is that the vessel would be operable for science work in 95% of the annual expected of sea conditions in central California waters.

4.6 Position Keeping

A preliminary dynamic positioning (DP) capability study was performed by Kongsberg and indicates 500 kW tunnel thrusters will provide satisfactory DP capability. The vessel is able to maintain position with 1 knot beam current and more than 25 knots wind and waves from any heading. With 2 knots beam current, the vessel can still maintain position with significant wind and waves at best heading. Figure 20 and Figure 21 show the DP capability plots for these conditions.

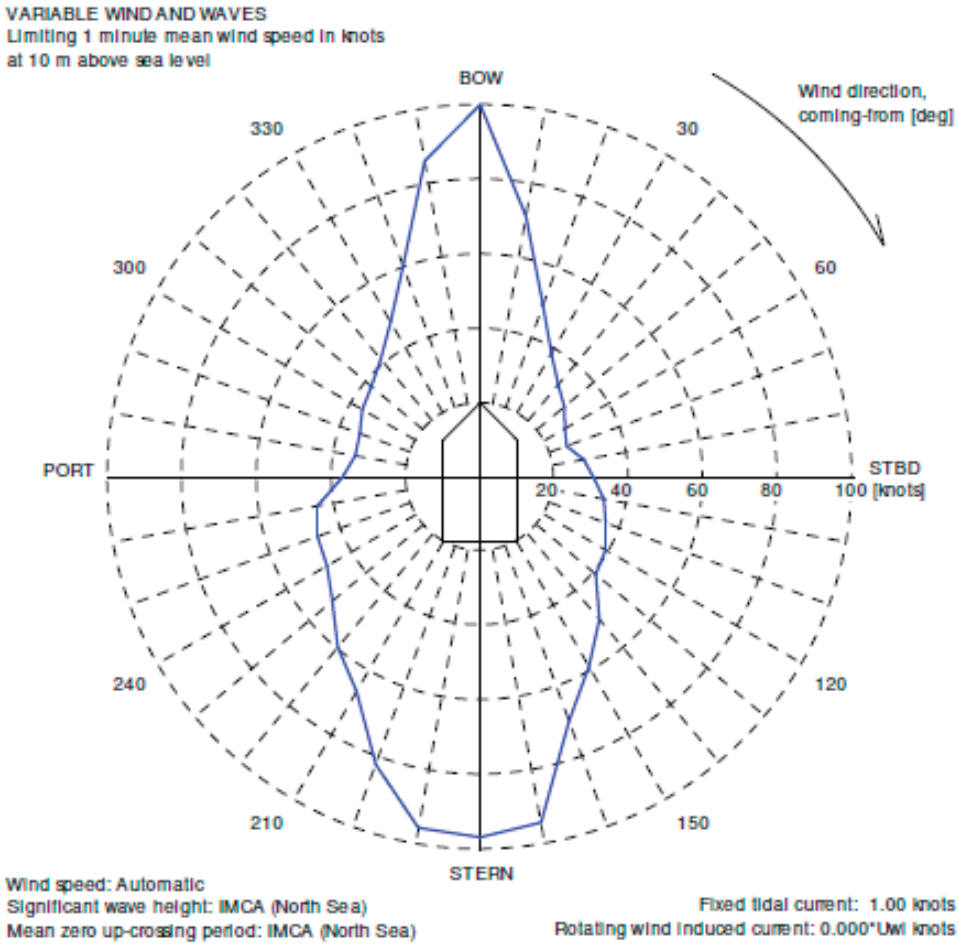

Figure 24 DP capability in one knot beam current

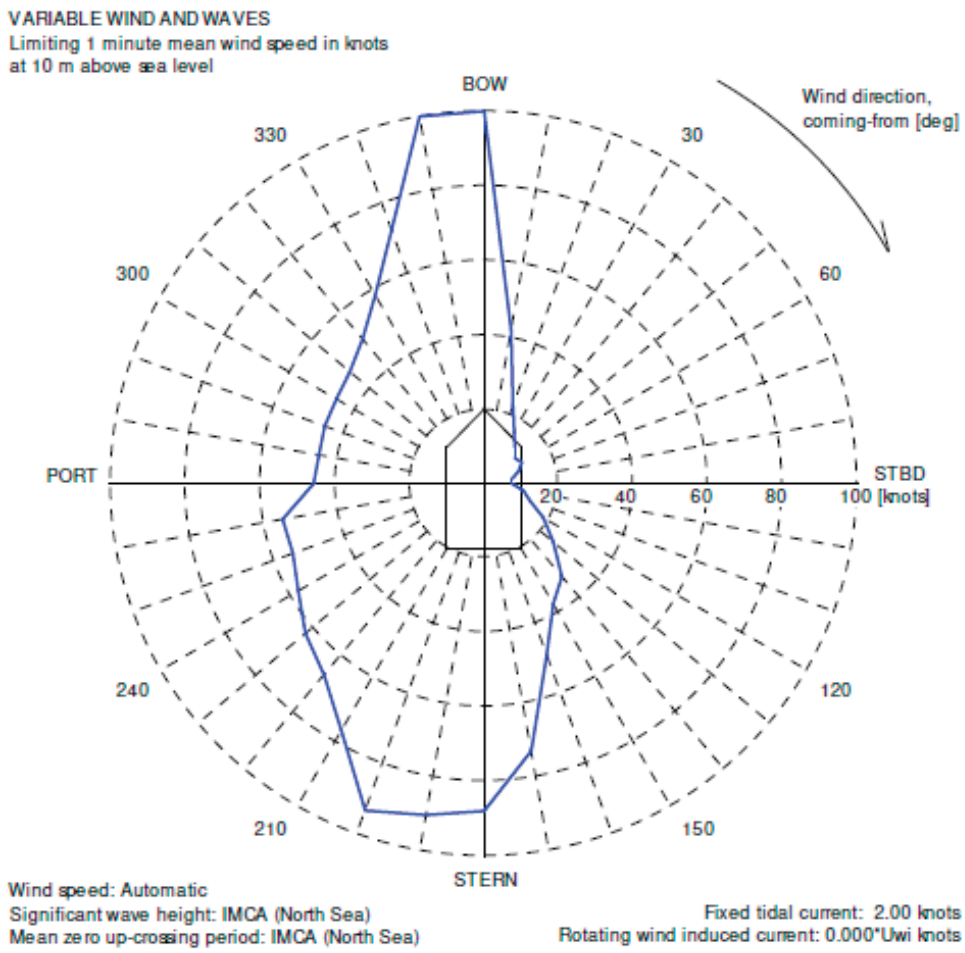

Figure 25 DP capability plot in two knots beam current

These DP capabilities are expected to be sufficient for performing the typical on-station work this vessel would engaged in.

4.7 Underwater Radiated Noise

One of the benefits of hydrogen fuel cells is that they are very quiet compared to diesel engines. The reduction in noise from elimination of diesel engines, one of the largest noise sources onboard conventional vessels, has two significant benefits. The reduction in airborne noise from the engine and the engine exhaust improves habitability both inside the vessel and on the working decks. Additionally, the reduction in noise helps the vessel achieve underwater radiated noise (URN) limits.

Low URN is very important for research vessels to avoid interference with scientific instruments such as sonars and to minimize detection from marine wildlife. Based on discussions with Scripps, the URN goal for the Zero-V is to meet the limits from the International Council for the Exploration of the Sea (ICES) Report 209 at a speed of 8 knots. The ICES Report 209 limits are a commonly used standard for URN limits of research vessels. Noise Control Engineering (NCE), a Glosten subsidiary, developed an estimate of the URN levels for the Zero-V. The estimate was developed using the URN predictions for the RCRV, developed for Oregon State University, as a baseline because the vessels are of similar size and propulsion power.

The RCRV URN analysis was done using the NCE-developed software program, DesignerNOISE ™. This software computes the individual sound contributions from Airborne (AB), First Structureborne (FSB) and Secondary Structureborne (SSB) noise paths.

DesignerNOISE ™ uses Statistical Energy Analysis (SEA) based algorithms and as such it computes the vibration on each of the elements within the vessel model. A hull vibration-to-underwater noise transfer function is then applied to compute URN at 1 meter from the hull.

To establish an estimate for the Zero-V, the RCRV URN predictions were adjusted to account for the removal of the noise source from the diesel engines. This method provides a relatively rough estimate, but as can be seen in Figure 26, the result suggests that, with noise treatments such as damping material on the hull and vibration isolation of large rotating machinery, the Zero-V can meet the limits in ICES Report 209. The Zero-V URN estimate was done for a steel hull and was not revised to account for the aluminum hull. The aluminum hull may require additional damping material to achieve ICES Report 209 limits. To establish a more accurate estimate, a full DesignerNOISE ™ model is required. This is beyond the scope of this feasibility study.

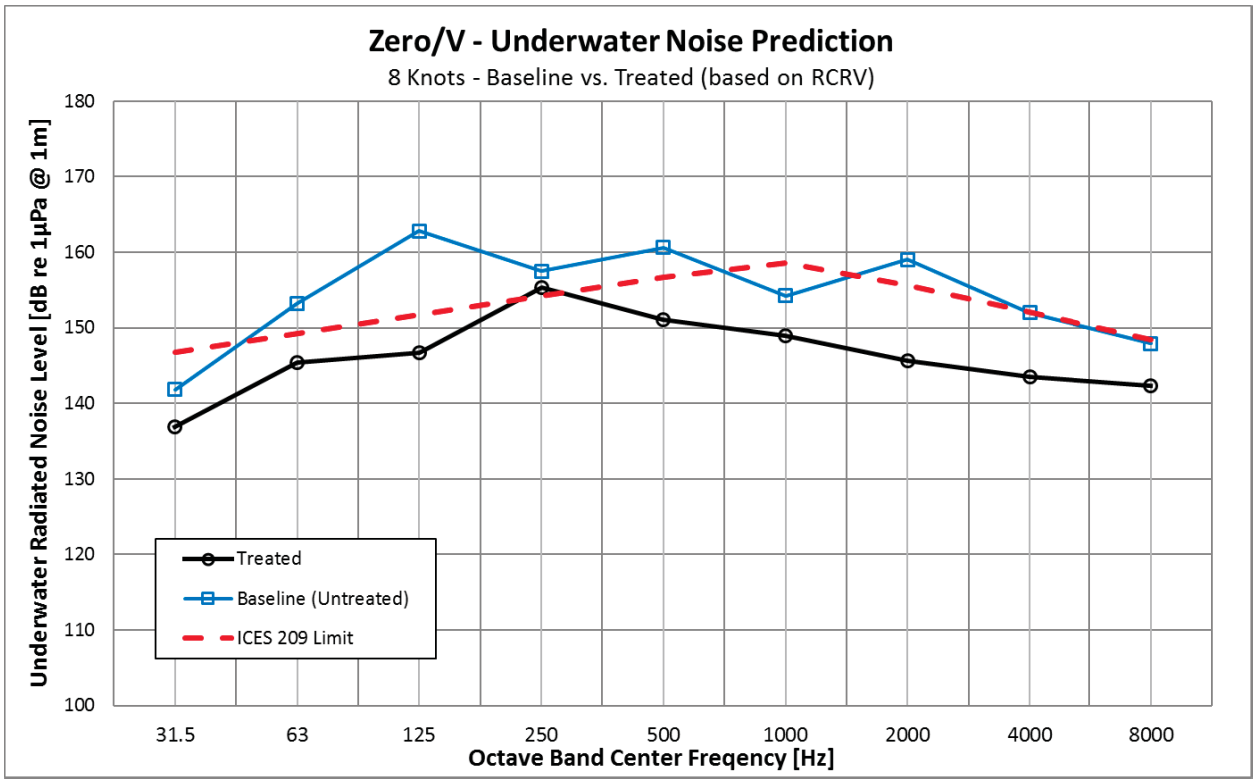

Figure 26 Zero-V Underwater Radiated Noise Prediction (estimate)

Section 5 Regulatory Review

As part of this study, Sandia and MARAD wish to establish a regulatory feasibility of the concept developed. A challenge for regulatory review of the Zero-V design is that there are currently no specific and comprehensive rules governing hydrogen installations on ships. Such rules are currently the subject of development by IMO, DNV GL, and other classification societies. The DNV GL rules for gas fueled vessels (Reference 1) and the IMO IGF code (Reference 2) govern gas fueled vessels, but are primarily specific to natural gas applications. The DNV GL rules do have some regulations pertaining to hydrogen in Part 6 Chapter 2 Section 3, of Reference 1. However, these rules are by no means comprehensive. 46 CFR are the federal regulations pertaining to design and operation of US flagged vessels which and are enforced by the United States Coast Guard (USCG). These federal regulations have no specific requirements for hydrogen fuel applications. Due to the lack of a comprehensive rule set, DNV GL and USCG have both indicated that the design would need to be developed as an alternative design approach whereby the equivalency of the vessel safety, reliability and dependability to that of a conventional oil-fueled vessel would need to be demonstrated. This approach requires a significant and time-consuming level of analysis that is well beyond the scope of this feasibility study.

In order to provide some basis for the design of the vessel, it was decided that the design would be developed for compliance with the DNV GL *Rules for Classification: Ships* with specific attention to Part 6 Chapter 2 Section 3, *Fuel Cell Installations* and Part 6 Chapter 2 Section 5, *Gas Fueled Ship Installations* as well as the IMO IGF Code Part A-1. While these rules are primarily for natural gas installation, they are considered to provide a reasonable baseline level of requirements for hydrogen fuel as well. There is the expectation that there will be additional requirements for hydrogen that will evolve as the rules are developed or as requirements become evident from rigorous risk analysis of a hydrogen fuel design. In addition to these rules, the general requirements of the vessel were developed from 46 CFR Subchapter U (USCG rules for oceanographic research vessels).

With the understanding of the aforementioned limitations on the available rules, the basic Zero-V design was submitted to both the US Coast Guard and DNV GL for review. The goal of the regulatory review is to identify any regulatory or safety areas of concern given consideration of the fundamental design. The following documents were provided.

- General Arrangement
- Preliminary Hazardous Zone Plan
- Electrical One-Line Diagram
- Concept Gas System Architecture
- Draft Design Study Report (including fire safety systems)

Both USCG and DNV GL provided review comments that are included in Appendix E. In general, the response from both reviewers was that while additional development would be necessary to gain approval as an alternative design, there were no identified fundamental concerns that would render the project infeasible. Furthermore, DNV GL provided a conditional approval in principle (CAIP), which is also provided in Appendix E.

Section 6 Cost Estimate

A preliminary construction cost estimate was developed for the Zero-V design. This cost estimate leveraged as a basis the cost estimate data from the Regional Class Research Vessel (RCRV) that Glosten designed for Oregon State University. The RCRV provided a good basis for the cost estimate for Zero-V because the size, outfitting, science mission equipment, and vessel capabilities are very similar and the RCRV project involved significant effort in development of cost estimates.

To develop the estimate, costs were broken down using the ship work breakdown structure to provide more discrete division and organization of the cost items. Cost were organized into eight SWBS groups (000 through 700) which were in turn broken down into major systems.

Table 10

SWBS No	Group	Major Components
000	Shipyard Engineering & Services	Production design engineering, planning & management, documentation, inspections/tests/trials, models and mockups
100	Structure	Hull, foundations, masts and other structures
200	Propulsion	Propulsion motors, shafting/bearing, propellers
300	Electric Plant	Fuel cells, batteries, switchgear, power distribution and conversion equipment, emergency generator, electric cables, lighting
400	Command and Surveillance	Navigation systems, machinery control, alarm and monitoring systems, communication systems, entertainment systems
500	Auxiliary Systems	Piping systems, HVAC, fuel storage, fuel systems, steering, bow/stern thrusters, anchors, mooring systems, pollution control systems, lifesaving equipment, small boats
600	Outfit & Furnishings	Paint and markings, joiner work, furnishings, ship fittings, doors/hatches/ladders, insulation
700	Science Outfit	Lab outfit, cranes, winches, over-the-side handling systems, science acoustic suite

The cost estimates for major systems were developed in one of several ways including built up from major equipment quotations, parametric from materials and dimensions, scaling and adjustment of RCRV estimated costs, or best engineering judgment estimates.

The cost estimate was developed considering the equipment and material costs as well as labor hours for construction or installation. While the material costs are considered constant, the labor rates for shipbuilding can vary significantly based on geographic location and economic climate in the shipbuilding industry. To capture this variation, the cost estimate was developed using both high ($75 per man-hour) and low ($60 per man-hour) labor rates to bracket the construction cost estimate. Included in the cost estimate was also a 15% shipyard markup on materials and subcontractors, the cost of builders risk insurance (1% of contract value), and a contingency allowance (15% of contract value). Table 9 contains the high-level summary of the construction cost estimate. A more detailed summary of the cost estimate is contained in Appendix D.

Table 11 Construction cost estimate in USD, Q2 2017

Construction at Low Labor Rate	
Construction cost at $75 per MH	$66,300,000
Builder's risk insurance (1%)	$663,000
Contingency (15%)	$9,300,000
Total	**$76,000,000**
Construction at High Labor Rate	
Construction cost at $60 per MH	$71,000,000
Builder's risk insurance (1%)	$713,000
Contingency (15%)	$10,000,000
Total	**$82,000,000**

A high-level examination of the construction cost compared to other vessels revealed that although somewhat more expensive, it is not unreasonable when compared to other modern research vessels of similar size and capabilities.

Section 7 Future Work

The vessel design process is often described as a design spiral. The project starts at the outside of the spiral and works around through the vessel requirements, design and performance. Each trip around the spiral takes the outcomes of the prior and refines them. In such a manner the project works inward through the spiral in ever increasing detail and rigor until the final design is achieved.

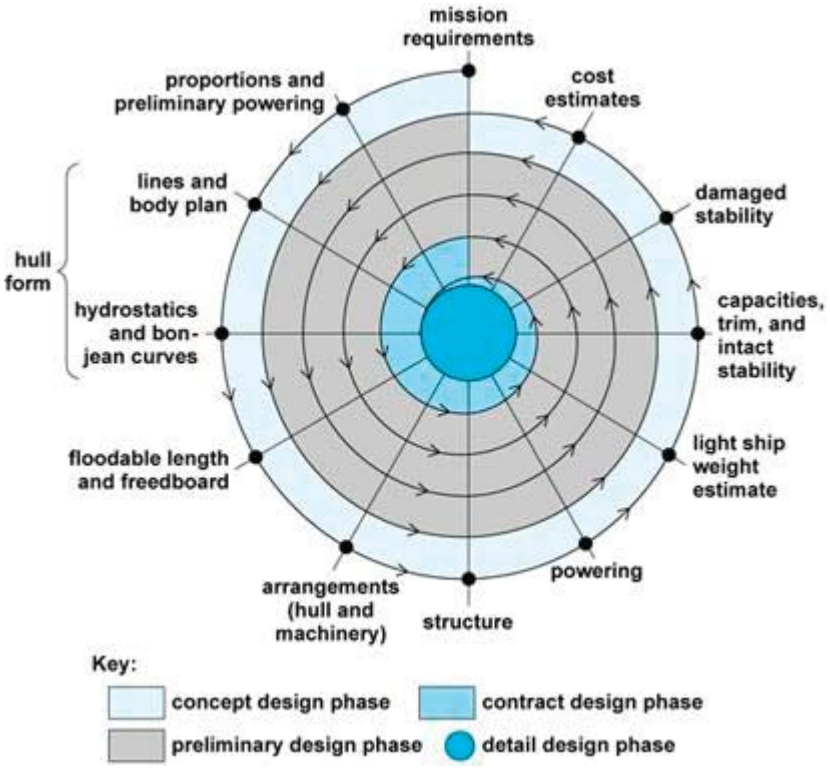

Figure 27 J. Evans visualized the ship design spiral in "Basic Design Concepts," Naval Engineers Journal, 1959

This project, to provide a very fundamental design basis as an evaluation of the feasibility of the vessel, represents the first trip around the design spiral. From this feasibility design, there is significant amount of additional work that is required to flesh out and refine the design especially in the areas peculiar to the gas system and the trimaran design. This section discusses some next steps required to further develop the design.

7.1 Gas System Development and Risk Assessment

A key step to moving the project forward is to conduct a risk assessment of the gas systems. Because the vessel must be developed and reviewed under the regulatory framework of an alternative design, both the US Coast Guard and classification societies will require a comprehensive and detailed risk assessment of gas systems and related fire and safety systems to demonstrate an equivalent level of operability and safety to a conventional oil fueled vessel. The first step of this is a comprehensive design of the systems. Following this, a hazard identification (HAZID) workshop involving major project and regulatory stakeholders would need to be held to identify potential risks and hazards. This would likely result in many specific areas requiring

further analysis to further asses the level of risk. It is anticipated that at a minimum the following analysis would be required:

- Failure modes and effects analysis (FMEA) of the gas system, fuel cells, propulsion electrical/control systems, gas detection systems, fire detection systems, ventilation systems, fire suppression systems, and emergency shutdown systems.
- Gas dispersion modeling of gas releases from the vent mast and leaks in enclosed spaces (i.e. fuel cell rack, Fuel Cell Room, tank connection space), and in the weather.
- Explosion analysis of the Fuel Cell Room.
- Probabilistic damage assessment of gas system.
- Fire risk assessment especially in way of the storage tanks.

7.2 CFD Analysis and Hull Form Optimization

Computational fluid dynamics analysis of resistance is important for future work because of the limited availability of parametric resistance estimation methods for trimarans, especially in low Froude number operating regimes. A comprehensive CFD study would provide improved confidence in resistance predictions as well as a more comprehensive understanding of the impact of hull form features, such as hull spacing, on the vessel resistance.

Additionally, CFD could be used to optimize the hull form. Because the fuel storage capacity is a large driver in the vessel design, minimizing resistance of the vessel is particularly critical for the Zero-V. In several Glosten vessel design projects, including research vessels, hull form optimization studies have been conducted using CFD. In these studies, the geometry of a parent hull form is manipulated within imposed constraints to seek a reduction in resistance. In past projects hull form optimization has resulted in resistance reductions of as much as 15%.

7.3 Structural Design

A structural design is required to take the design to the next phase of development. Because the hull structure is a significant driver of both the vessel weight and construction cost, developing a comprehensive hull structural arrangement would greatly improve accuracy of both the weight and cost estimates.

7.4 Vessel Systems Design and Energy Optimization

This feasibility study only examined vessel systems that are directly affected by or unique to the use of hydrogen fuel and fuel cells. Additionally these systems were only examined a high level to assess feasibility, not to develop the full system details. To take the vessel design forward, all vessel systems would require a preliminary level of design to develop the system requirements and sizing. Additionally, optimization of the energy efficiency to minimize the ship service electrical loads of the vessel will be very important for the Zero-V. Through a rigorous focus on reducing electrical energy use, it may be possible to realize significant improvement in range or reduction in required fuel storage tank size.

7.5 Seakeeping and Motions

To better define the seakeeping performance of the vessel, a computation seakeeping analysis is required. In this analysis a geometric model of the vessel will be analyzed in a seakeeping analysis software package to establish the expected vessel motions in a variety of sea states and to compare these motions to operation criteria.

Appendix A Drawings

General Arrangements

Hazardous Zones Plan

Electrical Oneline Diagram

Concept Gas System

(This page left intentionally blank.)

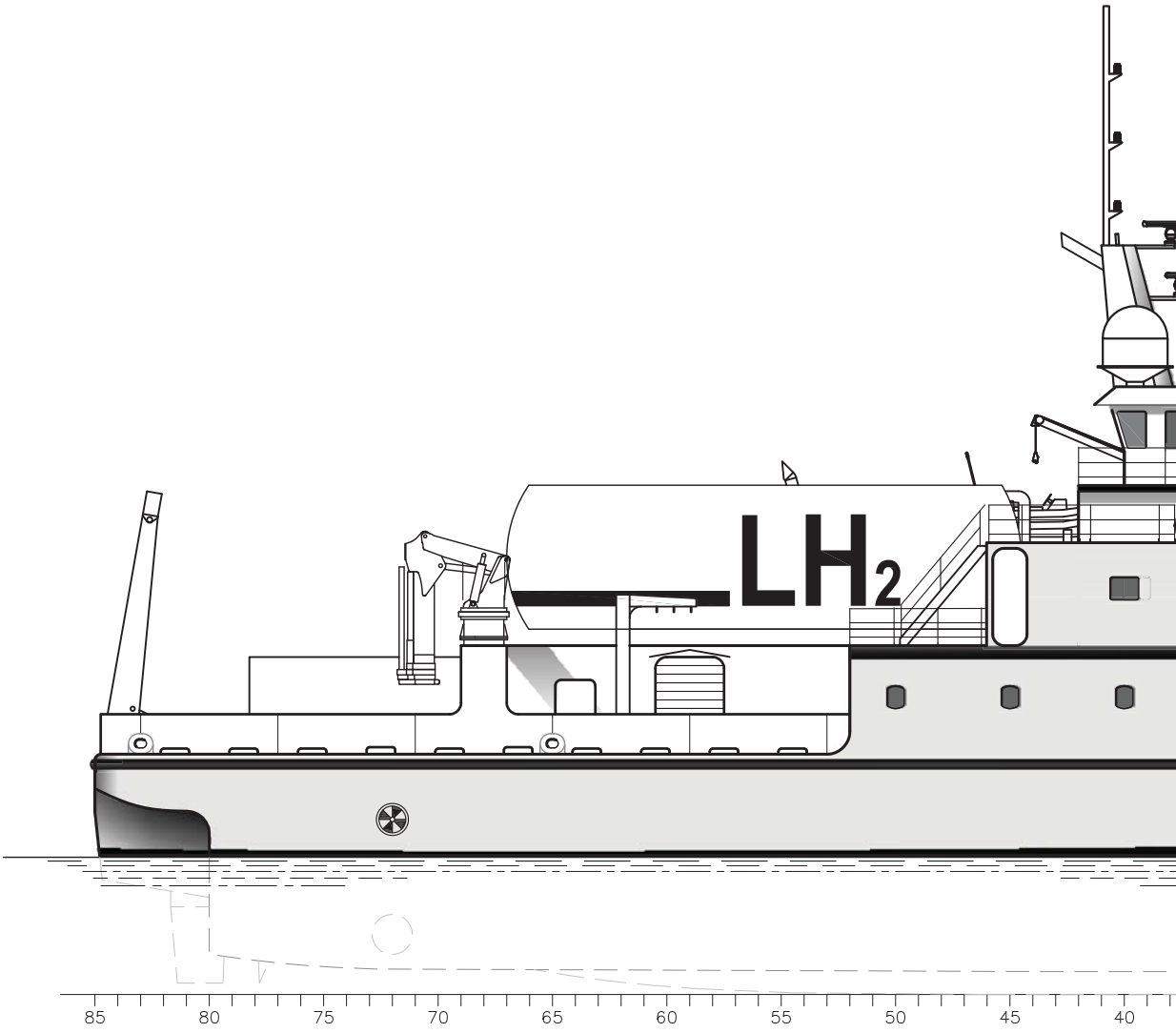

ELEVATION
OUTBOARD P
1/16"=1'-

VESSEL PARTICULARS	
LWL	162'–8"
LOA	170'–0"
BEAM	56'– 0"
HULL DEPTH	21'– 0"
DESIGN DRAFT	12'– 0"
AFT MAIN DECK W/O VANS ON DECK	1775 FT²
TOTAL AFT & SIDE DECKS W/O VANS ON DECK	2300 FT²
MAIN LAB	885 FT²
WET LAB	575 FT²
COMPUTER LAB	175 FT²
ELECTRICAL TECHNICIANS LAB	160 FT²
SCIENCE BERTHS	8 DOUBLE S/R 2 SINGLE S/R
CREW BERTHS	11 SINGLE S/R

GENERAL NOTES

ZO

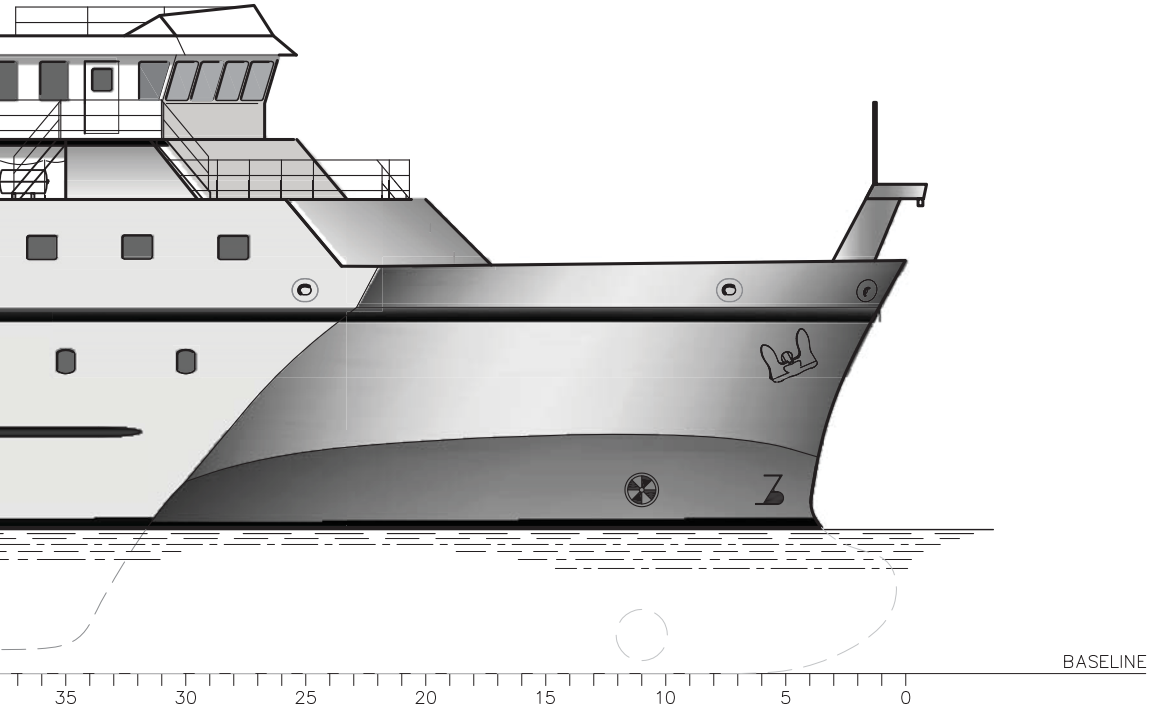

1–5A
PROFILE
-0"

REVISIONS

NE	REV	DESCRIPTION	DATE	APPD

REFERENCES

ROBERT T. MADSEN STATE OF WASHINGTON 48953 REGISTERED PROFESSIONAL ENGINEER
Digitally Signed 19-Oct-2017

SANDIA NATIONAL LABORATORIES
LIVERMORE, CALIFORNIA

ZERO–V
GENERAL ARRANGEMENT
OUTBOARD PROFILE SANDIA ZERO–V

Glosten | INNOVATIVE MARINE SOLUTIONS | 1201 WESTERN AVENUE, SUITE 200 SEATTLE, WASHINGTON 98101-2953 T 206.624.7850 GLOSTEN.COM

Drawn	Checked	Approved	Issue Date
IWM	RTM	TSL	10/3/2017

Scale	Drawing Number	Sheet	of	Revision
AS NOTED	17003.01–070–01	1	6	–

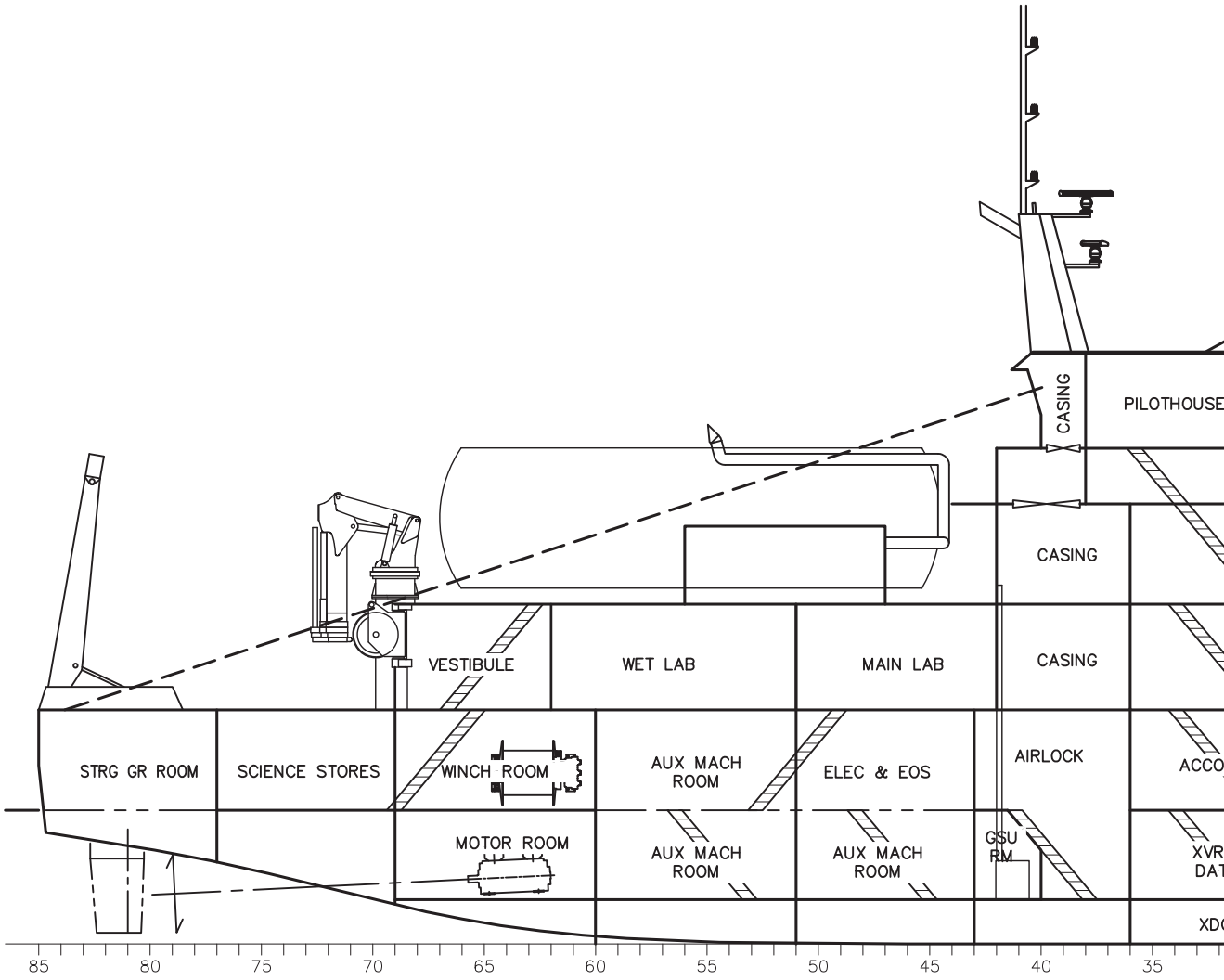

ELEVATION

INBOARD P

1/16"=1'

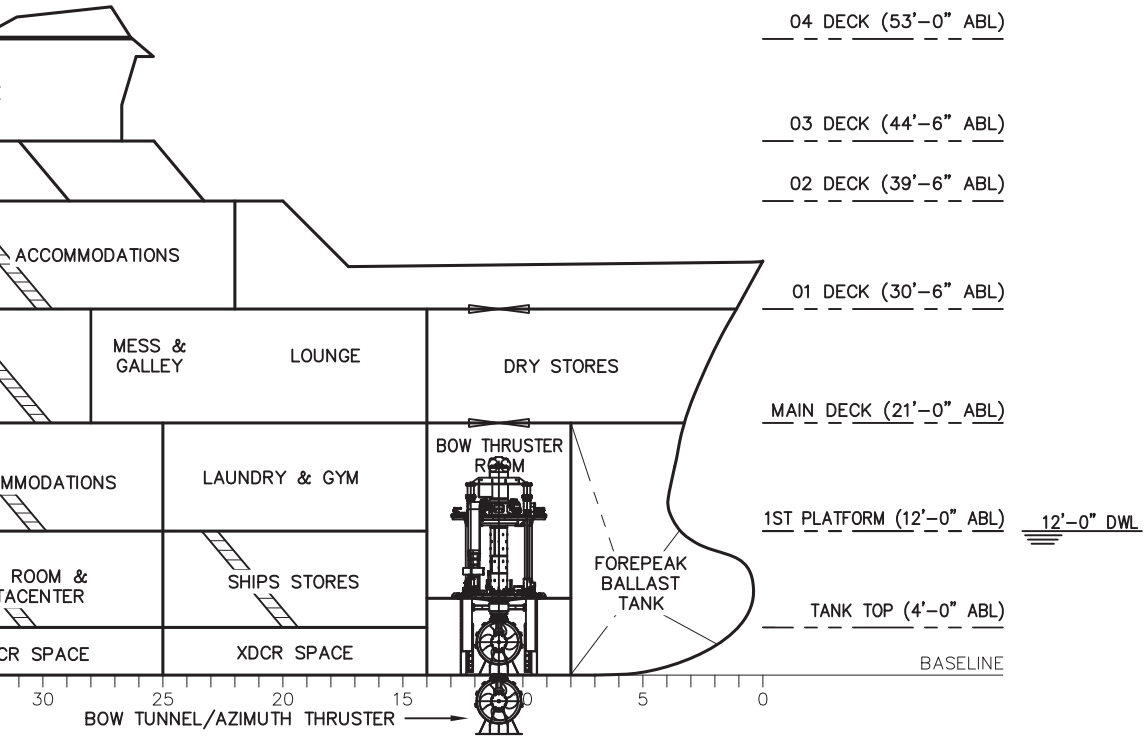

1 2–5A
PROFILE
'–0"

Digitally Signed 19-Oct-2017

SANDIA NATIONAL LABORATORIES
LIVERMORE, CALIFORNIA

ZERO–V
GENERAL ARRANGEMENT
INBOARD PROFILE SANDIA ZERO–V

Glosten | INNOVATIVE MARINE SOLUTIONS | 1201 WESTERN AVENUE, SUITE 200 SEATTLE, WASHINGTON 98101-2953 T 206.624.7850 GLOSTEN.COM

Drawn	Checked	Approved	Issue Date
IWM	RTM	TSL	10/3/2017

Scale	Drawing Number	Sheet	of	Revision
AS NOTED	17003.01–070–01	2	6	–

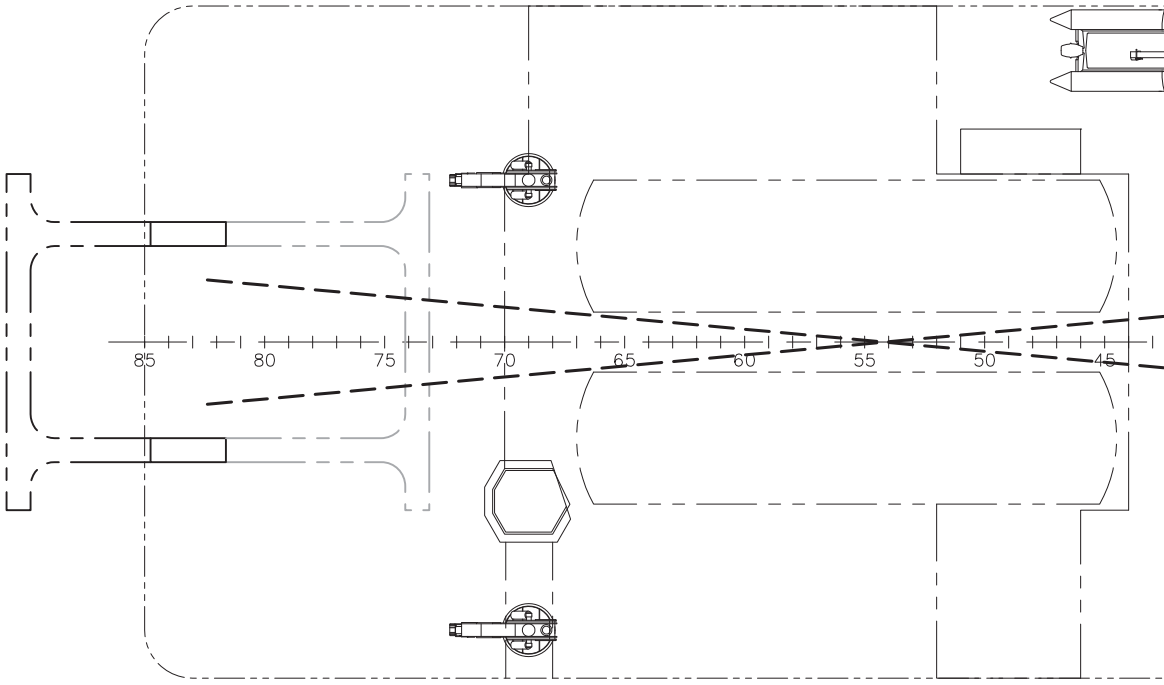
85
80
75
70
65
60
55
50
45

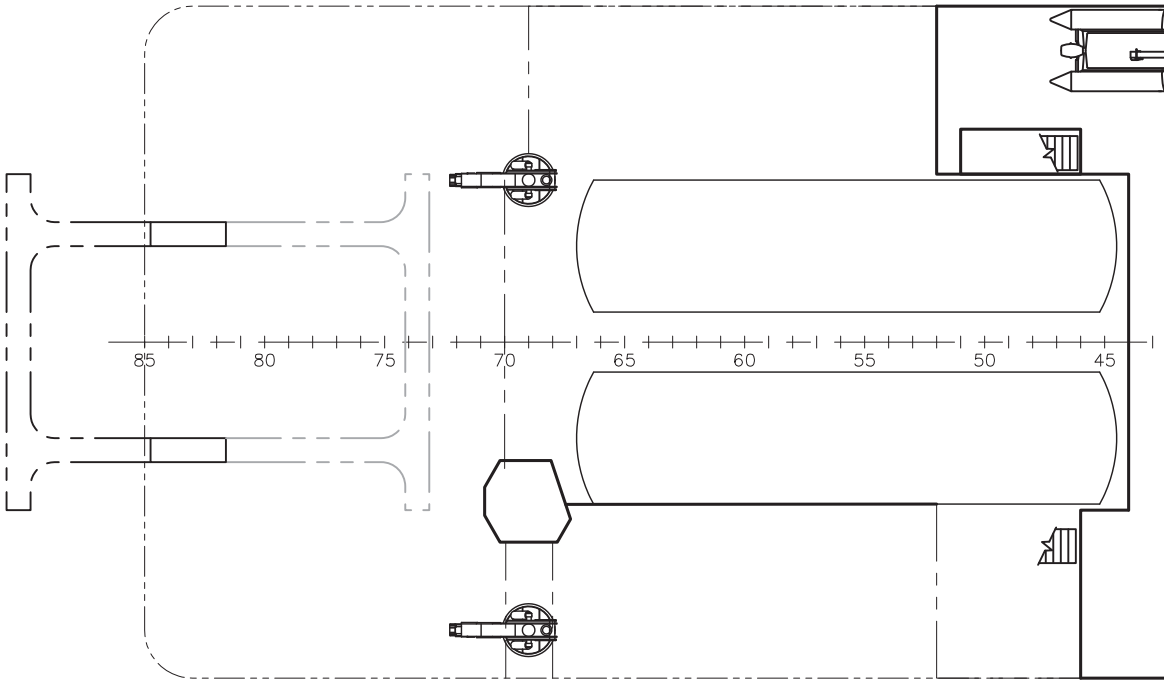
85
80
75
70
65
60
55
50
45

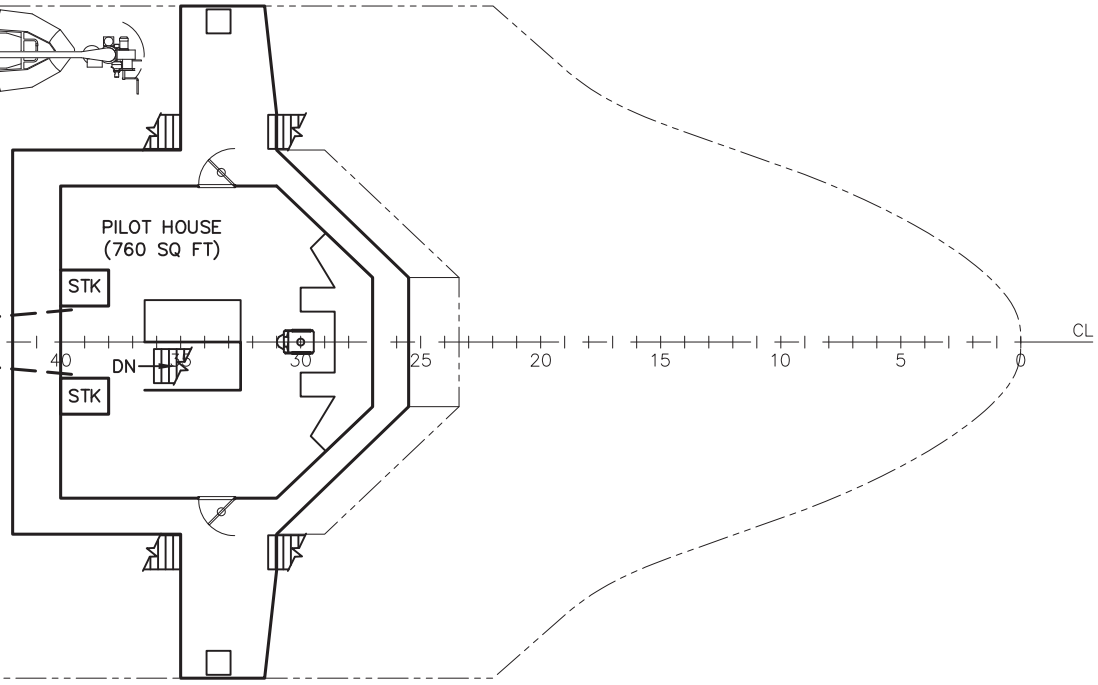

PLAN 3–3C

03 LEVEL (PILOTHOUSE)

1/16"=1'–0"

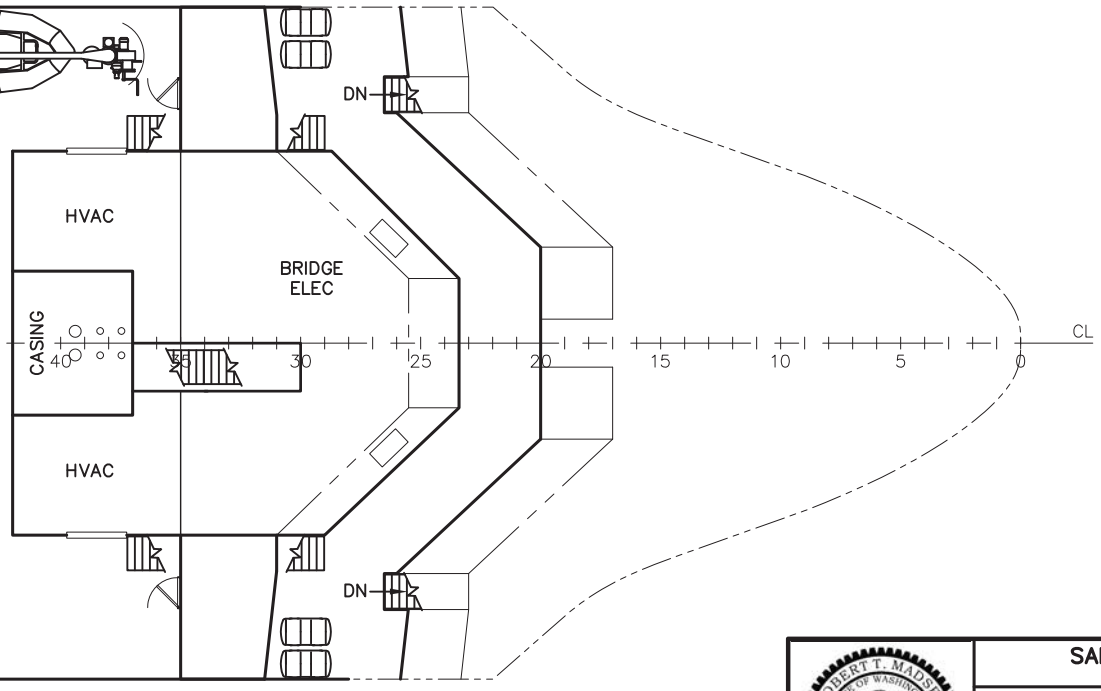

PLAN 3–3A

02 LEVEL

1/16"=1'–0"

ROBERT T. MADSEN
STATE OF WASHINGTON
18955
REGISTERED
PROFESSIONAL ENGINEER

Digitally Signed 19-Oct-2017

SANDIA NATIONAL LABORATORIES
LIVERMORE, CALIFORNIA

ZERO–V
GENERAL ARRANGEMENT
PLAN VIEWS – 02 03 04 LEVELS

Glosten | INNOVATIVE MARINE SOLUTIONS | 1201 WESTERN AVENUE, SUITE 200 SEATTLE, WASHINGTON 98101-2953 T 206.624.7850 GLOSTEN.COM

Drawn	Checked	Approved	Issue Date
IWM	RTM	TSL	10/3/2017

Scale	Drawing Number	Sheet	of	Revision
AS NOTED	17003.01–070–01	3	6	–

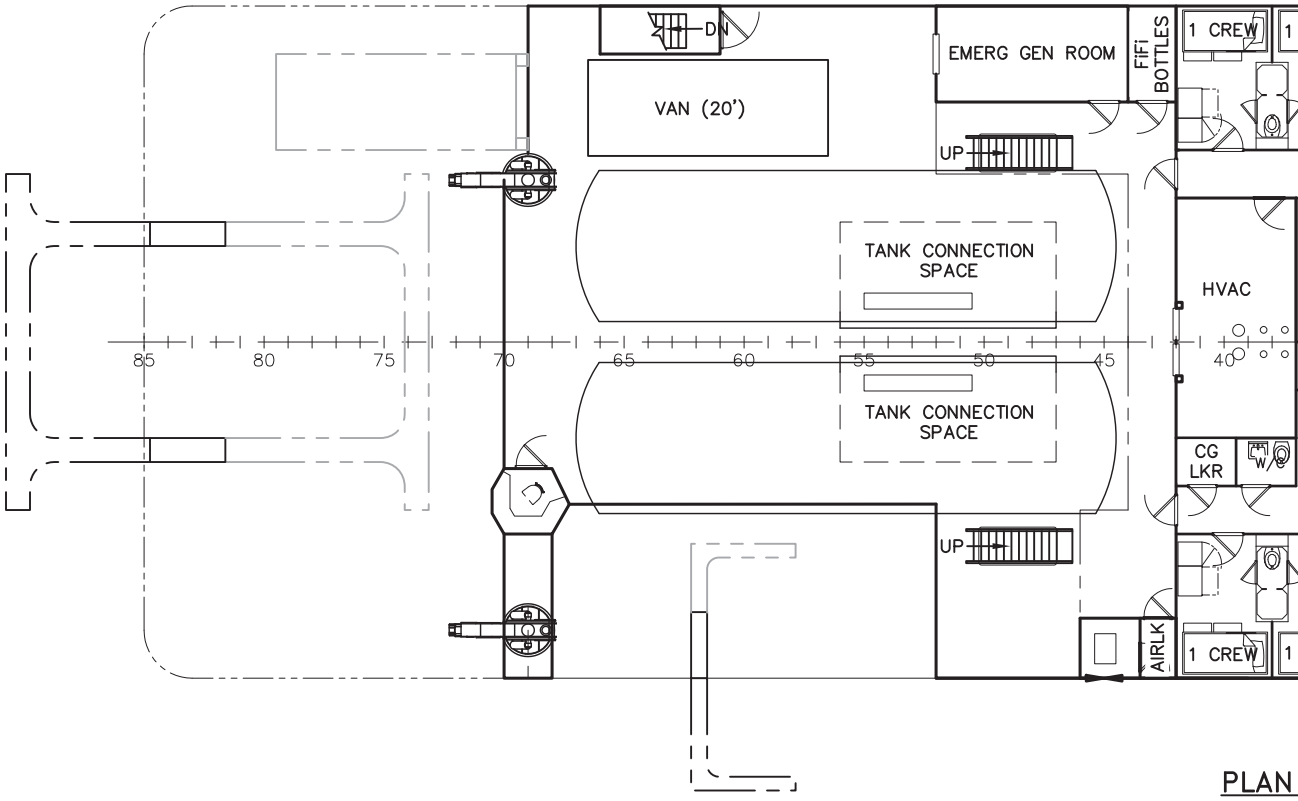

PLAN
01 L
1/16"

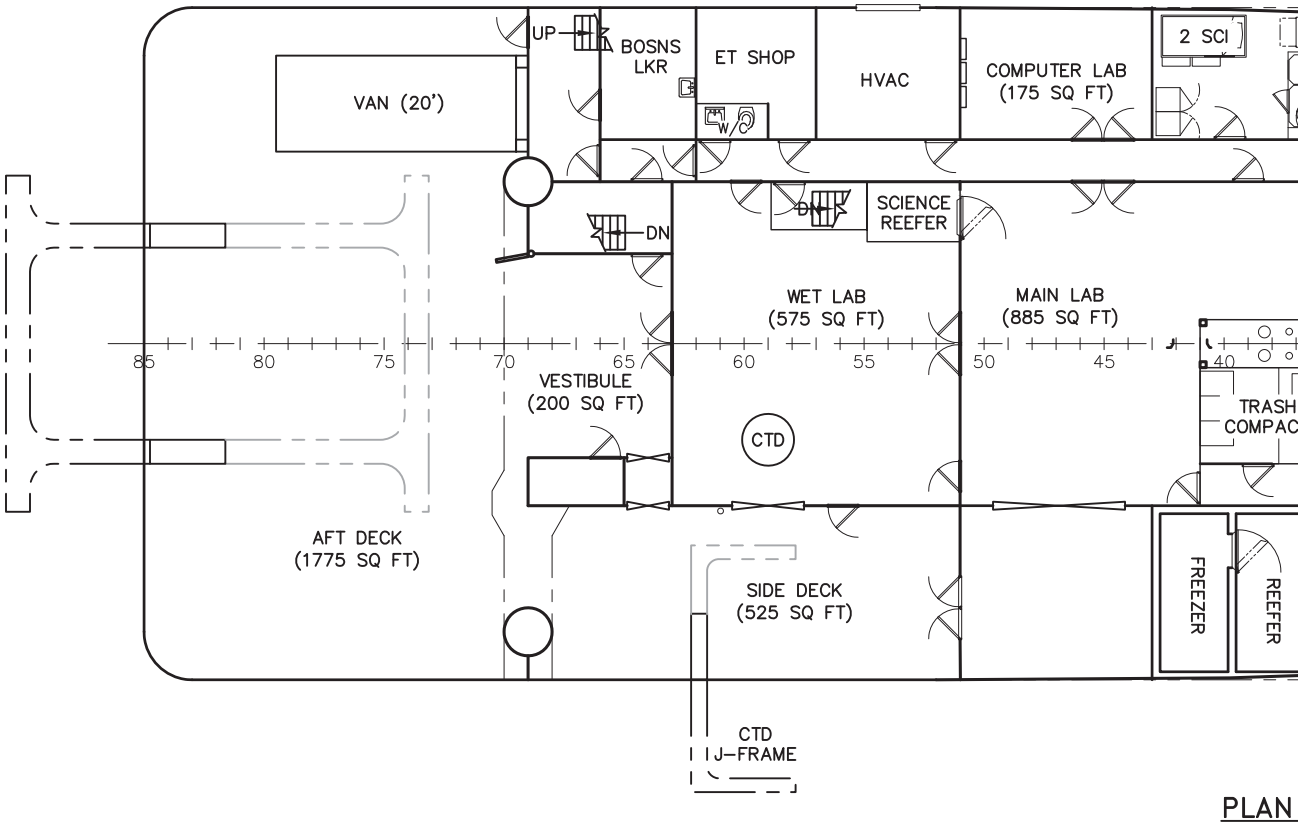

PLAN
MAIN
1/16"

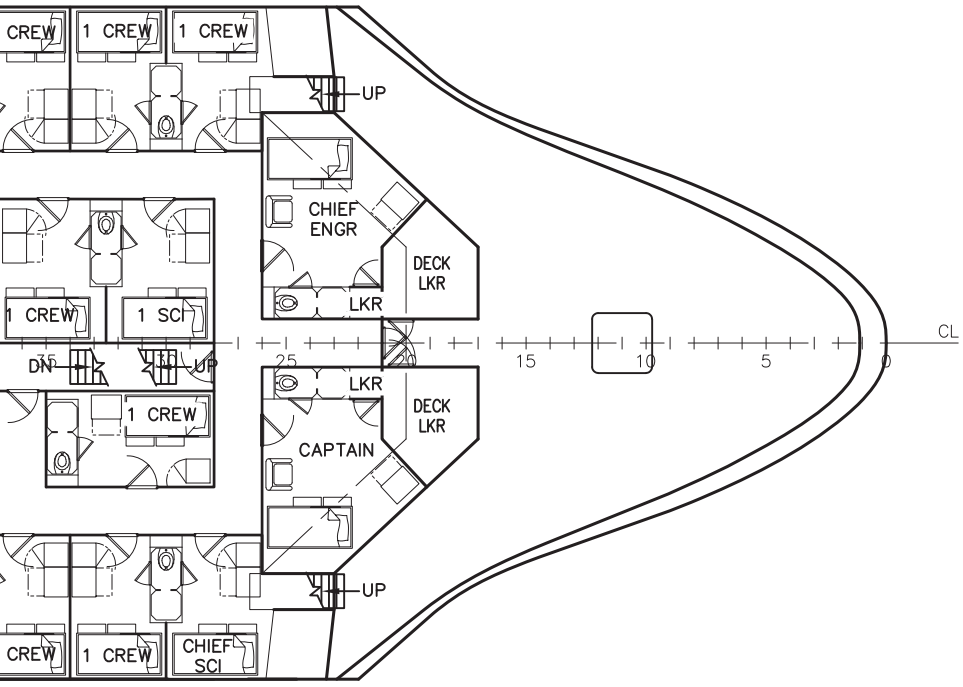

4–5C
LEVEL
"=1'–0"

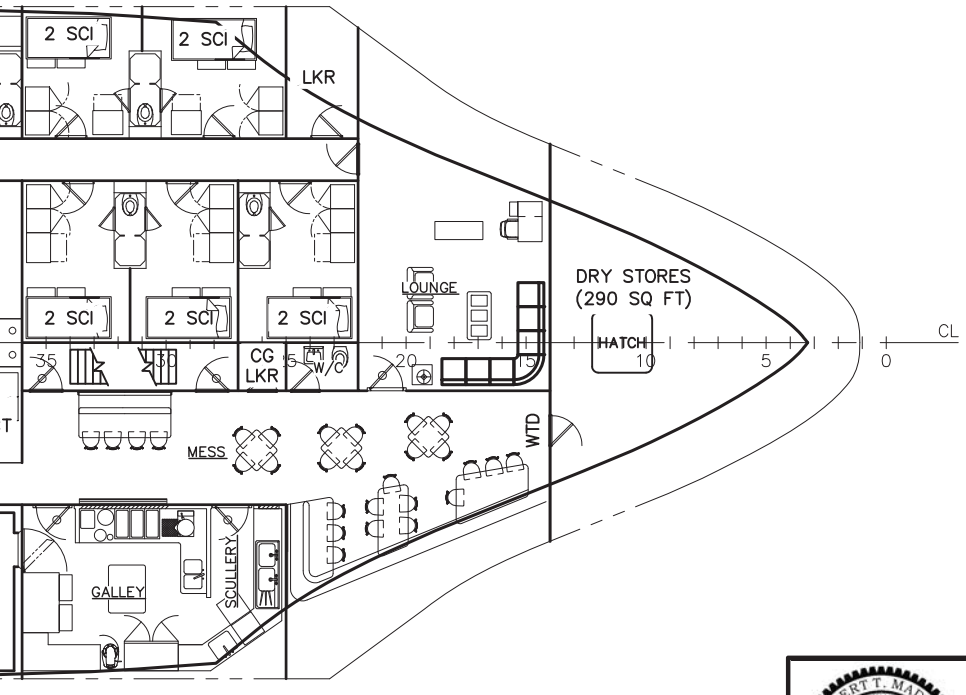

4–5A
DECK
"=1'–0"

Digitally Signed 19-Oct-2017

SANDIA NATIONAL LABORATORIES
LIVERMORE, CALIFORNIA

ZERO–V
GENERAL ARRANGEMENT
PLAN VIEWS – MAIN DECK & 01 LEVEL

Glosten | INNOVATIVE MARINE SOLUTIONS | 1201 WESTERN AVENUE, SUITE 200 SEATTLE, WASHINGTON 98101-2953 T 206.624.7850 GLOSTEN.COM

Drawn	Checked	Approved	Issue Date
IWM	RTM	TSL	10/3/2017

Scale	Drawing Number	Sheet	of	Revision
AS NOTED	17003.01–070–01	4	6	–

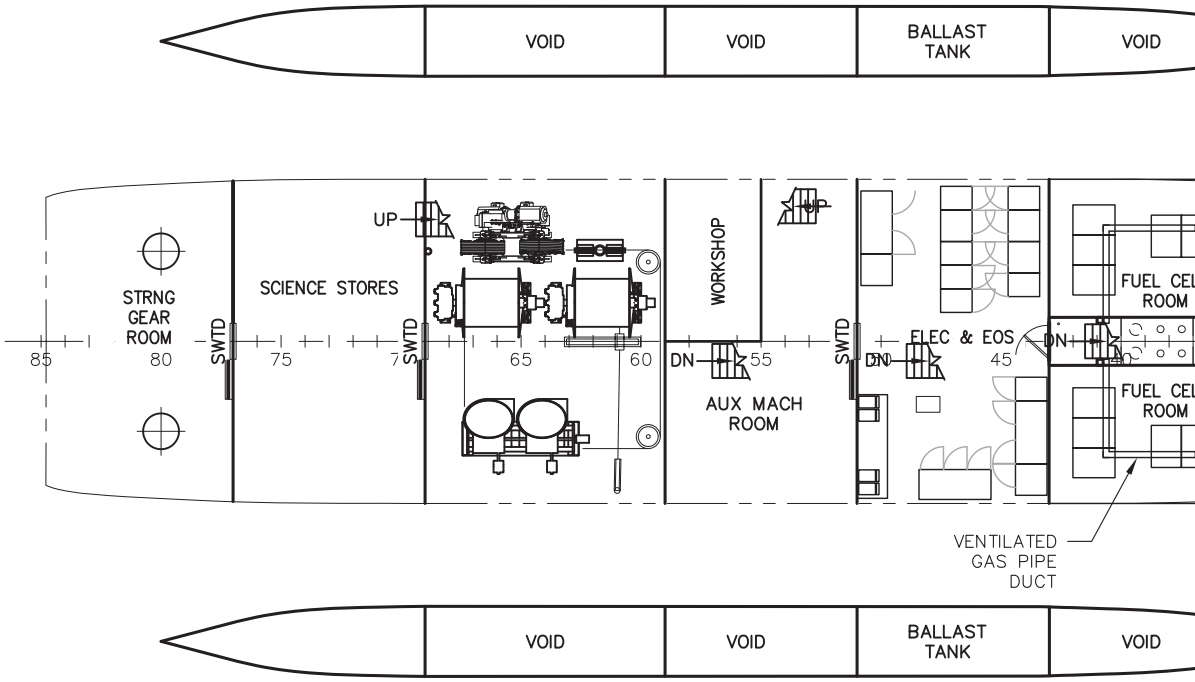

PLAN 5–5C
1ST PLATFORM
1/16"=1'–0"

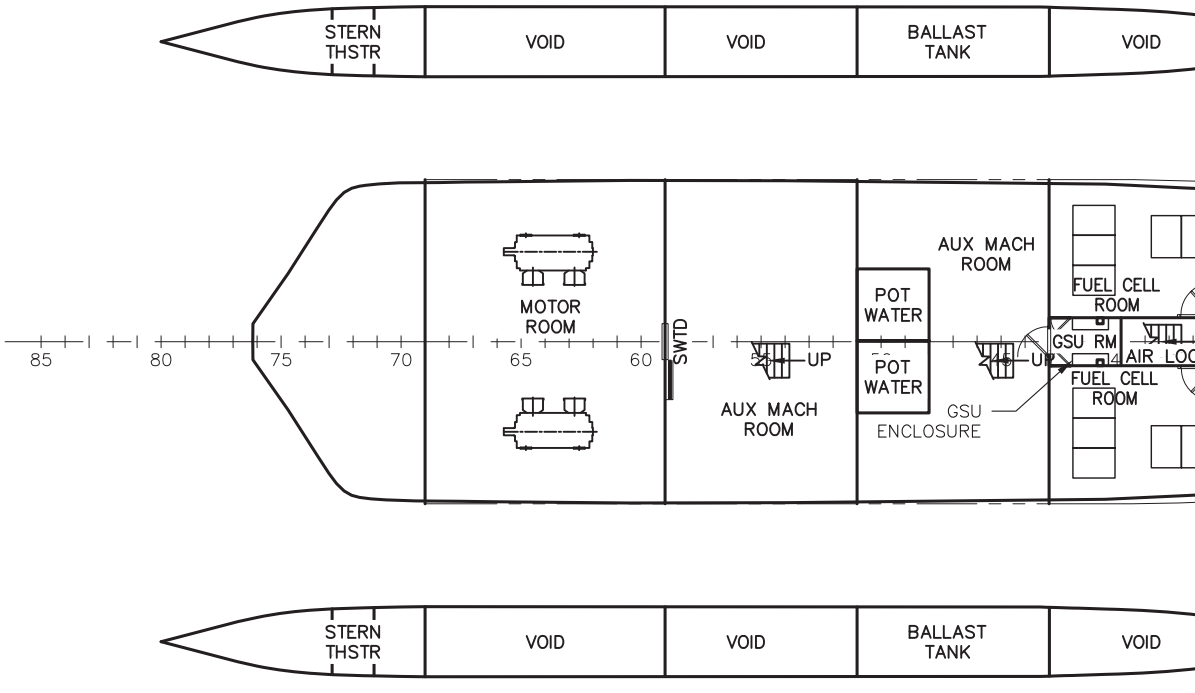

PLAN 5–5A
TANK TOP
1/16"=1'–0"

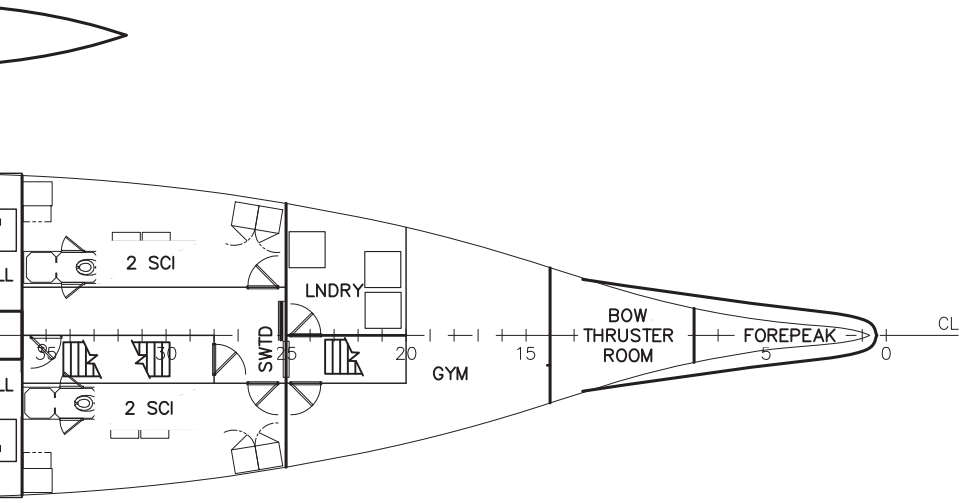

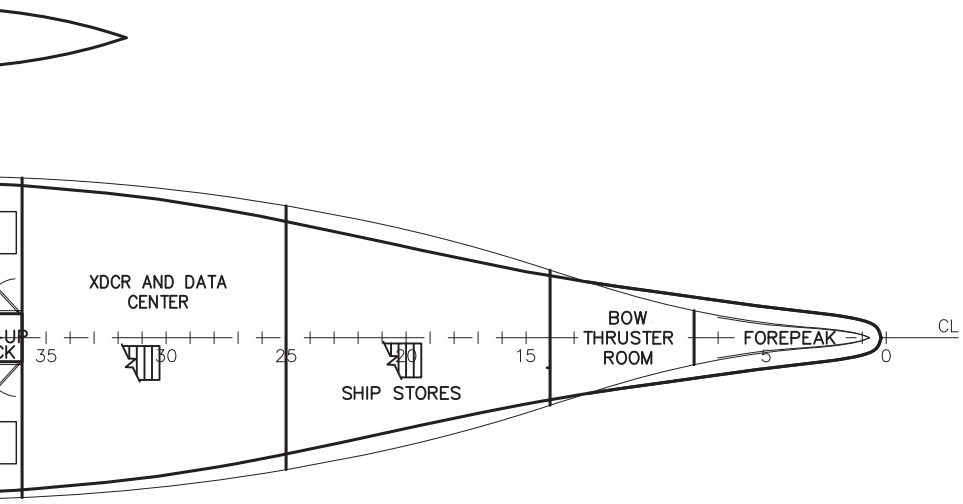

Digitally Signed 19-Oct-2017

SANDIA NATIONAL LABORATORIES
LIVERMORE, CALIFORNIA

ZERO–V
GENERAL ARRANGEMENT
PLAN VIEWS – TANKTOP HOLD & 1ST PLATFORM

Glosten
INNOVATIVE MARINE SOLUTIONS
1201 WESTERN AVENUE, SUITE 200
SEATTLE, WASHINGTON 98101-2953
T 206.624.7850 GLOSTEN.COM

Drawn	Checked	Approved	Issue Date
IWM	RTM	TSL	10/3/2017

Scale	Drawing Number	Sheet	of	Revision
AS NOTED	17003.01–070–01	5	6	–

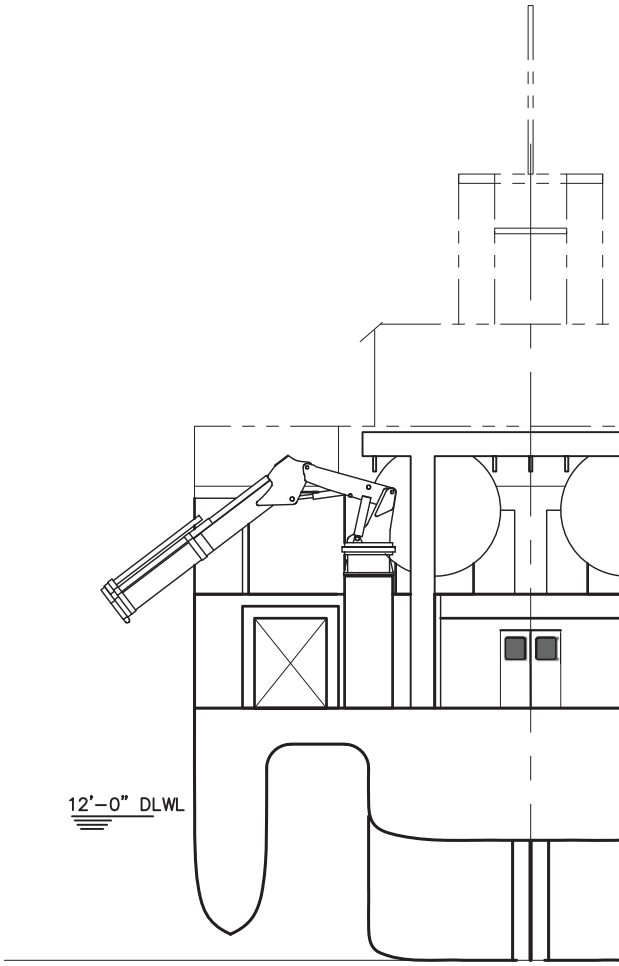

SECTION 6-5A

STERN

1/16"=1'-0"

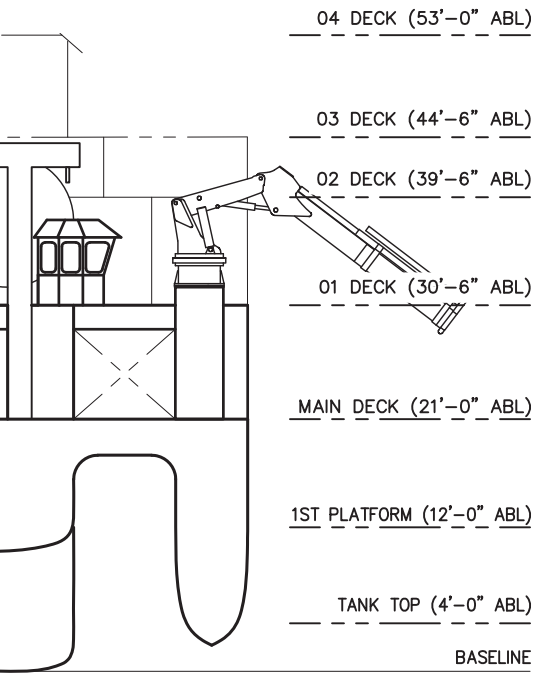

A

ROBERT T. MADSEN
STATE OF WASHINGTON
18955
REGISTERED
PROFESSIONAL ENGINEER

Digitally Signed 19-Oct-2017

SANDIA NATIONAL LABORATORIES
LIVERMORE, CALIFORNIA

ZERO–V
GENERAL ARRANGEMENT
SECTION VIEW – STERN

Glosten
INNOVATIVE MARINE SOLUTIONS
1201 WESTERN AVENUE, SUITE 200
SEATTLE, WASHINGTON 98101-2953
T 206.624.7850 GLOSTEN.COM

Drawn	Checked	Approved	Issue Date
IWM	RTM	TSL	10/3/2017

Scale	Drawing Number	Sheet	of	Revision
AS NOTED	17003.01–070–01	6	6	–

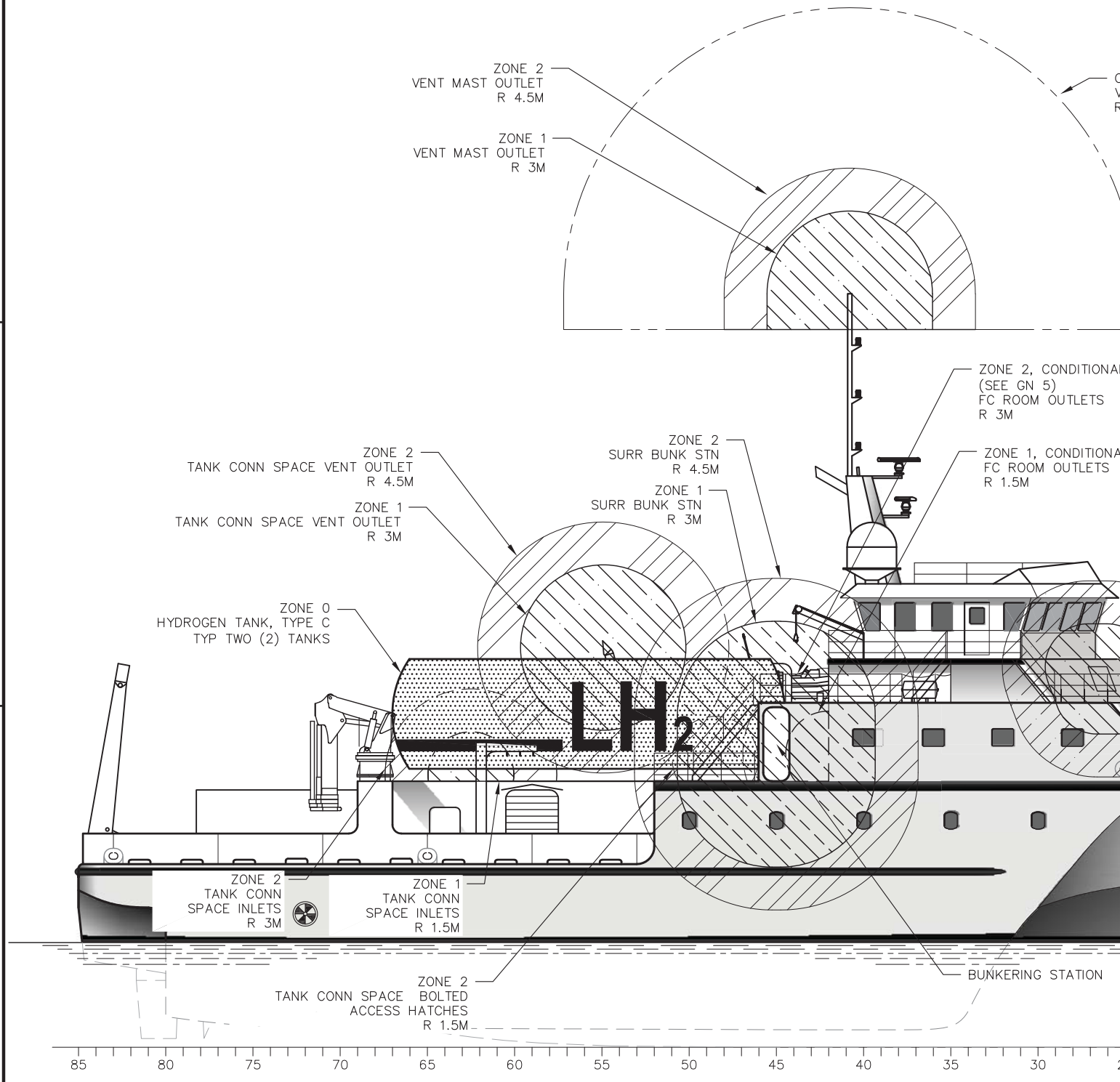

ZONE LEGEND

ZONE 0 AREA CLASSIFICATION

ZONE 1 AREA CLASSIFICATION

ZONE 2 AREA CLASSIFICATION

ELEVATION 1–5A

OUTBOARD PROFILE

1/16"=1'–0"

CLEARANCE TO VENTILATION INTAKES AND OPENINGS
VENT MAST OUTLET
R 10M

AL (SEE GN5)

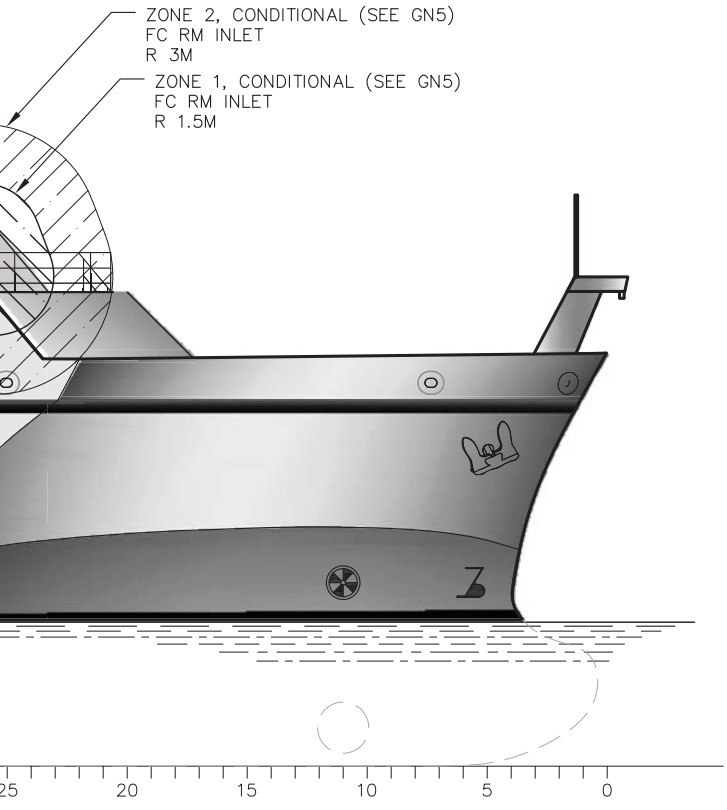

GENERAL NOTES

1. ELECTRICAL EQUIPMENT AND INSTALLATIONS WITHIN THE HAZARDOUS ZONES SHALL BE INTRINSICALLY SAFE, EXPLOSION–PROOF, FLAMEPROOF OR ANOTHER ACCEPTED PROTECTION METHOD IN ACCORDANCE WITH APPLICABLE USCG AND DNV–GL REQUIREMENTS PARTICULAR TO EACH ZONE'S HAZARD DESIGNATION.
2. THERE SHALL BE NO SPLICES IN ELECTRICAL CABLES IN HAZARDOUS AREAS EXCEPT IN INTRINSICALLY SAFE CIRCUITS.
3. FUEL TANKS AND ALL PIPING CONTAINING FUEL, INCLUDING PRESSURE RELIEF PIPING, IS CLASSIFIED AS A HAZARDOUS ZONE 0.
4. THE SPACE WITHIN THE SECONDARY ENCLOSURE AROUND FUEL PIPING IS CONSIDERED A HAZARDOUS ZONE 1 AREA. EQUIPMENT, INCLUDING GAS DETECTION, SHALL BE RATED ACCORDINGLY.
5. FUEL CELL ROOMS ARE PROTECTED BY EMERGENCY SHUTDOWN SYSTEMS (ESD). THEY ARE CONSIDERED NON–HAZARDOUS UNDER NORMAL CONDITIONS. ANY NON ESSENTIAL ELECTRICAL EQUIPMENT AND LIGHTING SHALL IN THE SPACE OR WITHIN THE HAZARDOUS AREAS ASSOCIATED WITH THE SPACE SHALL BE DE–ENERGIZED UPON DETECTION OF A GAS LEAK. ANY ESSENTIAL EQUIPMENT AND LIGHTING REQUIRED TO OPERATE FOLLOWING DETECTION OF GAS LEAKAGE SHALL BE SUITABLE FOR USE IN ZONE 1.
6. HYDROGEN VENT OUTLET RADIUS, SHOWN AS 10M (32'–10"), IS FOR CLEARANCES TO ENTRANCES, TO AIR INTAKES, OR TO OPENINGS TO ACCOMMODATIONS SPACES, SERVICE SPACES, CONTROL STATIONS AND OTHER NON–HAZARDOUS AREAS IN ACCORDANCE WITH DNV REGULATIONS.

REFERENCES

1. GLOSTEN, FILE NO. 17003.01–070–01, CONCEPT GENERAL ARRANGEMENT
2. INTERNATIONAL CODE OF SAFETY FOR SHIPS USING GASES OR OTHER LOW–FLASHPOINT FUEL (IGF CODE), INTERNATIONAL MARITIME ORGANIZATION, 1 JAN 2017
3. DNV–GL RULES FOR CLASSIFICATION OF SHIPS, PART 6 CH 2, SECTION 3, FUEL CELL INSTALLATIONS, 2016
4. DNV–GL RULES FOR CLASSIFICATION OF SHIPS, PART 6 CH 2, SECTION 5, GAS FUELED SHIP INSTALLATIONS, 2016

REVISIONS

ZONE	REV	DESCRIPTION	DATE	APPD

ROBERT T. MADSEN STATE OF WASHINGTON 18955 REGISTERED PROFESSIONAL ENGINEER
Digitally Signed 19-Oct-2017

SANDIA NATIONAL LABORATORIES
LIVERMORE, CALIFORNIA

ZERO–V
PRELIMINARY HAZARDOUS ZONES PLAN
OUTBOARD PROFILE

Glosten | INNOVATIVE MARINE SOLUTIONS | 1201 WESTERN AVENUE, SUITE 200 SEATTLE, WASHINGTON 98101-2953 T 206.624.7850 GLOSTEN.COM

Drawn	Checked	Approved	Issue Date
CMCF	RTM	TSL	10/3/2017

Scale	Drawing Number	Sheet	of	Revision
AS NOTED	17003.01–000–01	1	3	–

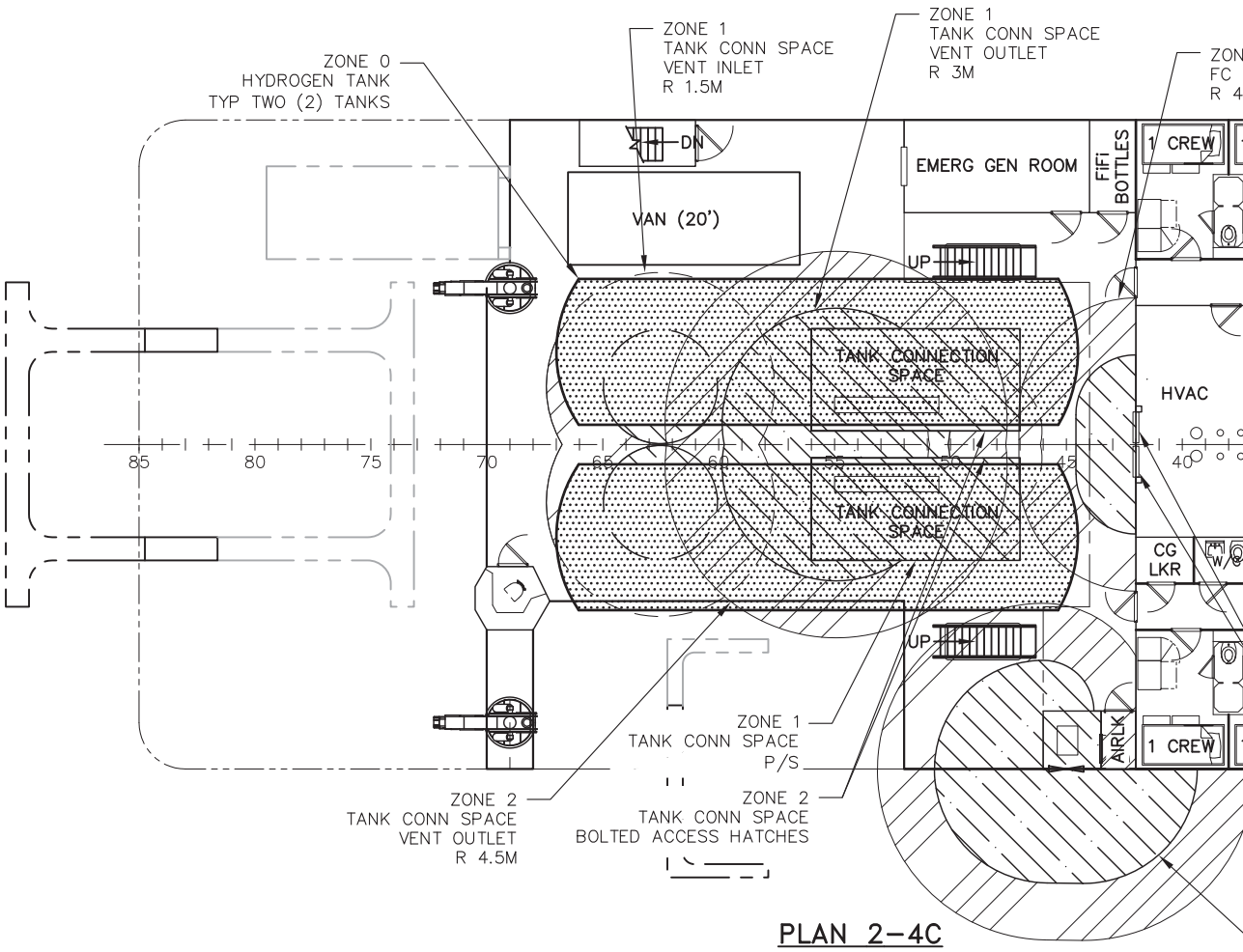

PLAN 2–4C
01 DECK
1/16"=1'–0"

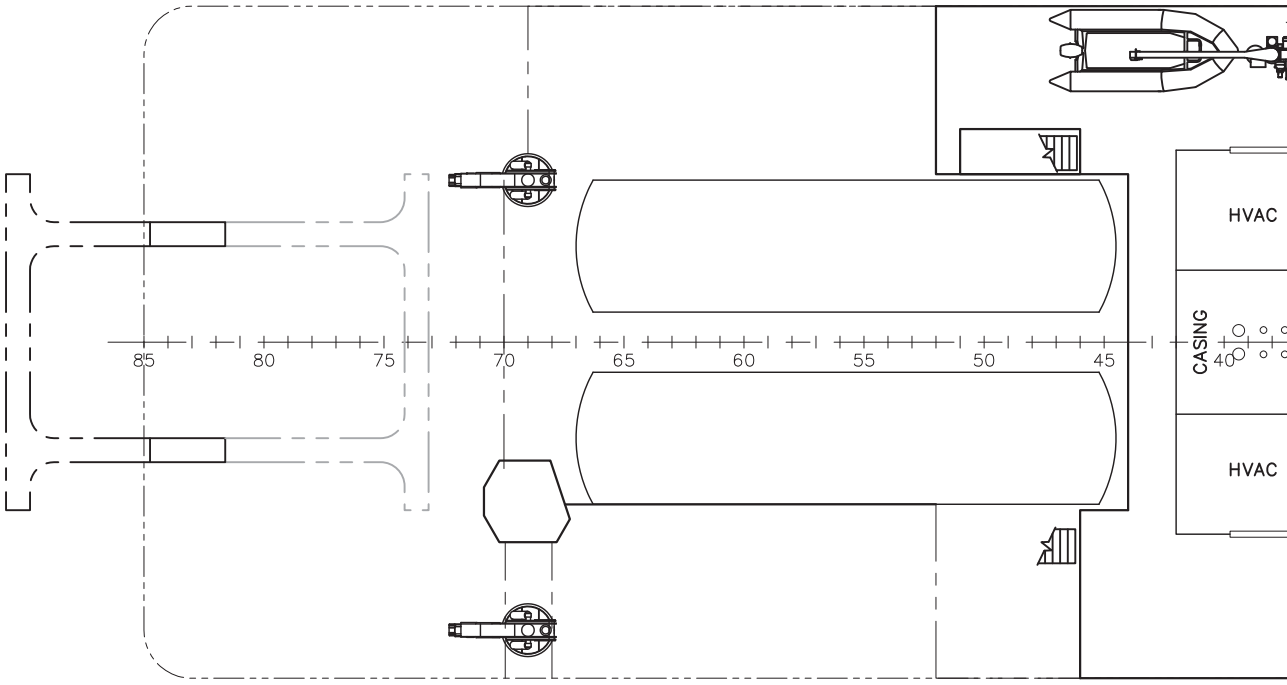

PLAN 2–4A
02 DECK
1/16"=1'–0"

E 2, CONDITIONAL (SEE GN5)
ROOM OUTLETS
.5M

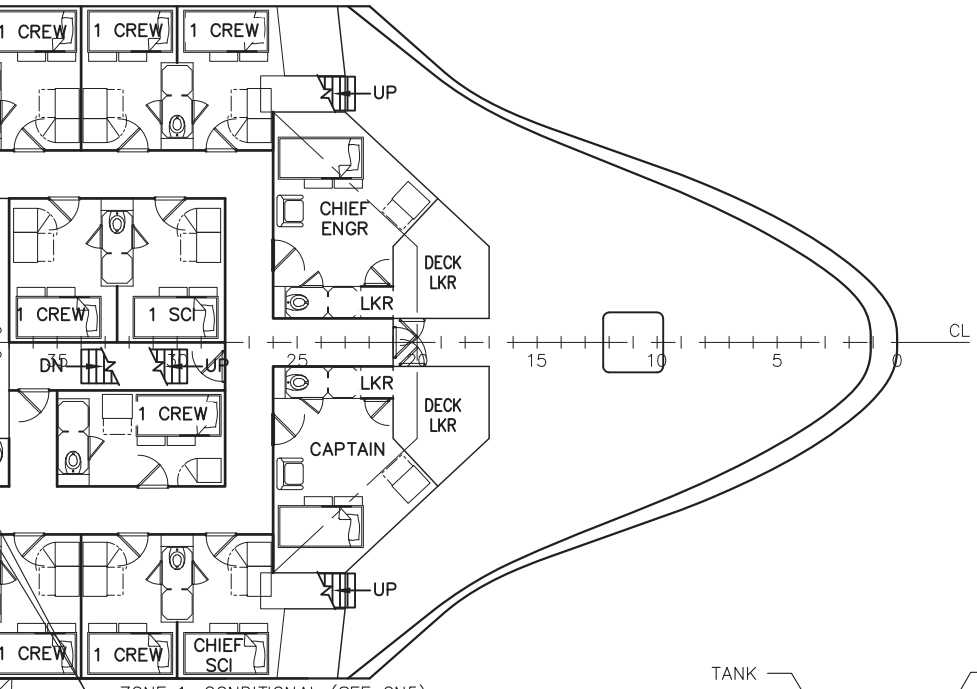

ZONE 1, CONDITIONAL (SEE GN5)
FC ROOM VENT OUTLETS
R 1.5M

ZONE 2
SURR BUNK STN
R 4.5M

ZONE 1
SURR BUNK STN
R 3M

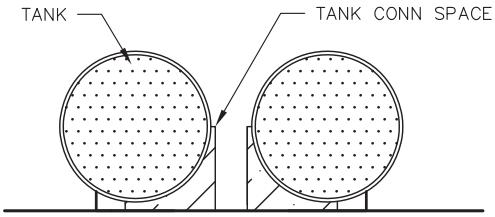

DETAIL 2–2B

LH2 TANKS AND TANK
CONNECTION SPACES
1/16"=1'–0"

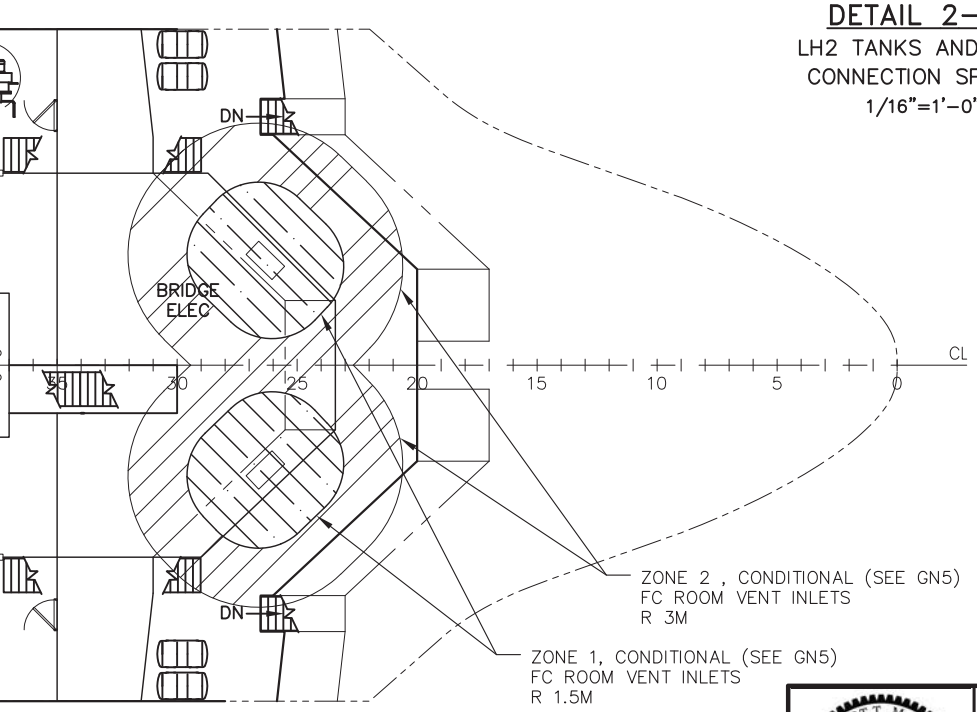

ZONE 2 , CONDITIONAL (SEE GN5)
FC ROOM VENT INLETS
R 3M

ZONE 1, CONDITIONAL (SEE GN5)
FC ROOM VENT INLETS
R 1.5M

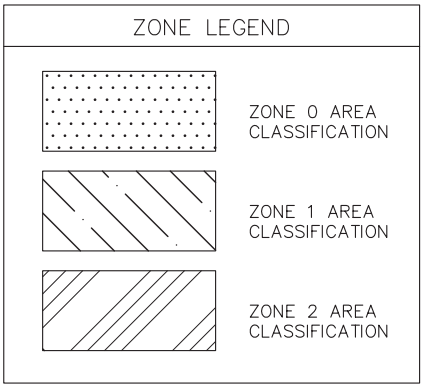

ROBERT T. MADSEN
STATE OF WASHINGTON
18955
REGISTERED
PROFESSIONAL ENGINEER
Digitally Signed 19-Oct-2017

SANDIA NATIONAL LABORATORIES
LIVERMORE, CALIFORNIA

ZERO–V
PRELIMINARY HAZARDOUS ZONES PLAN
01 & 02 DECKS

Glosten
INNOVATIVE MARINE SOLUTIONS
1201 WESTERN AVENUE, SUITE 200
SEATTLE, WASHINGTON 98101-2953
T 206.624.7850 GLOSTEN.COM

Drawn	Checked	Approved	Issue Date
CMCF	RTM	TSL	10/3/2017

Scale	Drawing Number	Sheet	of	Revision
AS NOTED	17003.01–000–01	2	3	–

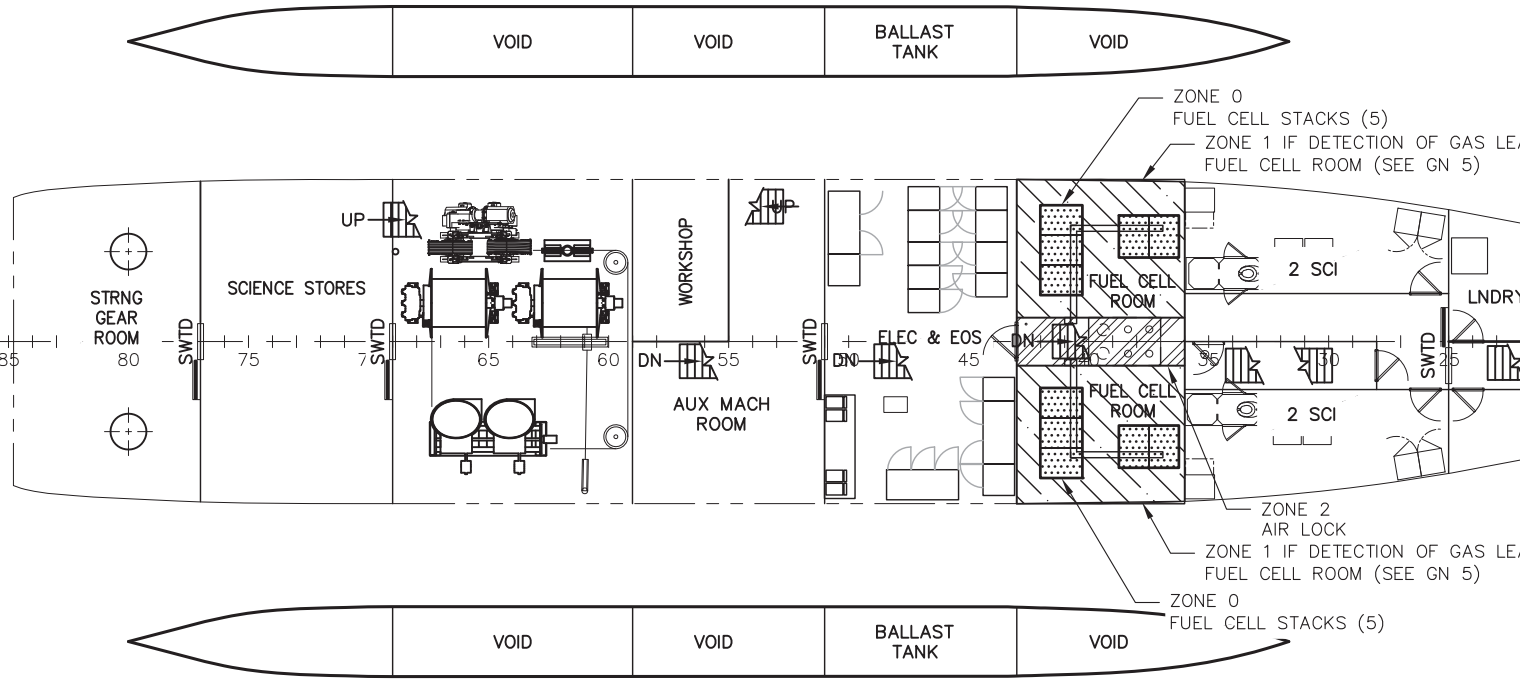

PLAN 3–6C
1ST PLATFORM
1/16"=1'–0"

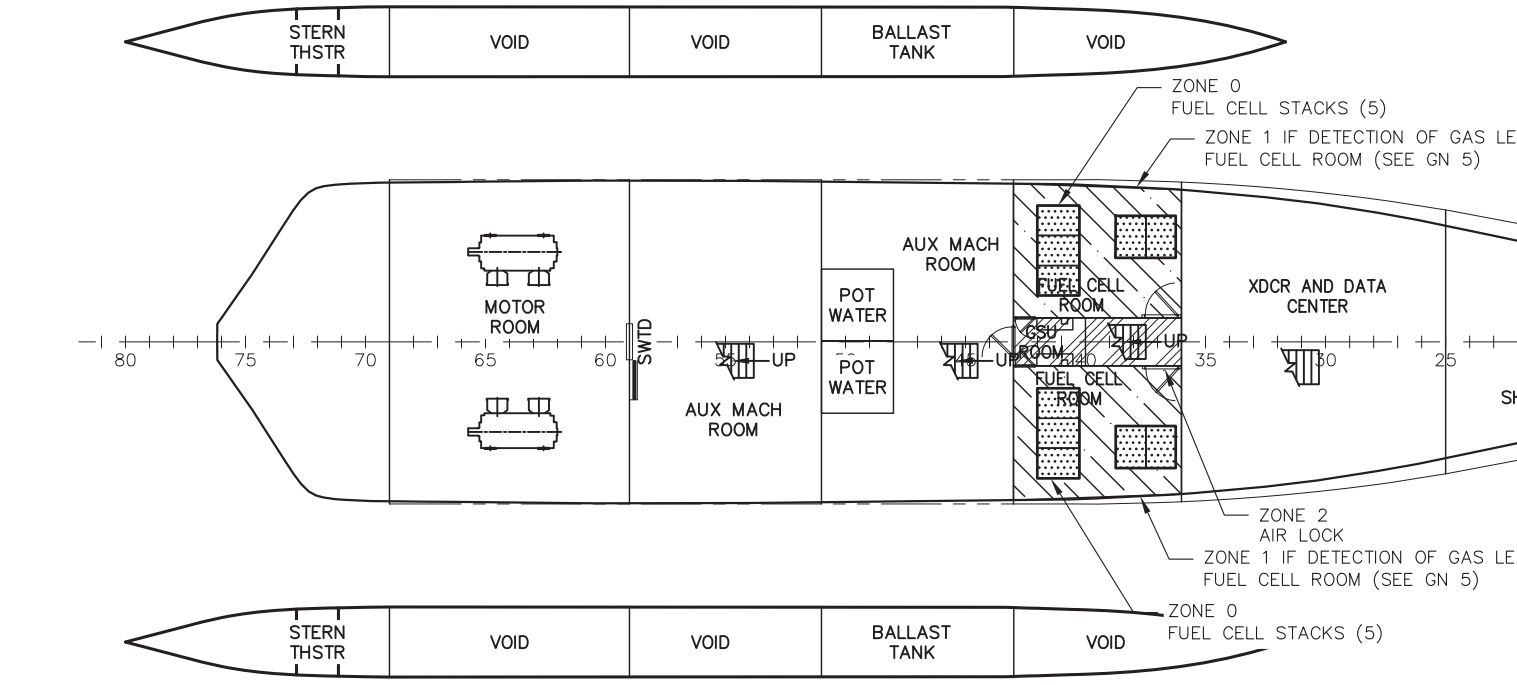

PLAN 3–6A
TANK TOP
1/16"=1'–0"

AKAGE

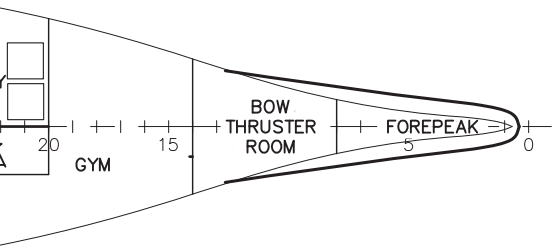

AKAGE

AKAGE

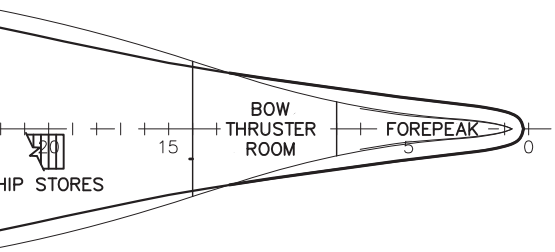

AKAGE

ZONE LEGEND

ZONE 0 AREA CLASSIFICATION

ZONE 1 AREA CLASSIFICATION

ZONE 2 AREA CLASSIFICATION

ROBERT T. MADSEN STATE OF WASHINGTON 18955 REGISTERED PROFESSIONAL ENGINEER

Digitally Signed 19-Oct-2017

SANDIA NATIONAL LABORATORIES
LIVERMORE, CALIFORNIA

ZERO–V
PRELIMINARY HAZARDOUS ZONES PLAN
HOLD LEVELS

Glosten
INNOVATIVE MARINE SOLUTIONS
1201 WESTERN AVENUE, SUITE 200
SEATTLE, WASHINGTON 98101-2953
T 206.624.7850 GLOSTEN.COM

Drawn	Checked	Approved	Issue Date
CMCF	RTM	TSL	10/3/2017

Scale	Drawing Number	Sheet	Revision
AS NOTED	17003.01–000–01	3 of 3	–

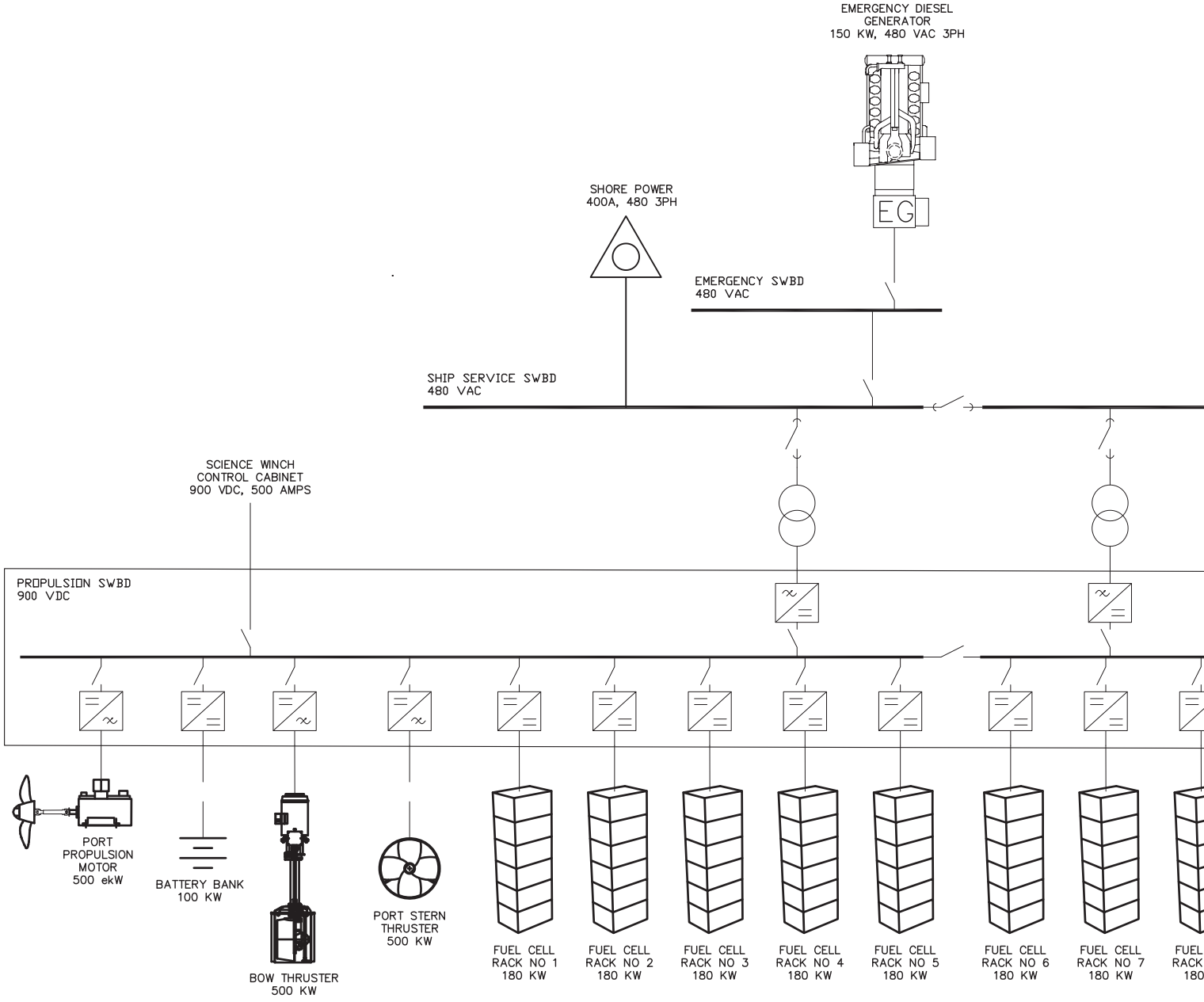
EMERGENCY DIESEL
GENERATOR
150 KW, 480 VAC 3PH
EG
SHORE POWER
400A, 480 3PH
EMERGENCY SWBD
480 VAC
SHIP SERVICE SWBD
480 VAC
SCIENCE WINCH
CONTROL CABINET
900 VDC, 500 AMPS
PROPULSION SWBD
900 VDC
PORT
PROPULSION
MOTOR
500 ekW
BATTERY BANK
100 KW
BOW THRUSTER
500 KW
PORT STERN
THRUSTER
500 KW
FUEL CELL
RACK NO 1
180 KW
FUEL CELL
RACK NO 2
180 KW
FUEL CELL
RACK NO 3
180 KW
FUEL CELL
RACK NO 4
180 KW
FUEL CELL
RACK NO 5
180 KW
FUEL CELL
RACK NO 6
180 KW
FUEL CELL
RACK NO 7
180 KW

GENERAL NOTES

1. MARINE HYDROGEN FUEL CELL INSTALLATIONS ARE AN EMERGING TECHNOLOGY AND CURRENTLY THERE IS NO APPLICABLE REGULATORY REVIEW PROCESS IN PLACE IN THE UNITED STATES. THIS DRAWING IS TO TO FACILITATE A REGULATORY FEASIBILITY DISCUSSION OF THE FUNDAMENTAL ELECTRICAL SYSTEM ARCHITECTURE.
2. ALL EQUIPMENT AND DESIGNS SHALL COMPLY WITH, BUT NOT BE LIMITED TO, THE REQUIREMENTS OF THE US COAST GUARD (USCG), DNVGL, AND THE RECOMMENDATIONS OF THE INSTITUTE OF ELECTRICAL AND ELECTRONIC ENGINEERS (IEEE) STANDARD 45.
3. ELECTRICAL EQUIPMENT AND INSTALLATIONS WITHIN THE HAZARDOUS ZONES SHALL BE INTRINSICALLY SAFE, EXPLOSION–PROOF, FLAMEPROOF OR ANOTHER ACCEPTED PROTECTION METHOD IN ACCORDANCE WITH APPLICABLE USCG AND DNV–GL REQUIREMENTS PARTICULAR TO EACH ZONE'S HAZARD DESIGNATION.
4. FUEL CELL ROOMS ARE PROTECTED BY EMERGENCY SHUTDOWN SYSTEMS (ESD). THEY ARE CONSIDERED NON–HAZARDOUS UNDER NORMAL CONDITIONS. ANY NON ESSENTIAL ELECTRICAL EQUIPMENT AND LIGHTING SHALL IN THE SPACE OR WITHIN THE HAZARDOUS AREAS ASSOCIATED WITH THE SPACE SHALL BE DE–ENERGIZED UPON DETECTION OF A GAS LEAK. ANY ESSENTIAL EQUIPMENT AND LIGHTING REQUIRED TO OPERATE FOLLOWING DETECTION OF GAS LEAKAGE SHALL BE SUITABLE FOR USE IN ZONE 1.

REFERENCES

1. GLOSTEN DWG 17003.01–000–01, PRELIMINARY HAZARDOUS ZONE PLAN, REV–
2. GLOSTEN DWG 17003.01–070–01, GENERAL ARRANGMENT, REV–

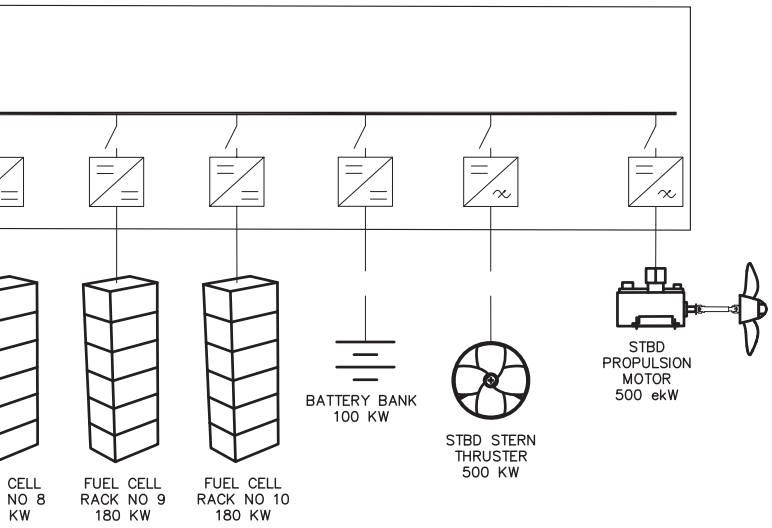

REVISIONS

ZONE	REV	DESCRIPTION	DATE	APPD

ROBERT T. MADSEN STATE OF WASHINGTON 48953 REGISTERED PROFESSIONAL ENGINEER

Digitally Signed 19-Oct-2017

SANDIA NATIONAL LABORATORIES
LIVERMORE, CALIFORNIA

ZERO–V
ELECTRICAL ONE–LINE DIAGRAM
CONCEPT SYSTEM ARCHITECTURE

Glosten — INNOVATIVE MARINE SOLUTIONS
1201 WESTERN AVENUE, SUITE 200
SEATTLE, WASHINGTON 98101-2953
T 206.624.7850 GLOSTEN.COM

Drawn	Checked	Approved	Issue Date
CMCF	RTM	TSL	10/3/2017

Scale	Drawing Number	Sheet	of	Revision
NO SCALE	17003.01–300–01	1	1	–

PIPING SYMBOL LIST

SYMBOL	DESCRIPTION
	DIRECTION OF FLOW ARROW
— GS —	PIPE – GAS SUPPLY
— SW —	PIPE – SEAWATER
— LB —	PIPE – LIQUID BUNKERING
— NS —	PIPE – NITROGEN SUPPLY
— VD —	DUCT – VENTILATION DUCT
— GV —	PIPE – GAS VENT
	VALVE, GLOBE
	VALVE, ANGLE, PRESSURE RELIEF (SELF ACTUATED)
	VALVE, MANUAL OVERRIDE

SYMBOL	DESCRIPTION
PT	PRESSURE TRANSMITTER
P	PRESSURE GAUGE
AF	AXIAL FAN
	GAS DETECTOR
	AIR INLET / OUTLET
	VALVE, SOLENOID OPERATED
M	VALVE, MOTOR OPERATED
NC	VALVE, NORMALLY CLOSED
	SPRAY NOZZLE

A

GSU – GAS S
PBU – PRESS
LH2 – LIQUEF
ACH – AIR C

CRONYM LIST

SUPPLY UNIT
SURE BUILD UNIT
FIED HYDROGEN GAS
HANGES PER HOUR

GENERAL NOTES

1. MARINE HYDROGEN FUEL CELL INSTALLATIONS ARE AN EMERGING TECHNOLOGY AND CURRENTLY THERE IS NO APPLICABLE REGULATORY REVIEW PROCESS IN PLACE IN THE UNITED STATES. THIS DRAWING IS TO BE USED ONLY TO FACILITATE A REGULATORY FEASIBILITY DISCUSSION OF THE FUNDAMENTAL GAS SYSTEMS ARCHITECTURE FOR THE SUBJECT VESSEL. THIS DRAWING IS NOT TO BE USED FOR THE DESIGN, CONSTRUCTION, MAINTENANCE OR OPERATION OF ANY MARINE, INDUSTRIAL OR OTHER GAS SYSTEM OR RELATED VENTILATION, GAS DETECTION OR SAFETY SYSTEMS.
2. PIPING SYSTEM DESIGN, MATERIAL, INSTALLATION, TESTING AND WORKMANSHIP WILL BE IN ACCORDANCE WITH REGULATORY BODY REQUIREMENTS OF U.S. COAST GUARD AND DNVGL
3. BULKHEAD AND DECK PIPING PENETRATIONS SHALL MAINTAIN THE WATERTIGHT, FUMETIGHT AND FIRE RATING OF THE BOUNDARY PER REGULATORY BODY REQUIREMENTS.
4. GAS SUPPLY, BUNKERING, AND PRESSURE RELIEF/VENT LINES SHALL BE CONTAINED IN A GAS TIGHT VENTILATED DUCT WHEN RUN THROUGH ENCLOSED SPACES.
5. LIQUID BUNKERING LINES SHALL BE DOUBLE-WALLED VACUUM INSULATED.
6. VENTILATION DUCTING SHALL BE A36 STEEL WELDED GAS TIGHT ALONG THE ENTIRE LENGTH.
7. ALL LIQUEFIED HYDROGEN PIPING SHALL BE SUFFICIENTLY INSULATED WHERE LOCATED WITHIN REACH OF PERSONNEL.
8. ALL PIPING CONTAINED IN TANK ROOMS SHALL BE CRYOGENIC COMPATIBLE.
9. ELECTRIC FAN MOTORS SHALL NOT BE LOCATED IN VENTILATION DUCTS FOR HAZARDOUS SPACES. FANS SHALL BE NON-SPARKING WITH EXPLOSION PROOF MOTORS SUITABLE FOR USE IN A HYDGOGEN GAS ATMOPSHER.
10. THE NUMBER AND POWER OF THE VENTILATION FANS SHALL BE SUCH THAT THE CAPACITY IS NOT REDUCED BY MORE THAN 50%, IF A FAN WITH A SEPARATE CIRCUIT FROM THE MAIN SWITCHBOARD OR EMERGENCY SWITCHBOARD OR A GROUP OF FANS WITH COMMON CIRCUIT FROM THE MAIN SWITCHBOARD OR EMERGENCY SWITCHBOARD, IS OUT OF ACTION.
11. ALL TANKS, PIPING, GASKETED PIPE JOINTS, AND HOSE CONNECTIONS SHALL BE ELECTRONICALLY BONDED TO THE SHIP'S STRUCTURE.

REFERENCES

1. GLOSTEN DWG NO. 9000-660-001-01, GENERAL ARRANGEMENT
2. DNV RULES FOR CLASSIFICATION OF SHIPS PART 6 CHAPTER 2 SECTION 3 "FUEL CELL INSTALLATIONS"
3. DNV RULES FOR CLASSIFICATION OF SHIPS PART 6 CHAPTER 2 Section 5 "GAS FUELED SHIP INSTALLATIONS"
4. IMO INTERNATIONAL CODE OF SAFETY FOR SHIPS USING GASES OR OTHER LOW-FLASHPOINT FUELS (IGF CODE), 2017

REVISIONS

ZONE	REV	DESCRIPTION	DATE	APPD

ROBERT T. MADSEN
STATE OF WASHINGTON
48955
REGISTERED
PROFESSIONAL ENGINEER
Digitally Signed 19-Oct-2017

SANDIA NATIONAL LABORATORIES
LIVERMORE, CALIFORNIA

ZERO-V
CONCEPT GAS SYSTEM ARCHITECTURE SKETCH
REFERENCES, NOTES, AND SYMBOLS

Glosten
INNOVATIVE MARINE SOLUTIONS
1201 WESTERN AVENUE, SUITE 200
SEATTLE, WASHINGTON 98101-2953
T 206.624.7850 GLOSTEN.COM

Drawn	Checked	Approved	Issue Date
RTM	SAC	TSL	10/3/2017

Scale	Drawing Number	Sheet	of	Revision
NO SCALE	17003.01-540-01	1	3	–

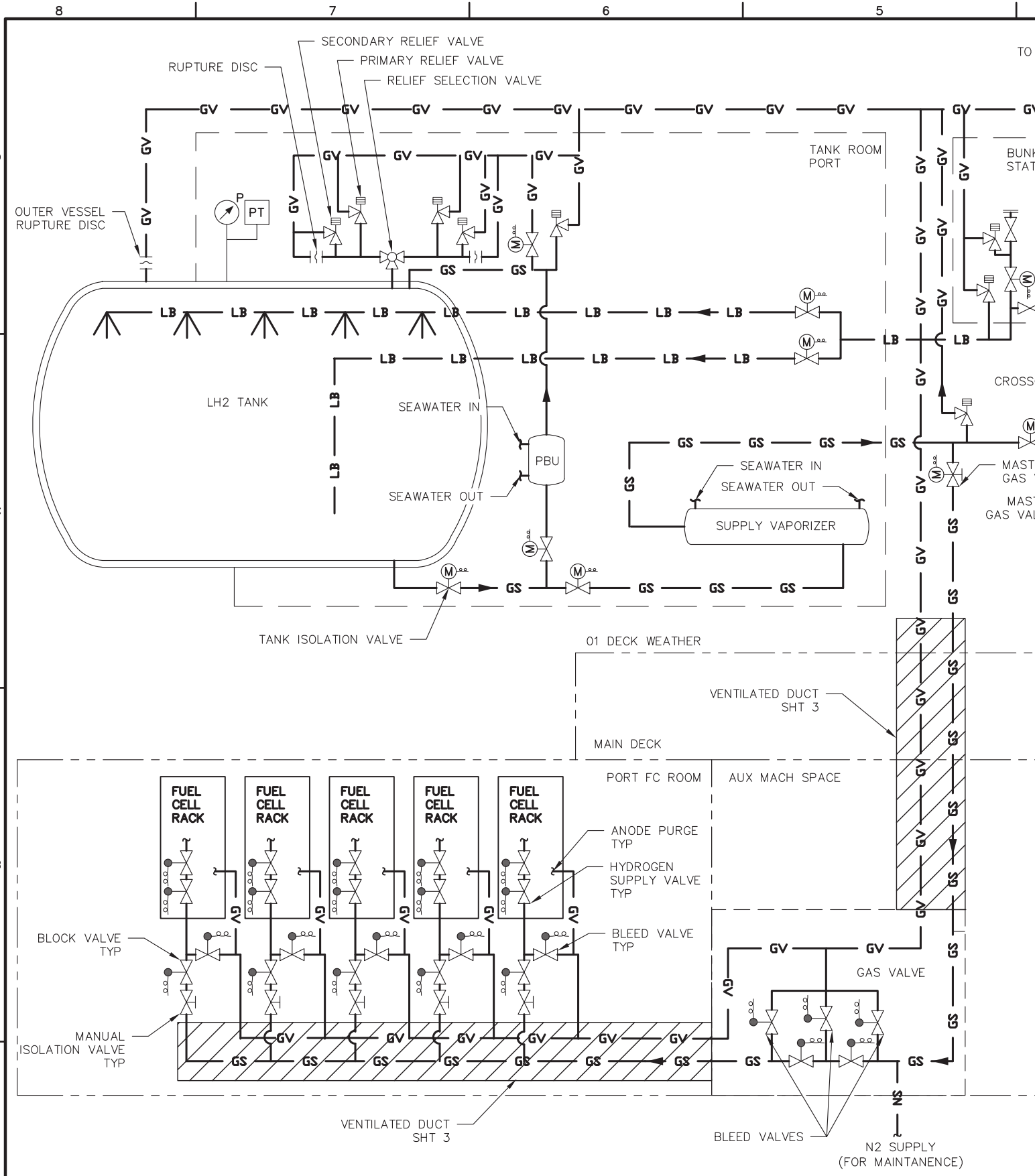
SECONDARY RELIEF VALVE
PRIMARY RELIEF VALVE
RELIEF SELECTION VALVE
RUPTURE DISC
OUTER VESSEL RUPTURE DISC
P
PT
TANK ROOM PORT
LH2 TANK
SEAWATER IN
SEAWATER OUT
PBU
SEAWATER IN
SEAWATER OUT
SUPPLY VAPORIZER
TANK ISOLATION VALVE
01 DECK WEATHER
VENTILATED DUCT SHT 3
MAIN DECK
PORT FC ROOM
AUX MACH SPACE
FUEL CELL RACK
ANODE PURGE TYP
HYDROGEN SUPPLY VALVE TYP
BLOCK VALVE TYP
BLEED VALVE TYP
GAS VALVE
MANUAL ISOLATION VALVE TYP
VENTILATED DUCT SHT 3
BLEED VALVES
N2 SUPPLY (FOR MAINTANENCE)
CROSS
GV
GS
LB
N2

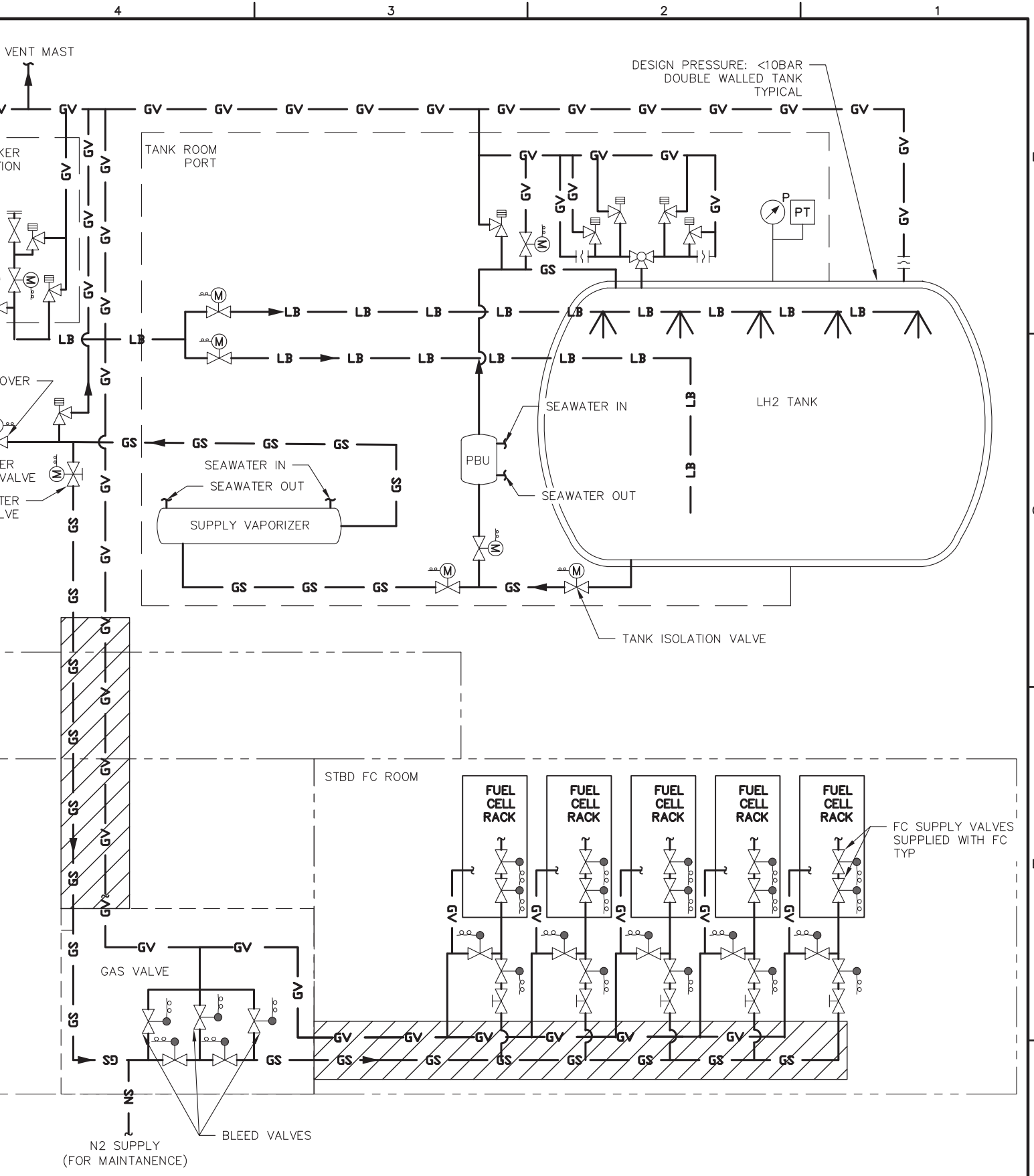

SANDIA NATIONAL LABORATORIES
LIVERMORE, CALIFORNIA

ZERO–V
CONCEPT GAS SYSTEM ARCHITECTURE SKETCH
FUEL GAS SYSTEM

ROBERT T. MADSEN STATE OF WASHINGTON 18955 REGISTERED PROFESSIONAL ENGINEER
Digitally Signed 19-Oct-2017

Glosten — INNOVATIVE MARINE SOLUTIONS
1201 WESTERN AVENUE, SUITE 200
SEATTLE, WASHINGTON 98101-2953
T 206.624.7850 GLOSTEN.COM

Drawn	Checked	Approved	Issue Date
RTM	SAC	TSL	10/3/2017

Scale	Drawing Number	Sheet	of	Revision
NO SCALE	17003.01–540–01	2	3	–

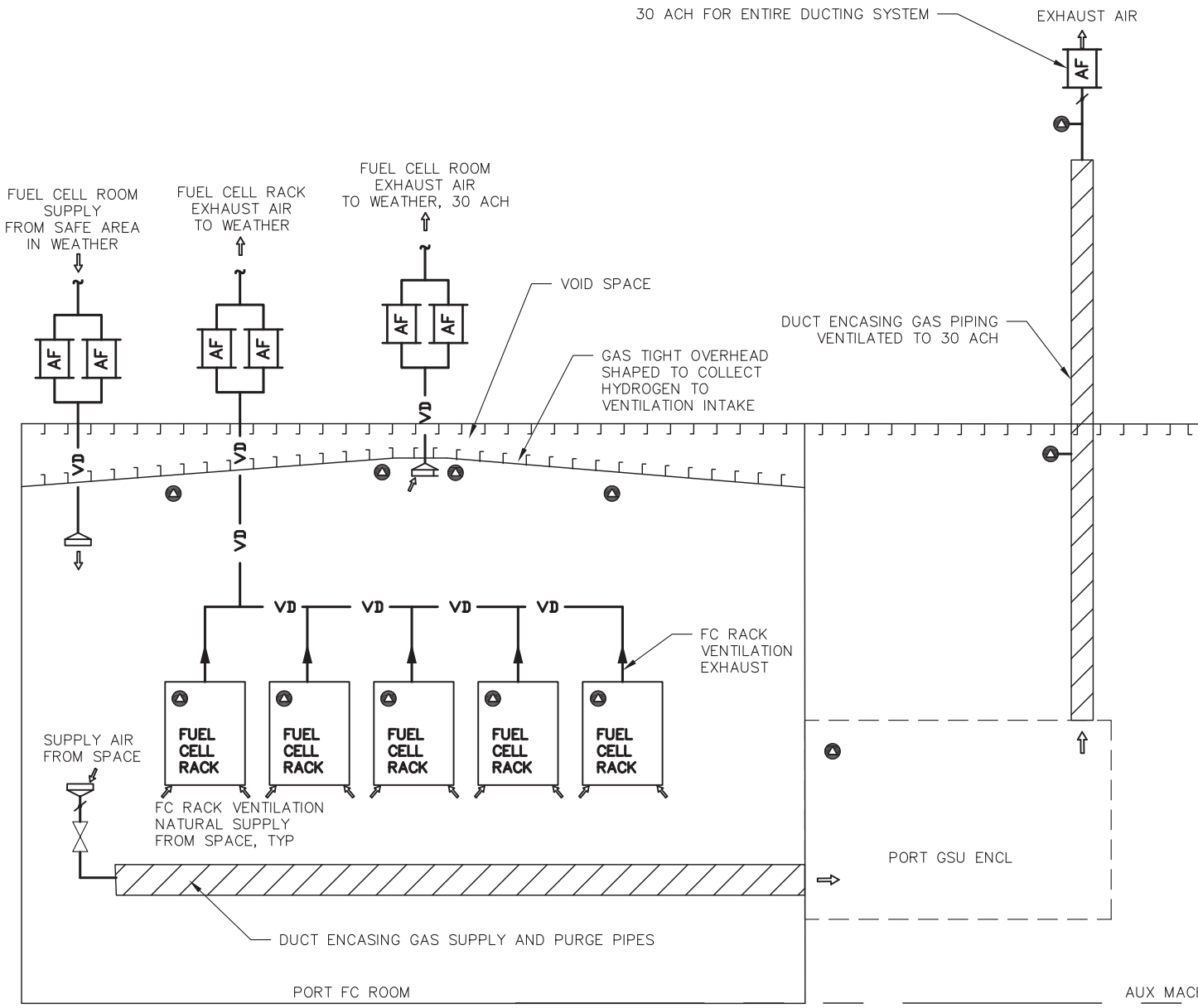
30 ACH FOR ENTIRE DUCTING SYSTEM
EXHAUST AIR
AF
FUEL CELL ROOM SUPPLY FROM SAFE AREA IN WEATHER
FUEL CELL RACK EXHAUST AIR TO WEATHER
FUEL CELL ROOM EXHAUST AIR TO WEATHER, 30 ACH
VOID SPACE
DUCT ENCASING GAS PIPING VENTILATED TO 30 ACH
GAS TIGHT OVERHEAD SHAPED TO COLLECT HYDROGEN TO VENTILATION INTAKE
VD
FC RACK VENTILATION EXHAUST
FUEL CELL RACK
SUPPLY AIR FROM SPACE
FC RACK VENTILATION NATURAL SUPPLY FROM SPACE, TYP
PORT GSU ENCL
DUCT ENCASING GAS SUPPLY AND PURGE PIPES
PORT FC ROOM
AUX MACH

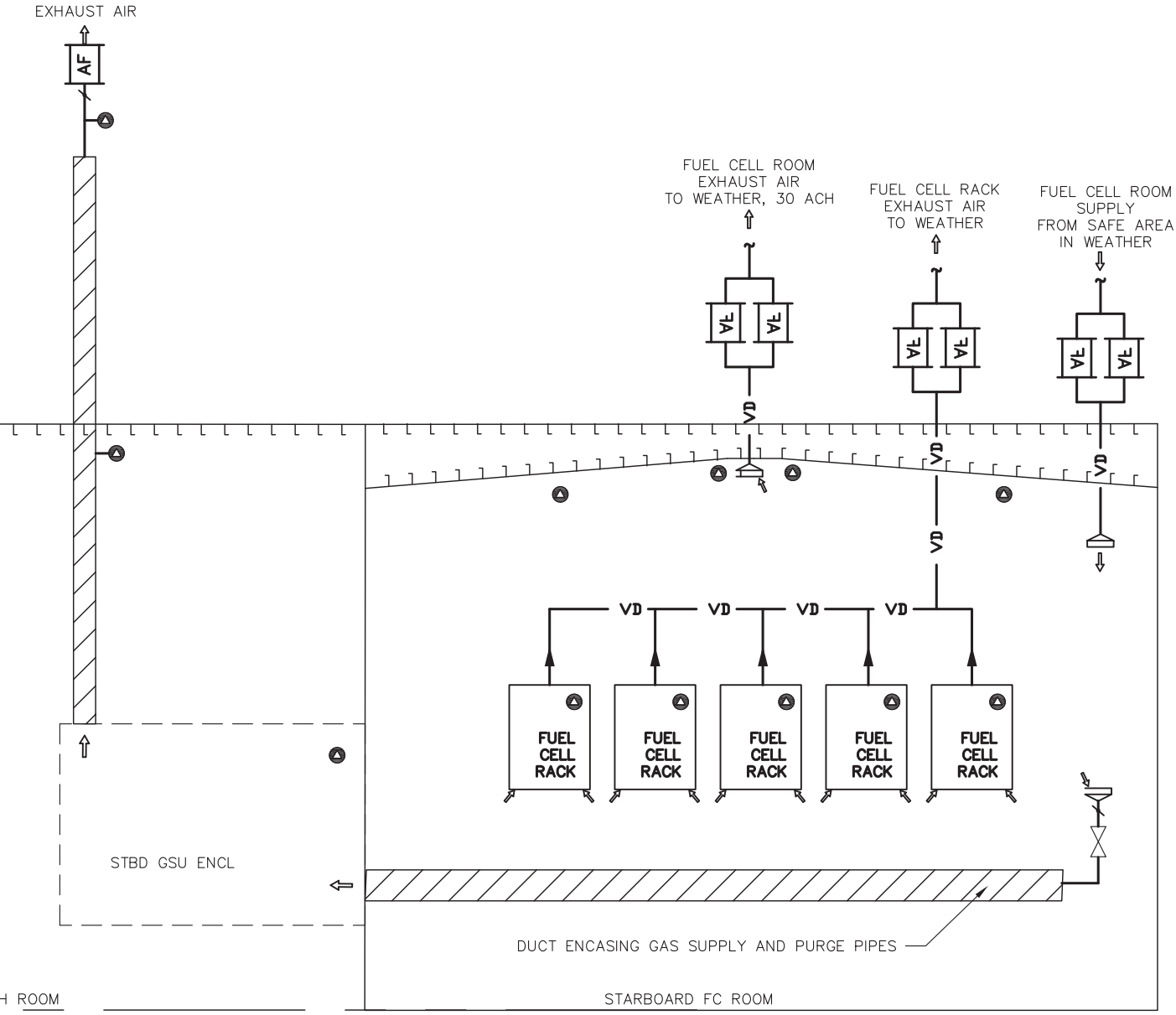

ROBERT T. MADSEN
STATE OF WASHINGTON
18955
REGISTERED
PROFESSIONAL ENGINEER

Digitally Signed 19-Oct-2017

SANDIA NATIONAL LABORATORIES
LIVERMORE, CALIFORNIA

ZERO-V
CONCEPT GAS SYSTEM ARCHITECTURE SKETCH
VENTILATION

Glosten
INNOVATIVE MARINE SOLUTIONS
1201 WESTERN AVENUE, SUITE 200
SEATTLE, WASHINGTON 98101-2953
T 206.624.7850 GLOSTEN.COM

Drawn	Checked	Approved	Issue Date
RTM	SAC	TSL	10/3/2017

Scale	Drawing Number	Sheet	Revision
NO SCALE	17003.01-540-01	3 of 3	–

Appendix B Calculations

Range and Endurance Calculations

Electrical Loads Analysis

Stability Analysis

Sandia National Laboratories
Zero-V
Operating Conditions

By: RTM
Checked: IWM/SAC
Date: October 3, 2017
Rev -
File 17003.01

Fuel Cell Efficiency	0.45	
Propulsion Motor Efficiency	0.958	**The Switch PMM500**
Switchgear Efficiency	0.96	
LH2 Density	70.9	**kg/m3**
LH2 LHV	119.96	**MJ/kg**
Tank Relief Valve Setting	8.00	**bar g**
Fuel Reserve (Heel)	5%	
Consumable Tank Volume	70.5%	
	392.4287	**ft3/kg**
gas density	0.08998	**g/L @ standard conditions (0°C, 1 atm)**

Condition	Sprint	Transit	Survey	Towing	Loiter	On Station	Science Ops
Speed (knots)	12	10	8	2	2	0	0
BHP	1220	501	234	151	20	300	300
Propulsion Power (skW)	454	187	87	56	7	112	111.75
Propulsion (ekW)	949	390	182	117	16	233	233
Bow Thrusters (ekW)	0	0	0	0	0	270	270
Traction Winch (ekW)	0	0	0	85	0	0	85
Ship Service (ekW)	250	250	250	250	250	250	250
Total Electrical (ekW)	1249	666	450	471	277	785	873
BSGC (MJ/kW-hr)	8.00	8.00	8.00	8.00	8.00	8.00	8.00
Fuel Consumption (MJ/hr)	9989.6	5330.1	3599.8	3770.2	2212.9	6277.5	6985.8
Fuel Consumption (kg/hr)	83.27	44.43	30.01	31.43	18.45	52.33	58.23
SCF/H	32679	17436	11776	12334	7239	20536	22853
Fuel Consumption (M3/hr)	1.18	0.63	0.42	0.44	0.26	0.74	0.82

Operating Profiles	Sprint	Transit	Survey	Towing	Loiter	On Station	On Station Science Ops	Totals		Required Total Tank Volume m3	Required Total Tank Volume Gal
	0	8		0	2		14	24	Operating hrs		
Coastal Mooring	0	355	0	0	37	0	815	1208	kg consumed	24	6386
	0	48	6	30	0	0	36	120	Operating hrs		
Deep Moorings (4000m) & towed sonar	0	2133	180	943	0	0	2096	5352	kg consumed	107	28300
	0	24	48	48	0	0	0	120	Operating hrs		
Mapping (multibeam & towed CHIRP)	0	1066	1440	1509	0	0	0	4015	kg consumed	80	21232
	0	3	3	3	0	0	3	12	Operating hrs		
Class Cruise biology	0	133	90	94	0	0	175	492	kg consumed	10	2603
	0	3	3	3			3	12	Operating hrs		
Class Cruise geology	0	133	90	94	0	0	175	492	kg consumed	10	2603
	0	3	3	3			3	12	Operating hrs		
Class Cruise ROV	0	133	90	94	0	0	175	492	kg consumed	10	2603
	0	48	6	30	12	0	72	168	Operating hrs		
ROV Survey	0	2133	180	943	221	0	4193	7670	kg consumed	154	40556
		24	24	0	0	0	72	120	Operating hrs		
Geology Sampling	0	1066	720	0	0	0	4193	5979	kg consumed	120	31618
		40	0	6	22	0	4	72	Operating hrs		
FLIP Anchor Handling	0	1777	0	189	406	0	233	2605	kg consumed	52	13773
		16	0	0	56	24	0	96	Operating hrs		
UAV Flight Ops	0	711	0	0	1033	1256	0	3000	kg consumed	60	15862
		16	8	0	72	0	0	96	Operating hrs		
AUV Ops (REMUS, Wave Flider, Spray etc)	0	711	240	0	1328	0	0	2279	kg consumed	46	12052
		48	24	24	24	0	72	192	Operating hrs		
Physical oceanography	0	2133	720	754	443	0	4193	8243	kg consumed	165	43586
		48	0	0	72	0	72	192	Operating hrs		
Biochemical Survey	0	2133	0	0	1328	0	4193	7654	kg consumed	153	40471
		240						**240**	Operating hrs		
Range Endurance	0	10664	0	0	0	0	0	**10664**	kg consumed	**213**	**56386**

Sandia National Laboratories
Zero-V
Range

By: RTM
Checked: IWM/SAC
Date: October 3, 2017
Rev -
File 17003.01

Fuel Cell Efficiency	0.45	
Propulsion Motor Efficiency	0.958	**The Switch PMM500**
Switchgear Efficiency	0.96	
LH2 Density	70.9	**kg/m3**
LH2 LHV	119.96	**MJ/kg**
Tank Relief Valve Setting	8.00	**bar g**
Fuel Reserve (Heel)	5%	
gas density	392.4287	**ft3/kg**
gas density	0.08998	**g/L @ standard conditions (0°C, 1 atm)**

Operating Conditions

Condition	**Transit**	**Cruise**
Speed (knots)	10	9
BHP	501	344
Propulsion Power (skW)	187	128
Propulsion (ekW)	390	268
Bow Thrusters (ekW)	0	0
Traction Winch (ekW)	0	0
Ship Service (ekW)	250	250
Total Electrical (ekW)	666	539
BSGC (MJ/kW-hr)	8.00	8.00
Fuel Consumption (MJ/hr)	5330.1	4312.6
Fuel Consumption (kg/hr)	44.43	35.95
SCF/H		
Fuel Consumption (M3/hr)	0.63	0.51

	Tanks Molded Volume (total)		**MARVS**	**Loading Limit**	**Heel**	**Consumable Fuel**				**Range**	**Heel Range (emergency reserve)**
Range	**Gal**	**m3**	**Bar a**	**%**	**%**	**%**	**Gal**	**m3**	**kg**	**nm**	**nm**
Standard Loading, 10 knots Calm Water	**57644**	**218**	**8**	**75.5%**	**5%**	**70.5%**	**40647**	**154**	**10902**	**2454**	**174**
Increased Loading Limit (85%), 10 knots Calm Water	**57644**	**218**	**8**	**85.0%**	**5%**	**80.0%**	**46115**	**175**	**12368**	**2784**	**174**
Max Increased Loading Limit (95%), 10 knots Calm Water	**57644**	**218**	**8**	**95.0%**	**5%**	**90.0%**	**51880**	**196**	**13914**	**3132**	**174**
Standard Loading, 9 knots Calm Water	**57644**	**218**	**8**	**75.5%**	**5%**	**70.5%**	**40647**	**154**	**10902**	**2729**	**194**
Increased Loading Limit (85%), 9 knots Calm Water	**57644**	**218**	**8**	**85.0%**	**5%**	**80.0%**	**46115**	**175**	**12368**	**3096**	**194**
Max Increased Loading Limit (95%), 9 knots Calm Water	**57644**	**218**	**8**	**95.0%**	**5%**	**90.0%**	**51880**	**196**	**13914**	**3483**	**194**

Electrical Load Analysis Sandia National Laboratories Zero-V	BY: CMCF CHECKED: RTM APPROVED: TSL
PREPARED FOR Sandia National Laboratories Livermore, California	FILE: 17003.01 DOCUMENT: 17003.01-300-02 REVISION: - DATE: 10/3/2017

Glosten | INNOVATIVE MARINE SOLUTIONS | 1201 WESTERN AVENUE, SUITE 200 SEATTLE, WASHINGTON 98101-2953 T 206.624.7850 GLOSTEN.COM

GENERAL NOTES

1. This document has been developed from information in References 1& 2.

2. Definitions and acronyms
   DF: Demand Factor, defined as the fraction of time that the load is operational in an operational profile.
   ekW: Electrical kilowatts
   FLA: Full Load Amperes
   HP: Horsepower
   kVA: Kilo Volt-Amperes
   Utilization Factor: the fraction of the connected load rating that is utilized during normal operation.
   V: Voltage
   ϕ: Number of phases

3. Calculation procedure: Profile Load = Connected * Utilization Factor * Demand Factor

4. This electrical load analysis is preliminary. It represents anticipated loads and demand factors for the Zero-V research vessel.

5. The main propulsion and ship service loads are supplied with power from 10 stacks of 6 fuel cells. The fuel cells provide a total of 1800 kW.

6. The fuel cell stacks supply DC power to the main propulsion switchboard at 360VDC - 720VDC. The propulsion switchboard supplies power to the propulsion motors, thrusters and ship service switchboard through an inverter and transformer.

7. There are seven operating profiles considered in the analysis. The In Transit scenario is applicable when the vessel is transiting between stations, and not performing science operations. The towing scenario represents when the vessel is moving at slow speed (2 knots) and using the towing winch. The Loitering and On Station profiles represent light and heavy DP respectively. In these scenarios, the bow and stern thrusters are being utilized, along with heavy science equipment demands. The In Port scenario represents the vessel's electrical demands while on shore power.

REFERENCES

1. Hydrogenics Fuel Cell Power Rack, Hydrogenics, November 25, 2014
2. Electrical One-Line Diagram, Glosten, File No. 17003.01-300-01

REVISIONS

REV.	SECTION	DESCRIPTION
-	ALL	ORIGINAL RELEASE

Electrical Load Analysis	FILE:	17003.01		BY:	CMCF
Sandia National Laboratories	REVISION:	-		CHECKED:	RTM
Zero-V	DATE:	18-May-17		APPROVED:	TSL
DOCUMENT:	17003.01-300-02				

PANEL:	**Propulsion Switchboard**
LOCATION:	**EOS**

LOAD DATA													Sprint			Tra
SWBS #	Load Description	V	Φ	HP	FLA	Power Factor	Connected ekW	Connected kVA	Utilization Factor	Utilized ekW	Utilized kVA	Load Notes	DF	ekW	kVA	DF
	Propulsion															
	Port Propulsion Motor	480	3		751.78	0.8	500.00	625.00	1.	500.00	625.00		1.	500.	625.	0.38
	Stbd Propulsion Motor	480	3		751.78	0.8	500.00	625.00	1.	500.00	625.00		1.	500.	625.	0.38
	Bow Thruster	480	3		751.78	0.8	500.00	625.00	1.	500.00	625.00		0.	0.	0.	0.
	Stern Thruster	480	3		751.78	0.8	500.00	625.00	1.	500.00	625.00		0.	0.	0.	0.
	Stern Thruster	480	3		751.78	0.8	500.00	625.00	1.	500.00	625.00		0.	0.	0.	0.
	Loads															
	Ship Service Loads	480	3		1804.27	0.9	1350.00	1500.00	1.	1350.00	1500.00		0.17	225.45	250.5	0.17
	Science Winch Loads	480	3		467.77	0.9	350.00	388.89	1.	350.00	388.89		0.	0.	0.	0.
	Emergency Loads	480	3		162.74	0.85	115.00	135.29	1.	115.00	135.29			0.	0.	
	Sub-Totals						4315.00	5149.18			5149.18			1225.5	1500.5	
	Design Ship Service Margin	10.0%					431.50	514.92			514.92			122.5	150.1	
	Growth Margin	10.0%					431.50	514.92			514.92			122.5	150.1	
	Totals						5178.00	6179.02			6179.02			1470.5	1800.6	

	FUEL CELLS	PF		ekW	kVA
	Fuel Cell Rack #1	1		180	180
	Fuel Cell Rack #2	1		180	180
	Fuel Cell Rack #3	1		180	180
	Fuel Cell Rack #4	1		180	180
	Fuel Cell Rack #5	1		180	180
	Fuel Cell Rack #6	1		180	180
	Fuel Cell Rack #7	1		180	180
	Fuel Cell Rack #8	1		180	180
	Fuel Cell Rack #9	1		180	180
	Fuel Cell Rack #10	1		180	180
	Total Ship Generating Power			1800	1800

	RACK LOADING	ekW	kVA	Configuration	Sprint	Tra
	1 Fuel Cell Racks	180	180		1000%	
	2 Fuel Cell Racks	360	360		500%	
	3 Fuel Cell Racks	540	540		333%	
	4 Fuel Cell Racks	720	720		250%	
	5 Fuel Cell Racks	900	900		200%	
	6 Fuel Cell Racks	1080	1080		167%	
	7 Fuel Cell Racks	1260	1260		143%	
	8 Fuel Cell Racks	1440	1440		125%	
	9 Fuel Cell Racks	1620	1620		111%	
	10 Fuel Cell Racks	1800	1800		100%	

	SHORE POWER	kVA
	Input Capacity	400

OPERATING PROFILES																			
nsit 10 knots		Survey 8 knots			Towing			Loitering (Light DP)			On Station (DP)			In Port			Emergency		
ekW	kVA	DF	ekW	kVA	DF	ekW	kVA	DF	ekW	kVA	DF	ekW	kVA	DF	ekW	kVA	DF	ekW	kVA
188.	235.	0.18	90.5	113.13	0.12	59.5	74.38	0.04	21.5	26.88	0.23	117.	146.25	0.	0.	0.	0.	0.	0.
188.	235.	0.18	90.5	113.13	0.12	59.5	74.38	0.04	21.5	26.88	0.23	117.	146.25	0.	0.	0.	0.	0.	0.
0.	0.	0.	0.	0.	0.	0.	0.	0.1	50.	62.5	0.25	125.	156.25	0.	0.	0.	0.	0.	0.
0.	0.	0.	0.	0.	0.	0.	0.	0.05	25.	31.25	0.15	75.	93.75	0.	0.	0.	0.	0.	0.
0.	0.	0.	0.	0.	0.	0.	0.	0.05	25.	31.25	0.15	75.	93.75	0.	0.	0.	0.	0.	0.
225.45	250.5	0.17	225.45	250.5	0.17	225.45	250.5	0.17	225.45	250.5	0.17	225.45	250.5	0.1	135.	150.	0.	0.	0.
0.	0.	0.1	35.	38.89	0.08	28.	31.11	0.25	85.75	95.28	0.25	85.75	95.28	0.	0.	0.	0.	0.	0.
0.	0.		0.	0.		0.	0.		0.	0.		0.	0.		0.	0.	1.	115.	135.29
601.5	720.5		441.5	515.6		372.5	430.4		454.2	524.5		820.2	982.		135.	150.		115.	135.3
60.1	72.1		44.1	51.6		37.2	43.		45.4	52.5		82.	98.2		13.5	15.		11.5	13.5
60.1	72.1											82.	98.2		13.5	15.		11.5	13.5
721.7	864.6		485.6	567.2		409.7	473.4		499.6	577.0		984.2	1178.4		162.0	180.0		138.0	162.4

nsit 10 knots	Survey 8 knots	Towing	Loitering (Light DP)	On Station (DP)	In Port	Emergency
480%	315%	263%	321%	655%	100%	90%
240%	158%	131%	160%	327%	50%	45%
160%	105%	88%	107%	218%	33%	30%
120%	79%	66%	80%	164%	25%	23%
96%	63%	53%	64%	131%	20%	18%
80%	53%	44%	53%	109%	17%	15%
69%	45%	38%	46%	94%	14%	13%
60%	39%	33%	40%	82%	13%	11%
53%	35%	29%	36%	73%	11%	10%
48%	32%	26%	32%	65%	10%	9%

												In Port	Emergency
												45%	41%

170x56x12 Trimaran
MAX VCG @ 900 LT
-0.5 DEG TRIM
USCG 170.173 PARAGRAPH B

RIGHTING ARMS vs HEEL ANGLE
LCG = 92.45a TCG = 0.00 VCG = 24.92

Origin Depth	Degrees of Trim	Heel	Displacement Weight(LT)	Righting Arms in Trim	in Heel	Area	Flood Pt Height
10.784	0.50f	0.00	900.00	0.00	0.000	0.00	16.03(3)
10.753	0.51f	5.00s	900.01	0.00	0.497	1.24	14.77(3)
10.657	0.55f	10.00s	899.99	0.00	1.035	5.06	13.45(3)
10.526	0.64f	15.00s	899.77	0.00	1.627	11.69	12.09(3)
10.485	0.79f	17.81s	899.85	0.00	1.752	16.47	11.43(3)
10.410	0.94f	20.00s	899.67	0.00	1.677	20.22	10.99(3)
10.119	1.28f	25.00s	900.23	0.00	1.671	28.68	10.01(3)
9.568	1.57f	30.00s	900.01	0.00	1.751	37.21	9.07(3)
9.453	1.60f	30.76s	899.99	0.00	1.752	38.54	8.92(3)
8.681	1.75f	35.00s	900.00	0.00	1.722	45.93	8.11(3)
7.525	1.86f	40.00s	899.99	0.00	1.682	54.46	6.00(1)
6.269	1.97f	45.00s	899.99	0.00	1.536	62.54	3.66(1)
5.027	2.09f	50.00s	899.99	0.00	1.134	69.32	1.31(1)
4.330	2.17f	52.82s	899.96	0.00	0.823	72.09	-0.00(1)
3.792	2.23f	55.00s	899.98	0.00	0.547	73.59	-1.02(1)
2.835	2.33f	58.86s	900.02	0.00	0.000	74.67	-2.80(1)
2.551	2.36f	60.00s	899.99	0.00	-0.175	74.57	-3.32(1)

Distances in FEET.------Specific Gravity = 1.025.----------Area in Ft-Deg.

Critical Points		LCP	TCP	VCP
(1) Vent Louver	FLOOD	145.00a	28.00	35.00
(3) CTD Wire Chase	FLOOD	122.00a	14.00	25.75

LIM 170.173 Paragraph b CRITERION		Min/Max		Attained	
(1) GM Upright	>	0.49	Ft	5.43	P
(2) Righting Arm at 30 deg or MaxRA	>	0.66	Ft	1.75	P
(3) Absolute Angle at MaxRA	>	25.00	deg	30.76	P
(4) Area from abs 0.000 deg to 30	>	10.30	Ft-deg	37.21	P
(5) Area from abs 0.000 deg to 40 or Flood	>	16.90	Ft-deg	54.46	P
(6) Area from 30 deg to 40 or Flood	>	5.60	Ft-deg	17.25	P

Relative angles measured from 0.000

900 24.92

170x56x12 Trimaran
MAX VCG @ 900 LT
-0.5 DEG TRIM
USCG 170.173 PARAGRAPH B

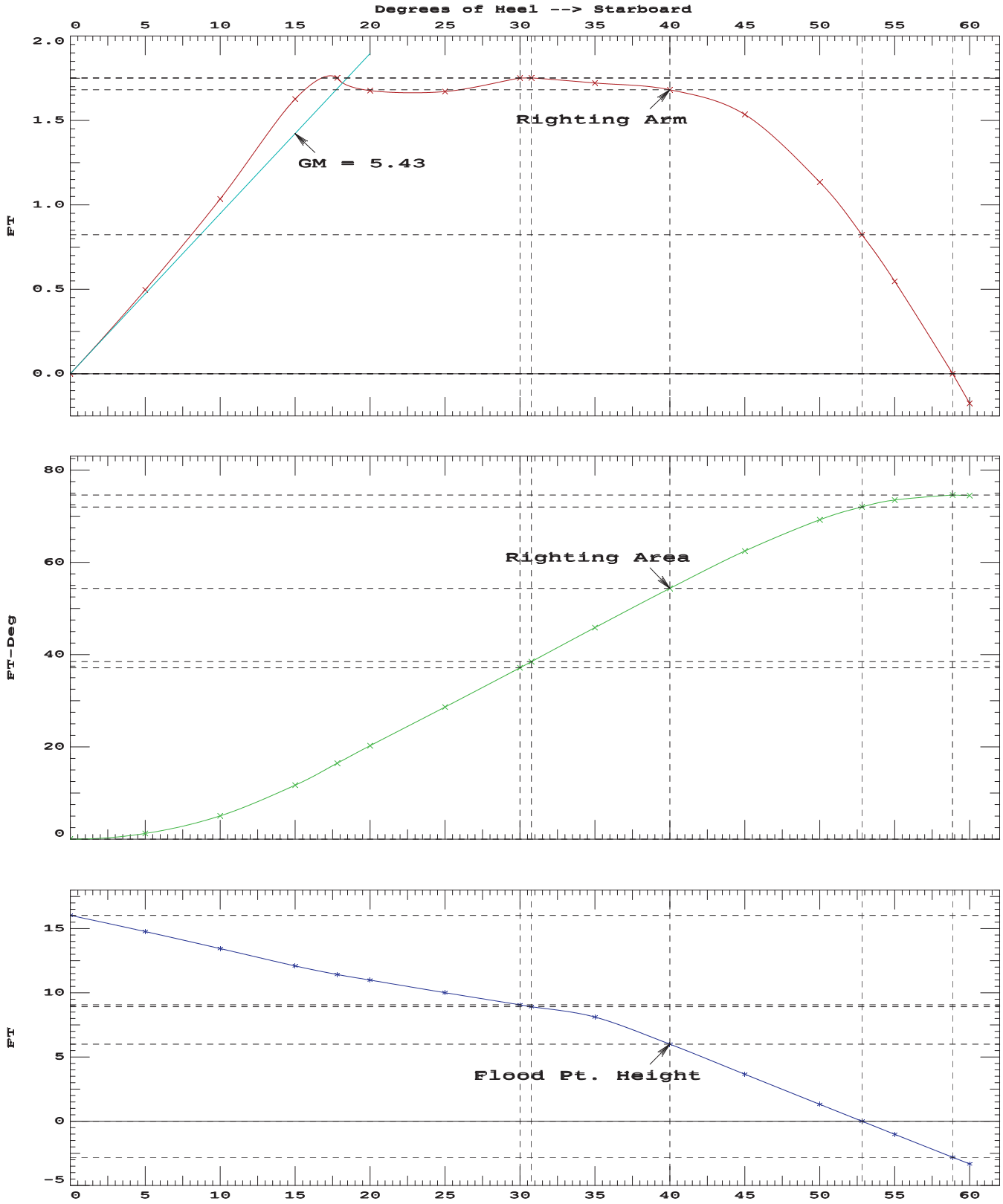

170x56x12 Trimaran
MAX VCG @ 925 LT
-0.5 DEG TRIM
USCG 170.173 PARAGRAPH B

RIGHTING ARMS vs HEEL ANGLE
LCG = 92.64a TCG = 0.00 VCG = 24.99

Origin Depth	Degrees of Trim	Heel	Displacement Weight(LT)	Righting Arms in Trim	in Heel	Area	Flood Pt Height
10.983	0.50f	0.00	925.00	0.00	0.000	0.00	15.83(3)
10.954	0.52f	5.00s	925.02	0.00	0.453	1.13	14.58(3)
10.852	0.55f	10.00s	924.98	0.00	0.945	4.61	13.25(3)
10.714	0.64f	15.00s	924.83	0.00	1.508	10.72	11.90(3)
10.654	0.80f	18.15s	924.77	0.00	1.680	15.78	11.15(3)
10.580	0.92f	20.00s	924.77	0.00	1.621	18.83	10.77(3)
10.255	1.24f	25.00s	925.29	0.00	1.615	27.01	9.81(3)
9.657	1.51f	30.00s	925.00	0.00	1.680	35.22	8.84(3)
9.565	1.53f	30.58s	924.99	0.00	1.681	36.20	8.73(3)
8.731	1.67f	35.00s	924.70	0.00	1.644	43.58	7.87(3)
7.551	1.76f	40.00s	924.99	0.00	1.593	51.69	5.71(1)
6.287	1.85f	45.00s	924.99	0.00	1.415	59.26	3.34(1)
5.040	1.97f	50.00s	924.99	0.00	0.985	65.37	0.98(1)
4.522	2.02f	52.09s	924.96	0.00	0.749	67.18	-0.00(1)
3.801	2.09f	55.00s	924.98	0.00	0.377	68.84	-1.37(1)
3.144	2.16f	57.65s	925.08	0.00	0.000	69.33	-2.61(1)
2.557	2.22f	60.00s	924.99	0.00	-0.361	68.91	-3.69(1)

Distances in FEET.------Specific Gravity = 1.025.----------Area in Ft-Deg.

Critical Points		LCP	TCP	VCP
(1) Vent Louver	FLOOD	145.00a	28.00	35.00
(3) CTD Wire Chase	FLOOD	122.00a	14.00	25.75

LIM 170.173 Paragraph b CRITERION		Min/Max		Attained	
(1) GM Upright	>	0.49	Ft	4.93	P
(2) Righting Arm at 30 deg or MaxRA	>	0.66	Ft	1.68	P
(3) Absolute Angle at MaxRA	>	25.00	deg	30.58	P
(4) Area from abs 0.000 deg to 30	>	10.30	Ft-deg	35.22	P
(5) Area from abs 0.000 deg to 40 or Flood	>	16.90	Ft-deg	51.69	P
(6) Area from 30 deg to 40 or Flood	>	5.60	Ft-deg	16.46	P

Relative angles measured from 0.000

925 24.99

170x56x12 Trimaran
MAX VCG @ 925 LT
-0.5 DEG TRIM
USCG 170.173 PARAGRAPH B

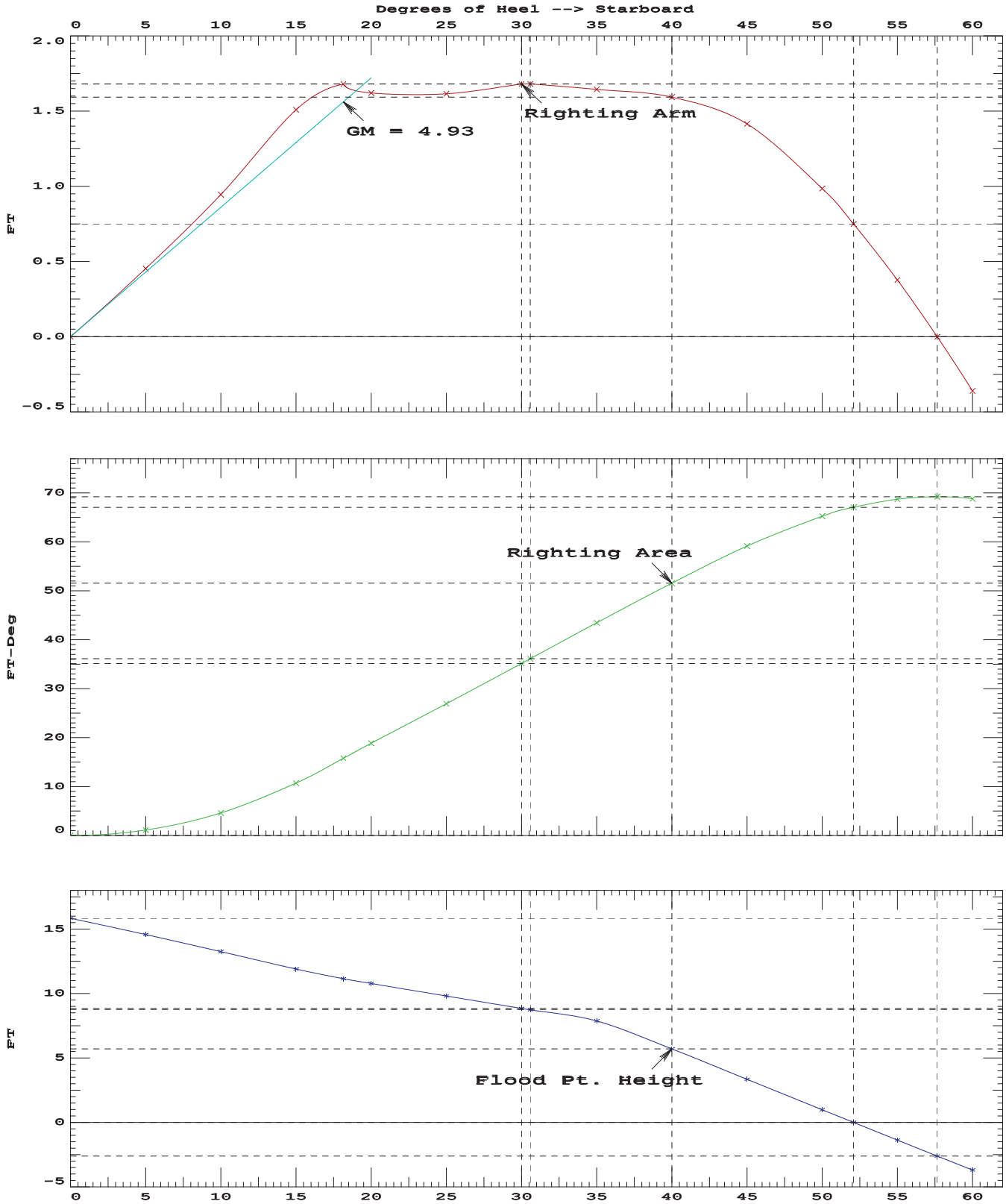

170x56x12 Trimaran
MAX VCG @ 950 LT
-0.5 DEG TRIM
USCG 170.173 PARAGRAPH B

RIGHTING ARMS vs HEEL ANGLE
LCG = 92.83a TCG = 0.00 VCG = 25.04

Origin Depth	Degrees of Trim	Heel	Displacement Weight(LT)	Righting Arms in Trim	in Heel	Area	Flood Pt Height
11.181	0.50f	0.00	950.00	0.00	0.000	0.00	15.63(3)
11.148	0.51f	5.00s	950.00	0.00	0.412	1.03	14.38(3)
11.047	0.55f	10.00s	949.98	0.00	0.865	4.21	13.05(3)
10.903	0.64f	15.00s	949.87	0.00	1.400	9.84	11.70(3)
10.820	0.80f	18.47s	949.87	0.00	1.620	15.12	10.87(3)
10.748	0.90f	20.00s	949.84	0.00	1.578	17.56	10.56(3)
10.383	1.21f	25.00s	950.00	0.00	1.572	25.53	9.60(3)
9.741	1.44f	30.00s	950.24	0.00	1.620	33.49	8.62(3)
8.779	1.58f	35.00s	949.80	0.00	1.578	41.52	7.64(3)
7.578	1.66f	40.00s	949.93	0.00	1.518	49.27	5.42(1)
6.310	1.74f	45.00s	950.00	0.00	1.309	56.40	3.04(1)
5.059	1.85f	50.00s	950.00	0.00	0.853	61.91	0.66(1)
4.712	1.88f	51.39s	949.96	0.00	0.694	62.98	-0.00(1)
3.814	1.96f	55.00s	949.98	0.00	0.225	64.67	-1.71(1)
3.423	2.00f	56.58s	950.11	0.00	0.000	64.84	-2.45(1)
2.564	2.08f	60.00s	950.00	0.00	-0.526	63.94	-4.06(1)

Distances in FEET.------Specific Gravity = 1.025.----------Area in Ft-Deg.

Critical Points		LCP	TCP	VCP
(1) Vent Louver	FLOOD	145.00a	28.00	35.00
(3) CTD Wire Chase	FLOOD	122.00a	14.00	25.75

LIM 170.173 Paragraph b CRITERION		Min/Max		Attained	
(1) GM Upright	>	0.49	Ft	4.48	P
(2) Righting Arm at 30 deg or MaxRA	>	0.66	Ft	1.62	P
(3) Absolute Angle at MaxRA	>	25.00	deg	30.00	P
(4) Area from abs 0.000 deg to 30	>	10.30	Ft-deg	33.49	P
(5) Area from abs 0.000 deg to 40 or Flood	>	16.90	Ft-deg	49.27	P
(6) Area from 30 deg to 40 or Flood	>	5.60	Ft-deg	15.78	P

Relative angles measured from 0.000

950 25.04

170x56x12 Trimaran
MAX VCG @ 950 LT
-0.5 DEG TRIM
USCG 170.173 PARAGRAPH B

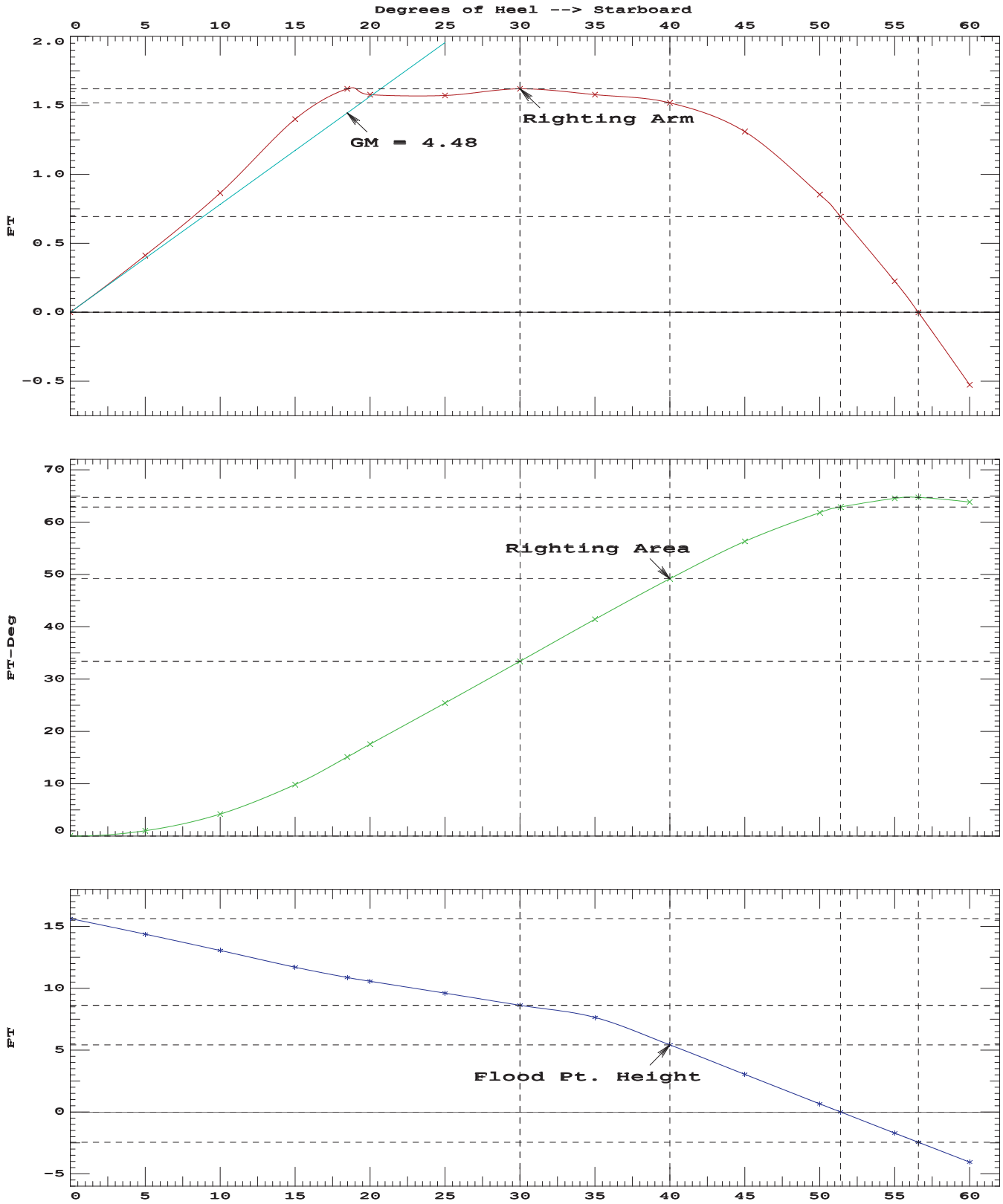

170x56x12 Trimaran
MAX VCG @ 975 LT
-0.5 DEG TRIM
USCG 170.173 PARAGRAPH B

RIGHTING ARMS vs HEEL ANGLE
LCG = 93.02a TCG = 0.00 VCG = 25.06

Origin Depth	Degrees of Trim	Heel	Displacement Weight(LT)	Righting Arms in Trim	in Heel	Area	Flood Pt Height
11.378	0.50f	0.00	975.00	0.00	0.000	0.00	15.44(3)
11.344	0.51f	5.00s	975.00	0.00	0.377	0.94	14.18(3)
11.243	0.55f	10.00s	975.00	0.00	0.794	3.85	12.86(3)
11.092	0.64f	15.00s	974.88	0.00	1.305	9.06	11.51(3)
10.983	0.80f	18.75s	974.99	0.00	1.576	14.49	10.61(3)
10.915	0.88f	20.00s	974.90	0.00	1.550	16.45	10.36(3)
10.512	1.17f	25.00s	974.70	0.00	1.543	24.29	9.40(3)
9.819	1.38f	30.00s	975.03	0.00	1.577	32.07	8.41(3)
8.832	1.50f	35.00s	974.99	0.00	1.528	39.87	7.41(3)
7.610	1.56f	40.00s	974.96	0.00	1.462	47.35	5.14(1)
6.337	1.63f	45.00s	975.00	0.00	1.225	54.14	2.74(1)
5.081	1.73f	50.00s	975.00	0.00	0.746	59.16	0.34(1)
4.903	1.74f	50.71s	974.98	0.00	0.663	59.67	0.00(1)
3.829	1.83f	55.00s	975.01	0.00	0.101	61.35	-2.05(1)
3.654	1.85f	55.70s	975.07	0.00	0.000	61.38	-2.39(1)
2.569	1.93f	60.00s	975.01	0.00	-0.662	59.99	-4.42(1)

Distances in FEET.------Specific Gravity = 1.025.----------Area in Ft-Deg.

Critical Points		LCP	TCP	VCP
(1)	Vent Louver	FLOOD 145.00a	28.00	35.00
(3)	CTD Wire Chase	FLOOD 122.00a	14.00	25.75

LIM	170.173 Paragraph b CRITERION	Min/Max		Attained
(1)	GM Upright	> 0.49	Ft	4.10 P
(2)	Righting Arm at 30 deg or MaxRA	> 0.66	Ft	1.58 P
(3)	Absolute Angle at MaxRA	> 25.00	deg	30.00 P
(4)	Area from abs 0.000 deg to 30	> 10.30	Ft-deg	32.07 P
(5)	Area from abs 0.000 deg to 40 or Flood	> 16.90	Ft-deg	47.35 P
(6)	Area from 30 deg to 40 or Flood	> 5.60	Ft-deg	15.28 P

Relative angles measured from 0.000

975 25.06

170x56x12 Trimaran
MAX VCG @ 975 LT
-0.5 DEG TRIM
USCG 170.173 PARAGRAPH B

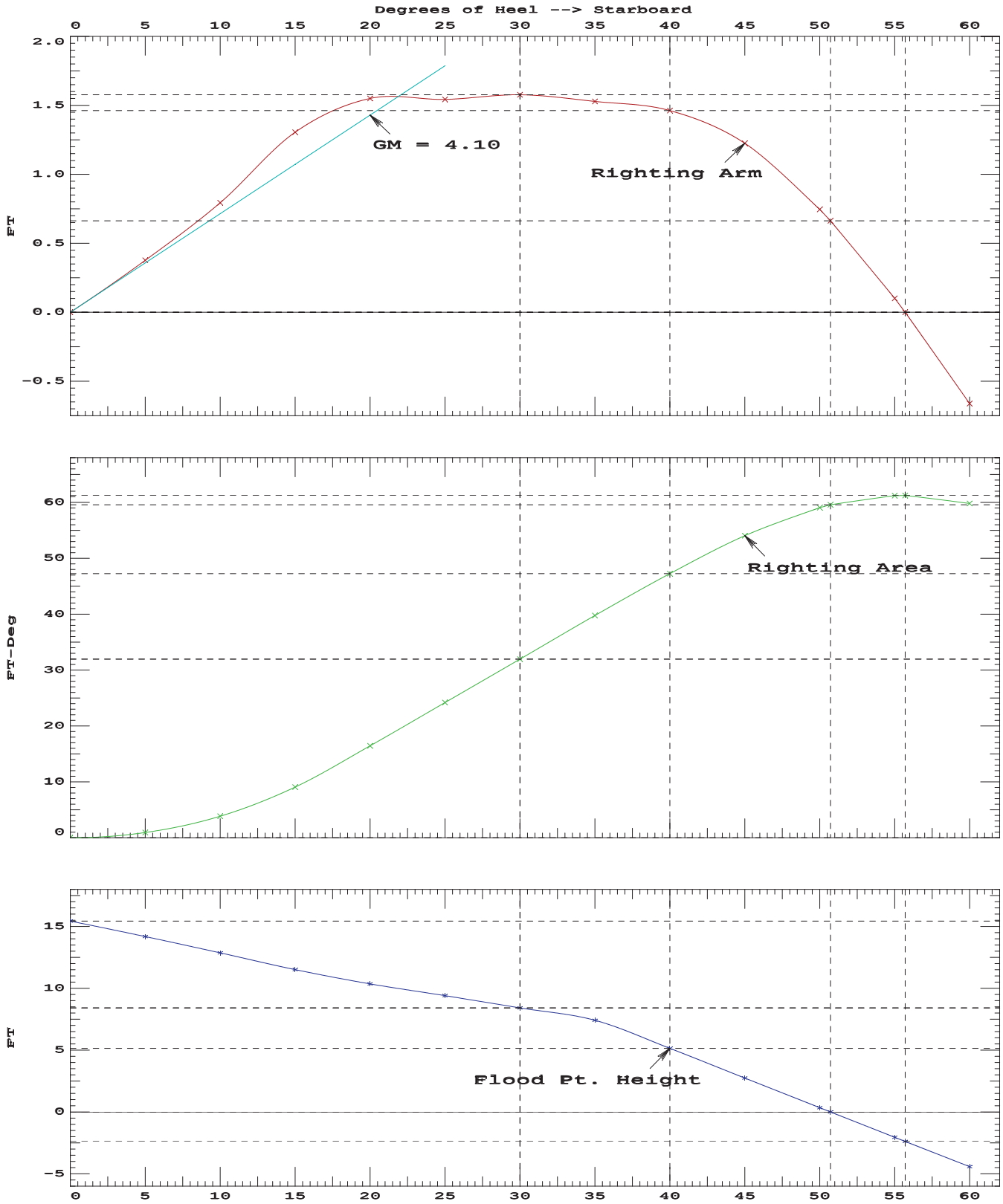

170x56x12 Trimaran
MAX VCG @ 1000 LT
-0.5 DEG TRIM
USCG 170.173 PARAGRAPH B

RIGHTING ARMS vs HEEL ANGLE
LCG = 93.20a TCG = 0.00 VCG = 25.11

Origin Depth	Degrees of Trim	Heel	Displacement Weight(LT)	Righting Arms in Trim	in Heel	Flood Pt ---> Area	Height
11.573	0.50f	0.00	1,000.0	0.00	0.000	0.00	15.24(3)
11.538	0.51f	5.00s	1,000.0	0.00	0.340	0.85	13.99(3)
11.436	0.55f	10.00s	1,000.0	0.00	0.722	3.49	12.67(3)
11.278	0.63f	15.00s	999.9	0.00	1.208	8.27	11.32(3)
11.077	0.86f	20.00s	1,000.1	0.00	1.518	15.16	10.15(3)
10.637	1.14f	25.00s	999.7	0.00	1.504	22.85	9.20(3)
9.893	1.31f	30.00s	1,000.0	0.00	1.519	30.39	8.20(3)
8.882	1.41f	35.00s	1,000.0	0.00	1.463	37.87	7.19(3)
7.644	1.46f	40.00s	1,000.0	0.00	1.386	45.01	4.87(1)
6.367	1.53f	45.00s	1,000.0	0.00	1.119	51.35	2.45(1)
5.103	1.61f	50.00s	1,000.0	0.00	0.616	55.79	0.03(1)
5.090	1.61f	50.05s	1,000.0	0.00	0.610	55.82	0.00(1)
3.921	1.69f	54.67s	1,000.0	0.00	0.000	57.28	-2.24(1)
3.838	1.70f	55.00s	1,000.0	0.00	-0.047	57.27	-2.39(1)
2.569	1.79f	60.00s	1,000.0	0.00	-0.822	55.15	-4.79(1)

Distances in FEET.------Specific Gravity = 1.025.----------Area in Ft-Deg.

Critical Points		LCP	TCP	VCP
(1)	Vent Louver	FLOOD 145.00a	28.00	35.00
(3)	CTD Wire Chase	FLOOD 122.00a	14.00	25.75

LIM	170.173 Paragraph b CRITERION	Min/Max		Attained
(1)	GM Upright	> 0.49	Ft	3.70 P
(2)	Righting Arm at 30 deg or MaxRA	> 0.66	Ft	1.52 P
(3)	Absolute Angle at MaxRA	> 25.00	deg	30.00 P
(4)	Area from abs 0.000 deg to 30	> 10.30	Ft-deg	30.39 P
(5)	Area from abs 0.000 deg to 40 or Flood	> 16.90	Ft-deg	45.01 P
(6)	Area from 30 deg to 40 or Flood	> 5.60	Ft-deg	14.62 P

Relative angles measured from 0.000

1000 25.11

170x56x12 Trimaran
MAX VCG @ 1000 LT
-0.5 DEG TRIM
USCG 170.173 PARAGRAPH B

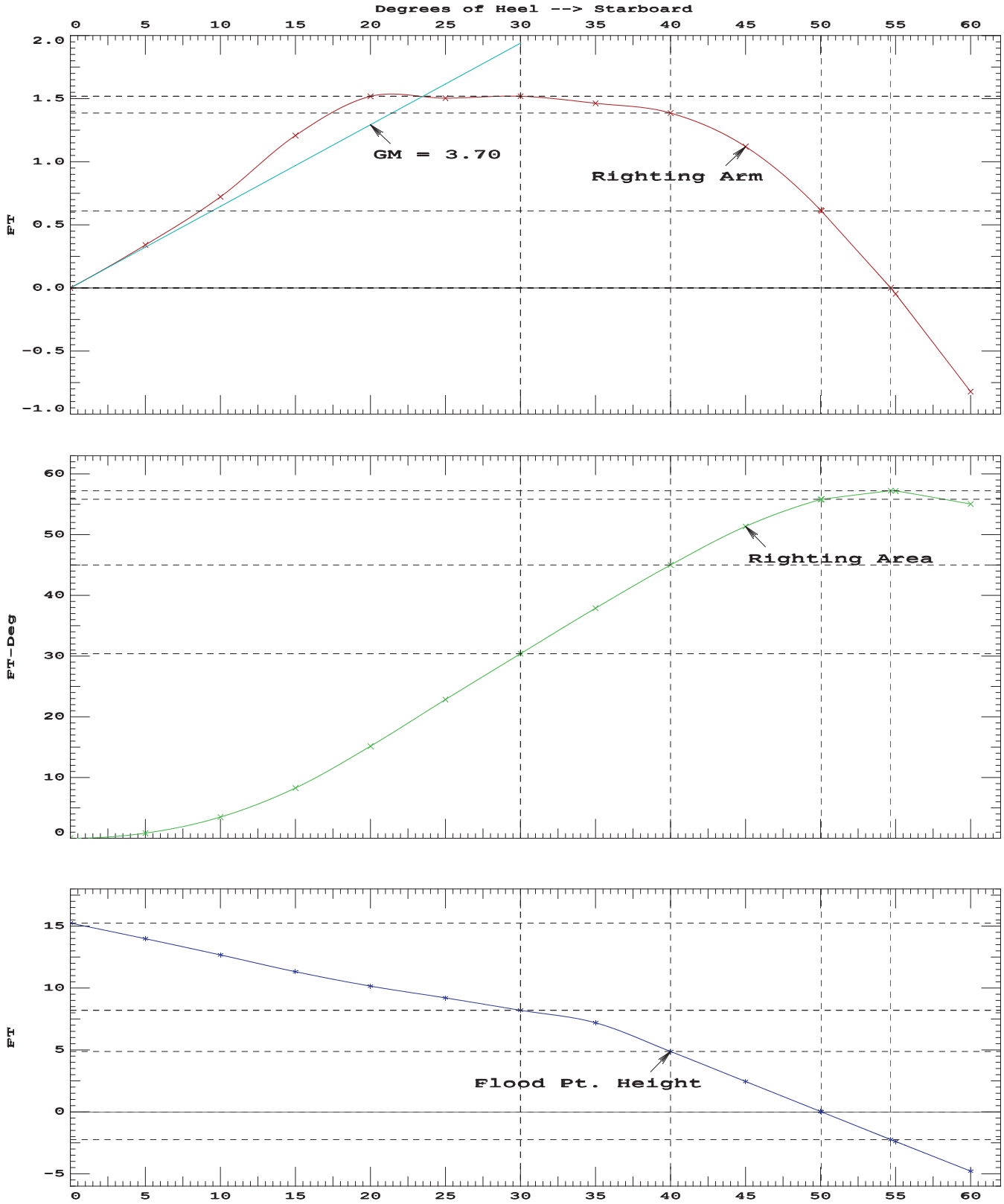

170x56x12 Trimaran
MAX VCG @ 1025 LT
-0.5 DEG TRIM
USCG 170.173 PARAGRAPH B

RIGHTING ARMS vs HEEL ANGLE
LCG = 93.39a TCG = 0.00 VCG = 24.98

Origin Depth	Degrees of Trim	Heel	Displacement Weight(LT)	Righting Arms in Trim	in Heel	Flood Pt ---> Area	Height
11.768	0.50f	0.00	1,025.0	0.00	0.000	0.00	15.05(3)
11.732	0.51f	5.00s	1,025.0	0.00	0.322	0.80	13.79(3)
11.626	0.55f	10.00s	1,025.0	0.00	0.685	3.31	12.48(3)
11.462	0.63f	15.00s	1,024.9	0.00	1.163	7.88	11.13(3)
11.236	0.84f	20.00s	1,025.2	0.00	1.551	14.70	9.95(3)
10.756	1.10f	25.00s	1,024.8	0.00	1.542	22.60	9.00(3)
9.966	1.25f	30.00s	1,025.0	0.00	1.551	30.32	7.99(3)
8.931	1.33f	35.00s	1,025.0	0.00	1.501	37.98	6.97(3)
7.678	1.37f	40.00s	1,025.0	0.00	1.426	45.31	4.60(1)
6.395	1.43f	45.00s	1,025.0	0.00	1.141	51.81	2.16(1)
5.272	1.48f	49.40s	1,025.0	0.00	0.696	55.92	0.00(1)
5.119	1.49f	50.00s	1,025.0	0.00	0.625	56.31	-0.29(1)
3.925	1.56f	54.68s	1,025.0	0.00	0.000	57.84	-2.58(1)
3.844	1.57f	55.00s	1,025.0	0.00	-0.046	57.83	-2.74(1)
2.564	1.64f	60.00s	1,025.0	0.00	-0.824	55.70	-5.16(1)

Distances in FEET.------Specific Gravity = 1.025.----------Area in Ft-Deg.

Critical Points		LCP	TCP	VCP
(1) Vent Louver	FLOOD	145.00a	28.00	35.00
(3) CTD Wire Chase	FLOOD	122.00a	14.00	25.75

LIM 170.173 Paragraph b CRITERION		Min/Max		Attained	
(1) GM Upright	>	0.49	Ft	3.52	P
(2) Righting Arm at 30 deg or MaxRA	>	0.66	Ft	1.55	P
(3) Absolute Angle at MaxRA	>	25.00	deg	30.00	P
(4) Area from abs 0.000 deg to 30	>	10.30	Ft-deg	30.32	P
(5) Area from abs 0.000 deg to 40 or Flood	>	16.90	Ft-deg	45.31	P
(6) Area from 30 deg to 40 or Flood	>	5.60	Ft-deg	14.98	P

----------Relative angles measured from 0.000 ----------

1025 24.98

170x56x12 Trimaran
MAX VCG @ 1025 LT
-0.5 DEG TRIM
USCG 170.173 PARAGRAPH B

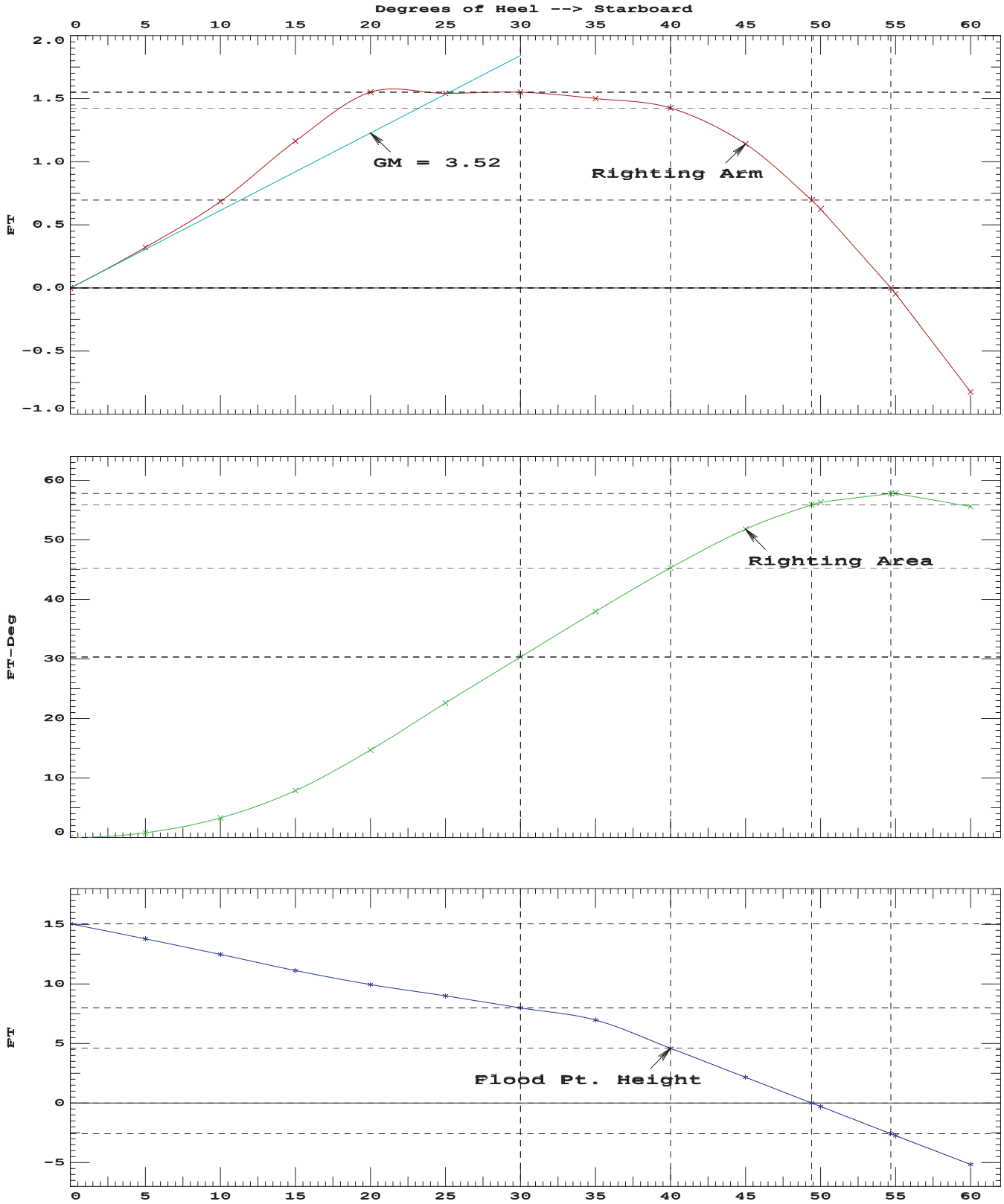

170x56x12 Trimaran
MAX VCG @ 1050 LT
-0.5 DEG TRIM
USCG 170.173 PARAGRAPH B

RIGHTING ARMS vs HEEL ANGLE
LCG = 93.57a TCG = 0.00 VCG = 24.85

Origin Depth	Degrees of Trim	Heel	Displacement Weight(LT)	Righting Arms in Trim	in Heel	Area	Flood Pt Height
11.961	0.50f	0.00	1,050.0	0.00	0.000	0.00	14.85(3)
11.925	0.51f	5.00s	1,050.0	0.00	0.306	0.76	13.60(3)
11.814	0.55f	10.00s	1,050.0	0.00	0.652	3.14	12.28(3)
11.643	0.63f	15.00s	1,049.9	0.00	1.124	7.53	10.95(3)
11.389	0.82f	20.00s	1,050.3	0.00	1.585	14.30	9.75(3)
10.869	1.06f	25.00s	1,049.9	0.00	1.582	22.41	8.81(3)
10.036	1.19f	30.00s	1,049.7	0.00	1.585	30.33	7.79(3)
8.980	1.25f	35.00s	1,050.0	0.00	1.540	38.16	6.75(3)
7.714	1.28f	40.00s	1,050.0	0.00	1.464	45.68	4.34(1)
6.420	1.32f	45.00s	1,050.0	0.00	1.162	52.34	1.87(1)
5.451	1.36f	48.76s	1,050.0	0.00	0.781	56.03	0.00(1)
5.131	1.37f	50.00s	1,050.0	0.00	0.634	56.91	-0.61(1)
3.922	1.43f	54.70s	1,050.0	0.00	0.000	58.46	-2.94(1)
3.846	1.43f	55.00s	1,050.0	0.00	-0.044	58.46	-3.09(1)
2.556	1.49f	60.00s	1,050.0	0.00	-0.825	56.32	-5.53(1)

Distances in FEET.------Specific Gravity = 1.025.----------Area in Ft-Deg.

Critical Points		LCP	TCP	VCP
(1)	Vent Louver	FLOOD 145.00a	28.00	35.00
(3)	CTD Wire Chase	FLOOD 122.00a	14.00	25.75

LIM	170.173 Paragraph b CRITERION		Min/Max		Attained	
(1)	GM Upright	>	0.49	Ft	3.34	P
(2)	Righting Arm at 30 deg or MaxRA	>	0.66	Ft	1.58	P
(3)	Absolute Angle at MaxRA	>	25.00	deg	30.00	P
(4)	Area from abs 0.000 deg to 30	>	10.30	Ft-deg	30.33	P
(5)	Area from abs 0.000 deg to 40 or Flood	>	16.90	Ft-deg	45.68	P
(6)	Area from 30 deg to 40 or Flood	>	5.60	Ft-deg	15.35	P

--------------------Relative angles measured from 0.000 ----------

1050 24.85

170x56x12 Trimaran
MAX VCG @ 1050 LT
-0.5 DEG TRIM
USCG 170.173 PARAGRAPH B

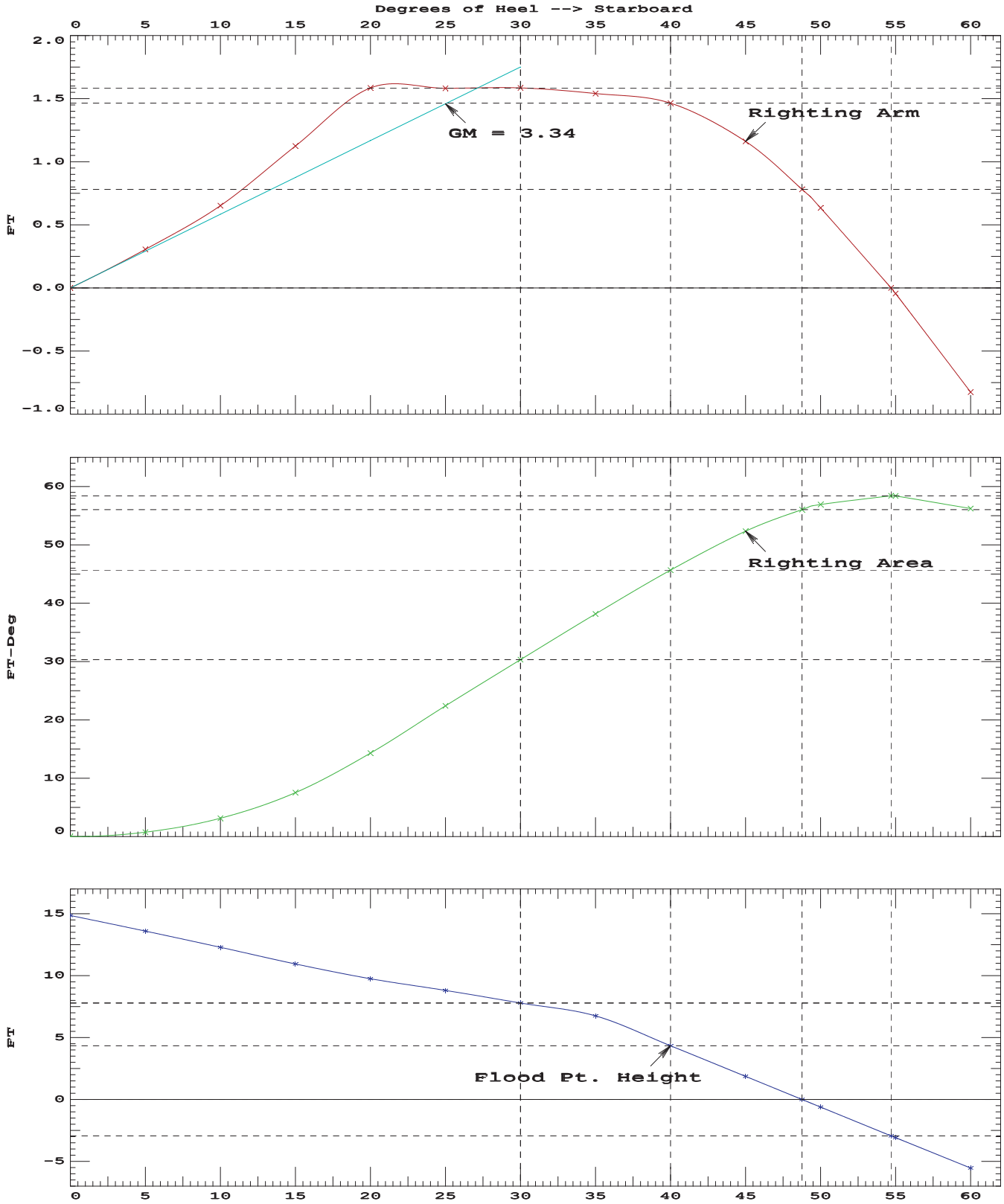

170x56x12 Trimaran
MAX VCG @ 1075 LT
-0.5 DEG TRIM
USCG 170.173 PARAGRAPH B

RIGHTING ARMS vs HEEL ANGLE
LCG = 93.75a TCG = 0.00 VCG = 24.63

Origin Depth	Degrees of Trim	Heel	Displacement Weight(LT)	Righting Arms in Trim	in Heel	Area	Flood Pt Height
12.155	0.50f	0.00	1,075.3	0.00	0.000	0.00	14.66(3)
12.116	0.51f	5.00s	1,075.0	0.00	0.299	0.75	13.41(3)
11.998	0.55f	10.00s	1,075.0	0.00	0.637	3.07	12.09(3)
11.820	0.63f	15.00s	1,074.9	0.00	1.114	7.39	10.76(3)
11.536	0.79f	20.00s	1,075.3	0.00	1.649	14.27	9.56(3)
11.149	0.97f	23.75s	1,075.0	0.00	1.663	20.59	8.85(3)
10.975	1.02f	25.00s	1,075.0	0.00	1.662	22.67	8.61(3)
10.344	1.10f	28.75s	1,075.0	0.00	1.664	28.94	7.84(3)
10.107	1.12f	30.00s	1,075.0	0.00	1.663	31.02	7.58(3)
9.028	1.18f	35.00s	1,075.0	0.00	1.631	39.25	6.54(3)
7.747	1.19f	40.00s	1,075.0	0.00	1.558	47.24	4.07(1)
6.439	1.21f	45.00s	1,075.0	0.00	1.245	54.35	1.57(1)
5.626	1.23f	48.13s	1,075.0	0.00	0.932	57.77	0.00(1)
5.140	1.25f	50.00s	1,075.0	0.00	0.713	59.31	-0.94(1)
3.842	1.29f	55.00s	1,075.0	0.00	0.033	61.25	-3.44(1)
3.787	1.29f	55.22s	1,075.3	0.00	-0.001	61.25	-3.55(1)
2.543	1.34f	60.00s	1,075.0	0.00	-0.746	59.50	-5.91(1)

Distances in FEET.------Specific Gravity = 1.025.----------Area in Ft-Deg.

Critical Points		LCP	TCP	VCP
(1) Vent Louver	FLOOD	145.00a	28.00	35.00
(3) CTD Wire Chase	FLOOD	122.00a	14.00	25.75

LIM 170.173 Paragraph b CRITERION		Min/Max		Attained	
(1) GM Upright	>	0.49	Ft	3.27	P
(2) Righting Arm at 30 deg or MaxRA	>	0.66	Ft	1.66	P
(3) Absolute Angle at MaxRA	>	25.00	deg	28.75	P
(4) Area from abs 0.000 deg to 30	>	10.30	Ft-deg	31.02	P
(5) Area from abs 0.000 deg to 40 or Flood	>	16.90	Ft-deg	47.24	P
(6) Area from 30 deg to 40 or Flood	>	5.60	Ft-deg	16.22	P

----------Relative angles measured from 0.000 ----------

1075 24.63

170x56x12 Trimaran
MAX VCG @ 1075 LT
-0.5 DEG TRIM
USCG 170.173 PARAGRAPH B

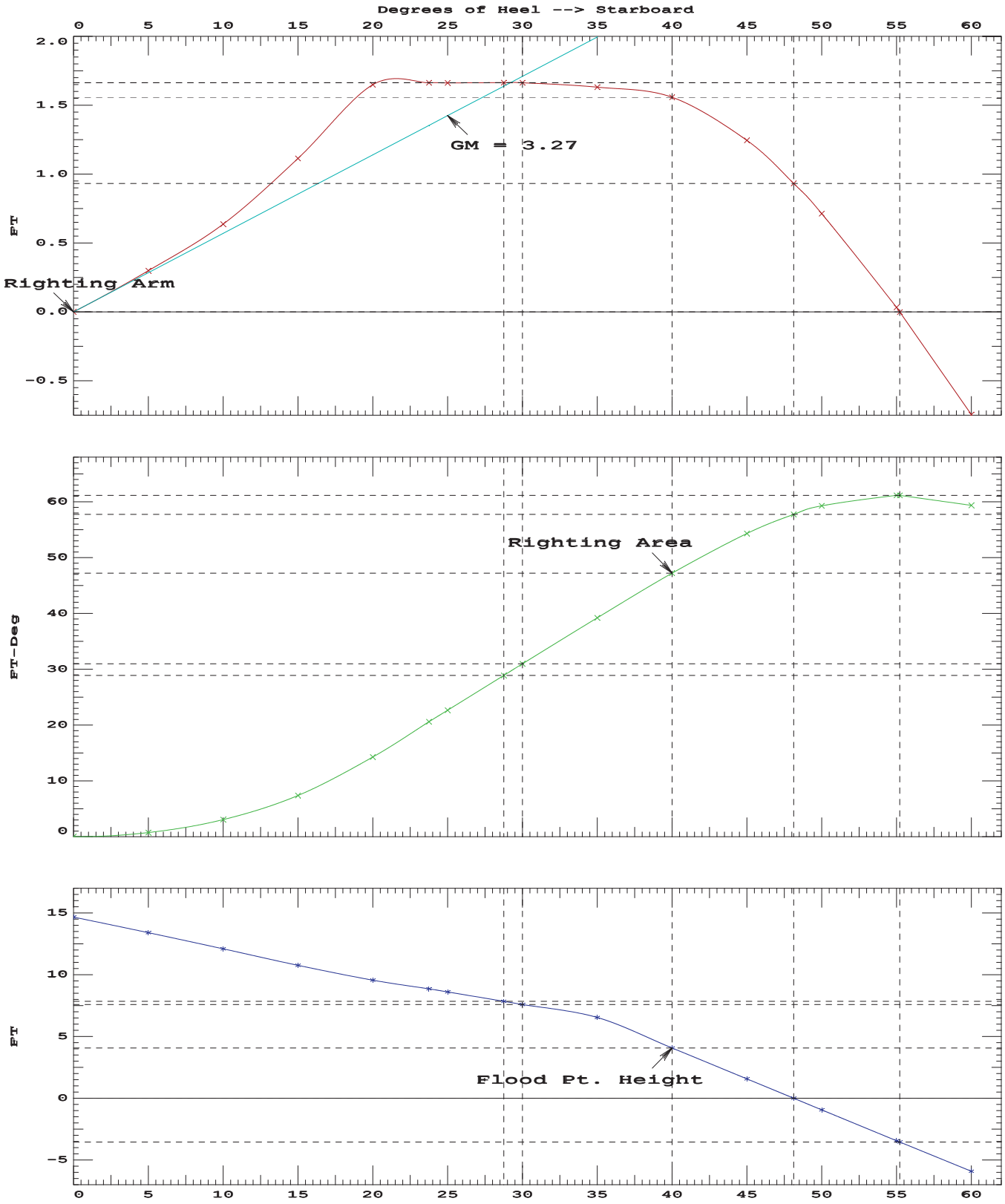

170x56x12 Trimaran
MAX VCG @ 1100 LT
-0.5 DEG TRIM
USCG 170.173 PARAGRAPH B

RIGHTING ARMS vs HEEL ANGLE
LCG = 93.93a TCG = 0.00 VCG = 24.40

Origin Depth	Degrees of Trim	Heel	Displacement Weight(LT)	Righting Arms in Trim	in Heel	Area	Flood Pt Height
12.346	0.50f	0.00	1,100.3	0.00	0.000	0.00	14.47(3)
12.305	0.51f	5.00s	1,100.0	0.00	0.294	0.74	13.22(3)
12.182	0.54f	10.00s	1,100.0	0.00	0.627	3.02	11.90(3)
11.996	0.62f	15.00s	1,099.9	0.00	1.112	7.31	10.58(3)
11.679	0.77f	20.00s	1,100.0	0.00	1.716	14.32	9.37(3)
11.076	0.97f	25.00s	1,100.0	0.00	1.749	23.22	8.41(3)
10.177	1.06f	30.00s	1,100.0	0.00	1.748	31.98	7.38(3)
9.078	1.10f	35.00s	1,099.9	0.00	1.727	40.68	6.32(1)
7.776	1.09f	40.00s	1,100.0	0.00	1.655	49.15	3.80(1)
6.458	1.10f	45.00s	1,100.0	0.00	1.334	56.73	1.27(1)
5.799	1.11f	47.51s	1,100.0	0.00	1.087	59.78	-0.00(1)
5.146	1.12f	50.00s	1,100.0	0.00	0.799	62.13	-1.26(1)
3.838	1.15f	55.00s	1,100.0	0.00	0.119	64.49	-3.79(1)
3.628	1.15f	55.80s	1,100.1	0.00	0.000	64.54	-4.19(1)
2.529	1.18f	60.00s	1,100.0	0.00	-0.657	63.19	-6.29(1)

Distances in FEET.------Specific Gravity = 1.025.----------Area in Ft-Deg.

Critical Points		LCP	TCP	VCP
(1)	Vent Louver	FLOOD 145.00a	28.00	35.00
(3)	CTD Wire Chase	FLOOD 122.00a	14.00	25.75

LIM 170.173 Paragraph b CRITERION		Min/Max		Attained
(1)	GM Upright	> 0.49	Ft	3.22 P
(2)	Righting Arm at 30 deg or MaxRA	> 0.66	Ft	1.75 P
(3)	Absolute Angle at MaxRA	> 25.00	deg	25.00 P
(4)	Area from abs 0.000 deg to 30	> 10.30	Ft-deg	31.98 P
(5)	Area from abs 0.000 deg to 40 or Flood	> 16.90	Ft-deg	49.15 P
(6)	Area from 30 deg to 40 or Flood	> 5.60	Ft-deg	17.17 P

----------Relative angles measured from 0.000 ----------

1100 24.4

170x56x12 Trimaran
MAX VCG @ 1100 LT
-0.5 DEG TRIM
USCG 170.173 PARAGRAPH B

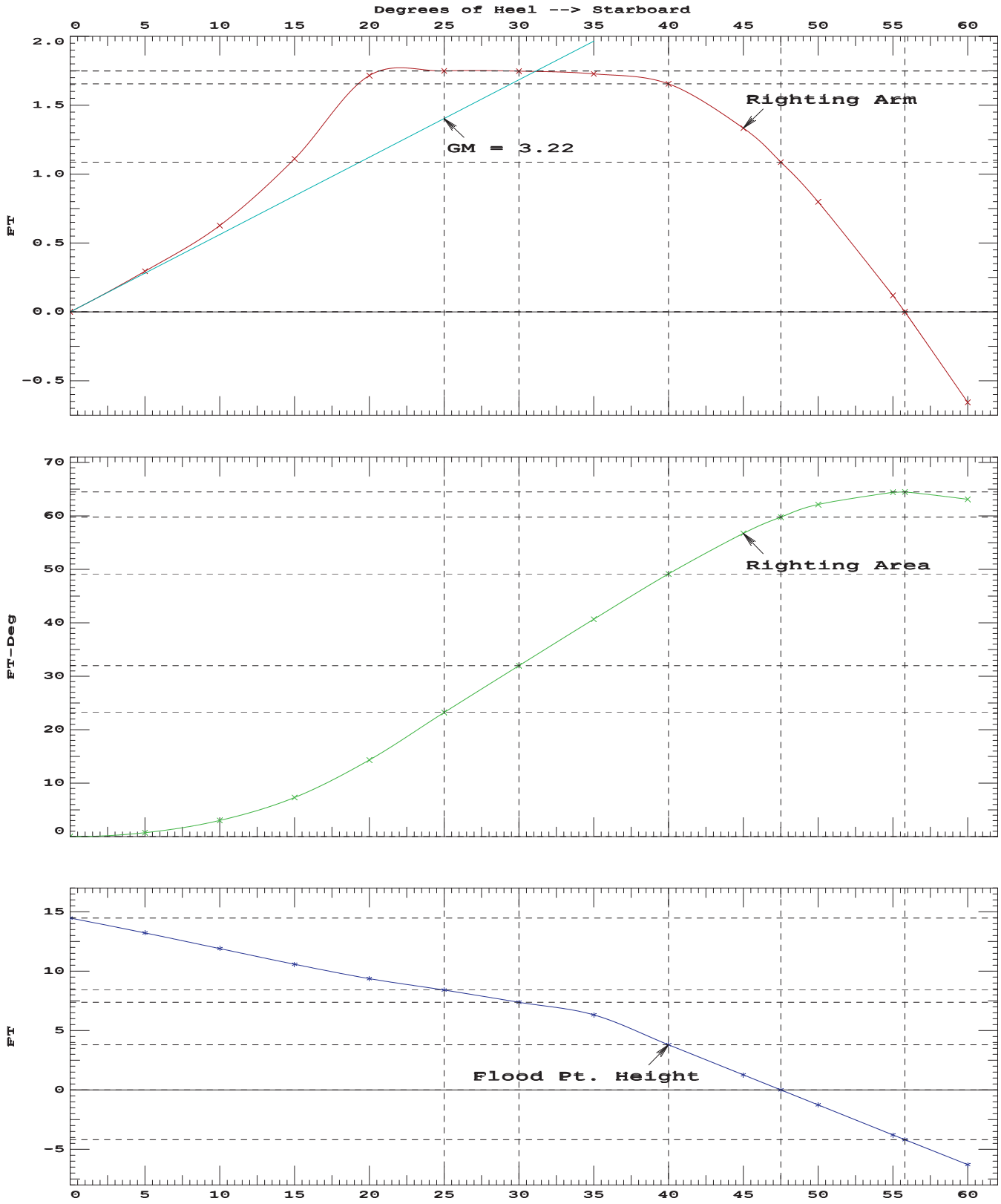

170x56x12 Trimaran
MAX VCG @ 1125 LT
-0.5 DEG TRIM
USCG 170.173 PARAGRAPH B

RIGHTING ARMS vs HEEL ANGLE
LCG = 94.10a TCG = 0.00 VCG = 24.18

Origin Depth	Degrees of Trim	Heel	Displacement Weight(LT)	Righting Arms in Trim	in Heel	Area	Flood Pt Height
12.536	0.50f	0.00	1,125.2	0.00	0.000	0.00	14.28(3)
12.494	0.51f	5.00s	1,125.0	0.00	0.291	0.73	13.03(3)
12.364	0.54f	10.00s	1,125.0	0.00	0.618	2.98	11.71(3)
12.170	0.62f	15.00s	1,124.9	0.00	1.112	7.24	10.39(3)
11.819	0.75f	20.00s	1,125.0	0.00	1.778	14.39	9.19(3)
11.174	0.93f	25.00s	1,125.0	0.00	1.833	23.67	8.22(3)
10.246	1.00f	30.00s	1,125.0	0.00	1.828	32.85	7.19(3)
9.125	1.02f	35.00s	1,125.0	0.00	1.817	41.96	6.07(1)
7.804	1.00f	40.00s	1,125.0	0.00	1.745	50.89	3.53(1)
6.473	0.99f	45.00s	1,125.0	0.00	1.415	58.90	0.97(1)
5.970	0.99f	46.90s	1,125.0	0.00	1.232	61.42	-0.00(1)
5.150	0.99f	50.00s	1,125.0	0.00	0.877	64.71	-1.59(1)
3.832	1.01f	55.00s	1,125.0	0.00	0.198	67.46	-4.14(1)
3.480	1.01f	56.33s	1,125.1	0.00	0.000	67.59	-4.82(1)
2.513	1.03f	60.00s	1,125.0	0.00	-0.575	66.56	-6.66(1)

Distances in FEET.------Specific Gravity = 1.025.----------Area in Ft-Deg.

Critical Points		LCP	TCP	VCP
(1)	Vent Louver	FLOOD 145.00a	28.00	35.00
(3)	CTD Wire Chase	FLOOD 122.00a	14.00	25.75

LIM	170.173 Paragraph b CRITERION		Min/Max		Attained	
(1)	GM Upright	>	0.49	Ft	3.18	P
(2)	Righting Arm at 30 deg or MaxRA	>	0.66	Ft	1.83	P
(3)	Absolute Angle at MaxRA	>	25.00	deg	25.00	P
(4)	Area from abs 0.000 deg to 30	>	10.30	Ft-deg	32.85	P
(5)	Area from abs 0.000 deg to 40 or Flood	>	16.90	Ft-deg	50.89	P
(6)	Area from 30 deg to 40 or Flood	>	5.60	Ft-deg	18.04	P

----------Relative angles measured from 0.000 ----------

1125 24.18

170x56x12 Trimaran
MAX VCG @ 1125 LT
-0.5 DEG TRIM
USCG 170.173 PARAGRAPH B

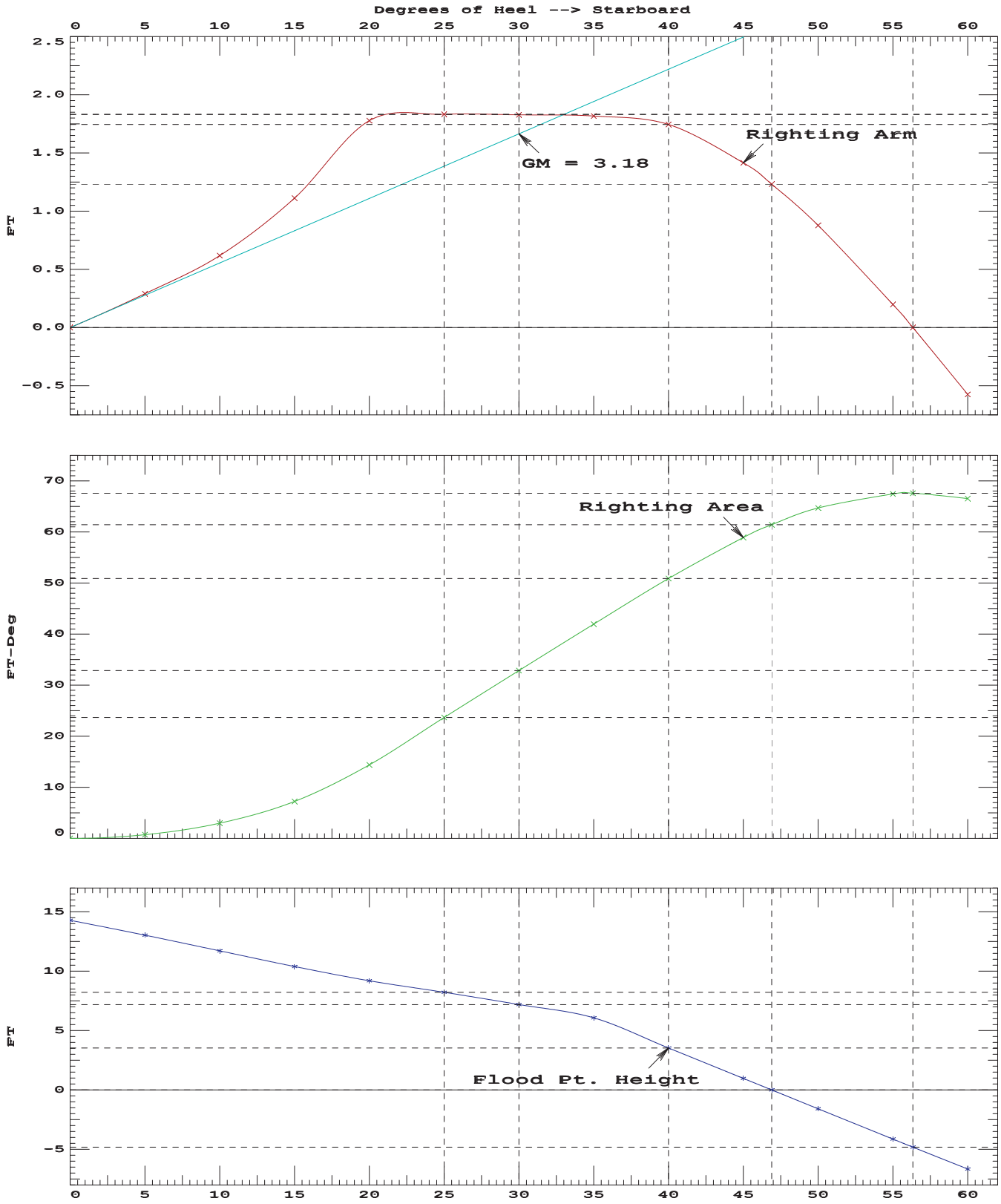

170x56x12 Trimaran
MAX VCG @ 1150 LT
-0.5 DEG TRIM
USCG 170.173 PARAGRAPH B

RIGHTING ARMS vs HEEL ANGLE
LCG = 94.27a TCG = 0.00 VCG = 23.92

Origin Depth	Degrees of Trim	Heel	Displacement Weight(LT)	Righting Arms in Trim	in Heel	Area	Flood Pt Height
12.725	0.50f	0.00	1,150.2	0.00	0.000	0.00	14.09(3)
12.681	0.51f	5.00s	1,150.0	0.00	0.291	0.73	12.84(3)
12.545	0.54f	10.00s	1,150.0	0.00	0.619	2.99	11.52(3)
12.340	0.61f	15.00s	1,149.9	0.00	1.128	7.28	10.21(3)
11.959	0.73f	20.00s	1,150.0	0.00	1.852	14.64	9.01(3)
11.269	0.88f	25.00s	1,150.0	0.00	1.935	24.38	8.03(3)
10.317	0.94f	30.00s	1,150.0	0.00	1.929	34.07	6.99(3)
9.170	0.95f	35.00s	1,150.0	0.00	1.928	43.71	5.83(1)
7.829	0.90f	40.00s	1,150.0	0.00	1.858	53.21	3.26(1)
6.485	0.87f	45.00s	1,150.0	0.00	1.524	61.77	0.67(1)
6.139	0.87f	46.30s	1,150.0	0.00	1.401	63.67	-0.00(1)
5.151	0.86f	50.00s	1,150.0	0.00	0.986	68.12	-1.92(1)
3.823	0.86f	55.00s	1,150.0	0.00	0.310	71.43	-4.50(1)
3.269	0.87f	57.08s	1,150.0	0.00	0.000	71.76	-5.56(1)
2.496	0.87f	60.00s	1,150.0	0.00	-0.457	71.10	-7.04(1)

Distances in FEET.------Specific Gravity = 1.025.----------Area in Ft-Deg.

Critical Points		LCP	TCP	VCP
(1) Vent Louver	FLOOD	145.00a	28.00	35.00
(3) CTD Wire Chase	FLOOD	122.00a	14.00	25.75

LIM 170.173 Paragraph b CRITERION		Min/Max		Attained
(1) GM Upright	>	0.49	Ft	3.18 P
(2) Righting Arm at 30 deg or MaxRA	>	0.66	Ft	1.93 P
(3) Absolute Angle at MaxRA	>	25.00	deg	25.00 P
(4) Area from abs 0.000 deg to 30	>	10.30	Ft-deg	34.07 P
(5) Area from abs 0.000 deg to 40 or Flood	>	16.90	Ft-deg	53.21 P
(6) Area from 30 deg to 40 or Flood	>	5.60	Ft-deg	19.14 P

Relative angles measured from 0.000

1150 23.92

170x56x12 Trimaran
MAX VCG @ 1150 LT
-0.5 DEG TRIM
USCG 170.173 PARAGRAPH B

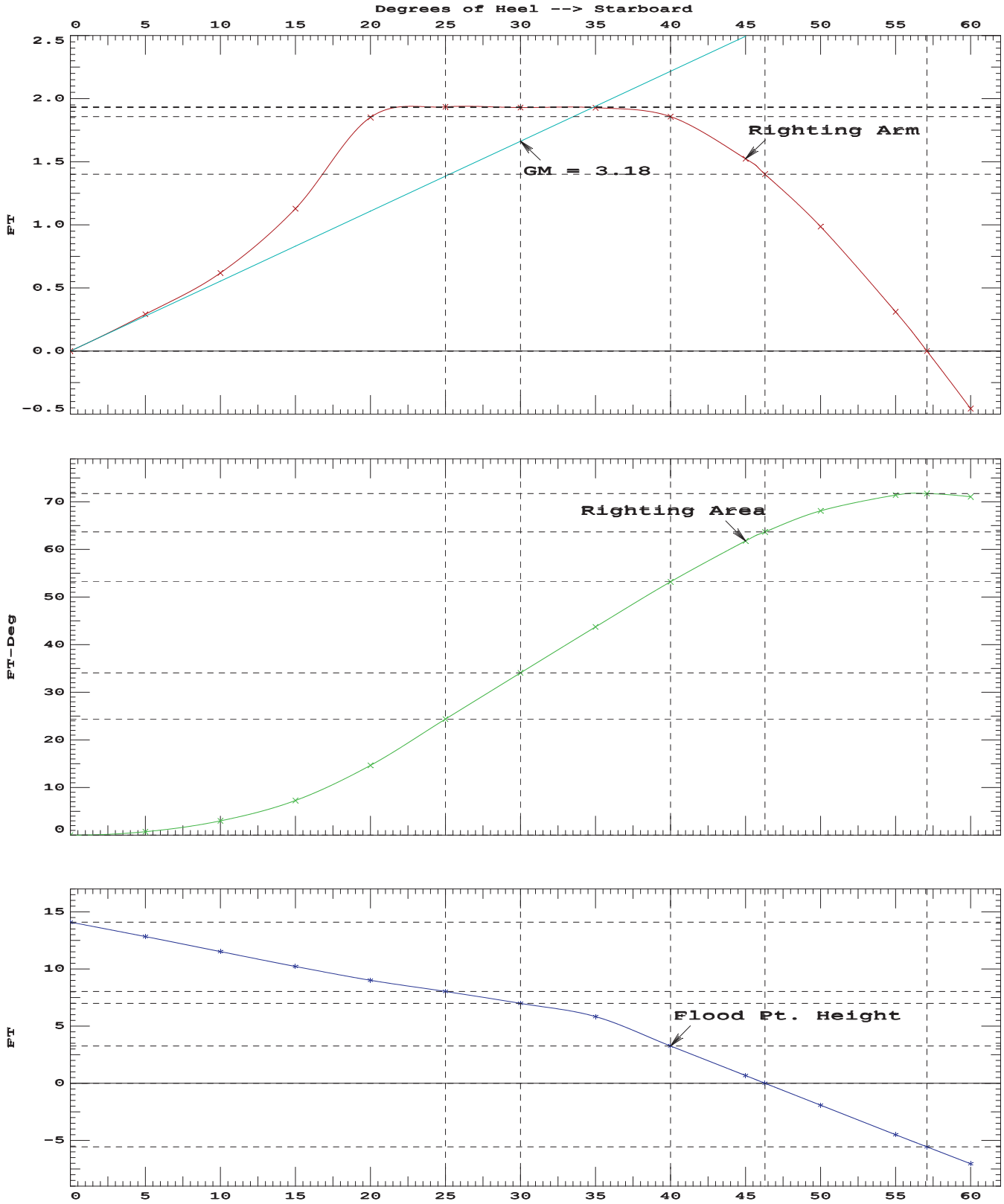

170x56x12 Trimaran
MAX VCG @ 1175 LT
-0.5 DEG TRIM
USCG 170.173 PARAGRAPH B

RIGHTING ARMS vs HEEL ANGLE
LCG = 94.44a TCG = 0.00 VCG = 23.66

Origin Depth	Degrees of Trim	Heel	Displacement Weight(LT)	Righting Arms in Trim	in Heel	Area	Flood Pt Height
12.914	0.50f	0.00	1,175.1	0.00	0.000	0.00	13.90(3)
12.867	0.51f	5.00s	1,175.0	0.00	0.293	0.73	12.65(3)
12.725	0.53f	10.00s	1,175.0	0.00	0.625	3.01	11.34(3)
12.508	0.61f	15.00s	1,174.9	0.00	1.149	7.36	10.03(3)
12.093	0.72f	20.00s	1,174.7	0.00	1.925	14.95	8.84(3)
11.486	0.83f	24.30s	1,175.0	0.00	2.038	23.65	7.98(3)
11.363	0.84f	25.00s	1,175.0	0.00	2.037	25.07	7.84(3)
10.388	0.89f	30.00s	1,175.0	0.00	2.030	35.37	6.80(3)
9.210	0.87f	35.00s	1,175.0	0.00	2.039	45.53	5.59(1)
7.852	0.80f	40.00s	1,175.0	0.00	1.969	55.59	2.99(1)
6.497	0.76f	45.00s	1,175.0	0.00	1.632	64.70	0.37(1)
6.306	0.75f	45.71s	1,175.0	0.00	1.567	65.83	-0.00(1)
5.151	0.73f	50.00s	1,175.0	0.00	1.096	71.59	-2.25(1)
3.812	0.72f	55.00s	1,175.0	0.00	0.424	75.46	-4.85(1)
3.053	0.71f	57.84s	1,175.0	0.00	0.000	76.07	-6.32(1)
2.475	0.71f	60.00s	1,175.0	0.00	-0.338	75.70	-7.42(1)

Distances in FEET.------Specific Gravity = 1.025.----------Area in Ft-Deg.

Critical Points		LCP	TCP	VCP
(1) Vent Louver	FLOOD	145.00a	28.00	35.00
(3) CTD Wire Chase	FLOOD	122.00a	14.00	25.75

LIM 170.173 Paragraph b CRITERION		Min/Max		Attained	
(1) GM Upright	>	0.49	Ft	3.22	P
(2) Righting Arm at 30 deg or MaxRA	>	0.66	Ft	2.04	P
(3) Absolute Angle at MaxRA	>	25.00	deg	35.00	P
(4) Area from abs 0.000 deg to 30	>	10.30	Ft-deg	35.37	P
(5) Area from abs 0.000 deg to 40 or Flood	>	16.90	Ft-deg	55.59	P
(6) Area from 30 deg to 40 or Flood	>	5.60	Ft-deg	20.22	P

----------Relative angles measured from 0.000 ----------

1175 23.66

170x56x12 Trimaran
MAX VCG @ 1175 LT
-0.5 DEG TRIM
USCG 170.173 PARAGRAPH B

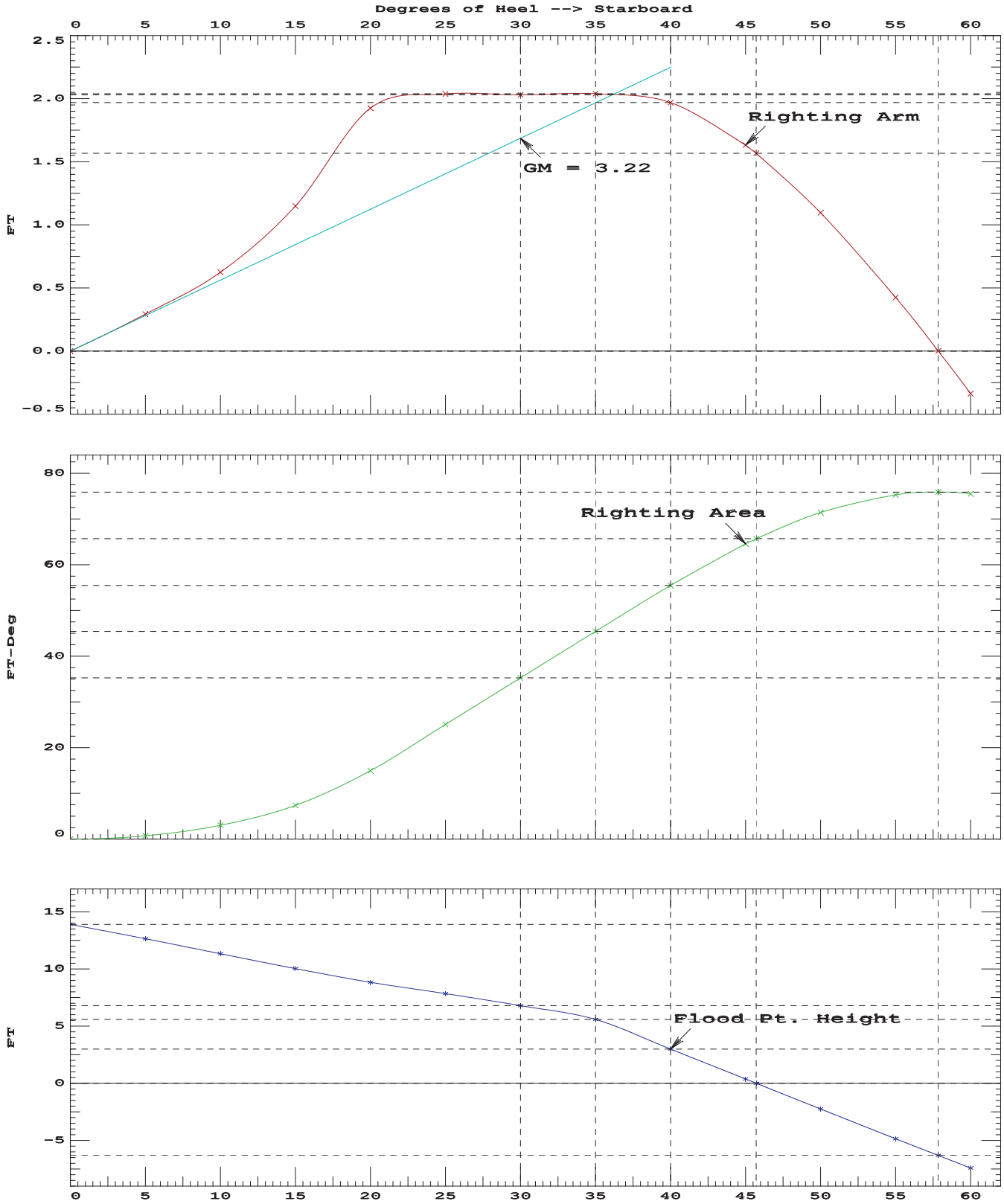

170x56x12 Trimaran
MAX VCG @ 1200 LT
-0.5 DEG TRIM
USCG 170.173 PARAGRAPH B

RIGHTING ARMS vs HEEL ANGLE
LCG = 94.60a TCG = 0.00 VCG = 23.44

Origin Depth	Degrees of Trim	Heel	Displacement Weight(LT)	Righting Arms in Trim	in Heel	Flood Pt ---> Area	Height
13.101	0.50f	0.00	1,200.1	0.00	0.000	0.00	13.71(3)
13.051	0.51f	5.00s	1,200.0	0.00	0.292	0.73	12.46(3)
12.905	0.53f	10.00s	1,200.0	0.00	0.627	3.01	11.15(3)
12.672	0.60f	15.00s	1,199.9	0.00	1.165	7.40	9.86(3)
12.226	0.70f	20.00s	1,199.8	0.00	1.981	15.15	8.66(3)
11.680	0.78f	23.75s	1,200.0	0.00	2.126	22.98	7.91(3)
11.457	0.80f	25.00s	1,200.0	0.00	2.123	25.64	7.66(3)
10.457	0.83f	30.00s	1,200.0	0.00	2.112	36.36	6.60(3)
9.247	0.78f	35.00s	1,200.0	0.00	2.124	46.94	5.34(1)
8.914	0.76f	36.23s	1,200.0	0.00	2.127	49.55	4.70(1)
7.872	0.70f	40.00s	1,200.0	0.00	2.052	57.45	2.71(1)
6.504	0.64f	45.00s	1,200.0	0.00	1.711	66.94	0.07(1)
6.471	0.64f	45.12s	1,200.0	0.00	1.699	67.15	-0.00(1)
5.148	0.60f	50.00s	1,200.0	0.00	1.174	74.23	-2.58(1)
3.799	0.57f	55.00s	1,200.0	0.00	0.506	78.49	-5.21(1)
2.888	0.56f	58.39s	1,200.0	0.00	0.000	79.36	-6.97(1)
2.452	0.55f	60.00s	1,200.0	0.00	-0.252	79.16	-7.80(1)

Distances in FEET.------Specific Gravity = 1.025.----------Area in Ft-Deg.

Critical Points		LCP	TCP	VCP
(1) Vent Louver	FLOOD	145.00a	28.00	35.00
(3) CTD Wire Chase	FLOOD	122.00a	14.00	25.75

LIM 170.173 Paragraph b CRITERION		Min/Max		Attained	
(1) GM Upright	>	0.49	Ft	3.23	P
(2) Righting Arm at 30 deg or MaxRA	>	0.66	Ft	2.13	P
(3) Absolute Angle at MaxRA	>	25.00	deg	36.23	P
(4) Area from abs 0.000 deg to 30	>	10.30	Ft-deg	36.36	P
(5) Area from abs 0.000 deg to 40 or Flood	>	16.90	Ft-deg	57.45	P
(6) Area from 30 deg to 40 or Flood	>	5.60	Ft-deg	21.09	P

Relative angles measured from 0.000

1200 23.44

170x56x12 Trimaran
MAX VCG @ 1200 LT
-0.5 DEG TRIM
USCG 170.173 PARAGRAPH B

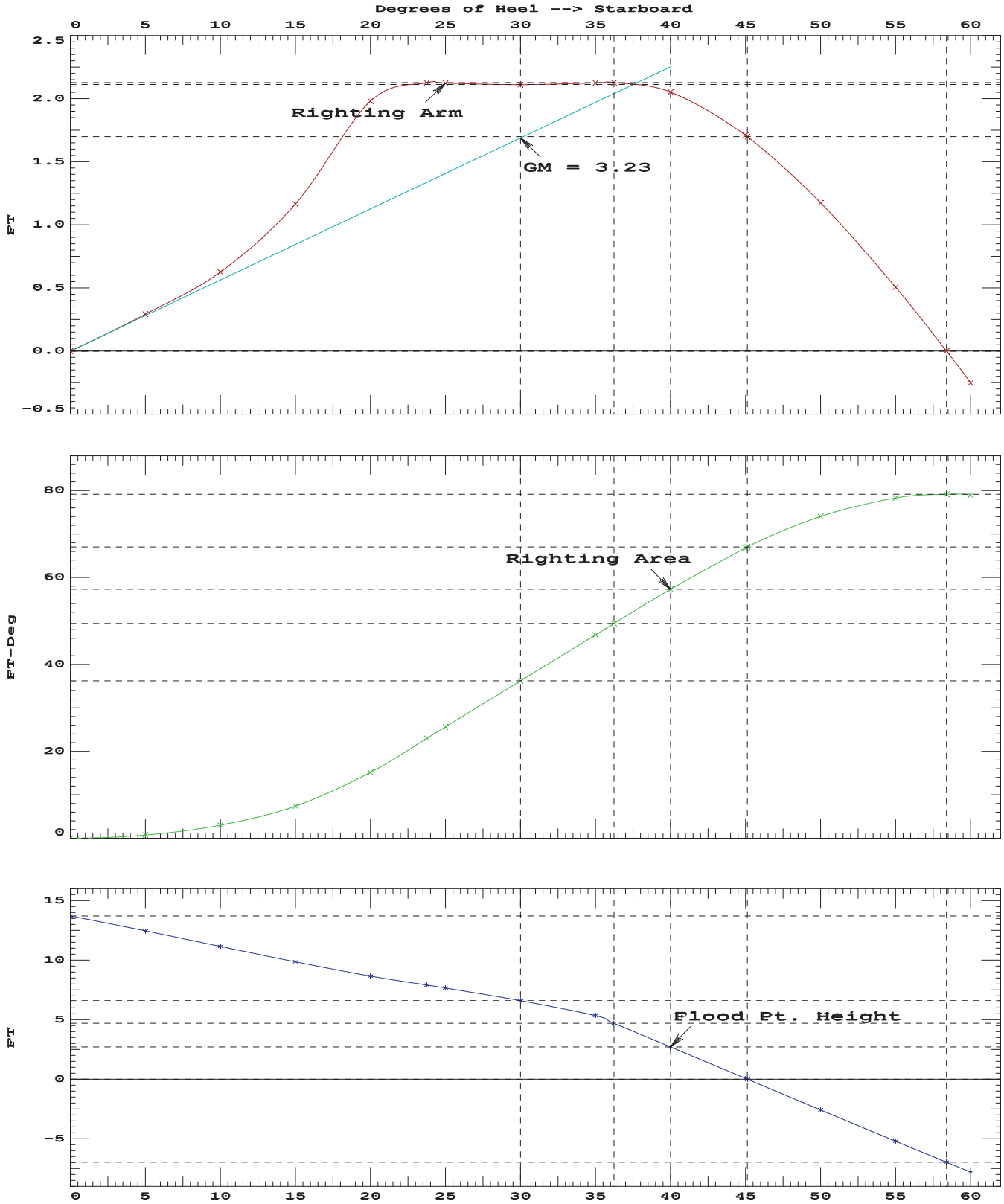

170x56x12 Trimaran
MAX VCG @ 900 LT
0. DEG TRIM
USCG 170.173 PARAGRAPH B

RIGHTING ARMS vs HEEL ANGLE
LCG = 93.98a TCG = 0.00 VCG = 24.79

Origin Depth	Trim	Heel	Displacement Weight(LT)	Righting Arms in Trim	in Heel	Area	Flood Pt Height
9.915	0.00	0.00	900.00	0.00	0.000	0.00	15.83(3)
9.889	0.02f	5.00s	900.00	0.00	0.516	1.29	14.58(3)
9.810	0.07f	10.00s	899.99	0.00	1.075	5.25	13.26(3)
9.697	0.16f	15.00s	899.80	0.00	1.712	12.18	11.90(3)
9.653	0.33f	18.16s	899.99	0.00	1.882	17.91	11.15(3)
9.600	0.46f	20.00s	899.75	0.00	1.824	21.32	10.78(3)
9.345	0.81f	25.00s	900.00	0.00	1.833	30.56	9.80(3)
8.818	1.10f	30.00s	900.26	0.00	1.884	39.84	8.82(3)
7.949	1.28f	35.00s	899.66	0.00	1.841	49.19	7.84(3)
6.819	1.40f	40.00s	899.80	0.00	1.793	58.28	5.53(1)
5.569	1.50f	45.00s	899.99	0.00	1.662	66.95	3.17(1)
4.334	1.62f	50.00s	899.99	0.00	1.273	74.40	0.82(1)
3.906	1.67f	51.75s	899.96	0.00	1.089	76.47	-0.00(1)
3.106	1.76f	55.00s	899.97	0.00	0.695	79.39	-1.52(1)
1.903	1.88f	59.84s	900.00	0.00	0.000	81.13	-3.77(1)
1.864	1.88f	60.00s	900.00	0.00	-0.025	81.13	-3.84(1)

Distances in FEET.------Specific Gravity = 1.025.----------Area in Ft-Deg.

Critical Points		LCP	TCP	VCP
(1) Vent Louver	FLOOD	145.00a	28.00	35.00
(3) CTD Wire Chase	FLOOD	122.00a	14.00	25.75

LIM 170.173 Paragraph b CRITERION		Min/Max		Attained	
(1) GM Upright	>	0.49	Ft	5.68	P
(2) Righting Arm at 30 deg or MaxRA	>	0.66	Ft	1.88	P
(3) Absolute Angle at MaxRA	>	25.00	deg	30.00	P
(4) Area from abs 0.000 deg to 30	>	10.30	Ft-deg	39.84	P
(5) Area from abs 0.000 deg to 40 or Flood	>	16.90	Ft-deg	58.28	P
(6) Area from 30 deg to 40 or Flood	>	5.60	Ft-deg	18.44	P

----------Relative angles measured from 0.000 ----------

900 24.79

170x56x12 Trimaran
MAX VCG @ 900 LT
0. DEG TRIM
USCG 170.173 PARAGRAPH B

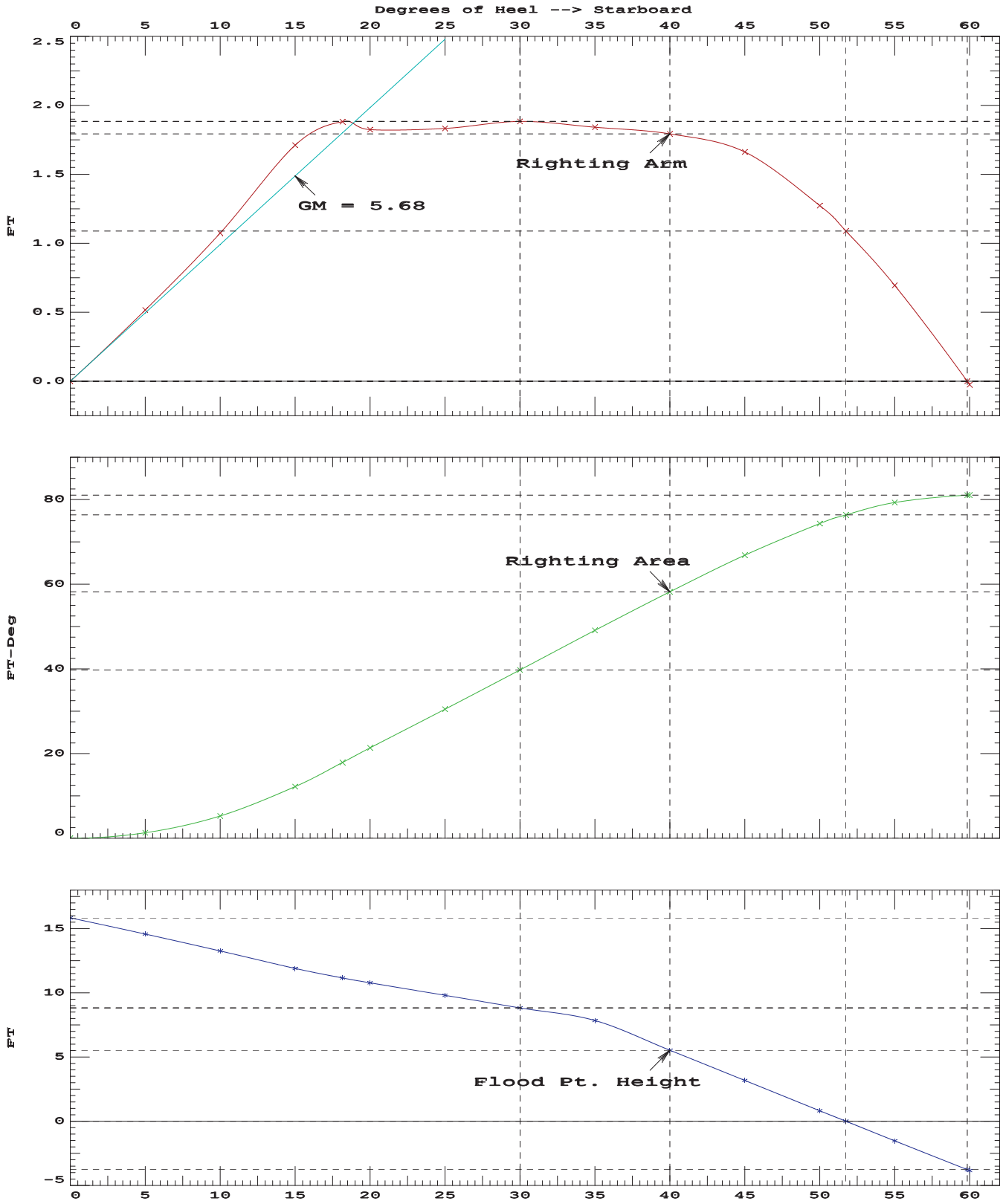

170x56x12 Trimaran
MAX VCG @ 925 LT
0. DEG TRIM
USCG 170.173 PARAGRAPH B

RIGHTING ARMS vs HEEL ANGLE
LCG = 94.15a TCG = 0.00 VCG = 24.83

Origin Depth	Degrees of Trim	Heel	Displacement Weight(LT)	Righting Arms in Trim	in Heel	Flood Pt Area	Height
10.111	0.00	0.00	925.00	0.00	0.000	0.00	15.64(2)
10.084	0.02f	5.00s	925.00	0.00	0.474	1.19	14.38(3)
10.004	0.07f	10.00s	924.98	0.00	0.990	4.83	13.06(3)
9.887	0.16f	15.00s	924.83	0.00	1.598	11.26	11.71(3)
9.825	0.34f	18.44s	924.73	0.00	1.819	17.19	10.89(3)
9.773	0.44f	20.00s	924.83	0.00	1.773	19.99	10.57(3)
9.484	0.78f	25.00s	924.72	0.00	1.782	28.98	9.60(3)
8.906	1.04f	30.00s	925.02	0.00	1.821	37.97	8.60(3)
8.009	1.20f	35.00s	924.98	0.00	1.773	46.99	7.61(3)
6.853	1.30f	40.00s	924.87	0.00	1.719	55.73	5.25(1)
5.598	1.39f	45.00s	925.00	0.00	1.560	63.97	2.87(1)
4.357	1.51f	50.00s	925.00	0.00	1.144	70.83	0.50(1)
4.098	1.53f	51.06s	924.98	0.00	1.030	71.99	0.00(1)
3.123	1.63f	55.00s	925.00	0.00	0.545	75.12	-1.86(1)
2.179	1.72f	58.79s	925.05	0.00	0.000	76.18	-3.64(1)
1.871	1.74f	60.00s	925.00	0.00	-0.188	76.07	-4.21(1)

Distances in FEET.------Specific Gravity = 1.025.----------Area in Ft-Deg.

Critical Points	LCP	TCP	VCP
(1) Vent Louver	FLOOD 145.00a	28.00	35.00
(2) A-Frame Wire Chase	FLOOD 138.00a	7.50	25.75
(3) CTD Wire Chase	FLOOD 122.00a	14.00	25.75

LIM 170.173 Paragraph b CRITERION	Min/Max		Attained	
(1) GM Upright	>	0.49	Ft	5.22 P
(2) Righting Arm at 30 deg or MaxRA	>	0.66	Ft	1.82 P
(3) Absolute Angle at MaxRA	>	25.00	deg	30.00 P
(4) Area from abs 0.000 deg to 30	>	10.30	Ft-deg	37.97 P
(5) Area from abs 0.000 deg to 40 or Flood	>	16.90	Ft-deg	55.73 P
(6) Area from 30 deg to 40 or Flood	>	5.60	Ft-deg	17.75 P

----------Relative angles measured from 0.000 ----------

925 24.83

170x56x12 Trimaran
MAX VCG @ 925 LT
0. DEG TRIM
USCG 170.173 PARAGRAPH B

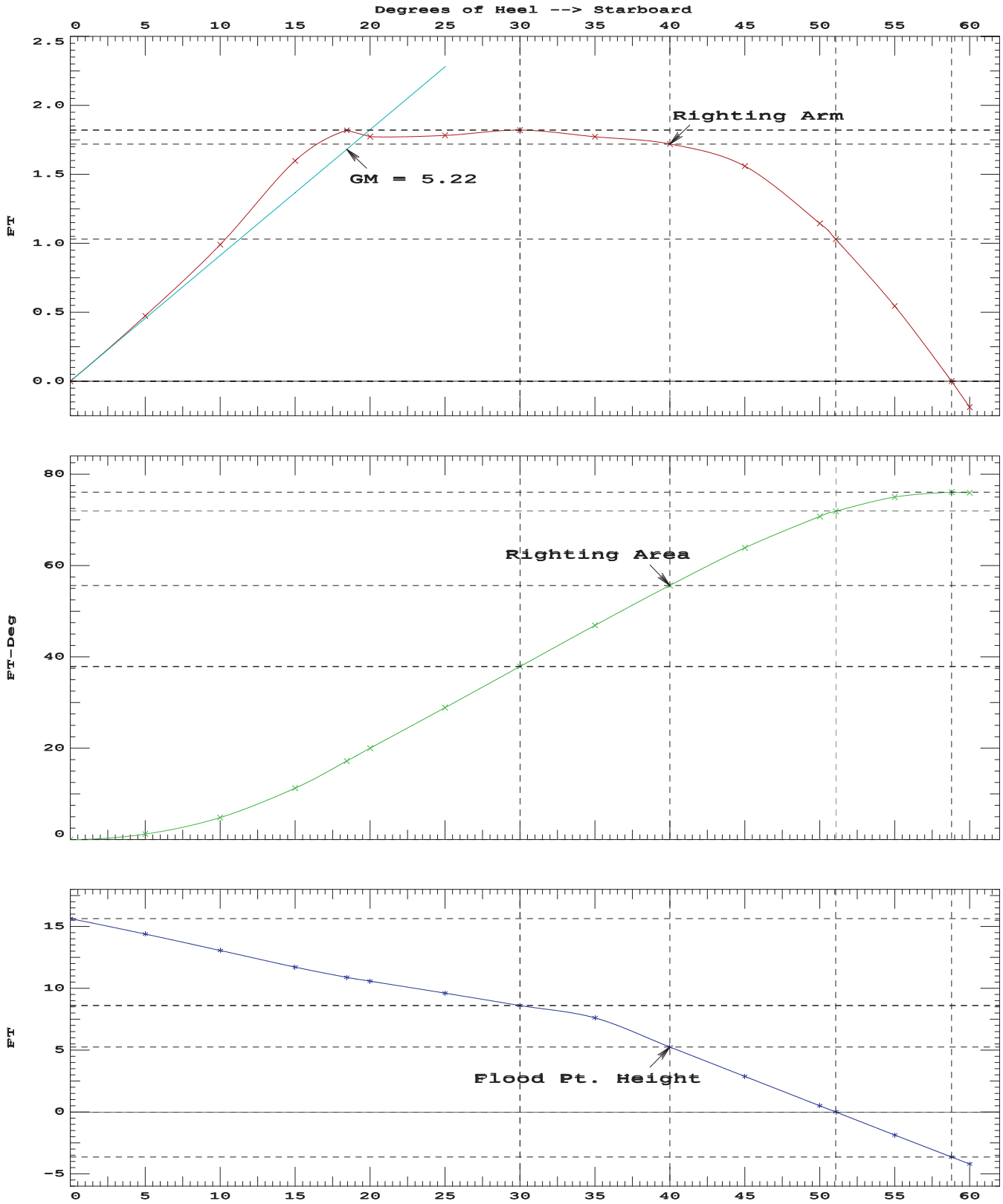

170x56x12 Trimaran
MAX VCG @ 950 LT
0. DEG TRIM
USCG 170.173 PARAGRAPH B

RIGHTING ARMS vs HEEL ANGLE
LCG = 94.31a TCG = 0.00 VCG = 24.84

Origin Depth	Degrees of Trim	Heel	Displacement Weight(LT)	Righting Arms in Trim	in Heel	Area	Flood Pt Height
10.306	0.00	0.00	950.00	0.00	0.000	0.00	15.44(2)
10.279	0.02f	5.00s	950.00	0.00	0.437	1.09	14.19(3)
10.195	0.06f	10.00s	949.98	0.00	0.916	4.46	12.87(3)
10.076	0.16f	15.00s	949.84	0.00	1.498	10.45	11.52(3)
9.995	0.34f	18.73s	950.00	0.00	1.770	16.59	10.62(3)
9.943	0.42f	20.00s	949.89	0.00	1.739	18.81	10.37(3)
9.619	0.75f	25.00s	949.73	0.00	1.745	27.63	9.40(3)
8.998	0.98f	30.00s	950.03	0.00	1.772	36.42	8.39(3)
8.066	1.12f	35.00s	949.98	0.00	1.723	45.19	7.38(1)
6.889	1.21f	40.00s	949.91	0.00	1.666	53.66	4.97(1)
5.630	1.29f	45.00s	950.00	0.00	1.479	61.58	2.58(1)
4.383	1.39f	50.00s	950.00	0.00	1.039	67.98	0.19(1)
4.287	1.40f	50.39s	950.01	0.00	0.996	68.38	0.00(1)
3.136	1.50f	55.00s	950.01	0.00	0.422	71.70	-2.20(1)
2.404	1.56f	57.92s	950.07	0.00	0.000	72.33	-3.59(1)
1.877	1.60f	60.00s	950.00	0.00	-0.322	71.99	-4.57(1)

Distances in FEET.------Specific Gravity = 1.025.----------Area in Ft-Deg.

Critical Points		LCP	TCP	VCP
(1) Vent Louver	FLOOD	145.00a	28.00	35.00
(2) A-Frame Wire Chase	FLOOD	138.00a	7.50	25.75
(3) CTD Wire Chase	FLOOD	122.00a	14.00	25.75

LIM 170.173 Paragraph b CRITERION		Min/Max		Attained	
(1) GM Upright	>	0.49	Ft	4.82	P
(2) Righting Arm at 30 deg or MaxRA	>	0.66	Ft	1.77	P
(3) Absolute Angle at MaxRA	>	25.00	deg	30.00	P
(4) Area from abs 0.000 deg to 30	>	10.30	Ft-deg	36.42	P
(5) Area from abs 0.000 deg to 40 or Flood	>	16.90	Ft-deg	53.66	P
(6) Area from 30 deg to 40 or Flood	>	5.60	Ft-deg	17.25	P

Relative angles measured from 0.000

950 24.84

170x56x12 Trimaran
MAX VCG @ 950 LT
0. DEG TRIM
USCG 170.173 PARAGRAPH B

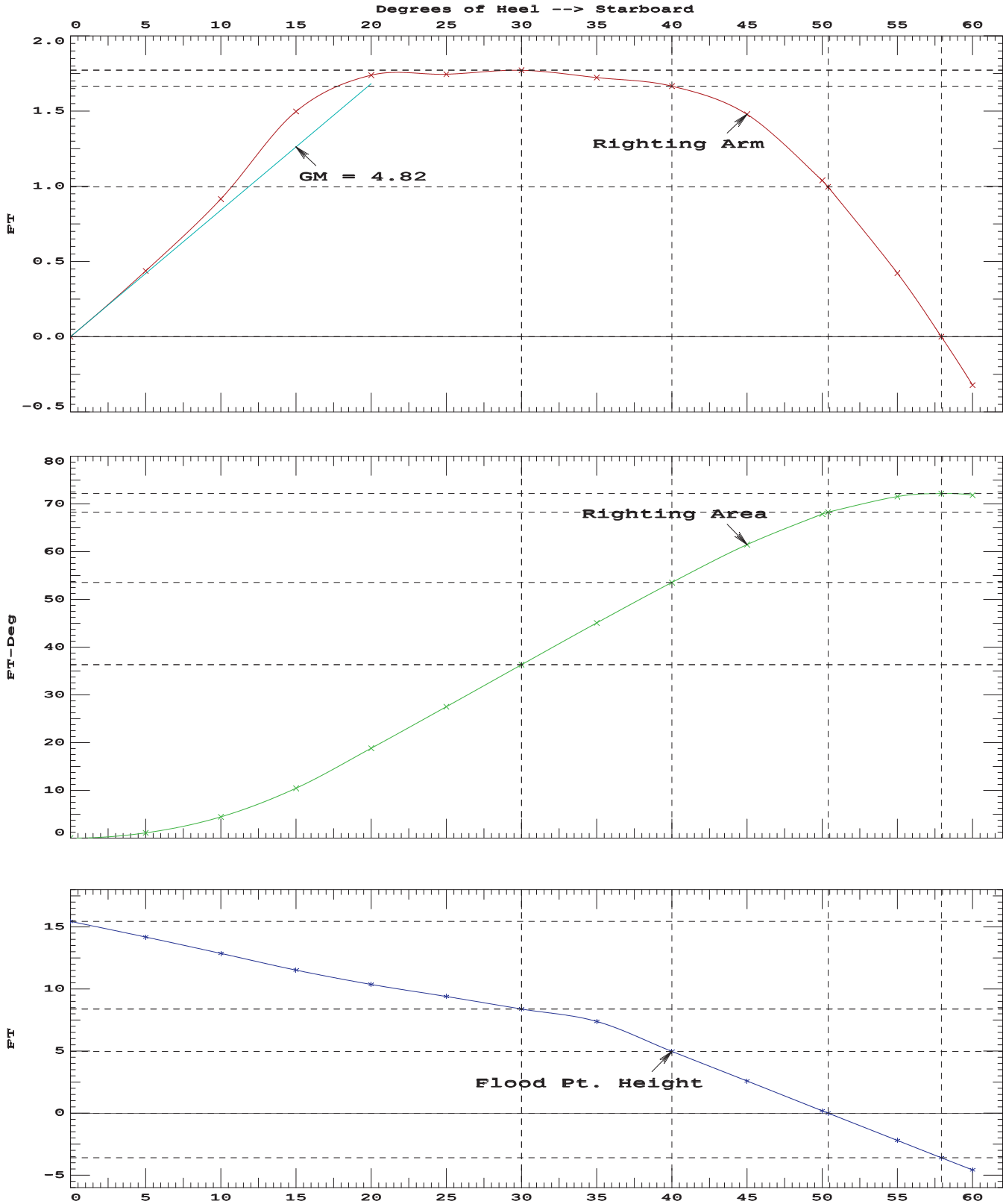

170x56x12 Trimaran
MAX VCG @ 975 LT
0. DEG TRIM
USCG 170.173 PARAGRAPH B

RIGHTING ARMS vs HEEL ANGLE
LCG = 94.48a TCG = 0.00 VCG = 24.94

Origin Depth	Trim	Heel	Displacement Weight(LT)	Righting Arms in Trim	in Heel	Area	Flood Pt Height
10.500	0.00	0.00	975.00	0.00	0.000	0.00	15.25(2)
10.473	0.02f	5.00s	975.00	0.00	0.395	0.99	13.99(3)
10.384	0.06f	10.00s	974.98	0.00	0.830	4.03	12.68(3)
10.262	0.16f	15.00s	974.87	0.00	1.380	9.51	11.33(3)
10.109	0.40f	20.00s	975.04	0.00	1.679	17.26	10.16(3)
9.749	0.72f	25.00s	974.70	0.00	1.673	25.77	9.20(3)
9.085	0.92f	30.00s	975.26	0.00	1.679	34.14	8.18(3)
8.123	1.04f	35.00s	974.99	0.00	1.623	42.43	7.13(1)
6.928	1.11f	40.00s	974.95	0.00	1.555	50.38	4.70(1)
5.662	1.19f	45.00s	975.00	0.00	1.334	57.67	2.29(1)
4.471	1.27f	49.73s	975.02	0.00	0.896	63.03	0.00(1)
4.404	1.27f	50.00s	975.00	0.00	0.865	63.26	-0.13(1)
3.145	1.37f	55.00s	975.01	0.00	0.227	66.07	-2.55(1)
2.749	1.39f	56.57s	975.11	0.00	0.000	66.24	-3.31(1)
1.877	1.45f	60.00s	975.00	0.00	-0.532	65.35	-4.94(1)

Distances in FEET.------Specific Gravity = 1.025.----------Area in Ft-Deg.

Critical Points		LCP	TCP	VCP
(1)	Vent Louver	FLOOD 145.00a	28.00	35.00
(2)	A-Frame Wire Chase	FLOOD 138.00a	7.50	25.75
(3)	CTD Wire Chase	FLOOD 122.00a	14.00	25.75

LIM	170.173 Paragraph b CRITERION	Min/Max		Attained	
(1)	GM Upright	>	0.49	Ft	4.35 P
(2)	Righting Arm at 30 deg or MaxRA	>	0.66	Ft	1.68 P
(3)	Absolute Angle at MaxRA	>	25.00	deg	30.00 P
(4)	Area from abs 0.000 deg to 30	>	10.30	Ft-deg	34.14 P
(5)	Area from abs 0.000 deg to 40 or Flood	>	16.90	Ft-deg	50.38 P
(6)	Area from 30 deg to 40 or Flood	>	5.60	Ft-deg	16.23 P

Relative angles measured from 0.000

975 24.94

170x56x12 Trimaran
MAX VCG @ 975 LT
0. DEG TRIM
USCG 170.173 PARAGRAPH B

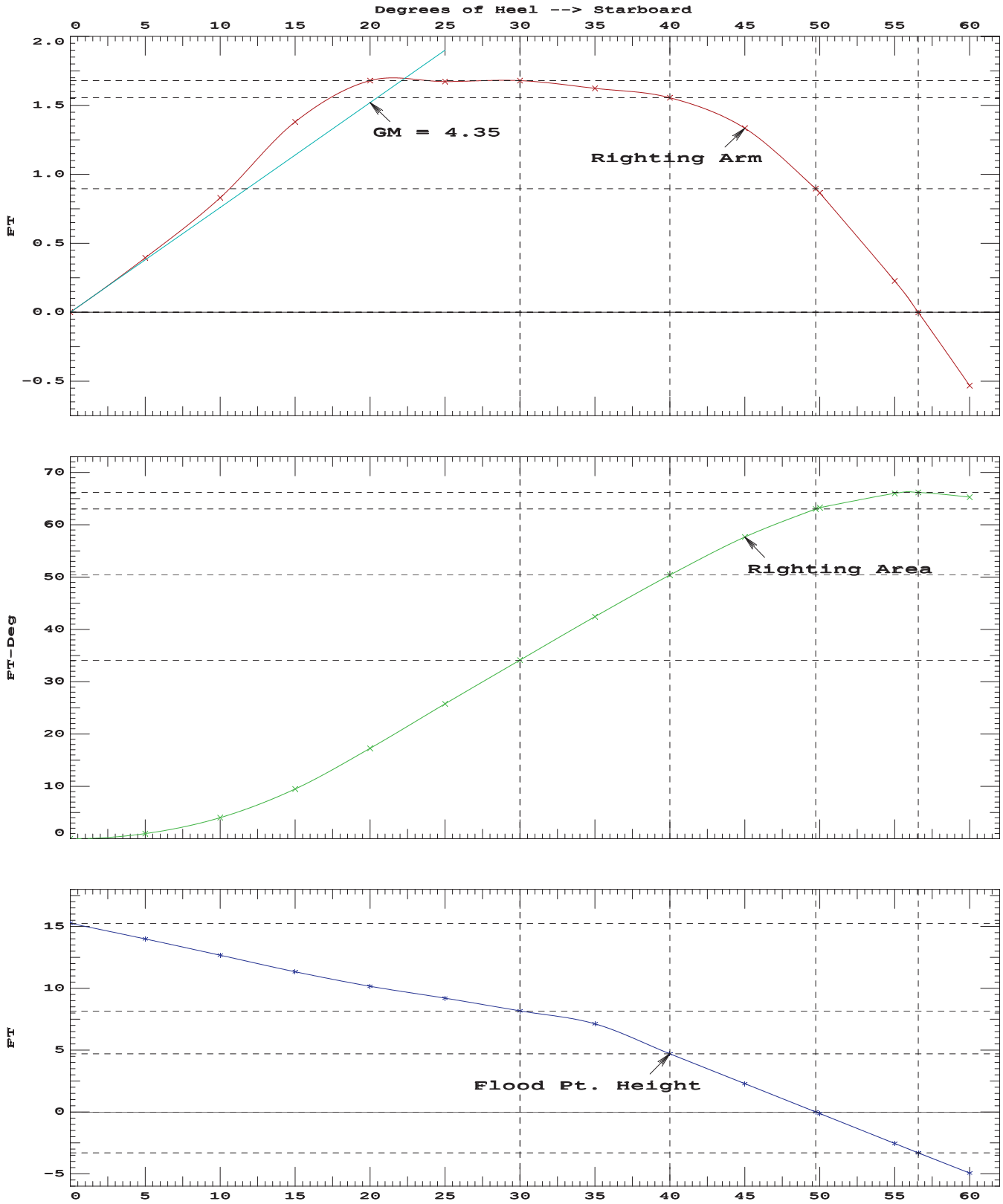

170x56x12 Trimaran
MAX VCG @ 1000 LT
0. DEG TRIM
USCG 170.173 PARAGRAPH B

RIGHTING ARMS vs HEEL ANGLE
LCG = 94.64a TCG = 0.00 VCG = 24.81

Origin Depth	Degrees of Trim	Heel	Displacement Weight(LT)	Righting Arms in Trim	in Heel	Area	Flood Pt Height
10.694	0.00	0.00	1,000.1	0.00	0.000	0.00	15.06(2)
10.665	0.02f	5.00s	1,000.0	0.00	0.375	0.94	13.80(3)
10.570	0.06f	10.00s	1,000.0	0.00	0.789	3.83	12.48(3)
10.446	0.16f	15.00s	999.9	0.00	1.328	9.07	11.14(3)
10.273	0.39f	20.00s	1,000.0	0.00	1.704	16.71	9.96(3)
9.874	0.68f	25.00s	999.8	0.00	1.700	25.38	9.00(3)
9.160	0.86f	30.00s	1,000.0	0.00	1.705	33.89	7.97(3)
8.178	0.97f	35.00s	1,000.0	0.00	1.656	42.31	6.88(1)
6.966	1.02f	40.00s	1,000.0	0.00	1.592	50.44	4.44(1)
5.689	1.08f	45.00s	1,000.0	0.00	1.352	57.87	2.00(1)
4.652	1.14f	49.08s	1,000.0	0.00	0.972	62.67	0.00(1)
4.418	1.15f	50.00s	1,000.0	0.00	0.869	63.52	-0.45(1)
3.148	1.23f	55.00s	1,000.0	0.00	0.222	66.32	-2.90(1)
2.760	1.25f	56.53s	1,000.1	0.00	0.000	66.49	-3.64(1)
1.872	1.31f	60.00s	1,000.0	0.00	-0.540	65.57	-5.32(1)

Distances in FEET.------Specific Gravity = 1.025.----------Area in Ft-Deg.

Critical Points		LCP	TCP	VCP
(1) Vent Louver	FLOOD	145.00a	28.00	35.00
(2) A-Frame Wire Chase	FLOOD	138.00a	7.50	25.75
(3) CTD Wire Chase	FLOOD	122.00a	14.00	25.75

LIM 170.173 Paragraph b CRITERION		Min/Max		Attained	
(1) GM Upright	>	0.49	Ft	4.13	P
(2) Righting Arm at 30 deg or MaxRA	>	0.66	Ft	1.71	P
(3) Absolute Angle at MaxRA	>	25.00	deg	30.00	P
(4) Area from abs 0.000 deg to 30	>	10.30	Ft-deg	33.89	P
(5) Area from abs 0.000 deg to 40 or Flood	>	16.90	Ft-deg	50.44	P
(6) Area from 30 deg to 40 or Flood	>	5.60	Ft-deg	16.55	P

Relative angles measured from 0.000

1000 24.81

170x56x12 Trimaran
MAX VCG @ 1000 LT
0. DEG TRIM
USCG 170.173 PARAGRAPH B

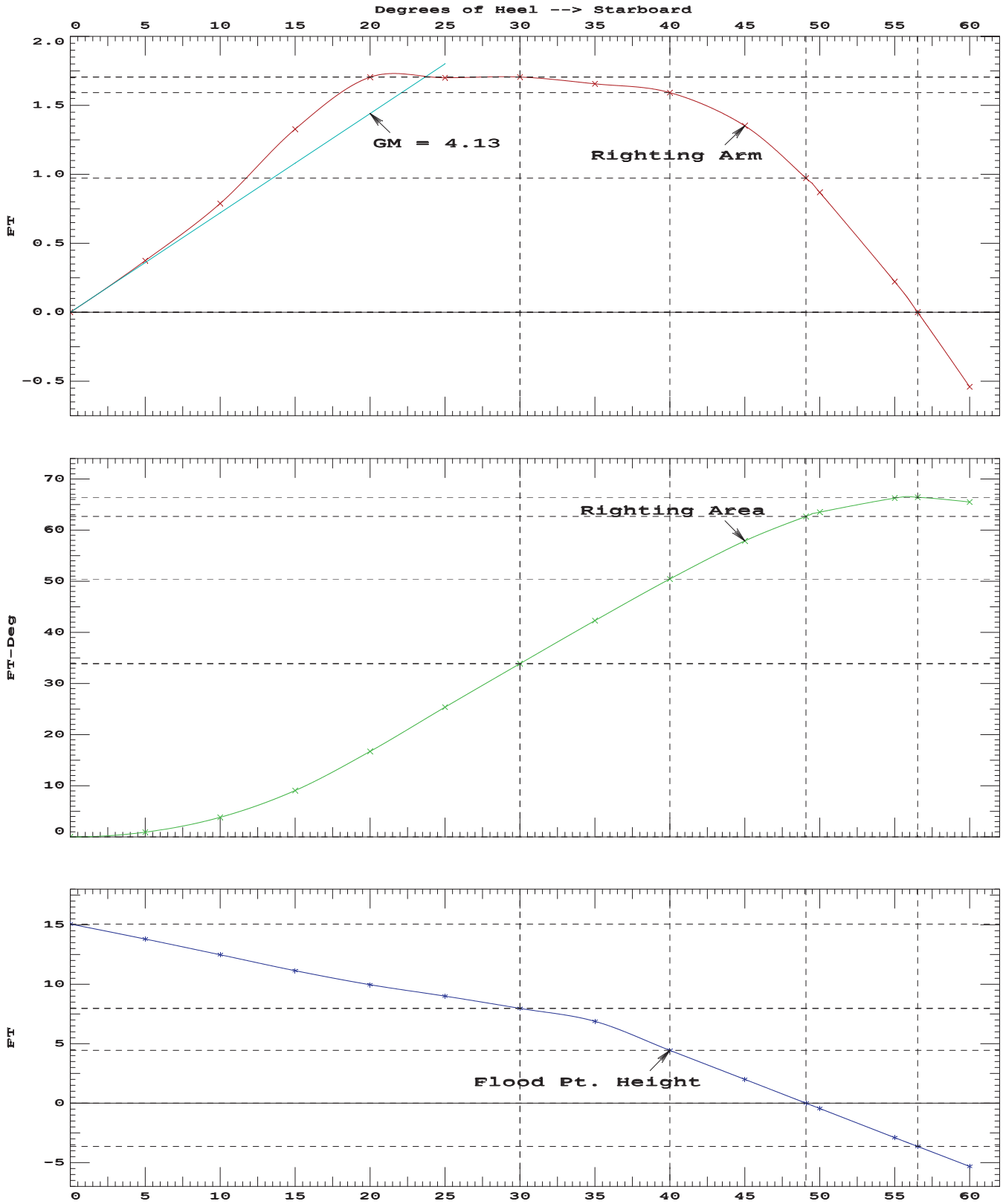

170x56x12 Trimaran
MAX VCG @ 1025 LT
0. DEG TRIM
USCG 170.173 PARAGRAPH B

RIGHTING ARMS vs HEEL ANGLE
LCG = 94.80a TCG = 0.00 VCG = 24.67

Origin Depth	Degrees of Trim	Heel	Displacement Weight(LT)	Righting Arms in Trim	in Heel	Area	Flood Pt Height
10.885	0.00	0.00	1,025.0	0.00	0.000	0.00	14.86(2)
10.855	0.02f	5.00s	1,025.0	0.00	0.357	0.89	13.61(3)
10.755	0.06f	10.00s	1,025.0	0.00	0.752	3.65	12.29(3)
10.628	0.16f	15.00s	1,024.9	0.00	1.283	8.68	10.96(3)
10.432	0.37f	20.00s	1,025.2	0.00	1.736	16.26	9.76(3)
9.996	0.65f	25.00s	1,025.0	0.00	1.733	25.12	8.80(3)
9.238	0.80f	30.00s	1,025.0	0.00	1.737	33.80	7.77(3)
8.233	0.89f	35.00s	1,024.9	0.00	1.696	42.40	6.63(1)
7.003	0.94f	40.00s	1,025.0	0.00	1.635	50.73	4.18(1)
5.713	0.98f	45.00s	1,025.0	0.00	1.375	58.34	1.71(1)
4.830	1.01f	48.44s	1,025.0	0.00	1.055	62.55	0.00(1)
4.431	1.03f	50.00s	1,025.0	0.00	0.881	64.06	-0.77(1)
3.149	1.09f	55.00s	1,025.0	0.00	0.227	66.91	-3.24(1)
2.752	1.11f	56.55s	1,025.1	0.00	0.000	67.08	-4.01(1)
1.863	1.15f	60.00s	1,025.0	0.00	-0.538	66.17	-5.69(1)

Distances in FEET.------Specific Gravity = 1.025.----------Area in Ft-Deg.

Critical Points		LCP	TCP	VCP
(1) Vent Louver	FLOOD	145.00a	28.00	35.00
(2) A-Frame Wire Chase	FLOOD	138.00a	7.50	25.75
(3) CTD Wire Chase	FLOOD	122.00a	14.00	25.75

LIM 170.173 Paragraph b CRITERION		Min/Max		Attained	
(1) GM Upright	>	0.49	Ft	3.93	P
(2) Righting Arm at 30 deg or MaxRA	>	0.66	Ft	1.74	P
(3) Absolute Angle at MaxRA	>	25.00	deg	30.00	P
(4) Area from abs 0.000 deg to 30	>	10.30	Ft-deg	33.80	P
(5) Area from abs 0.000 deg to 40 or Flood	>	16.90	Ft-deg	50.73	P
(6) Area from 30 deg to 40 or Flood	>	5.60	Ft-deg	16.94	P

Relative angles measured from 0.000

1025 24.67

170x56x12 Trimaran
MAX VCG @ 1025 LT
0. DEG TRIM
USCG 170.173 PARAGRAPH B

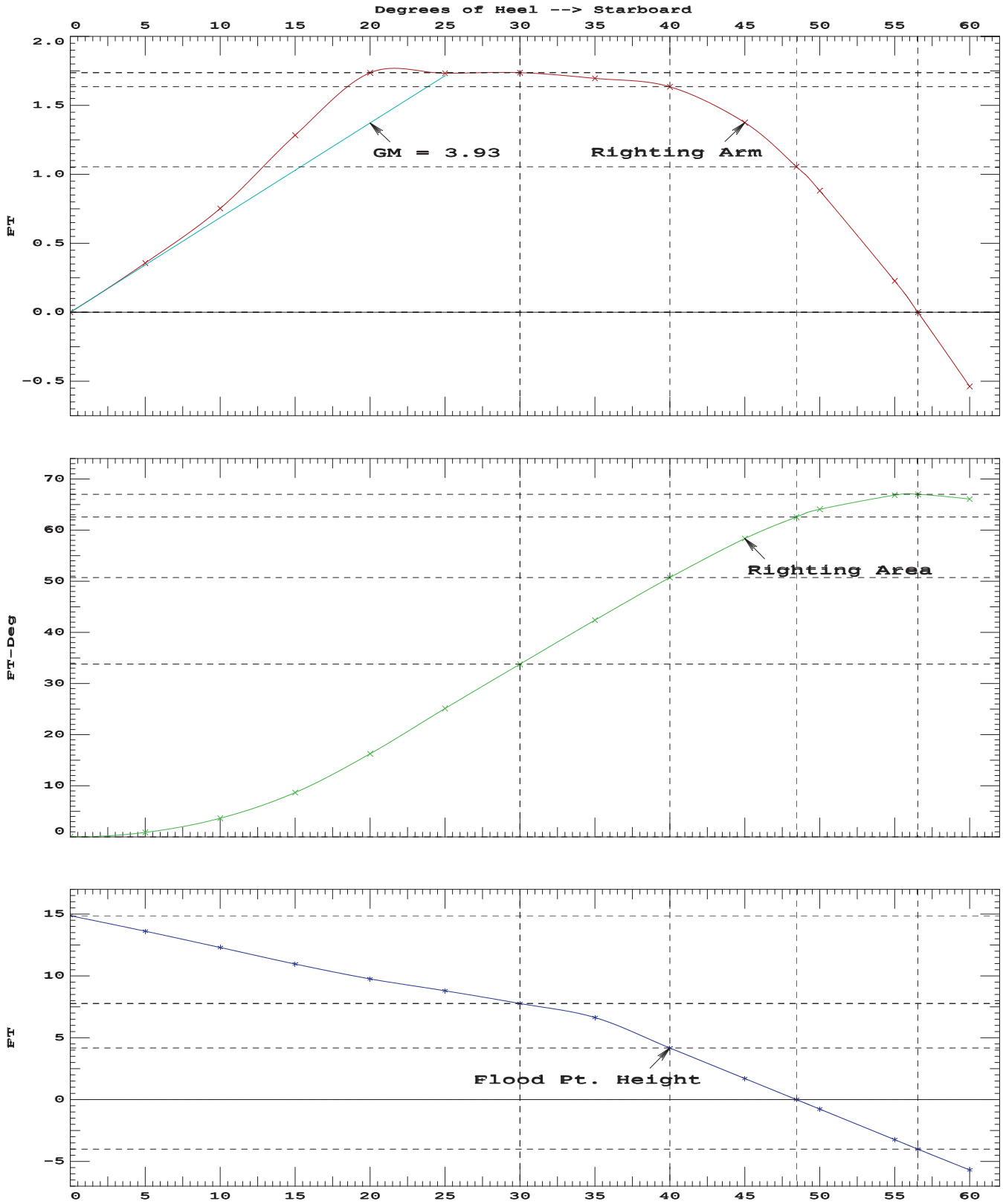

170x56x12 Trimaran
MAX VCG @ 1050 LT
0. DEG TRIM
USCG 170.173 PARAGRAPH B

RIGHTING ARMS vs HEEL ANGLE
LCG = 94.96a TCG = 0.00 VCG = 24.46

Origin Depth	Degrees of Trim	Heel	Displacement Weight(LT)	Righting Arms in Trim	in Heel	Area	Flood Pt Height
11.076	0.00	0.00	1,050.0	0.00	0.000	0.00	14.67(2)
11.044	0.02f	5.00s	1,050.0	0.00	0.347	0.87	13.42(3)
10.937	0.05f	10.00s	1,050.0	0.00	0.732	3.55	12.10(3)
10.808	0.16f	15.00s	1,049.9	0.00	1.262	8.47	10.77(3)
10.588	0.35f	20.00s	1,050.3	0.00	1.793	16.11	9.57(3)
10.360	0.51f	22.80s	1,050.0	0.00	1.805	21.19	9.04(3)
10.113	0.61f	25.00s	1,049.9	0.00	1.798	25.16	8.60(3)
9.314	0.74f	30.00s	1,050.0	0.00	1.805	34.24	7.56(3)
8.290	0.82f	35.00s	1,050.0	0.00	1.776	43.21	6.39(1)
7.036	0.84f	40.00s	1,050.0	0.00	1.720	51.96	3.91(1)
5.733	0.87f	45.00s	1,050.0	0.00	1.448	59.97	1.41(1)
5.005	0.89f	47.81s	1,050.0	0.00	1.189	63.69	0.00(1)
4.439	0.91f	50.00s	1,050.0	0.00	0.947	66.03	-1.10(1)
3.146	0.95f	55.00s	1,050.0	0.00	0.290	69.19	-3.60(1)
2.637	0.97f	56.97s	1,050.1	0.00	0.000	69.48	-4.57(1)
1.850	1.00f	60.00s	1,050.0	0.00	-0.473	68.77	-6.07(1)

Distances in FEET.------Specific Gravity = 1.025.----------Area in Ft-Deg.

Critical Points		LCP	TCP	VCP
(1) Vent Louver	FLOOD	145.00a	28.00	35.00
(2) A-Frame Wire Chase	FLOOD	138.00a	7.50	25.75
(3) CTD Wire Chase	FLOOD	122.00a	14.00	25.75

LIM 170.173 Paragraph b CRITERION		Min/Max		Attained	
(1) GM Upright	>	0.49	Ft	3.83	P
(2) Righting Arm at 30 deg or MaxRA	>	0.66	Ft	1.81	P
(3) Absolute Angle at MaxRA	>	25.00	deg	30.00	P
(4) Area from abs 0.000 deg to 30	>	10.30	Ft-deg	34.24	P
(5) Area from abs 0.000 deg to 40 or Flood	>	16.90	Ft-deg	51.96	P
(6) Area from 30 deg to 40 or Flood	>	5.60	Ft-deg	17.72	P

Relative angles measured from 0.000

1050 24.46

170x56x12 Trimaran
MAX VCG @ 1050 LT
0. DEG TRIM
USCG 170.173 PARAGRAPH B

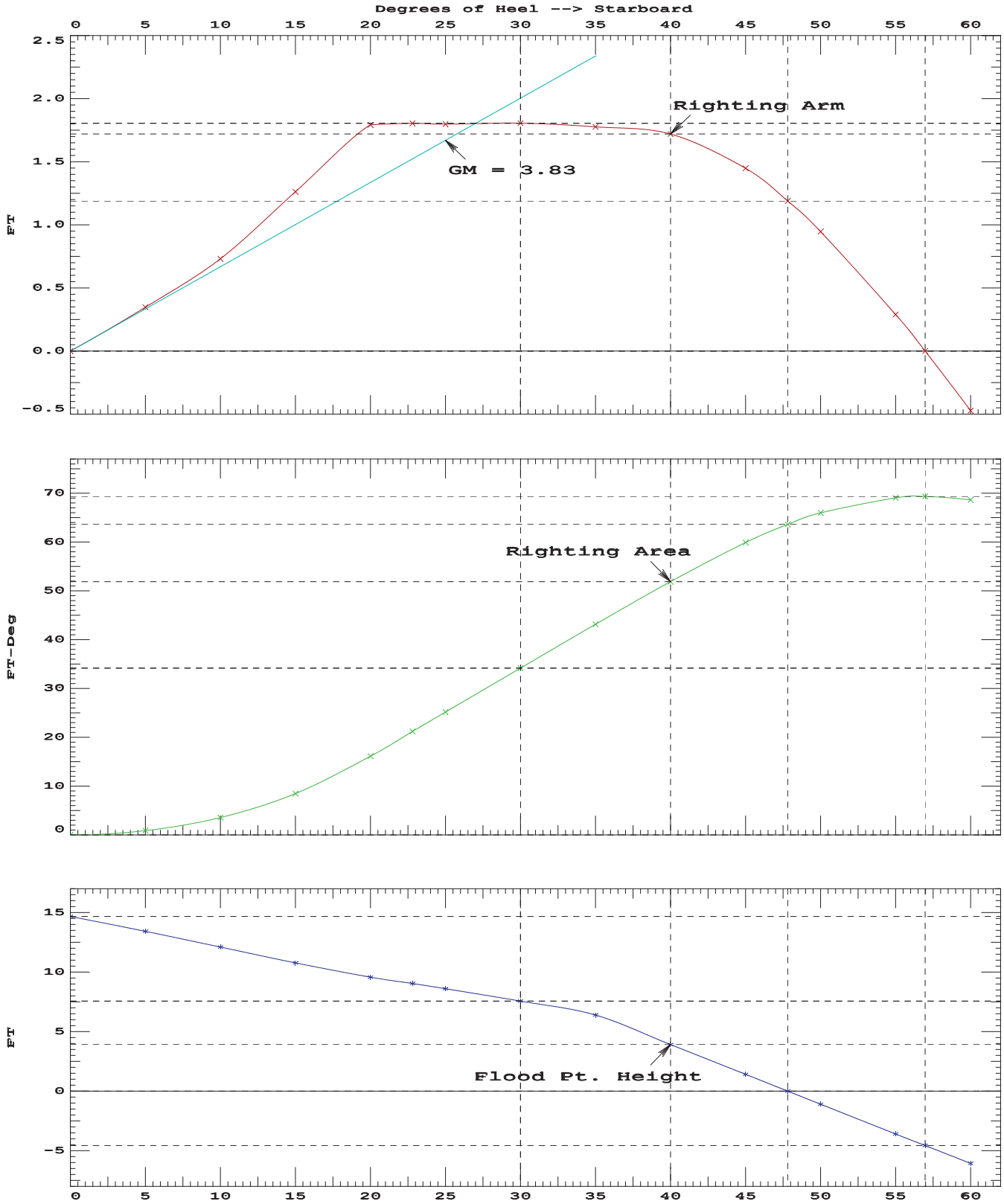

170x56x12 Trimaran
MAX VCG @ 1075 LT
0. DEG TRIM
USCG 170.173 PARAGRAPH B

RIGHTING ARMS vs HEEL ANGLE
LCG = 95.12a TCG = 0.00 VCG = 24.28

Origin Depth	Degrees of Trim	Heel	Displacement Weight(LT)	Righting Arms in Trim	in Heel	Area	Flood Pt Height
11.266	0.00	0.00	1,075.0	0.00	0.000	0.00	14.48(2)
11.232	0.01f	5.00s	1,075.0	0.00	0.336	0.84	13.23(3)
11.118	0.05f	10.00s	1,075.0	0.00	0.709	3.44	11.91(3)
10.986	0.15f	15.00s	1,074.9	0.00	1.239	8.24	10.59(3)
10.742	0.33f	20.00s	1,075.3	0.00	1.839	15.91	9.38(3)
10.457	0.50f	23.13s	1,075.0	0.00	1.860	21.77	8.78(3)
10.224	0.57f	25.00s	1,074.9	0.00	1.853	25.24	8.41(3)
9.389	0.68f	30.00s	1,075.0	0.00	1.860	34.61	7.37(3)
9.243	0.70f	30.77s	1,075.0	0.00	1.861	36.04	7.20(3)
8.344	0.75f	35.00s	1,075.0	0.00	1.838	43.87	6.15(1)
7.065	0.75f	40.00s	1,075.0	0.00	1.783	52.94	3.64(1)
5.751	0.76f	45.00s	1,075.0	0.00	1.498	61.24	1.11(1)
5.178	0.76f	47.19s	1,075.0	0.00	1.298	64.31	-0.00(1)
4.444	0.78f	50.00s	1,075.0	0.00	0.990	67.54	-1.42(1)
3.140	0.81f	55.00s	1,075.0	0.00	0.330	70.91	-3.95(1)
2.557	0.83f	57.24s	1,075.1	0.00	0.000	71.29	-5.07(1)
1.835	0.85f	60.00s	1,075.0	0.00	-0.432	70.70	-6.44(1)

Distances in FEET.------Specific Gravity = 1.025.----------Area in Ft-Deg.

Critical Points		LCP	TCP	VCP
(1) Vent Louver	FLOOD	145.00a	28.00	35.00
(2) A-Frame Wire Chase	FLOOD	138.00a	7.50	25.75
(3) CTD Wire Chase	FLOOD	122.00a	14.00	25.75

LIM 170.173 Paragraph b CRITERION	Min/Max		Attained	
(1) GM Upright	>	0.49	Ft	3.69 P
(2) Righting Arm at 30 deg or MaxRA	>	0.66	Ft	1.86 P
(3) Absolute Angle at MaxRA	>	25.00	deg	30.77 P
(4) Area from abs 0.000 deg to 30	>	10.30	Ft-deg	34.61 P
(5) Area from abs 0.000 deg to 40 or Flood	>	16.90	Ft-deg	52.94 P
(6) Area from 30 deg to 40 or Flood	>	5.60	Ft-deg	18.33 P

Relative angles measured from 0.000

1075 24.28

170x56x12 Trimaran
MAX VCG @ 1075 LT
0. DEG TRIM
USCG 170.173 PARAGRAPH B

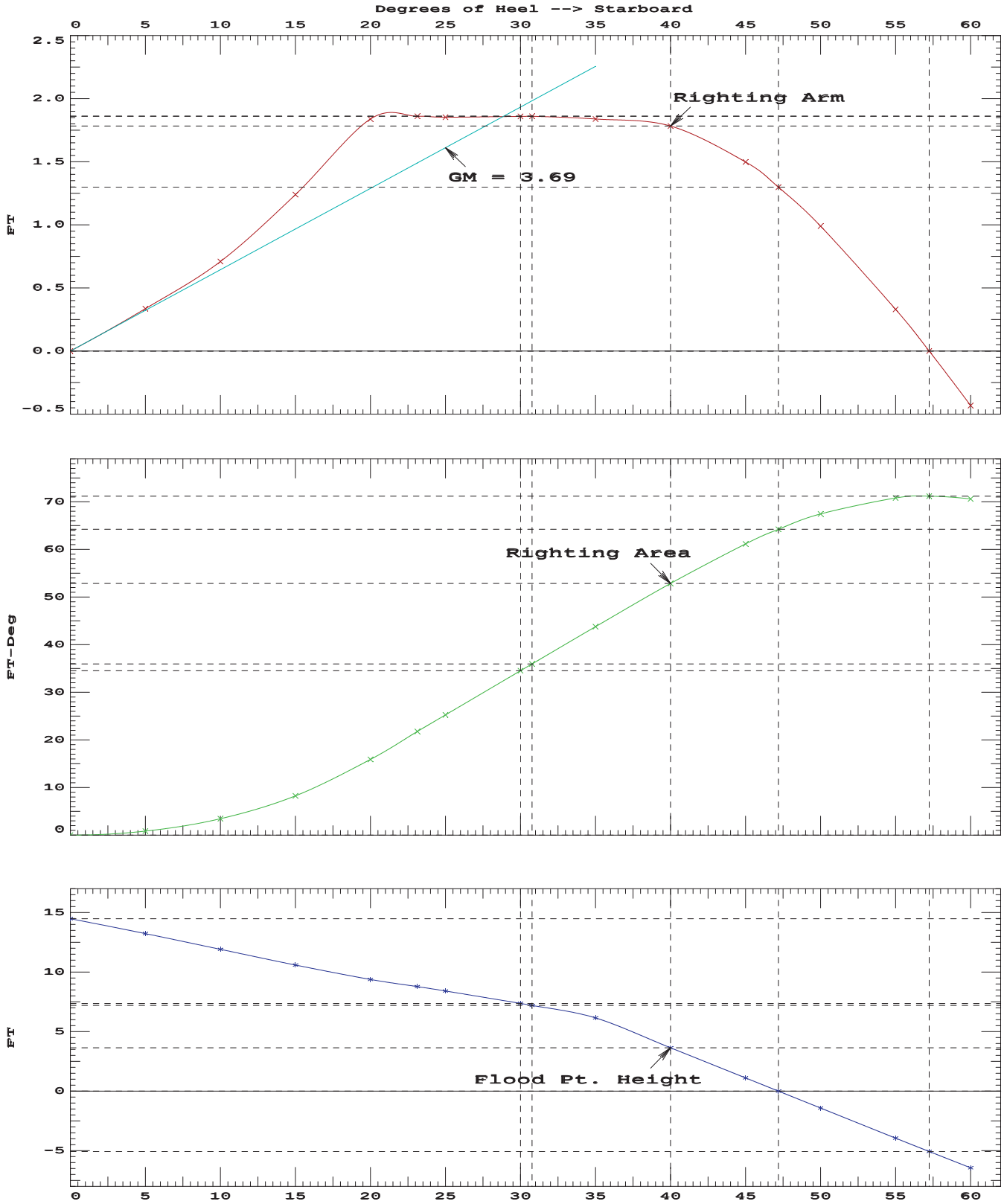

170x56x12 Trimaran
MAX VCG @ 1100 LT
0. DEG TRIM
USCG 170.173 PARAGRAPH B

RIGHTING ARMS vs HEEL ANGLE
LCG = 95.28a TCG = 0.00 VCG = 24.10

Origin Depth	Degrees of Trim	Heel	Displacement Weight(LT)	Righting Arms in Trim	in Heel	Area	Flood Pt Height
11.456	0.00	0.00	1,100.1	0.00	0.000	0.00	14.29(2)
11.418	0.01f	5.00s	1,100.0	0.00	0.327	0.82	13.04(3)
11.299	0.04f	10.00s	1,100.0	0.00	0.691	3.35	11.72(3)
11.162	0.15f	15.00s	1,099.9	0.00	1.221	8.06	10.41(3)
10.891	0.32f	20.00s	1,100.0	0.00	1.885	15.77	9.20(3)
10.543	0.48f	23.44s	1,100.0	0.00	1.917	22.42	8.53(3)
10.330	0.53f	25.00s	1,100.0	0.00	1.910	25.39	8.21(3)
9.464	0.63f	30.00s	1,100.0	0.00	1.916	35.05	7.17(3)
9.258	0.64f	31.07s	1,100.0	0.00	1.917	37.09	6.94(3)
8.393	0.67f	35.00s	1,100.0	0.00	1.900	44.61	5.91(1)
7.092	0.65f	40.00s	1,100.0	0.00	1.845	53.98	3.37(1)
5.764	0.64f	45.00s	1,100.0	0.00	1.548	62.57	0.81(1)
5.347	0.64f	46.58s	1,100.0	0.00	1.405	64.90	0.00(1)
4.447	0.65f	50.00s	1,100.0	0.00	1.033	69.10	-1.75(1)
3.131	0.67f	55.00s	1,100.0	0.00	0.372	72.68	-4.30(1)
2.471	0.68f	57.51s	1,100.1	0.00	0.000	73.15	-5.57(1)
1.817	0.69f	60.00s	1,100.0	0.00	-0.390	72.67	-6.82(1)

Distances in FEET.------Specific Gravity = 1.025.----------Area in Ft-Deg.

Critical Points		LCP	TCP	VCP
(1) Vent Louver	FLOOD	145.00a	28.00	35.00
(2) A-Frame Wire Chase	FLOOD	138.00a	7.50	25.75
(3) CTD Wire Chase	FLOOD	122.00a	14.00	25.75

LIM 170.173 Paragraph b CRITERION	Min/Max		Attained	
(1) GM Upright	>	0.49	Ft	3.61 P
(2) Righting Arm at 30 deg or MaxRA	>	0.66	Ft	1.92 P
(3) Absolute Angle at MaxRA	>	25.00	deg	31.07 P
(4) Area from abs 0.000 deg to 30	>	10.30	Ft-deg	35.05 P
(5) Area from abs 0.000 deg to 40 or Flood	>	16.90	Ft-deg	53.98 P
(6) Area from 30 deg to 40 or Flood	>	5.60	Ft-deg	18.93 P

Relative angles measured from 0.000

1100 24.1

170x56x12 Trimaran
MAX VCG @ 1100 LT
0. DEG TRIM
USCG 170.173 PARAGRAPH B

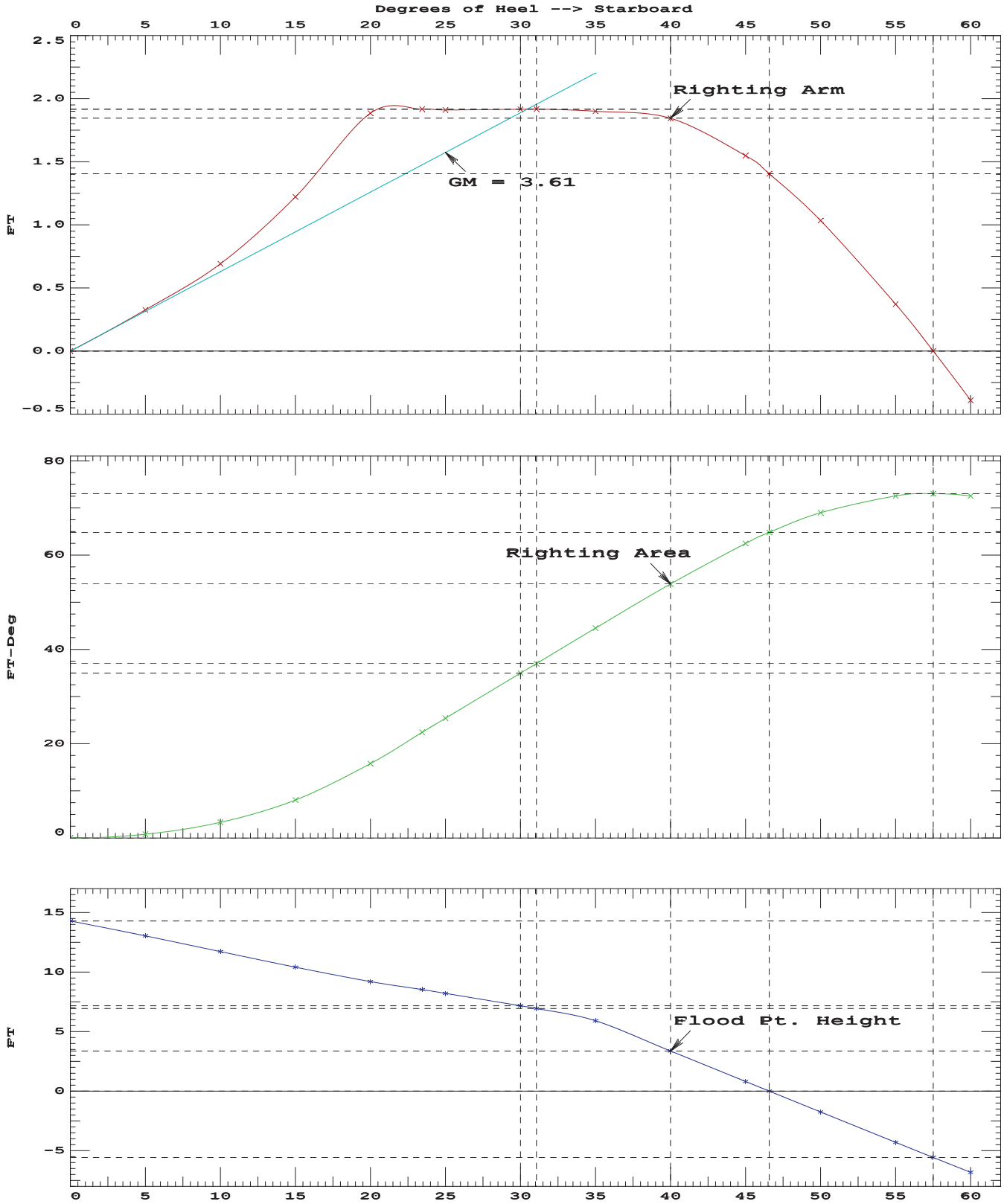

170x56x12 Trimaran
MAX VCG @ 1125 LT
0. DEG TRIM
USCG 170.173 PARAGRAPH B

RIGHTING ARMS vs HEEL ANGLE
LCG = 95.44a TCG = 0.00 VCG = 23.90

Origin Depth	Degrees of Trim	Heel	Displacement Weight(LT)	Righting Arms in Trim	in Heel	Flood Pt Area	Height
11.644	0.00	0.00	1,125.0	0.00	0.000	0.00	14.11(2)
11.602	0.01f	5.00s	1,125.0	0.00	0.320	0.80	12.85(3)
11.480	0.04f	10.00s	1,125.0	0.00	0.681	3.28	11.54(3)
11.335	0.15f	15.00s	1,124.8	0.00	1.214	7.95	10.23(3)
11.036	0.30f	20.00s	1,125.0	0.00	1.935	15.74	9.02(3)
10.618	0.45f	23.75s	1,125.0	0.00	1.983	23.22	8.27(3)
10.431	0.49f	25.00s	1,125.0	0.00	1.979	25.70	8.02(3)
9.540	0.57f	30.00s	1,125.0	0.00	1.982	35.71	6.98(3)
9.311	0.58f	31.14s	1,125.0	0.00	1.983	37.98	6.73(3)
8.438	0.59f	35.00s	1,125.0	0.00	1.972	45.61	5.67(1)
7.115	0.55f	40.00s	1,125.0	0.00	1.917	55.34	3.10(1)
5.774	0.53f	45.00s	1,125.0	0.00	1.611	64.27	0.51(1)
5.515	0.53f	45.98s	1,125.0	0.00	1.524	65.80	0.00(1)
4.446	0.52f	50.00s	1,125.0	0.00	1.093	71.11	-2.08(1)
3.121	0.52f	55.00s	1,125.0	0.00	0.431	74.98	-4.66(1)
2.350	0.53f	57.90s	1,125.0	0.00	0.000	75.62	-6.14(1)
1.796	0.53f	60.00s	1,125.0	0.00	-0.329	75.27	-7.20(1)

Distances in FEET.------Specific Gravity = 1.025.----------Area in Ft-Deg.

Critical Points		LCP	TCP	VCP
(1) Vent Louver	FLOOD	145.00a	28.00	35.00
(2) A-Frame Wire Chase	FLOOD	138.00a	7.50	25.75
(3) CTD Wire Chase	FLOOD	122.00a	14.00	25.75

LIM 170.173 Paragraph b CRITERION	Min/Max		Attained	
(1) GM Upright	>	0.49	Ft	3.54 P
(2) Righting Arm at 30 deg or MaxRA	>	0.66	Ft	1.98 P
(3) Absolute Angle at MaxRA	>	25.00	deg	31.14 P
(4) Area from abs 0.000 deg to 30	>	10.30	Ft-deg	35.71 P
(5) Area from abs 0.000 deg to 40 or Flood	>	16.90	Ft-deg	55.34 P
(6) Area from 30 deg to 40 or Flood	>	5.60	Ft-deg	19.63 P

Relative angles measured from 0.000

1125 23.9

170x56x12 Trimaran
MAX VCG @ 1125 LT
0. DEG TRIM
USCG 170.173 PARAGRAPH B

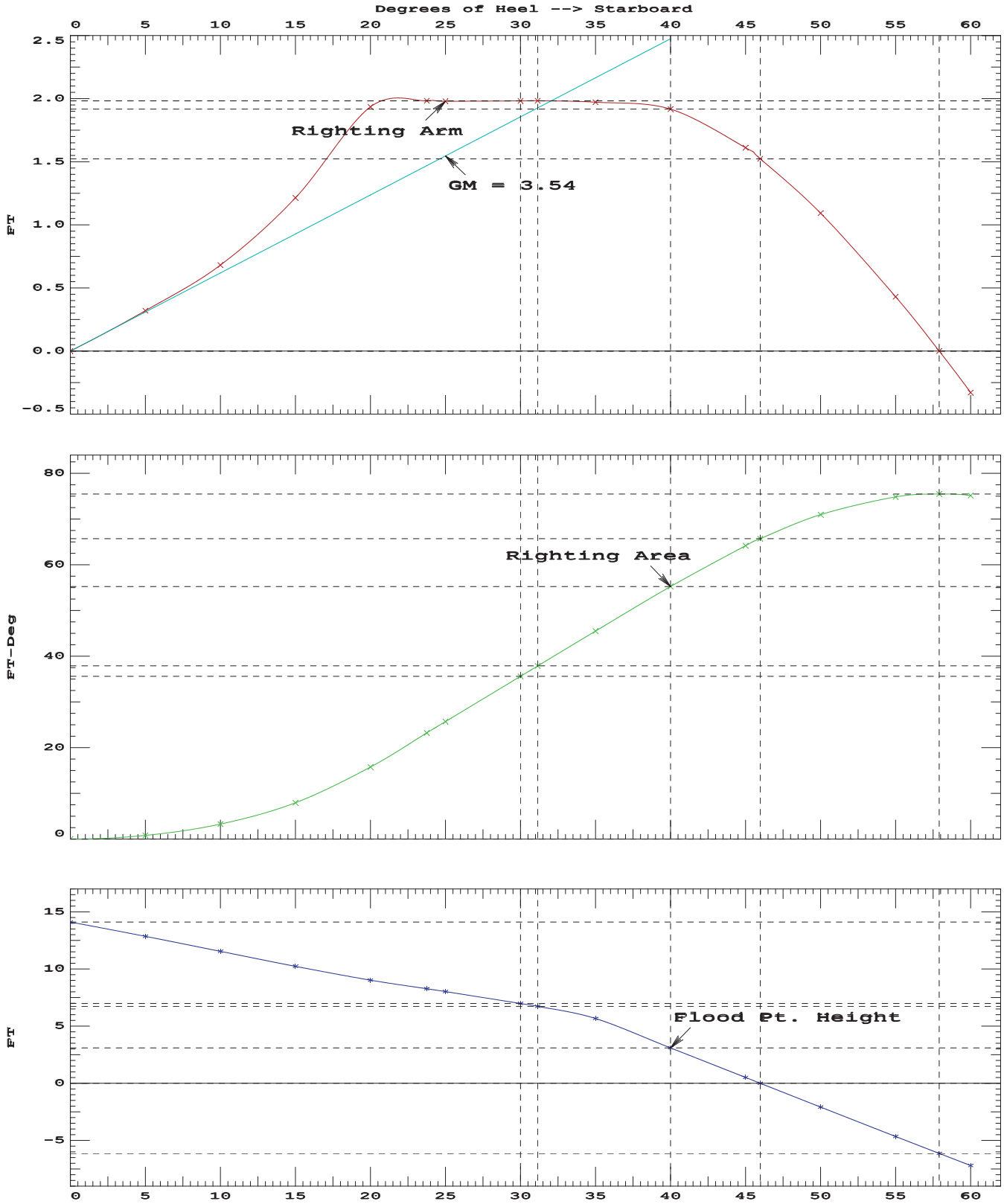

170x56x12 Trimaran
MAX VCG @ 1150 LT
0. DEG TRIM
USCG 170.173 PARAGRAPH B

RIGHTING ARMS vs HEEL ANGLE
LCG = 95.59a TCG = 0.00 VCG = 23.65

Origin Depth	Degrees of Trim	Heel	Displacement Weight(LT)	Righting Arms in Trim	in Heel	Flood Pt Area	Height
11.831	0.00	0.00	1,150.0	0.00	0.000	0.00	13.92(2)
11.786	0.01f	5.00s	1,150.0	0.00	0.319	0.80	12.66(3)
11.662	0.04f	10.00s	1,150.0	0.00	0.682	3.28	11.35(3)
11.506	0.14f	15.00s	1,149.8	0.00	1.225	7.97	10.05(3)
11.181	0.29f	20.00s	1,150.0	0.00	1.998	15.94	8.84(3)
10.728	0.42f	23.75s	1,150.0	0.00	2.074	23.70	8.09(3)
10.529	0.44f	25.00s	1,150.0	0.00	2.072	26.30	7.83(3)
9.613	0.51f	30.00s	1,150.0	0.00	2.073	36.78	6.78(3)
9.180	0.52f	32.04s	1,150.0	0.00	2.075	41.00	6.33(3)
8.479	0.51f	35.00s	1,150.0	0.00	2.072	47.15	5.42(1)
7.136	0.45f	40.00s	1,150.0	0.00	2.019	57.39	2.82(1)
5.784	0.41f	45.00s	1,150.0	0.00	1.709	66.81	0.20(1)
5.680	0.41f	45.39s	1,150.0	0.00	1.675	67.47	-0.00(1)
4.444	0.39f	50.00s	1,150.0	0.00	1.190	74.14	-2.41(1)
3.107	0.38f	55.00s	1,150.0	0.00	0.532	78.51	-5.02(1)
2.153	0.37f	58.58s	1,150.2	0.00	-0.001	79.47	-6.86(1)
1.773	0.37f	60.00s	1,150.2	0.00	-0.224	79.31	-7.58(1)

Distances in FEET.------Specific Gravity = 1.025.----------Area in Ft-Deg.

Critical Points		LCP	TCP	VCP
(1) Vent Louver	FLOOD	145.00a	28.00	35.00
(2) A-Frame Wire Chase	FLOOD	138.00a	7.50	25.75
(3) CTD Wire Chase	FLOOD	122.00a	14.00	25.75

LIM 170.173 Paragraph b CRITERION	Min/Max		Attained	
(1) GM Upright	>	0.49	Ft	3.53 P
(2) Righting Arm at 30 deg or MaxRA	>	0.66	Ft	2.08 P
(3) Absolute Angle at MaxRA	>	25.00	deg	32.04 P
(4) Area from abs 0.000 deg to 30	>	10.30	Ft-deg	36.78 P
(5) Area from abs 0.000 deg to 40 or Flood	>	16.90	Ft-deg	57.39 P
(6) Area from 30 deg to 40 or Flood	>	5.60	Ft-deg	20.61 P

Relative angles measured from 0.000

1150 23.65

170x56x12 Trimaran
MAX VCG @ 1150 LT
0. DEG TRIM
USCG 170.173 PARAGRAPH B

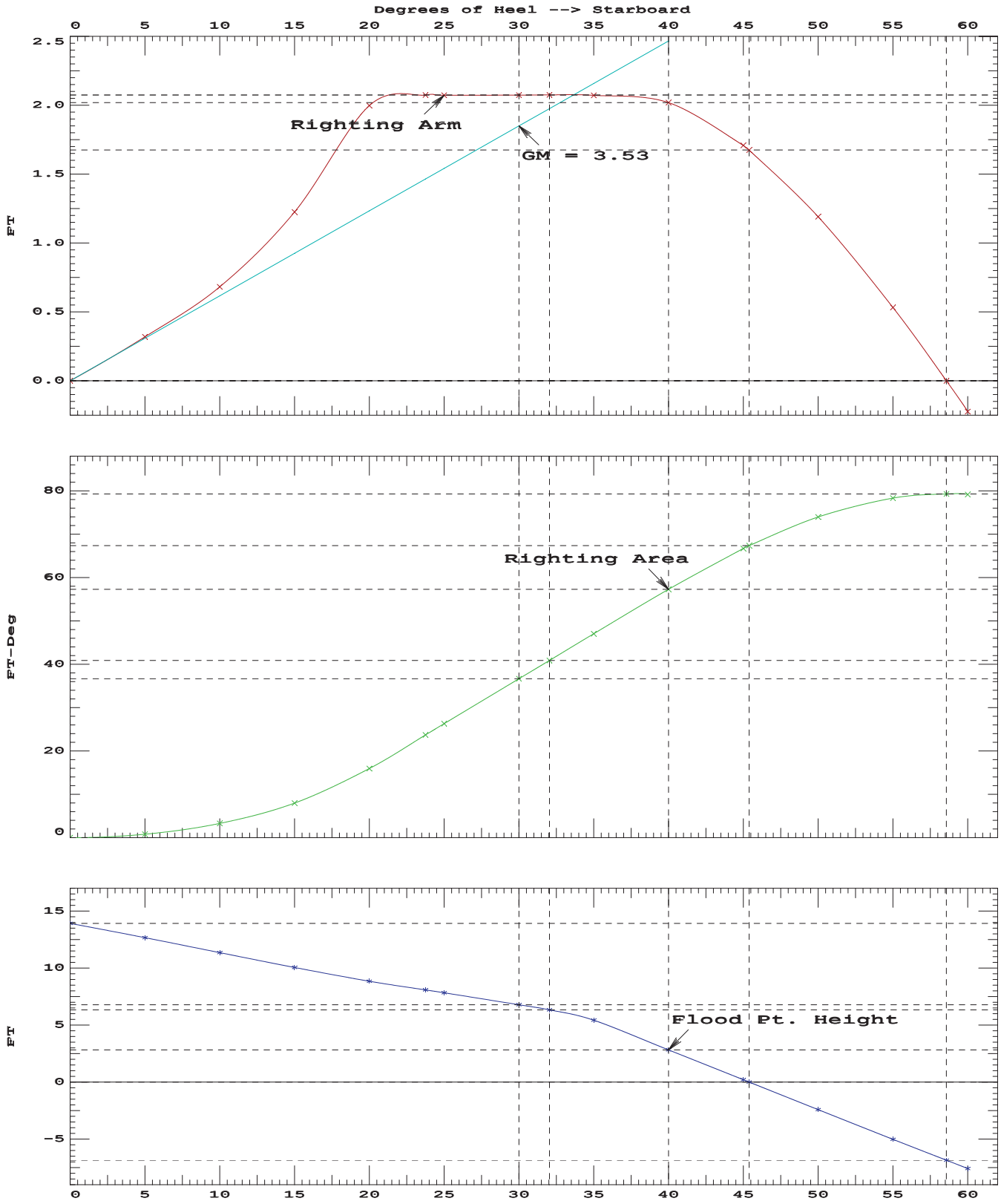

170x56x12 Trimaran
MAX VCG @ 1175 LT
0. DEG TRIM
USCG 170.173 PARAGRAPH B

RIGHTING ARMS vs HEEL ANGLE
LCG = 95.74a TCG = 0.00 VCG = 23.42

Origin Depth	Degrees of Trim	Heel	Displacement Weight(LT)	Righting Arms in Trim	in Heel	Flood Pt Area	Height
12.018	0.00	0.00	1,175.0	0.00	0.000	0.00	13.73(2)
11.973	0.01f	5.00s	1,175.2	0.00	0.317	0.79	12.47(3)
11.844	0.04f	10.00s	1,175.0	0.00	0.683	3.27	11.17(3)
11.676	0.14f	15.00s	1,174.8	0.00	1.236	7.99	9.87(3)
11.323	0.27f	20.00s	1,175.0	0.00	2.049	16.10	8.67(3)
10.834	0.38f	23.75s	1,175.0	0.00	2.160	24.12	7.90(3)
10.628	0.40f	25.00s	1,175.0	0.00	2.158	26.82	7.65(3)
9.683	0.46f	30.00s	1,175.0	0.00	2.154	37.73	6.59(3)
8.517	0.43f	35.00s	1,175.0	0.00	2.159	48.51	5.18(1)
8.133	0.41f	36.45s	1,175.0	0.00	2.161	51.63	4.42(1)
7.156	0.35f	40.00s	1,175.0	0.00	2.106	59.23	2.55(1)
5.844	0.30f	44.81s	1,175.0	0.00	1.807	68.71	0.00(1)
5.791	0.29f	45.00s	1,175.0	0.00	1.791	69.05	-0.10(1)
4.441	0.26f	50.00s	1,175.0	0.00	1.273	76.80	-2.75(1)
3.093	0.23f	55.00s	1,175.0	0.00	0.617	81.58	-5.37(1)
1.979	0.21f	59.15s	1,175.0	0.00	0.000	82.88	-7.52(1)
1.749	0.21f	60.00s	1,175.0	0.00	-0.133	82.83	-7.96(1)

Distances in FEET.------Specific Gravity = 1.025.----------Area in Ft-Deg.

Critical Points		LCP	TCP	VCP
(1) Vent Louver	FLOOD	145.00a	28.00	35.00
(2) A-Frame Wire Chase	FLOOD	138.00a	7.50	25.75
(3) CTD Wire Chase	FLOOD	122.00a	14.00	25.75

LIM 170.173 Paragraph b CRITERION	Min/Max		Attained	
(1) GM Upright	>	0.49	Ft	3.51 P
(2) Righting Arm at 30 deg or MaxRA	>	0.66	Ft	2.16 P
(3) Absolute Angle at MaxRA	>	25.00	deg	36.45 P
(4) Area from abs 0.000 deg to 30	>	10.30	Ft-deg	37.73 P
(5) Area from abs 0.000 deg to 40 or Flood	>	16.90	Ft-deg	59.23 P
(6) Area from 30 deg to 40 or Flood	>	5.60	Ft-deg	21.50 P

Relative angles measured from 0.000

1175 23.42

170x56x12 Trimaran
MAX VCG @ 1175 LT
0. DEG TRIM
USCG 170.173 PARAGRAPH B

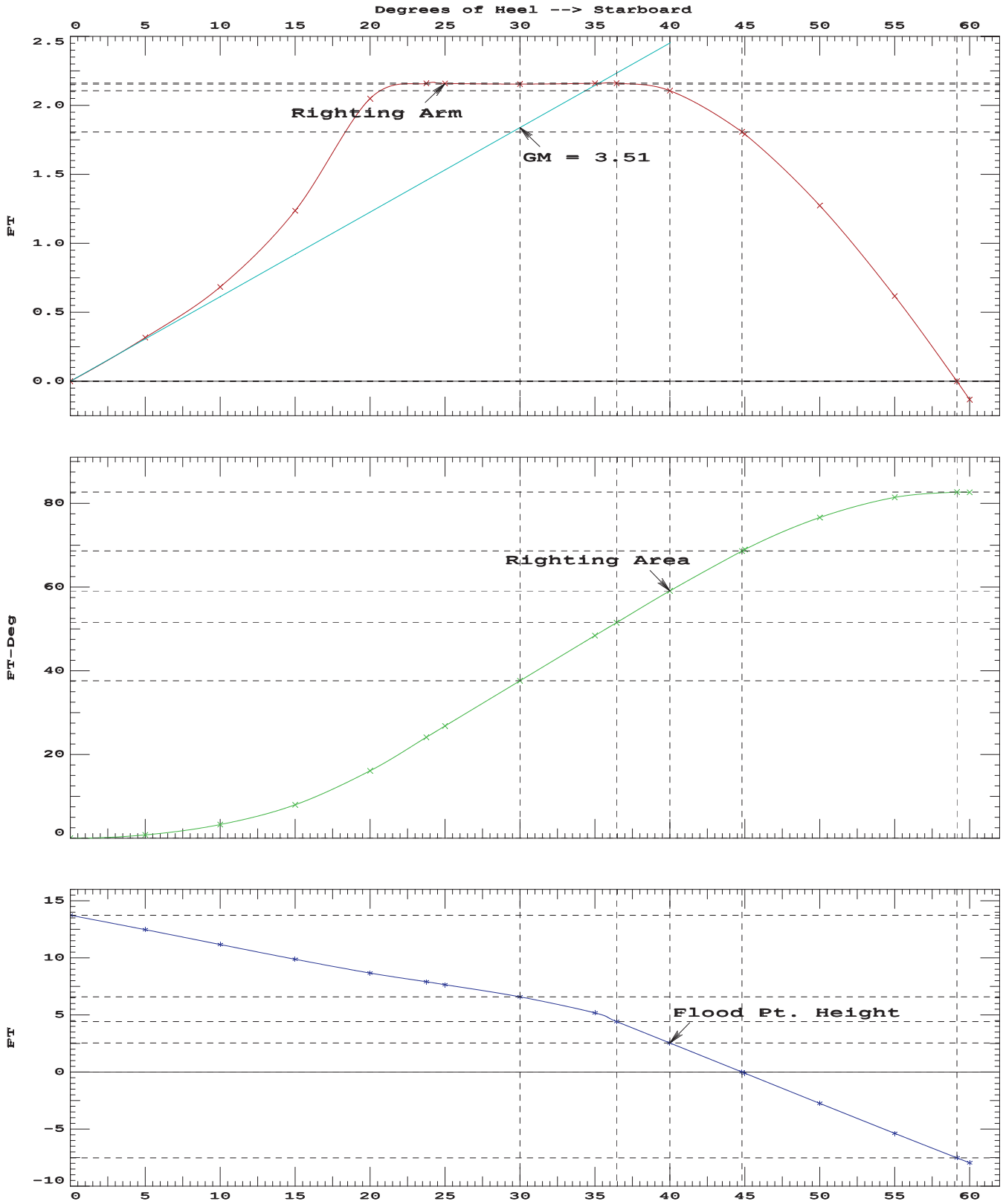

170x56x12 Trimaran
MAX VCG @ 1200 LT
0. DEG TRIM
USCG 170.173 PARAGRAPH B

RIGHTING ARMS vs HEEL ANGLE
LCG = 95.88a TCG = 0.00 VCG = 23.21

Origin Depth	Degrees of Trim	Heel	Displacement Weight(LT)	Righting Arms in Trim	in Heel	Area	Flood Pt Height
12.205	0.00	0.00	1,200.0	0.00	0.000	0.00	13.54(2)
12.157	0.01f	5.00s	1,200.2	0.00	0.314	0.79	12.29(3)
12.027	0.04f	10.00s	1,200.0	0.00	0.684	3.26	10.98(3)
11.845	0.14f	15.00s	1,199.8	0.00	1.248	8.01	9.69(3)
11.459	0.26f	20.00s	1,199.6	0.00	2.092	16.24	8.50(3)
10.942	0.34f	23.75s	1,200.0	0.00	2.239	24.49	7.72(3)
10.729	0.36f	25.00s	1,200.0	0.00	2.237	27.29	7.47(3)
9.752	0.40f	30.00s	1,200.2	0.00	2.224	38.58	6.39(3)
8.553	0.34f	35.00s	1,200.0	0.00	2.234	49.72	4.93(1)
8.151	0.32f	36.48s	1,200.0	0.00	2.239	53.03	4.14(1)
7.174	0.25f	40.00s	1,200.0	0.00	2.179	60.82	2.27(1)
6.006	0.18f	44.24s	1,200.0	0.00	1.922	69.56	-0.00(1)
5.798	0.17f	45.00s	1,200.0	0.00	1.859	71.00	-0.41(1)
4.437	0.12f	50.00s	1,200.0	0.00	1.340	79.00	-3.08(1)
3.079	0.08f	55.00s	1,200.0	0.00	0.687	84.12	-5.73(1)
1.829	0.05f	59.62s	1,200.0	0.00	0.000	85.74	-8.15(1)
1.725	0.05f	60.00s	1,200.0	0.00	-0.058	85.73	-8.34(1)

Distances in FEET.------Specific Gravity = 1.025.----------Area in Ft-Deg.

Critical Points		LCP	TCP	VCP
(1) Vent Louver	FLOOD	145.00a	28.00	35.00
(2) A-Frame Wire Chase	FLOOD	138.00a	7.50	25.75
(3) CTD Wire Chase	FLOOD	122.00a	14.00	25.75

LIM 170.173 Paragraph b CRITERION		Min/Max		Attained	
(1) GM Upright	>	0.49	Ft	3.48	P
(2) Righting Arm at 30 deg or MaxRA	>	0.66	Ft	2.24	P
(3) Absolute Angle at MaxRA	>	25.00	deg	36.48	P
(4) Area from abs 0.000 deg to 30	>	10.30	Ft-deg	38.58	P
(5) Area from abs 0.000 deg to 40 or Flood	>	16.90	Ft-deg	60.82	P
(6) Area from 30 deg to 40 or Flood	>	5.60	Ft-deg	22.23	P

Relative angles measured from 0.000

1200 23.21

170x56x12 Trimaran
MAX VCG @ 1200 LT
0. DEG TRIM
USCG 170.173 PARAGRAPH B

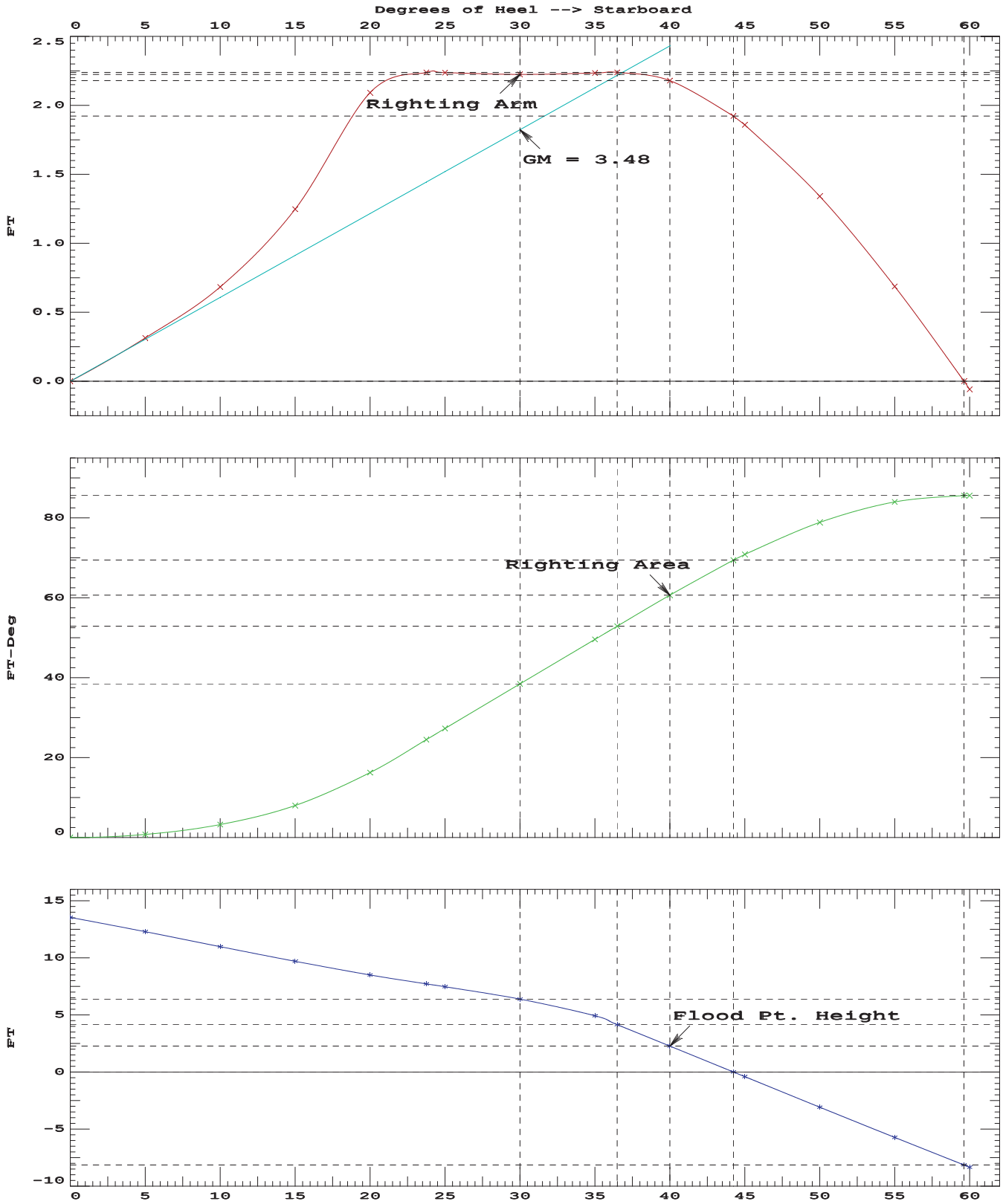

170x56x12 Trimaran
MAX VCG @ 900 LT
0.5 DEG TRIM
USCG 170.173 PARAGRAPH B

RIGHTING ARMS vs HEEL ANGLE
LCG = 95.59a TCG = 0.00 VCG = 24.63

Origin Depth	Degrees of Trim	Heel	Displacement Weight(LT)	Righting Arms in Trim	in Heel	Flood Pt Area	Height
9.039	0.50a	0.00	900.00	0.00	0.000	0.00	15.51(2)
9.019	0.48a	5.00s	900.00	0.00	0.541	1.35	14.39(3)
8.950	0.43a	10.00s	899.97	0.00	1.123	5.49	13.07(3)
8.859	0.31a	15.00s	899.79	0.00	1.810	12.78	11.72(3)
8.809	0.13a	18.53s	900.11	0.00	2.031	19.63	10.88(3)
8.774	0.03a	20.00s	900.07	0.00	1.992	22.58	10.58(3)
8.552	0.34f	25.00s	899.74	0.00	2.012	32.70	9.60(3)
8.039	0.62f	30.00s	900.25	0.00	2.033	42.82	8.58(3)
7.194	0.80f	35.00s	899.97	0.00	1.980	52.88	7.44(1)
6.089	0.92f	40.00s	899.79	0.00	1.925	62.64	5.06(1)
4.845	1.02f	45.00s	899.99	0.00	1.811	72.01	2.69(1)
3.610	1.14f	50.00s	900.00	0.00	1.436	80.23	0.32(1)
3.444	1.16f	50.68s	900.00	0.00	1.368	81.19	0.00(1)
2.377	1.26f	55.00s	900.01	0.00	0.866	86.06	-2.04(1)
1.113	1.37f	60.00s	900.02	0.00	0.145	88.66	-4.39(1)

Distances in FEET.------Specific Gravity = 1.025.----------Area in Ft-Deg.

Critical Points		LCP	TCP	VCP
(1) Vent Louver	FLOOD	145.00a	28.00	35.00
(2) A-Frame Wire Chase	FLOOD	138.00a	7.50	25.75
(3) CTD Wire Chase	FLOOD	122.00a	14.00	25.75

LIM 170.173 Paragraph b CRITERION	Min/Max		Attained	
(1) GM Upright	>	0.49	Ft	6.02 P
(2) Righting Arm at 30 deg or MaxRA	>	0.66	Ft	2.03 P
(3) Absolute Angle at MaxRA	>	25.00	deg	30.00 P
(4) Area from abs 0.000 deg to 30	>	10.30	Ft-deg	42.82 P
(5) Area from abs 0.000 deg to 40 or Flood	>	16.90	Ft-deg	62.64 P
(6) Area from 30 deg to 40 or Flood	>	5.60	Ft-deg	19.83 P

Relative angles measured from 0.000

900 24.63

170x56x12 Trimaran
MAX VCG @ 900 LT
0.5 DEG TRIM
USCG 170.173 PARAGRAPH B

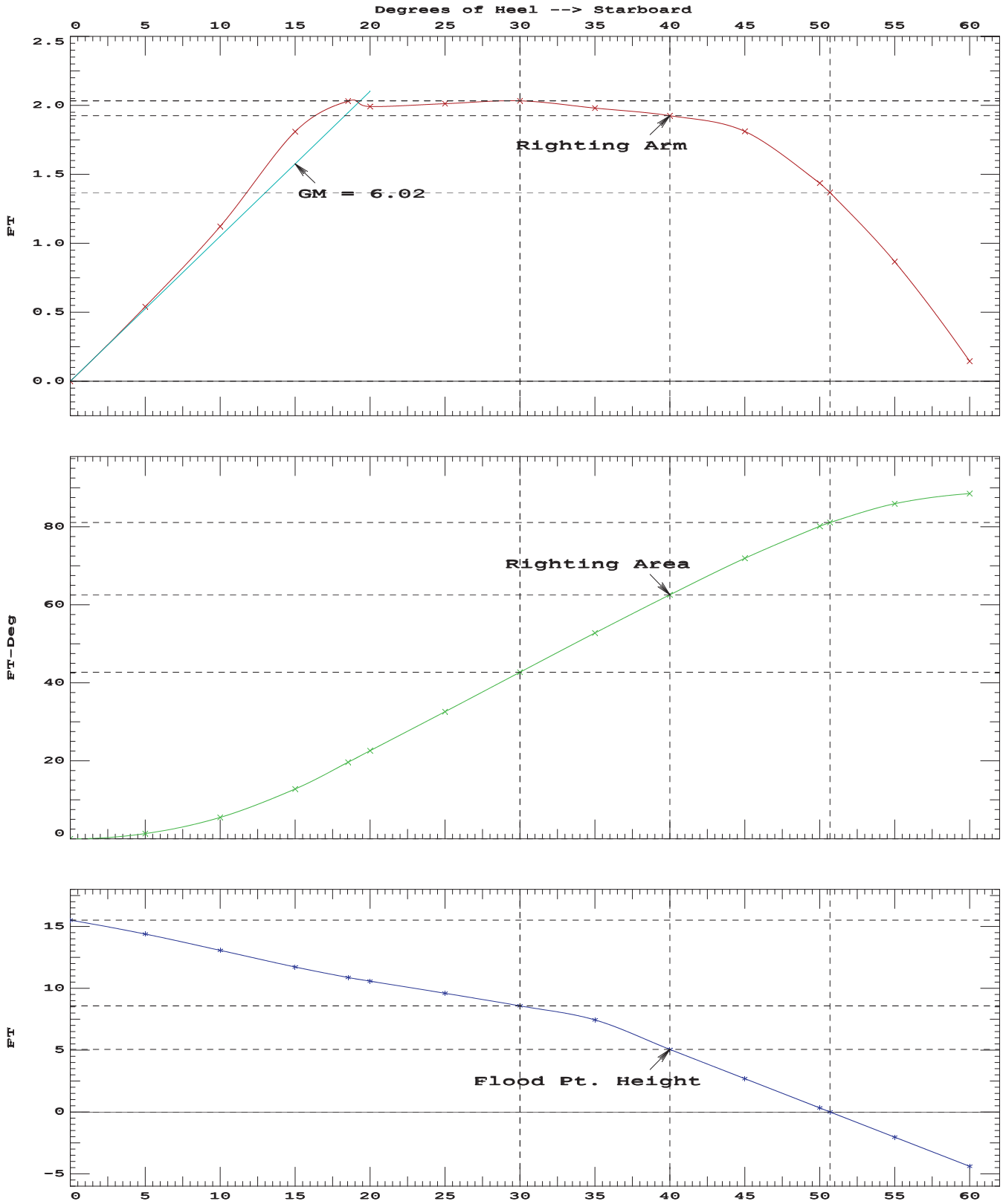

170x56x12 Trimaran
MAX VCG @ 925 LT
0.5 DEG TRIM
USCG 170.173 PARAGRAPH B

RIGHTING ARMS vs HEEL ANGLE
LCG = 95.74a TCG = 0.00 VCG = 24.63

Origin Depth	Degrees of Trim	Heel	Displacement Weight(LT)	Righting Arms in Trim	in Heel	Area	Flood Pt Height
9.233	0.50a	0.00	925.00	0.00	0.000	0.00	15.31(2)
9.212	0.48a	5.00s	925.00	0.00	0.502	1.26	14.20(3)
9.138	0.43a	10.00s	924.98	0.00	1.044	5.11	12.88(3)
9.047	0.32a	15.00s	924.82	0.00	1.704	11.93	11.53(3)
8.982	0.13a	18.75s	925.08	0.00	1.980	18.89	10.63(3)
8.946	0.04a	20.00s	925.05	0.00	1.950	21.35	10.37(3)
8.690	0.31f	25.00s	924.74	0.00	1.967	31.26	9.39(3)
8.132	0.56f	30.00s	925.02	0.00	1.980	41.14	8.37(3)
7.257	0.73f	35.00s	924.98	0.00	1.929	50.94	7.19(1)
6.130	0.83f	40.00s	924.83	0.00	1.873	60.44	4.79(1)
4.881	0.92f	45.00s	925.00	0.00	1.733	69.49	2.40(1)
3.633	1.02f	50.00s	925.00	0.00	1.332	77.26	0.01(1)
3.633	1.03f	50.01s	925.01	0.00	1.331	77.28	0.00(1)
2.389	1.13f	55.00s	925.01	0.00	0.744	82.53	-2.39(1)
1.116	1.23f	60.00s	925.02	0.00	0.013	84.48	-4.76(1)

Distances in FEET.------Specific Gravity = 1.025.----------Area in Ft-Deg.

Critical Points		LCP	TCP	VCP
(1) Vent Louver	FLOOD	145.00a	28.00	35.00
(2) A-Frame Wire Chase	FLOOD	138.00a	7.50	25.75
(3) CTD Wire Chase	FLOOD	122.00a	14.00	25.75

LIM 170.173 Paragraph b CRITERION		Min/Max		Attained	
(1) GM Upright	>	0.49	Ft	5.59	P
(2) Righting Arm at 30 deg or MaxRA	>	0.66	Ft	1.98	P
(3) Absolute Angle at MaxRA	>	25.00	deg	30.00	P
(4) Area from abs 0.000 deg to 30	>	10.30	Ft-deg	41.14	P
(5) Area from abs 0.000 deg to 40 or Flood	>	16.90	Ft-deg	60.44	P
(6) Area from 30 deg to 40 or Flood	>	5.60	Ft-deg	19.31	P

Relative angles measured from 0.000

925 24.63

170x56x12 Trimaran
MAX VCG @ 925 LT
0.5 DEG TRIM
USCG 170.173 PARAGRAPH B

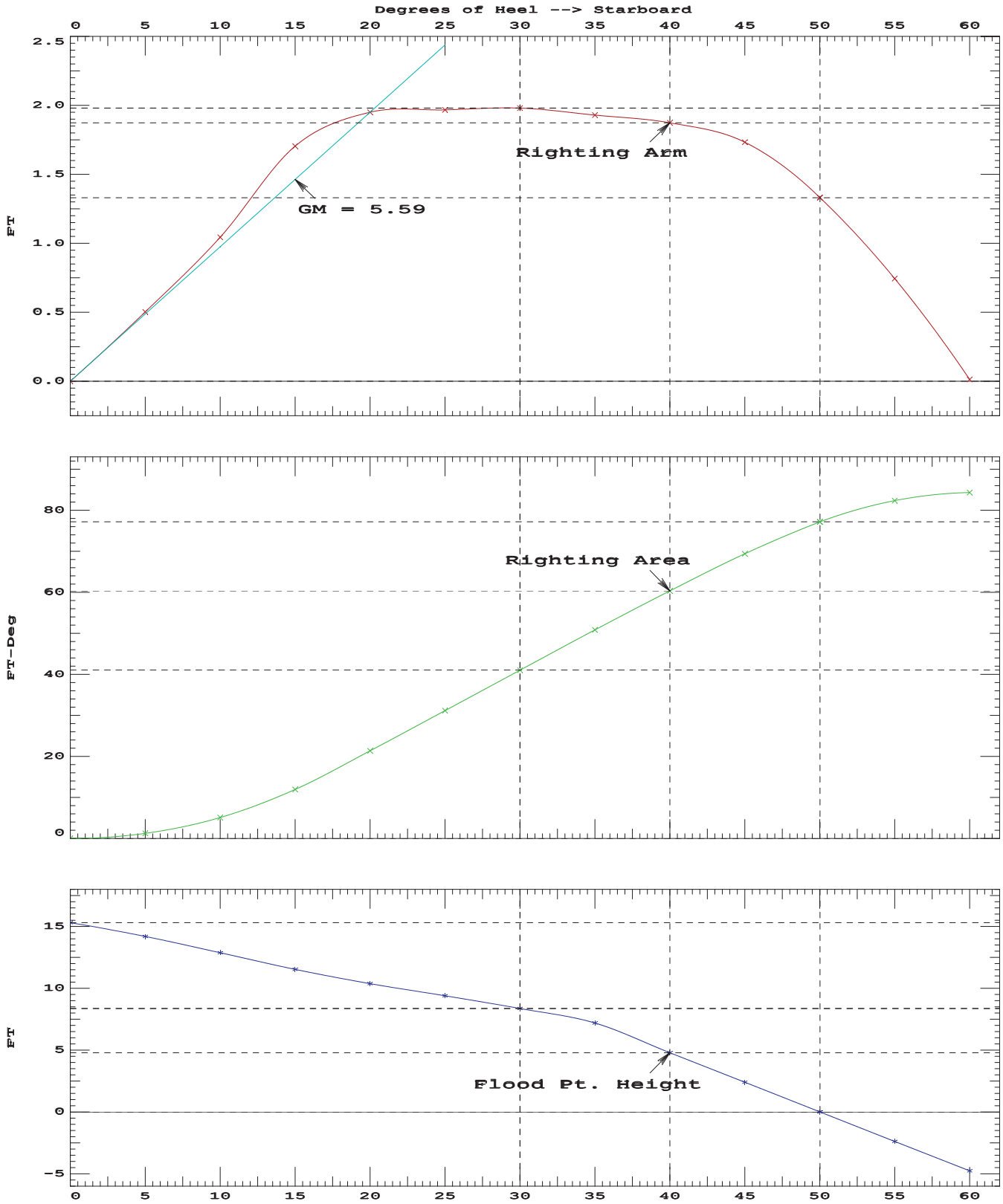

170x56x12 Trimaran
MAX VCG @ 950 LT
0.5 DEG TRIM
USCG 170.173 PARAGRAPH B

RIGHTING ARMS vs HEEL ANGLE
LCG = 95.88a TCG = 0.00 VCG = 24.59

Origin Depth	Trim	Heel	Displacement Weight(LT)	Righting Arms in Trim	in Heel	Area	Flood Pt Height
9.425	0.50a	0.00	950.00	0.00	0.000	0.00	15.12(2)
9.403	0.48a	5.00s	950.00	0.00	0.469	1.17	14.00(3)
9.323	0.43a	10.00s	949.98	0.00	0.977	4.77	12.68(3)
9.233	0.32a	15.00s	949.83	0.00	1.615	11.20	11.34(3)
9.157	0.14a	18.75s	949.99	0.00	1.948	17.92	10.42(3)
9.115	0.06a	20.00s	950.04	0.00	1.928	20.35	10.17(3)
8.825	0.28f	25.00s	949.77	0.00	1.942	30.15	9.19(3)
8.225	0.51f	30.00s	950.01	0.00	1.949	39.88	8.15(3)
7.320	0.65f	35.00s	949.98	0.00	1.903	49.53	6.94(1)
6.175	0.75f	40.00s	949.97	0.00	1.848	58.91	4.52(1)
4.912	0.82f	45.00s	950.00	0.00	1.683	67.79	2.11(1)
3.815	0.89f	49.35s	950.00	0.00	1.326	74.41	0.00(1)
3.653	0.91f	50.00s	950.01	0.00	1.260	75.25	-0.31(1)
2.395	1.00f	55.00s	950.00	0.00	0.657	80.12	-2.73(1)
1.248	1.07f	59.49s	950.00	0.00	0.000	81.64	-4.89(1)
1.114	1.08f	60.00s	950.00	0.00	-0.082	81.62	-5.13(1)

Distances in FEET.------Specific Gravity = 1.025.----------Area in Ft-Deg.

Critical Points		LCP	TCP	VCP
(1) Vent Louver	FLOOD	145.00a	28.00	35.00
(2) A-Frame Wire Chase	FLOOD	138.00a	7.50	25.75
(3) CTD Wire Chase	FLOOD	122.00a	14.00	25.75

LIM 170.173 Paragraph b CRITERION		Min/Max		Attained	
(1) GM Upright	>	0.49	Ft	5.22	P
(2) Righting Arm at 30 deg or MaxRA	>	0.66	Ft	1.95	P
(3) Absolute Angle at MaxRA	>	25.00	deg	30.00	P
(4) Area from abs 0.000 deg to 30	>	10.30	Ft-deg	39.88	P
(5) Area from abs 0.000 deg to 40 or Flood	>	16.90	Ft-deg	58.91	P
(6) Area from 30 deg to 40 or Flood	>	5.60	Ft-deg	19.03	P

Relative angles measured from 0.000

950 24.59

170x56x12 Trimaran
MAX VCG @ 950 LT
0.5 DEG TRIM
USCG 170.173 PARAGRAPH B

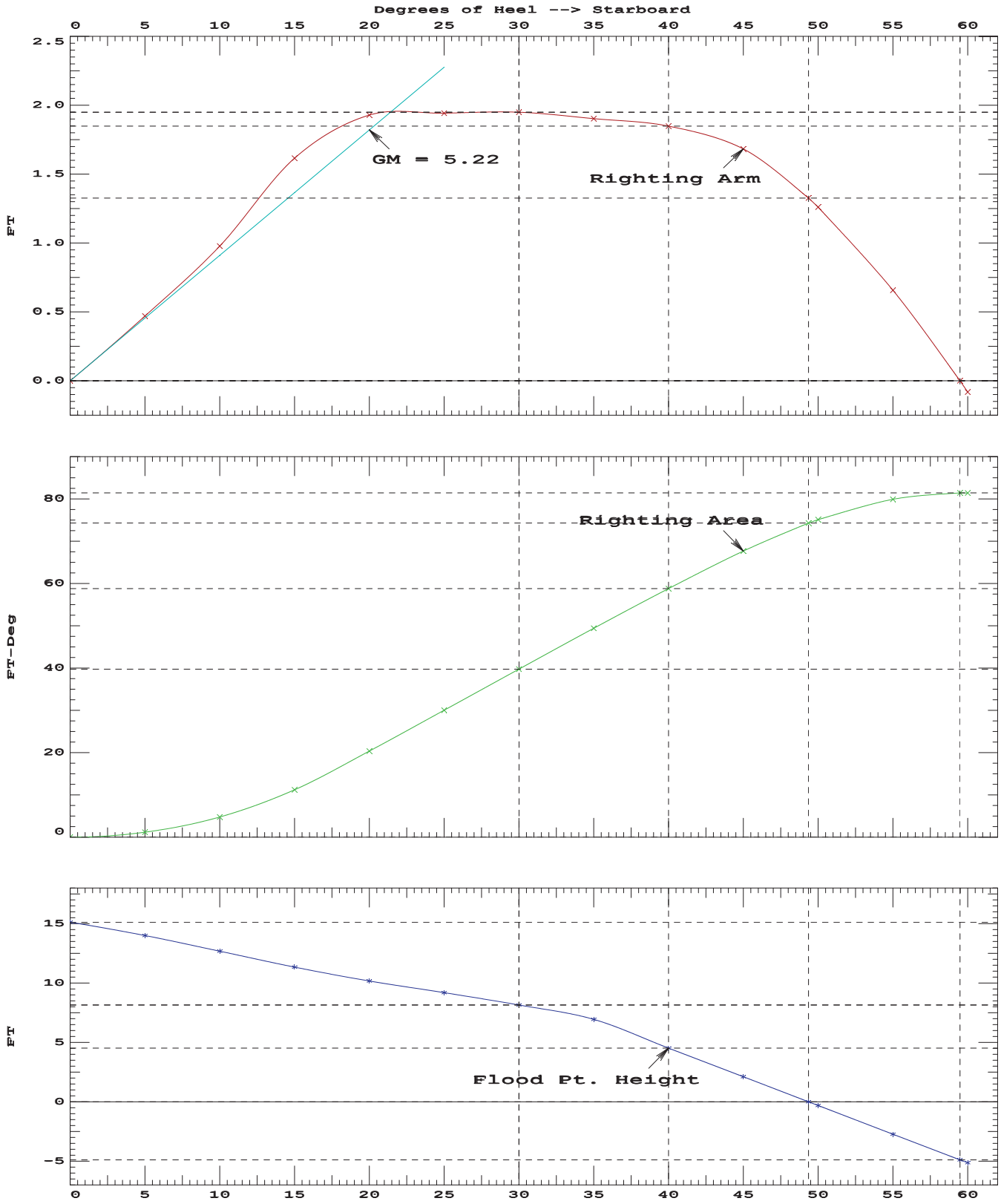

170x56x12 Trimaran
MAX VCG @ 975 LT
0.5 DEG TRIM
USCG 170.173 PARAGRAPH B

RIGHTING ARMS vs HEEL ANGLE
LCG = 96.02a TCG = 0.00 VCG = 24.58

Origin Depth	Trim	Heel	Displacement Weight(LT)	Righting Arms in Trim	in Heel	Area	Flood Pt Height
9.619	0.50a	0.00	975.32	0.00	0.000	0.00	14.93(2)
9.591	0.48a	5.00s	975.00	0.00	0.436	1.09	13.81(3)
9.505	0.44a	10.00s	974.98	0.00	0.910	4.44	12.49(3)
9.416	0.32a	15.00s	974.83	0.00	1.524	10.47	11.16(3)
9.282	0.07a	20.00s	975.03	0.00	1.902	19.13	9.97(3)
9.066	0.18f	23.75s	975.00	0.00	1.906	26.34	9.24(3)
8.957	0.25f	25.00s	974.96	0.00	1.906	28.73	8.99(3)
8.313	0.45f	30.00s	974.90	0.00	1.906	38.31	7.95(3)
7.383	0.58f	35.00s	974.98	0.00	1.861	47.75	6.69(1)
6.216	0.66f	40.00s	974.99	0.00	1.804	56.92	4.26(1)
4.939	0.71f	45.00s	975.00	0.00	1.611	65.51	1.82(1)
3.994	0.76f	48.71s	975.00	0.00	1.301	70.95	-0.00(1)
3.668	0.78f	50.00s	975.03	0.00	1.166	72.55	-0.63(1)
2.397	0.86f	55.00s	975.00	0.00	0.547	76.91	-3.08(1)
1.438	0.91f	58.74s	975.00	0.00	0.000	77.96	-4.90(1)
1.107	0.93f	60.00s	975.00	0.00	-0.199	77.83	-5.51(1)

Distances in FEET.------Specific Gravity = 1.025.----------Area in Ft-Deg.

Critical Points		LCP	TCP	VCP
(1) Vent Louver	FLOOD	145.00a	28.00	35.00
(2) A-Frame Wire Chase	FLOOD	138.00a	7.50	25.75
(3) CTD Wire Chase	FLOOD	122.00a	14.00	25.75

LIM 170.173 Paragraph b CRITERION		Min/Max		Attained	
(1) GM Upright	>	0.49	Ft	4.84	P
(2) Righting Arm at 30 deg or MaxRA	>	0.66	Ft	1.91	P
(3) Absolute Angle at MaxRA	>	25.00	deg	25.00	P
(4) Area from abs 0.000 deg to 30	>	10.30	Ft-deg	38.31	P
(5) Area from abs 0.000 deg to 40 or Flood	>	16.90	Ft-deg	56.92	P
(6) Area from 30 deg to 40 or Flood	>	5.60	Ft-deg	18.60	P

Relative angles measured from 0.000

975 24.58

170x56x12 Trimaran
MAX VCG @ 975 LT
0.5 DEG TRIM
USCG 170.173 PARAGRAPH B

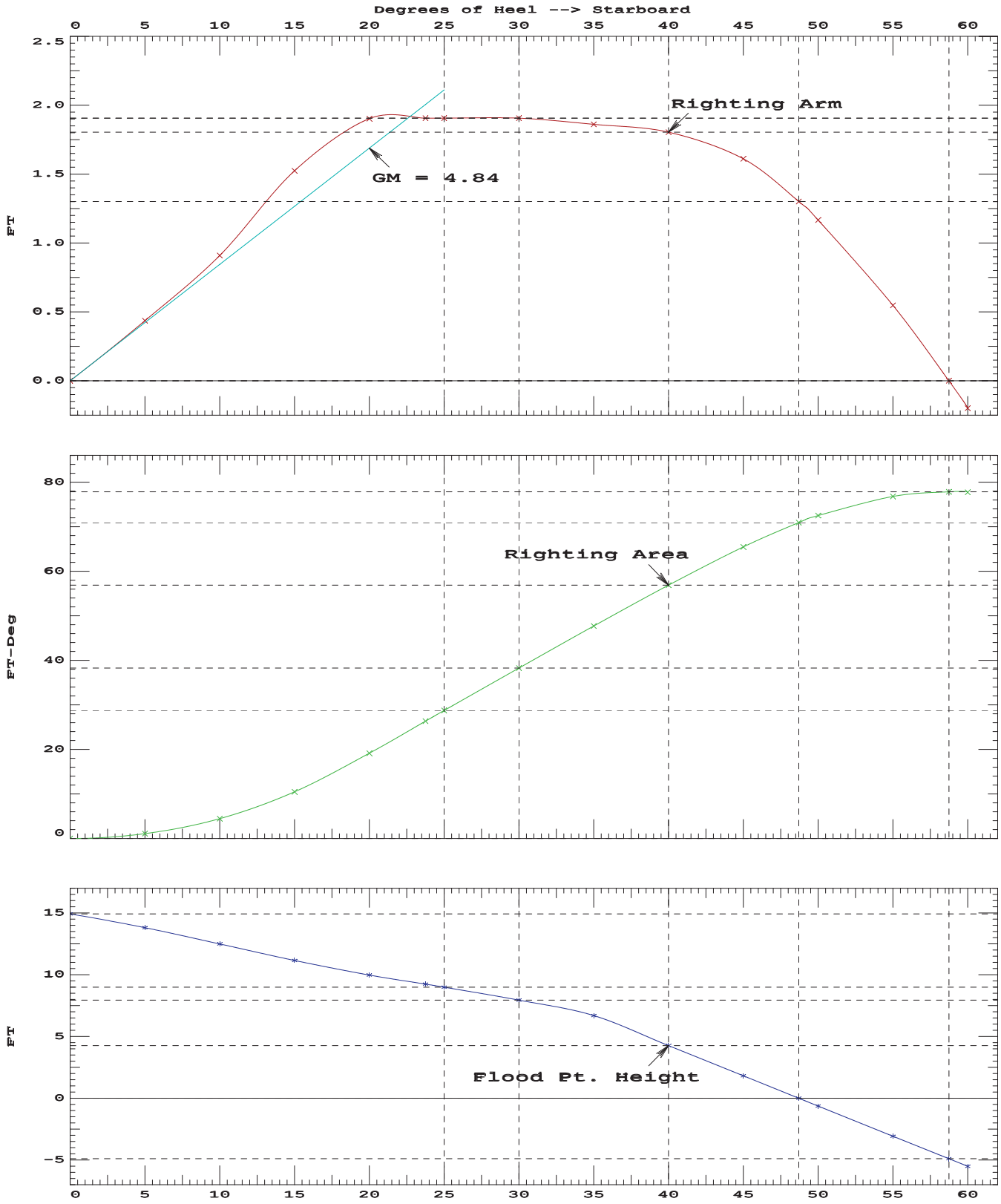

170x56x12 Trimaran
MAX VCG @ 1000 LT
0.5 DEG TRIM
USCG 170.173 PARAGRAPH B

RIGHTING ARMS vs HEEL ANGLE
LCG = 96.16a TCG = 0.00 VCG = 24.42

Origin Depth	Degrees of Trim	Heel	Displacement Weight(LT)	Righting Arms in Trim	in Heel	Area	Flood Pt Height
9.809	0.50a	0.00	1,000.3	0.00	0.000	0.00	14.74(2)
9.779	0.48a	5.00s	1,000.0	0.00	0.418	1.04	13.62(3)
9.687	0.44a	10.00s	1,000.0	0.00	0.872	4.25	12.30(3)
9.599	0.32a	15.00s	999.8	0.00	1.477	10.06	10.97(3)
9.448	0.09a	20.00s	1,000.2	0.00	1.934	18.65	9.77(3)
9.283	0.09f	22.77s	1,000.0	0.00	1.940	24.05	9.24(3)
9.083	0.21f	25.00s	999.8	0.00	1.937	28.38	8.79(3)
8.398	0.39f	30.00s	999.9	0.00	1.940	38.14	7.74(3)
7.447	0.51f	35.00s	1,000.0	0.00	1.907	47.77	6.46(1)
6.253	0.57f	40.00s	1,000.0	0.00	1.855	57.18	3.99(1)
4.962	0.61f	45.00s	1,000.0	0.00	1.645	66.00	1.52(1)
4.173	0.64f	48.07s	1,000.0	0.00	1.388	70.68	0.00(1)
3.679	0.66f	50.00s	1,000.1	0.00	1.188	73.16	-0.96(1)
2.397	0.72f	55.00s	1,000.0	0.00	0.562	77.62	-3.43(1)
1.408	0.77f	58.83s	1,000.0	0.00	0.000	78.72	-5.31(1)
1.097	0.78f	60.00s	1,000.0	0.00	-0.185	78.61	-5.88(1)

Distances in FEET.------Specific Gravity = 1.025.----------Area in Ft-Deg.

Critical Points		LCP	TCP	VCP
(1) Vent Louver	FLOOD	145.00a	28.00	35.00
(2) A-Frame Wire Chase	FLOOD	138.00a	7.50	25.75
(3) CTD Wire Chase	FLOOD	122.00a	14.00	25.75

LIM 170.173 Paragraph b CRITERION		Min/Max		Attained	
(1) GM Upright	>	0.49	Ft	4.62	P
(2) Righting Arm at 30 deg or MaxRA	>	0.66	Ft	1.94	P
(3) Absolute Angle at MaxRA	>	25.00	deg	30.00	P
(4) Area from abs 0.000 deg to 30	>	10.30	Ft-deg	38.14	P
(5) Area from abs 0.000 deg to 40 or Flood	>	16.90	Ft-deg	57.18	P
(6) Area from 30 deg to 40 or Flood	>	5.60	Ft-deg	19.05	P

Relative angles measured from 0.000

1000 24.42

170x56x12 Trimaran
MAX VCG @ 1000 LT
0.5 DEG TRIM
USCG 170.173 PARAGRAPH B

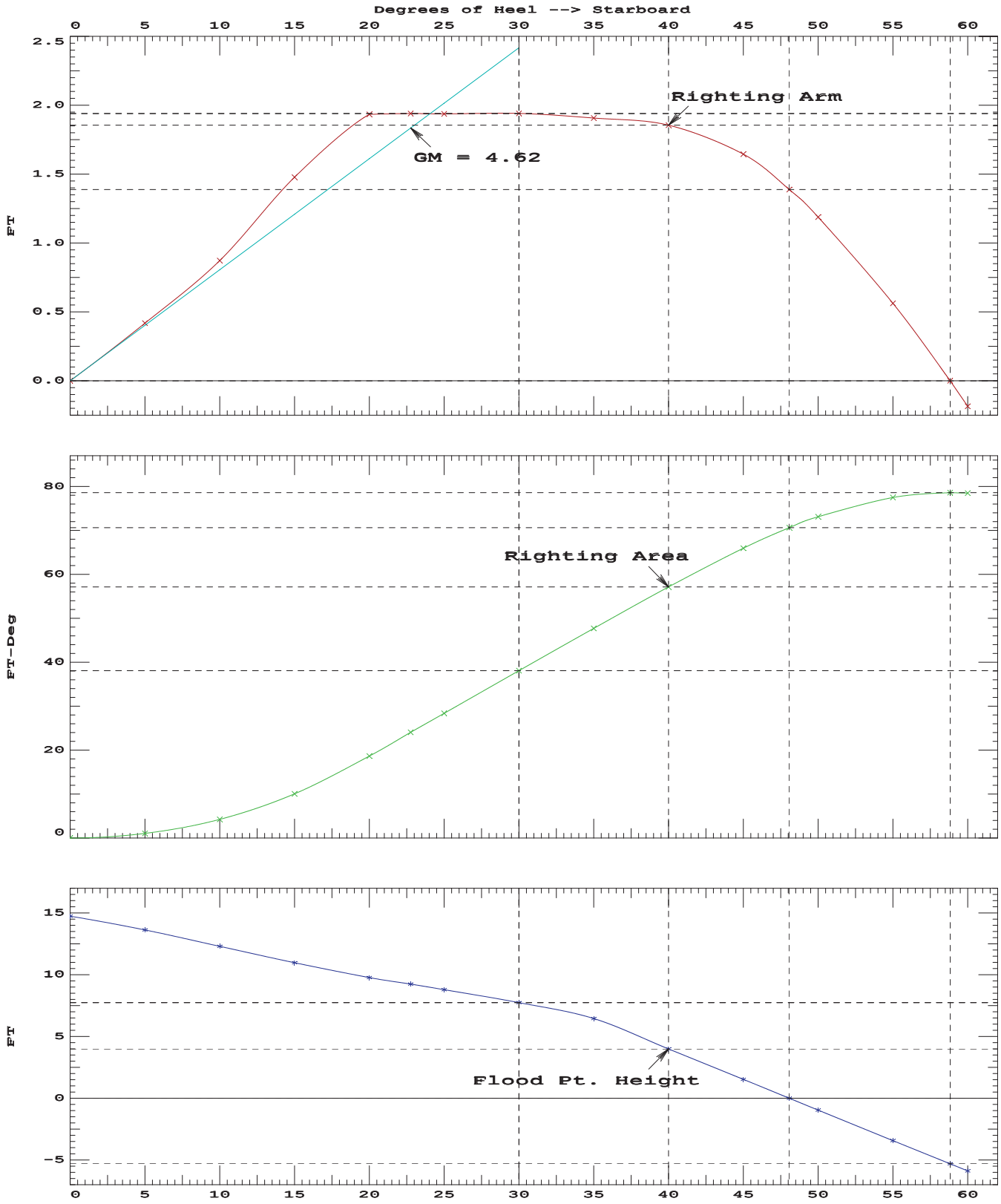

170x56x12 Trimaran
MAX VCG @ 1025 LT
0.5 DEG TRIM
USCG 170.173 PARAGRAPH B

RIGHTING ARMS vs HEEL ANGLE
LCG = 96.30a TCG = 0.00 VCG = 24.26

Origin Depth	Degrees of Trim	Heel	Displacement Weight(LT)	Righting Arms in Trim	in Heel	Area	Flood Pt Height
9.999	0.50a	0.00	1,025.2	0.00	0.000	0.00	14.55(2)
9.966	0.49a	5.00s	1,025.0	0.00	0.401	1.00	13.43(3)
9.868	0.45a	10.00s	1,025.0	0.00	0.839	4.09	12.11(3)
9.780	0.32a	15.00s	1,024.8	0.00	1.436	9.71	10.79(3)
9.611	0.10a	20.00s	1,025.2	0.00	1.967	18.25	9.58(3)
9.436	0.06f	22.64s	1,025.0	0.00	1.978	23.48	9.07(3)
9.205	0.18f	25.00s	1,024.8	0.00	1.970	28.15	8.59(3)
8.480	0.34f	30.00s	1,024.9	0.00	1.977	38.09	7.54(3)
8.343	0.36f	30.78s	1,025.0	0.00	1.978	39.64	7.37(3)
7.509	0.44f	35.00s	1,025.0	0.00	1.952	47.94	6.22(1)
6.288	0.47f	40.00s	1,025.3	0.00	1.904	57.59	3.72(1)
4.983	0.50f	45.00s	1,025.0	0.00	1.677	66.62	1.23(1)
4.348	0.51f	47.44s	1,025.0	0.00	1.474	70.48	-0.00(1)
3.686	0.54f	50.00s	1,025.0	0.00	1.210	73.92	-1.28(1)
2.394	0.58f	55.00s	1,025.0	0.00	0.579	78.47	-3.78(1)
1.372	0.62f	58.93s	1,025.0	0.00	0.000	79.64	-5.73(1)
1.088	0.62f	60.00s	1,025.2	0.00	-0.170	79.54	-6.26(1)

Distances in FEET.------Specific Gravity = 1.025.----------Area in Ft-Deg.

Critical Points		LCP	TCP	VCP
(1) Vent Louver	FLOOD	145.00a	28.00	35.00
(2) A-Frame Wire Chase	FLOOD	138.00a	7.50	25.75
(3) CTD Wire Chase	FLOOD	122.00a	14.00	25.75

LIM 170.173 Paragraph b CRITERION	Min/Max		Attained	
(1) GM Upright	>	0.49	Ft	4.46 P
(2) Righting Arm at 30 deg or MaxRA	>	0.66	Ft	1.98 P
(3) Absolute Angle at MaxRA	>	25.00	deg	30.78 P
(4) Area from abs 0.000 deg to 30	>	10.30	Ft-deg	38.09 P
(5) Area from abs 0.000 deg to 40 or Flood	>	16.90	Ft-deg	57.59 P
(6) Area from 30 deg to 40 or Flood	>	5.60	Ft-deg	19.50 P

Relative angles measured from 0.000

1025 24.26

170x56x12 Trimaran
MAX VCG @ 1025 LT
0.5 DEG TRIM
USCG 170.173 PARAGRAPH B

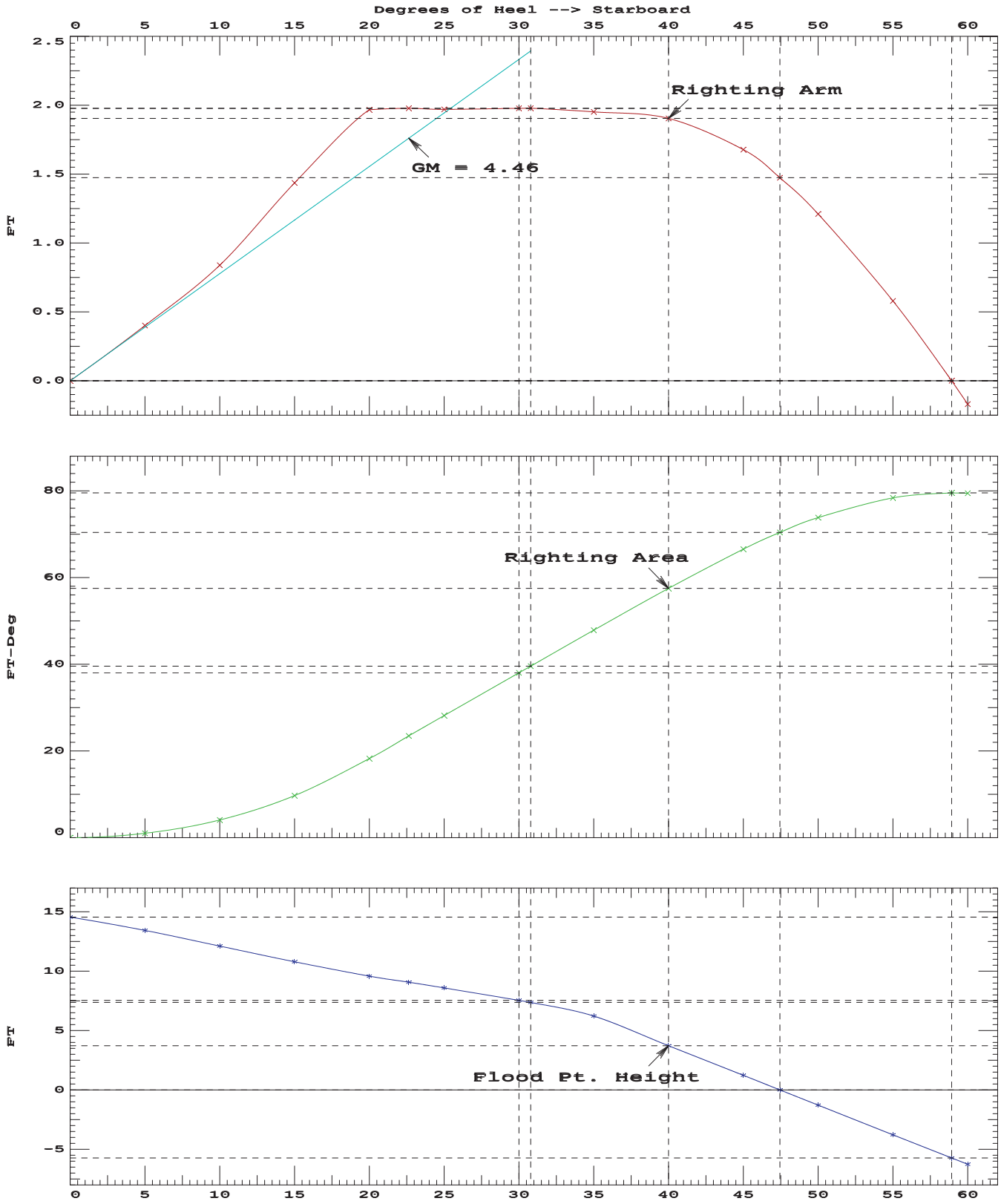

170x56x12 Trimaran
MAX VCG @ 1050 LT
0.5 DEG TRIM
USCG 170.173 PARAGRAPH B

RIGHTING ARMS vs HEEL ANGLE
LCG = 96.44a TCG = 0.00 VCG = 24.11

Origin Depth	Degrees of Trim	Heel	Displacement Weight(LT)	Righting Arms in Trim	in Heel	Flood Pt Area	Height
10.187	0.50a	0.00	1,050.2	0.00	0.000	0.00	14.36(2)
10.151	0.49a	5.00s	1,050.0	0.00	0.385	0.96	13.24(3)
10.049	0.45a	10.00s	1,050.0	0.00	0.810	3.93	11.92(3)
9.958	0.32a	15.00s	1,049.8	0.00	1.398	9.39	10.60(3)
9.768	0.12a	20.00s	1,050.0	0.00	1.998	17.87	9.39(3)
9.576	0.03f	22.62s	1,050.0	0.00	2.014	23.17	8.88(3)
9.324	0.14f	25.00s	1,049.9	0.00	2.002	27.95	8.40(3)
8.564	0.29f	30.00s	1,050.0	0.00	2.011	38.06	7.34(3)
8.334	0.31f	31.28s	1,050.0	0.00	2.014	40.64	7.07(3)
7.565	0.37f	35.00s	1,050.0	0.00	1.991	48.09	5.97(1)
6.315	0.38f	40.00s	1,050.0	0.00	1.946	57.95	3.46(1)
5.000	0.39f	45.00s	1,050.0	0.00	1.702	67.15	0.93(1)
4.520	0.39f	46.83s	1,050.0	0.00	1.551	70.13	-0.00(1)
3.692	0.41f	50.00s	1,050.0	0.00	1.226	74.56	-1.61(1)
2.387	0.44f	55.00s	1,050.0	0.00	0.589	79.17	-4.14(1)
1.343	0.46f	58.99s	1,050.2	0.00	-0.001	80.36	-6.13(1)
1.073	0.47f	60.00s	1,050.2	0.00	-0.161	80.28	-6.64(1)

Distances in FEET.------Specific Gravity = 1.025.----------Area in Ft-Deg.

Critical Points		LCP	TCP	VCP
(1) Vent Louver	FLOOD	145.00a	28.00	35.00
(2) A-Frame Wire Chase	FLOOD	138.00a	7.50	25.75
(3) CTD Wire Chase	FLOOD	122.00a	14.00	25.75

LIM 170.173 Paragraph b CRITERION		Min/Max		Attained	
(1) GM Upright	>	0.49	Ft	4.28	P
(2) Righting Arm at 30 deg or MaxRA	>	0.66	Ft	2.01	P
(3) Absolute Angle at MaxRA	>	25.00	deg	31.28	P
(4) Area from abs 0.000 deg to 30	>	10.30	Ft-deg	38.06	P
(5) Area from abs 0.000 deg to 40 or Flood	>	16.90	Ft-deg	57.95	P
(6) Area from 30 deg to 40 or Flood	>	5.60	Ft-deg	19.89	P

Relative angles measured from 0.000

1050 24.11

170x56x12 Trimaran
MAX VCG @ 1050 LT
0.5 DEG TRIM
USCG 170.173 PARAGRAPH B

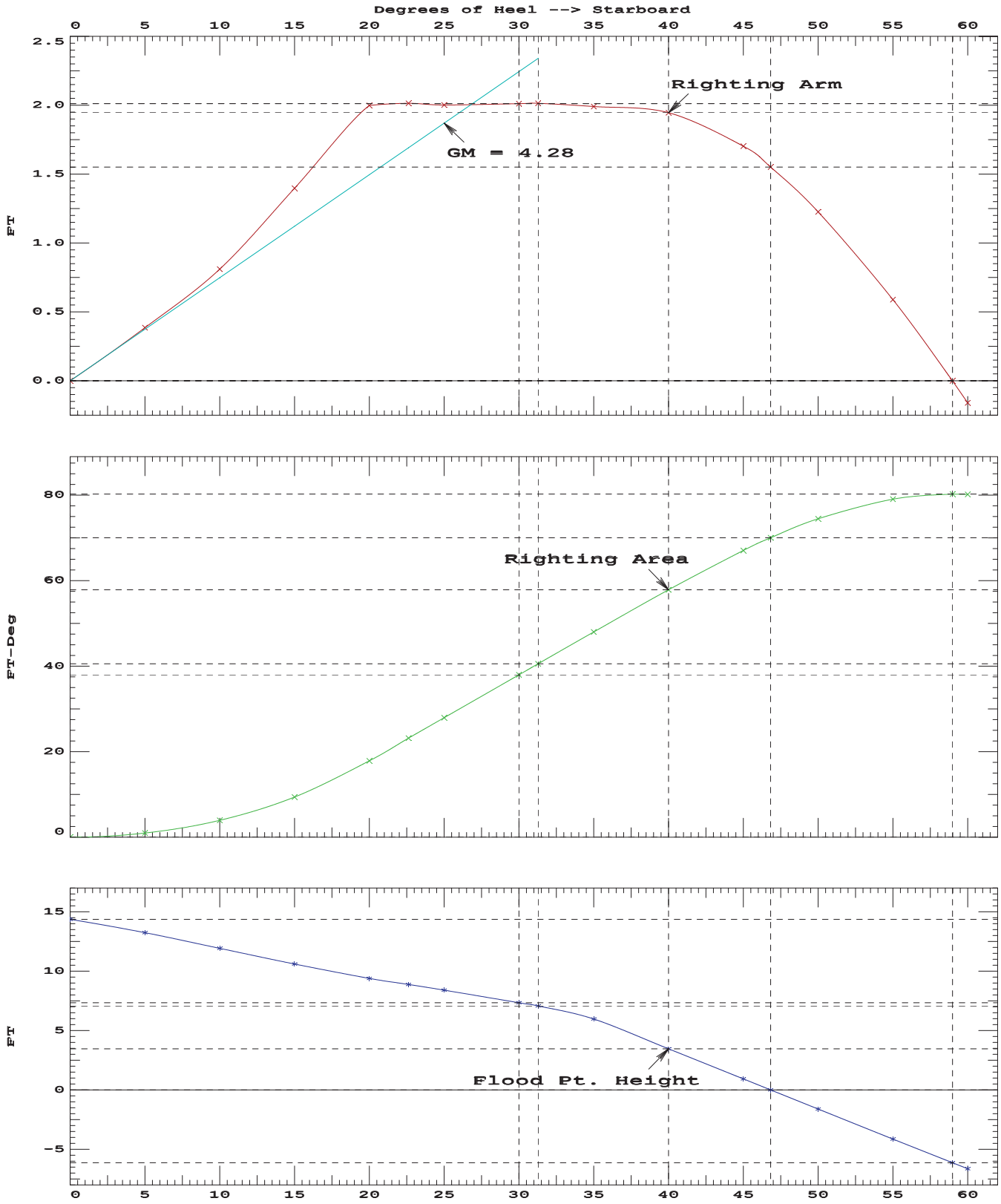

170x56x12 Trimaran
MAX VCG @ 1075 LT
0.5 DEG TRIM
USCG 170.173 PARAGRAPH B

RIGHTING ARMS vs HEEL ANGLE
LCG = 96.57a TCG = 0.00 VCG = 23.94

Origin Depth	Trim	Heel	Displacement Weight(LT)	Righting Arms in Trim	in Heel	Area	Flood Pt Height
10.375	0.50a	0.00	1,075.1	0.00	0.000	0.00	14.17(2)
10.336	0.49a	5.00s	1,075.0	0.00	0.372	0.93	13.05(3)
10.231	0.45a	10.00s	1,075.0	0.00	0.788	3.81	11.74(3)
10.135	0.32a	15.00s	1,074.8	0.00	1.370	9.14	10.42(3)
9.928	0.13a	20.00s	1,075.0	0.00	2.035	17.62	9.21(3)
9.692	0.02f	22.80s	1,074.8	0.00	2.059	23.41	8.65(3)
9.440	0.11f	25.00s	1,074.9	0.00	2.045	27.92	8.20(3)
8.649	0.23f	30.00s	1,075.0	0.00	2.057	38.26	7.15(3)
8.389	0.26f	31.38s	1,075.0	0.00	2.060	41.11	6.85(3)
7.618	0.29f	35.00s	1,075.0	0.00	2.040	48.53	5.73(1)
6.343	0.28f	40.00s	1,075.0	0.00	1.998	58.64	3.19(1)
5.014	0.27f	45.00s	1,075.0	0.00	1.741	68.07	0.63(1)
4.691	0.27f	46.22s	1,075.0	0.00	1.640	70.14	0.00(1)
3.695	0.28f	50.00s	1,075.0	0.00	1.256	75.65	-1.94(1)
2.379	0.30f	55.00s	1,075.0	0.00	0.617	80.41	-4.49(1)
1.278	0.31f	59.17s	1,075.2	0.00	-0.001	81.72	-6.60(1)
1.056	0.31f	60.00s	1,075.2	0.00	-0.131	81.66	-7.01(1)

Distances in FEET.------Specific Gravity = 1.025.----------Area in Ft-Deg.

Critical Points		LCP	TCP	VCP
(1) Vent Louver	FLOOD	145.00a	28.00	35.00
(2) A-Frame Wire Chase	FLOOD	138.00a	7.50	25.75
(3) CTD Wire Chase	FLOOD	122.00a	14.00	25.75

LIM 170.173 Paragraph b CRITERION		Min/Max		Attained	
(1) GM Upright	>	0.49	Ft	4.14	P
(2) Righting Arm at 30 deg or MaxRA	>	0.66	Ft	2.06	P
(3) Absolute Angle at MaxRA	>	25.00	deg	31.38	P
(4) Area from abs 0.000 deg to 30	>	10.30	Ft-deg	38.26	P
(5) Area from abs 0.000 deg to 40 or Flood	>	16.90	Ft-deg	58.64	P
(6) Area from 30 deg to 40 or Flood	>	5.60	Ft-deg	20.37	P

Relative angles measured from 0.000

1075 23.94

170x56x12 Trimaran
MAX VCG @ 1075 LT
0.5 DEG TRIM
USCG 170.173 PARAGRAPH B

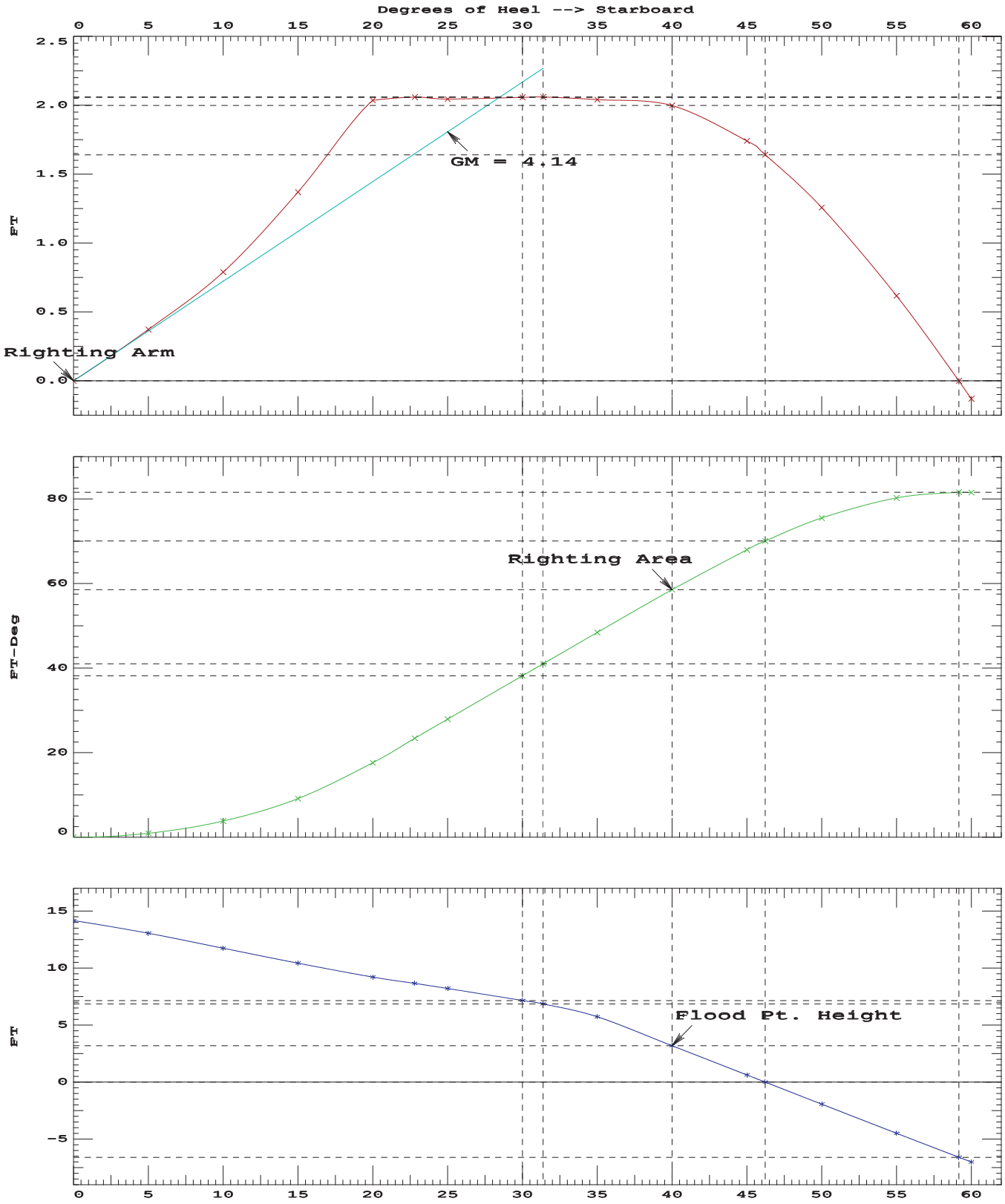

170x56x12 Trimaran
MAX VCG @ 1100 LT
0.5 DEG TRIM
USCG 170.173 PARAGRAPH B

RIGHTING ARMS vs HEEL ANGLE
LCG = 96.70a TCG = 0.00 VCG = 23.77

Origin Depth	Trim	Heel	Displacement Weight(LT)	Righting Arms in Trim	in Heel	Area	Flood Pt Height
10.562	0.50a	0.00	1,100.1	0.00	0.000	0.00	13.98(2)
10.520	0.49a	5.00s	1,100.0	0.00	0.360	0.90	12.86(3)
10.414	0.45a	10.00s	1,100.0	0.00	0.770	3.71	11.55(3)
10.313	0.33a	15.00s	1,099.8	0.00	1.347	8.93	10.24(3)
10.085	0.14a	20.00s	1,100.0	0.00	2.069	17.41	9.03(3)
9.790	0.00	23.12s	1,100.0	0.00	2.103	24.00	8.40(3)
9.554	0.07f	25.00s	1,099.9	0.00	2.091	27.94	8.01(3)
8.730	0.18f	30.00s	1,100.0	0.00	2.102	38.52	6.96(3)
8.454	0.20f	31.42s	1,100.0	0.00	2.104	41.50	6.65(3)
7.668	0.22f	35.00s	1,100.0	0.00	2.089	49.02	5.49(1)
6.368	0.19f	40.00s	1,100.0	0.00	2.048	59.37	2.91(1)
5.027	0.16f	45.00s	1,100.0	0.00	1.779	69.03	0.32(1)
4.861	0.16f	45.63s	1,100.0	0.00	1.728	70.13	0.00(1)
3.697	0.15f	50.00s	1,100.0	0.00	1.288	76.79	-2.27(1)
2.371	0.15f	55.00s	1,100.0	0.00	0.645	81.69	-4.85(1)
1.209	0.16f	59.36s	1,100.1	0.00	-0.001	83.13	-7.07(1)
1.036	0.15f	60.00s	1,100.1	0.00	-0.101	83.10	-7.39(1)

Distances in FEET.------Specific Gravity = 1.025.----------Area in Ft-Deg.

Critical Points		LCP	TCP	VCP
(1) Vent Louver	FLOOD	145.00a	28.00	35.00
(2) A-Frame Wire Chase	FLOOD	138.00a	7.50	25.75
(3) CTD Wire Chase	FLOOD	122.00a	14.00	25.75

LIM 170.173 Paragraph b CRITERION		Min/Max		Attained	
(1) GM Upright	>	0.49	Ft	4.01	P
(2) Righting Arm at 30 deg or MaxRA	>	0.66	Ft	2.10	P
(3) Absolute Angle at MaxRA	>	25.00	deg	31.42	P
(4) Area from abs 0.000 deg to 30	>	10.30	Ft-deg	38.52	P
(5) Area from abs 0.000 deg to 40 or Flood	>	16.90	Ft-deg	59.37	P
(6) Area from 30 deg to 40 or Flood	>	5.60	Ft-deg	20.85	P

Relative angles measured from 0.000

1100 23.77

170x56x12 Trimaran
MAX VCG @ 1100 LT
0.5 DEG TRIM
USCG 170.173 PARAGRAPH B

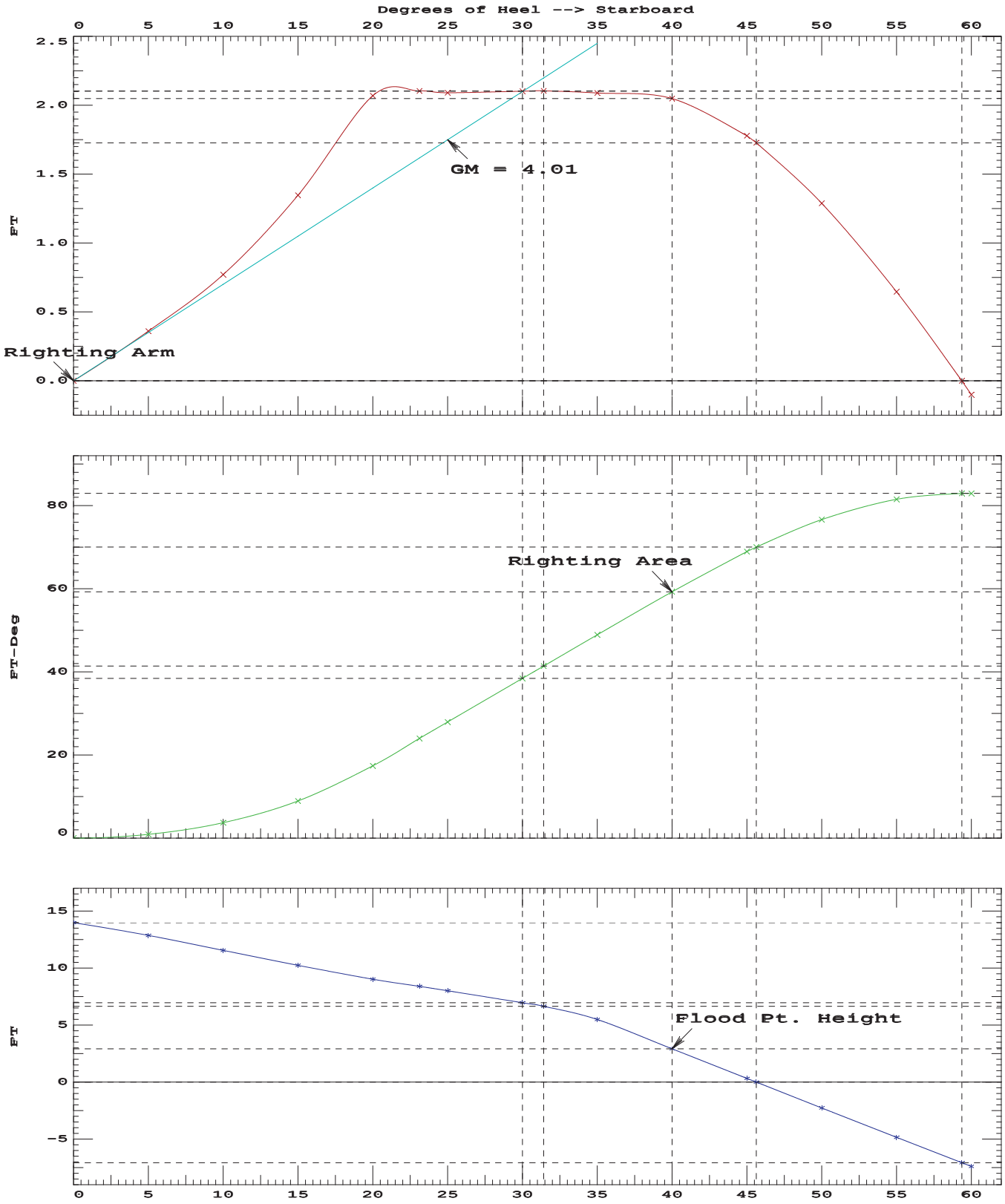

170x56x12 Trimaran
MAX VCG @ 1125 LT
0.5 DEG TRIM
USCG 170.173 PARAGRAPH B

RIGHTING ARMS vs HEEL ANGLE
LCG = 96.83a TCG = 0.00 VCG = 23.60

Origin Depth	Degrees of Trim	Heel	Displacement Weight(LT)	Righting Arms in Trim	in Heel	Flood Pt Area	Height
10.750	0.50a	0.00	1,125.1	0.00	0.000	0.00	13.80(2)
10.705	0.49a	5.00s	1,125.0	0.00	0.350	0.88	12.68(3)
10.598	0.45a	10.00s	1,125.0	0.00	0.756	3.62	11.37(3)
10.490	0.33a	15.00s	1,124.8	0.00	1.329	8.76	10.06(3)
10.239	0.15a	20.00s	1,125.0	0.00	2.097	17.24	8.85(3)
9.854	0.01a	23.64s	1,125.0	0.00	2.148	25.09	8.11(3)
9.667	0.03f	25.00s	1,124.9	0.00	2.140	28.02	7.83(3)
8.807	0.13f	30.00s	1,125.0	0.00	2.147	38.84	6.76(3)
8.547	0.14f	31.29s	1,125.0	0.00	2.148	41.62	6.48(3)
7.715	0.14f	35.00s	1,125.0	0.00	2.137	49.57	5.24(1)
6.391	0.09f	40.00s	1,125.0	0.00	2.096	60.16	2.64(1)
5.040	0.04f	45.00s	1,125.0	0.00	1.816	70.04	0.02(1)
5.028	0.04f	45.04s	1,125.0	0.00	1.812	70.12	0.00(1)
3.699	0.02f	50.00s	1,125.0	0.00	1.320	77.97	-2.60(1)
2.360	0.01f	55.00s	1,125.0	0.00	0.676	83.02	-5.20(1)
1.137	0.00	59.56s	1,125.0	0.00	0.000	84.60	-7.55(1)
1.018	0.00a	60.00s	1,125.3	0.00	-0.070	84.58	-7.78(1)

Distances in FEET.------Specific Gravity = 1.025.----------Area in Ft-Deg.

Critical Points		LCP	TCP	VCP
(1) Vent Louver	FLOOD	145.00a	28.00	35.00
(2) A-Frame Wire Chase	FLOOD	138.00a	7.50	25.75
(3) CTD Wire Chase	FLOOD	122.00a	14.00	25.75

LIM 170.173 Paragraph b CRITERION		Min/Max		Attained	
(1) GM Upright	>	0.49	Ft	3.89	P
(2) Righting Arm at 30 deg or MaxRA	>	0.66	Ft	2.15	P
(3) Absolute Angle at MaxRA	>	25.00	deg	31.29	P
(4) Area from abs 0.000 deg to 30	>	10.30	Ft-deg	38.84	P
(5) Area from abs 0.000 deg to 40 or Flood	>	16.90	Ft-deg	60.16	P
(6) Area from 30 deg to 40 or Flood	>	5.60	Ft-deg	21.32	P

Relative angles measured from 0.000

1125 23.6

170x56x12 Trimaran
MAX VCG @ 1125 LT
0.5 DEG TRIM
USCG 170.173 PARAGRAPH B

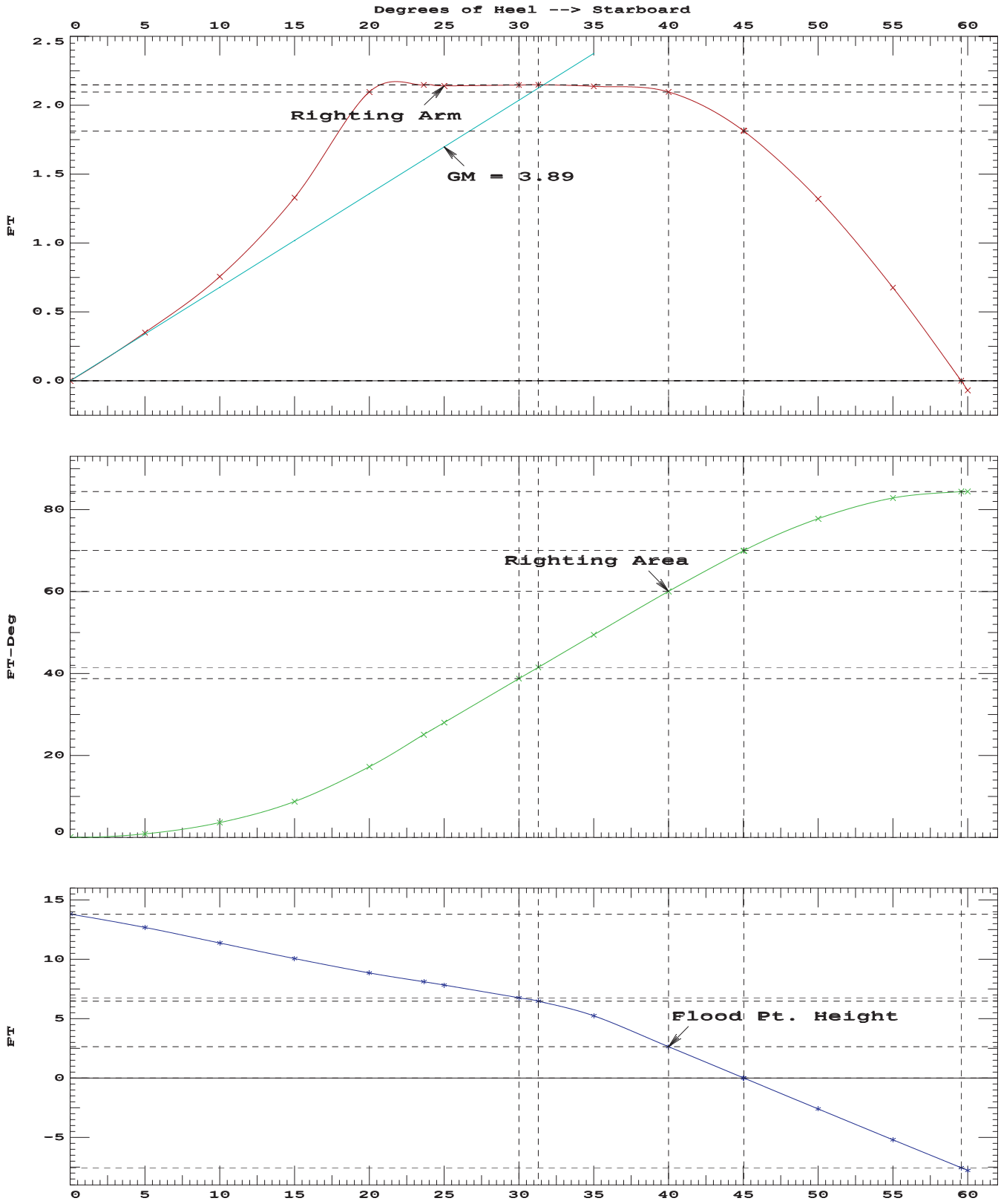

170x56x12 Trimaran
MAX VCG @ 1150 LT
0.5 DEG TRIM
USCG 170.173 PARAGRAPH B

RIGHTING ARMS vs HEEL ANGLE
LCG = 96.95a TCG = 0.00 VCG = 23.37

Origin Depth	Degrees of Trim	Heel	Displacement Weight(LT)	Righting Arms in Trim	in Heel	Flood Pt Area	Height
10.937	0.50a	0.00	1,150.1	0.00	0.000	0.00	13.61(2)
10.892	0.49a	5.00s	1,150.2	0.00	0.346	0.87	12.49(3)
10.784	0.45a	10.00s	1,150.0	0.00	0.755	3.59	11.18(3)
10.667	0.33a	15.00s	1,149.7	0.00	1.333	8.74	9.89(3)
10.391	0.16a	20.00s	1,150.0	0.00	2.142	17.33	8.67(3)
9.961	0.03a	23.75s	1,150.0	0.00	2.223	25.66	7.90(3)
9.779	0.00	25.00s	1,150.0	0.00	2.221	28.43	7.64(3)
8.881	0.07f	30.00s	1,150.0	0.00	2.221	39.66	6.57(3)
8.446	0.07f	32.06s	1,150.0	0.00	2.223	44.24	6.10(3)
7.757	0.06f	35.00s	1,150.0	0.00	2.219	50.77	5.00(1)
6.413	0.01a	40.00s	1,150.0	0.00	2.182	61.78	2.37(1)
5.194	0.07a	44.47s	1,150.0	0.00	1.937	71.06	0.00(1)
5.050	0.07a	45.00s	1,150.0	0.00	1.895	72.08	-0.28(1)
3.697	0.11a	50.00s	1,150.0	0.00	1.398	80.40	-2.93(1)
2.349	0.14a	55.00s	1,150.0	0.00	0.757	85.85	-5.56(1)
0.998	0.16a	60.00s	1,150.0	0.00	0.017	87.83	-8.15(1)

Distances in FEET.------Specific Gravity = 1.025.----------Area in Ft-Deg.

Critical Points		LCP	TCP	VCP
(1) Vent Louver	FLOOD	145.00a	28.00	35.00
(2) A-Frame Wire Chase	FLOOD	138.00a	7.50	25.75
(3) CTD Wire Chase	FLOOD	122.00a	14.00	25.75

LIM 170.173 Paragraph b CRITERION	Min/Max		Attained	
(1) GM Upright	>	0.49	Ft	3.85 P
(2) Righting Arm at 30 deg or MaxRA	>	0.66	Ft	2.22 P
(3) Absolute Angle at MaxRA	>	25.00	deg	32.06 P
(4) Area from abs 0.000 deg to 30	>	10.30	Ft-deg	39.66 P
(5) Area from abs 0.000 deg to 40 or Flood	>	16.90	Ft-deg	61.78 P
(6) Area from 30 deg to 40 or Flood	>	5.60	Ft-deg	22.12 P

Relative angles measured from 0.000

1150 23.37

170x56x12 Trimaran
MAX VCG @ 1150 LT
0.5 DEG TRIM
USCG 170.173 PARAGRAPH B

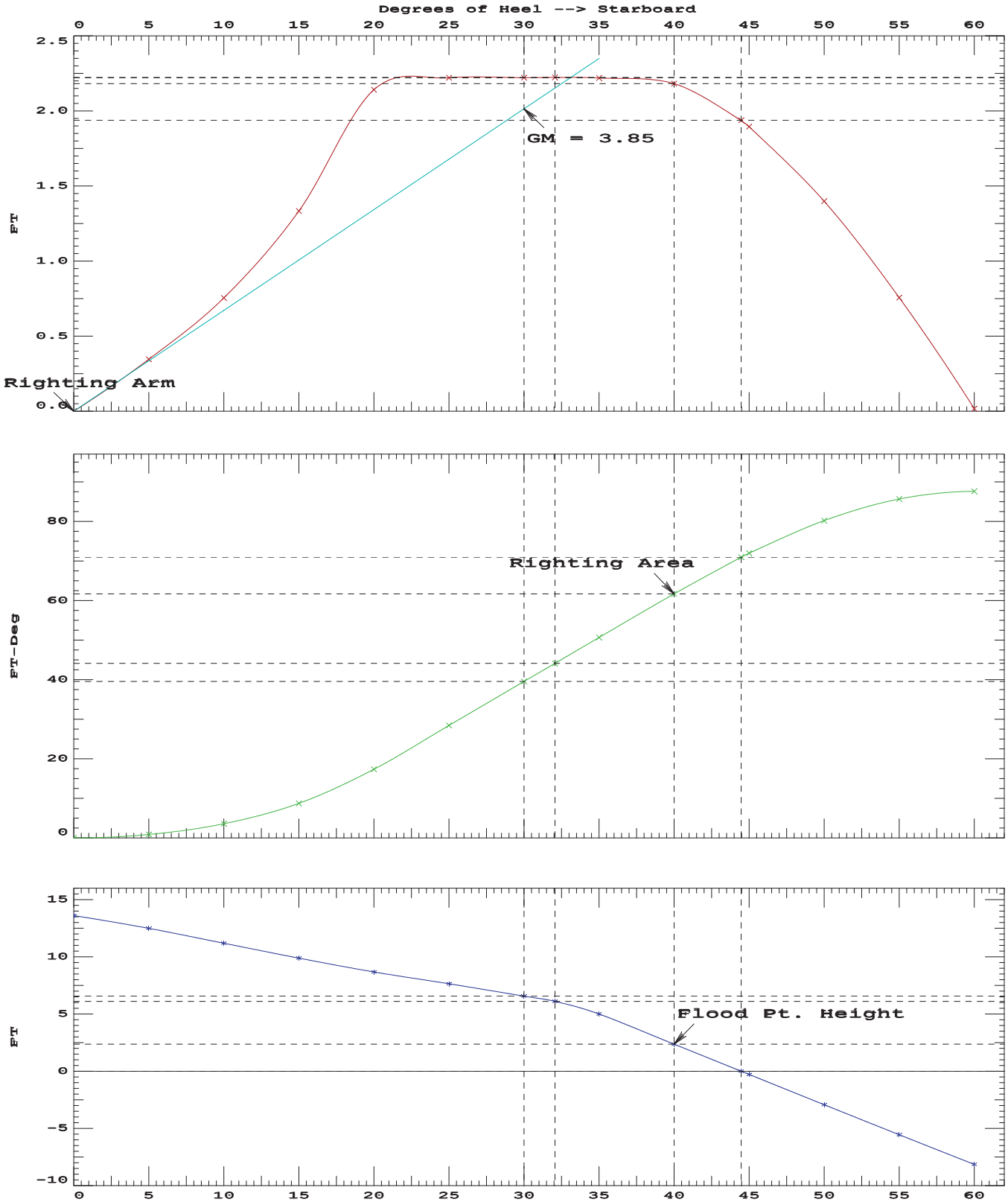

170x56x12 Trimaran
MAX VCG @ 1175 LT
0.5 DEG TRIM
USCG 170.173 PARAGRAPH B

RIGHTING ARMS vs HEEL ANGLE
LCG = 97.07a TCG = 0.00 VCG = 23.14

Origin Depth	Degrees of Trim	Heel	Displacement Weight(LT)	Righting Arms in Trim	in Heel	Area	Flood Pt Height
11.123	0.50a	0.00	1,175.1	0.00	0.000	0.00	13.42(2)
11.076	0.49a	5.00s	1,175.2	0.00	0.344	0.86	12.30(3)
10.971	0.45a	10.00s	1,175.0	0.00	0.757	3.58	11.00(3)
10.843	0.33a	15.00s	1,174.7	0.00	1.343	8.76	9.71(3)
10.540	0.17a	20.00s	1,175.0	0.00	2.183	17.47	8.50(3)
10.082	0.06a	23.75s	1,175.0	0.00	2.304	26.02	7.72(3)
9.888	0.03a	25.00s	1,175.0	0.00	2.301	28.90	7.46(3)
8.953	0.01f	30.00s	1,175.0	0.00	2.296	40.52	6.37(3)
7.798	0.02a	35.00s	1,175.0	0.00	2.300	52.01	4.75(1)
7.342	0.05a	36.72s	1,175.0	0.00	2.304	55.97	3.84(1)
6.434	0.11a	40.00s	1,175.0	0.00	2.265	63.47	2.09(1)
5.357	0.18a	43.91s	1,175.0	0.00	2.058	71.95	-0.00(1)
5.059	0.19a	45.00s	1,175.0	0.00	1.974	74.15	-0.59(1)
3.697	0.24a	50.00s	1,175.0	0.00	1.477	82.78	-3.26(1)
2.338	0.28a	55.00s	1,175.0	0.00	0.838	88.63	-5.91(1)
0.977	0.32a	60.00s	1,175.0	0.00	0.104	91.03	-8.53(1)

Distances in FEET.------Specific Gravity = 1.025.----------Area in Ft-Deg.

Critical Points		LCP	TCP	VCP
(1) Vent Louver	FLOOD	145.00a	28.00	35.00
(2) A-Frame Wire Chase	FLOOD	138.00a	7.50	25.75
(3) CTD Wire Chase	FLOOD	122.00a	14.00	25.75

LIM 170.173 Paragraph b CRITERION		Min/Max		Attained	
(1) GM Upright	>	0.49	Ft	3.82	P
(2) Righting Arm at 30 deg or MaxRA	>	0.66	Ft	2.30	P
(3) Absolute Angle at MaxRA	>	25.00	deg	36.72	P
(4) Area from abs 0.000 deg to 30	>	10.30	Ft-deg	40.52	P
(5) Area from abs 0.000 deg to 40 or Flood	>	16.90	Ft-deg	63.47	P
(6) Area from 30 deg to 40 or Flood	>	5.60	Ft-deg	22.95	P

Relative angles measured from 0.000

1175 23.14

170x56x12 Trimaran
MAX VCG @ 1175 LT
0.5 DEG TRIM
USCG 170.173 PARAGRAPH B

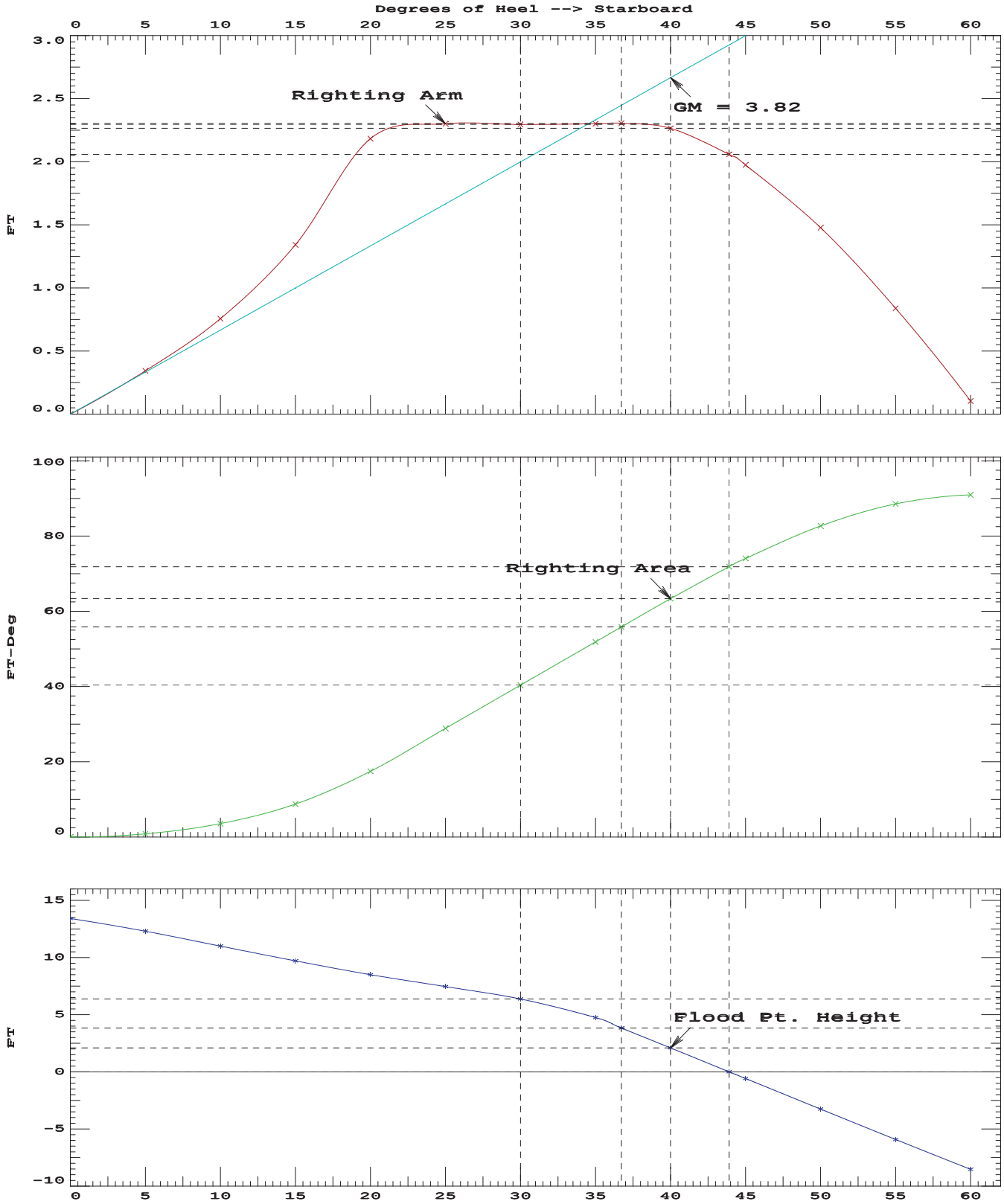

170x56x12 Trimaran
MAX VCG @ 1200 LT
0.5 DEG TRIM
USCG 170.173 PARAGRAPH B

RIGHTING ARMS vs HEEL ANGLE
LCG = 97.19a TCG = 0.00 VCG = 22.93

Origin Depth	Degrees of Trim	Heel	Displacement Weight(LT)	Righting Arms in Trim	in Heel	Area	Flood Pt Height
11.309	0.50a	0.00	1,200.1	0.00	0.000	0.00	13.24(2)
11.261	0.49a	5.00s	1,200.2	0.00	0.341	0.85	12.12(3)
11.159	0.44a	10.00s	1,200.0	0.00	0.757	3.56	10.82(3)
11.020	0.32a	15.00s	1,199.7	0.00	1.353	8.77	9.54(3)
10.691	0.18a	20.00s	1,200.2	0.00	2.216	17.58	8.33(3)
10.199	0.09a	23.75s	1,200.0	0.00	2.378	26.32	7.54(3)
9.993	0.07a	25.00s	1,200.0	0.00	2.373	29.29	7.28(3)
9.022	0.05a	30.00s	1,200.0	0.00	2.360	41.27	6.17(3)
7.836	0.11a	35.00s	1,200.0	0.00	2.370	53.08	4.50(1)
7.354	0.15a	36.78s	1,200.1	0.00	2.378	57.31	3.54(1)
6.453	0.22a	40.00s	1,200.0	0.00	2.334	64.90	1.81(1)
5.522	0.28a	43.35s	1,200.0	0.00	2.162	72.46	0.00(1)
5.067	0.31a	45.00s	1,200.0	0.00	2.039	75.92	-0.89(1)
3.695	0.37a	50.00s	1,200.0	0.00	1.541	84.87	-3.59(1)
2.326	0.43a	55.00s	1,200.0	0.00	0.905	91.04	-6.27(1)
0.956	0.48a	60.00s	1,200.0	0.00	0.175	93.78	-8.91(1)

Distances in FEET.------Specific Gravity = 1.025.----------Area in Ft-Deg.

Critical Points		LCP	TCP	VCP
(1) Vent Louver	FLOOD	145.00a	28.00	35.00
(2) A-Frame Wire Chase	FLOOD	138.00a	7.50	25.75
(3) CTD Wire Chase	FLOOD	122.00a	14.00	25.75

LIM 170.173 Paragraph b CRITERION		Min/Max		Attained	
(1) GM Upright	>	0.49	Ft	3.78	P
(2) Righting Arm at 30 deg or MaxRA	>	0.66	Ft	2.38	P
(3) Absolute Angle at MaxRA	>	25.00	deg	36.78	P
(4) Area from abs 0.000 deg to 30	>	10.30	Ft-deg	41.27	P
(5) Area from abs 0.000 deg to 40 or Flood	>	16.90	Ft-deg	64.90	P
(6) Area from 30 deg to 40 or Flood	>	5.60	Ft-deg	23.64	P

----------Relative angles measured from 0.000 ----------

1200 22.93

170x56x12 Trimaran
MAX VCG @ 1200 LT
0.5 DEG TRIM
USCG 170.173 PARAGRAPH B

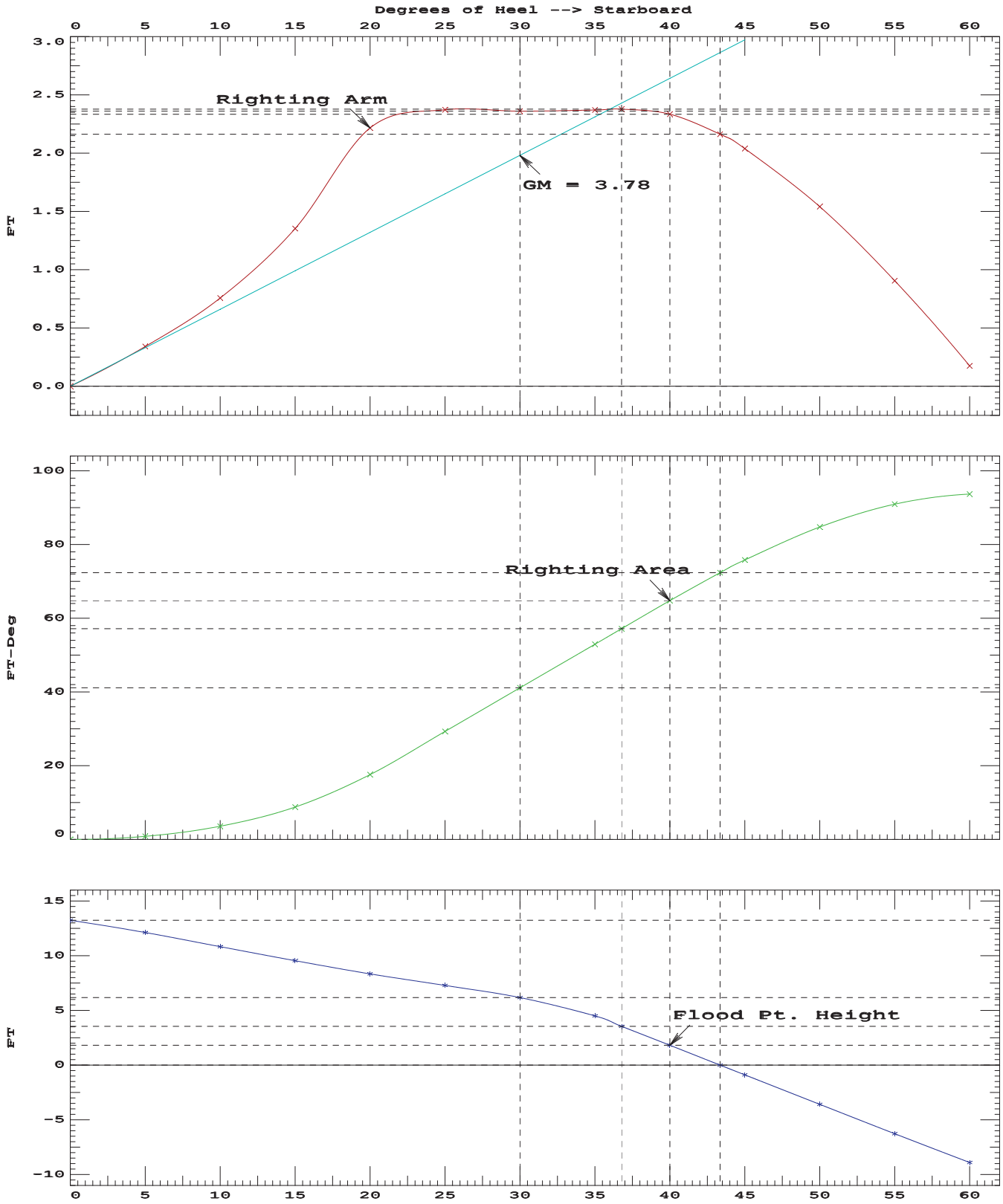

US Coast Guard Weather Criteria 170.170

Displacement (LT)	MaxVCG (ft)
900	26.4889
925	26.1133
950	25.7603
975	25.4286
1000	25.1042
1025	24.7931
1050	24.5033
1075	24.2056
1100	23.9542
1125	23.7014
1150	23.4471
1175	23.1981
1200	22.9565

Appendix C Weight Estimate

SWBS	Entry Description		Weight (LT)	LCG (ft-FR 0)	TCG (ft-CL +S)	VCG (ft-ABL)
100	Hull Structure		270.00	91.71	-0.88	19.00
	Welding Allowance	1.5%	4.05	91.71	-0.88	19.00
	Mill Tolerance Allowance	2.0%	5.40	91.71	-0.88	19.00
	Brackets, Inserts and Doublers Allowance	2.0%	5.40	91.71	-0.88	19.00
	Total Hull Structure		284.85	91.71	-0.88	19.00
	Weight/VCG Margin	18.0%	51.27		12.0%	2.28
	Total Hull Structure w/ margins		**336.12**	**91.71**	**-0.88**	**21.28**
200	Propulsion System		10.94	137.74	0.00	6.21
	Weight/VCG Margin	18.0%	1.97		12.0%	0.74
	Propulsion System w/ margins		**12.91**	**137.74**	**0.00**	**6.95**
300	Electrical System		59.26	90.22	0.70	18.69
	Weight/VCG Margin	18.0%	10.67		12.0%	2.24
	Electrical System w/ margins		**69.93**	**90.22**	**0.70**	**20.93**
400	Command and Surveillance		9.07	66.57	-1.24	38.29
	Weight/VCG Margin	18.0%	1.63		12.0%	4.60
	Command and Surveillance w/ margins		**10.71**	**66.57**	**-1.24**	**42.89**
500	Auxiliary Systems		198.74	73.31	-0.23	20.02
	Weight/VCG Margin	18.0%	35.77		12.0%	2.40
	Auxiliary Systems w/ margins		**234.52**	**73.31**	**-0.23**	**22.43**
600	Outfitting and Furnishings		152.26	77.36	-0.93	24.78
	Weight/VCG Margin	18.0%	27.41		12.0%	2.97
	Outfitting and Furnishings w/ margins		**179.67**	**77.36**	**-0.93**	**27.76**
700	Mission Equipment		69.43	137.70	4.98	26.52
	Weight/VCG Margin	18.0%	12.50		12.0%	3.18
	Mission Equipment w/ margins		**81.93**	**137.70**	**4.98**	**29.70**
	Lightship Subtotal w/o margins		**784.56**	**88.57**	**-0.08**	**21.07**
	Net Margins	18.0%	141.22		12%	2.53
	Lightship at Delivery w/ margins		**925.78**	**88.57**	**-0.08**	**23.60**

1200	Post Delivery Outfit		14.99	109.85	9.19	16.53
	Weight/VCG Margin	6.7%	1.00		3.03%	0.50
	Post Delivery Outfit w/ margins		**15.99**	**109.85**	**9.19**	**17.03**
	Operational Lightship Subtotal w/o margins		**799.55**	**88.97**	**0.09**	**20.98**
	Operational Lightship w/margins		**941.77**	**88.94**	**0.08**	**23.49**

Contract Modification & Service Life Allowance	60.00			
End Of Life Lightship	**1001.77**	**88.94**	**0.08**	**23.49**
Operational Weights				
Science Payload	50.00	160.00	0.00	21.00
Crew&Effects	5.00	60.00	0.00	30.00
Fuel	20.00	112.50	0.00	37.50
Misc. Tanks	25.00	90.00	0.00	5.00
Consumables	12.50	90.00	0.00	21.00
Total Operational Weights	112.50	123.78	0.00	20.78
New Departure Weight	**1054.27**	**92.65**	**0.07**	**23.20**
Total End of Life Departure Weight	**1114.27**	**92.45**	**0.07**	**23.21**

Appendix D Cost Estimate

Zero-V Research Vessel - Engineers Cost Estimate (Low Labor Rate)					
SWBS NUMBER	SWBS GROUP DESCRIPTION	LABOR (HOURS)	MATERIALS ($)	SUBCONTRACTS ($)	SUB-TOTAL ($)
000	Shipyard Engineering & Services	97,583	2,216,538	5,472,445	13,543,963
100	Structure	122,445	3,287,833	0	10,634,532
200	Propulsion	2,124	419,300	25,000	571,740
300	Electric Plant	27,771	7,825,956	0	9,492,216
400	Command and Surveillance	16,651	1,793,814	601,250	3,394,124
500	Auxiliary Systems	43,518	6,180,142	3,096,003	11,887,195
600	Outfit & Furnishings	19,995	1,237,441	2,951,400	5,388,517
700	Science Outfit	5,426	6,237,271	406,000	6,968,807
	SUB-TOTAL	335,512	29,198,294	12,552,098	61,881,093
	Labor Rate	$60	per hour		
	Material Markup (for shipping, receiving, taxes, storage)	15%			4,379,744
	CONSTRUCTION COST SUBTOTAL				66,260,838
	Builders Risk Insurance	1.0%			662,608
	Estimating Allowance (Contingency)	15%			9,282,164
	TOTAL CONSTRUCTION COST ESTIMATE				**$76,205,610**

Zero-V Research Vessel - Engineers Cost Estimate (High Labor Rate)					
SWBS NUMBER	SWBS GROUP DESCRIPTION	LABOR (HOURS)	MATERIALS ($)	SUBCONTRACTS ($)	SUB-TOTAL ($)
000	Shipyard Engineering & Services	97,583	2,216,538	5,472,445	15,007,708
100	Structure	122,445	3,287,833	0	12,471,207
200	Propulsion	2,124	419,300	25,000	603,600
300	Electric Plant	27,771	7,825,956	0	9,908,781
400	Command and Surveillance	16,651	1,793,814	601,250	3,643,889
500	Auxiliary Systems	43,518	6,180,142	3,096,003	12,539,957
600	Outfit & Furnishings	19,995	1,237,441	2,951,400	5,688,436
700	Science Outfit	5,426	6,237,271	406,000	7,050,191
	SUB-TOTAL	335,512	29,198,294	12,552,098	66,913,769
	Labor Rate	$75	per hour		
	Material Markup (for shipping, receiving, taxes, storage)	15%			4,379,744
	CONSTRUCTION COST SUBTOTAL				71,293,513
	Builders Risk Insurance	1.0%			712,935
	Estimating Allowance (Contingency)	15%			10,037,065
	TOTAL CONSTRUCTION COST ESTIMATE				**$82,043,513**

Appendix E Regulatory Review

United States Coast Guard Comments

DNV GL Comments and Statement of Conditional Approval in Principal

U.S. Department of Homeland Security
United States Coast Guard

Commandant
United States Coast Guard

2703 Martin Luther King Jr. Ave SE
Washington, DC 20593-7430
Staff Symbol: CG-ENG
Phone: (202) 372-1365
Fax: (202) 372-1925
Email: timothy.e.meyrs@uscg.mil

16710/ZERO-V
2017845
August 28, 2017

Glosten
Attn: Mr. Robin Madsen, P.E.
1201 Western Ave, Suite 200
Seattle, WA 98101-2953

Subj: ZERO-V Hydrogen-Fueled Research Vessel Design Study Review

Ref: (a) Glosten email, "*Zero-V Hydrogen Research Vessel Design Review*", dated July 5, 2017
(b) Glosten Memo, Job/File No. 17003.01, "*Zero/V Regulatory Review*", dated July 5, 2017
(c) *General Arrangement*, Glosten, Drawing No. 17003.01-070-01, Rev. P5, 5 July 2017
(d) *Preliminary Hazardous Zone Plan*, Glosten, Drawing No. 17003.01-000-01, Rev. P1, 5 July 2017
(e) *Concept Gas System Architecture*, Glosten, Drawing No. 17003.01-540-01, Rev. P0, 5 July 2017
(f) *Electrical One-line Diagram: System Architecture*, Glosten, Drawing No. 17003.01-300-01, Rev. P1, 5 July 2017
(g) *Hazardous Zone 3d View*, Glosten, File 17003.01-000-02_Hazardous Zones 3DView_P1.pdf
(h) *Rules for Classification: Ships*, Part 6 Chapter 2, DNVGL, January 2017
(i) *International Code of Safety for Ships Using Gases or Other Low-Flashpoint Fuels (IGF Code)* as Amended by Resolution MSC.391 (95), International Maritime Organization (IMO)
(j) Commandant (CG-ENG) Policy Letter 01-12, CH-1, *Equivalency Determination – Design Criteria for Natural Gas Fuel Systems (Change-1)*, 12 July 2017

Dear Mr. Madsen:

We have reviewed references (a) through (g) regarding the feasibility study of a proposed hydrogen fuel cell powered research vessel that you are conducting on behalf of Sandia National Laboratories (Sandia) and the US Maritime Administration (MARAD). We understand from your memo that it is a goal of Sandia and MARAD to ultimately obtain approval of a Design Basis from the Coast Guard for this proposed vessel design. In this letter we are providing feedback and comments on what you have provided so far. However, since your project is still in the feasibility study phase, we are not able to issue a Design Basis Letter at this time. If the project progresses from feasibility to preliminary design, with an owner/operator dedicated to moving forward with this project, the owner/operator may submit a proposal through the Marine Safety Center requesting a Design Basis from the Coast Guard.

In general, we find no noteworthy issues with the concept as presented. As an oceanographic research vessel, the proposed vessel would be regulated under 46 CFR Subchapter U. Neither the use of liquid hydrogen as a fuel, nor fuel cells as a source for propulsion power, is specifically addressed in Subchapter U. However, 46 CFR 188.15 – *Equivalents*, allows the Coast Guard to accept a vessel of unusual, unique, special, or exotic design provided that the vessel is shown to be at least as safe as any vessel which meets the standards required by Subchapter U.

Your proposal to use the IGF Code in conjunction with DNV-GL rules seems a reasonable approach based on the nature of liquid hydrogen as a low-flashpoint fuel. The IGF Code is an internationally accepted standard that has already been incorporated by Coast Guard policy, in reference (j), and applied to the design of natural gas fueled vessels. While the vessel proposed in your study would use liquid hydrogen as fuel, not natural gas, there are many similarities in the physical properties and risks presented by these two fuels. Furthermore, the use of class rules from a Coast Guard recognized classification society such as DNV-GL, which specifically address hydrogen fuel cell installations, provides a solid foundation for requirements we could apply to such a vessel.

Details of the specific framework of standards and requirements to be applied to the proposed hydrogen fueled research vessel would need to be specified in a Design Basis Letter issued by the Coast Guard, with special attention given to the differences between liquid hydrogen, and liquefied natural gas (LNG). As mentioned above, this would need to be initiated by a request and proposal from an owner/operator who has an established intent to move forward with the project.

We offer the following comments based on a review of your submission:

IGF Code and alternative design analysis – We agree that while there are no existing requirements specific to hydrogen fuel in the IGF Code, it does provide a good baseline design standard for the hydrogen-fueled propulsion plant and associated safety systems on the vessel proposed in your study. Section 2.3 – "Alternative Design" of the IGF Code provides a framework for evaluating designs using fuels such as liquid hydrogen, which are not specifically addressed within the code. This section references the alternatives methodology in SOLAS II-1/55, as a means of meeting the goals and functional requirements contained within the code. Furthermore, IMO has developed *Guidelines on Alternative Design and Arrangements for SOLAS II-1 and III (MSC.1/Circ.1212)*, which provides additional details for the engineering analysis required in SOLAS II-1/55. This guidance would be instrumental for a potential owner/operator in developing a Design Basis proposal for Coast Guard review as described above.

IGF Code Risk Assessment – Section 4.2 of the IGF Code requires a risk assessment be conducted to ensure that risks arising from the use of low-flashpoint fuels affecting persons on board, the environment, the structural strength or the integrity of the ship are addressed. While this risk assessment is limited in scope to those areas specified under 4.2.2 for vessels that use natural gas fuel, this is not the case for other low-flashpoint fuels which must undergo a more

comprehensive risk assessment. The risk assessment submitted to the Coast Guard should follow an assessment plan with representatives from relevant disciplines and stakeholders that can identify hazards, categorize the risk, and ensure proper safeguards are utilized to reduce risks where necessary. The scope should be broad enough to adequately cover hazards associated with the specific novel design being proposed, and should be conducted in conjunction with or following the alternative design analysis mentioned above. The risk assessment should be conducted in accordance with relevant guidance of a recognized risk advisory body such as: classification society (e.g. ABS, DNV-GL); industry association (e.g. American Institute of Chemical Engineers, Society of Fire Protection Engineers, National Fire Protection Association); or another acceptable alternative that would be referred to in the assessment plan.

Fuel cell installation requirements – We note your intended use of the DNV-GL Rules for fuel cell installations in reference (h). The IMO is also in the process of developing fuel cell requirements as an upcoming amendment to the IGF Code. A draft of the requirements being considered should be available from IMO as an annex to the CCC Subcommittee Report following their upcoming meeting scheduled for September, 2017. In addition to reference (h), requirements from this draft fuel cell amendment to the IGF Code may prove useful in developing a Design Basis proposal for the vessel under study.

Hazardous areas – We note that the hazardous areas depicted in references (d) and (g) in general follow the prescriptive zones for natural gas specified in Section 12.5 of the IGF Code, which may not be suitable for hydrogen due to the differences in density, dispersion, and flammable range between the two fuels. If moving forward with this project, the alternative design analysis mentioned above should address whether the IGF Code's natural gas hazardous zones are sufficiently conservative to address hydrogen, or whether they should be modified based on dispersion analysis, or some other method, for application to the vessel proposed in your study. The hazardous areas standards in IEC 60079-10-1:2015, provide one possible source for a more detailed methodology of classifying hazardous areas, as well as providing specific considerations for hydrogen in Annex H of the standard.

Fire protection systems – While applying IGF Code requirements for natural gas is a good starting point, it is difficult to provide substantive comments on appropriate fire protection systems for a hydrogen fueled vessel without the support of engineering analysis, such as that prescribed under the IGF Code's alternative design section. Section 3.8.2 of the draft Design Study Report, included in reference (b), for example shows the use of a water spray system located within the fuel cell spaces. Water spray systems are typically used on a vessel's exterior surfaces to provide a cooling effect to protect boundaries of sensitive interior spaces such as accommodation, service or control spaces. The use of a water spray system on an interior compartment such as a fuel cell space should be supported by engineering analysis that compares it with other alternatives to determine an appropriate solution that satisfies the functional requirements in the IGF Code.

The Coast Guard recently issued an update to our policy letter on design of U.S.-flag LNG fueled vessels, reference (j), to incorporate the new IGF Code as a baseline standard. While reference (j) is only applicable to LNG fuel systems, it should prove instructive as a reference in providing

general insight into Coast Guard interpretation of IGF Code requirements, especially in those areas of the code that are left to "the Administration".

We heartily commend the innovative approach by Glosten, in collaboration with Sandia and MARAD to advance the state-of-the-art for marine power systems and look forward to seeing this novel technology mature over time. We recognize that hydrogen fuel cell technology has potential air emissions benefits, and applaud the work you and your team have accomplished in providing alternative arrangements for vessels as the marine transportation system pivots toward cleaner and more sustainable energy.

For further clarification on any of these issues, please feel free to contact Tim Meyers of my staff at (202) 372-1365 or timothy.e.meyers@uscg.mil.

Sincerely,

John H. Miller

J. H. MILLER, P.E.
Commander, U.S. Coast Guard
Chief, Systems Engineering Division
By direction

Copy: Commanding Officer, Marine Safety Center (MSC-2)
Detachment Chief, U.S. Coast Guard Liquefied Gas Carrier National Center of Expertise

STATEMENT OF CONDITIONAL APPROVAL IN PRINCIPLE

Glosten/Sandia National Laboratories
Zero-V Hydrogen Research Vessel

This is to certify that Zero-V Hydrogen Research Vessel is granted *Conditional Approval in Principle (CAIP).*

The approval is based on the prospective DNVGL Rules for Classification of Ships Pt. 6 Ch. 2 Sec. 3 – *Fuel Cell Ship Installations – FC* (01-2018 edition), IGF Code – *International code of safety for ships using gases or other low-flashpoint fuels*, Part A.

Acknowledging that the current regulatory status does not allow for a conventional approval of hydrogen as fuel and fuel cells on maritime applications, this CAIP is a precursor to the more extensive alternative design process as described by the applicable statutory instruments.
No deviations have been identified that would be considered to be major show-stoppers from a regulatory point of view, given the available information in the design drawings in Appendix 2. Compliance with/clarifications of comments in Appendix 1 is a condition for the Approval in Principle, but comments need not be clarified/solved at this stage of the project.

Classification and Certification of specific installations may be granted subject to plan approval and survey as specified by the Rules, findings in future HAZIDS, risk assessments, explosion analysis etc.

DNV GL
Høvik, 2017-11-01

Digitally Signed By: Torill Grimstad Osberg
DNV GL Høvik, Norway
2017-11-01

Torill Grimstad Osberg
Head of Section, MCANO385 LNG, Cargo Handling and Piping Systems

Appendix 1: Drawing status and comments
Appendix 2: Drawings included in the Approval in Principle

Robin Madsen
Att: rtmadsen@glosten.com

DNV GL AS Approval
LNG, Cargo Handling & Piping Systems
P.O. Box 300
1322 Høvik
Norway
Tel: +47 67 57 90 26

Date:	**Our reference**:	**Your reference**:	**Job ID:**
2017-11-01	MCANO385/HCKW/ P26305-J-3		MCANO385-Zero/V-1

HØVIK LNG, CARGO HANDLING & PIPING SYSTEMS, Id. No. P26305
Zero-V conditional AIP review

Reference is made to your letter dated 2017-10-21. The following documents are stamped 2017-11-01 and given the status as shown below:

Document No	Rev	DNV GL No	Title	Code	Status
		1	LH2 Tank Vent Diagram for Hans-Christian		For Inf.
		2	Hydrogenics Power Rack Pictures and Diagrams		For Inf.
		3	Documentation on PEM Fuel Cells and Hydrogenics Fuel Cell Racks		For Inf.
		4	17003.01-540-01 Concept Gas System_Rev -_Signed		Examined w/comm
		5	17003.01-300-01 Electrical Oneline Diagram_Rev-_Signed		Examined
		6	17003.01-070-01_General Arrangement Rev -_Signed		Examined w/comm
		7	17003.01-000-01_ Hazardous Zones Plan_Rev-_Signed		Examined w/comm
		8	17003.01 Sandia Design Study Report Rev P2		For Inf.

Document No. **(empty)**, "LH2 Tank Vent Diagram for Hans-Christian" has the following comments:

2 **LH2 Tanks - Loss of vacuum insulation** **Important Note**

Reference is made to sheet 3. The rate of boil-off should be evaluated to document the statements regarding the capacities of the pressure relief valves, including the 3-way transfer valve.

Loss of vacuum insulation will lead to a colder outer shell, the effect of cryogenic cooling of supports and deck structures should be evaluated and documented.

7 **3 way valve** **Important Note**

The 3 way valve will be subject to special consideration, with respect to reliability and potential for

erronous operation (human error).

Document No. **(empty)**, "Documentation on PEM Fuel Cells and Hydrogenics Fuel Cell Racks" has the following comment:

9 Certification of fuel cells Important Note

The fuel cells are subject to certification, and should be delivered with a product certificate. The test programme can be based on the IEC standard 62282-3-1 "Stationary fuel cell power systems - Safety". Environmental and operating conditions in a ship shall also be taken into account. Please also note that according to DNVGL Rules, use of flammable materials is only acceptable for electrical isolating purposes and shall be minimized as far as practicable.

Document No. **(empty)**, "17003.01-540-01 Concept Gas System_Rev -_Signed" has been reviewed in accordance with DNVGL Rules for Ships Pt. 6 Ch. 2, IGF Code Pt. A, with the following comments:

3 Tank rooms/tank connection spaces Important Note

The IGF Code requires that a tank connection space (TCS) shall be able to fully contain LNG leakages. Given the differences in environmental impact between natural gas and hydrogen, and the high evaporation rate of the latter, it should be evaluated whether the tank rooms/TCSs should be closed and able to contain LH2 leakages, or if it is more suitable to construct a semi open TCS, providing natural ventilation and mechanical and environmental protection.

If fully closed tank room/TCS are selected, a pressure build-up analysis in case of major LH2 leakages should be provided.

8 Isolated pipe segments Important Note

Pipe segments and components that may be isolated in a liquid condition shall be provided with pressure relief valves. This applies for any part of piping from the tank isolation valve in the gas supply lines up to the first isolation valve after the liquid H2 is fully vaporized. If the vaporizers can be isolated, these should also be fitted with pressure relief valves.

10 Materials Important Note

On a general note, austenitic stainless steel should be used for materials in contact with hydrogen fuel. Use of other materials should be subject to special consideration. Materials and other piping specifications have not been reviewed at this stage, but will be subject to approval at the detailed design stage.

13 Double-block-and-bleed arrangement Important Note

The N2 supply should be installed to prevent the return of hydrogen to any non-hazardous spaces

15 Pressure relief valve maintenance Important Note

Stop valves shuold be fitted before and after the pressure relief valves at the tanks. These shall enable in-service maintenance without the risk of release of hydrogen gas through the (potentially) open pipe. Therefore, each group of relief valves/rupture disc should be possible to isolate from the vent mast. The stop valves shall be arranged to minimize the possibility that all pressure relief valves for one tank are isolated simultaneously. Physical interlocks shall be included to this effect. Reference is made to DNVGL Rules Pt. 6 Ch. 2 Sec. 5 (Gas fuelled ship installations). Although these rules are, as the IGF Code,

written for use with natural gas, it is considered that the safety philosophy in this specific issue should be the same.

Document No. **(empty)**, "17003.01-300-01 Electrical Oneline Diagram_Rev-_Signed" has been reviewed in accordance with DNVGL Rules for Ships Pt. 6 Ch. 2, IGF Code Pt. A

Document No. **(empty)**, "17003.01-070-01_General Arrangement Rev -_Signed" has been reviewed in accordance with DNVGL Rules for Ships Pt. 6 Ch. 2, IGF Code Pt. A, with the following comments:

1 **LH2 Tanks - Mechanical damage** **Important Note**

It is assumed that the tank location fulfills the probabilistic and deterministic criteria as described in the IGF Code [5.3] for collision protection. It is also assumed that the applicability of the requirements, as they are developed for natural gas, will be considered at the detailed design stage.

The need for mechanical protection of the tanks should be assessed, with respect to cargo operations, ship operations, green sea etc.

4 **Cryogenic cooling** **Important Note**

The effects of cryogenic cooling of decks and structures below any LH2 leakage points should be evaluated in the detailed design stage.

14 **Bunkering lines** **Action Required**

In general, bunkering lines should be arranged as self-draining towards the tank. If this is impractical due to the location of the tanks on the 01 Deck, other suitable means should be provided to relieve the pressure and remove liquid contents from the bunker lines.

It must be ensured in the detailed design stage that the bunkering manifold is designed to withstand the external loads it is subjected to during bunkering. This shall include the forces on the manifold in a scenario where the bunkering line is released by a breakaway coupling.

Please address follow-up to the approval expert

Document No. **(empty)**, "17003.01-000-01_ Hazardous Zones Plan_Rev-_Signed" has been reviewed in accordance with DNVGL Rules for Ships Pt. 6 Ch. 2, IGF Code Pt. A, with the following comments:

5 **Extent of hazardous zones** **Important Note**

It is noted that the hazardous zone classification described for natural gas is used. As the properties of hydrogen differs from those of natural gas, the extent of the zones should be evaluated.

Around the vent mast, the Code specifies a hazardous zone of 4.5 meters. This is justified by the requirements for tank holding times and boil-off gas management systems. As the application of hydrogen may introduce a different approach to these safety measures, the zone around the vent mast should be given special consideration.

6 **Flanges and valves** **Important Note**

During the detailed design of the vessel, it must be taken into account that all flanges, valves and other leakage points in the hydrogen system generates hazardous spaces. The hazardous zones will affect locations of other ship systems and accommodation, service stations etc. This has not been evaluated at this stage.

12 **ESD Concept** **Action Required**

It is noted the ESD Concept will be applied to the fuel cell spaces. It should be noted that the ESD philosophy is developed for use in connection with natural gas systems, and will not necessarily fulfill the safety requirements for hydrogen systems. Applying the ESD concept will be subject to special consideration in the next stage of the project.

Please address follow-up to the approval expert

Document No. **(empty)**, "17003.01 Sandia Design Study Report Rev P2" has the following comment:

11 **Safety/reliability philosophy** **Important Note**

Before the detailed design stage of the project, a safety/reliability philosophy document should be developed. The overall design should ensure that any single failure in the fuel cell power installation will not lead to an unacceptable loss of power (for definition, please see: DNVGL Rules Pt. 6 Ch. 2 Sec. 5 Table 1). Further, any safety actions required by rules, regulations or findings in a HAZID/Risk assessment shall not lead to an unacceptable loss of power.

Approval Expert for this approval is Hans-Christian Koch-Wintervoll.

Sincerely
for DNV GL AS

Torill Grimstad Osberg
Head of Section

Hans-Christian Koch-Wintervoll
Contact Person

Appendix: C

Emissions of Radiation Trapping Gases and Criteria Pollutants

As discussed previously, hydrogen has the potential to form the basis for a zero-CO_2 (eq.) energy system. This section assesses the impact on GHG (infrared radiation trapping gases) and criteria pollutant emissions of using hydrogen PEM fuel cell technology in the Zero-V research vessel application. Greenhouse gas (GHG) and criteria pollutant emissions are determined and directly compared with those from an equivalent diesel-powered vessel, as well as a vessel fueled with biodiesel fuel.

In order to calculate the GHG and criteria pollutant emissions associated with vessel operation, the thermal efficiency of the power generating equipment must be known at various partial load states to calculate the fuel demand. Figure 1 gives the thermal efficiency, as a percentage of the LHV of the input fuel, for the PEM fuel cells and the diesel engines across their operating ranges. The figure assumes a LHV value of hydrogen of 119.96 MJ/kg, and a LHV value for diesel fuel of 43.4 MJ/kg. The PEM fuel cell data is from Hydrogenics specifications for the HD-30 PEM fuel cell [1, 2], which is the core fuel cell component for the Zero-V PEM fuel cell power system. The HD-30 has a maximal power rating of 33 kW. In Figure 1, we show a typical (generic) results for the partial-load thermal efficiency of a large diesel engine which would power a diesel vessel equivalent to the Zero-V. For this analysis, we assumed the maximum diesel engine thermal efficiency was 41.91%, with a partial load profile nominally following that of Figure 1.

The maximal efficiency of the PEM fuel cell is 53.3%, for a fuel cell power about 25% of the full rated power, or 8.25 kW in Figure 2. There are 60 HD-30 fuel cell units on the Zero-V (10 fuel cell racks, with each rack holding six HD-30 fuel cell units). As a result, for any power demand greater than 8.25 kW and less than 60 x 8.25 kW = 495 kW, the power load can be distributed amongst the fuel cells so that the optimal 53.3% efficiency is maintained.

Using these considerations, we calculated the annual fuel consumption for the Zero-V and for the equivalent diesel-fueled vessel in performing the 14 Scripps science missions described previously. In a year, the Zero-V will consume 142,459 kg of hydrogen. The equivalent diesel-fueled vessel would consume 504,638 kg of diesel fuel. This quantity of hydrogen

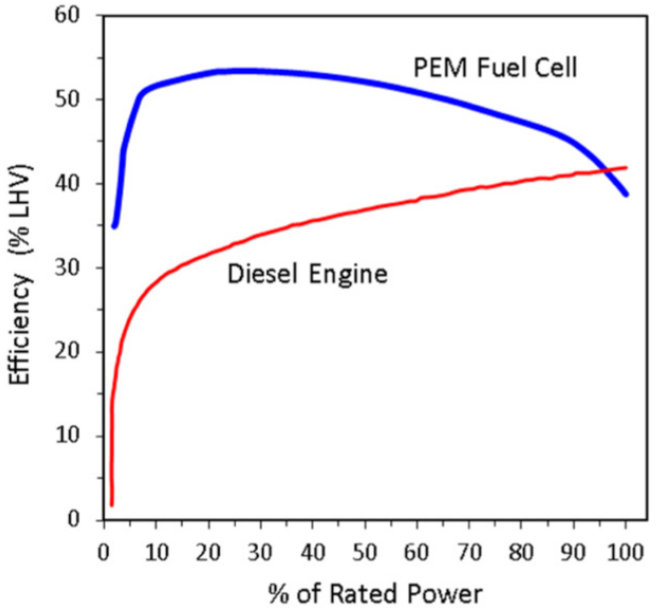

Figure 1: Thermal efficiency of the Zero-V HD-30 PEM fuel cell (thick blue line) and that for the diesel engine (thin red line) used for the "equivalent" diesel vessel performing the same mission as the Zero-V. For the HD-30, the maximal power (100% load) is 33 kW. For one of the diesel engines, the maximal power is 1700 kW. The figure assumes a LHV value of hydrogen of 119.96 MJ/kg, and a LHV value for diesel fuel of 43.4 MJ/kg.

corresponds (using LHV) to 1.709 x 10^7 MJ of hydrogen fuel energy. Concomitantly, this quantity of diesel fuel corresponds (using LHV) to 2.19x10^7 MJ of fuel energy. Thus, we see right away that the Zero-V running on hydrogen is about 22% more energy efficient than the equivalent diesel vessel.

Water is the only product of PEM fuel cell operation. There is no formation of CO_2, NO_x, SO_x, or particulate matter (PM), making the PEM fuel cell a zero-emissions power plant. As a result, the GHG emissions associated with Zero-V consist entirely of the emissions associated with the production and transport of LH_2 to the vessel. This fuel pathway is referred to as "well-to-tank" (WTT). Analogously, GHG emissions are also associated with the production and delivery of diesel fuel. If the diesel fuel originates from petroleum, then there is the additional GHG emissions associated with releasing CO_2 upon combustion. As a result, GHG emissions from the "diesel equivalent vessel" involve two sources: 1) the WTT production and delivery of the diesel fuel and 2) the combustion of the fuel assuming the diesel is derived from petroleum. For light-duty vehicles, this entire pathway is referred

to as "well-to-wheels" as it includes combustion of the fuel onboard the vehicle. For our maritime application, we refer to this pathway as "well-to-waves" (WTW).

Our GHG estimates rely on the WTT GHG analysis conducted by the European commission for automotive fuels in 2007 [3], which were updated in 2013 [4]. These studies considered a wide variety of pathways (both fossil fuel and renewable) for generating hydrogen. As described in Reference [3], the WTT analysis considers the process of producing, transporting, manufacturing and distributing a number of fuels, including hydrogen, diesel, and biodiesel fuel. The study covers all steps in producing and delivering a final fuel product to the storage tank of an end use (vehicle, vessel) with the steps defining a WTT pathway. Energy costs and GHG emissions are assessed along various fuel production/delivery pathways. The study assumes the infrastructure for fuel production and delivery already exists, hence it does not consider GHG emissions associated with construction or decommissioning of plants (which are relatively negligible anyway. For fuels of biomass origin, such as biodiesel or hydrogen from wood gasification, the predicted GHG emissions do not include emissions caused by land use change, but do include N_2O emissions from use of fertilizer and N_2O release from agricultural lands.

The prior SF-BREEZE project report [5] and a recent publication [6] reviews the 4 general categories defining a WTT pathway. The Production and Conditioning at Source category captures all operations required to extract, capture or cultivate the primary energy source at its point of capture. The Transportation to Processing Plant category captures the transportation of the primary energy carrier to the processing plant where the primary energy carrier is refined into finished fuel. The Processing at Plant category captures the energy and GHG emissions involved in processing and transforming

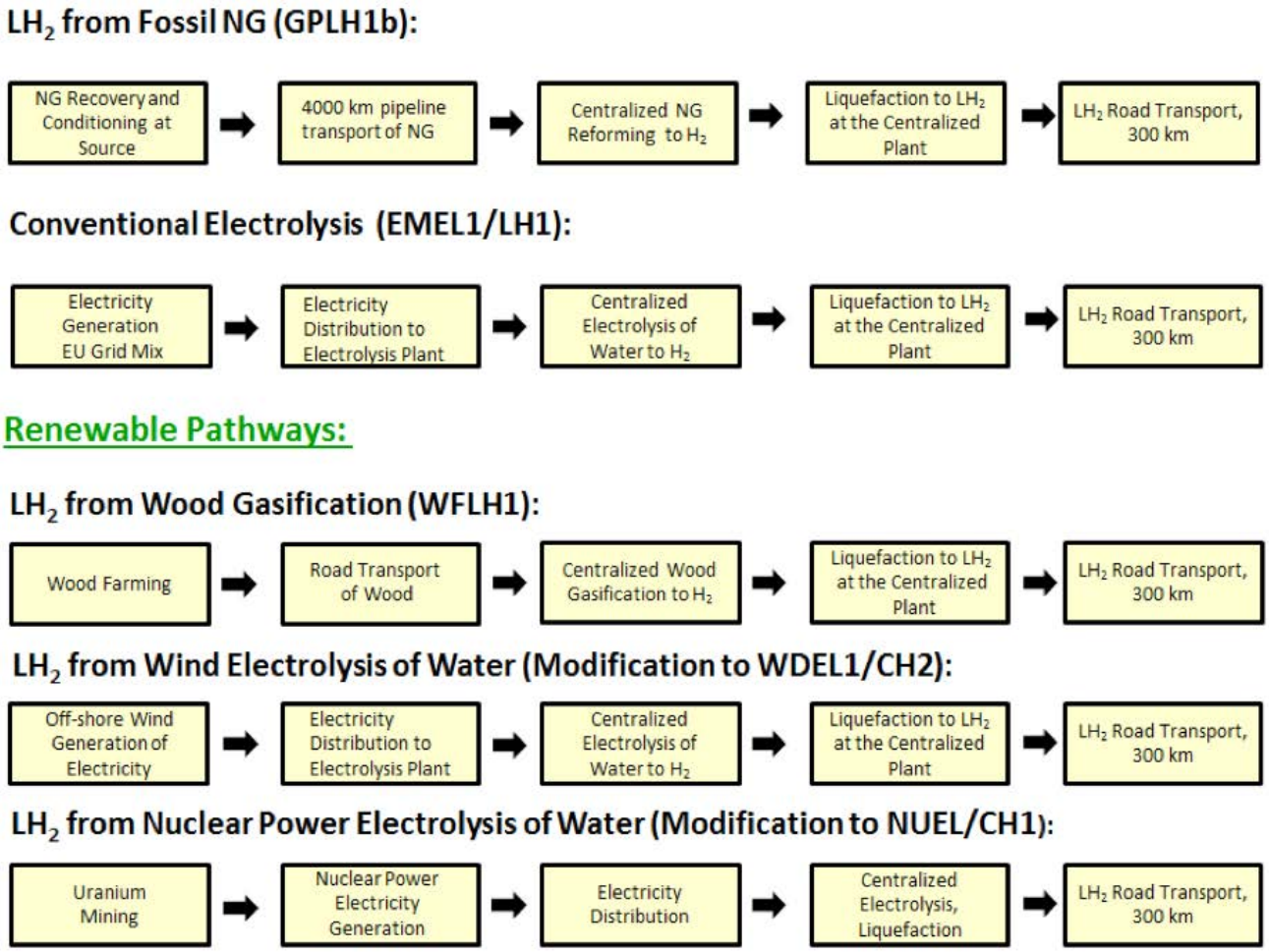

Figure 2: WTT LH_2 pathways considered in the GHG analysis of the Zero-V. Pathway codes in parenthesis identify the pathway describe in detail in the European Commission Reports [3, 4].

the product into a final fuel to an agreed upon specification near the final market. Furthermore, if the hydrogen needs to be liquefied (as it does for the Zero-V), liquefaction also takes place at the centralized plant and involves significant energy input with associated GHG emissions. The Distribution category captures the energy and GHG emissions associated with transport to the final customer end use. While hydrogen may one day be delivered by pipeline, for the Zero-V application, we consider LH_2 to be initially delivered by road tanker carrying LH_2. Taken together, the emissions associated with these four categories are added together to form the WTT pathway emissions, which is the emissions already released by the time the fuel is delivered to the vessel. If in using the fuel the vessel has emissions, then these need to be added to the WTT emissions to form the well-to-waves (WTW) emissions, which capture the entire emissions associated with fuel production and delivery as well as vessel use.

The major GHGs accounted for in the study are carbon dioxide (CO_2), methane (CH_4) and nitrous oxide (N_2O). The results are expressed as "CO_2 equivalence" (CO_2 (eq.)) and each gas is assigned a CO_2 (eq.) "weighting factor." CO_2 has a weighting factor of 1, whereas CH_4 has a factor of 23 and N_2O has a weighting factor of 296. Thus methane is 23 times more potent a GHG than carbon dioxide, which makes NG leakage a significant concern for GHG emissions associated with NG transport. Carbon dioxide is produced in gigantic quantities by combustion of fossil fuels. Nitrous oxide emission derives primarily from nitrogen fertilizer production and release from open agricultural fields. Although produced in relatively smaller amounts, N_2O is an important GHG because of its very large weighting factor of 296. In contrast to CO_2, CH_4, and N_2O, H_2 is not a GHG, so leaks of hydrogen, while an economic loss, have no environmental impact.

The LH_2 WTT pathways considered in this study are depicted in Figure 2 and have also been presented elsewhere [5, 6]. Approximately 90% of the hydrogen used today comes from the steam reforming of fossil NG. Steam methane reforming to LH_2 is identified in the EU Commission study as pathway GPLH1b. The NG is conditioned at the source, transported via NG pipeline 4000 km, reformed at a central reforming facility, liquefied at the plant, and then transported as a liquid in a road tanker a distance of 300 km. Since all of the carbon in fossil-based NG is released into the atmosphere during pathway GPLH1b, we anticipate large GHG emissions from the Zero-V using LH_2 from this pathway.

A second LH_2 production pathway is electrolysis of water using grid power, in this case, the grid mix of the European Union. This pathway is indicated in Figure 2, and identified in the EU Commission report as pathway EMEL1/LH1. Table 1 compares the 2007 EU grid mix assumed for the study [3], and that of the State of California in 2014 [7]. There are

Grid Resource	2007 EU Mix (%)	2014 State of CA (%)
Nuclear	37.5	8.5
Coal	22.4	6.4
Oil	9.6	0
Natural Gas	15.5	44.5
Hydroelectric	12.4	5.5
Wind	0.4	8.1
Waste	1.8	2.5
Other Renewables	0.3	9.5
Other	0.1	15

Table 1: A comparison of the 2007 EU grid mix assumed in the studies of Reference [3] with the 2014 State of California grid mix described in Reference [7].

distinct differences between the two grid mixes. The EU has more low-carbon nuclear, while the State of CA has considerably less high-carbon coal. The State of CA has more low-carbon wind, but less zero-carbon hydroelectric power. Overall, we judge these two grid mixes to be comparable as bases for GHG calculations. More recent assessments of the EU grid mix in 2013 show only small variations from the grid mix of 2007 [4].

"Renewable Pathways" of hydrogen production are those that don't involve the release of carbon, or if carbon is released, then it came recently from CO_2 in the air, making the pathway "carbon neutral." The EU commission studies [3, 4] incorporated one renewable pathway that led directly to LH_2, namely wood gasification (WFLH1). Other renewable pathways to hydrogen include using offshore wind to electrolyze water (WDEL1/CH_2) and using nuclear generated electricity to electrolyze water (NUEL/CH1), as depicted in Figure 2. For these later two pathways, compressed hydrogen gas was produced, not LH_2. To estimate a GHG emission number for the pathway that would have led to LH_2, we modified the path to include a hydrogen liquefaction step, and increased the GHG emissions reported by the EU commission for the renewable compressed hydrogen product by a factor of 1.286 to reflect increased emissions associated with liquefaction using renewable energy. This factor was determined by taking the ratio of the GHG emissions reported for making LH_2 by fossil NG reforming (GPLH1b), 126.3 g CO_2 (eq.)/MJ_{fuel} to the GHG emissions reported for making compressed hydrogen by fossil NG reforming (GPCH$_2$b), 98.2 g CO_2 (eq.)/MJ_{fuel}. That ratio is 1.286 and is used to correct renewable pathway GHG emission reported for compressed gas to obtain the GHG emission for producing LH_2 via the same production method.

The results for the EU Commission report for total WTT GHG emissions in CO_2 (eq.) for the LH_2 production pathways of Figure 2 are reported in Figure 3. Only the total GHG figure is given. The EU Commission report [3] can be consulted for

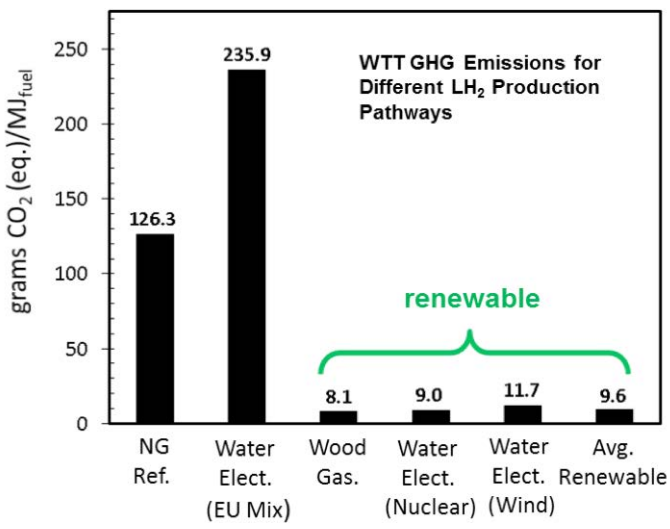

Figure 3: Total fuel pathway (WTT) GHG emissions in grams CO_2 (eq.)/MJ_{fuel} for the LH_2 production pathways considered in this study: (L-R); NG reforming, electrolysis of water using the EU grid mix, wood gasification, water electrolysis using nuclear-based electricity, water electrolysis using wind-based electricity, and the average of the renewable paths. The figure reports the GHG emissions associated with producing one MJ of finished fuel on a LHV basis, MJ_{fuel}. GHG emissions in units of grams CO_2 (eq.)/MJ_{fuel} are given for the LH_2 production pathways considered in this study. The figures report the GHG emissions associated with producing one MJ of finished fuel on a LHV basis, MJ_{fuel}.

the breakdown in the GHG emissions according to each pathway step (production at source, transportation to processing plant, processing to fuel, and fuel transport to market).

Figure 3 shows that the current commercial method of making LH_2, namely NG reforming to hydrogen followed by liquefaction (GPLH1b) produces 126.3 grams of CO_2 (eq.) per megajoule of LH_2 on a LHV basis. Recall that the LHV of hydrogen is 119.96 MJ/kg. Thus, 15.1 kg of CO_2 (eq.) emissions are released in the production of 1 kg of LH_2.

Water electrolysis using conventional grid power comprised of the EU mix produces 235.9 grams of CO_2 (eq.)/MJ_{fuel}, significantly worse than the fossil NG reforming route. This is because water electrolysis is very energy intensive. The EU Commission reports that it takes 1.13 MJ of process energy for every 1.0 MJ of LH_2 fuel produced by NG reforming. In contrast, it takes 4.22 MJ of process energy to make 1.0 MJ of LH_2 via water electrolysis. Thus, if the current carbon-rich electrical grid is used to perform the electrolysis, LH_2 production via water electrolysis is not competitive from a GHG perspective with steam methane reforming. We will not consider water electrolysis via the grid further.

Figure 3 shows that when renewable sources of hydrogen are available, then fuel pathway GHG emissions are dramatically reduced. Wood gasification (WFLH1) yields 8.1 grams of CO_2(eq.) for every 1.0 MJ (LHV) of LH_2. Electrolysis of water using low-carbon electricity sources such as nuclear power or wind also yield very low GHG emission values of 9.0 and 11.7 g CO_2 (eq.)/MJ_{fuel} , respectively. Taking the average of these renewable paths, we get an average renewable GHG emissions for the production and delivery of renewable LH_2 as 9.6 grams CO_2(eq.)/MJ_{fuel}. Since PEM fuel cells produce no emissions of any kind at the point of use, these WTT LH_2 production numbers provide the entire basis for estimating GHG emissions from the Zero-V. In other words, since the PEM fuel cell is zero emissions, the WTT emissions equal the WTW emissions for hydrogen PEM fuel cell technology.

In contrast, the use of diesel fuel on the "equivalent diesel-powered vessel " has two components of GHG emission. The first component lies in the production and delivery of diesel fuel. The EU Commission study reports that GHG emissions associated with diesel production is 14.2 g CO_2 (eq.)/MJ_{fuel}. Recalling the LHV of diesel is 43.4 MJ/kg, and noting the density of diesel fuel is 0.832 kg/L, making one gallon of diesel fuel releases 1.94 kg CO_2 (eq.) per gallon produced. This figure is significantly less than the 15.1 kg of CO_2 (eq.) emissions released in the production of 1 kg of LH_2 by fossil NG reforming. The emissions for manufacture of diesel fuel are less because there is dramatically less process energy used in refining petroleum to diesel fuel than in steam reforming NG to hydrogen. The EU Commission reports that it takes 0.16 MJ of process energy to make 1.0 MJ of diesel fuel. This can be compared to the 1.13 MJ of process energy it takes to make 1.0 MJ of LH_2 fuel by NG reforming. Only a portion of the process energy is tied up in liquefaction of hydrogen. The EU reports that to make and deliver 1.0 MJ of hydrogen compressed to 880 bar (pathway GPCH$_2$b) still requires 0.72 MJ of process energy. Summarizing, making LH_2 is very energy intensive compared to making diesel fuel, even when using the least-energy-intensive pathway for making hydrogen, namely steam reforming of fossil NG.

Since the carbon atoms in fossil diesel fuel came from the atmosphere millions of years ago, its combustion represents a significant addition to CO_2 already in the atmosphere. The EU commission reports that burning diesel fuel produces 73.2 g CO_2 (eq.)/MJ_{fuel}. This is nearly all produced as CO_2, assuming the average chemical formula for diesel fuel is $C_{12}H_{23}$. Thus, the total WTW GHG emissions from making and burning (to completion) 1.0 MJ (LHV) of fossil-derived diesel fuel is 14.2 g CO_2 (eq.) + 73.2 g CO_2 (eq.) = 87.4 g CO_2 (eq.)/MJ_{fuel}.

We consider "biodiesel fuel," specifically fatty acid methyl ester (FAME), to be the "renewable" fuel that could be used in an "equivalent biodiesel vessel." We don't anticipate there would be dramatic changes to the engines, fuel tanks, fueling systems or passenger capacity upon using biodiesel. With

the hardware, weight and passenger allotment of the vessel remaining the same, we can use the same general vessel design as the "equivalent diesel vessel" assess GHG emission for an equivalent vessel to the Zero-V, only running on biodiesel.

The EU Commission reports [3, 4] the energy and GHG emissions associated with making and delivering biodiesel fuel, with the most updated figures from the 2013 Report [4]. In Europe, biodiesel is mostly produced from rapeseed with some production using sunflower seeds as the feedstock. Since the carbon in these living materials came recently from atmospheric CO_2, burning biodiesel with CO_2 release is considered carbon neutral, and the WTW GHG emissions equal the WTT GHG emissions for biodiesel. However, the WTT GHG emissions for making and delivering biodiesel are not zero, since significant process energy is needed for farming the seeds and converting the biomass to fuel. Making biofuels from these seeds takes 1.20 MJ of process energy for every megajoule of biodiesel fuel produced. This is 7.5 times more process energy than it takes to make the energy equivalent of diesel fuel from petroleum (0.16 MJ/MJ_{fuel}). The WTT GHG emissions associated with making biodiesel fuel by the rapeseed and sunflower pathways is (taking the average of the two feedstocks) 55.0 g CO_2 (eq.)/MJ_{fuel} [4]. Although burning biodiesel does not release net CO_2, criteria pollutants are created, such as NO_x, HC and PM.

With this information in hand about the WTT GHG emissions associated with making and delivering LH_2 via the pathways of Figure 3, the WTT GHG emissions associated with making and delivering fossil diesel and biodiesel, as well as the GHG

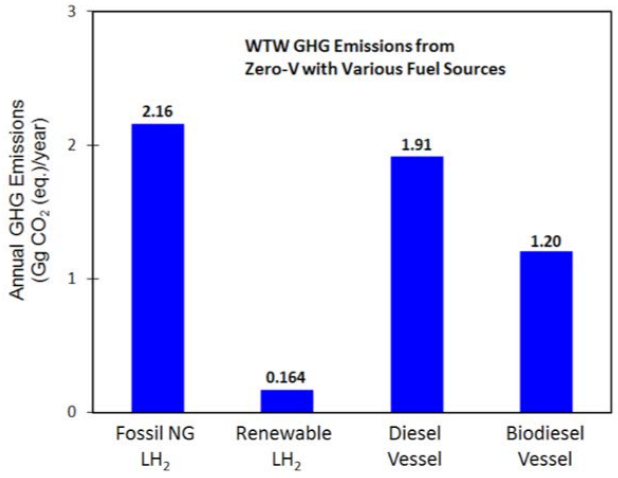

Figure 4: Predicted well-to-waves (WTW) GHG emissions per year for the Zero-V operating on fossil-based and renewable LH_2, compared to an equivalent diesel or biodiesel vessel.

emissions associated with burning fossil diesel, we can now assess and compare the well-to-waves GHG emissions from the Zero-V, an "equivalent diesel vessel" and "an equivalent biodiesel vessel" all in performing the same 14 Scripps science mission in a given year. The results are shown in Figure 4. Figure 4 shows that the annual WTW GHG emissions from the Zero-V fueled with LH_2 from fossil NG would be 2.16 Gigagrams (Gg) of CO_2 (eq.) per year, produced entirely during the production and delivery of the LH_2 fuel. Recall that a "Gigagram" is $1x10^9$ grams. This is slightly worse than the equivalent vessel running on fossil diesel, with WTW GHG emissions of 1.91 Gg CO_2 (eq.)/year, despite the fact that the Zero-V is 22% more energy efficient than the equivalent diesel vessel. The reason for this increase is the fact that making hydrogen is energy intensive in the first place, and hydrogen liquefaction involves significant energy and associated GHG emissions. This produces undesirable GHG emissions for the Zero-V along the fuel production and delivery path.

The situation is dramatically improved using renewable hydrogen. Taking the average value of the renewable production pathways, 9.6 g CO_2 (eq.)/MJ_{fuel} in Figure 3, Figure 4 shows the annual WTW GHG emissions from the Zero-V using renewable LH_2 becomes 0.164 Gg CO_2 (eq.)/year. This is 91.4% less than the WTW GHG emissions from the Diesel Vessel running on conventional diesel fuel. Figures 3 and 4 show that the real potential in hydrogen technology to reduce GHG lies NOT in the use of hydrogen derived from fossil NG, but rather in using renewable hydrogen. The renewable hydrogen considered for Figures 3 and 4 is nearly 100% renewable. In our discussions with the gas suppliers, renewable LH_2 can be made available to the Zero-V today in the quantities required, and are currently working to make renewable hydrogen more broadly available.

One could consider using biodiesel to power an "equivalent biodiesel vessel." Figure 4 shows that the well-to-waves GHG emissions are indeed reduced, from 1.91 Gg CO_2 (eq.)/year for diesel fuel to 1.20 Gg CO_2 (eq.)/year for biodiesel. This represents a 37% reduction in GHG emissions. The reduction is not as large as one might expect from a biofuel because making biodiesel is energy intensive. The analysis does not take into account that more biodiesel would have to be stored on the equivalent vessel because the LHV of biodiesel is ~ 37 MJ/kg [8], down from 43.4 MJ/kg for diesel fuel. The extra biodiesel fuel needing to be stored would increase the weight of the vessel, increasing the energy demand in the performance of the 14 Scripps science missions. Also, we note here that the biodiesel results in Figure 4 are for the particular FAME biodiesel productions paths considered in Ref. [4]. Biodiesel production paths can vary considerably, especially with regard to the fertilizer and water requirements. The WTW GHG emissions for a particular biodiesel pathway differing from those of Ref. [4] would have to be evaluated separately.

Traditional biodiesel is the fatty acid methyl ester product that results from the transesterification of vegetable oil or animal fats with methanol. The oils themselves are not compatible with diesel engine operation due to their higher viscosities, thus requiring the transesterification processing. In the ~2010 timeframe, there emerged alternative methods of oil processing that produced fuels whose composition more closely resembled fossil diesel. These products are called "renewable diesel" or "green diesel". Renewable diesel is produced primarily by "hydrodeoxygenation" in which the oil or fat feedstock is treated with hydrogen at elevated temperatures and pressures to produce long chain alkanes (not the esters of biodiesel) that resemble the components of fossil diesel fuel. In Europe, the product is called "hydrotreated vegetable oil" (HVO). The 2013 EU commission study [4] reports that the WTT GHG emissions (grams CO_2 (eq.)/MJ_{fuel}) for HVO and biodiesel are essentially the same. This means that the WTW GHG emissions for the "equivalent vessel" operating on renewable diesel would be essentially the same as that depicted in Figure 4 for biodiesel.

Summarizing the GHG results of Figure 4, hydrogen PEM fuel cell technology can dramatically reduce the GHG emissions from a high-performance research vessel. However, nearly 100% renewable hydrogen must be used to achieve the desired deep cuts in GHG emissions that are commensurate with the challenge presented by increased levels of infra-red radiation trapping gases in the atmosphere.

1.1.1.1 Results: Criteria Pollutant Emissions

Criteria pollutant emissions from the combustion of fossil fuels, among them nitrogen oxides (NO_x), hydrocarbons (HC) and particulate matter (PM) continues to be of concern due to their immediate adverse health effects. Since the PEM fuel cell does not involve combustion, it is incapable of producing criteria pollutants at the point of use. As a result, any criteria pollutant emissions associated with the Zero-V arise entirely from emissions associated with the production and transport of LH_2 to the vessel, namely the WTT criteria pollutant emissions. Criteria pollutant emissions can arise from combustion used to create the process heat needed to heat the reactants of the SMR process or as a byproduct of the SMR process. Alternatively, combustion could be used to generate the electricity used in hydrogen liquefaction.

Analogously, criteria pollutant emissions are associated with the production and delivery of diesel fuel. For example, the diesel-fueled tanker truck delivering diesel fuel is a source of diesel pathway criteria pollutant emissions. If the diesel fuel originates from petroleum ("fossil diesel"), then there is the additional criteria pollutant emissions associated with burning the fuel in the research vessel diesel engines. As a result, criteria pollutant emissions from an equivalent diesel-powered vessel using fossil diesel fuel involve two sources: (1) production and delivery of the diesel fuel and (2) combustion of the fuel onboard the vessel. If the diesel fuel originates from biomass ("biodiesel"), there are still criteria pollutant emissions released on the vessel, even though biodiesel reduces GHG emissions because the carbon released on the vessel originated recently from CO_2 in the air.

The European commission WTT analysis for automotive fuels in 2007 [3], updated in 2013 [4], were used as the basis for our GHG analysis. However, these studies did not provide information on criteria pollutant WTT emissions. For WTT fuel pathway criteria pollutant emissions, we use a 2007 analysis conducted by Unnasch and Pont of TIAX LLC for the California Energy Commission (CEC).[9]

The TIAX WTT study provides estimates for criteria pollutant emissions based on the energy consumption of various fuel paths, including the production and delivery of LH_2, diesel fuel and biodiesel. Combustion energy consumption is the principle source of criteria emission in these fuel pathways. The study reports emissions from the perspective of exposure to an individual in California, and thus is somewhat California specific. This is an advantage of the analysis for the present purposes as we consider the case of the Zero-V initially operating along the California coastline.

The TIAX study generally follows the spirit of the pathways indicated in Figure 2. The pathway for production of LH_2 from fossil NG is similar to that in Figure 2 (labeled GPLH1b from the European Commission study), except that the distance for LH_2 road transport was assumed to be 80.5 km (50 miles) instead of 300 km. The renewable pathways for LH_2 production shown in Figure 2, namely wood gasification, wind electrolysis of water and nuclear power electrolysis of water, were not considered in the TIAX criteria pollutant emissions analyses.

Fuel Pathway	NO_x (g/GJ_{fuel})	HC (g/GJ_{fuel})	PM (g/GJ_{fuel})
Fossil NG LH_2 Fuel Pathway	45.0	3.5	5.0
70% Renewable LH_2 Fuel Pathway	2.1	2.0	3.9
100% Renewable LH_2 Fuel Pathway	0.83	0.083	0.029
Fossil Diesel Fuel Pathway	1.4	3.5	0.06
Biodiesel Fuel Pathway	4.5	3.4	0.18

Table 2: WTT criteria pollutant emissions for fuel pathways on a LHV basis. GJ_{fuel} represents the lower heating value (LHV) of the indicated fuel in gigajoules (GJ). 1 GJ = 1 x 10^9 J. The 100% Renewable LH_2 fuel pathway assumes the hydrogen is delivered 80.5 km (50 miles) in a diesel-fueled trailer.

However, there was an analysis performed for criteria emissions associated with conventional water electrolysis (labeled EMEL1/CH1 from the European Commission study) producing gaseous hydrogen using 70% renewable power at an on-site facility (i.e. no road transport). We multiply the criteria pollutant emissions for this 70% renewable path by the factor 1.286 to account for emissions associated with liquefaction using renewable energy, and also add emissions associated with tanker transport of the LH_2 over a distance of 80.5 km (50 miles). We adopt this revised pathway to represent criteria pollutant emissions associated with "70% Renewable LH_2."

Using 100% renewable electricity for the fuel manufacturing, the WTW criteria pollutant emissions for the Zero-V would collapse to those for LH_2 trailer transport operating on diesel fuel. If the LH_2 trailer ran on 100% renewable hydrogen instead of diesel fuel, the criteria pollutant emissions could be essentially eliminated.

Table 2 reports the WTT criteria pollutant emissions associated with the fuel pathways for LH_2 produced by steam methane reforming of fossil NG, 70% renewable LH_2, 100% renewable LH_2 (with diesel truck transport), fossil diesel fuel and biodiesel. The results are reported in terms of grams of pollutant emitted per gigajoule (LHV) of the fuel energy.

	NO_x (kg/year)	HC (kg/year)	PM_{10} (kg/year)
Zero-V Fossil NG LH_2 Fuel Pathway, WTT	769.05	59.82	85.45
Zero-V 70% Renewable LH_2 Fuel Pathway, WTT	35.89	34.18	66.65
Zero-V 100% Renewable LH_2 Fuel Pathway, WTT	14.24	1.42	0.50
Zero-V Fuel Cell Engine	0.00	0.00	0.00
Zero-V Fossil NG LH_2 Total (Pathway + Engine), WTW	769.05	59.82	85.45
Zero-V 70% Renewable LH_2 Total (Pathway + Engine), WTW	35.89	34.18	66.65
Zero-V 100% Renewable LH_2 Total (Pathway + Engine), WTW	14.24	1.42	0.50
Diesel Fuel Pathway, WTT	30.66	76.65	1.31
Biodiesel Fuel Pathway, WTT	98.55	74.46	3.94
***Diesel Vessel* Tier 4 Engine**	4090.50	433.60	89.99
***Diesel Vessel* Tier 4 Diesel Total (Pathway + Engine), WTW**	4121.16	510.25	91.30
***Biodiesel Vessel* Tier 4 Biodiesel**	4189.05	508.06	93.93

Table 3: Fuel pathway (WTT) criteria pollutant emissions and well-to-waves (pathway + engine, WTW) emissions on a kilograms/year basis calculated for the Zero-V and the equivalent diesel research vessel and the equivalent biodiesel research vessel. The engine criteria pollutant emissions of the equivalent diesel and equivalent biodiesel research vessels are set to the Tier 4 limits for engine operation.

The "Fossil NG LH_2 Fuel Pathway" has sizeable criteria pollutant emissions. This is due to the use of combustion (typically of NG) to heat the SMR reactor to the required ~ 900 °C. In addition, combustion is used to provide electricity for the process equipment via the California grid (of which 50.9% is derived from burning NG or coal, see Table 1), and combustion is used to power the LH_2 tanker truck as it drives 80.5 km in delivering LH_2. In the TIAX study [9] it was noted for this fuel pathway that there exists somewhat high PM emissions for natural gas combined cycle power plants which constitute 44.5% of the California grid mix. The origin is not the increased (~ 2x) PM emissions associated with LH_2 trailer transport compared to diesel fuel transport [9]. Indeed, the PM release from trailer transport of 4000 kg of LH_2 a distance of 80.5 km is predicted [9] to be only 0.029 g/GJ_{fuel} ; ~0.6% of the overall WTT PM emissions of 5.0 g/GJ_{fuel} for the Fossil NG LH_2 Fuel Pathway reported in Table 2. It is the energy intensity of hydrogen production, not transport, which drives the associated WTT criteria pollutant emissions.

The "70% Renewable LH_2 Fuel Pathway" has substantially reduced NO_x emissions because the electrolysis of water does not require the high process heat of the SMR production method. However, as stated previously, electrolysis of water is very energy intensive. Recall that it takes 4.22 MJ of process energy to make 1.0 MJ of LH_2 (LHV) via water electrolysis. The 30% of the energy that is not renewable (fossil-fuel based), combined with the large requirement for electrolysis process energy, produce non-zero amounts of NO_x, HC and PM emissions per GJ_{fuel}, as shown in Table 2. Using 100% renewable electricity for the fuel manufacturing, the WTW criteria pollutant emissions for the Zero-V collapses to those for LH_2 trailer transport operating on diesel fuel. It is conceivable that hydrogen-powered trailers, running on 100% renewable hydrogen, will one day be the preferred delivery method for hydrogen. For this case, the emissions associated with 100% Renewable LH_2 would essentially vanish.

Table 2 also lists the WTT criteria pollutants associated with making and delivering fossil diesel and biodiesel. The criteria pollutant emissions for biodiesel are generally higher than for fossil diesel because of the increased process energy needed to make biodiesel fuel, as mentioned earlier.

Using these values in Table 2, we can calculate the annual fuel pathway (WTT) criteria pollutant emissions for the Zero-V

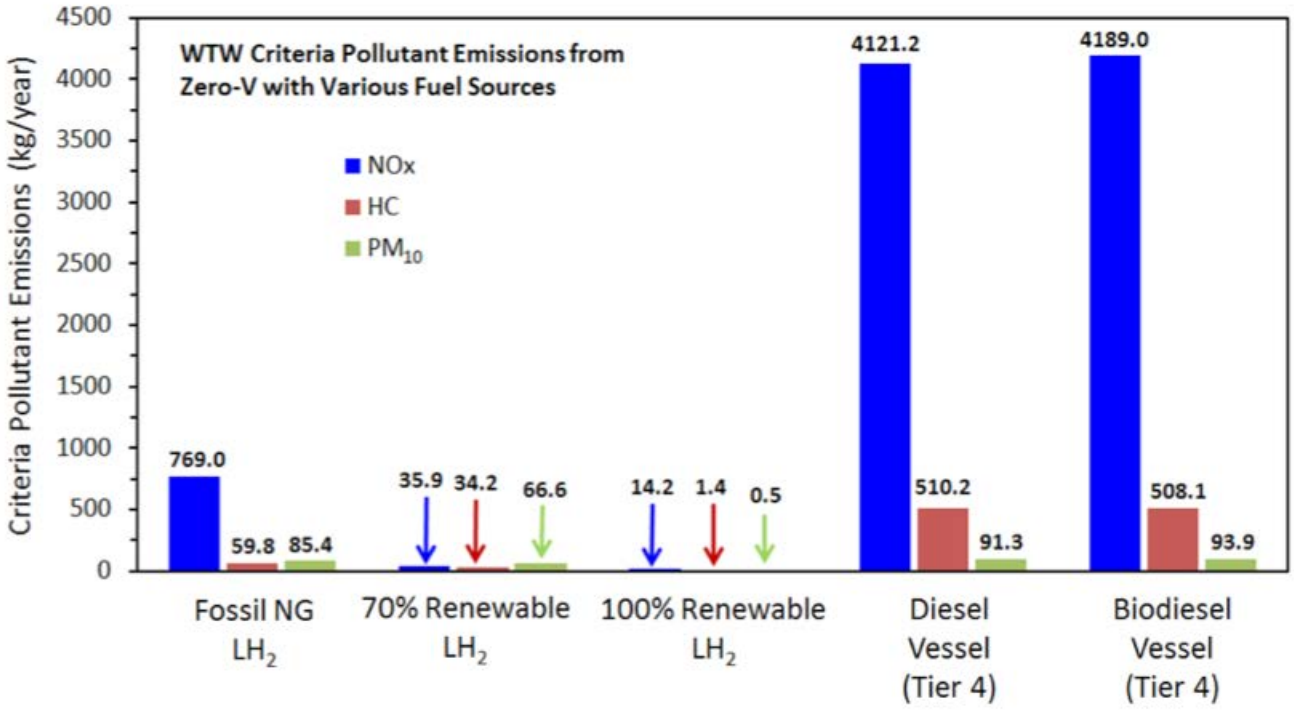

Figure 5 : Predicted annual well-to-waves (WTW) criteria pollutant emissions for the Zero-V operating on various hydrogen fuels, and the equivalent diesel and biodiesel vessels constrained to Tier 4 emission limits.

and again compare to the equivalent diesel vessel and the equivalent biodiesel vessel. We do this by combining the WTT criteria pollutant emission values in Table 2 with the vessel fuel use numbers for the Zero-V and the equivalent diesel vessel. These results are shown in Table 3 for the Zero-V and equivalent diesel and biodiesel research vessels. Well-to-waves (WTW) criteria pollutant emissions (pathway + engine) for the Zero-V are equal to the LH_2 well-to-tank (WTT) fuel pathway emissions because the PEM fuel cell criteria pollutant emissions are zero.

For Table 3 we constrain both the diesel and biodiesel engine emissions of the Vallejo to be at the Tier 4 criteria pollutant emission limits. In this way, we are comparing the Zero-V to a new vessel build (one based on either fossil diesel or biodiesel) which must meet the Tier 4 limits by regulation. While the hydrogen PEM fuel cell technology automatically satisfies the Tier 4 criteria emission requirements because it is zero-emission technology at the point of use, the WTW hydrogen analyses capture important fuel production pathway and delivery emissions.

The results for WTW criteria pollutant emissions shown in Table 3 are presented graphically in Figure 5. The first aspect of Figure 5 to notice is that the WTW criteria pollutant emissions for the "equivalent vessel" running on diesel fuel or biodiesel are very nearly the same. Although the WTT criteria pollutant emissions for the production and delivery of biodiesel are higher than those for fossil diesel (see Table 3) due to the increased process energy required, the WTT criteria pollutant emissions are only a small fraction of the overall WTW criteria pollutant emissions, as indicated in Table 3. This finding, combined with the onboard criteria emissions for the equivalent vessel running on fossil diesel or biodiesel set equal to each other at the Tier 4 limits, produces the similarity for these fuels seen in Figure 5.

The TIAX report [9] did not examine criteria emissions from renewable diesel because it was a barely emerging technology at the time of the report. There have been no published analyses of the WTT criteria pollutant emissions associated with the production and delivery of renewable diesel. However, the EU Commission study [4] reports that the WTT energy required to make HVO (renewable diesel) and biodiesel are very nearly the same. This suggests that the WTW criteria pollutant emissions from the equivalent vessel operating on renewable diesel would be similar to that reported in Table 3 and Figure 5 for the vessel operating on biodiesel. This finding is analogous to the similarity of renewable diesel and biodiesel in the WTW GHG emissions discussed previously in connection with Figure 4.

Table 3 and Figure 5 show that the Zero-V operating on LH_2 derived from NG SMR reduces WTW NO_x by ~ 81.3% below

that of the equivalent vessel operating on fossil diesel fuel (but held to Tier 4 emission standards). Using 70% Renewable LH_2 on the SF-BREEZE, the WTW NO_x is reduced 99.1% below the equivalent vessel fossil diesel levels. These reductions in NO_x can be traced to relatively less NOx being produced when NG is burned for SMR process heat, and dramatically less NO_x associated with electrolysis of water using 70% renewable electricity [9]. WTW HC is reduced ~ 88.3% below that of the equivalent vessel operating on fossil diesel fuel (but held to Tier 4 emission standards) when the Zero-V is operated on LH_2 derived from NG SMR. Using 70% Renewable LH_2, the WTW HC is reduced 93.3% below the Tier 4 equivalent vessel fossil diesel levels.

Figure 5 shows that the WTW PM emissions associated with the Zero-V using 70% Renewable LH_2 are only slightly smaller than the WTW PM emissions of the equivalent vessel running on fossil diesel. In the TIAX study [9] it was noted for this fuel pathway that there exists somewhat high PM emissions for natural gas combined cycle power plants which constitute 44.5% of the California grid mix.

Using 100% renewable electricity, the WTW criteria pollutant emissions for the Zero-V collapse to those for LH_2 trailer transport operating on diesel fuel. Thus, using 100% renewable electricity, the Zero-V WTW emissions would represent a 99.6% reduction in NO_x, a 99.7% reduction in HC and a 99.4% reduction in PM compared to the equivalent vessel running on diesel fuel with Tier 4 emission constraints. If the LH_2 trailer ran on 100% renewable hydrogen instead of diesel fuel, the criteria pollutant emissions could be essentially eliminated.

Summarizing these criteria pollutant emission results, the Zero-V goes far beyond the Tier 4 criteria pollutant emissions requirements for new vessel construction in the U.S. because the powerplant is zero emissions at the point of use. Hydrogen PEM fuel cell technology can dramatically reduce WTW NO_x and HC emissions below the most advanced Tier 4 criteria pollutant emissions requirements regardless of whether the hydrogen is made by NG reforming or using more renewable means. Overall, the results show that operating a hydrogen fuel cell ferry on nearly 100% renewable hydrogen provides the dramatic reduction in vessel GHG and criteria pollutant emissions commensurate with the problems of global climate change and increasing maritime air pollution worldwide.

References

[1.] Personal communication with R. Sookhoo, Director New Initiatives at Hydrogenics, 2016-2017.

[2]. "*HyPM-HD Power Modules for light to heavy duty mobility,*" Hydrogenics, 2015. Available: http://www.hydrogenics.com/docs/default-source/default-document-library/hypm-hd-8pg-jan2015-lr.pdf?sfvrsn=0,

[3]. R. Edwards, J.-F. Larive, V. Mahieu, and P. Rouveirolles, "*Well-to-Wheels Analysis of Future Automotive Fuels and Powertrains in the European Context: Well-to-Tank Report, Version 2C*," Joint Research Center of the European Commission, 2007.

[4]. R. Edwards, J.-F. Larive, D. Rickeard, and W. Weindorf, "*Well-to-Wheels Analysis of Future Automotive Fuels and Powertrains in the European Context: Well-to-Tank Report, Version 4*," Joint Research Center of the European Commission, 2013.

[5]. J.W. Pratt and L.E. Klebanoff, "*Feasibility of the SF-BREEZE: A Zero-Emission, Hydrogen Fuel Cell, High-Speed Passenger Ferry,*" Sandia National Laboratories Report: SAND2016-9719, September 2016.

[6]. L.E. Klebanoff , J.W. Pratt, C.M. Leffers, K.T. Sonerholm, T. Escher, J. Burgard, and S. Ghosh, "*Comparison of the Greenhouse Gas and Criteria Pollutant Emissions from the SF-BREEZE High-Speed Fuel-Cell Ferry with a Diesel Ferry*," Transportation Research D **54**, 250 (2017).

[7]. California Energy Commission, "*Utility Annual Power Content Labels for 2014*," State of California, 2016. Available: http://www.energy.ca.gov/pcl/labels/index.html, Accessed May 24, 2016.

[8]. P. S. Mehta and K. Anand, "*Estimation of a Lower Heating Value of Vegetable Oil and Biodiesel Fuel,*" Energy and Fuels **23**, 3893-3898, 2009.

[9]. S. Unnasch and J. Pont, "*Full Fuel Cycle Assessment Well to Tank Energy Inputs, Emissions, and Water Impacts,*" TIAX, LLC, for the California Energy Commission, CEC-600-2007-002-D,2007.

Appendix: D

TRD Article on CO_2(eq.) and Criteria Pollutant Emissions from the SF-BREEZE

Presented here is a paper published in Transportation Research Part D that discusses in detail the CO_2(eq.) and criteria pollutant emissions from the SF-BREEZE fuel cell ferry. The article is referenced: "Comparison of the Greenhouse Gas and Criteria Pollutant Emissions from the SF-BREEZE High-Speed Fuel-Cell Ferry with a Diesel Ferry," L.E. Klebanoff , J.W. Pratt, C.M. Leffers, K.T. Sonerholm, T. Escher, J. Burgard, and S. Ghosh, Transportation Research D **54**, 250 (2017).

Comparison of the Greenhouse Gas and Criteria Pollutant Emissions from the SF-BREEZE High-Speed Fuel-Cell Ferry with a Diesel Ferry

L.E. Klebanoff *,[1], J.W. Pratt1, C.M. Leffers[2], K.T. Sonerholm[2], T. Escher[3], J. Burgard[3], and S. Ghosh[4]

[1]Sandia National Laboratories, 7011 East Avenue, Livermore CA 94551 USA

[2]Elliott Bay Design Group, 5305 Shilshole Avenue NW, Seattle WA 98107 USA

[3]Red and White Fleet, 43 The Embarcadero, San Francisco, CA 94105 USA

[4]U.S. Maritime Administration, 1200 New Jersey Avenue SE, Washington D.C. 20590 USA

*author to whom correspondence should be addressed: lekleba@sandia.gov

Keywords: Hydrogen, PEM Fuel Cell, GHG Emissions, Ferry Emissions, Criteria Pollutant Emissions

Transportation Research Part D 54 (2017) 250–268

Contents lists available at ScienceDirect

Transportation Research Part D

journal homepage: www.elsevier.com/locate/trd

Comparison of the greenhouse gas and criteria pollutant emissions from the SF-BREEZE high-speed fuel-cell ferry with a diesel ferry

L.E. Klebanoff [a,*], J.W. Pratt [a], C.M. Leffers [b], K.T. Sonerholm [b], T. Escher [c], J. Burgard [c], S. Ghosh [d]

[a] Sandia National Laboratories, 7011 East Avenue, Livermore, CA 94551, USA
[b] Elliott Bay Design Group, 5305 Shilshole Avenue NW, Seattle, WA 98107, USA
[c] Red and White Fleet, 43 The Embarcadero, San Francisco, CA 94105, USA
[d] U.S. Maritime Administration, 1200 New Jersey Avenue SE, Washington, D.C. 20590, USA

ARTICLE INFO

Article history:

Keywords:
Hydrogen
PEM fuel cell
GHG emissions
Ferry emissions
Criteria pollutant emissions

ABSTRACT

A theoretical comparison is made of the "well to waves" (WTW) greenhouse gas (GHG) and criteria pollutant emissions from the SF-BREEZE high-speed hydrogen PEM fuel cell ferry and the VALLEJO ferry powered by traditional diesel engine technology but constrained to Tier 4 emissions standards. The emissions were calculated for a common maritime mission, the current ferry route between Vallejo CA and San Francisco CA. Calculations are made of the energy required for the SF-BREEZE and VALLEJO to perform the mission route profile. The SF-BREEZE requires 10.1% more fuel energy than the VALLEJO, primarily due to the SF-BREEZE being heavier. Estimates are made for the SF-BREEZE GHG emissions associated with five LH_2 fuel production pathways including renewable and non-renewable (fossil-fuel based) methods. Estimates are also made for GHG emissions associated with fossil-diesel production and delivery as well as those for biodiesel, which can be considered a renewable "drop-in" fuel replacement for conventional diesel fuel. We find that the GHG emissions for the SF-BREEZE using non-renewable LH_2 are significantly higher than for the Tier 4 diesel-fueled VALLEJO on a per passenger basis. However, using renewable LH_2, the GHG emissions for the SF-BREEZE ferry are reduced 75.8% compared to the diesel-fueled VALLEJO operating at Tier 4 emissions standards. We also compare the criteria pollutant emissions (NO_x, HC, PM_{10}) for the SF-BREEZE to that of the VALLEJO held to Tier 4 emissions standards fueled by diesel fuel or biodiesel. Hydrogen PEM fuel cell technology dramatically reduces NO_x and HC emissions below the most advanced Tier 4 criteria pollutant emissions requirements regardless of whether the LH_2 is made by NG reforming or via water electrolysis using 70% renewable energy. Renewable LH_2 made with greater than 84% renewable process energy is needed to also drop the SF-BREEZE PM_{10} emissions below that of Tier 4 for high-speed fuel cell ferry transportation. Overall, the results show that operating a hydrogen fuel cell ferry on nearly 100% renewable hydrogen provides the dramatic reduction in GHG and criteria pollutant emissions commensurate with the problems of global climate change and maritime air pollution worldwide.

* Corresponding author.
E-mail address: lekleba@sandia.gov (L.E. Klebanoff).

http://dx.doi.org/10.1016/j.trd.2017.05.012
1361-9209/

Abstract

A theoretical comparison is made of the "well to waves" (WTW) greenhouse gas (GHG) and criteria pollutant emissions from the SF-BREEZE high-speed hydrogen PEM fuel cell ferry and the VALLEJO ferry powered by traditional diesel engine technology but constrained to Tier 4 emissions standards. The emissions were calculated for a common maritime mission, the current ferry route between Vallejo CA and San Francisco CA. Calculations are made of the energy required for the SF-BREEZE and VALLEJO to perform the mission route profile. The SF-BREEZE requires 10.1% more fuel energy than the VALLEJO, primarily due to the SF-BREEZE being heavier. Estimates are made for the SF-BREEZE GHG emissions associated with five LH_2 fuel production pathways including renewable and non-renewable (fossil-fuel based) methods. Estimates are also made for GHG emissions associated with fossil-diesel production and delivery as well as those for bio-

diesel, which can be considered a renewable "drop-in" fuel replacement for conventional diesel fuel. We find that the GHG emissions for the SF-BREEZE using non-renewable LH_2 are significantly higher than for the Tier 4 diesel-fueled VALLEJO on a per passenger basis. However, using renewable LH_2, the GHG emissions for the SF-BREEZE ferry are reduced 75.8% compared to the diesel-fueled VALLEJO operating at Tier 4 emissions standards. We also compare the criteria pollutant emissions (NO_x, HC, PM_{10}) for the SF-BREEZE to that of the VALLEJO held to Tier 4 emissions standards fueled by diesel fuel or biodiesel. Hydrogen PEM fuel cell technology dramatically reduces NO_x and HC emissions below the most advanced Tier 4 criteria pollutant emissions requirements regardless of whether the LH_2 is made by NG reforming or via water electrolysis using 70% renewable energy. Renewable LH_2 made with greater than 84% renewable process energy is needed to also drop the SF-BREEZE PM_{10} emissions below that of Tier 4 for high-speed fuel cell ferry transportation. Overall, the results show that operating a hydrogen fuel cell ferry on nearly 100% renewable hydrogen provides the dramatic reduction in GHG and criteria pollutant emissions commensurate with the problems of global climate change and maritime air pollution worldwide.

Introduction

Keller et al. have described [1] the growing problem of greenhouse gas (GHG) emissions (such as CO_2, CH_4, N_2O), its origin in the early 1900s, and how hydrogen can form the basis for a zero-carbon energy system. Unless we have new transportation technology with emissions reductions approaching 80% or more, the emission reductions will not be robust against growth in either population, or in the intensity with which technology uses energy [1]. Such deep cuts are consistent with recommendations from the Intergovernmental Panel on Climate Change (IPCC) [2] and U.S National Academy of Sciences studies [3]. While use of fossil-based hydrogen allows the introduction of the hydrogen-based power conversion technology [4], ultimately renewable hydrogen may be required to provide the GHG reduction commensurate with the global climate change problem.

Criteria pollutant emissions from the combustion of fossil fuels, among them nitrogen oxides (NO_x), hydrocarbons (HC) and particulate matter (PM) continue to be of concern due to their immediate adverse health effects. These adverse health effects include worsening of asthma, chronic bronchitis, respiratory tract infection, heart disease and stroke [5]. Although criteria pollutant emissions have been regulated from land-based transportation since the 1960's, regulation of criteria pollutant marine emissions has only existed since 1999 when the U.S. EPA introduced the Tier 1 Marine Engine Standards.

Psaraftis and Kontovas [6] estimated that in 2007, aggregate CO_2 emissions from all marine vessels (including crude oil tankers, cargo vessels, Ro-Ro vessels, and passenger ships) summed to 943.4 million metric tonnes (MMT), with 89% of the marine CO_2 emissions coming from large international cargo vessels. Boden and coworkers [7] have estimated that global GHG emissions in 2007 were 31,284 MMT CO_2 (eq.). Thus, worldwide maritime transportation accounts for ~ 3.0% of global GHG emissions. Excluding large international cargo vessels, marine transportation accounts for 0.33% of global GHG emissions.

Since January 2013 energy efficiency regulations have been in place for large new ocean-going vessels such as tankers, bulk carriers, gas carriers and container ships. Known as the "Amendments to MARPOL Annex VI," the Energy Efficiency Design Index (EEDI) is the first legally binding global mandatory GHG emission reduction regulation since the 1997 Kyoto Protocols. The regulation requires a "phased in" increase in vessel energy efficiency, thereby reducing both GHG and criteria pollutant emissions, to an ultimate target of 30% improvement by 2025 and beyond [8]. Unfortunately, the benefits derived from the 30% reduction in emissions will be eroded by expected increase in the size of the fleet of such vessels in the near future. There has yet to be established GHG regulations for the smaller passenger vessels ("ferries") being considered here.

The International Maritime Organization's (IMO) Third IMO GHG Study 2014 [9] comprehensively describes the expected increases in worldwide shipping emissions over the next 35 years as global GDP increases and marine transportation increases along with it. The study examines various cases of shipping types, efficiency improvements, and fuel types and concludes that even with projected improvements, in 2050 GHG emissions from shipping will be ~ 50% to 250% higher than 2012 levels. Particularly important are the following observations about GHG emission projections [9]:

"The emissions projections show that improvements in efficiency are important in mitigating emissions growth but even the most significant improvements modelled do not result in a downward trend. Compared to regulatory or market-driven improvements in efficiency, changes in the fuel mix have a limited impact on GHG emissions, assuming that fossil fuels remain dominant."

In other words, despite reductions in per-unit GHG emissions due to fuel changes and efficiency improvements, the increase in maritime transportation activity will still result in an overall increase in sector GHG emissions as long as fossil

fuels are the primary fuel. An analogous conclusion was also drawn for the light-duty vehicle market [1]. The only way to truly reduce GHG emissions in the face of increasing transportation activity is to transition to a zero GHG-emitting mode of transportation.

On a more local level, the California Air Resources Board (ARB) has estimated [10] that the total GHG emissions for the State of California in 2014 were 441.5 MMT CO_2 (eq.). ARB has also made emissions estimates for "harbor craft," defined as all vessels that operate within California coastal waters and inland waterways, and has a home port located in California. By definition, harbor craft excludes the large international cargo vessels, but includes ferries. The California ARB estimates harbor craft GHG emissions in 2014 were 1.548 MMT CO_2 (eq.) [10]. Thus, in California, harbor craft account for 0.35% of the statewide California GHG emissions, in good accord with the 2007 global estimate [6] for fractional GHG emissions from such vessels.

As for criteria pollutant emissions, ARB data indicate that harbor craft emitted 2.8% of the NO_x emissions in the State of California, 0.095% of the HC emissions, and 0.10% of the PM emissions in the State. Although these numbers may seem small, as noted by Corbett and Farrell [11], emissions from passenger ferries constitute a highly visible pollution source in close proximity to dense population areas where emissions most adversely affect human health. Indeed, the California ARB considers passenger ferries, along with other commercial harbor craft, to be important sources of pollutant emissions in California, especially in coastal areas with high marine activity. In 2004, ARB estimated that emissions from commercial harbor craft in the San Francisco Bay Area Air Quality Management District (BAAQMD) were equivalent to nearly 60% of the heavy-duty diesel trucks in the area [12].

Consequently, criteria pollutant emissions from harbor craft have come under increasing levels of regulation [13]. In 1999, the U.S. Environmental Protection Agency (EPA) instituted the Tier 1 Marine Engine Standards [14]. These regulations were enforced on engines built in the model year 2004. Stricter U.S. EPA Tier 2 regulations were created to cover marine engines built in model year 2007. These criteria emission regulations were followed by the U.S. EPA Tier 3 Marine Standards for marine diesel Category 1 engines, with the Tier 3 standards imposed on engines built in the 2012 – 2014 timeframe. The current U.S. EPA regulations for criteria pollutant emissions from marine propulsion engines are the Tier 4 Marine Standards [15]. Any new build of a passenger ferry in the U.S. must adhere to the Tier 4 emission standards. For the passenger ferry discussed here, the Tier 4 emission limits are set per propulsion engine output energy: NO_x = 1.8 g/kW-hr, HC = 0.19 g/kW-hr and PM = 0.04 g/kW-hr.

Recently, there has been increasing efforts to understand not only GHG and criteria pollutant emissions associated with larger Emission Control Areas (ECAs) (e.g. Baltic Sea, North Sea), [16] but also for specific ports as well [17-22]. Port emissions derive from trucks transporting shipping containers [17,18], landside equipment and emissions from vessels [19-22]. For vessels, Chang and co-workers have examined the emission inventory for a variety of fossil-fuel vessels at the Port of Incheon Korea for both criteria pollutants [19] and CO_2 [20]. Song considered the GHG and criteria pollutant emission inventories and associated social costs for the Yangshan Port south of Shanghai China [21]. Tzannatos has examined the criteria pollution emissions from passenger vessel traffic at the Port of Piraeus in Greece [22].

Amongst the different types of vessels at ports, there is increased interest in passenger ferries as a way to relieve the oversubscription of land transportation modes. This interest generates renewed focus on the GHG and criteria pollutant emissions coming from ferries. In this work, we examine the impact on the GHG and criteria pollutant emissions of using hydrogen PEM fuel cell technology in a high-speed ferry application. Emissions are directly compared with those from a present day diesel-powered high-speed ferry considered to be operating under Tier 4 emission constraints fueled with either traditional diesel fuel or biodiesel. Since we use a fuel-cell ferry designed to match the mission of the analogous diesel ferry, the emission comparisons should be quite accurate for the high-speed class of ferries.

Our objective is not to conduct an inventory of emissions in the San Francisco Bay Area, or for any specific geographic region. Rather, the results reported here provide the first technical input for hydrogen fuel-cell vessel emissions that will inform future studies calculating the vessel emission inventories for ports and larger ECAs in which hydrogen infrastructure and technology has been introduced or is being contemplated. Our work also emphasizes that emissions associated with fuel production must be explicitly examined for future studies of marine emissions derived from hydrogen use, and we present the first such "well-to-waves" (WTW) analysis associated with hydrogen vessel operation

Background on Hydrogen and Proton Exchange Membrane Fuel Cells

As reviewed by Klebanoff et al. [4], high efficiency hydrogen energy conversion devices that convert hydrogen into electrical or shaft power are powerful drivers for hydrogen technology. Proton Exchange Membrane (PEM) fuel cells in particular are already finding use in light-duty fuel-cell vehicles and other mobility power applications. A hydrogen fuel cell is an

electrochemical device that executes the hydrogen/oxygen reaction (1) without direct combustion [4]:

$$2H_2\,(g) + O_2\,(g) \rightarrow 2H_2O\,(g) + Q, \qquad (1)$$

where hydrogen (H_2) is stored in some fashion, oxygen (O_2) typically comes from the air, and Q is the energy released by the reaction, apportioned between electrical work and thermal energy. The PEM fuel cell is perhaps the simplest of the fuel cells [4].

The most gravimetrically and volumetrically efficient way of storing large amounts of hydrogen is as liquid hydrogen (LH_2). LH_2 is very similar to liquid natural gas (LNG) in its physical properties, with LH_2 being colder. Both LH_2 and LNG are cryogenic fuels stored in sturdy double-walled vacuum-insulated vessels, and vaporize readily to gases that are lighter than air. Both hydrogen/air and natural gas/air mixtures can be ignited easily by weak ignition sources such as static electric discharges and hot surfaces. A detailed comparison of the safety-related physical and combustion properties of LH_2 and LNG has recently been published by Klebanoff and co-workers [23].

Figure 1 shows the relevant reactions in a H_2 PEM fuel cell

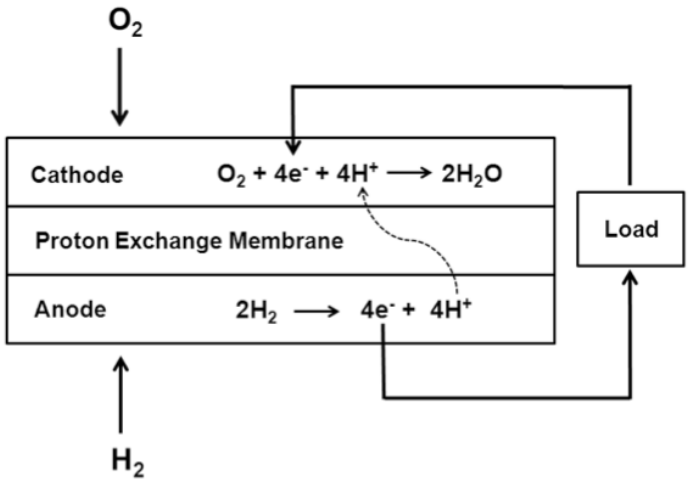

Figure 1: Schematic diagram of a PEM fuel cell, reproduced with permission from Reference 4.

[4]. At the anode, hydrogen gas ionizes, releasing protons to the membrane and electrons to the external circuit. At the cathode, oxygen molecules are reduced in an acidic environment by electrons from the circuit, forming water molecules. Protons pass through the proton exchange membrane, from anode to cathode, completing the circuit while electrons are driven through the load by the electromotive force of reaction (1).

Commercial fuel cell units consist of "stacks" of the fundamental PEM fuel cell unit shown in Figure 1. The PEM fuel cell generates electricity with a thermal efficiency (electrical work out/fuel energy in) of ~ 41 – 53%, depending on the load. It uses pure hydrogen (typically > 99.95% pure) at the anode, and can operate at relatively low temperatures (50 – 100 °C), using a catalyst (typically platinum) to increase the reaction kinetics. PEM fuel cells are dramatically quieter than internal combustion engine (ICE) technology [4]. Since there is no combustion occurring in the fuel cell and the fuel is pure hydrogen, there is zero NO_x emission, zero SO_x, zero hydrocarbons (HC) and zero particulate emission. The PEM fuel cell is certified as a zero-emissions power system by the California ARB. The PEM fuel cell offers high power density, high efficiency, the potential for good cold and transient performance and is amongst the lightest and most compact of fuel cells. Furthermore, the PEM fuel cell is commercially available with an excellent performance track record. These advantages, combined with it being a zero-emission source, made the PEM fuel cell the hydrogen engine of choice for the San Francisco Bay Renewable Energy Electric Vessel with Zero Emissions (SF-BREEZE).

The thermal efficiency of the electrochemical process can be significantly higher than traditional internal combustion engines (ICEs), due to engine materials limits to the temperature at which combustion can be conducted. However, in the absence of such limits, both ICEs and fuel cells have equivalent thermal efficiencies [24-26]. Whereas traditional gasoline combustion has a thermal efficiency of ~35%, limited by the temperatures achievable in traditional combustion systems, the thermal efficiency of the electrochemical process can exceed ~ 50%. Thus, 50% of the energy released by reaction (1) can be converted to electricity, with the remaining 50% constituting "waste heat" which is removed from the system by cooling air or liquid. In "combined cycle" fuel cell systems, this waste heat can be captured and used, which would increase the effective fuel-cell system thermal efficiency beyond 50%.

Theory/Calculations

Design of the SF-BREEZE

The SF-BREEZE is a high-speed hydrogen fuel-cell ferry designed for commercial use on the San Francisco Bay. As depicted in its current design shown in Figure 2, the SF-BREEZE combines hydrogen fuel, PEM fuel cell technology, and a catamaran hull design to provide high-speed ferry service for 150 passengers at 35-knot top speed. The feasibility of such a vessel has been recently proven in a project funded by the Maritime Administration (MARAD) within the U.S. Department of Transportation. We report elsewhere details of the initial design of the vessel by the Elliott Bay Design Group (EBDG,

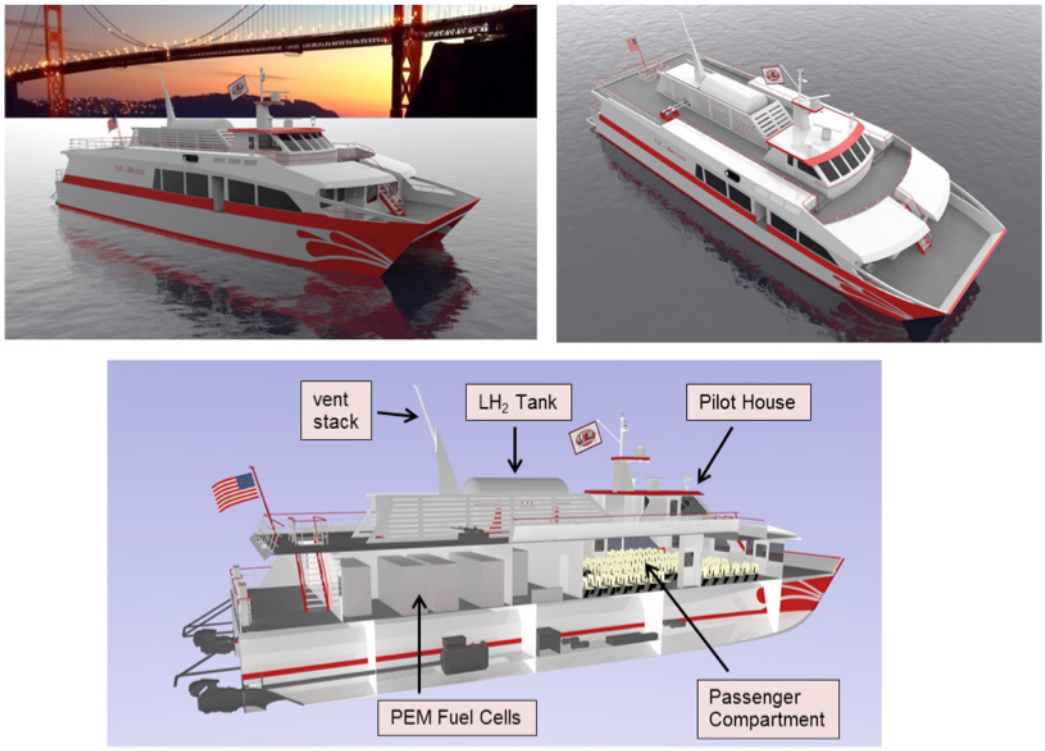

Figure 2: Engineering Models of the SF-BREEZE. The Top Deck holds the LH_2 storage tank, the associated vent stack, evaporation equipment, and the Pilot House of the vessel. The Main Deck holds the PEM fuel cell power racks and the passenger compartment.

the project's naval architect), as well as assessments of the technical and economic feasibility [27].

The SF-BREEZE Top Deck holds a cylindrical 1200 kg capacity liquid hydrogen (LH_2) tank, with enough hydrogen for 4 hours of continuous operation. The plan to refuel only two times per day drives the 1200 kg capacity specification. The high-speed (35 knots) specification requires the lightest method of storing 1200 kg of hydrogen, namely LH_2 storage in a DOT-approved double-walled cryogenic tank. The forty-one 120 kW PEM fuel cell racks, each rack containing 4 fuel cell units of nominal power 30 kW, are located on the Main Deck, adjacent to the passenger compartment. Although PEM fuel cells can use "industrial grade" hydrogen (99.95% pure), LH_2 is typically 99.9995% pure.

Diesel Ferry (VALLEJO) Specifications

We will be comparing the GHG and criteria pollutant emissions of the SF-BREEZE with a conventional diesel-powered ferry. Figure 3 shows pictures and information for the SF-BREEZE and the VALLEJO, a diesel-fueled ferry currently in service on the San Francisco Bay. The VALLEJO was chosen as a comparison because it represents typical ferries in use around the world today and operates on a route that is well-characterized and appropriate for the SF-BREEZE. This choice in no way was intended to find fault with the VALLEJO, the transit agency that operates it, or the public that supports it.

The feasibility study for the SF-BREEZE targeted a "Subchapter T" vessel, which has a passenger limit of 150 passengers. Subchapter T regulatory requirements are somewhat relaxed compared to the larger Subchapter K vessels with a passenger limit of 600, which was thought to facilitate design approval by the U.S. Coast Guard and the American Bureau of Shipping (ABS). Although the VALLEJO is a larger vessel, carrying twice the passengers as the SF-BREEZE, the two vessels can be compared for their GHG and criteria pollutant emissions on a per passenger basis.

For this analysis, the Hydrogenics HD-30 fuel cell was adopted as representative of PEM fuel cells in general [28]. The HD-30 has a rated maximum power of 33 kW. Four HD-30 units are assembled per rack, giving a nominal rack power of 120 kW. With forty-one 120 kW racks onboard, the maximum power for the SF-BREEZE is 4920 kW, with 4400 kW propulsion power required to achieve 35-knot speed.

The VALLEJO is powered by two MTU 16V4000 Diesel Engines [29] with a maximum power each of 1700 kW, giving a total installed propulsion power of 3400 kW. Both vessels are assumed to have a "hotel" or ship service power of 120 kW, which is needed for normal vessel electrical needs such as navigation, lights, and propulsion cooling systems for both vessels.

SF-BREEZE

Top Speed: 35 knots
Power Plant: PEM fuel cells
Fuel: Liquid Hydrogen
Passenger Capacity: 150

VALLEJO

Top Speed: 35 knots
Power Plant: Two diesel engines
Fuel: Diesel
Passenger Capacity: 300

Figure 3: (Top): Engineering model for the SF-BREEZE. (Bottom): Photograph of the VALLEJO ferry.

Route Profile and Energy

The GHG and criteria pollutant emissions analyses for the SF-BREEZE and the VALLEJO are based on the energy expended by each vessel performing the same maritime mission. The existing Vallejo to San Francisco route was chosen for the maritime mission. This route is shown in Figure 4, with detailed route information given in Figure 5 and Table I. The Vallejo to San Francisco route involves passenger loading at the Vallejo Ferry Terminal, maneuvering the vessel away from the Vallejo Terminal within the Mare Island Channel, navigation at slow speeds through the Mare Island Channel, high-speed crossing on the open San Francisco Bay, maneuvering at the Port of San Francisco Ferry Building Terminal, and passenger unloading. Figure 5 gives the trip profile (speed vs. time) for the existing Vallejo-SF ferry service, while Table I gives additional information on the distances involved.

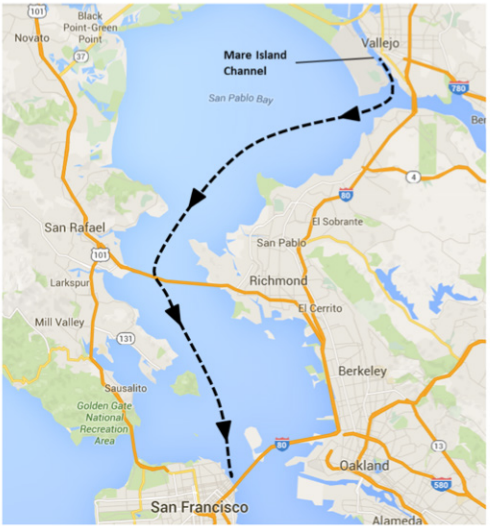

Figure 4: Existing ferry route for the VALLEJO, providing ferry service between Vallejo, CA and San Francisco, CA.

The Vallejo to San Francisco route was chosen to provide a stiff challenge to the fuel-cell ferry design. First, the existing service requires a top speed of 35 knots, the fastest vessel in regular service on the San Francisco Bay. Second, the route is 24 nautical miles long, the longest ferry route currently in service on the bay, which places demands on the SF-BREEZE design range. An additional benefit of using this route for the maritime mission is that detailed information (step duration, speed) is available for this route, which formed the basis for Figure 5 and Table I.

The SF-BREEZE design generated by EBDG, public information about the VALLEJO ferry, along with Figure 5 and Table I allow a calculation of the energy needed by both the SF-BREEZE and the VALLEJO ferries to perform the Vallejo to San Francisco maritime mission. These energy calculations are shown in Tables II and III for the SF-BREEZE and the VALLEJO ferries, respectively, and form the basis for the GHG and criteria pollutant emissions estimates for these vessels. These energy estimates assume vessel operation in a quiescent sea state, but with a 13.5 knot head wind. No other energy margins are assumed. The SF-BREEZE energy requirements take into account the efficiencies of the electric drive components powered by the fuel cells, including DC-DC converters for power conditioning, DC-AC inverters and AC permanent

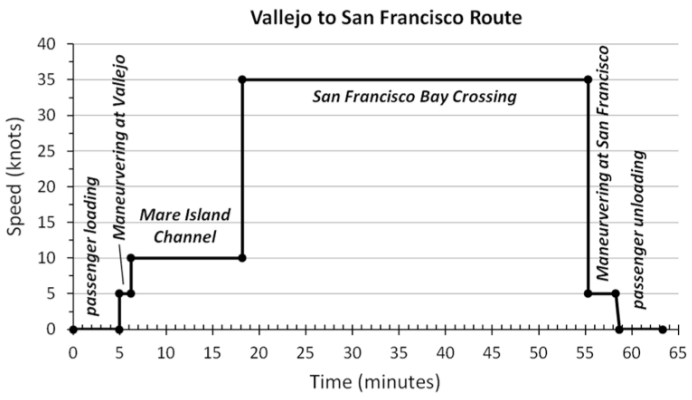

Figure 5: Route profile (speed versus time) for a one-way trip from the Vallejo CA Ferry Terminal to the San Francisco Ferry Building Terminal onboard the VALLEJO ferry.

magnet electric motors that provide shaft power [27]. The propulsor (water jet) efficiency is also taken into account.

Power Plant Efficiencies

Tables II and III list the total energy required for each step of the Vallejo-SF trip. In order to calculate the GHG and criteria pollutant emissions associated with vessel operation, the thermal efficiency of the power generating equipment must be known at various partial load states to calculate the fuel demand. Figure 6 gives the thermal efficiency, as a percentage of the LHV of the input fuel, for the PEM fuel cells and the diesel engines across their operating ranges.

	Passenger Loading	Maneuvering at Vallejo	Mare Island	SF Bay Crossing	Maneuvering at SF	Passenger Unloading
Step Distance, (nm)	0	0.1	2.0	21.65	0.25	0
Cumulative Distance, (nm)	0	0.1	2.1	23.75	24	24
Speed, (knots)	0	5	10	35	5	0
Step Duration, (mins)	5	1.2	12	37.1	3	5
Cumulative Time, (mins)	5	6.2	18.2	55.3	58.3	63.3

Table I: Vallejo To San Francisco Ferry Route Details: Step Distance (in nautical miles, nm), Cumulative Distance, Step Speed, Step Duration and Cumulative Time are shown for a one-way trip onboard the VALLEJO from the Vallejo Ferry Terminal in Vallejo CA to the San Francisco Ferry Building Terminal in San Francisco, CA.

The maximal efficiency of the PEM fuel cell is 53.3%, for a fuel cell power about 25% of the full rated power, or 8.25 kW in Figure 6. There are 164 HD-30 fuel cell units on the SF-BREEZE (41 fuel cell racks, with each rack holding four HD-30 fuel cell units). As a result, for any power demand greater than 8.25 kW and less than 164 x 8.25 kW = 1353 kW, the power load can be distributed amongst the fuel cells so that the optimal 53.3% efficiency is maintained. This is an important inherent advantage of having many fuel cells as opposed to a few large diesel engines – the number of fuel cells producing power can be controlled. At part load, the operator can choose to use more cells at lower power to achieve maximal efficiency and reduce fuel cost, or can choose to operate fewer cells at higher power to reduce the number of hours each cell operates on average. As shown

SF-BREEZE Step	Duration (min)	Service Power (kW)	Propulsion Power (kW)	Total Energy for Step (J)	FC Efficiency for Step (%)	H_2 LHV Needed (J)
Passenger Loading	5	120	0	3.60×10^7	53.3	6.75×10^7
Maneuvering	1.2	120	470	4.25×10^7	53.3	7.97×10^7
Mare Island Channel	12	120	1180	9.36×10^8	53.3	1.76×10^9
SF Bay Crossing	37.1	120	4400	1.01×10^{10}	46.6	2.17×10^{10}
Maneuvering at SF	3	120	470	1.06×10^8	53.3	1.99×10^8
Passenger Unloading	5	120	0	3.60×10^7	53.3	6.75×10^7

Table II: Vallejo to San Francisco Energy Requirements for the SF-BREEZE: The energy demands on the SF-BREEZE for performing each step of the Vallejo to San Francisco Ferry route are listed. The lower heating value (LHV) of the LH_2 fuel needed to perform the step is also shown, which is a function of the fuel cell (FC) thermal efficiency appropriate for that step. The hydrogen lower heating value (LHV) is 119.96 MJ/kg. The total engine energy (service energy + propulsion energy) needed for the one-way trip is 1.125×10^{10} J. The total hydrogen fuel energy (LHV) needed for the one-way trip is 2.39×10^{10} J.

VALLEJO Step	Duration (min)	Service Power (kW)	Propulsion Power (kW)	Total Energy for Step (J)	Diesel Engine Efficiency for Step (%)	Diesel LHV Needed (J)
Passenger Loading	5	120	0	3.60×10^7	21.6	1.66×10^8
Maneuvering	1.2	120	363.3	3.48×10^7	28.7	1.21×10^8
Mare Island Channel	12	120	912.1	7.43×10^8	33.2	2.24×10^9
SF Bay Crossing	37.1	120	3400	7.84×10^9	41.9	1.87×10^{10}
Maneuvering at SF	3	120	363.3	8.70×10^7	28.7	3.03×10^8
Passenger Unloading	5	120	0	3.60×10^7	21.6	1.66×10^8

Table III: The energy demands on the VALLEJO ferry for performing each step of the Vallejo to San Francisco Ferry route. The lower heating value (LHV) of the diesel fuel needed to perform the step is also shown, which is a function of the diesel engine thermal efficiency appropriate for that step. The fossil diesel fuel LHV is 43.4 MJ/kg. The total engine energy (service energy + propulsion energy) needed for the one-way trip is 8.78×10^9 J. The total diesel fuel energy (LHV) needed for the one-way trip is 2.17×10^{10} J.

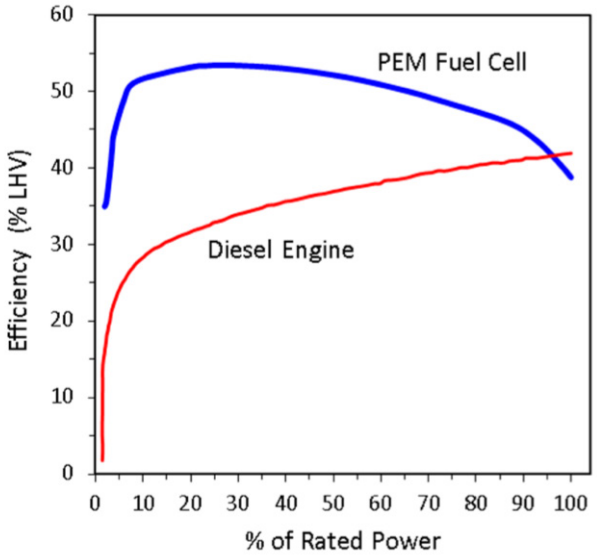

Figure 6: Thermal efficiency of the SF-BREEZE HD-30 PEM fuel cell (thick blue line) and the VALLEJO's MTU 16V4000 diesel engine (thin red line) as a function of the partial load. For the HD-30, the maximal power (100% load) is 33 kW. For one of the MTU 16V4000 diesel engines, the maximal power is 1700 kW. The figure assumes a LHV value of hydrogen of 119.96 MJ/kg, and a LHV value for diesel fuel of 43.4 MJ/kg.

in Table II, for all trip steps except for the San Francisco Bay Crossing, the fuel cells operate at the maximal efficiency of 53.3%. For total power loads greater than 1353 kW, there is a steady decline in PEM fuel cell thermal efficiency suggested by Figure 6. At full SF-BREEZE power, required for the SF-Bay crossing, the fuel cell thermal efficiency is 46.6% with all the fuel cells sharing the power equally.

This fuel cell power distribution architecture is conceptually different than that of the VALLEJO. With two diesel engines on the VALLEJO driving the water jets independently of each other, for any given propulsion power, the propulsion load is assumed to be split evenly between the two diesel engines for the vessel to track in a straight line (except for low power maneuvering of the vessel in port). Thus, during operation at less than maximal load, the two diesel engines are operating at the same sub-maximal thermal efficiencies as listed in Table III. The highest diesel engine efficiency, 41.9%, is achieved for the SF-Bay crossing.

Tables II and III show that the crossing of San Francisco Bay consumes the vast majority of the energy needed for this maritime mission. For the SF-BREEZE, the crossing requires 89.8% of the total mission energy; for the VALLEJO, the percentage is 89.3%. Thus, the SF Bay crossing drives ~ 90% of the GHG and criteria pollutant emissions from these vessels during the voyage. The total fuel energy required for the trip, combined with the LHV numbers for the two fuels allows a calculation of the total fuel consumption for each vessel. For the SF-BREEZE, the LH_2 consumption per trip is 199.2 kg. For the VALLEJO, the diesel fuel consumption per trip is 500.0 kg, or 601.0 L (158.8 gallons).

The fuel energy (on a LHV basis) per trip required for the SF-BREEZE is 10.1% more than for the VALLEJO. This is a consequence of the SF-BREEZE being heavier. Despite the fact that hydrogen is the lightest fuel, the weights of the fuel cell power racks, liquid hydrogen tank, evaporator and other "balance-of-plant" items are heavier than the two diesel engines with their associated balance-of-plant. Although the fuel cells on the SF-BREEZE are more efficient than the two diesel engines on the VALLEJO, the higher weight tips the fuel energy consumption balance in favor of the VALLEJO.

Results and Discussion

GHG Emissions

As described by Eq. (1), water is the only product of PEM fuel cell operation. There is no formation of CO_2, NO_x, SO_x, or PM, making the PEM fuel cell a zero-emissions power plant. As a result, the GHG emissions associated with SF-BREEZE consist entirely of the emissions associated with the production and transport of LH_2 to the vessel. This fuel pathway is referred to as "well-to-tank" (WTT). Analogously, GHG emissions are associated with the production and delivery of diesel fuel. If the diesel fuel originates from petroleum, then there is the additional GHG emissions associated with releasing CO_2 upon combustion. As a result, GHG emissions from the VALLEJO involve two sources: the WTT production and delivery of the diesel fuel, and combustion of the fuel assuming the diesel is derived from petroleum. For light-duty vehicles, this entire pathway is referred to as "well-to-wheels" as it includes combustion of the fuel onboard the vehicle. For our maritime application, we refer to this pathway as "well-to-waves" (WTW).

Our GHG estimates rely on the WTT GHG analysis conducted by the European Commission for automotive fuels in 2007 [30], which were updated in 2013 [31]. We chose this study because its authors come from a variety of stakeholders including automakers (Ford, Renault, Volvo, Fiat, etc.), energy companies (Exxon/Mobile, BP, Shell, etc.) and environmental experts from across the EU. In addition, the study considered a wide variety of pathways (both fossil fuel and renewable) for generating hydrogen. There is also a greater cumulative experience with diverse energy pathways in Europe than elsewhere in the world, which provides confidence in the study results.

As described in Reference 30, the WTT analysis considers the process of producing, transporting, manufacturing and distributing a number of fuels, including hydrogen, diesel and

biodiesel fuel. The study covers all steps in producing and delivering a final fuel product to the storage tank of an end use (vehicle, vessel) with the steps defining a WTT pathway. Energy costs and GHG emissions are assessed along various fuel production/delivery pathways. The study assumes the infrastructure for fuel production and delivery already exists, hence it does not consider GHG emissions associated with construction or decommissioning of plants. It turns out the GHG contributions from these infrastructures are relatively small and within the uncertainty of the estimates. For fuels of biomass origin, such as biodiesel or hydrogen from wood gasification, the predicted GHG emissions do not include emissions caused by land use change, but do include N_2O emissions from use of fertilizer and N_2O release from agricultural lands.

There are 4 general categories defining a WTT pathway:

Production and Conditioning at Source: Generally a fuel can be produced from a number of different primary energy sources, obtained by extraction (as in hydrocarbons or fissile material for nuclear power), capture (as in solar or wind), or growing (as in biomass). The Production and Conditioning at Source category captures all operations required to extract, capture or cultivate the primary energy source at its point of capture. For example, petroleum needs to be extracted from the ground. Typically this is done using the natural pressure of the oil field, but it can also require deliberate gas injection to boost pressure. The extracted or harvested primary energy carrier typically requires some form of treatment or conditioning before it can be safely transported elsewhere. For example, water may need to be separated out. The energy and GHG emissions associated with such operations at the source are examined in the EU Commission study in this category.

Transportation to Processing Plant: This category captures the

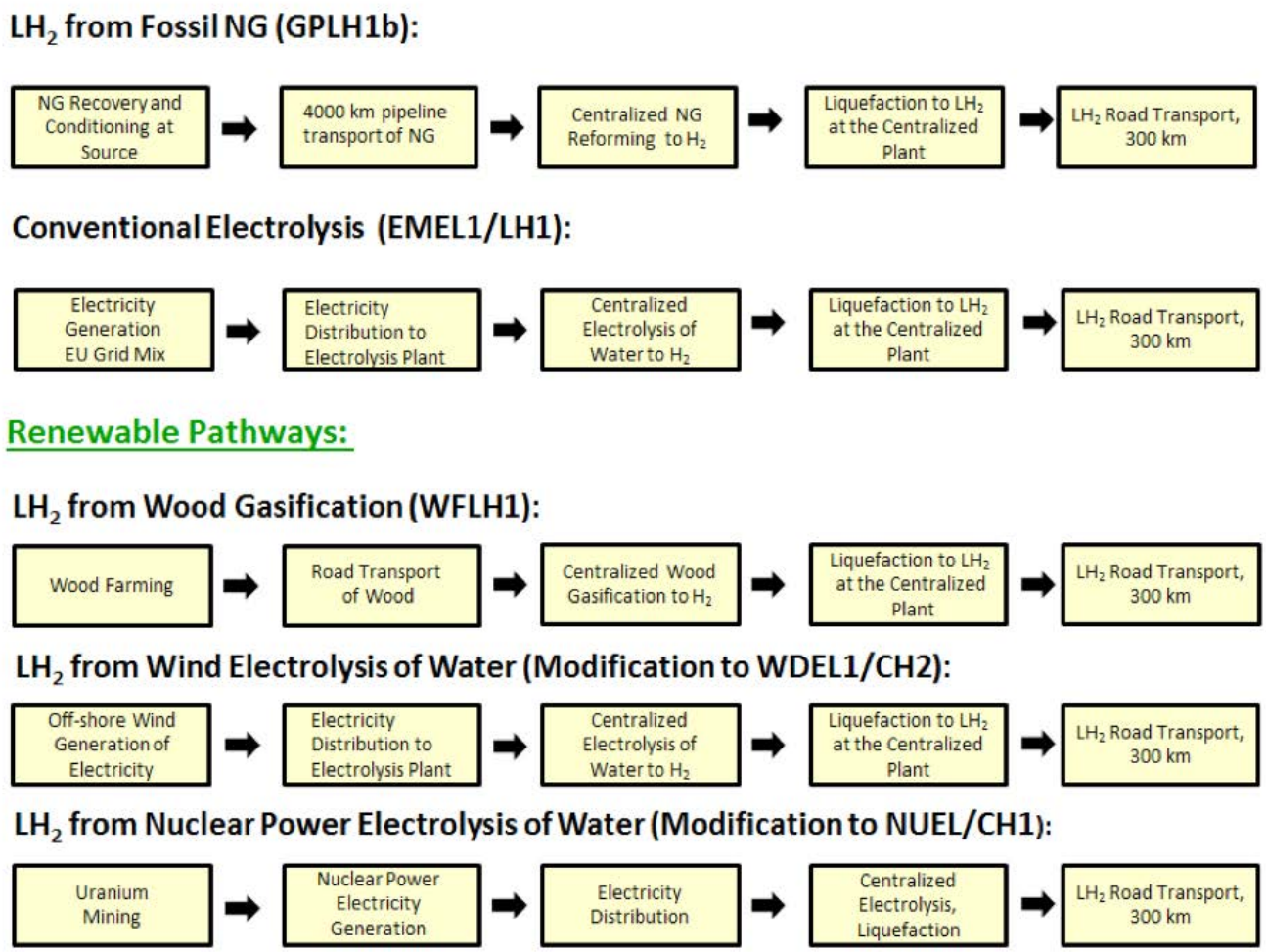

Figure 7: WTT LH_2 pathways considered in the GHG analysis of the SF-BREEZE. Pathway codes in parenthesis identify the pathway described in detail in the European Commission studies of References 30 and 31.

transportation of the primary energy carrier to the processing plant where the primary energy carrier is refined into finished fuel. Since this refining is typically not conducted near the source, the transportation distances can be quite long. For natural gas (NG), transportation represents the largest energy requirement. Western Siberian fields are ~ 7000 km from Europe. Pipelines require compression stations at regular intervals along the transport path, consuming energy and producing associated GHG emissions. Leakage in NG pipelines also represents a transportation pathway source of GHG emissions. This has direct relevance for hydrogen, as steam methane reforming (SMR) of NG is currently the dominant method of producing hydrogen.

Processing at Plant: This category captures the energy and GHG emissions involved in processing and transforming the product into a final fuel to an agreed upon specification near the final market. For the example of hydrogen generation from NG, steam methane reforming takes place at the processing plant and requires significant energy input to produce the furnace temperatures (~ 900 °C) needed for the reformation process. Furthermore, if the hydrogen needs to be liquefied (as it does for the SF-BREEZE), liquefaction also takes place at the centralized plant and involves significant energy input with associated GHG emissions.

Distribution: This category captures the energy and GHG emissions associated with transport to the final customer end use. For NG, distribution is made via an extensive pipeline distribution network. Hydrogen can also delivered by pipeline, but for delivery to hydrogen stations serving light-duty fuel cell vehicles, or a hydrogen station serving the SF-BREEZE, the hydrogen will initially be delivered by road tanker carrying LH_2. For some light-duty vehicle hydrogen stations, hydrogen is delivered as a compressed gas.

The major GHGs accounted for in the study are carbon dioxide (CO_2), methane (CH_4) and nitrous oxide (N_2O). The results are expressed as "CO_2 equivalence" (CO_2 (eq.)) and each gas is assigned a CO_2 (eq.) "weighting factor." CO_2 has a weighting factor of 1, whereas CH_4 has a factor of 23 and N_2O has a weighting factor of 296. Thus methane is 23 times more potent a GHG than carbon dioxide, which makes NG leakage a significant concern for GHG emissions associated with NG transport. Carbon dioxide is produced in gigantic quantities by combustion of fossil fuels. Nitrous oxide emission derives primarily from nitrogen fertilizer production and release from open agricultural fields. Although produced in relatively smaller amounts, N_2O is an important GHG because of its very large weighting factor of 296. In contrast to CO_2, CH_4 and N_2O, hydrogen is not a GHG, so leaks of hydrogen, while an economic loss and a safety concern, have no environmental impact.

The LH_2 WTT pathways considered in this study are depicted in Figure 7. Approximately 90% of the hydrogen used today comes from the steam reforming of fossil NG. Steam methane reforming to LH_2 is identified in the EU Commission study as pathway GPLH1b. The NG is conditioned at the source, transported via NG pipeline 4000 km, reformed at a central reforming facility, liquefied at the plant, and then transported as a liquid in a road tanker a distance of 300 km. Since all of the carbon in fossil-based NG is released into the atmosphere during pathway GPLH1b, we anticipate large GHG emissions from the SF-BREEZE using LH_2 from this pathway.

A second LH_2 production pathway is conventional electrolysis of water using grid power, in this case, the grid mix of the European Union. This pathway is indicated in Figure 7, and identified as pathway EMEL1/LH1. Table IV compares the 2007 EU grid mix assumed for the study [30], and that of the State of California in 2014 [32].

There are distinct differences between the two grid mixes. The EU has more low-carbon nuclear, while the State of CA has considerably less high-carbon coal. The State of CA has

Grid Resource	2007 EU Mix (%)	2014 State of CA (%)
Nuclear	37.5	8.5
Coal	22.4	6.4
Oil	9.6	0
Natural Gas	15.5	44.5
Hydroelectric	12.4	5.5
Wind	0.4	8.1
Waste	1.8	2.5
Other Renewables	0.3	9.5
Other	0.1	15

Table IV: A comparison of the 2007 EU grid mix assumed in the studies of Reference 30 with the 2014 State of California grid mix from Reference 32.

more low-carbon wind, but less zero-carbon hydroelectric power. Overall, we judge these two grid mixes to be comparable as bases for GHG calculations. While we note the overall comparability of the grid mixes in Table IV, we emphasize that we are not attempting to predict emission inventories for a particular geographic region, but rather to compare emission differences between a high-speed hydrogen fuel-cell ferry and the analogous diesel and biodiesel vessels performing the same route profile. Using the common EU commission analyses for these fuels allows this comparison for the GHG emissions to be made.

"Renewable Pathways" of hydrogen production are those that don't involve the release of carbon, or if carbon is released, then it came recently from CO_2 in the air, making the pathway "carbon neutral." The EU commission studies [30,31] incorporated one renewable pathway that led directly to LH_2, namely wood gasification (WFLH1). Other renewable pathways to hydrogen include using offshore wind to electrolyze water (WDEL1/CH_2) and using nuclear generated electricity to electrolyze water (NUEL/CH1), as depicted in Figure 7. For these later two pathways, compressed hydrogen gas was produced, not LH_2. To estimate a GHG emission number for the pathway that would have led to LH_2, we modified the path to include a hydrogen liquefaction step, and increased the GHG emissions reported by the EU commission for the renewable compressed hydrogen product by a factor of 1.286 to reflect increased emissions associated with liquefaction using renewable energy. This factor was determined by taking the ratio of the GHG emissions reported for making

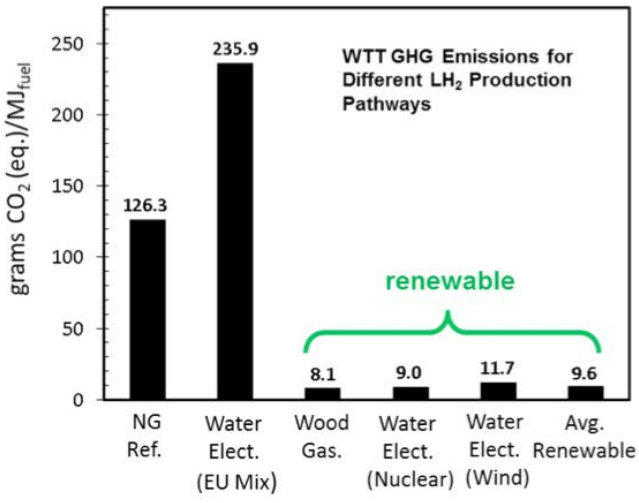

Figure 8: Total fuel pathway (WTT) GHG emissions in grams CO_2 (eq.)/MJ_{fuel} for the LH_2 production pathways considered in this study: (L-R); NG reforming, electrolysis of water using the EU grid mix, wood gasification, water electrolysis using nuclear-based electricity, water electrolysis using wind-based electricity, and the average of the renewable paths. The figure reports the GHG emissions associated with producing one MJ of finished fuel on a LHV basis, MJ_{fuel}.

LH_2 by fossil NG reforming (GPLH1b), 126.3 g CO_2 (eq.)/MJ_{fuel} to the GHG emissions reported for making compressed hydrogen by fossil NG reforming (GP-CH_2b), 98.2 g CO_2 (eq.)/MJJ_{fuel}. That ratio is 1.286 and is used to correct renewable pathway GHG emission reported for compressed gas to obtain the GHG emission for producing LH_2 via the same production method.

The results for the EU Commission report for total WTT GHG emissions in CO_2 (eq.) for the LH_2 production pathways of Figure 7 are reported in Figure 8. The report [30] can be consulted for the breakdown in the GHG emissions according to each pathway step (production at source, transportation to processing plant, processing to fuel, and fuel transport to market).

Figure 8 shows that the current commercial method of making LH_2, namely NG reforming to hydrogen followed by liquefaction (GPLH1b) produces 126.3 grams of CO_2 (eq.) per megajoule of LH_2 on a LHV basis. Recall that the LHV of hydrogen is 119.96 MJ/kg. Thus, 15.1 kg of CO_2 (eq.) emissions are released in the production of 1 kg of LH_2. Water electrolysis using conventional grid power produces 235.9 grams of CO_2 (eq.)/MJ_{fuel}, significantly worse than the fossil NG reforming route. This is because water electrolysis is very energy intensive. The EU Commission reports that it takes 1.13 MJ of process energy for every 1.0 MJ of LH_2 fuel produced by NG reforming. In contrast, it takes 4.22 MJ of process energy to make 1.0 MJ of LH_2 via water electrolysis. Thus, if the current carbon-rich electrical grid is used to perform the electrolysis, LH_2 production via water electrolysis is not competitive from a GHG perspective with steam methane reforming. We will not consider water electrolysis via the grid further, but will assess its GHG and criteria pollutant emissions when low-carbon (renewable) sources of electricity are available.

Figure 8 shows that when renewable sources of hydrogen are available, then fuel pathway GHG emissions are dramatically reduced. Wood gasification (WFLH1) yields 8.1 grams of CO_2(eq.) for every 1.0 MJ (LHV) of LH_2. Electrolysis of water using low-carbon electricity sources such as nuclear power or wind also yield very low GHG emission values of 9.0 and 11.7 g CO_2 (eq.)/MJ_{fuel} , respectively. Taking the average of these renewable paths, we get an average renewable GHG emissions for the production and delivery of renewable LH_2 as 9.6 grams CO_2(eq.)/MJ_{fuel}. Since PEM fuel cells produce no emissions of any kind at the point of use, these WTT LH_2 production numbers provide the entire basis for estimating GHG emissions from the SF-BREEZE. In other words, since the PEM fuel cell is zero emissions, the WTT emissions equal the WTW emissions.

In contrast, the use of diesel fuel on the VALLEJO has two components of GHG emission. The first component lies in the

production and delivery of diesel fuel. The EU Commission study reports that GHG emissions for diesel production is 14.2 g CO_2 (eq.)/MJ_{fuel}. Recalling the LHV of diesel is 43.4 MJ/kg, and noting the density of diesel fuel is 0.832 kg/L, making one gallon of diesel fuel releases 1.94 kg CO_2 (eq.) per gallon produced. This figure is significantly less than the 15.1 kg of CO_2 (eq.) emissions released in the production of 1 kg of LH_2 by fossil NG reforming. The emissions for manufacture of diesel fuel are less because there is dramatically less process energy used in refining petroleum to diesel fuel than in steam reforming NG to hydrogen. The EU Commission reports that it takes 0.16 MJ of process energy to make 1.0 MJ of diesel fuel. This can be compared to the 1.13 MJ of process energy it takes to make 1.0 MJ of LH_2 fuel by NG reforming. Only a portion of the process energy is tied up in liquefaction of hydrogen. The EU reports that to make and deliver 1.0 MJ of hydrogen compressed to 880 bar (pathway GPCH_2b) still requires 0.72 MJ of process energy. Summarizing, making LH_2 is very energy intensive compared to making diesel fuel, even when using the least-energy-intensive pathway for making hydrogen, namely steam reforming of fossil NG.

Since the carbon atoms in fossil diesel fuel came from the atmosphere millions of years ago, its combustion represents a significant addition to CO_2 already in the atmosphere. The EU commission reports that burning diesel fuel produces 73.2 g CO_2 (eq.)/MJ_{fuel}. This is nearly all produced as CO_2 itself. Thus, the total WTW GHG emissions from making and burning (to completion) 1.0 MJ (LHV) of fossil-derived diesel fuel is 14.2 g CO_2 (eq.) + 73.2 g CO_2 (eq.) = 87.4 g CO_2 (eq.)/MJ_{fuel}. Thus, fuel production accounts for 16.2% of the total GHG emissions associated with producing and using diesel fuel.

We consider biodiesel fuel to be the "renewable" version of diesel fuel that could be used in the VALLEJO. Since biodiesel could be to first approximation a "drop in" fuel for the VALLEJO, we can consider the impact of fueling the VALLEJO with a renewable biodiesel because we don't anticipate there would be very significant changes to the engines, fuel tanks, fueling systems or passenger capacity. With the hardware, weight and passenger allotment of the vessel remaining the same, we can use the same values of "step energy" shown in Table III to assess the WTW GHG emission for the VALLEJO running on biodiesel.

The EU Commission reports [30,31] the energy and GHG emissions associated with making and delivering biodiesel fuel, with the most updated figures from the 2013 Report [31]. In Europe, biodiesel is mostly produced from rapeseed with some production using sunflower seeds as the feedstock. Since the carbon in these living materials came recently from atmospheric CO_2, burning biodiesel with CO_2 release is considered carbon neutral, and the WTW GHG emissions equal the WTT GHG emissions for biodiesel. However, the WTT GHG emissions for making and delivering biodiesel are considerable, since significant process energy is needed for farming the seeds and converting the biomass to fuel. Making biofuels from these seeds takes 1.20 MJ of process energy for every megajoule of biodiesel fuel produced. This is 7.5 times more process energy than it takes to make the energy equivalent of diesel fuel from petroleum (0.16 MJ/MJ_{fuel}). The WTW GHG emissions associated with making biodiesel by the rapeseed and sunflower pathways is (taking the average of the two feedstocks) 55.0 g CO_2 (eq.)/MJ_{fuel} [31]. Although burning biodiesel does not release net CO_2, criteria pollutants are created, such as NO_x, HC and PM.

With this information in hand about the GHG emissions associated with making and delivering LH_2 via the pathways of Figure 7, the GHG emissions associated with making and delivering fossil diesel and biodiesel, as well as the GHG emissions associated with burning fossil diesel, we can now assess the well-to-waves GHG emissions from both the SF-BREEZE and the VALLEJO in travelling from Vallejo CA to San Francisco CA. The results are shown in Figure 9.

Figure 9 shows that the GHG emissions from the SF-BREEZE fueled with LH_2 from fossil NG would be 20.12 kg CO_2 (eq.)/passenger/trip, produced entirely during the production and delivery of the LH_2 fuel. This is significantly worse than the VALLEJO running on fossil diesel, with GHG emissions of 6.32 kg CO_2 (eq.)/passenger/trip. The reasons for this increase are that the SF-BREEZE carries half the number of passengers as the VALLEJO and also requires more fuel energy. Since the

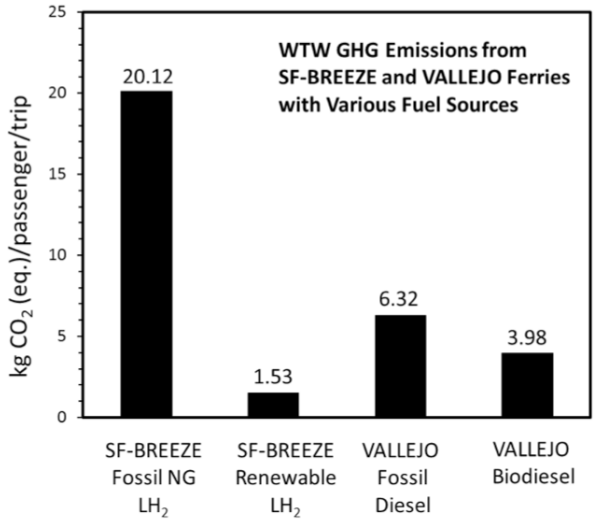

Figure 9: Predicted well-to-waves (WTW) GHG emissions per passenger for the SF-BREEZE and the VALLEJO for the Vallejo-San Francisco route described in Figures 4 and 5 and in Table I. Emissions are given based on a one-way trip. Note the change in vertical scales units from Figure 8 to Figure 9.

GHG results are normalized to the number of passengers, this produces a factor-of-two increase for the SF-BREEZE GHG emissions based on passenger capacity alone. Further increases in the GHG emissions come from the fact that making hydrogen is energy intensive in the first place, and hydrogen liquefaction involves significant energy and associated GHG emissions. Thus, the reduced passenger count, the higher fuel energy consumption, and GHG penalties associated with making hydrogen from fossil NG and liquefying it, produce undesirable GHG emissions for the SF-BREEZE along the hydrogen fuel production and delivery path.

The situation is dramatically improved using renewable hydrogen. Taking the average value of the renewable production pathways, 9.6 g CO_2 (eq.)/MJ_{fuel} in Figure 8, Figure 9 shows the GHG emissions from the SF-BREEZE becomes 1.53 kg CO_2 (eq.)/passenger/trip. This is 75.8% less than the GHG emissions from the VALLEJO running on conventional diesel fuel on a per passenger, per trip basis.

Figures 8 and 9 show that the real potential in hydrogen technology to reduce GHG lies NOT in the use of hydrogen derived from fossil NG, but in using renewable hydrogen. The renewable hydrogen considered for Figures 8 and 9 is nearly 100% renewable. In California, the current mandate is that all state-funded hydrogen stations being built in the State for light-duty fuel-cell vehicles need to provide hydrogen that is at least 33% renewable. That percentage must increase significantly to make the cuts in GHG emissions needed to properly address global climate change. In our discussions with the gas suppliers, renewable LH_2 can be made available to the SF-BREEZE today. The major gas suppliers are currently working to make renewable hydrogen more broadly available.

One could consider using biodiesel as a drop-in renewable fuel for the VALLEJO. Figure 9 shows that the GHG emissions are indeed reduced, from 6.32 kg CO_2 (eq.)/passenger/trip for diesel fuel to 3.98 kg CO_2 (eq.)/passenger/trip for biodiesel. The analysis does not take into account that more biodiesel would have to be stored on the VALLEJO because the LHV of biodiesel is ~ 37 MJ/kg [33], down from 43.4 MJ/kg for diesel fuel. The extra biodiesel fuel needing to be stored would increase the weight of the VALLEJO, increasing the energy demand for the trip from Vallejo to San Francisco. Also, we note here that the biodiesel results in Figure 9 are for the particular biodiesel productions paths considered in Reference 30. Biodiesel production paths can vary considerably, especially with regard to the fertilizer and water requirements. The GHG emissions for a particular biodiesel pathway differing from those of Reference 31 would have to be evaluated separately.

Summarizing the GHG results of Figure 9, hydrogen PEM fuel cell technology can dramatically reduce the GHG emissions from high-speed ferry operations. However, nearly 100% renewable hydrogen must be used to achieve the desired deep cuts (76%) in GHG emissions that are commensurate with the challenge presented by global climate change.

Criteria Pollutant Emissions

Criteria pollutant emissions from the combustion of fossil fuels, among them nitrogen oxides (NO_x), hydrocarbons (HC) and particulate matter (PM) continues to be of concern due to their immediate adverse health effects. Since the PEM fuel cell does not involve combustion, it is incapable of producing criteria pollutants at the point of use. As a result, any criteria pollutant emissions associated with the SF-BREEZE arise entirely from emissions associated with the production and transport of LH_2 to the vessel, namely the WTT criteria pollutant emissions. Criteria pollutant emissions can arise from combustion used to create the process heat needed to heat the reactants of the SMR process or as a byproduct of the SMR process. Alternatively, combustion could be used to generate the electricity used in hydrogen liquefaction.

Analogously, criteria pollutant emissions are associated with the production and delivery of diesel fuel. For example, the diesel-fueled tanker truck delivering diesel fuel is a source of diesel pathway criteria pollutant emissions. If the diesel fuel originates from petroleum ("fossil diesel"), then there is the additional criteria pollutant emissions associated with burning the fuel in the ferry diesel engines. As a result, criteria pollutant emissions from the VALLEJO using fossil diesel fuel involve two sources: (1) production and delivery of the diesel fuel and (2) combustion of the fuel onboard the vessel. If the diesel fuel originates from biomass ("biodiesel"), there are still criteria pollutant emissions released on the vessel, even though biodiesel reduces GHG emissions because the carbon released on the vessel originated recently from CO_2 in the air. Indeed, combustion of biodiesel can lead to increased levels of criteria pollutant emissions because its heating value is lower than fossil diesel.

Although the European Commission WTT analysis for automotive fuels in 2007 [30], updated in 2013 [31], were used as the basis for our GHG analysis, these studies do not provide information on criteria pollutant WTT emissions. For fuel pathway criteria pollutant emissions, we use a 2007 analysis conducted by TIAX LLC for the California Energy Commission (CEC) [34].

The TIAX WTT study provides estimates for criteria pollutant emissions based on the energy consumption of various fuel paths, including the production and delivery of LH_2, diesel fuel and biodiesel. Combustion energy consumption is the principle source of criteria emission in these fuel pathways. The study reports emissions from the perspective of expo-

sure to an individual in California, and thus is somewhat California specific. For example the electricity grid mix employed was that of California, and California emissions standards on stationary equipment were assumed [34]. Our objective, however, is not to predict a criteria pollutant inventory of maritime emissions for California, but rather to compare emissions for the hydrogen high-speed ferry technology with the analogous diesel ferry (constrained to Tier 4 limits). Using the common TIAX WTT analyses allows this comparison for the criteria pollutant emissions to be made.

The TIAX study generally follows the spirit of the pathways indicated in Figure 7. The pathway for production of LH_2 from fossil NG is similar to that in Figure 7 (labeled GPLH1b from the European Commission study), except that the distance for LH_2 road transport was assumed to be 80.5 km (50 miles) instead of 300 km. The renewable pathways for LH_2 production shown in Figure 7, namely wood gasification, wind electrolysis of water and nuclear power electrolysis of water, were not considered in the TIAX criteria pollutant emissions analyses. However, there was an analysis performed for criteria emissions associated with conventional water electrolysis producing gaseous hydrogen using 70% renewable power at an on-site facility (i.e. no road transport). We multiply the criteria pollutant emissions for this 70% renewable path by the factor 1.286 to account for emissions associated with liquefaction using renewable energy, and also add emissions associated with tanker transport of the LH_2 over a distance of 80.5 km. We adopt this revised pathway to represent criteria pollutant emissions associated with "70% Renewable LH_2."

Table V reports the WTT criteria pollutant emissions associated with the fuel pathways for LH_2 produced by SMR of fossil NG, 70% renewable LH_2, fossil diesel fuel and biodiesel. The results are reported in terms of grams of pollutant emitted per gigajoule (LHV) of the fuel energy. The TIAX study reported PM emissions as PM_{10} (particles with diameter less than 10 μm).

The "Fossil NG LH_2 Fuel Pathway" has sizeable criteria pollutant emissions. This is due to the use of combustion (typically of NG) to heat the SMR reactor to the required ~ 900 °C. In addition, combustion is used to provide electricity for the process equipment via the California grid (of which 50.9% is derived from burning NG or coal, see Table IV), and combustion is used to power the LH_2 tanker truck as it drives 80.5 km in delivering LH_2. In the TIAX study [34] it was noted for this fuel pathway that there exists somewhat high PM_{10} emissions for natural gas combined cycle power plants which constitute 44.5% of the California grid mix. The origin is not the increased (~ 2x) PM10 emissions associated with LH_2 trailer transport compared to diesel fuel transport [34]. Indeed, the PM_{10} release from trailer transport of 4000 kg of LH_2 a distance of 80.5 km is predicted to be only 0.029 g/GJ_{fuel} ; ~ 0.6% of the overall WTT PM_{10} emissions of 5.0 g/GJ_{fuel} for the Fossil NG LH_2 Fuel Pathway reported in Table V. It is the energy intensity of hydrogen production, not transport, that drives the associated WTT criteria pollutant emissions.

Fuel Pathway	NO_x (g/GJ_{fuel})	HC (g/GJ_{fuel})	PM_{10} (g/GJ_{fuel})
Fossil NG LH_2 Fuel Pathway	45.0	3.5	5.0
70% Renewable LH_2 Fuel Pathway	2.1	2.0	3.9
Fossil Diesel Fuel Pathway	1.4	3.5	0.06
Biodiesel Fuel Pathway	4.5	3.4	0.18

Table V: WTT criteria pollutant emissions for fuel pathways on a LHV basis. GJ_{fuel} represents the lower heating value (LHV) of the indicated fuel in gigajoules (GJ). 1 GJ = 1 x 10^9 J.

The "70% Renewable LH_2 Fuel Pathway" has substantially reduced NO_x emissions because the electrolysis of water does not require the high process heat of the SMR production method. However, as stated previously, electrolysis of water is very energy intensive. The 30% of the energy that is not renewable (fossil-fuel based), combined with the large requirement for electrolysis process energy, produce non-zero amounts of NO_x, HC and PM emissions per GJ_{fuel}, as shown in Table V.

Table V also lists the WTT criteria pollutants associated with making and delivering fossil diesel and biodiesel. The criteria pollutant emissions for biodiesel are generally higher than for fossil diesel because of the increased process energy needed to make biodiesel fuel.

Using these values in Table V, combined with the vessel energy use numbers for the SF-BREEZE and the VALLEJO reported in Tables II and III, respectively, we can calculate the fuel pathway (WTT) and well-to-waves (WTW) criteria pollutant emissions on a per passenger per trip basis. These results are shown in Table VI for the SF-BREEZE and the VALLEJO. Well-to-waves (WTW) criteria pollutant emissions (pathway + engine) for the SF-BREEZE are equal to the LH_2 well-to-tank (WTT) fuel pathway emissions because the PEM fuel cell criteria pollutant emissions are zero. The results for WTW criteria pollutant emissions shown in Table VI are presented graphically in Figure 10. For Table VI and Figure 10, we constrain the diesel and biodiesel engine emissions of the VALLEJO to be at the Tier 4 criteria pollutant emission limits. Brynolf and co-workers have described some emission compliance strategies for diesel-fueled vessels [35]. While the hydrogen PEM fuel cell technology automatically satisfies the Tier 4 criteria emission requirements because it is zero-emission technology at the point of use, the WTW analysis captures important

	NO_x (g/passenger/trip)	HC (g/passenger/trip)	PM_{10} (g/passenger/trip)
SF-BREEZE Fossil NG LH_2 Fuel Pathway, WTT	7.17	0.557	0.796
SF-BREEZE 70% Renewable LH_2 Fuel Pathway, WTT	0.338	0.321	0.620
SF-BREEZE Fuel Cell Engine	0.00	0.00	0.00
SF-BREEZE Fossil NG LH_2 Pathway + Engine, WTW	7.17	0.557	0.796
SF-BREEZE 70% Renewable LH_2, Pathway + Engine, WTW	0.338	0.321	0.620
Diesel Fuel Pathway, WTT	0.101	0.253	0.00433
Biodiesel Fuel Pathway, WTT	0.322	0.246	0.0130
VALLEJO Tier 4 Engine	14.63	1.54	0.325
VALLEJO Tier 4 Diesel Pathway + Engine, WTW	14.73	1.79	0.329
VALLEJO Tier 4 Biodiesel Pathway + Engine, WTW	14.95	1.79	0.338

Table VI: Fuel pathway (WTT) criteria pollutant emissions and well-to-waves (pathway + engine, WTW) emissions on a grams per passenger/trip basis calculated for the SF-BREEZE and the VALLEJO for the Vallejo to San Francisco route of Figure 4. The SF-BREEZE carries 150 passengers, while the VALLEJO carries 300 passengers. The engine criteria pollutant emissions of the VALLEJO are set to the Tier 4 limits for both fossil diesel and biodiesel operation.

fuel production pathway and delivery emissions.

The first aspect of Figure 10 to notice is that the WTW criteria pollutant emissions for the VALLEJO running on diesel fuel or biodiesel are very nearly the same. Although the WTT criteria pollutant emissions for the production and delivery of biodiesel are higher than those for fossil diesel (see Table VI) due to the increased process energy required, the WTT criteria pollutant emissions are only a small fraction of the overall WTW criteria pollutant emissions, as indicated in Table VI.

Thus, the WTW criteria pollutant emissions are very nearly the same for the VALLEJO operating on fossil diesel fuel or biodiesel. In practice, the criteria pollutant emissions from the VALLEJO running on biodiesel would be somewhat larger than the VALLEJO running on fossil diesel fuel even when using Tier 4 engines because the LHV of biodiesel is less than that of fossil diesel [33], requiring the burning of a higher mass of biodiesel in the engine for a given energy output. This subtlety was not taken into account in our analysis.

Table VI and Figure 10 show that the SF-BREEZE operating on LH_2 derived from NG SMR reduces NO_x by ~ 51.3% below that of the VALLEJO operating on fossil diesel fuel (but held to Tier 4 emission standards). Using 70% Renewable LH_2 on the SF-BREEZE, the NO_x is reduced 97.7% below the Tier 4 VALLEJO levels. These reductions in NO_x can be traced to relatively less NO_x being produced when NG is burned for SMR process heat, and dramatically less NO_x associated with electrolysis of water using 70% renewable electricity [34]. Turning to HC emissions, we see that HC is reduced ~ 68.8% below that of the VALLEJO operating on fossil diesel fuel (but held to Tier 4 emission standards) when the SF-BREEZE is operated on LH_2 derived from NG SMR. Using 70% Renewable LH_2, the HC is reduced 82.1% below the Tier 4 VALLEJO levels.

Figure 10 shows that the PM_{10} emissions associated with the SF-BREEZE using 70% Renewable LH_2 are higher than that of the PM emissions of the VALLEJO running on fossil diesel. If the production of LH_2 from water electrolysis were conducted using 84% renewable electricity or higher, the PM_{10} emissions would fall below that for the VALLEJO running on diesel fuel with Tier 4 compliance. Using 100% renewable electricity, the criteria pollutant emissions for the SF-BREEZE would collapse to those for LH_2 trailer transport operating on diesel fuel, giving SF-BREEZE NO_x , HC and PM_{10} emissions of 0.133 grams/passenger/trip, 0.0133 grams/passenger/trip and 0.00465 grams/passenger/trip, respectively. Thus, using 100% renewable electricity, the SF-BREEZE emissions would represent a 99.1% reduction in NO_x, a 99.2% reduction in HC and a 98.6% reduction in PM_{10} compared to the VALLEJO running on diesel fuel with Tier 4 emission constraints. If the LH_2 trailer ran on 100% renewable hydrogen instead of diesel fuel, the criteria pollutant emissions could be essentially eliminated.

Summarizing these criteria pollutant emission results, the SF-BREEZE goes far beyond the Tier 4 criteria pollutant emissions requirements for new ferry construction in the U.S. because the powerplant is zero emissions at the point of use. Hydrogen PEM fuel cell technology can dramatically reduce NOx and HC emissions below the most advanced Tier 4 criteria pollutant emissions requirements regardless of whether the hydrogen is made by NG reforming or via water electrolysis using 70% or greater renewable energy. Renewable LH_2 made with greater than 84% renewable process energy is required to also drop the SF-BREEZE PM_{10} emissions below that equivalent to Tier 4 requirements for high-speed fuel cell ferry transportation.

Our work takes place against the backdrop of prior measurements of maritime criteria pollutant emissions. These prior studies [36-39] report emissions per engine power or energy output, in units of g/MJ or g/kW-hr, respectively. For comparison to this prior work, we summarize in Table VII the criteria pollutant (NO_x, HC and PM_{10}) and GHG (CO_2 (eq.)) emissions per trip for the SF-BREEZE running on LH_2 derived from fossil NG and renewable LH_2, as well as for the VALLEJO running on fossil diesel fuel and biodiesel constrained to the Tier 4 criteria pollutant emission limits. This comparison does not normalize for the number of passengers being carried.

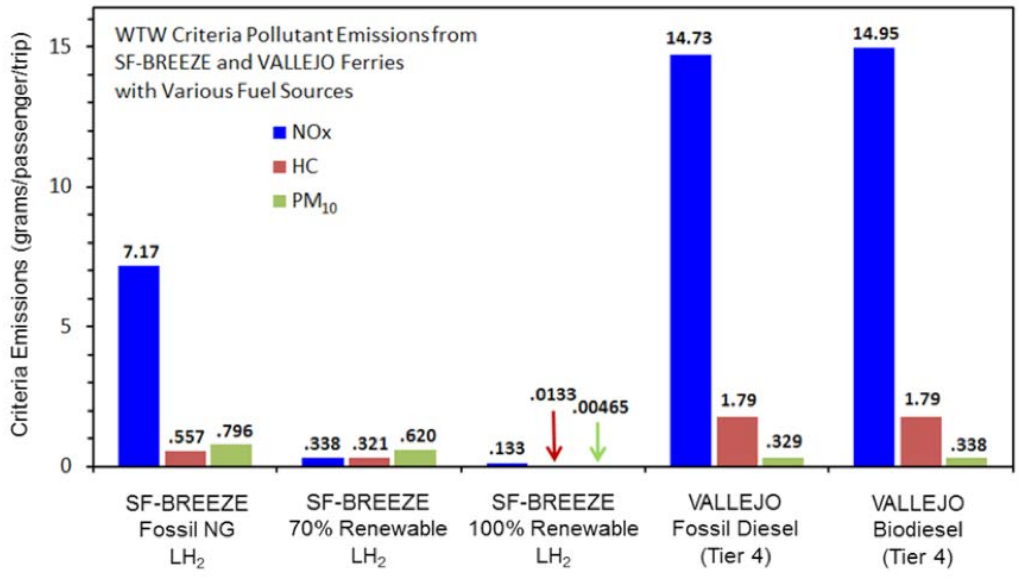

Figure 10: Predicted well-to-waves (WTW) criteria pollutant emissions per passenger for the SF-BREEZE and the VALLEJO on the Vallejo-San Francisco route described in Figures 4 and 5 and in Table I. Emissions are given based on a one-way trip. The SF-BREEZE carries 150 passengers, while the VALLEJO carries 300 passengers. The VALLEJO engine emissions are set equal to the Tier 4 limits for both fossil diesel and biodiesel operation.

Rather, it is a direct comparison of criteria and GHG emission on a "total engine energy" basis for these vessels performing one trip from Vallejo to San Francisco using the route profile of Figure 5. Recall that the total engine energy required (service energy + propulsion energy) of the SF-BREEZE to execute the Vallejo to San Francisco route is 1.125 x 10^{10} J (see Table II) and that for the VALLEJO running the same route is 8.78 x 10^{9} J (see Table III).

Per Trip Emission per Engine Power and Energy	SF-BREEZE Fossil NG LH_2	SF-BREEZE Renewable LH_2	VALLEJO Fossil Diesel	VALLEJO Biodiesel
NO_x (g/MJ)	0.0956	0.00450[a]	0.503	0.511
NO_x (g/kW-hr)	0.344	0.0162[a]	1.81	1.84
HC (g/MJ)	0.00743	0.00427[a]	0.0614	0.0612
HC (g/kW-hr)	0.0267	0.0154[a]	0.221	0.220
PM_{10} (g/MJ)	0.0106	0.00826[a]	0.0113	0.0115
PM_{10} (g/kW-hr)	0.0382	0.0298[a]	0.0407	0.0414
CO_2 (eq.) (g/MJ)	268.27	20.395[b]	216.00	135.93
CO_2 (eq.) (g/kW-hr)	965.77	73.422[b]	777.60	489.35

a) Criteria pollutant (NO_x, HC, PM_{10}) emissions per trip for SF-BREEZE fueled with Renewable LH_2 based on TIAX WTT input data [34] assuming 70% renewable energy used in the production of LH_2.

b) CO_2 (eq.) emissions per trip for SF-BREEZE fueled with Renewable LH_2 based on EU WTT input data [30] assuming fully renewable energy used in the production of LH_2.

Table VII: Well-to-waves (WTW) criteria pollutant and GHG emissions (in grams) reported per integrated engine output energy (in MJ and kW-hr) for the SF-BREEZE and the VALLEJO for the Vallejo-San Francisco route described in Figures 4 and 5 and in Table I.

The results of the measurements of criteria pollutant emissions [36 - 39] from various vessels report NOx emissions in the range 12 -15 g/kW-hr, HC in the range 0.027 – 0.208 g/kW-hr, and PM in the range 0.11 – 0.29 g/kW-hr. These emissions reflect engine pollution without selective catalytic reduction (SCR). Nuszkowski and co-workers [36] conducted a study in which engine emissions were measured with and without SCR treatment. The study found that SCR reduced NO_x emissions from 15.35 g/kW-hr to 5.54 g/kW-hr. These post-treatment emissions are generally consistent with observations by Cooper [37] in which NO_x measurements for a marine diesel engine with SCR was observed to be 2.0 g/kW-hr. Since none of these marine engines were under Tier 4 constraints, their criteria pollutant emissions are larger than those estimated for the SF-BREEZE using fossil NG LH_2 or renewable LH_2, as well as those estimated for the VALLEJO using fossil diesel fuel or biodiesel under Tier 4 emission constraints. Note that the experiments measure emissions from the engine output only, and do not include fuel pathway criteria pollutant emissions.

Our intent is that these results provide useful input data for future efforts to calculate GHG and criteria pollutant emissions for ports and larger ECAs involving hydrogen vessels and infrastructure. However, we caution that the results are for a specific maritime application, that of a high-speed (35 knot) 24-nm range commuter ferry carrying 100 to 300 passengers. Although any hydrogen fuel-cell vessel would have zero emissions from the vessel itself, from the well-to-waves perspective, the emission comparison between hydrogen vessels and the diesel and biodiesel vessels (constrained to Tier 4 limits) is likely to be different for different combinations of vessel route speed, range, and passenger capacity; vessels which could also enter into the vessel inventory for a specific

port. Indeed, in a follow-on project, we are currently examining how the fuel-cell ferry benefits change over a wide range of vessel size, speed, range and passenger capacity.

Our criteria pollutant emission results report PM10 emissions. This was necessitated by our use of the TIAX criteria pollutant emissions for hydrogen, diesel and biofuel production that reported particulate matter emissions in the form of PM_{10}. An improved analysis would result if particle emissions for fuel production pathways were available specifying the more dangerous smaller particle sizes, such as $PM_{2.5}$. A review of particulate matter emissions from marine diesel engines is provided by Di Natale and Carotenuto [40].

In our analysis, we have placed fuel production pathway emissions on an equal footing with emissions coming from the vessel itself, which is inherent in the WTW formalism. This approach is reasonable and indeed responsible. Figure 10 shows that for the SF-BREEZE operating on 100% renewable LH_2, dramatic reductions in criteria pollutant emissions below Tier 4 limits are achieved. However, there are some marine applications where zero-emissions from the vessel are the overriding priority, even if emissions occur elsewhere from fuel production. Lack and Corbett have discussed [41] the problem of "black carbon," defined as the subset of particulate emissions with average particle diameter ~ 0.2 micron that possesses high carbon content and strongly absorbs light. Black carbon (BC) can produce significant localized heating when deposited on snow and ice [41], making BC a particular threat to the Arctic environment. Although scrubbers can remove BC from the diesel engine exhaust stream, the efficiency of removal for the small 0.2 micron particles is uncertain [41]. Thus, for vessels currently operating in Arctic waters and the increasing marine traffic expected for the Arctic as polar sea ice recedes, zero BC emissions from the vessel itself will become a top priority. A hydrogen fuel-cell vessel by its nature provides zero emissions of PM, NO_x and HC at the point of use.

Conclusions

A theoretical comparison was made between the WTW GHG and criteria pollutant emissions from the SF-BREEZE high-speed hydrogen PEM fuel cell ferry and the VALLEJO Ferry, powered by traditional diesel engine technology. The emissions were calculated for a common maritime mission, the current ferry route between Vallejo CA and San Francisco CA. This route is challenging for the design of the fuel-cell vessel because it is a long ferry route (24 nautical miles) and demands a high transit speed of 35 knots. Calculations were made of the fuel energy required for the SF-BREEZE and VALLEJO to perform the mission route profile, taking into account the varying engine efficiencies in effect during different parts of the voyage. It was found that the SF-BREEZE requires 10.1% more fuel energy (LHV) than the VALLEJO, primarily due to the SF-BREEZE being heavier. Since the PEM fuel cell is a zero-emissions power plant, the GHG emissions for the Vallejo to San Francisco route are determined entirely by the GHG emissions associated with hydrogen production. In contrast, for the VALLEJO, if fossil-based diesel fuel is used, the vessel GHG emissions are determined by the sum of the GHG emissions associated with diesel fuel production and delivery plus the carbon released in diesel combustion onboard the vessel.

A description was given of the 2007/2013 European Commission studies of GHG emissions associated with hydrogen, diesel and biodiesel fuel production. Using this prior work, estimates were made for the SF-BREEZE GHG emissions associated with five LH_2 production pathways. We also examined the VALLEJO GHG emissions associated with fossil-diesel production and use, as well as that for biodiesel which can be considered a renewable "drop-in" fuel replacement for conventional diesel fuel. The GHG results show that hydrogen PEM fuel cell technology can dramatically reduce the GHG emissions from high-speed ferry operations. However, nearly 100% renewable hydrogen must be used to achieve the desired deep cuts (76%) in GHG emissions that are commensurate with the challenge presented by global climate change.

We also compared the criteria (NO_x, HC, PM_{10}) pollutant emissions for the SF-BREEZE to that of the VALLEJO constrained to Tier 4 emissions standards fueled by diesel fuel or biodiesel. While the hydrogen PEM fuel cell technology goes far beyond the Tier 4 criteria emission requirements because it is zero-emission technology at the point of use, it is important to consider the fuel production pathway and delivery emissions in a well to waves (WTW) analysis. Using estimates for criteria pollutant emissions from a study by TIAX associated with the production of LH_2 (by both renewable and non-renewable means) diesel and biodiesel, we compared the WTW criteria pollutant (NO_x, HC, PM_{10}) emissions for the SF-BREEZE to that of the VALLEJO fueled by diesel fuel or biodiesel. Compared to VALLEJO Tier 4 emissions using diesel fuel, the SF-BREEZE using LH_2 derived from steam reforming of fossil natural gas reduces NO_x by 51.3%, HC by 68.8%, but PM_{10} emissions increase a factor of 2.5 times. Renewable LH_2 made with greater than 84% renewable process energy is required to also dramatically drop the SF-BREEZE WTW PM_{10} emissions below that of the equivalent Tier 4 for high-speed fuel cell ferry transportation. Using 100% renewable electricity, there would be a 99.1% reduction in NO_x, a 99.2% reduction in HC and a 98.6% reduction in PM compared to the VALLEJO running on diesel fuel with Tier 4 emission constraints.

Summarizing, the results show that operating a hydrogen fuel cell ferry on nearly 100% renewable hydrogen provides

the dramatic reduction in vessel GHG and criteria pollutant emissions commensurate with the problems of global climate change and increasing maritime air pollution worldwide. These results can be used in future analyses of GHG and criteria pollutant emission in areas where hydrogen vessels and infrastructure have been introduced.

Glossary of Abbreviations

ARB: Air Resources Board (California)

BAAQMD: Bay Area Air Quality Management District

BC: Black Carbon

CEC: California Energy Commission

DOT: U.S. Department of Transportation

EBDG: Elliott Bay Design Group

EEDI: Energy Efficiency Design Index

GHG: Greenhouse Gas

HC: Hydrocarbons

ICE: Internal Combustion Engine

LH_2: Liquid Hydrogen

LHV: Lower Heating Value

LNG: Liquid Natural Gas

MARAD: Maritime Administration (U.S.)

MMT: million metric tonne

NG: Natural Gas

NO_x: Oxides of nitrogen

PEM: Proton Exchange Membrane

PM: Particulate Matter

PM_{10}: Particulate matter with diameter less than 10 micrometers.

$PM_{2.5}$: Particulate matter with diameter less than 2.5 micrometers

SF-BREEZE: San Francisco Bay Renewable Energy Electric Vessel with Zero Emissions

SMR: Steam methane reforming

WTT: Well-to-Tank

WTW: Well-to-Waves

Acknowledgements:

The U.S. Department of Transportation (DOT), Maritime Administration (MARAD) funded the SF-BREEZE project. The views expressed here are not necessarily those of the DOT. Information and helpful discussions with Ryan Sookhoo of Hydrogenics are much appreciated. Thanks are extended to Kirk Rosenkranz and John Lee of the California Air Resources Board for very helpful information and discussion. We are grateful to Dr. Samantha Lawrence (Sandia) and Thomas Klebanoff (Duke University) for assistance with some aspects of the data handling and figure production. We very much appreciate constructive comments from Tom Felter of Sandia regarding criteria pollutant emissions associated with hydrogen production paths, and Rich Berman of the Port of San Francisco for helpful and encouraging discussions. Finally, the authors thank the anonymous journal reviewers for very constructive comments on the manuscript.

The work was performed at Sandia National Laboratories, which is a multi-program laboratory managed and operated by Sandia Corporation, a wholly owned subsidiary of Lockheed Martin Corporation, for the U.S. Department of Energy's National Nuclear Security Administration under contract DE-AC04-94AL85000.d

References:

[1]. J. Keller, L. Klebanoff, S. Schoenung and M. Gillie, "*The Need for Hydrogen-based Energy Technologies in the 21st Century,*" Chapter 1 in Hydrogen Storage Technology, Materials and Applications, Ed. L.E. Klebanoff (Boca Raton: Taylor & Francis; 2012), p. 3.

[2]. IPCC (Intergovernmental Panel on Climate Change) Report: "*Climate Change 2007: The Physical Science Basis. Contribution of Working Group I to the Fourth Assessment Report of the IPCC*," S. Solomon, D. Qin, M. Manning, Z. Chen, M. Marquis, K. B. Averyt, M. Tignor, and H. L. Miller, eds. Cambridge, U.K.: Cambridge University Press, p. 996.

[3]. "*America's Climate Choices, Panel on Advancing the Science of Climate Change*," National Research Council, ISBN: 0-309-14589-9 (2010).

[4]. L. Klebanoff, J. Keller, M. Fronk and P. Scott, "*Hydrogen Conversion Technologies and Automotive Applications,*" Chapter 2 in Hydrogen Storage Technology, Materials and Applications, Ed. L.E. Klebanoff (Boca Raton: Taylor & Francis; 2012), p. 31.

[5]. A. Sydbom, A. Blomberg, S. Parnia, N. Stenfors, T. Sandström and S.E. Dahlen, "*Health Effects of Diesel Exhaust Emissions,*" European Respiratory Journal, **17**(4), 733 (2001).

[6]. H. N. Psaraftis and C.A. Kontovas, "*CO_2 Emission Statistics for the World Commercial Fleet,*" WMU J. of Maritime Affairs **8**, 1 (2009).

[7]. T.A. Boden, R.J. Andres and G. Marland, "*Global, Regional and National Fossil-Fuel CO_2 Emissions,*" available at: http://cdiac.ornl.gov/trends/emis/tre_glob_2013.html

[8]. The EEDI amendments to MARPOL Annex VI can be found at: http://www.imo.org/en/MediaCentre/HotTopics/GHG/Documents/eedi%20amendments%20RESOLUTION%20MEPC203%2062.pdf

[9]. "*Third IMO GHG Study 2014: Executive Summary and Final Report, June 2014,*" International Maritime Organization, Marine Environment Protection Committee MEPC 67/INF.32014.

[10]. The 2012 Estimated Annual Average Emissions Statewide can be found at the California Air Resources Board Website: http://www.arb.ca.gov/app/emsinv/2013/emssumcat_query.php?F_YR=2012&F_DIV=-4&F_SEASON=A&SP=2013&F_AREA=CA#8

[11]. J. J. Corbett and A. Farrell, "*Mitigating Air Pollution Impacts of Passenger Ferries,*" Transportation Research Part D **7**, 197 (2002).

[12]. California ARB document *"Appendix B: Emissions Estimation Methodology for Commercial Harbor Craft Operating in California,"* available at: http://www.arb.ca.gov/regact/2007/chc07/appb.pdf

[13]. A link to the California ARB's commercial harbor craft regulations can be found at: https://govt.westlaw.com/calregs/Document/I0FD137A0A3C111E0BACCB30E82542E24?viewType=FullText&originationContext=documenttoc&transitionType=CategoryPageItem&contextData=%28sc.Default%29 Subsection 93118.5(e)(4) and (e)(5) are subsections that set forth the regulatory requirements new ferries need to meet.

[14]. Tier 1 regulations set forth by the U.S. EPA in "*Control of Emissions of Air Pollution from New Marine Compression-Ignition Engines at or Above 37 kW,*" 64 Federal Register (FR) 73299-73373, December 29, 1999 (40 CFR Part 94).

[15]. Tier 4 regulations set forth by the U.S. EPA in "*Final Rule: Control of Emissions of Air Pollution from Locomotive and Marine Compression-Ignition Engines Less than 30 Liters Per Cylinder*" (73 FR 25245 et seq., May 6, 2008)(40 CFR Part 1042).

[16]. K. Cullinane and R. Bergqvist, "*Emission Control Areas and Their Impact on Maritime Transport,*" Transportation Research Part D **28**, 1 (2014).

[17]. B.C. Hartman and C.B. Clott, "*An Economic Model for Sustainable Harbor Trucking*," Transportation Research Part D **17**, 354 (2012).

[18]. C.-H. Liao, P.-H. Tseng, K. Cullinane and C.-S. Lu, "*The Impact of An Emerging Port on the Carbon Dioxide Emissions of Inland Container Transport: An Empirical Study of Taipei Port,*" Energy Policy **38**. 5251 (2010).

[19]. Y.-T. Chang, Y. Roh and H. Park, "*Assessing Noxious Gases of Vessel Operations in a Potential Emission Control Area*," Transportation Research Part D **28**, 91 (2014).

[20]. Y.-T. Chang, Y. Song and Y. Roh, "*Assessing Greenhouse Gas Emissions from Port Vessel Operations at the Port of Incheon,*" Transportation Research Part D **25**, 1 (2013).

[21]. S. Song, "*Ship Emissions Inventory, Social Cost and Eco-efficiency in Shanghai Yangshan Port,*" Atmospheric Environment **82**, 288 (2014).

[22]. E. Tzannatos, "*Ship Emissions and their Externalities for the Port of Piraeus-Greece*," Atmospheric Environment **44**, 400 (2010).

[23]. L.E. Klebanoff, J.W. Pratt and C.B. LaFleur, "*Comparison of the Safety-related Physical and Combustion Properties of Liquid Hydrogen and Liquid Natural Gas in the Context of the SF-BREEZE High-Speed Fuel-Cell Ferry,*" Int. Journal of Hydrogen Energy **42**, 757 (2017).

[24]. A.E. Lutz, R.S. Larson and J.O. Keller, "*Thermodynamic Comparison of Fuel Cells to the Carnot Cycle,*" International J. of Hydrogen Energy **27**, 1103 (2002).

[25]. J. Larminie and A. Dicks, in *"Fuel Cell Systems Explained,"* (John Wiley & Sons Ltd., New York, 2000).

[26]. S.E. Wright, *"Comparison of the Theoretical Performance Potential of Fuel Cells and Heat Engines,"* Renewable Energy **29**, 179 (2004).

[27]. J.W. Pratt, L.E. Klebanoff, T. Escher, J. Burgard, C. Leffers and K. Sonerholm, *"Design of the SF-BREEZE High-Speed Fuel-Cell Ferry,"* in preparation.

[28]. Details of the HD-30 PEM Fuel Cell were provided courtesy of Ryan Sookhoo of Hydrogenics. The HD-30 specifications can also be found at the website: http://www.hydrogenics.com/docs/default-source/pdf/2-3-1-hypm_hd30_one-pager_en_a4_rev00.pdf?sfvrsn=2

[29]. Information on the MTU 16V4000 diesel engine can be found at: https://www.mtu-online.com/fileadmin/fm-dam/mtu-global/technical-info/operating-instructions/neu_17_08_2012/en/M015241_03E.pdf

[30]. R. Edwards, J.-F. Larive, V. Mahieu and P. Rouveirolles, *"Well-to-Wheels Analysis of Future Automotive Fuels and Powertrains in the European Context: Well-to-Tank Report",* Version 2C, Technical Report by the Joint Research Center of the European Commission March 2007.

[31]. R. Edwards, J.-F. Larive, D. Rickeard and W. Weindorf, *"Well-to-Wheels Analysis of Future Automotive Fuels and Powertrains in the European Context: Well-to-Tank Report,"* Version 4, Technical Report by the Joint Research Center of the European Commission, July 2013.

[32]. A description of the State of California 2014 Electrical Grid resource mix can be found at: http://energyalmanac.ca.gov/electricity/total_system_power.html

[33] P.S. Mehta and K. Anand, *"Estimation of a Lower Heating Value of Vegetable Oil and Biodiesel Fuel,"* Energy and Fuels **23**, 3893 (2009).

[34]. S. Stoner, T. Olson, M. Addy, R. Tuvell, R. Shapiro and B.B. Blevins, *"Full Fuel Cycle Assessment Well to Tank Energy Inputs, Emissions and Water Impacts,"* California Energy Commission Report CEC-600-2007-002-D, 2007. Available at: http://www.energy.ca.gov/2007publications/CEC-600-2007-002/CEC-600-2007-002-D.PDF

[35]. S. Brynolf, M. Magnusson, E. Fridell and K. Anderson, "*Compliance Possibilities for the Future ECA Regulations Through the Use of Abatement Technologies or Change of Fuels,*" Transportation Research Part D **28**, 6 (2014).

[36]. J. Nuszkowski, N.N. Clark, T.K. Spencer, D.K. Carder, M. Gautam, T.H. Balon and P.J. Moynihan, "*Atmospheric Emissions from a Passenger Ferry with Selective Catalytic Reduction,*" J. Air &Waste Manage. Assoc. **59**, 18 (2009).

[37]. D.A. Cooper, "*Exhaust Emissions from High Speed Passenger Ferries,*" Atmospheric Environment **35**, 4189 (2001).

[38]. D.A. Cooper and K. Andreasson, *"Predictive NO_x Emission Monitoring On-board a Passenger Ferry,"* Atmospheric Environment **33**, 4637 (1999).

[39]. D.A. Cooper, K. Peterson and D. Simpson, *"Hydrocarbon, PAH and PCB Emissions from Ferries: A Case Study in the Skagerak-Kattegatt-Oresund Region,"*Atmospheric Environment, **30** 2463 (1996).

[40]. F. Di Natale and C. Carotenuto, *"Particulate Matter in Marine Diesel Engines Exhausts: Emissions and Control Strategies,"* Transportation Research D **40**, 166 (2015).

[41]. D.A. Lack and J.J. Corbett, *"Black Carbon from Ships: A Review of the Effects of Ship Speed, Fuel Quality and Exhaust Gas Scrubbing,"* Atmos. Chem. Phys. **12** 3985 (2012).

Appendix: E

Annual Operations Cost Estimates for the Zero-V

Base the Zero-V annual operating and maintenance cost estimate from the 2014 Annual Budget Estimate for the *New Horizon*, provided to Lennie Klebanoff from Bruce Appelgate on 8/10/17.

New Horizon

Built: 1978
Mid-Life: 1996
Length: 170’
Beam: 36’
Draft (max): 12’
ITC Gross Tonnage: 797 tons
ITC Net Tonnage: 239 tons
Registered Tonnage, Gross: 297 tons
Registered Tonnage, Net: 202 tons
Loaded Displacement: 1,007 long tons
Crew: 12
Scientific berting: 19
Main Engines: Two D398, 850 hp Catepillar Models
Bow Thruster: LIPS Variable-Speed Electric Tunnel 200kW
Propulsion: Two, controllable pitch
Water Capacity: 2,300 gal
Ship Service Generators: Two 230 kW
Fuel Consumption: 1,000 gal/day (average)
Transit Speed for Cruise Planning: 9.0 knots (variable with speed/time estimates)
Minimum Speed: variable to 0
Endurance: 40 days max (fuel)
Range: 9,600 miles (fuel)
Fuel Capacity: 40,000 (planning)
Radio Call Sign: WKWB
Laboratory Space: 1,265 sq. ft
Main Deck Working Area: 1,730 sq. ft.
Freeboard: 3.5 ft.

Zero-V

Design Speed: 10 knots
Main Laboratory” 670 sq. ft.
Wet Lab: 650 sq. ft. (Total = 1320 sq. ft.)
Main Deck Working Area (Aft. + Side): 2300 sq. ft.
Freeboard: 9 ft.

Zero-V Mission:
- Zero emissions
- General purpose R/V
- Coastal operations - CA
- 2400nm range
- Dynamic positioning18 scientists, 11 crew
- Large lab spaces
- Large working deck
- Substantial over-the-side handling systems
- Low underwater noise
- Capable hydro acoustic suite

Vessel Particulars:
Length: 170’-0”
Beam: 56’-0
Draft: 12’-0”
Depth: 21’-0”
Fuel Cell Power: ~1.8 MW
LH_2: ~ 11,000 kg

New Horizon Baseline Figures

***New Horizon* Days at Sea: 179**

Total Ships Payroll: $1,228,455
(12 crew, includes all salaries, overtime, fringe benefits)

Maintenance and Repair: $565,667
($400,000/yr for 5-year engine overhaul + $165,667 normal M&R)

Fuel (diesel, $3.50/gal): $625,305
For our estimate, use the Robin Madsen's diesel consumption for the Zero-V of 504,638 kg (158, 691 gallons) @ $3.50/gallon = $555,419.

Other Ship Costs: $621,141
(food, insurance, stores, travel)

Total Ship Costs = Payroll + M&R + Fuel + Other Ship Costs: $2,970,682.

Total Distributed Costs: $371,316
(Salaries, Employee Benefits, Shore Support)

Total Direct Costs = Total Ship Costs + Total Distributed Costs: $3,341,998

Indirect Cost: $614,139

Total *New Horizon* O&M Cost = Total Direct Costs + Indirect Cost: $3,956,137

Adjustments to this baseline for the Zero-V

Fuel Cell Refurbishment: We have 60 Hydrogenics HD30 fuel cell units on the Zero-V. The number of days the vessel is operating is 152 from Robin. This corresponds to 3648 hours of operation in a year. The fuel cell lifetime is reported to be 10,000 – 15,000 hours from Hydrogenics. Let's assume 12,500 hours. Thus if all of the fuel cells were being used during the 3648 hours of operation, then all of the fuel cells would need to be replaced every 3.43 years.

However, this is not the case. Robin has calculated that the total energy output of the Zero-V fuel cells over the 152 days in performing the Scripps science mission is 2,272, 525 kW-hours. Thus, over the 3648 hours in the 152 days of use, the average power is (2,272,525 kW-hrs)/3648 hours = 623 kW. Thus, it turns out that on average only 34.6% of the 1.8 MW of installed fuel cell power is being used over the course of a year. Of course, some vessel operations require all the fuel cells to be used. Other operations require a lot less. But the average is 34.6%. This means that instead of all the fuel cells needing to be replaced in 3.43 years, they will need to be replaced in 9.91 years. This new consideration leads to a considerably reduced O&M cost.

The cost to replace an HD30 fuel cell unit is estimated to be (in current dollars) $30,000/unit. Thus, to replace all 60 HD 30 units on the Zero-V would require $1,800,000. If all of the fuel cells are replaced every 9.91 years, then the annual cost is $1,800,000/9.91 years = $181,635.

Fuel Cell Balance of Plant (BOP) Maintenance

Hydrogenics reports we should use a budget of 2.5% of the fuel cell powerplant capital cost to cover the yearly BOP maintenance. Hence, $3.96M x 0.025 = $99,000/year for fuel cell BOP maintenance.

LH_2 Fuel Costs

Robin has estimated that to perform the science missions indicated by Scripps, the total amount of LH_2 fuel used would be 142,459 kg in a year. For non-renewable hydrogen produced from natural gas, we use a delivered LH_2 price of $6.87/kg$H_2$. Thus, the yearly cost of LH_2 (non-renewable) would be: 142,459 kgH_2 x $6.87/kg = $978,693 per year. If we used renewable LH_2, we have a quoted price of $16.38/kg at today's prices. If we used renewable LH_2, the fuel costs would be 142,459 kgH_2 x $16.38/kg = $2,333,478 per year.

Implementing Adjustments

Let's assume that for the *New Horizon* M&R budget of $565,667, that $165,667 of this budget is for equipment unrelated to the diesel engines, so we have to keep that number and add the H-related expenses. The new M&R budget for the Zero-V would be $165,667 (non-diesel engine M&R) + $181,635 (fuel cell replacement) + $99,000 (fuel cell BOP) = $445,635.

The LH_2 fuel cost would be: $978,693 /year for NG-derived hydrogen. The LH_2 fuel cost would be $2,333,478 per year using renewable LH_2. Thus, for the Zero-V annual budget, we have:

Zero-V Baseline Figures

Days at Sea : 152

Total Ships Payroll: $1,228,455
(includes all salaries, overtime, fringe benefits)

Maintenance and Repair: $445,635
(including fuel cell overhaul)

Fuel (LH_2, non-renewable, $6.87/kg): $978,693
(Renewable LH_2: $2,333,478, $16.38/kg)

Other Ship Costs: $621,141
(food, insurance, stores, travel)

Total Ship Costs = Payroll + M&R + Fuel + Other Ship Costs: $3,273,924
(Renewable: $4,628,709)

Total Distributed Costs: $371,316
(Salaries, Employee Benefits, Shore Support)

Total Direct Costs = Total Ship Costs + Total Distributed Costs: $3,645,240.
(Renewable: $5,000,025)

Indirect Cost: $614,139

Total Zero-V O&M Cost (NG LH_2) = Total Direct Costs + Indirect Cost: $4,259,379

Increase in Total Annual Operations Cost for Zero-V relative to *New Horizon* = $4,259,379/$3,956,137= 1.077 at today's prices for NG LH_2.

Total Zero-V O&M Cost (Renewable LH_2) = Total Direct Costs + Indirect Cost: $5,614, 164.

Increase in Total Annual Operations Cost for Zero-V relative to *New Horizon* = $5,614, 164/$3,956,137 = 1.419 at today's prices for renewable LH_2.

But, you are getting: Zero-emission operation, no fuel spills, quieter operation, 33% increase in deck working area, 4.3% increase in lab space, 11% increase in speed, but 75% reduction in range.

Appendix: F

Feasibility of Refueling the Zero-V at Identified Sites

The Zero-V will primarily operate along the coast of California, although it has the range to transit from San Francisco to Honolulu. The vessel holds two LH_2 tanks with storage capacity 5840 kg each, or a total of 11,680 kg. The usable hydrogen capacity is 10,900 kg (see Appendix B). Since road LH_2 trailers typically can deliver 4,000 kg each, three trailers will be required to refuel the Zero-V at maximum. We recognize that many refueling operations would require only two trailers, as half of the vessel's missions involve less fuel consumption. The first feasibility question to be answered is if this supply of LH_2 (both fossil NG based hydrogen and renewable hydrogen) could be supplied by the gas suppliers. A second feasibility question is if the Zero-V refueling operation could physically take place at the sites identified as likely refueling sites. For example is there sufficient space for a couple of LH_2 trailers to be refueling the Zero-V at the same time? A third refueling question is if the refueling could take place within the desired time. Scripps indicated that the preferred refueling time was 8 hours or less, as this is the duration of a typical work shift.

A picture of a Linde LH_2 tanker refueling a stationary LH_2 tank at the Emeryville CA hydrogen station is shown in Figure 1 below.

In addition to LH_2 refueling, there are other activities onboard the Zero-V that must be accommodated by the refueling site. These activities include:

- Bringing 18-wheel trucks onto the site to deliver science equipment.
- Using forklifts to off-load equipment from the Zero-V, and loading new equipment onboard.
- Using cranes to load/off-load science equipment.
- Storing science equipment in anticipation of vessel arrival in a onsite warehouse (or other enclosed structure).

Needed facilities in support of this work includes power, sewage, water, internet, all of which must be provided at the refueling location. Another activity is adding/replacing crew and scientists for work on the vessel, which should be supported by proximity to hotels and restaurants.

Figure 1: (a) Linde LH_2 Refueling Trailer providing hydrogen to the Emeryville CA hydrogen station stationary LH_2 tank. (b) Linde personnel preparing hose connection; (c) Linde LH_2 Refueling Trailer. Pictured (L-R) are Kyle McKeown and Nitan Natesan (Linde), Lennie Klebanoff (Sandia), and Tom Escher and Joe Burgard of the Red and White Fleet.

With these issues in mind, we examined the feasibility of refueling the Zero-V. We start with the questions concerning LH_2 supply and refueling rates and overall refueling logistics and requirements. Two industrial gas suppliers were contacted with regard to the Zero-V refueling: Linde Gas and Air Products. The meeting with Kyle McKeown (Linde) took place on March 21, 2017 in their Pleasanton CA offices. The conversation with Dave Farese and Brian Bonner (both Air Products) took place on the telephone on March 23, 2017.

Beginning with Linde, Kyle walked us through the typical high-level tank filling operations for a hydrogen fueling station.

1. Truck arrives on site and makes connections
2. Truck builds pressure in the trailer tank using the truck's pressure build coil.
3. Truck purges air out of hoses and pipes with cold hydrogen gas, the gas also serves to cool down the hoses. During purging and cool down, gas is vented to the fueling station vent mast.
4. Once hoses are cooled, the truck starts pushing liquid to the storage tanks.
5. Once liquid transfer is complete, the truck used cold gas to push liquid out of lines into the storage tank.
6. Truck drops the trailer tank pressure by venting gas to the fueling station vent mast.
7. Hose connection is broken using non-sparking tools and hoses are capped.
8. Truck departs.

Our conversations with Linde and Air Products centered on how this procedure could be adapted for refueling the Zero-V, and what the requirements are for the refueling site. Summaries of these discussions are provided below.

Questions and Answers in Meeting with Linde (Kyle McKeown)

How much deliverable LH_2 does a Linde tanker (of nominal 4,000 kg storage) actually deliver?

Kyle believes the deliverable LH_2 from the trailer is 3870 kg. To deliver the total fuel complement of 11,680 kg will require 3 LH_2 trailers, which will deliver 11,610 kg or 99.4 percent of the required fuel.

Can we refuel the Zero-V in 8 hours using three LH_2 tanker trucks?

Kyle says it takes 1.5 hours to set up for a fill, and then once set up, the LH_2 is typically delivered at 22 kg/min for one trailer. If we have two trailers, this would double to 44 kg/min. So, to deliver 7740 kg with 2 trucks fueling in parallel = 2.93 hrs of full flow. At the end of the fill, it takes about 15 mins to disconnect one trailer (or 30 minutes for two trailers). It would take about 45 mins to bring in and attach the third trailer, 2.93 hr to fuel the remaining 3870 kg with one trailer, and then another 15 mins to disconnect. Total time to get to 11610 kg into 2 tanks = 1.5 hr + 2.93 hr + 0.50 hr + 0.75 hr + 2.93 hr + 0.25 hr = 8.86 hours, or rounding to a whole number, 9 hours.

Should we refuel the Zero-V tanks independently? One trailer filling one tank in parallel?

Kyle answered affirmatively, this way you don't have to worry about the two LH_2 lines having different pressures. Fill independently, one trailer filling one tank is the best procedure to follow.

Can we refuel with two tanker trucks simultaneously? Would there be scheduling problems getting three Linde tankers to a location at the start of a refueling window?

Yes, refueling with two LH_2 trailers simultaneously, with each trailer devoted to refueling one Zero-V LH_2 tank, should be straightforward, and there are no regulatory barriers to doing so. There are no technical hurdles to scheduling three LH_2 trailers to arrive on the same day with about 10 days advanced notice.

Would we be better off going to a permanent Zero-V LH_2 storage facility to increase hydrogen flow rate and decouple the Zero-V from the Linde truck schedule?

Kyle strongly felt that refueling with mobile trailers is the better option. We would also need to deploy a fueling stanchion which would be the union between the trailer LH_2 hose and the hose coming from the Zero-V. A fueling stanchion would provide a stationary fueling port that the trailers could connect to, avoiding complications from boat motion during fueling. In addition, the fueling stanchion could be portable (for example on a truck). This could be very attractive for Port operations, as all refueling infrastructure is brought in for refueling, and removed from the Port after refueling is complete. In addition, the trailer delivery should be cheaper and the liquid quality better for fueling (subcooled).

What are the requirements for a location to receive the LH_2 tankers? Weight and access only?

The weight of each LH_2 trailer is 76,000 lbs fully loaded and they have 5 axles. So, on any prospective fueling location,

we needs space for 3 such LH_2 trailers, a mobile refueling stanchion and be able to handle the weight of three trailers (228,000 lbs).

If we demanded "renewable" LH_2 be delivered, can Linde provide it?

Kyle does not know where they would source the renewable LH_2, but he thought they could provide it. The Zero/V using renewable LH_2 would dramatically impact the way Linde looks at renewable LH_2 in the U.S. because the Zero-V would be a large and reliable customer of renewable LH_2.

What is your assessment of refueling the Zero-V at Wharf 5 within the Port of Redwood City?

Wharf 5 looks very good. One detail is that we might have to upgrade the lights to be protected from H_2 leaks. Wharf 5 looks to have easy access for LH_2 tanks to come onto and off the Wharf. One important San Francisco Bay Area refueling note: Currently, LH_2 trailers are forbidden from traveling on the San Francisco Bay Bridge. However, this restriction does not affect refueling at Pier 54 in San Francisco, or Wharf 5 at the Port of Redwood City.

Would Linde be OK moving a trailer that is pressurized (say to 100 psig) a few hundred feet to a "depressurization station" after Zero-V refueling is complete? That way, we can perform trailer depressurization (required before the trailer goes back on public roads) away from the Zero-V, to another part of the Port.

Kyle can't speak for all of Linde or its distribution operations, however, he does not think moving a 100 psig trailer would be a concern. His understanding is that it's a very common practice.

Questions and Answers in Meeting with Air Products (Dave Farese and Brian Bonner)

How much deliverable LH_2 does an Air Products tanker (of nominal 4,000 kg storage) actually deliver?

A typical deliverable load is up to 4,000 kg. Thus, two trailers filling simultaneously can deliver 8,000 kg, followed by a third truck for final refueling to 11,680 kg. The easiest way is to have each trailer fuel one tank independently. The ground under the trailer should be concrete or gravel. Spill pans for temporary filling can be used, but are not preferred. Typical trailer vacuum insulated hose lengths can be up to 14 feet, with internal diameters (ID) and outside diameters (OD) of typically 1" ID and 3" OD, respectively.

How long would it take to refuel 11,680 kg for the Zero-V?

A typical "all in" delivery time to dispense 4,000 kg is 3.5 hours for a single trailer. This time includes hookup, line purging and cool-down. Thus, for 11,680 kg, the refueling time would be 10.22 hours, just outside the 8 hours of a single work shift. However, Air Products recommends dual fueling stanchions to permit simultaneous unloading. These fueling points should maintain a 25 feet separation for the trailers. There should be no trailer movement while each trailer is fueling. Ship-to-shore transfer distances of 50-60 feet are not an issue. Some extended fill lines have been up to 100 feet, but it takes longer to cool everything down and transfer losses may increase slightly.

Can we refuel with two LH_2 tanker trucks simultaneously? Are there any restrictions, either technical or regulatory, or in Air Products scheduling? How much lead time does Air Products need to be notified for a refueling operation?

Air Products responded that they can refuel with 2 trailers simultaneously, and there are no restrictions other than the 25 foot separation guidance between trailers. Trailers can fuel from the rear, or from the side. With 1 week notice, Air Products can get LH_2 product almost anywhere, and be there on a given day at a certain time. Previous aerospace requirements have required as many as 9 LH_2 trailers to be on call for delivery with tight schedules.

Would we be better off going to a permanent LH_2 storage facility to get increased hydrogen flow rate and decouple the Zero-V from the Air Products truck schedule?

That is an option, but mobile refueling can also meet the need. For example, Air Products services submarines, delivering LH_2 to various ports and locations. Although the hydrogen is vaporized and compressed, since submarines receive gaseous H_2, the hydrogen arrives at these locations as LH_2, delivered by tanker truck. Air Products designs and builds fueling hardware. Gardner Cryogenics is an example vendor who manufactures tanks.

What are the requirements for a location to receive two LH_2 tankers simultaneously?

NFPA 55 and NFPA 2 provide guidelines for LH_2 storage and delivery. There are standoff distances for buildings, electrical equipment, flammable materials, etc. For example, ordinary electrical equipment can't be within 25 feet. The area must be large enough to allow for maneuvering of trailers that are up to 48 feet long and weigh up to 80,000 lbs.

If we required "renewable" LH_2 be delivered to the Zero-V, can Air Products provide this in the quantities required?

Air Products responded yes, but the hydrogen will be more expensive.

What is your assessment about refueling the Zero-V at Wharf 5 within the Port of Redwood City?

Air Products responded that this site, pending an official site evaluation could meet the requirements. In fact, Wharf 5 looks very similiar to the locations where they refuel submarines with hydrogen gas from LH_2 trailers.

Summarizing these discussions with the gas providers Linde Gas and Air Products, there was very good agreement on how the Zero-V refueling could be conducted. Fully refueling the Zero-V with 11,680 kg of LH_2 is best performed using LH_2 tankers directly, so infrastructure burden on the Ports can be minimized. The refueling can potentially be completed in 9 - 10 hours using three LH_2 trailers, slightly beyond the duration of a single work shift. The trailers can be reliably delivered with 7 – 10 days' notice, and both gas companies can provide renewable LH_2 in order to reduce well-to-waves GHG emissions, although renewable hydrogen would be more expensive. A fueling stanchion is recommended for ease and security of refueling hose connection.

The next set of feasibility questions concerned the locations for the refueling. The feasibility questions include: Can the Zero-V vessel dock comfortably? Can two LH_2 tankers with refueling stanchion be accommodated? Are the standoff requirements satisfied? Would the Ports even want LH_2 and the Zero-V visiting their locations? Are the required water depths (the draught of the Zero-V is 12 feet) at these locations sufficient to allow safe operation of the Zero-V? These and other questions were discussed with personnel from Nimitz Marine Facility (MarFac) of the Scripps Institution of Oceanography, with Mike Prince from the Moss Landing Marine Laboratory (MLML) and Monterey Bay Aquarium Research Institute (MBARI), with Rich Berman from the Port of San Francisco and with Mike Giari and Giorgio Garilli from the Port of Redwood City.

Nimitz Marine Facility (MarFac), San Diego, CA

The home port for the Zero-V would be the Nimitz Marine Facility (MarFac) of the Scripps Institution of Oceanography in San Diego CA. Figure 2(a) shows the general location of MarFac within the greater San Diego area. Figure 2(b) provides a general view of MarFac facility with the Zero-V docked while Figure 2(c) gives a close-up view of the Zero-V docked at MarFac along two LH_2 trailers and refueling stanchion show in red. The refueling stanchion recommended by the gas providers is notional only. The relative sizes of the Zero-V, LH_2 trailers and docks are properly rendered to allow an assessment of available space for the LH_2 refueling operation.

Figure 2 shows that there is ample room at MarFac to refuel the Zero-V. The water depth off the pier is 17-25 feet, more than enough to accommodate the 12 foot draught of the Zero-V. The facility already allows for refueling and restocking of research vessels, and there is ample room for all of the activities anticipated for the Zero-V, as suggested by Figure

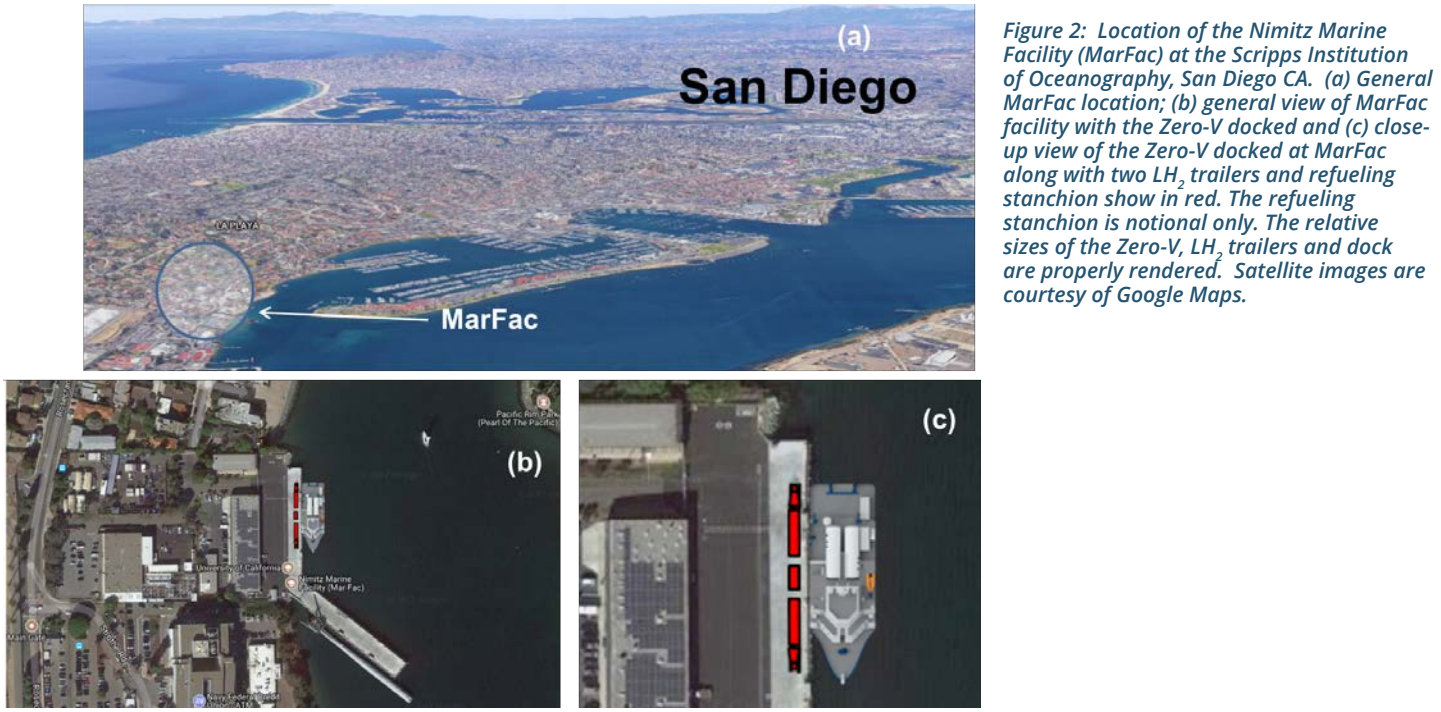

Figure 2: Location of the Nimitz Marine Facility (MarFac) at the Scripps Institution of Oceanography, San Diego CA. (a) General MarFac location; (b) general view of MarFac facility with the Zero-V docked and (c) close-up view of the Zero-V docked at MarFac along with two LH_2 trailers and refueling stanchion show in red. The refueling stanchion is notional only. The relative sizes of the Zero-V, LH_2 trailers and dock are properly rendered. Satellite images are courtesy of Google Maps.

2(c). Paul Mauricio, the Port Engineer at MarFac after hearing a full briefing on the Zero-V, concluded that all aspects of Zero-V refueling are readily accommodated at MarFac. One advantage of the hydrogen fuel-cell technology of the Zero-V is the complete absence of fuel spills. When asked about concerns about diesel fuel spills with conventional research vessels, and the absence of that with the Zero-V, Paul responded that they worry a lot about diesel spills, although it does not happen often (a cup full of diesel has spilled in the water that last 16 years). It is, however, a "big deal" when diesel spills, either on the water or on the deck. Spills incur a lot of costs, and people can lose their jobs. Bruce Appelgate confirmed they worry a lot about diesel spills, and added that if they spill it, they (or their contractor) must clean it up, which is expensive, and fines are given out, which is also expensive. From that standpoint, a fuel like LH_2 that disperses in seconds, and is not itself a GHG is very attractive.

Moss Landing Marine Laboratories (MLML) and Monterey Bay Aquarium Research Institute (MBARI), Moss Landing, CA

The MLML is a graduate school in Marine Sciences of the California State University System (CSU) located within Moss Landing Harbor, approximately 15 miles north of Monterey California. The Monterey Bay Aquarium Research Institute (MBARI) is a private, non-profit research center, funded by The David and Lucile Packard Foundation also located in Moss Landing with pier facilities supporting research vessels. Since the Zero-V can perform science missions in support of MLML and MBARI oceanographic research and educational objectives, we anticipate the Zero-V will need to dock and refuel at the MBARI Pier indicated in Figure 3.

The Zero-V can successfully transit to and from the MBARI Pier. However, the MBARI Pier is much more physically constrained than the other refueling sites, both with regard to vessel navigation from the sea through Moss Landing Harbor, to docking at the MBARI Pier. In addition, there are buildings near the berth, which must be examined with regard to the fire and safety codes NFPA 55 and NFPA 2.

Pier 54, Port of San Francisco, San Francisco, CA

The Zero-V project was briefed to Rich Berman of the Port of San Francisco on April 7, 2017 by Lennie Klebanoff. The Port of San Francisco was very enthusiastic and supportive. In addition to being a way of bringing zero-emission maritime technology to San Francisco Bay, they also were attracted by the educational component. Bay Area universities working with Scripps are:

U.C. Berkeley, Stanford, San Francisco State, San Jose State and U.C. Santa Cruz. Scripps is the oceanographic lead for all the U.C. schools. There is a current initiative to increase collaboration between the U.C. and Cal State Universities in

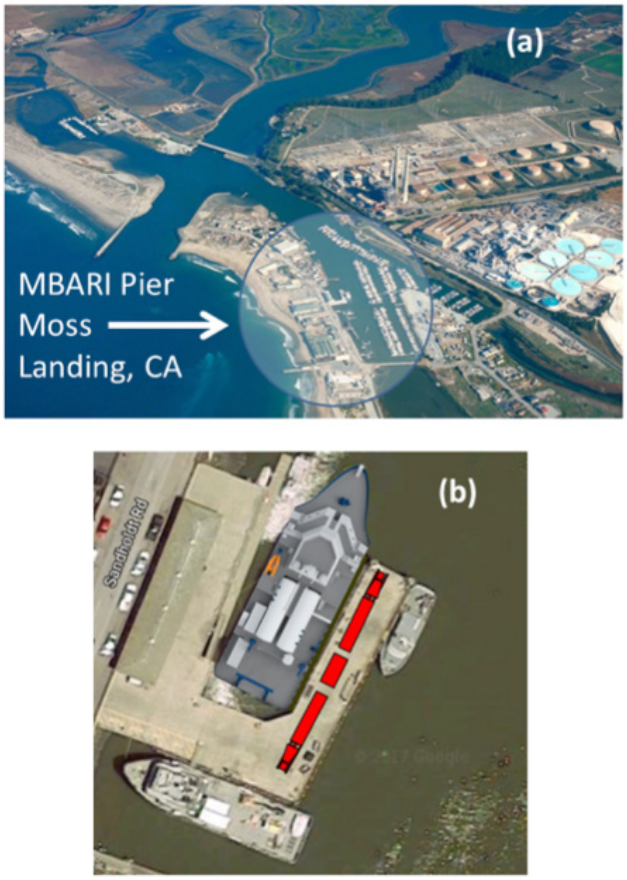

Figure 3: Location of the Monterey Bay Aquarium Research Institute (MBARI), within Moss Landing, 15 miles north of Monterey CA. (a) General MBARI location; (b) close-up view of the Zero-V docked at MBARI Pier along with two LH_2 trailers and refueling stanchion show in red. The refueling stanchion is notional only. The relative sizes of the Zero-V, LH_2 trailers and dock are properly rendered. Satellite images are courtesy of Google Maps.

the area of ocean science and the Port of San Francisco was excited to be host to such a zero-emissions hydrogen vessel that can support this research.

The Port of San Francisco recommended using Pier 54, as shown in Figure 4. Figure 4 shows that there is sufficient space at Pier 54 to refuel the Zero-V. Pier 54 is leased short-term and does not have any existing development plans. Pier 54 has direct vessel access from the San Francisco Bay. It has significant amount of Port-owned land at its base, which is currently being used as a parking lot. The area where it is located tends to be business/light and industrial dominant. The area is currently home to the UC San Francisco Medical Center. Both the City of San Francisco and the Port of San Francisco expect significant development in the years ahead. For example, The Chase Center, a new arena that will become home to the NBA's Golden State Warriors basketball team, is

Figure 4: Location of Pier 54, San Francisco CA. (a) General Pier 54 location relative to the City of San Francisco; (b) general view of Pier 54 with the Zero-V docked and (c) close-up view of the Zero-V docked at Pier 54 along with two LH_2 trailers and refueling stanchion show in red. The refueling stanchion is notional only. The relative sizes of the Zero-V, LH_2 trailers and dock are properly rendered. Satellite images are courtesy of Google Maps.

in the process of being built near to Pier 54. With the existence of medical facilities, and numerous hotels and restaurants nearby, Pier 54 is an attractive option in support of the Zero-V crew and scientists.

There are three aspects of Pier 54 that need to be considered. First, the south side is exposed to very rough swells during storms so the ideal location for the bunkering is on the north side, as indicated in Figures 4(b) and 4(c). Second, a structural assessment performed by the Port of San Francisco in 2013 revealed deterioration of some piles and other concrete support members on Pier 54. As a result, the pier was classified as Restricted Use and there is currently a 10-ton (gross) limit on vehicle traffic. This means that repairs are needed if the pier is to support the weight three LH_2 refueling trailers. Nonetheless, such repairs would be straightforward. Third, the current depth of the water on the north side of Pier 54 is estimated to be 10 - 12 feet, not enough for the Zero-V with a draught of 12 feet. The Port said they would need to take soundings and develop the bathymetry on the north side of Pier 54 to be sure. The Port of San Francisco's permit to dredge the bottom to 35 feet was renewed in 2013, so the Port has the authority to dredge, but it will be costly. Despite these aspects that need resolution, the Port of San Francisco has determined that Pier 54 is a feasible and preferred location for the Zero-V hydrogen bunkering operation provided the Pier's structure is repaired so as to allow multiple LH_2 trailers on the dock.

Wharf 5, Port of Redwood City, Redwood City, CA

The Port of Redwood City is in the South San Francisco Bay, and is another option for Zero-V refueling in the San Francisco Bay. It is an attractive destination because of its proximity to universities in the area (Stanford, San Jose State, U.C. Berkeley and U.C. Santa Cruz) with oceanographic research interests. In addition there are ample hotels and restaurants nearby to support Zero-V crew exchange. The Zero-V project was briefed to Mike Giari (Port Director) and Giorgio Garilli (Assistant Manager of Operations) on May 9, 2017. In attendance were also Joe Pratt (Sandia) and Joe Burgard (Red and White Fleet).

The Port of Redwood City is a deep-water port. Mike Giari and Giorgio Garilli agreed that amongst the Port's Wharfs, that Wharf 5 would be the best location for Zero-V refueling. Wharf 5 is shown in Figure 5.

Wharf 5 is a large open, structurally-sound pier. It had an engineering assessment performed in 2016 and is certified to be structurally sound, although the fenders need to be replaced. Wharf 5 is 60 feet wide, and access is excellent - an LH_2 trailer could come in one side and drive out the other

(Figure 5(b)). Wharf 5 has security already in place (fences), electricity, and has about 75 feet of space between the dock and the land which aids in meeting the setback distances required for LH_2 refueling operations. There is also the possibility of creating a parking lot near Wharf 5 as shown in Figure 5. It is close to the major freeway, CA-101, allowing easy transport of LH_2 via tanker trailer.

The depth of the water at Wharf 5 is adequate for the Zero-V, with minimum depth of 18 – 20 feet at the and 30 feet within the channel connecting the dock to the San Francisco Bay. There has not been a water depth survey for a few years, so another survey would be needed to confirm. Channel is regularly dredged for ships by Army Corps of Engineers every year or two. Near the dock the dredging is performed by the Port.

The Wharf 5 deck is 14' above water at 0-tide. The Zero-V has a 9-foot freeboard (21-feet deck to keel, with 12-foot draught). This would necessitate putting a floating dock in between, but a floating dock would be less stable. There is nothing unusual about fueling a 170 foot vessel (such as the Zero-V) at Wharf 5. There is ample room to locate a small truck crane on the Wharf, and the while it would not be permissible to permanently store science equipment on the dock, there is good storage space on the land side of Wharf 5. In fact, the space is already used by the U.S. Geological Survey (USGS) to store science equipment.

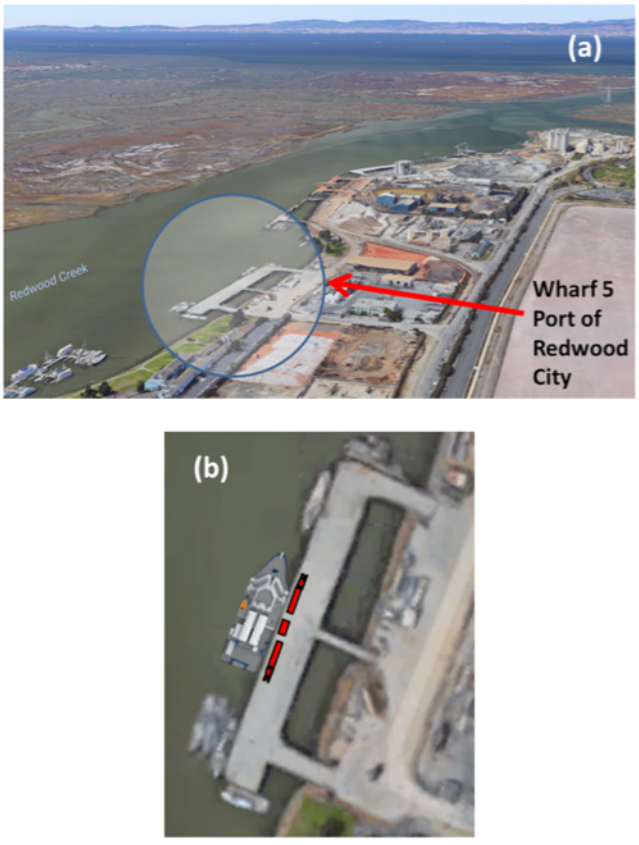

Figure 5: Location of Wharf 5, Port of Redwood City, Redwood City CA. (a) General Wharf 5 location relative to the San Francisco Bay; (b) close-up view of the Zero-V docked at Wharf 5 along with two LH_2 trailers and refueling stanchion show in red. The refueling stanchion is notional only. The relative sizes of the Zero-V, LH_2 trailers and dock are properly rendered. Satellite images are courtesy of Google Maps.

Wharf 5 is currently set up for shore-power of 480V/60A as this is what prior vessels used. Zoltan Kelety of Scripps stated that 480V/400A is more typical for research vessels like the Zero-V. Thus we anticipate an upgrade to the Wharf 5 electrical facilities would be needed. Wharf 5 has city water supply. There is no sewage connection on the dock but there is a sewer connection on shore. For Zero-V refueling, Wharf 5 could be set up with a line and pump to provide sewage offloading needs for the Zero-V. The Port of Redwood City likes the idea of refueling via LH_2 tanker with portable fueling stanchion, as this preserves on a day-to-day basis the Wharf 5 area. The weight limit for Wharf 5 is 500 lbs/ft^2. This is more than sufficient as the LH_2 trailers have a weight footprint of ~ 150 lbs/ft^2.

There is a history of smaller research vessels berthing at Wharf 5. The USGS used to use Wharf 5 for their Polaris research vessel, which is a 90-foot vessel. The Polaris moved to another location because the Wharf 5 fenders need replacing. The USGS now has a 60-65' research vessel for in-bay research, whose equipment is stored at the land side of Wharf 5.

Overall, Wharf 5 is under-utilized, with about 20 calls per year. Each call typically lasts one day, with a range of from 4 hours to 1 week. Barges that dock at Wharf 5 can be moved around to accommodate other vessels such as the Zero-V.

Appendix: G

DNV GL Statement of Conditional Approval in Principle and USCG Feedback

STATEMENT OF CONDITIONAL APPROVAL IN PRINCIPLE

Glosten/Sandia National Laboratories
Zero-V Hydrogen Research Vessel

This is to certify that Zero-V Hydrogen Research Vessel is granted *Conditional Approval in Principle (CAIP).*

The approval is based on the prospective DNVGL Rules for Classification of Ships Pt. 6 Ch. 2 Sec. 3 – *Fuel Cell Ship Installations – FC* (01-2018 edition), IGF Code – *International code of safety for ships using gases or other low-flashpoint fuels*, Part A.

Acknowledging that the current regulatory status does not allow for a conventional approval of hydrogen as fuel and fuel cells on maritime applications, this CAIP is a precursor to the more extensive alternative design process as described by the applicable statutory instruments.
No deviations have been identified that would be considered to be major show-stoppers from a regulatory point of view, given the available information in the design drawings in Appendix 2. Compliance with/clarifications of comments in Appendix 1 is a condition for the Approval in Principle, but comments need not be clarified/solved at this stage of the project.

Classification and Certification of specific installations may be granted subject to plan approval and survey as specified by the Rules, findings in future HAZIDS, risk assessments, explosion analysis etc.

DNV GL
Høvik, 2017-11-01

Digitally Signed By: Torill Grimstad Osberg
DNV GL Høvik, Norway
2017-11-01

Torill Grimstad Osberg
Head of Section, MCANO385 LNG, Cargo Handling and Piping Systems

Appendix 1: Drawing status and comments
Appendix 2: Drawings included in the Approval in Principle

Robin Madsen
Att: rtmadsen@glosten.com

DNV GL AS Approval
LNG, Cargo Handling & Piping Systems
P.O. Box 300
1322 Høvik
Norway
Tel: +47 67 57 90 26

Date:	**Our reference**:	**Your reference**:	**Job ID:**
2017-11-01	MCANO385/HCKW/ P26305-J-3		MCANO385-Zero/V-1

HØVIK LNG, CARGO HANDLING & PIPING SYSTEMS, Id. No. P26305
Zero-V conditional AIP review

Reference is made to your letter dated 2017-10-21. The following documents are stamped 2017-11-01 and given the status as shown below:

Document No	Rev	DNV GL No	Title	Code	Status
		1	LH2 Tank Vent Diagram for Hans-Christian		For Inf.
		2	Hydrogenics Power Rack Pictures and Diagrams		For Inf.
		3	Documentation on PEM Fuel Cells and Hydrogenics Fuel Cell Racks		For Inf.
		4	17003.01-540-01 Concept Gas System_Rev -_Signed		Examined w/comm
		5	17003.01-300-01 Electrical Oneline Diagram_Rev-_Signed		Examined
		6	17003.01-070-01_General Arrangement Rev -_Signed		Examined w/comm
		7	17003.01-000-01_ Hazardous Zones Plan_Rev-_Signed		Examined w/comm
		8	17003.01 Sandia Design Study Report Rev P2		For Inf.

Document No. **(empty)**, "LH2 Tank Vent Diagram for Hans-Christian" has the following comments:

2 **LH2 Tanks - Loss of vacuum insulation** **Important Note**

Reference is made to sheet 3. The rate of boil-off should be evaluated to document the statements regarding the capacities of the pressure relief valves, including the 3-way transfer valve.
Loss of vacuum insulation will lead to a colder outer shell, the effect of cryogenic cooling of supports and deck structures should be evaluated and documented.

7 **3 way valve** **Important Note**

The 3 way valve will be subject to special consideration, with respect to reliability and potential for

erronous operation (human error).

Document No. **(empty)**, "Documentation on PEM Fuel Cells and Hydrogenics Fuel Cell Racks" has the following comment:

9 Certification of fuel cells Important Note

The fuel cells are subject to certification, and should be delivered with a product certificate. The test programme can be based on the IEC standard 62282-3-1 "Stationary fuel cell power systems - Safety". Environmental and operating conditions in a ship shall also be taken into account. Please also note that according to DNVGL Rules, use of flammable materials is only acceptable for electrical isolating purposes and shall be minimized as far as practicable.

Document No. **(empty)**, "17003.01-540-01 Concept Gas System_Rev -_Signed" has been reviewed in accordance with DNVGL Rules for Ships Pt. 6 Ch. 2, IGF Code Pt. A, with the following comments:

3 Tank rooms/tank connection spaces Important Note

The IGF Code requires that a tank connection space (TCS) shall be able to fully contain LNG leakages. Given the differences in environmental impact between natural gas and hydrogen, and the high evaporation rate of the latter, it should be evaluated whether the tank rooms/TCSs should be closed and able to contain LH2 leakages, or if it is more suitable to construct a semi open TCS, providing natural ventilation and mechanical and environmental protection.
If fully closed tank room/TCS are selected, a pressure build-up analysis in case of major LH2 leakages should be provided.

8 Isolated pipe segments Important Note

Pipe segments and components that may be isolated in a liquid condition shall be provided with pressure relief valves. This applies for any part of piping from the tank isolation valve in the gas supply lines up to the first isolation valve after the liquid H2 is fully vaporized. If the vaporizers can be isolated, these should also be fitted with pressure relief valves.

10 Materials Important Note

On a general note, austenitic stainless steel should be used for materials in contact with hydrogen fuel. Use of other materials should be subject to special consideration. Materials and other piping specifications have not been reviewed at this stage, but will be subject to approval at the detailed design stage.

13 Double-block-and-bleed arrangement Important Note

The N2 supply should be installed to prevent the return of hydrogen to any non-hazardous spaces

15 Pressure relief valve maintenance Important Note

Stop valves shuold be fitted before and after the pressure relief valves at the tanks. These shall enable in-service maintenance without the risk of release of hydrogen gas through the (potentially) open pipe. Therefore, each group of relief valves/rupture disc should be possible to isolate from the vent mast. The stop valves shall be arranged to minimize the possibility that all pressure relief valves for one tank are isolated simultaneously. Physical interlocks shall be included to this effect. Reference is made to DNVGL Rules Pt. 6 Ch. 2 Sec. 5 (Gas fuelled ship installations). Although these rules are, as the IGF Code,

written for use with natural gas, it is considered that the safety philosophy in this specific issue should be the same.

Document No. **(empty)**, "17003.01-300-01 Electrical Oneline Diagram_Rev-_Signed" has been reviewed in accordance with DNVGL Rules for Ships Pt. 6 Ch. 2, IGF Code Pt. A

Document No. **(empty)**, "17003.01-070-01_General Arrangement Rev -_Signed" has been reviewed in accordance with DNVGL Rules for Ships Pt. 6 Ch. 2, IGF Code Pt. A, with the following comments:

1 **LH2 Tanks - Mechanical damage** **Important Note**

It is assumed that the tank location fulfills the probabilistic and deterministic criteria as described in the IGF Code [5.3] for collision protection. It is also assumed that the applicability of the requirements, as they are developed for natural gas, will be considered at the detailed design stage.

The need for mechanical protection of the tanks should be assessed, with respect to cargo operations, ship operations, green sea etc.

4 **Cryogenic cooling** **Important Note**

The effects of cryogenic cooling of decks and structures below any LH2 leakage points should be evaluated in the detailed design stage.

14 **Bunkering lines** **Action Required**

In general, bunkering lines should be arranged as self-draining towards the tank. If this is impractical due to the location of the tanks on the 01 Deck, other suitable means should be provided to relieve the pressure and remove liquid contents from the bunker lines.

It must be ensured in the detailed design stage that the bunkering manifold is designed to withstand the external loads it is subjected to during bunkering. This shall include the forces on the manifold in a scenario where the bunkering line is released by a breakaway coupling.

Please address follow-up to the approval expert

Document No. **(empty)**, "17003.01-000-01_ Hazardous Zones Plan_Rev-_Signed" has been reviewed in accordance with DNVGL Rules for Ships Pt. 6 Ch. 2, IGF Code Pt. A, with the following comments:

5 **Extent of hazardous zones** **Important Note**

It is noted that the hazardous zone classification described for natural gas is used. As the properties of hydrogen differs from those of natural gas, the extent of the zones should be evaluated.

Around the vent mast, the Code specifies a hazardous zone of 4.5 meters. This is justified by the requirements for tank holding times and boil-off gas management systems. As the application of hydrogen may introduce a different approach to these safety measures, the zone around the vent mast should be given special consideration.

6 **Flanges and valves** **Important Note**

During the detailed design of the vessel, it must be taken into account that all flanges, valves and other leakage points in the hydrogen system generates hazardous spaces. The hazardous zones will affect locations of other ship systems and accommodation, service stations etc. This has not been evaluated at this stage.

12 **ESD Concept** **Action Required**

It is noted the ESD Concept will be applied to the fuel cell spaces. It should be noted that the ESD philosophy is developed for use in connection with natural gas systems, and will not necessarily fulfill the safety requirements for hydrogen systems. Applying the ESD concept will be subject to special consideration in the next stage of the project.

Please address follow-up to the approval expert

Document No. **(empty)**, "17003.01 Sandia Design Study Report Rev P2" has the following comment:

11 **Safety/reliability philosophy** **Important Note**

Before the detailed design stage of the project, a safety/reliability philosophy document should be developed. The overall design should ensure that any single failure in the fuel cell power installation will not lead to an unacceptable loss of power (for definition, please see: DNVGL Rules Pt. 6 Ch. 2 Sec. 5 Table 1). Further, any safety actions required by rules, regulations or findings in a HAZID/Risk assessment shall not lead to an unacceptable loss of power.

Approval Expert for this approval is Hans-Christian Koch-Wintervoll.

Sincerely
for DNV GL AS

Torill Grimstad Osberg
Head of Section

Hans-Christian Koch-Wintervoll
Contact Person

U.S. Department of Homeland Security
United States Coast Guard

Commandant
United States Coast Guard

2703 Martin Luther King Jr. Ave SE
Washington, DC 20593-7430
Staff Symbol: CG-ENG
Phone: (202) 372-1365
Fax: (202) 372-1925
Email: timothy.e.meyrs@uscg.mil

16710/ZERO-V
2017845
August 28, 2017

Glosten
Attn: Mr. Robin Madsen, P.E.
1201 Western Ave, Suite 200
Seattle, WA 98101-2953

Subj: ZERO-V Hydrogen-Fueled Research Vessel Design Study Review

Ref: (a) Glosten email, "*Zero-V Hydrogen Research Vessel Design Review*", dated July 5, 2017
(b) Glosten Memo, Job/File No. 17003.01, "*Zero/V Regulatory Review*", dated July 5, 2017
(c) *General Arrangement*, Glosten, Drawing No. 17003.01-070-01, Rev. P5, 5 July 2017
(d) *Preliminary Hazardous Zone Plan*, Glosten, Drawing No. 17003.01-000-01, Rev. P1, 5 July 2017
(e) *Concept Gas System Architecture*, Glosten, Drawing No. 17003.01-540-01, Rev. P0, 5 July 2017
(f) *Electrical One-line Diagram: System Architecture*, Glosten, Drawing No. 17003.01-300-01, Rev. P1, 5 July 2017
(g) *Hazardous Zone 3d View*, Glosten, File 17003.01-000-02_Hazardous Zones 3DView_P1.pdf
(h) *Rules for Classification: Ships*, Part 6 Chapter 2, DNVGL, January 2017
(i) *International Code of Safety for Ships Using Gases or Other Low-Flashpoint Fuels (IGF Code)* as Amended by Resolution MSC.391 (95), International Maritime Organization (IMO)
(j) Commandant (CG-ENG) Policy Letter 01-12, CH-1, *Equivalency Determination – Design Criteria for Natural Gas Fuel Systems (Change-1)*, 12 July 2017

Dear Mr. Madsen:

We have reviewed references (a) through (g) regarding the feasibility study of a proposed hydrogen fuel cell powered research vessel that you are conducting on behalf of Sandia National Laboratories (Sandia) and the US Maritime Administration (MARAD). We understand from your memo that it is a goal of Sandia and MARAD to ultimately obtain approval of a Design Basis from the Coast Guard for this proposed vessel design. In this letter we are providing feedback and comments on what you have provided so far. However, since your project is still in the feasibility study phase, we are not able to issue a Design Basis Letter at this time. If the project progresses from feasibility to preliminary design, with an owner/operator dedicated to moving forward with this project, the owner/operator may submit a proposal through the Marine Safety Center requesting a Design Basis from the Coast Guard.

In general, we find no noteworthy issues with the concept as presented. As an oceanographic research vessel, the proposed vessel would be regulated under 46 CFR Subchapter U. Neither the use of liquid hydrogen as a fuel, nor fuel cells as a source for propulsion power, is specifically addressed in Subchapter U. However, 46 CFR 188.15 – *Equivalents*, allows the Coast Guard to accept a vessel of unusual, unique, special, or exotic design provided that the vessel is shown to be at least as safe as any vessel which meets the standards required by Subchapter U.

Your proposal to use the IGF Code in conjunction with DNV-GL rules seems a reasonable approach based on the nature of liquid hydrogen as a low-flashpoint fuel. The IGF Code is an internationally accepted standard that has already been incorporated by Coast Guard policy, in reference (j), and applied to the design of natural gas fueled vessels. While the vessel proposed in your study would use liquid hydrogen as fuel, not natural gas, there are many similarities in the physical properties and risks presented by these two fuels. Furthermore, the use of class rules from a Coast Guard recognized classification society such as DNV-GL, which specifically address hydrogen fuel cell installations, provides a solid foundation for requirements we could apply to such a vessel.

Details of the specific framework of standards and requirements to be applied to the proposed hydrogen fueled research vessel would need to be specified in a Design Basis Letter issued by the Coast Guard, with special attention given to the differences between liquid hydrogen, and liquefied natural gas (LNG). As mentioned above, this would need to be initiated by a request and proposal from an owner/operator who has an established intent to move forward with the project.

We offer the following comments based on a review of your submission:

IGF Code and alternative design analysis – We agree that while there are no existing requirements specific to hydrogen fuel in the IGF Code, it does provide a good baseline design standard for the hydrogen-fueled propulsion plant and associated safety systems on the vessel proposed in your study. Section 2.3 – "Alternative Design" of the IGF Code provides a framework for evaluating designs using fuels such as liquid hydrogen, which are not specifically addressed within the code. This section references the alternatives methodology in SOLAS II-1/55, as a means of meeting the goals and functional requirements contained within the code. Furthermore, IMO has developed *Guidelines on Alternative Design and Arrangements for SOLAS II-1 and III (MSC.1/Circ.1212)*, which provides additional details for the engineering analysis required in SOLAS II-1/55. This guidance would be instrumental for a potential owner/operator in developing a Design Basis proposal for Coast Guard review as described above.

IGF Code Risk Assessment – Section 4.2 of the IGF Code requires a risk assessment be conducted to ensure that risks arising from the use of low-flashpoint fuels affecting persons on board, the environment, the structural strength or the integrity of the ship are addressed. While this risk assessment is limited in scope to those areas specified under 4.2.2 for vessels that use natural gas fuel, this is not the case for other low-flashpoint fuels which must undergo a more

comprehensive risk assessment. The risk assessment submitted to the Coast Guard should follow an assessment plan with representatives from relevant disciplines and stakeholders that can identify hazards, categorize the risk, and ensure proper safeguards are utilized to reduce risks where necessary. The scope should be broad enough to adequately cover hazards associated with the specific novel design being proposed, and should be conducted in conjunction with or following the alternative design analysis mentioned above. The risk assessment should be conducted in accordance with relevant guidance of a recognized risk advisory body such as: classification society (e.g. ABS, DNV-GL); industry association (e.g. American Institute of Chemical Engineers, Society of Fire Protection Engineers, National Fire Protection Association); or another acceptable alternative that would be referred to in the assessment plan.

Fuel cell installation requirements – We note your intended use of the DNV-GL Rules for fuel cell installations in reference (h). The IMO is also in the process of developing fuel cell requirements as an upcoming amendment to the IGF Code. A draft of the requirements being considered should be available from IMO as an annex to the CCC Subcommittee Report following their upcoming meeting scheduled for September, 2017. In addition to reference (h), requirements from this draft fuel cell amendment to the IGF Code may prove useful in developing a Design Basis proposal for the vessel under study.

Hazardous areas – We note that the hazardous areas depicted in references (d) and (g) in general follow the prescriptive zones for natural gas specified in Section 12.5 of the IGF Code, which may not be suitable for hydrogen due to the differences in density, dispersion, and flammable range between the two fuels. If moving forward with this project, the alternative design analysis mentioned above should address whether the IGF Code's natural gas hazardous zones are sufficiently conservative to address hydrogen, or whether they should be modified based on dispersion analysis, or some other method, for application to the vessel proposed in your study. The hazardous areas standards in IEC 60079-10-1:2015, provide one possible source for a more detailed methodology of classifying hazardous areas, as well as providing specific considerations for hydrogen in Annex H of the standard.

Fire protection systems – While applying IGF Code requirements for natural gas is a good starting point, it is difficult to provide substantive comments on appropriate fire protection systems for a hydrogen fueled vessel without the support of engineering analysis, such as that prescribed under the IGF Code's alternative design section. Section 3.8.2 of the draft Design Study Report, included in reference (b), for example shows the use of a water spray system located within the fuel cell spaces. Water spray systems are typically used on a vessel's exterior surfaces to provide a cooling effect to protect boundaries of sensitive interior spaces such as accommodation, service or control spaces. The use of a water spray system on an interior compartment such as a fuel cell space should be supported by engineering analysis that compares it with other alternatives to determine an appropriate solution that satisfies the functional requirements in the IGF Code.

The Coast Guard recently issued an update to our policy letter on design of U.S.-flag LNG fueled vessels, reference (j), to incorporate the new IGF Code as a baseline standard. While reference (j) is only applicable to LNG fuel systems, it should prove instructive as a reference in providing

general insight into Coast Guard interpretation of IGF Code requirements, especially in those areas of the code that are left to "the Administration".

We heartily commend the innovative approach by Glosten, in collaboration with Sandia and MARAD to advance the state-of-the-art for marine power systems and look forward to seeing this novel technology mature over time. We recognize that hydrogen fuel cell technology has potential air emissions benefits, and applaud the work you and your team have accomplished in providing alternative arrangements for vessels as the marine transportation system pivots toward cleaner and more sustainable energy.

For further clarification on any of these issues, please feel free to contact Tim Meyers of my staff at (202) 372-1365 or timothy.e.meyers@uscg.mil.

Sincerely,

John H. Miller

J. H. MILLER, P.E.
Commander, U.S. Coast Guard
Chief, Systems Engineering Division
By direction

Copy: Commanding Officer, Marine Safety Center (MSC-2)
Detachment Chief, U.S. Coast Guard Liquefied Gas Carrier National Center of Expertise

Appendix: H

Zero-V Project Report-Out Meetings at the Scripps Institution of Oceanography, San Diego, CA

On September 28, 2017 two meetings were held at the Scripps Institution of Oceanography to present the Zero-V project results to the Scripps science community (in the morning) and to the Scripps research vessel operations staff (in the afternoon). Each meeting began with a summary presentation of the feasibility results, followed by a question and answer session, and lasted approximately 2 hours each. This summary captures the questions raised and the answers given.

Figure 1: Robin Madsen (Glosten) presents results from the Zero-V study.

Morning Meeting Summary (Scripps science community)

For the morning meeting, beginning at 9:00 am, there were 18 in attendance, including representatives of the Scripps science staff, Lt. William Hawn from the U.S. Coast Guard as well as a representative from Clean Cities organization of San Diego. Sujit Ghosh from MARAD attended by telephone. These questions followed a Zero-V summary presentation given by Bruce Appelgate, Lennie Klebanoff, Robin Madsen and Sean Caughlan, as shown in Figure 1.

Is there a stability issue for the Zero-V with having the LH_2 tanks up high?

Answer: No, there is no stability issue. Also, it was commented from Glosten that the Zero-V would not need ballast water because the fully fueled and fuel-empty weights of the vessel are similar.

Could we introduce a small flight deck on the Zero-V to allow for UAV flight applications? This would be very useful. Could it be placed above the LH_2 tanks (to make use of unused space)?

Answer: This is something we could think about, however, a flight deck above the LH_2 tanks presents some concerns with visibility to the aft deck and with locating such equipment in a hazardous area above the tanks. However, a small flight deck could in principle be introduced near the front of the vessel. This approach has been taken with other research vessels.

Are there limitations associated with the hazardous area surrounding the LH_2 tanks?

Answer: It was discussed that much of the area surrounding the LH_2 tanks is classified as a hazardous area. This means that there are restrictions on electrical equipment in that area. It was discussed that this might have some impacts on the van location adjacent to the tanks. However, following additional review after the meeting, it is noted that the van site is in fact entirely outside of the hazardous areas as currently defined.

Where is the acoustic equipment located on the Zero-V?.

Answer: The multibeam sonar transducers are in the bottom center hull towards the bow of the vessel. The transceivers are in a space immediately above the transducers. It was discussed that based on model testing of the RCRV hull form with the same draft and a similar bow shape, that bubble sweepdown would not be a problem at the transducer location. It was noted that bubble sweepdown model testing can certainly be performed at a later stage of development as the project progresses.

Dr. Gabi Laske (UCSD) questioned the relative position of the winch and the LH_2 tank, specifically that a snapped winch cables could hit the LH_2 tank.

Answer: There would likely be some sort of robust fencing

around the LH_2 tanks that allows ventilation, but protects the tanks from being struck by objects.

Is there room for additional sonars up front?

Answer: Yes

Dr. Mark Ohman (UCSD) commented that the Zero-V was an interesting an innovative design, had ample laboratory space and the Zero-V would be a versatile research vessel. It should be seriously considered.

Answer: We appreciate this supportive comment.

Is the Scripps Administration on-board with the Zero-V?

Answer (from Bruce Appelgate): If there was sufficient funding for it, then yes, there is institutional support.

What kind of specialized training would be required for the crew of the Zero-V?

Answer: There would have to be training in monitoring the fuel-cell control system and the H_2 safety related sensors. With such training, the engineers who operate a modern diesel electric plant would be able to operate this vessel.

What is the expected crew size for the Zero-V, noting in comparison that both the New Horizon and the Gordon Sproul vessels are uninspected, and the Zero-V would most likely be an inspected vessel?

Answer: The vessel would almost certainly be USCG inspected regardless of tonnage because of the use of liquid hydrogen as a fuel. The anticipated crew for Zero-V is 12. The crewing impacts of this were not considered because it was our understanding that typically research vessels sail with a full crew even when not necessarily required by the Certificate of Inspection (COI). The USCG officer at the meeting noted that the crewing required by USCG is a function of the vessel tonnage. Having a periodically unattended machinery space does not reduce the minimum crew required. The USCG also noted in response to discussion about bunkering that it would not be hard to fuel both tanks simultaneously.

Mike Prince (Moss Landing Marine Laboratory) asked how much the Moss Landing facility requirements drove the design and cost?

Answer: It had a definite influence on the design, but Robin felt that that while the vessel solution might look different (i.e. a longer or deeper monohull), the capital expenditure (CapEx) and operational expenses (OpEx) for a vessel that did not have the Moss Landing design constraints may not be all that different from the Zero-V. Bruce noted that we've demonstrated that, in order to have 2,400 nm range, we cannot make a smaller vessel. In that respect, the Moss Landing harbor constraints don't matter at all.

Dr. Mark Ohman (UCSD) commented that the 2400 nm range was the absolute minimum that would be acceptable for the Scripps community.

Answer: We agreed.

Can the Zero-V be refueled from a water-borne vessel?

Answer: The answer is yes. LH_2 is currently transported by NASA by barge, and that the Viking Grace cruise ship in Finland is refueled with LNG via a floating LNG refueler. While there are no water-borne LH_2 refuelers currently in existence, it should be possible. Bruce noted that diesel refueling is possible over water too, but for all sorts of other operational reasons it is almost never done.

Lennie then asked the audience, about what new science would be enabled if a vessel like the Zero-V were used that had zero emissions, zero chance of polluting fuel spills and low noise?

Answer (from Dr. Ken Melville (UCSD)): The collection of aerosol samples would be greatly improved, because they worry a lot about contamination of samples. Bruce commented that the zero-emissions is a really good advantage because air sampling is a big deal on RVs, and this would be a great capability. Other benefits for the Zero-V are quiet operations and making plenty of deionized water on the vessel (from the fuel cell exhaust).

The feedback on noise was that the lower the noise, the better. Lower noise always helps, but the audience questioned if anyone would pay for it. The overall sense was that the low noise would not enable a qualitatively different kind of science mission than is performed today with diesel vessels. In response to the lack of fuel spills, someone said that the prospects for diesel spills does not deter research vessels from going anywhere, they simply impose costs on these vessels for spill response. Bruce commented that if diesel fuel is spilled, Scripps or the contractor has to clean it up, which is expensive. In addition, fines are incurred with diesel spills, which can get expensive. From that standpoint, a fuel like LH_2 that cleans itself up in a matter of seconds, and is not a GHG, is very attractive.

Would the Zero-V have a diesel-fueled limp-home mode of operation?

Answer: While a limp-home mode would be possible to establish on the Zero-V with the installation of an emergency diesel generator, it is not necessary. There is redundancy in the Zero-V hydrogen fuel cell propulsion systems.

How does the freeboard of the Zero-V impact recovery of overboard packages? Specifically the difficulty of recovery on the Kilo Moana was noted.

Answer: A lot of the challenge with the Kilo Moana is due to the shape of the hull at the side rather than the freeboard. Because it is a SWATH, the Kilo Moana has a very slender hull at the water plan and wide overhanging haunches. The Zero-V by contrast is wall sided in the area of the side deck. This will make launch and recover similar to a monohull. Bruce noted that launch and recovery is fine on the Roger Revelle research vessel that has the same freeboard as the Zero-V.

Dr. Rob Pinkel (UCSD) asked if the FLIP vessel is an opportunity for introduction of hydrogen fuel cell power?

Answer (from Bruce Appelgate): It's a great idea. One could remove all the diesel generators from FLIP and replace with hydrogen fuel cell systems. FLIP does not have propulsion, and uses generators to make electricity. The point of FLIP is to be as quiet and benign as possible – and the generators are noisy and smell bad. If FLIP continues to be supported for use (questionable because it's 53 years old), introducing hydrogen fuel cell power would be a great upgrade.

After the morning meeting, the following Zero-V group photo was taken, shown in Figure 2:

Figure 2: (L-R): Bruce Appelgate (Scripps), Ryan Sookhoo (Hydrogenics), Tim Leach (Glosten), Sean Caughlan (Glosten), Lennie Klebanoff (Sandia) and Robin Madsen (Glosten).

Summary of Q&A Sessions for the Zero-V Afternoon Meeting at Scripps

At 3:00 pm in the afternoon of September 28, 2017, a presentation was given to the Scripps operations staff. There were 16 in attendance, including Scripps operations staff, Mike Prince from Moss Landing Marine Laboratories, Ryan Sookhoo from Hydrogenics, Joe Pratt from Sandia and a representative from Clean Cities San Diego. This summary captures the questions raised and the answers given. Photos from the presentation are given as Figures 3 and 4.

Figure 3: Sean Caughlan (Glosten) presents Zero-V research results to the Scripps operations staff.

What can you use the fuel cell waste water for?

Answer from Ryan Sookhoo (Hydrogenics): With a little treatment, the water from the fuel-cell reaction is drinkable. It is considered deionized water upon exit from the fuel-cell stack. Lennie noted that the shuttle astronauts drank treated water from PEM fuel cells. Bruce added that many scientific applications require ultrapure water. Scripps has ultrapure water generators on all of their ships to produce this. Having ultrapure (or nearly so) water to start with is an advantage.

Can the fuel cells be upgraded and keep the same form factor? In other words, if the Zero-V were built today, but in 5 years the fuel cells are better, will it be easy to replace the old fuel cells?

Answer from Ryan Sookhoo: Yes, the balance-of-plant (water cooling, waste water handling, hydrogen input requirements) will all be the same. As for the fuel cells themselves, it should be possible to just remove old units and insert new and improved ones. Hydrogenics is working in that direction currently.

Are there any exotic and therefore expensive materials in a fuel cell that would make them a target of crime?

Answer from Ryan Sookhoo: There are small amounts of platinum in the fuel cells, but they will be in the fuel cell cars too (which have larger exposure to theft). Lennie noted that he had never heard of fuel cells being targeted for their platinum, and he didn't think the amounts in the fuel cell are significant. Also, it is highly dispersed, difficult to recover.

Will there be special training for the crews of fuel-cell vessels?

Answer: Yes, there will be training in understanding the fuel-cell monitoring systems, and also training in hydrogen technology. The Gas Suppliers will do the bunkering, but the vessel crew needs to be trained in bunkering issues too, and monitoring the fuel transfer. Robin Madsen added with regard to LH_2 refueling that marine bunkering is probably a little different than industrial facility filling. The chief engineer is overall responsible for the bunkering operation and safety of the vessel. It will be very much a coordinated effort between the gas supplier and the ship's crew. Likely during bunkering, the gas supplier would be operating the truck and ship's personnel will be at the bunker manifold and monitoring the vessel tanks.

Why doesn't the nitrogen in the air react within the fuel cell?

Answer: Nitrogen is too stable (because of its N-N triple bond) to react with hydrogen under the conditions of temperature and pressure of fuel cell operations.

Question from Lennie to the group, does anyone see a worrisome problem arising from hydrogen fuel cell use on the Zero-V as described?

Answer: No, nobody identified a worrisome problem, it all looks manageable.

What are the hydrogen pressures on the Zero-V?

Answer: The Zero-V pressures are less than or equal to ~ 150 psig. Zoltan Kelety commented this was a relatively low pressure.

Are the ventilation systems and fuel cell racks designed for proper operation in rough seas?

Answer: Robin Madsen answered that the classification societies (ABS, DNVGL) would require the fuel cells to go through "shake and bake" tests. Ryan Sookhoo added that Hydrogenics PEM fuel cell systems have already been tested for stability (shake and bake) for aircraft applications, and that they have been tested under launch stress conditions for the Canadian Space Agency.

Can Hydrogen Explode?

Answer: Lennie Klebanoff described the physical and combustion properties of hydrogen that relate to explosion, indicating that you need confinement, an explosive H_2/air mix and a blasting cap (high energy ignition source) to get hydrogen to directly explode. It is possible to get a deflagration to detonation transition (DDT) in hydrogen given sufficient run-up distance (> 10 meters) and turbulence-inducing structure. The fuel-cell rooms in the Zero-V have physical dimensions less than 10 meters. Zoltan Kelety commented that with lead acid battery use on a submarine, that the hydrogen release (from batteries) is being handled routinely. The strategy is to keep the H_2/air mix below the lower flammability limit (LFL) of 4%, ventilate, and you have no problems.

Question from Lennie Klebanoff to Paul Mauricio during the Gordon Sproul Tour: Given the refueling described for the Zero-V (3 LH_2 trailers, etc.), and moving the trailer off the pier for trailer depressurization, do you see any issues performing these refueling activities at MARFAC?.

Answer: No, sounds easily accommodated. They have a lot of 18 wheelers coming onto the staging area/pier now.

Question from Lennie Klebanoff to Paul Mauricio during the Gordon Sproul Tour: Do you worry about diesel fuel spills?

Answer: Yes. Although it does not happen often (a cup full of diesel has spilled in the water in the last 16 years), it is a big deal when diesel fuel does spill, either on the water or on the deck. It is expensive, and people can lose their jobs over it. Scripps operations staff worries a lot about it. Bruce Appelgate confirmed that Scripps worries a lot about oil spills.

If fuel or oil is spilled, Scripps or the contractor has to clean it up, which is expensive. In addition, fines need to be paid, which is expensive. From that standpoint, a fuel such as LH_2 that can evaporate in ~ 10 – 15 seconds and is not a GHG is very attractive.

After the afternoon meeting, a Zero-V group photo was taken, shown in Figure 4.

Figure 4: (L-R) Tim Leach, Robin Madsen, Lennie Klebanoff, Sean Caughlan, Bruce Appelgate, Joe Pratt, Ryan Sookhoo.

(This page left intentionally blank.)

For more information, please contact:

Sandia National Laboratories

Leonard E. Klebanoff
E-mail: lekleba@sandia.gov
Phone: (925) 294-3471
Website: http://energy.sandia.gov/transportation-energy/hydrogen/market-transformation/maritime-fuel-cells/